AD NUMBER

ADB083264

NEW LIMITATION CHANGE

TO

Approved for public release, distribution unlimited

FROM

Distribution authorized to U.S. Gov't. agencies only; Test and Evaluation; July 1983. Other requests shall be referred to AFWAL/MLBC, Wright-Patterson Air Force Base, Ohio 45433.

AUTHORITY

WL/MLBC fax, 13 Jan 1985.

AFWAL-TR-83-4124

PROCESSING SCIENCE OF EPOXY RESIN COMPOSITES

R. A. BRAND
G. G. BROWN
E. L. MC KAGUE
GENERAL DYNAMICS CONVAIR DIVISION
P.O. BOX 85357
SAN DIEGO, CALIFORNIA 92138

JANUARY 1984

FINAL REPORT FOR PERIOD AUGUST 1980 – DECEMBER 1983

SUBJECT TO EXPORT CONTROL LAWS

This document contains information for manufacturing or using munitions of war. Export of the information contained herein, or release to foreign nationals within the United States, without first obtaining an export license, is a violation of the International Traffic-in-Arms Regulations. Such violation is subject to a penalty of up to 2 years imprisonment and a fine of $100,000 under 22 USC 2778.

Include this notice with any reproduced portion of this document.

MATERIALS LABORATORY
AIR FORCE WRIGHT AERONAUTICAL LABORATORIES
Air Force Systems Command
Wright-Patterson Air Force Base, Ohio 45433

NOTICE

When Government drawings, specifications, or other data are used for any purpose other than in connection with a definitely related Government procurement operation, the United States Government thereby incurs no responsibility nor any obligation whatsoever; and the fact that the government may have formulated, furnished, or in any way supplied the said drawings, specifications, or other data, is not to be regarded by implication or otherwise as in any manner licensing the holder or any other person or corporation, or conveying any rights or permission to manufacture, use, or sell any patented invention that may in any way be related thereto.

This technical report has been reviewed and is approved for publication.

C.E. BROWNING, Technical Area Manager
Structural Materials Branch
Nonmetallic Materials Division

R.L. RAPSON, Chief
Structural Materials Branch
Nonmetallic Materials Division

FOR THE COMMANDER

F.D. CHERRY, Chief
Nonmetallic Materials Division

"If your address has changed, if you wish to be removed from our mailing list, or if the addressee is no longer employed by your organization please notify AFWAL/MLBC, W-P AFB, OH 45433 to help maintain a current mailing list."

Copies of this report should not be returned unless return is required by security considerations, contractual obligations, or notice on a specific document.

UNCLASSIFIED

SECURITY CLASSIFICATION OF THIS PAGE (When Data Entered)

REPORT DOCUMENTATION PAGE

READ INSTRUCTIONS BEFORE COMPLETING FORM

1. REPORT NUMBER: AFWAL-TR-83-4124	2. GOVT ACCESSION NO.: AD-B083264L
3. RECIPIENT'S CATALOG NUMBER:	
4. TITLE (and Subtitle): PROCESSING SCIENCE OF EPOXY RESIN COMPOSITES	5. TYPE OF REPORT & PERIOD COVERED: Final Report August 1980 - December 1983
	6. PERFORMING ORG. REPORT NUMBER:
7. AUTHOR(s): R. A. Brand, G. G. Brown, E. L. McKague	8. CONTRACT OR GRANT NUMBER(s): F33615-80-C-5021
9. PERFORMING ORGANIZATION NAME AND ADDRESS: General Dynamics Convair Division, P.O. Box 85357, San Diego, California 92138	10. PROGRAM ELEMENT, PROJECT, TASK AREA & WORK UNIT NUMBERS: P.E. 62102F, 2419-03-19
11. CONTROLLING OFFICE NAME AND ADDRESS: AFWAL/MLBC, WPAFB, OH 45433	12. REPORT DATE: January 15, 1984
	13. NUMBER OF PAGES: 318
14. MONITORING AGENCY NAME & ADDRESS (if different from Controlling Office)	15. SECURITY CLASS. (of this report): Uncl
	15a. DECLASSIFICATION/DOWNGRADING SCHEDULE:

16. DISTRIBUTION STATEMENT (of this Report)

Distribution limited to US Government Agencies only; test and evaluation; July 1983. Other requests for this document must be referred to AFWAL/MLBC, Wright-Patterson Air Force Base, Ohio 45433.

17. DISTRIBUTION STATEMENT (of the abstract entered in Block 20, if different from Report)

18. SUPPLEMENTARY NOTES

19. KEY WORDS (Continue on reverse side if necessary and identify by block number)

Epoxy, Processing, Mathematical Modeling, Resin Characterization, Internal Pressure Cure, Bagless Cure, Diffusivity, Solubility, Moisture Absorption, Void Etiology

20. ABSTRACT (Continue on reverse side if necessary and identify by block number)

The "Processing Science of Epoxy Resin Composites" program investigated the interrelationships between the resin and prepreg physical and chemical properties of 177C (350F) curing epoxy resin systems and how these properties ultimately affected the processing characteristics of the material.

The primary influence in affecting laminate quality was determined to be the volatiles in the resin. The major volatile was determined to be water. The

(Cont.)

DD FORM 1 JAN 73 1473 EDITION OF 1 NOV 65 IS OBSOLETE

UNCLASSIFIED

SECURITY CLASSIFICATION OF THIS PAGE (When Data Entered)

20. Abstract Continued

situation, however, was more complicated than just the quantity of volatiles that were in a resin or prepreg. Rather, the point of volatile release and local concentrations played a significant role in void formation. Associated also with void formation was vacuum application during processing.

Mathematical models have been developed to describe the collective effects of diffusivity, solubility, surface tension, resin flow, and pressure on the removal of volatile material and entrapped air within a laminate.

Two techniques were developed to insure pressure translation into the resin during processing, i.e., (1) bagless curing of consolidated parts and (2) internal bag pressurization. These processes have proven to be quite successful in part fabrication, if prior processing cycles were employed.

Validation articles comprised the final phase of the program. The F-16 vertical stabilizer skin was selected as the validation article along with a small 0.61 m by 0.91 m internal ply drop-off laminate employed as a material screening laminate by Fort Worth Division.

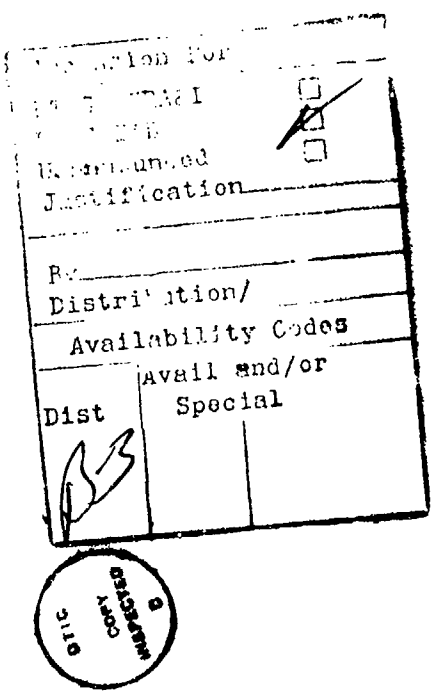

SUMMARY

The "Processing Science of Epoxy Resin Composites" program investigated the interrelationships between the resin and prepreg physical and chemical properties of 177C (350F) curing epoxy resin systems and how these properties ultimately affected the processing characteristics of the material.

The primary influence in affecting laminate quality was determined to be the volatiles in the resin. The major volatile was determined to be water. The situation, however, was more complicated than just the quantity of volatiles that were in a resin or prepreg. Rather, the point of volatile release and local concentrations played a significant role in void formation. Associated also with void formation was vacuum application during processing.

Mathematical models have been developed to describe the collective effects of diffusivity, solubility, surface tension, resin flow, and pressure on the removal of volatile material and entrapped air within a laminate.

Two techniques were developed to insure pressure translation into the resin during processing, i.e., (1) bagless curing of consolidated parts and (2) internal bag pressurization. These processes have prover to be quite successful in part fabrication, if proper processing cycles were employed.

Validation articles comprised the final phase of the program. The F-16 vertical stabilizer skin was selected as the validation article along with a small 0.61 m by 0.91 m internal ply drop-off laminate employed as a material screening laminate by Fort Worth Division.

FOREWORD

This report describes the work performed under Contract F33615-80-C-5021 during the period from 18 August 1980 to 19 December 1983. The program was administered under the technical direction of Dr. C. E. Browning, AFWAL/MLBC, Aeroanutical Systems Division, Wright-Patterson Air Force Base, Ohio 45433.

The Convair Division of General Dynamics Corporation was the prime contractor with Dr. R. A. Brand serving as program manager. The Fort Worth Division of General Dynamics Corporation was under subcontract and was directed by E. L. McKague.

Dr. J. L. Kardos and Dr. M. P. Dudukovic of Washington University (St. Louis) were consultants for the mathematical model development portion of the program and developed the modeling computer program.

Acknowledgments are extended to M. Lehman, Principal Investigator on the program at Fort Worth Division and C. F. Ochoa, Chemist at the Convair Division for their outstanding contributions to the program.

Acknowledgments are also extnded to Dr. R. J. Hinrichs, Applied Polymer Technology, and W. A. Wilson, NARMCO Corporation, for their contributions to the program effort.

TABLE OF CONTENTS

TABLE OF CONTENTS (Continued)

LIST OF FIGURES

LIST OF FIGURES (Continued)

LIST OF FIGURES (Continued)

LIST OF FIGURES (Continued)

LIST OF FIGURES (Continued)

LIST OF FIGURES (Continued)

LIST OF FIGURES (Continued)

LIST OF TABLES

1.0 PROGRAM OVERVIEW

1.1 OBJECTIVES

The objectives of the Processing Science of Epoxy Resin Composites program were to establish and understand the fundamental interrelationships between the material, processing, and environmental parameters of graphite/epoxy material systems. This was accomplished through a multi-phase program designed to (1) develop an understanding of the behavior of the graphite/epoxy material during the various processing steps, (2) determine what material characteristics and processing parameters were critical and controllable for consistent processing, and (3) develop a methodology where critical materials and processing parameters were defined and specified before manufacturing of a given composite part configuration. The information and data generated on this program was generic in nature and was applicable to many graphite/epoxy material systems. However, for this program, the 5208/T-300 system produced by Narmco Corporation was selected for initial evaluation.

The original progfam was structured in four phases. The first phase was directed toward the development and definition of the materials behavioral profiles as functions of various processing parameters associated with different resin formulations. Variations in resin formulations includdd high and low base resin viscosity, variations in curing agent content of +5 and -5 percent of nominal, and upper and lower limits of the processed resin viscosity. These variations in prepreg were then to be subjected to a spectrum of assembly and fabrication steps, including various final autoclave/vacuum bag cure procedures.

Two changes in the program structure were made with the concurrence of the Air Force program monitor. The first change was the elimination of the different

resin formulations and concentration on the normal or baseline 5208/T300 prepreg as produced by Narmco Corporation. The second change in the program was the inclusion of additional types of prepreg for evaluation. These additional materials were epoxy graphite, 3502/AS4, and 976/T300.

The second phase, which ran concurrently with the first, consisted of development of a mathematical model which quantified the various transport processes which occurred during the processing of laminates. This phase was conducted by the Fort Worth Division of General Dynamics. The third phase coupled the results of the first two phases into a general methodology encompassing part configuration, fabricability and material behavior characteristics. The fourth phase encompassed validation of the incorporated results of the first three phases by fabrication of parts under appropriate reciprocal variations in both process conditions and material behavioral characteristics. One of the validation parts was identified as a vertical tail skin for the F-16 aircraft. Various innovative process and cure techniques developed during this program were utilized in the curing of the vertical tail skin at the Fort Worth Division. Included in the fourth phase was also the preparation of a set of operating procedures for the utilization of the developed materials/processing methodologies.

2.0 PROGRAM RESULTS

2.1 STANDARD PREPREG AND BASE RESIN CHARACTERIZATION

The successful implementation of the Processing Science program was based on the understanding of the resin system employed and how the resin reacts to specific temeprature, pressure, time, and environmental influences. A fundamental resin characterization program initiated this study. In particular, General Dynamics was concerned with the initial ("as recieved") composition of the resin, what the resin's rheological profile was as a function of various processing conditions, what the basic kinetics of the polymerization of the resin were, and how the kinetics related to the rheology/processability of the resin.

2.1.1 PHYSICAL PROPERTIES OF STANDARD PREPREG. A standard batch (batch 716) of 150 pounds of 5208/T300 prepreg was received early in the program. From this initial shipment 95 pounds were retained at the Convair Division, 50 pounds were delivered to the Fort Worth Division and 5 pounds to AFWAL. In addition, 5 pounds of catalyzed resin was also received, and approximately 100 pounds of uncatalyzed resin were retained from the original resin batch and stored at -18C at Convair. This additional resin was to be used in the preparation of future prepreg requirements during the course of the program.

Physical properties were determined on the initial batch of prepreg and found to be within the specified ranges of the Purchase Order. Table 1 shows the fiber areal weight and resin content of the sampled rolls.

2.1.2 BASE RESIN CHARACTERIZATION. The viscosity profile of any epoxy resin at any time during a particular processing cycle is a reasonably uniform function of at least two variables: the degree of polymerization and

Table 1. Fiber Areal Weight and Resin Content

Spec. Value	Fiber Areal Weight (g/m^2) 157 ± 2	Resin Content (% by Weight) 32 ± 2
Roll 4A	158.1	32.34
Roll 3B	158.2	33.08

temperature. Of these two, the degree of polymerization affects all of the essential material characteristics that must be accounted for in optimizing a cure process. These characteristics include resin viscosity, surface tension, shrinkage, moisture diffusion rate, and a uniform heat transfer behavior.

It was therefore necessary to develop a measurement/characterization scheme that would establish viscosity, surface tension, shrinkage, and moisture diffusion coefficients as functions of the degree of polymerization. With these relationships and the cure reaction kinetics, we would then be able to establish the "process" variables at any point during any cure cycle. Conversely, if a particular viscosity must be achieved for adequate flow and devolatization to take place, then an appropriate cure cycle could be developed.

To quantify the degree of polymerization of the resin, a number of methods of analyses were investigated.

2.1.2.1 Wet Chemical Analysis. This was one of the first methods to be investigated. For this analysis we employed the accepted acetone/hydrochloric acid titration technique developed by Ciba-Geigy for determining epoxy content as a function of time at 121C. Acceptable results were obtained after the resin was reacted with the reagent overnight followed by back titration with a standard base.

Figure 1 shows these results. It can be seen that the change in epoxy number is linear with advancement time, out to as long as 165 minutes. We

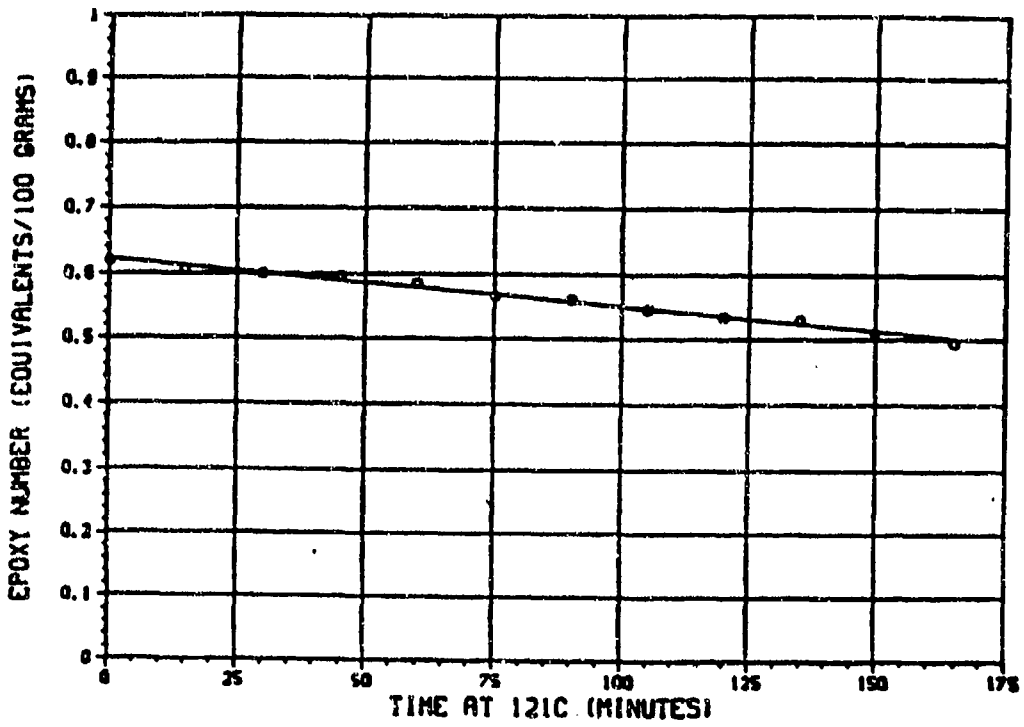

Figure 1. Epoxy Number as a Function of Time at 121C, 5208 (B-716)

previously established an estimate of 5.6 percent reaction of the initial epoxy group content during the resin mixing and staging procedures. Since fully cured material would ideally have a zero epoxy number, we can calcualte the degree of advancement in moving from 5.6 percent to 24.0 percent reaction during the 165 minute exposure at 121C. It should be noted that resin gellation occurs after approximately 30 to 40 percent epoxy group consumption.

2.1.2.2 High Pressure Liquid Chromatography (HPLC) Analysis. High pressure liquid chromatrography using standard techniques provided consistently good results when the major epoxy peak was calculated on a cocunts per microgram injected basis. A linear relationship through the range employed in the 165 minutes at 121C exposure is displayed in Figure 2. The translation to degree of cure (advancement) of the resin was applicable only through the range investigated. This analysis measured only the decrease in a single reacting species, the major epoxy group.

Figure 3 shows the correlation between the two techniques, providing a straight line plot of the epoxy equivalent number and the major epoxy HPLC counts per sample.

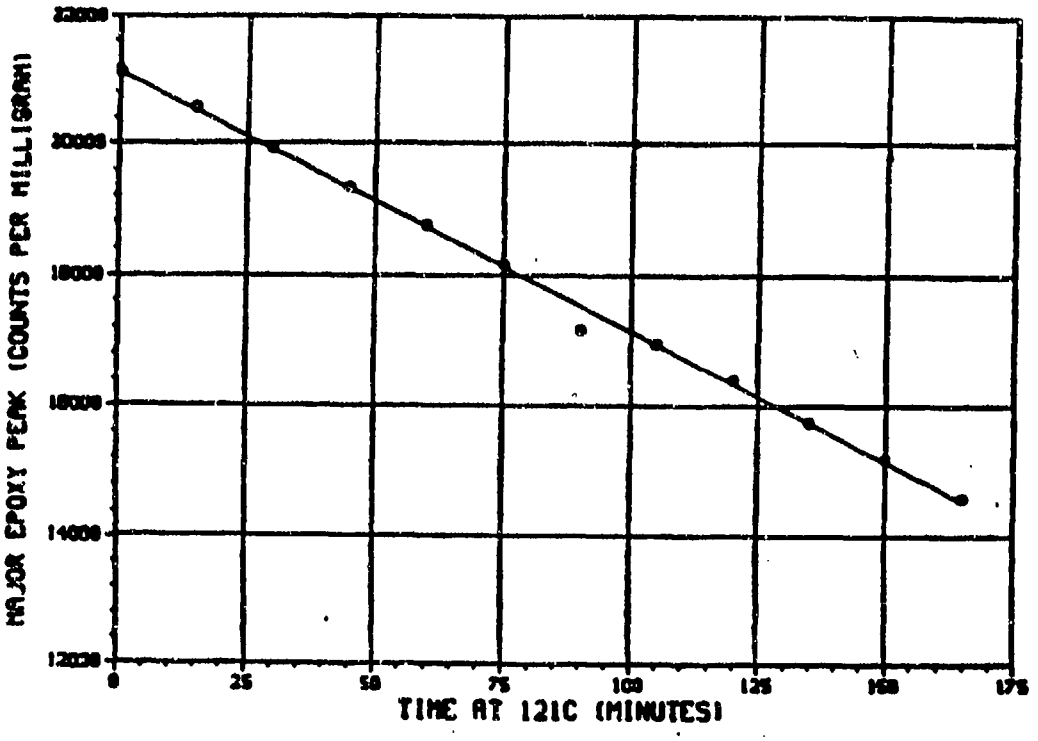

Figure 2. Major Epoxy (HPLC) as a Function of Time at 121C, 5208 (B-716)

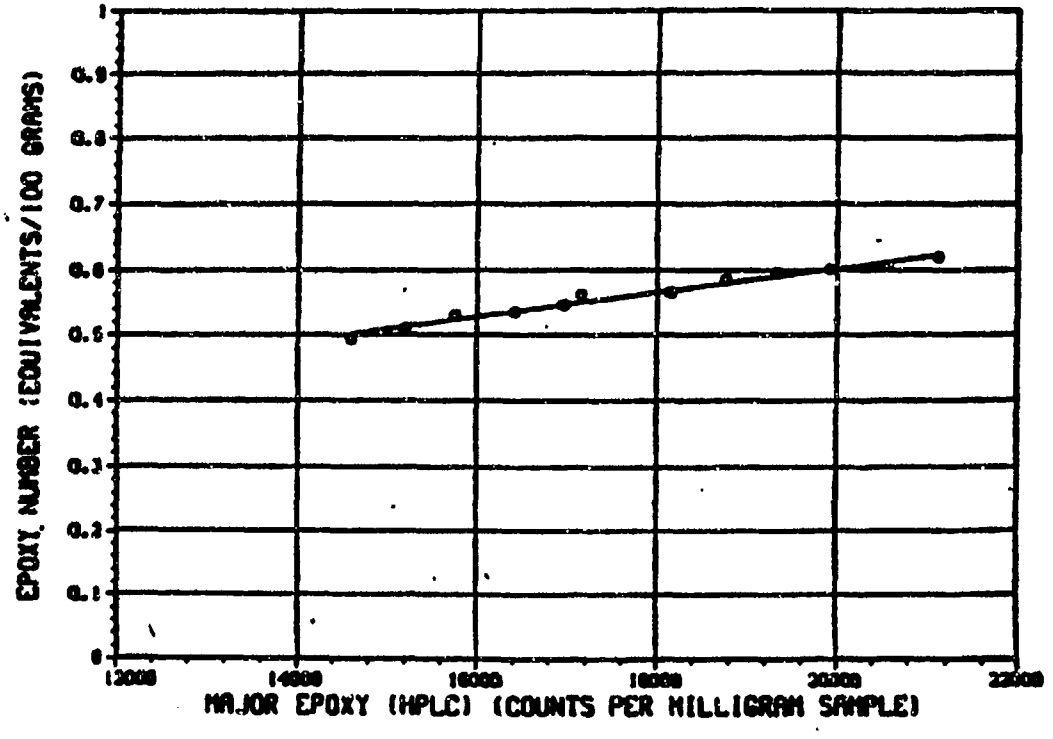

Figure 3. Epoxy Number as a Function of Major Epoxy Content (HPLC), 5208 (B-716)

An HPLC analysis was also performed on the resin used in a spot viscosity aging study. Samples were taken at approximately 22 minute intervals during the aging at 120 and 135C. Table 2 shows the change in the major and minor epoxy and the hardener as a function of the aging study.

Figures 4 and 5 show overlays of actual HPLC data showing the maximum change in peak heights between normal advancement levels and after maximum aging of 135 and 86 minutes respectively at 120 and 135C. HPLC data for intermediate levels of advancement are shown in Figures 6 through 8.

2.1.2.3 Infrared Analysis. An infrared analysis was performed on the 5208 resin, batch 716 after exposure to different degrees of cure (various exposure times at 121C). The analysis was done on a Nicolet Fourier Transform Infrared (FTIR), spectrometer, Model 7199.

The infrared region was scanned between 4,000 and 400 cm^{-1}. Figure 9, FTIR scan of the resin compares the aromatic absorption peaks at 1589 cm^{-1} and the epoxy absorption peak at 886 cm^{-1}. A plot of the ratios of these absorption peaks versus time of exposure at 121C, Figure 10, indicates that a considerable

Table 2. HPLC Analysis Results of Controlled Temperature Aging Samples

Sample	Age Temp, °C	Age Time, Minutes	% Reaction* Predicted	RDR Major Epoxy	%Chng.	RDR Minor Epoxy	% Chng.	RDR Hardener	% Chng.
Aging Blank	-	-	0	70.6	-	6.53	-	18.48	-
A-1	120	50	3.87	65.5	-7.2	5.30	-18.8	15.24	-17.5
A-2	120	100	7.74	54.3	-23.1	4.97	-23.9	10.87	-41.2
A-3	120	135	10.46	49.8	-29.5	4.92	-24.4	8.60	-53.5
A-4	120	150	11.62	47.8	-32.3	4.91	-24.8	7.19	-61.1
B-1	135	22.1	3.87	64.3	-8.9	5.25	-19.6	15.74	-14.8
B-2	135	44.2	7.75	57.0	-19.3	4.90	-25.0	11.31	-38.8
B-3	135	66.7	11.63	45.1	-36.1	4.79	-26.6	6.84	-63.0
B-4	135	85.7	15.0	40.3	-42.9	4.40	-32.6	4.33	-76.6

*Predicted by ln (Rate) = 19 6 - 8708/T

REVERSE-PHASE HPLC - ACETONITRILE/WATER GRADIENT MOBILE PHASE

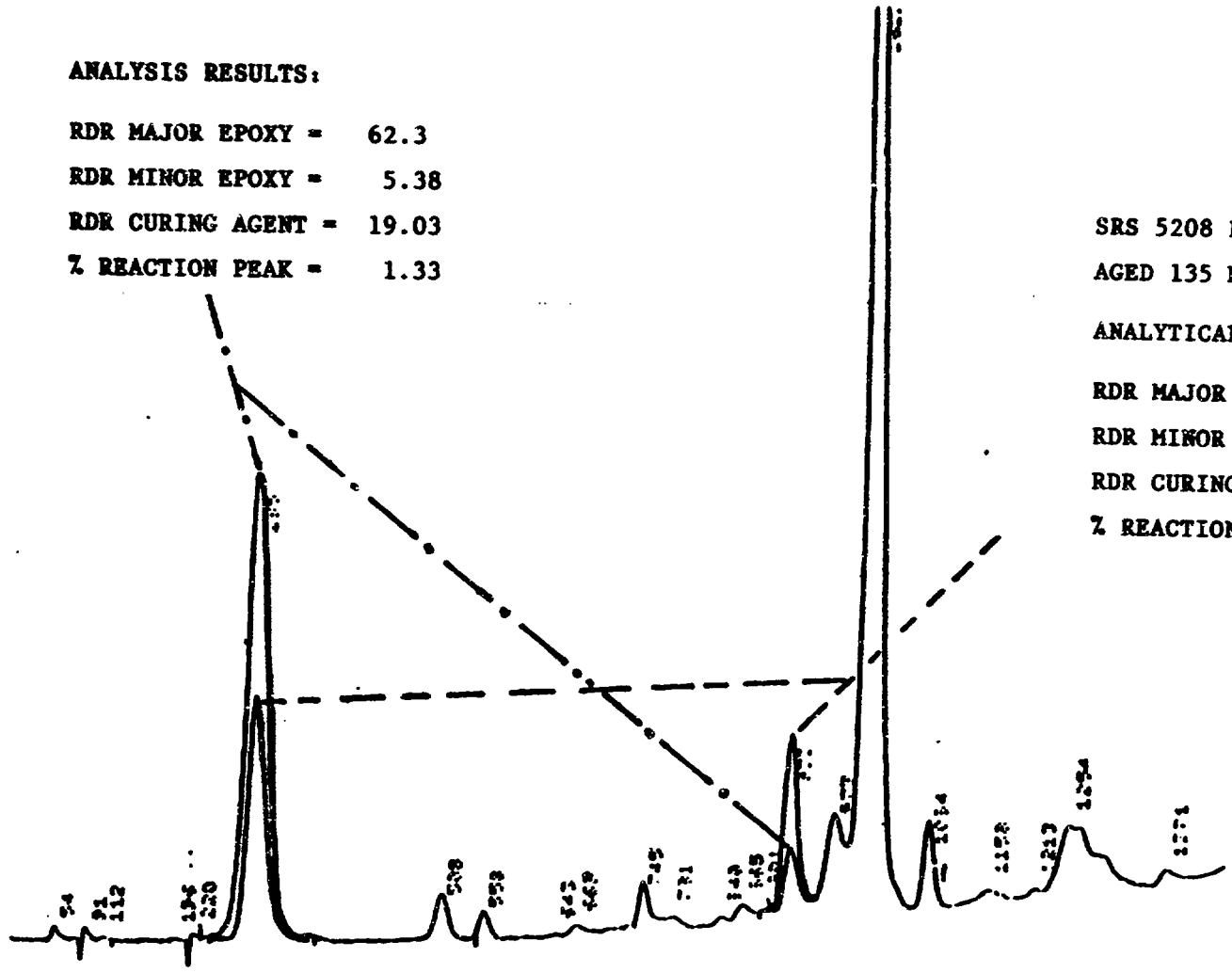

Figure 4. 5208 Batch 716 - Normal Level Advancement and Aged 135 Minutes at 120C

REVERSE PHASE HPLC - ACETONITRILE/WATER MOBILE PHASE

AGED 86 MINUTES AT 135C

ANALYSIS RESULTS:

RDR MAJOR EPXOY = 40.4
RDR MINOR EPOXY = 4.32
RDR CURING AGENT= 4.21
% REACTION PEAK = 3.04

NORMAL LEVEL

RDR MAJOR EPOXY = 62.3
RDR MINOR EPOXY = 5.38
RDR CURING AGENT = 19.03
% REACTION PEAK = 1.33

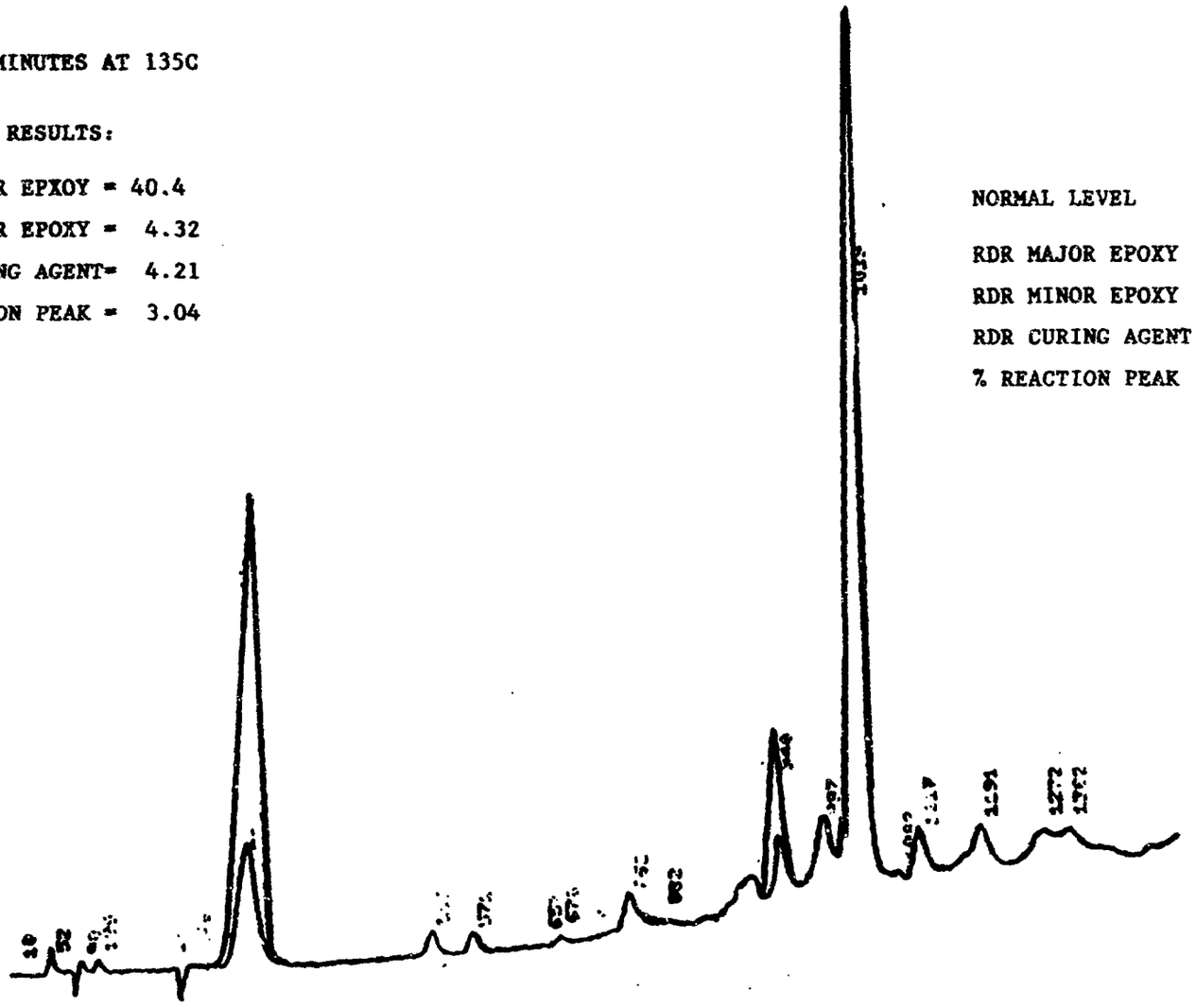

Figure 5. 5208 Batch 716 Sample B-4 - Aged 85.7 Minutes at 135C

REVERSE PHASE HPLC - ACETONITRILE/WATER GRADIENT MOBILE PHASE

ANALYSIS RESULTS:

RDR MAJOR EPOXY = 60.8

RDR MINOR EPOXY = 5.38

RDR CURING AGENT = 14.96

% REACTION PEAK = 2.94

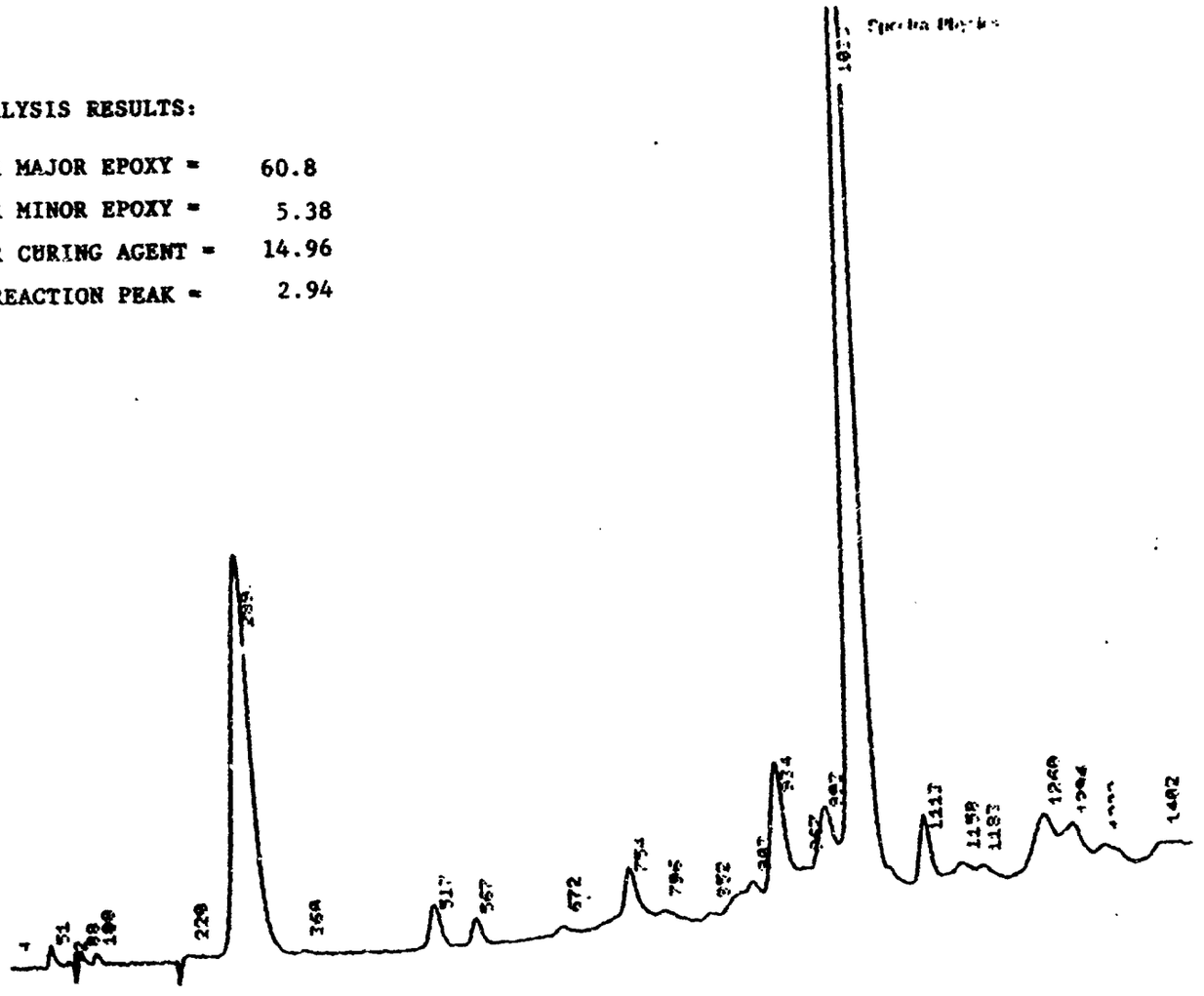

Figure 6. 5208, Batch 716 - Aged 50 Minutes at 120C

REVERSE-PHASE HPLC - ACETONITRILE/WATER GRADIENT MOBILE PHASE

ANALYTICAL RESULTS:

RDR MAJOR EPOXY = 54.3

RDR MINOR EPOXY = 4.97

RDR CURING AGENT = 10.87

% REACTION PEAK = 3.18

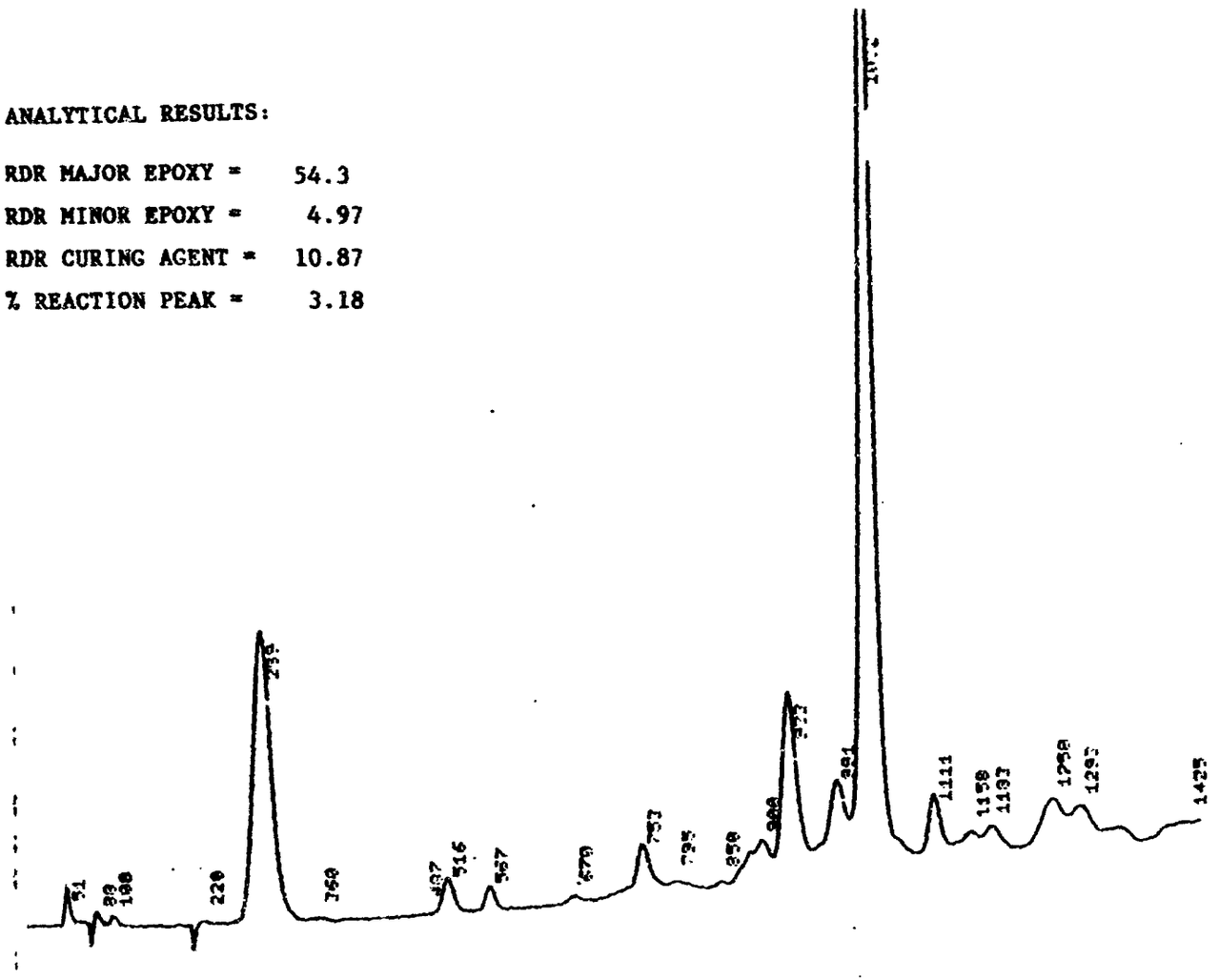

Figure 7. 5208 Batch 716 - Aged 100 Minutes at 120C

ANALYTICAL RESULTS:

RDR MAJOR EPOXY = 49.8

RDR MINOR EPOXY = 4.92

DRD CURING AGENT = 8.60

% REACTION PEAK = 4.31

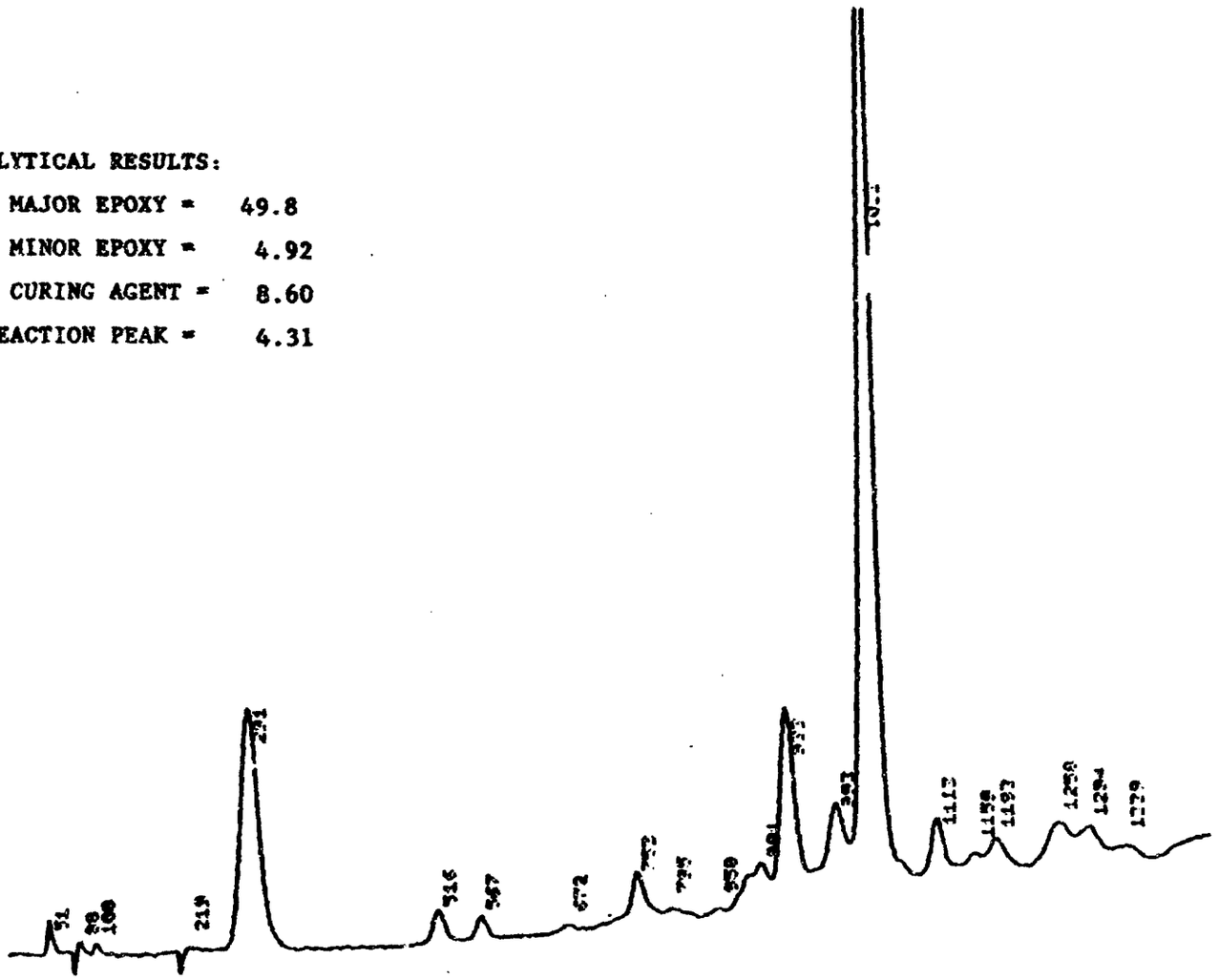

Figure 8. 5208 Batch 716 - Aged 135 Minutes at 120C

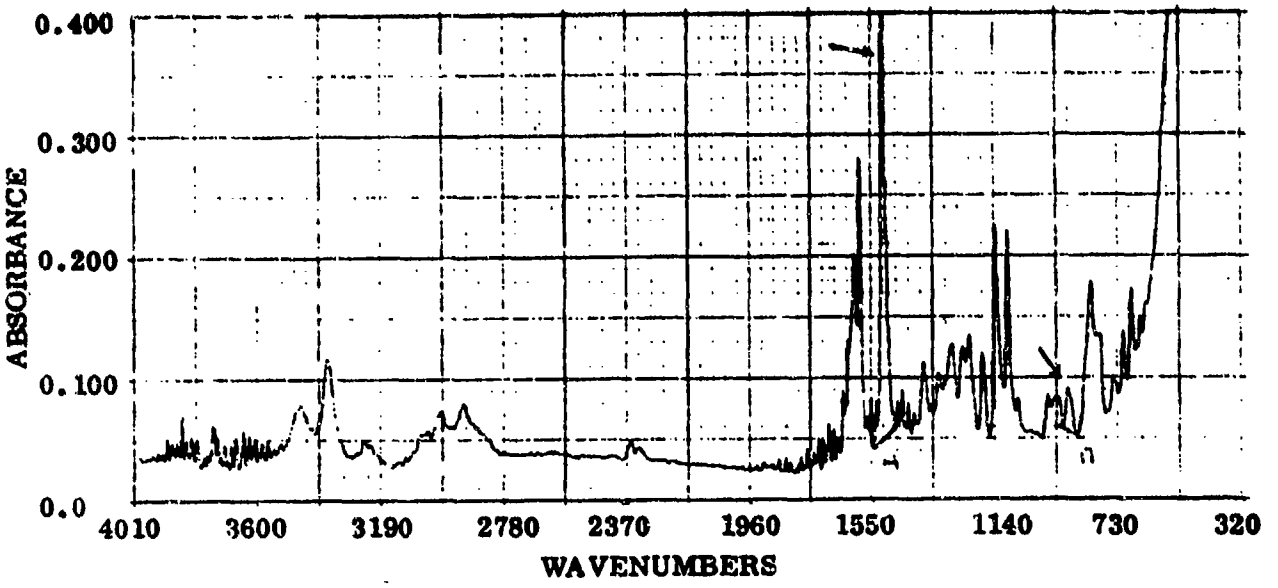

Figure 9. FTIR Spectrum of 5208 Resin Batch 716

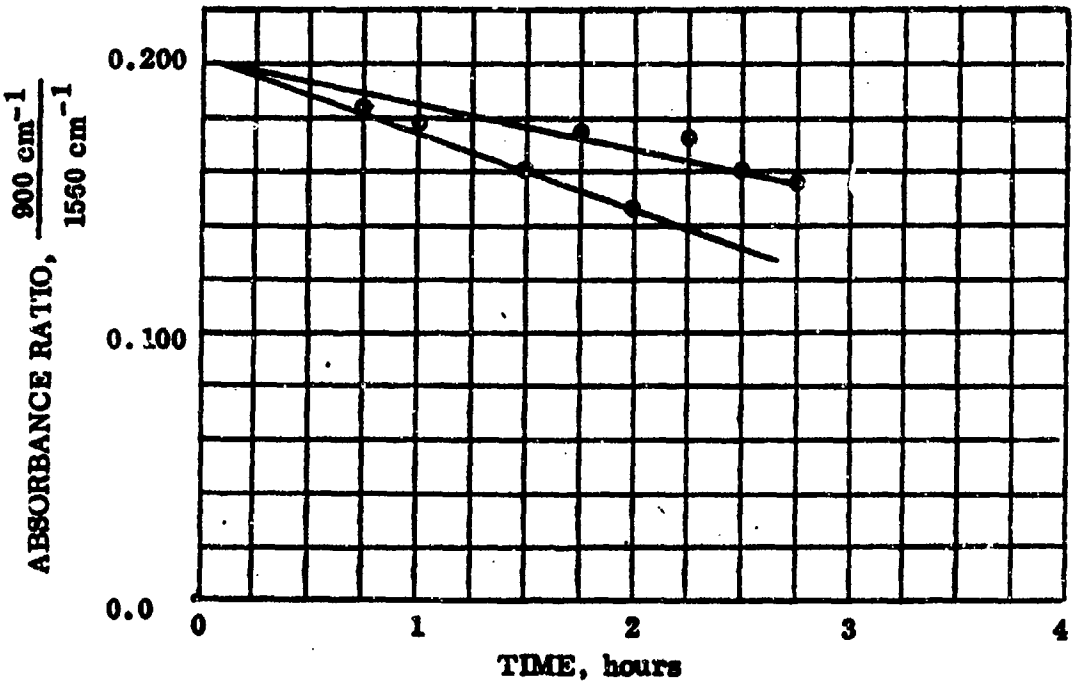

Figure 10. Infrared Analysis of Advancing 5208 (B-716) at 250F

amount of scatter in data points exists. This method does not appear to be an accurate procedure for determination of the degree of advancement for the 5208 resin.

Figure 9 clearly illustrated the absorption bands utilized in the analysis of the FTIR spectrum taken at a zero resin time (no advancement). The epoxy peak at 886 cm^{-1} is quite small and with staging, near resin gel, would only decrease by about 20 percent.

Therefore, small changes of peak intensity are difficult to observe and measure with accuracy. Another procedure investigated was the acquisition of absorption data in the near infrared. This method, however, was not as accurate as the HPLC or titration technique and was not used.

2.1.2.4 Differential Scanning Calorimeter (DCS) Analysis. A substantial amount of DSC work was done at relatively high scan rates (e.g., 5 to 20 C/min). The total quantity of heat given off during cure is one of the important measurements for our purposes since the extent of cure is an inverse function of the residual cure exotherm. A precision of about ±8 percent (135 ± 12 mcal/g) has been experienced in determination of total heat of reaction for 5208 resins at scan rates of 5C/minute or greater.

Straight line relationships are obtained between the logarithm of the scan rate and the reciprocal temperature for such features as peak exotherm initiation, and final temperatures of the cure exotherm.

The fit of the Arrhenius plot implies a correspondence between measurements made at the various scan rates. However, there is probably no change in the mechanism of the measured reaction regardless of the temperature region where the measurements are taken.

A DSC scan was run on MY-720 (the tetraglycidylether of methylene dianiline, the major epoxy constituent of most 177C (350F) epoxy resin systems) alone.

The amount of overlap between "cure" of MY-720 alone and 5208 was compared. Figure 11 shows the CSC results at 10C/minute. The same mateials run at 2C/minute are shown in Figure 12, where it can be seen that the cure of the formulated resin is well beyond half completed before the MY-720 begins to exotherm appreciably, around 225C. The implication is that scans run at higher rates may not reflect actual residual cure exotherm but may be skewed toward homopolymerization or decomposition of the MY-720 resin.

A study of DSC response to scan rate included 1, 2, 5 and 10C/min scan rates. Whie the values for residual heats of reaction appeared significantly higher (~ 145 to 155 mcal/g) for the slower scan rates, the scatter in repetitive runs is no better than normal scan rates (5 and 10C/min). A precision of only about 6 to 8 percent of the average value was not high enough to consider DSC as a sensitive measurement method for determining the extent of cure of the baseline resin.

2.1.2.5 Rheometric Viscosity Studies. Rheometric viscosity profiles of 5208 resin were completed for a number of different processing conditions. Viscosity measurements were taken throughout a process range which simulated different possible cure cycles for the 5208/T300 material. Heat-up rates were varied between 1C and 5C/min (1.8 and 11F/min) with hold times at temperatures which varied between 100 and 140 minutes. Changes in viscosity as a function of holding at four different temperatures, 88, 127, 135 and 143C (190, 260, 275,and 290F), were recorded.

Table 3 lists the test variables used in the Rheometric viscoelastic analysis. The analyses were performed on neat resin batch 716.

Figure 13 shows a typical plot of the viscosity change as a function of the heat-up rate, hold times, and hold temperatures. Figure 14 shows a

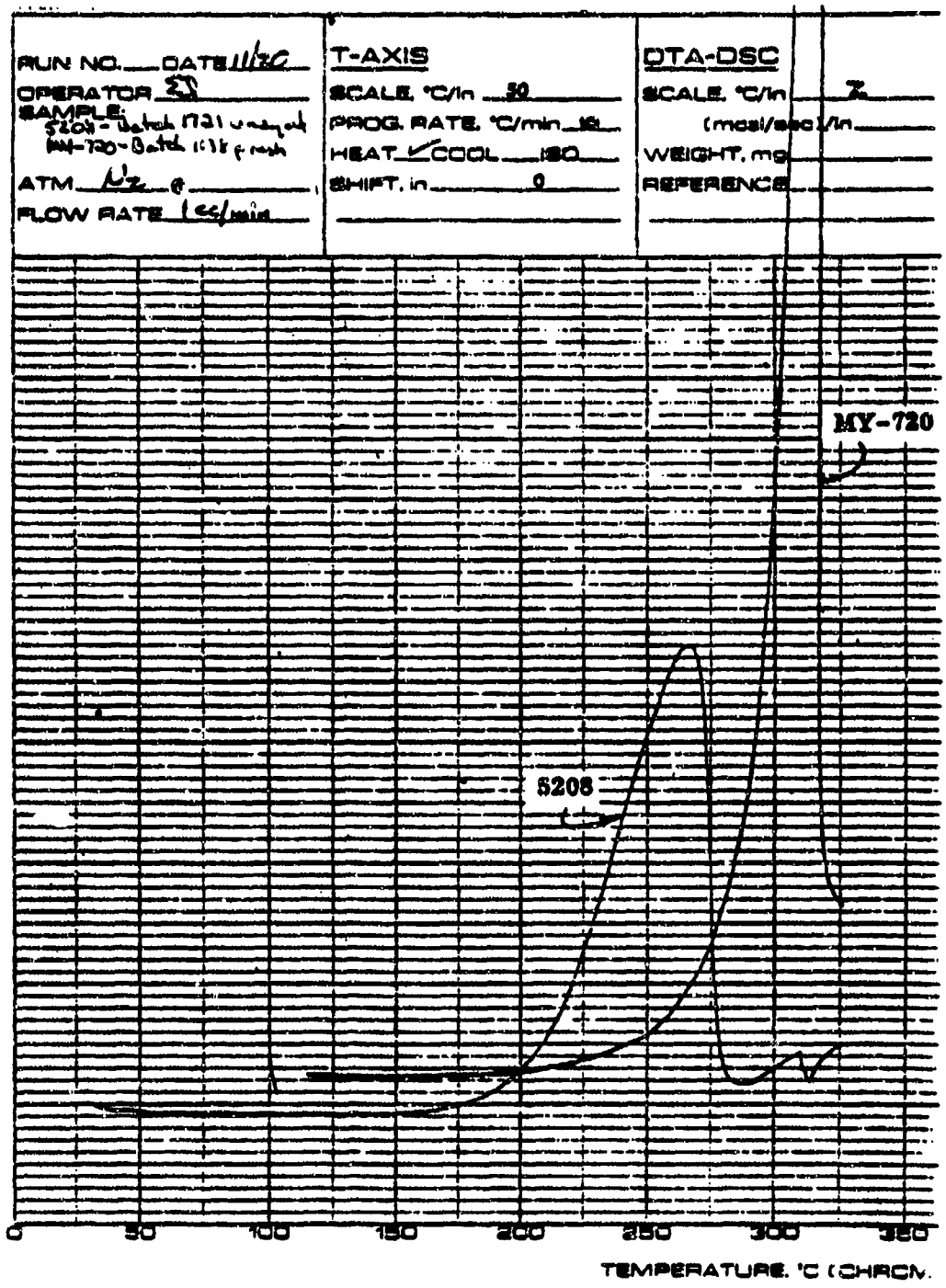

Figure 11. DSC Scan of 4208 and MY-720 at 10C/Min Heat-Up

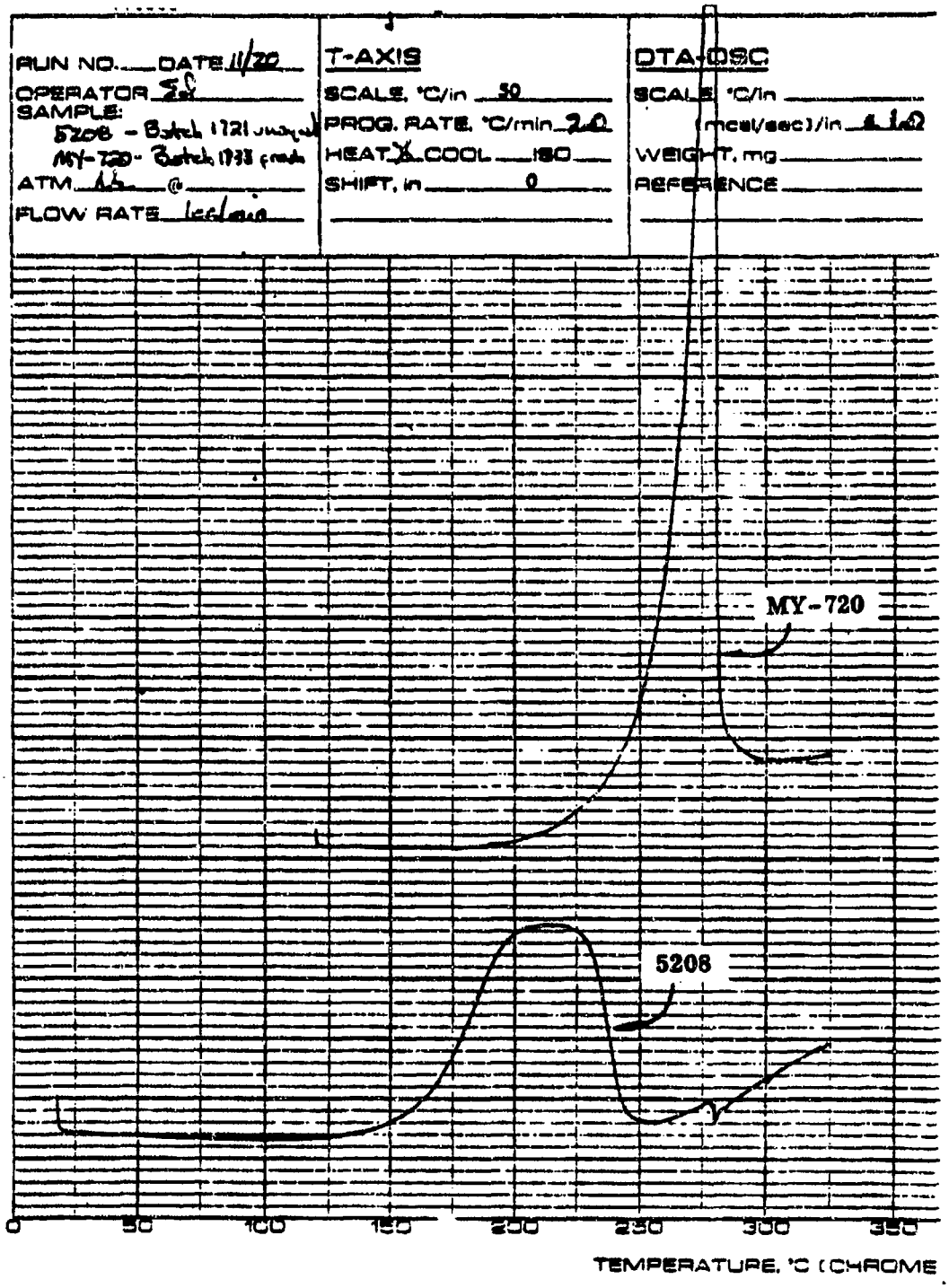

Figure 12. DSC Scan of 5208 and MY-720 at 2.0C/Min Heat-up

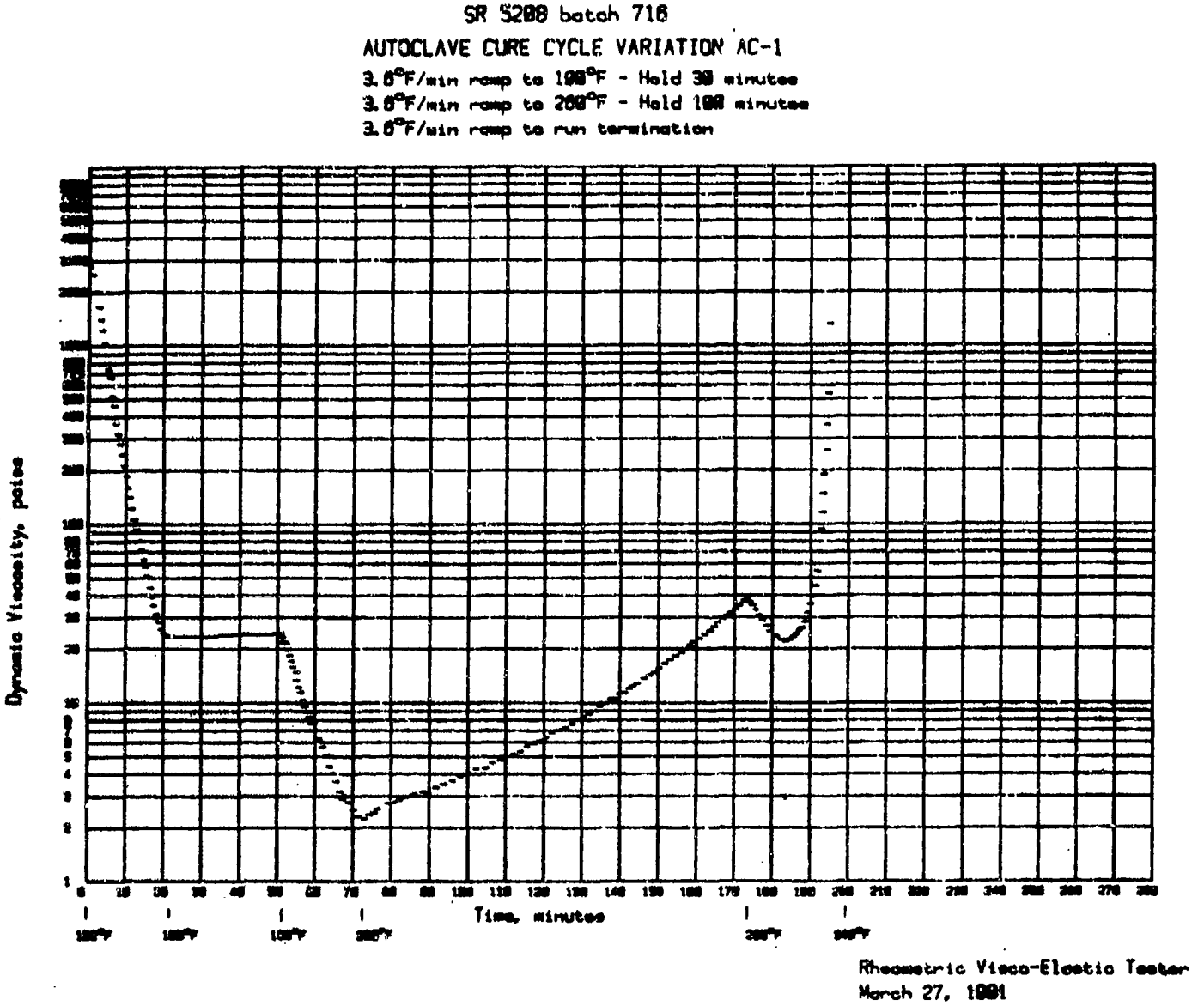

Figure 13. 5208 Batch 716, Autoclave Cure Cycle Variation AC-1

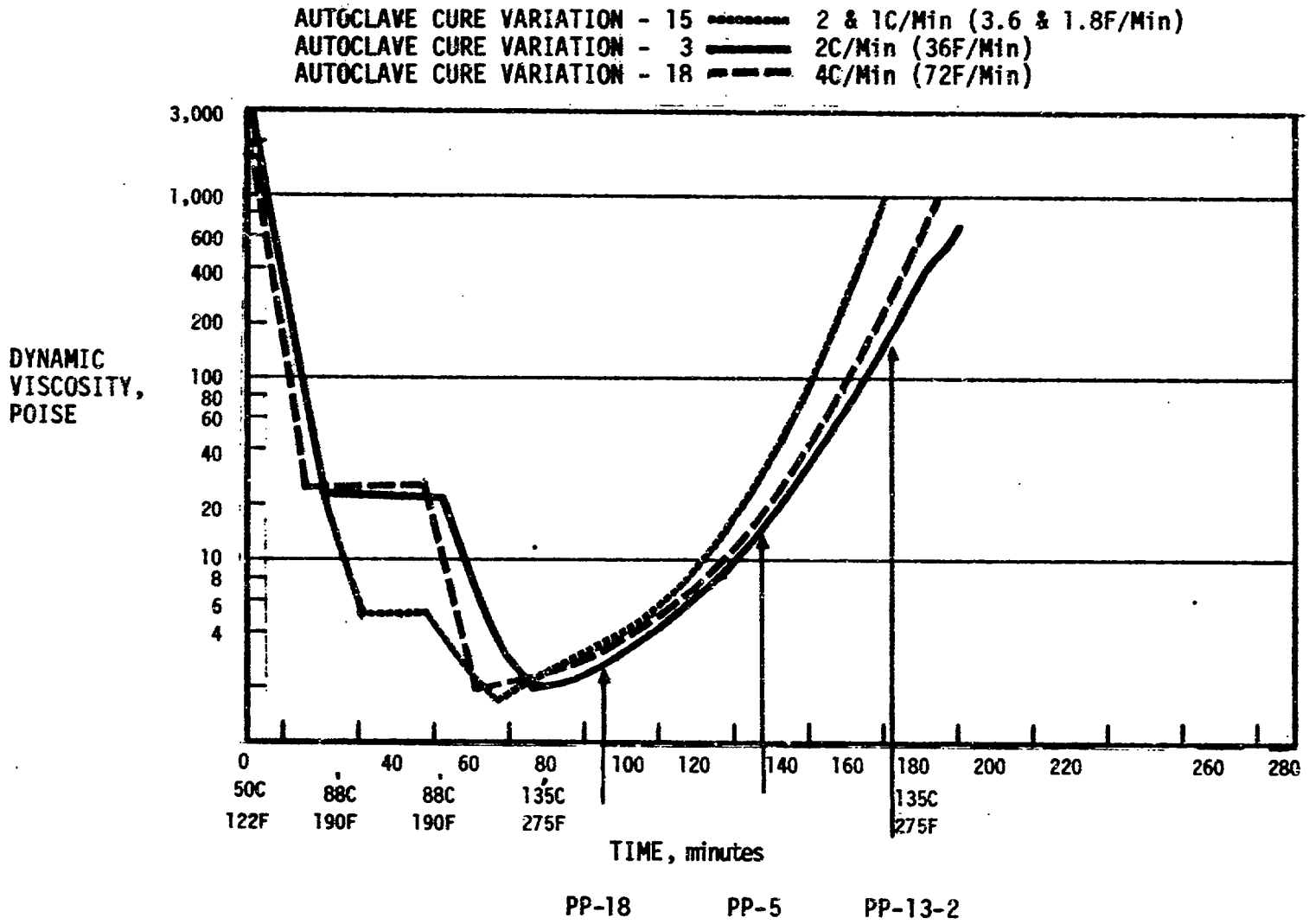

Figure 14. Rheometric Viscosity Comparison of Different Heat-up Rates

comparison of viscosity plots from different heat-up rates of 1.0, 2.0, and 4.0C/minute (1.8, 3.6, and 7.2F/minute).

One significant point was observed from all of the viscosity plots (with the exception of AC-19). There was essentially no difference between the plots in viscosity level during the ramp heat-up to 88C or to 127C, 135C, or 193C (190F or 260, 275, or 290F) regardless of the heat-up rate. With all plots, the viscosity at the 88C (190F) hold is approximately 250 cps, and 200 to 300 cps at the initial portion of the higher hold temperatures. This indicated, in conjucntion with the kinetics data which are discussed in more detail later, that the viscosity of the resin at the lower hold temperatures was a function of the temperature of the material and not the heat-up rate employed to get to the hold temperature. This was valid because of the very slow rate of polymerization (advancement) of the resin at the lower hold temperature. Viscosity plots of all of the processing variables shown in Table 3 are presented in the Appendix of this report as Figures A-1 through A-13.

2.1.2.6 Ambient to 52C (125F) Resin Viscosity. The precompaction or consolidation studies discovered that a prepreg lay-up or stack can be consolidated to a void-free condition with the application of moderate heat and adequate pressure. These results are discussed in more detail in the processing section of this report.

It became obvious, therefore, that the resin viscosity of typical 177C (350F) curing epoxy resin systems controlled, to a large degree, the facility or ease of the consolidation of the prepreg stack at this early stage of laminate curing.

Figure 15 shows the dynamic viscosity of the three different resin systems, 5208, 3502, and 976 at 52C (125F) and an extrapolation of viscosity back to 24C (75F). The 5208 resin system demonstrates a 2 to 4 times higher dynamic viscosity at both 24C (75F) and 52C (125F) than the 3502 and 976 resin systems. Additional viscosity work performed by Frances Abrams at the AFML laboratories

Table 3. Rheometric Viscosity Specimens for Evaluating Aerospace Cycle Variations

Spec. ID	Type of Specimen	Processing Conditions		
		Heatup Rates °C/Min	Hold Temperatures °C	Hold Times (Min)
AC1	Neat Resin	2	88 & 127	30 & 100
AC2	Neat Resin	2	88 & 127	30 & 140
AC3	Neat Resin	2	88 & 135	30 & 100
AC4	Neat Resin	2	88 & 135	30 & 140
AC6	Neat Resin	2	88 & 143	30 & 140
AC7	Neat Resin	1	88 & 127	30 & 100
AC8	Neat Resin	1	88 & 127	30 & 140
AC9	Neat Resin	1	88 & 135	30 & 100
AC11	Neat Resin	1	88 & 143	30 & 100
AC13	Neat Resin	2 1	88 & 135	30 & 100
AC14	Neat Resin	2 - 1	107 & 135	8 & 105
AC18	Neat Resin	4	79 & 135	30 & 100
AC19	Neat Resin	6	135	No hold

confirms (Figure 16) the extrapolated 976 viscosity data at 24C (75F).

In both types of testing, tack and ambient viscosity, the 5208 resin system and prepreg demonstrated between 2 to 6 times higher test values. Obviously, both viscosity of resin and degree of tack could play a significant part in the quality of an initial laminate compaction.

2.1.2.7 Resin Kinetics Study of Batch 716. The purpose of this study was to determine the kinetics of cure associated with the 5208 resin and to correlate the actual degree of polymerization to the rheological (viscoelastic) properties. The objectives were to predict the rate of reaction at any given temperature and time and to quantify the relationship between the degree of

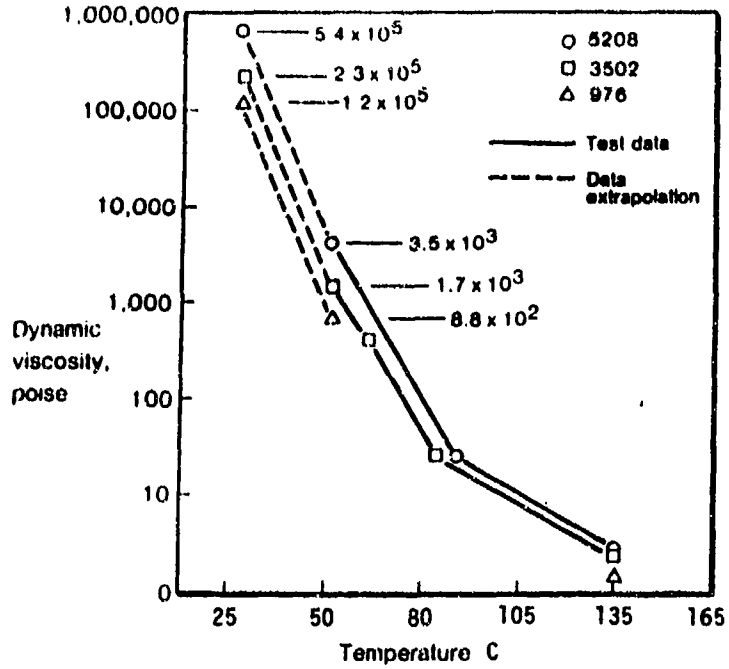

(High viscosity at lower temperatures, where initial vacuum compaction takes place, poses the question of how well ply drop-off areas are filled with prepreg or resin)

- Significant difference in viscosity noted between epoxy systems at 25° & 50C

Figure 15. Rheological Viscosity of Epoxy Resin Systems

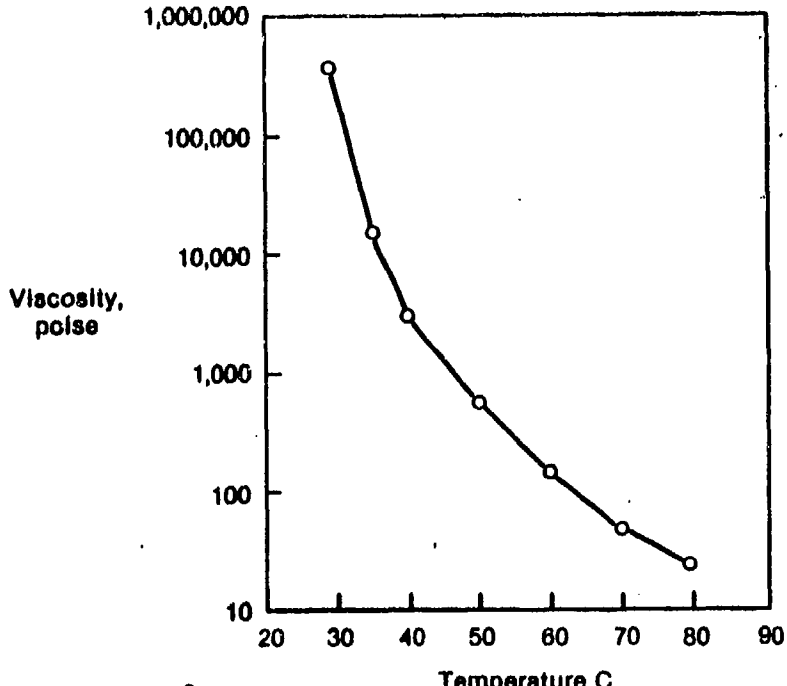

Source:
Frances Abrams
Charlie Browning

Figure 16. Viscosity vs Temperature, 976 Resin-AFML Data

polymerization and other parameters, such as dynamic viscosity, HPLC reaction peak data, and epoxy equivalent weight measurements.

The instrument employed for the kinetic study was the Acceleration Rate Calorimeter (ARC). The ARC is an instrument whose primary function is to maintain a resin sample in an adiabatic condition and permit it to undergo an exothermic reaction due to self heating, while recording the time/temperature relationships of the thermal cycle. The ARC consists of a sample container with an attached thermocouple suspended within a larger container which has embedded thermocouples and heating elements. The entire apparatus is controlled by a computer which constantly monitors the sample and jacket temperatures, and adds heat to the jacket whenever it lags behind the sample, thus maintaining a very close approximation to true adiabaticity. Data taken during the ARC run provides the following information:

1. adiabatic temperature rise,
2. temperature of maximum reaction rate, and
3. self-heat rate at any temperature for the experimental system.

Although these data are taken from an adiabatic experiment, most are directly applicable to isothermal or ramped temperature systems because they describe instantaneous kinetic parameters.

The main thrust of the kinetic experimentation is threefold:

1. Adiabatic self-heat reactions
2. Isothermal holds
3. Viscosity correlation

Samples of 5208 resin, approximately seven grams each, were step-heated in the ARC until it detected an exothermic reaction. They were then allowed to react to completion while the ARC maintained adiabatic conditions. This test was done for 5208 Batch 716 at normal advancement (Figure 17)

5208 Batch 716 - Normal Advancement Material

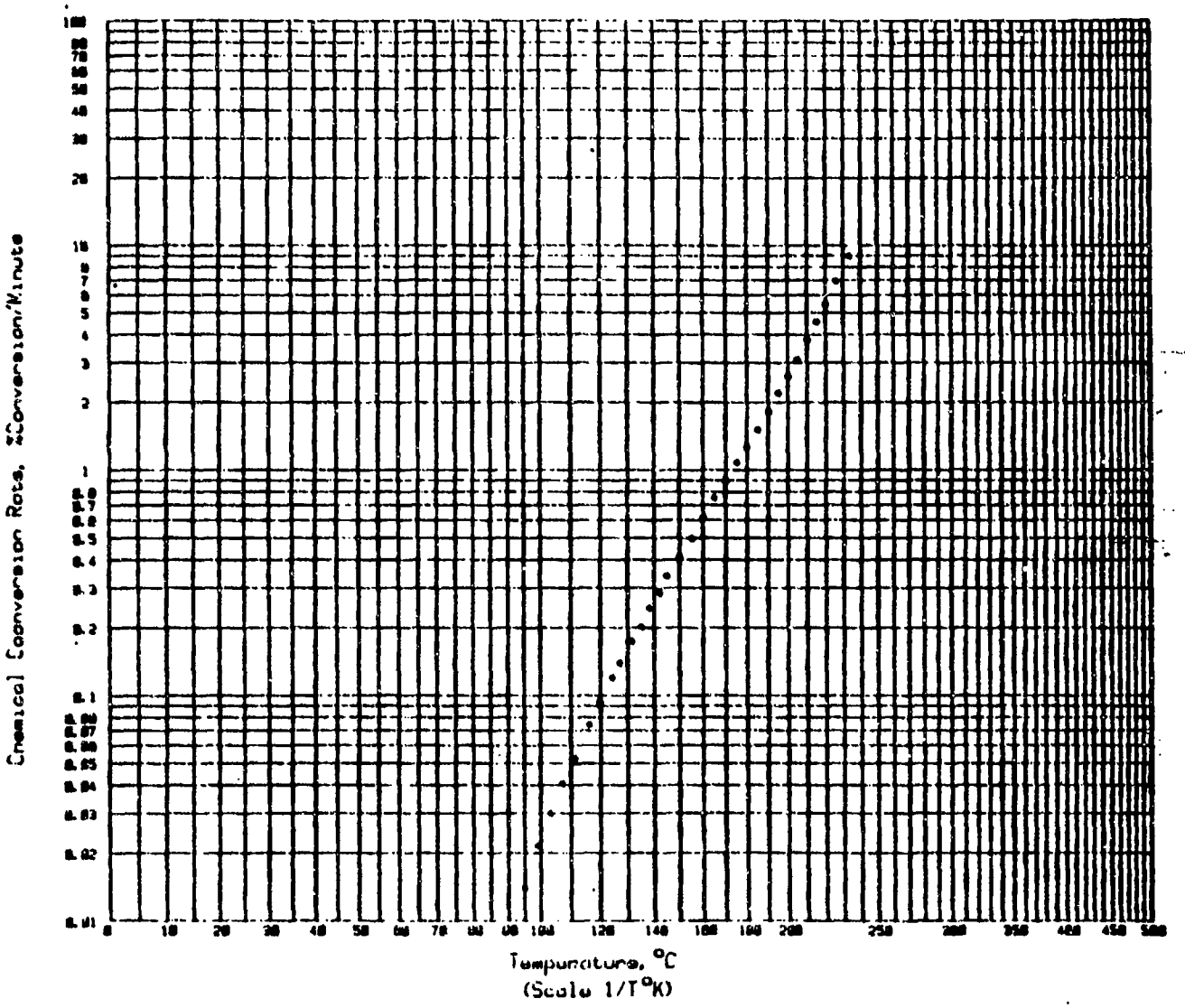

Figure 17. Chemical Conversion Rate vs Temperature, 5208 Batch 716 - Normal Advancement Material

and material advanced approximately 15 percent (85 percent epoxy groups unreacted, Figure 18). The data from Figure 18 was replotted as a graph of percent reaction rate versus 1/T degree K, shown in Figure 19.

It appeared from these experiments that advancement does not affect reaction rate at this level (less than approximately 20 percent reacted), since Figures 17 and 18 were essentially identical. This greatly simplified the description of the cure kinetics since the reaction rate was only a function of the temperature at the advancement levels found throughout the processing range of 5208 prepregs. A preliminary equation for rate of reactions as a function of absolute temperature has been derived by regression analysis of the data in Figure 19. It is as follows:

$$\ln (\text{Rate}) = 19.6 - 8708/T$$

where rate is expressed at percent total reaction/minute and T is in degrees Kelvin.

In another experiment, 10g samples of 5208 resin were held isothermally in the ARC at various temperatures for various lengths of time. The resin was spot sampled for viscosity and epoxide content, and in some cases the remainder of the resin (approximately 7 grams) was allowed to react to completion in the ARC apparatus.

The samples from the isothermal hold described above were analyzed for viscosity after aging at 120C (248F) and 135C (275F) and plots were made of the data. Figures 20 and 21 are plots showing the viscosity of the 5208 resin as a function of the percent of resin advancement at various isothermal temperatures. Viscosities were determined over 10C increases from 71 to 138C and correlated to the degree of resin advancement. The percent of resin advancement equals a little more than 50 percent of the possible total reaction of epoxide groups.

5208 Batch 716 - Normal Advancement Material

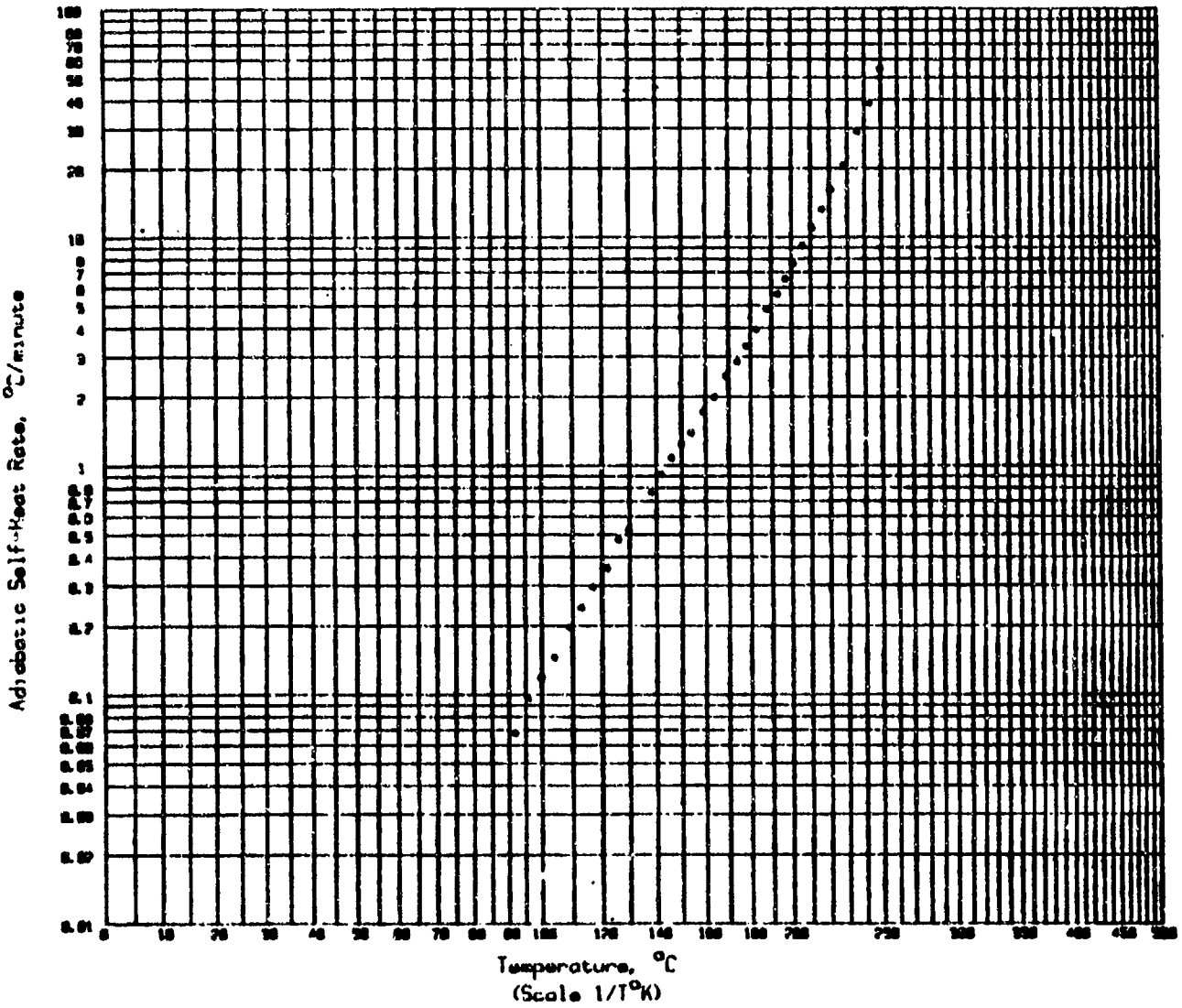

Figure 18. Adiabatic Self-Heat Vs Temperature, 5208 Batch 716 - Aged 135 Minutes at 120C

5208 Batch 716 - aged 135 minutes at 120°C

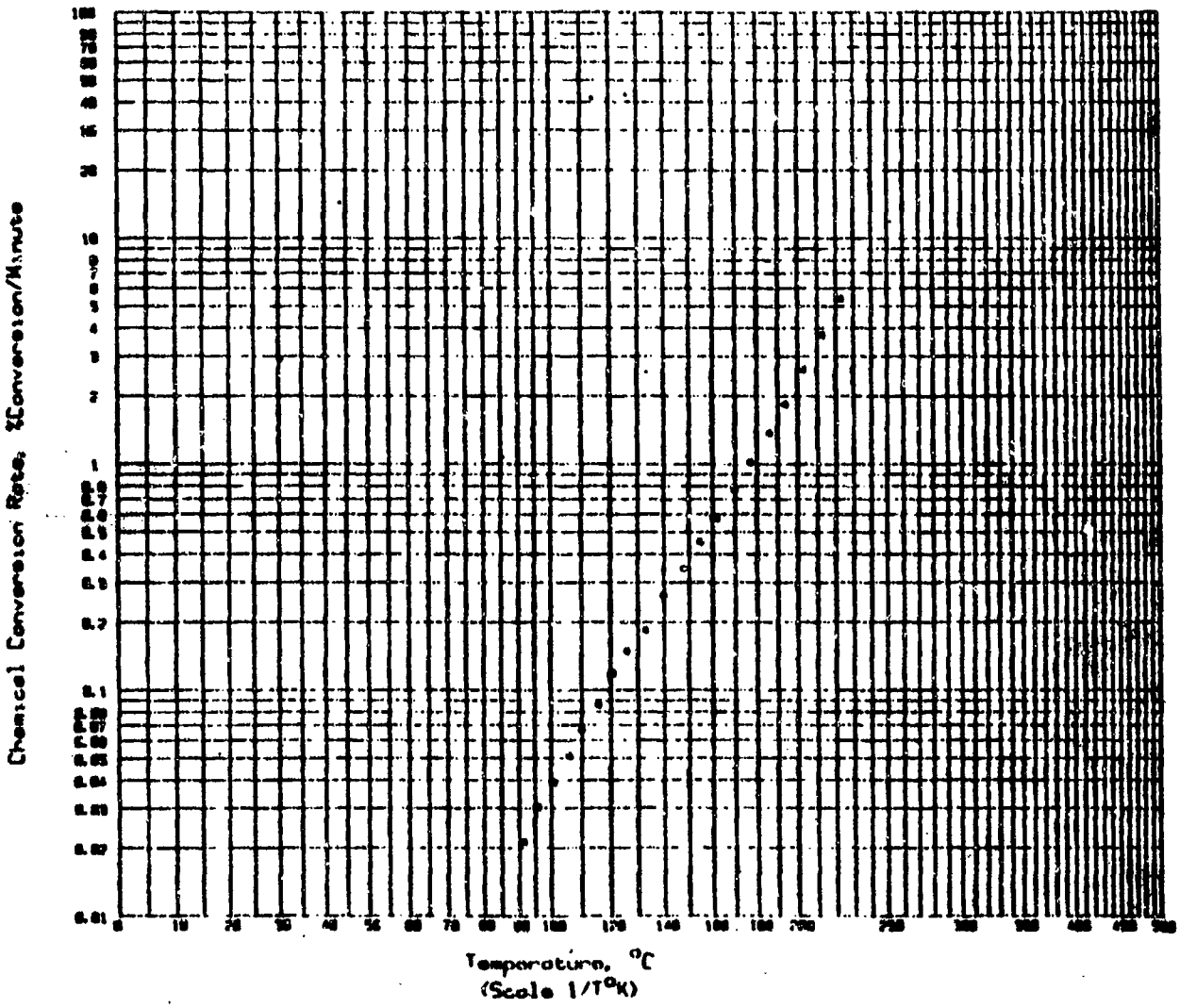

Figure 19. Chemical Conversion Rate vs Temperature, 5208 Batch 716 - Aged 235 Minutes at 120°C

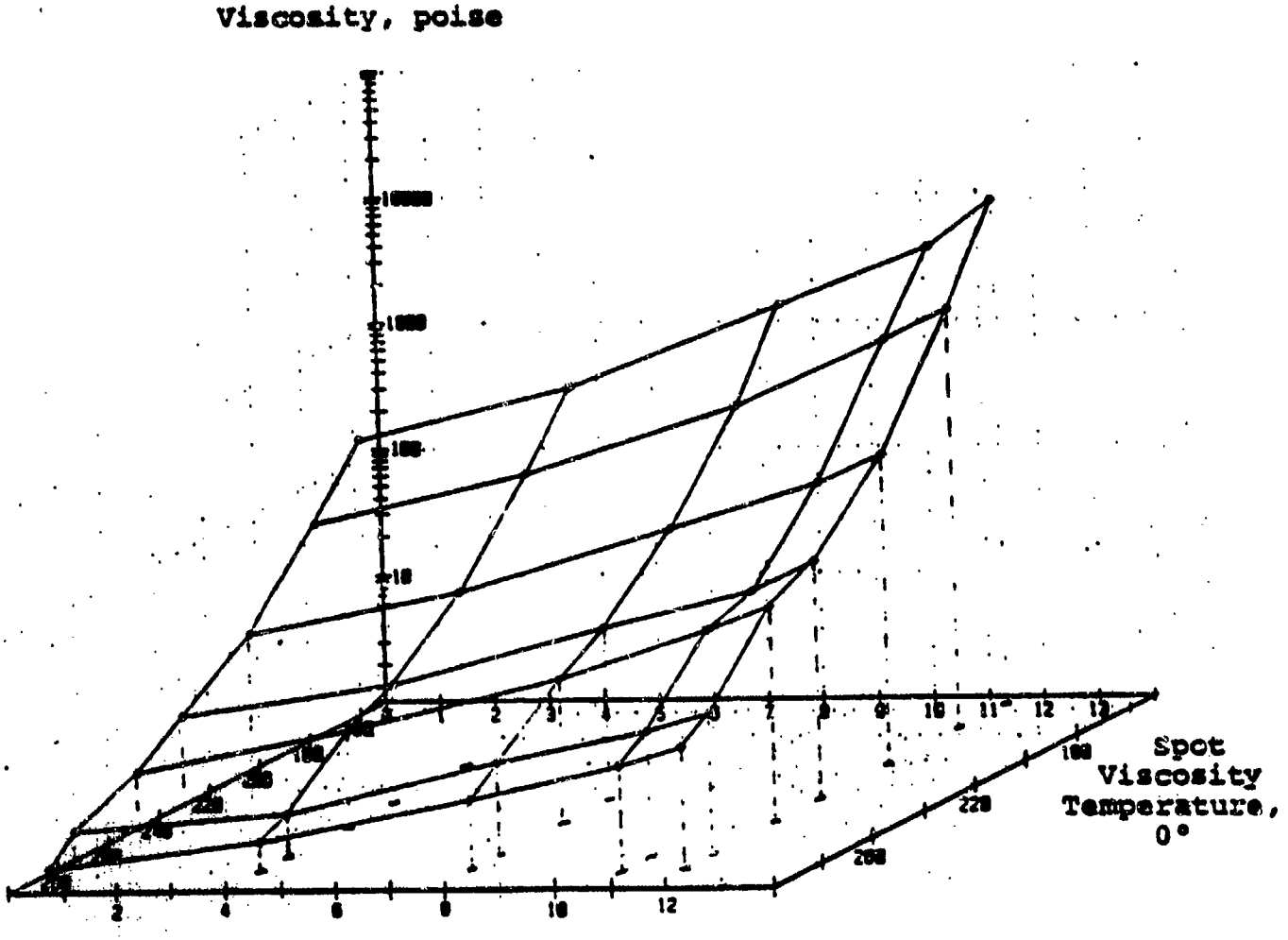

* Calculated by ln Rate = 19.6 - 8708/T

Figure 20. 5208, Batch 716, Aged at 120C Instantaneous Viscosity Versus Advancement as a Function of Temperature

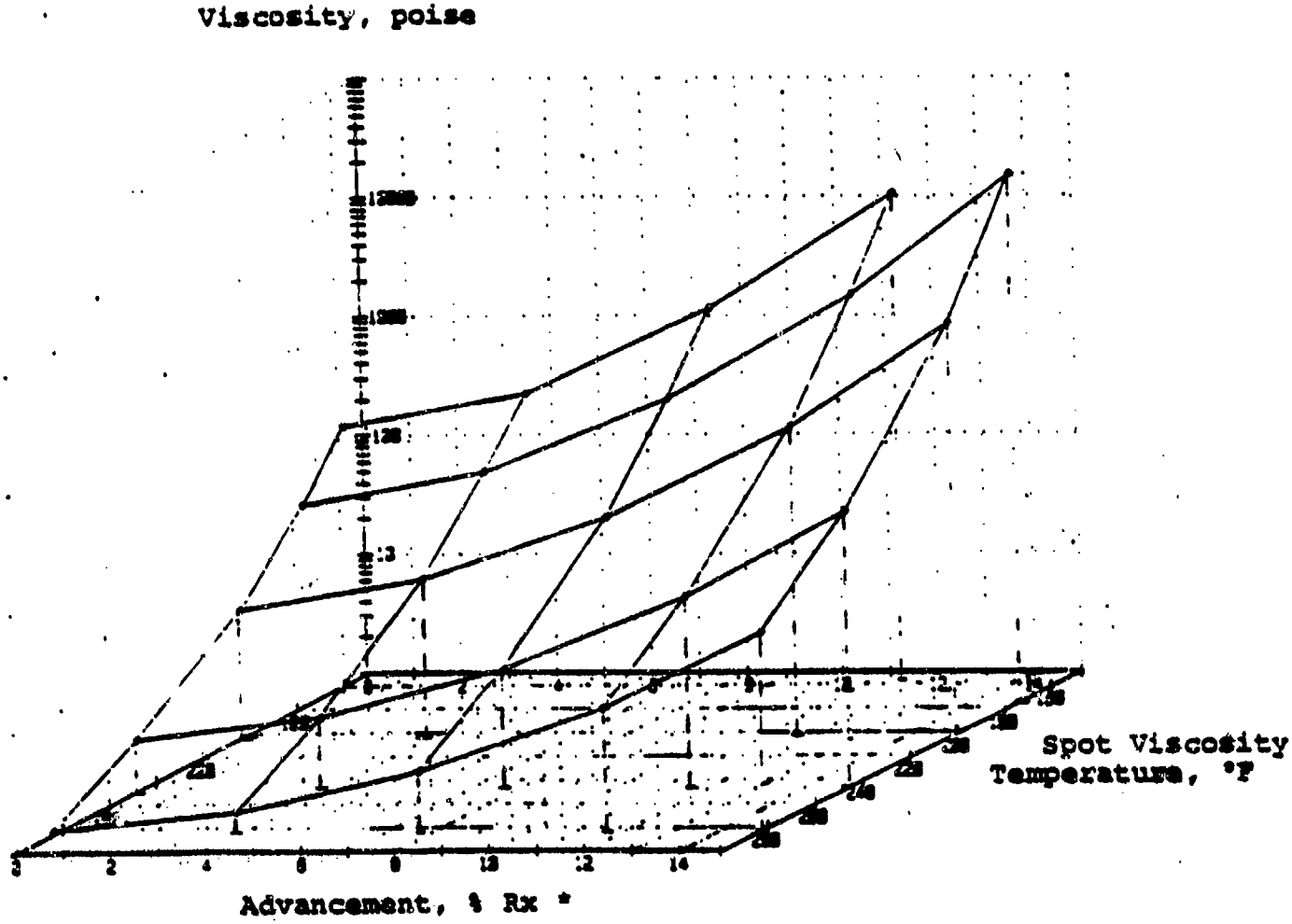

* Calculated by ln Rate = 19.6 - 8708/T

Figure 21. 5208, Batch 716, Aged at 135C, Instantaneous Viscosity Versus Advancement as a Function of Temperature

Some changes in viscosity levels were noted between the two aged specimens, Figures 22 and 23. The rate of viscosity increase at the higher temperature (135C) shows much higher viscosities for similar aging times. Aging time at 120C was 150 minutes and the aging time at 135C was 90 minutes to achieve the same viscosity (advancement level). Examination of these two plots revealed a significant increase in resin viscosity during aging at the elevated temperature.

2.2 LAMINATE FABRICATION

2.2.1 BASELINE LAMINATE FABRICATION. During the first portion of the program a total of 23 flat laminates were fabricated from prepreg batch 716; of those 23, 13 were 32 ply, seven were 64 ply, two were 96 ply, and one was a 16 ply laminate. All were pseudoisotropic with the exception of the 16 ply and one 32 ply laminate, both of which were unidirectional laminates. The layup sequence for all of the remaining laminates was $(0, +45, 90, -45)_{sN}$.

Three different cure cycles were used for final consolidation and curing of these laminates. The cure cycles differed only with the length of dwell at 135C (275F) prior to application of pressure. The basic cure cycle was: application of vacuum, heat at 2C (3.6F)/minute to 135C (275F) hold for 15 minutes for cure cycle 3, 60 minutes for cure cycle 1 and 90 minutes for cure cycle 2; apply 0.586 MPa (85 psi) and hold for 105 minutes; heat at 1C (2F)/minute to 180C (355F) and hold for two hours. The laminates were then cooled under pressure and vacuum to 52C (125F) before removal from the autoclave. Figure 24 shows the relative viscosity of the resin at the time of pressure application for laminates PP-18, PP-5 and PP-13-2 at the three different hold times at 135C (275F). All three 0.305 m by 0.305 m (1 ft by 1 ft), 32 ply laminates were of excellent quality and represented laminates where pressure application varied within a 75 minute time frame.

SR 5208, Batch 716

Viscosity at Various Temperatures

vs. Age Time at 120°C

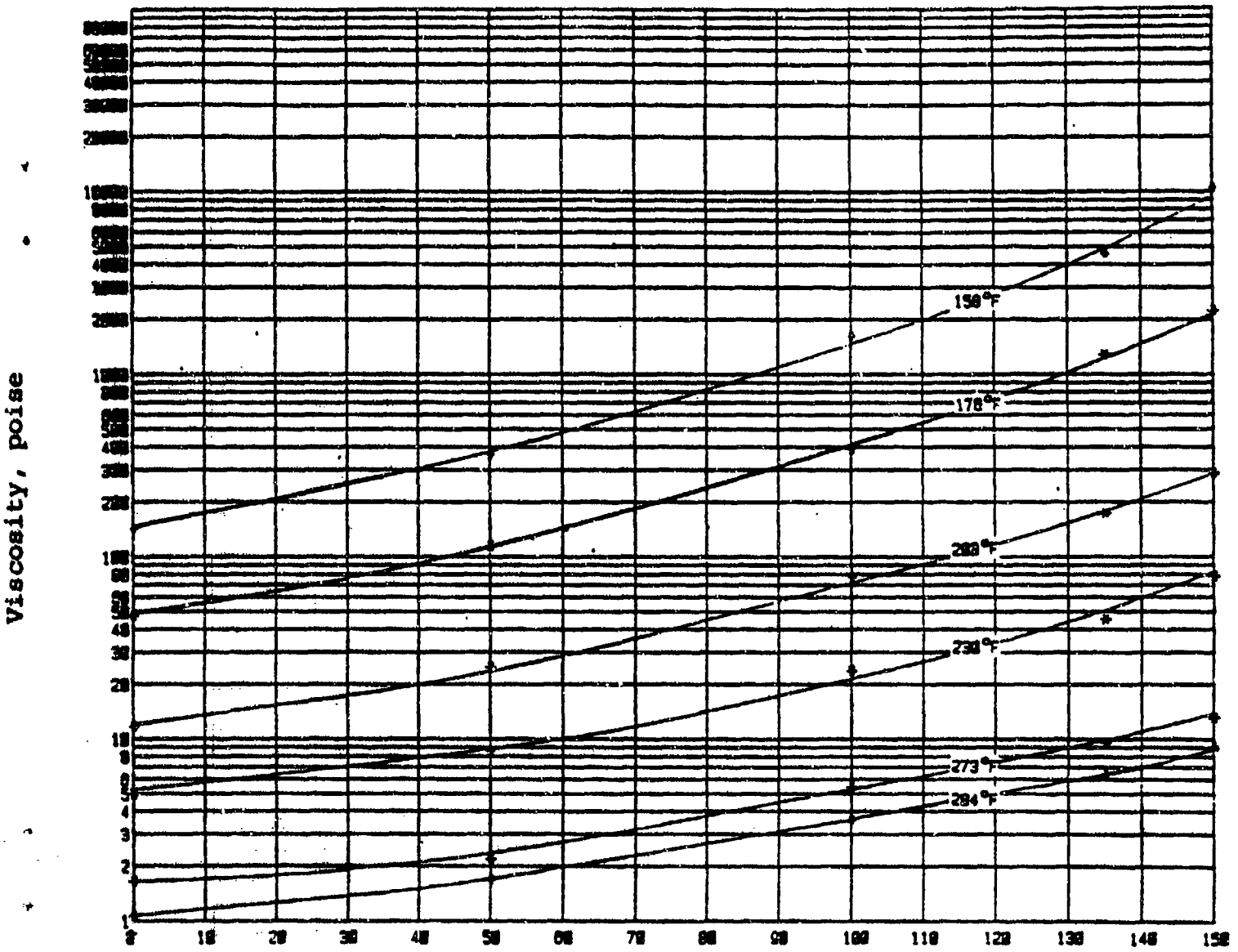

FIGURE 22.

SR 5208, Batch 716
Viscosity at Various Temperatures
vs. Age Time at 135°C

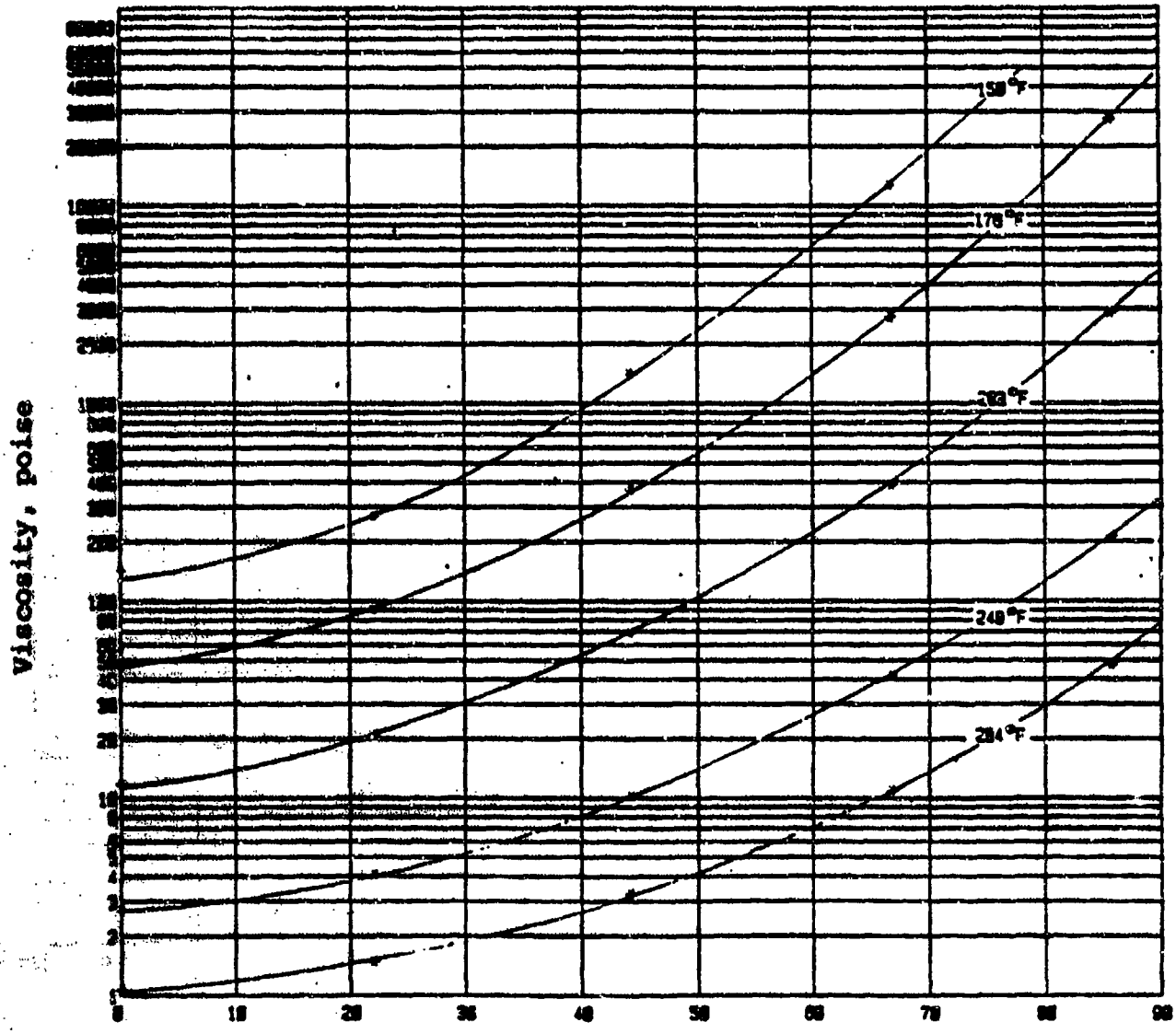

FIGURE 23.

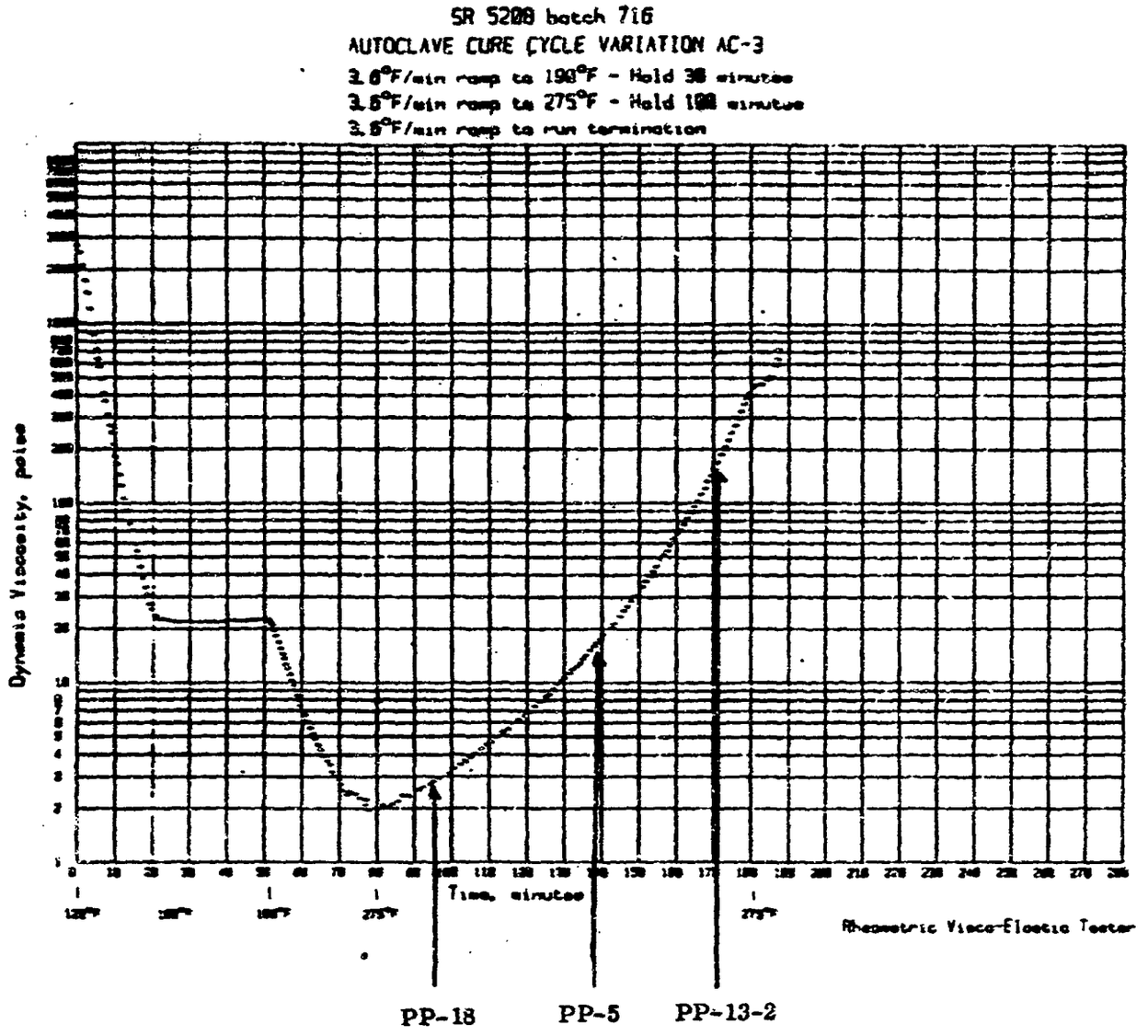

Figure 24. Pressure Application Points and Corresponding Viscosity for 5208, Batch 716, Autoclave Cure Cycle Variation AC-3

The desired cure cycle was fed into a programmable controller connected to the autoclave thus assuring identical heatup rates and cure cycles for all of the laminates.

Table 4 lists the 23 laminates fabricated. In addition, the laminate weights, thicknesses, densities, fiber volumes, resin contents, and void volumes are indicated. The C-scan results are also shown along with observations of the inspection of micropolished sections of the laminates.

The original baseline laminate geometry proposed for the program was 0.305 m by 0.305 m (1 ft by 1 ft) by 32 plies. A number of these lamiantes were cured using the three different cure cycles and all of the laminates were of high quality regardless of the length of hold at 135C (275F) prior to application of pressure. As shown in Figure 21, the resin viscosity at the three different pressure application points was quite different, ranging from 280 poise after 15 minutes at 135C (275F) to almost 18,000 poise after 75 minutes at 135C (275F).

This data indicated that for this particular laminate configuration there is a time window of approximately 75 minutes where pressure can be applied, and a high quality laminate will result if pressure was applied at any time within that 75 minute hold period.

Thicker laminates of the same ply configuration as the 32-ply laminate were also prepared in an attempt to produce an unacceptable, void containing laminate; four 64-ply and two 96-ply laminates, 0.305 m by 0.305 m (1 ft by 1 ft), were fabricated.

These thicker laminates, however, were of a high quality yielding good C-scans and micropolished sections.

Laminates identified in Table 4 as PP-21 and PP-28 were both thicker laminates being 64 and 52 plies, respectively. The major difference between these two and the prior 64-ply laminates is that both PP-21 and PP-28 were 0.61

Table 4. Processing Science of Epoxy Resin Composites Laminate Test Data

LAMINATE	PLYS	WEIGHT,g	THICKNESS CM	THICKNESS IN.	DENSITY g/cm3	F.V.,%	R.C.,%	V.V.,%	C-SCAN	MICRO POLISH	CURE	COMMENTS
PP-1	32p	(1,099.7) 628.4	0.421 ±0.005	0.166 ±0.002	1.588	66.3	26.7	0.2	Good	Void Free		
PF-5	32p	631.5	0.427 ±0.005	0.158 ±0.002	1.588	66.2	26.8	0.2	Good	Void Free		
PP-7	32p	(1,082) 618	0.419 ±0.0025	0.165 ±0.001	1.597	68.0	25.2	0.2	Good	Void Free		
PP-8	32u	621.8	0.414 ±0.013	0.163 ±0.005	1.598	67.2	25.9	0	Good		1	
PP-9	16u	542.6	0.211 ±0.0025	0.083 ±0.001	1.595	67.1	26.0	0			1	0.305 x 0.305m (1 ft x 1 ft)
PP-11	64p	1,266	0.853 ±0.015	0.336 ±0.006	1.588	66.3	26.7	0.2	Good		1	
PP-12	96p	1,927.7	1.303 ±0.023	0.513 ±0.009	1.580	66.6	26.4	0.8	Possible Voids	Minor Voids	1	Acceptable Gradient
PP-13-1	32p	633.6	0.429 ±0.005	0.169 ±0.002	1.591	66.5	26.5	0	Good		3	
PP-14	64p	1,237.4	0.838 ±0.010	0.330 ±0.004	1.593	67.7	25.5	0	Good	Void Free	3	
PP-15	96p	1,926.2	1.300 ±0.030	0.512 ±0.012	1.585				Possible Voids	Minor Voids	3	Acceptable Gradient
PP-17*	32p	628.5	0.424 ±0.008	0.167 ±0.003	1.589	65.8	27.1	0	Good		3	Pressure 60 min. into 135C (275F) hold.
PP-18**	32p	611.0	0.409 ±0.005	0.161 ±0.002	1.602	69.0	24.3	0	Good		3	Pressure 15 min. into 135C (275F) hold.
PP-19	64p	1,257	0.838 ±0.010	0.330 ±0.004	1.590	68.1	25.1	0.6			1	No caul plate, but in same location
PP-20	64p	1,253	0.851 ±0.008	0.335 ±0.003	1.591	67.5	25.6	0	Good	Void Free	3	No caul plate, staggered butts
PP-13-2	32p	629.6	0.424 ±0.005	0.167 ±0.002	1.590	66.3	26.7	0	Good		2 (3)	Late pressure 30 minutes late
PP-21	64p	5,095	0.858	0.338	1.579	65.9	27.7	0.8	Bad	Major Voids	3	0.61 x 0.61 m (2 ft x 2 ft) Laminate
PP-22	32p	624.2	0.424 ±0.013	0.167 ±0.005	1.591	67.1	26.0	0.3	Good		3	1 ply bleeder
PP-23	32p								Good	Void Free	3	
PP-24	64p								Good	Void Free	3	
PP-25	32p								Good	Void Free	3	
PP-26	32p								Good	Void Free	3	
PP-27	32p								Good	Void Free	3	0.305 x 0.305 m (1 ft x 1 ft) laminate Ft Worth reject.
PP-28	64p								Bad	Major voids	3	0.610 x 0.610 m (2 ft x 2 ft) laminate Ft Worth reject.

m by 0.61 m (2 ft by 2 ft) in size. Both laminates were determined to be unacceptable both from C-scan and microsection analysis.

A portion of a C-scan of PP-21, as shown in Figure 25, is representative of both halves of the laminate, and reveals relatively large void areas located generally in the center area of the 0.61 m by 0.61 m (2 ft by 2 ft) laminates. There was a 0.15 m (6 in) periphery around each laminate which appeared to be relatively void free.

Sections were removed from those areas identified as containing voids, and were polished for micro analysis. Examination of those sections revealed two interesting facts; (1) the voids occurred only between plies, never at a fiber resin interface or within a ply, and (2) voids occurred only between the 10th and 25th plies of the 64 ply laminate. The first ply is identified as being closest to the tool surface.

Laminate PP-27, a 0.305 m by 0.305 m (1 ft by 1 ft) 32-ply panel was cured under the same vacuum bag as PP-28 (an unacceptable laminate) and was determined to be of high quality.

It is quite evident from this laminate study that there is a very definite effect of laminate geometry, particularly laminate area rather than thickness, on the resulting laminate quality.

2.2.2 LARGE LAMINATE FABRICATION. The fabrication and evaluation of larger, 0.61 m by 0.61 m (2 ft by 2 ft) by 64-ply laminates was initiated to discern and evaluate incoming prepreg. The evaluation to date has included six large laminates. One laminate was made from prepreg that had been dried for six days at room temperature in an environmental chamber containing phosphorous pentoxide (a desicant); the second laminate was prepared from deaerated prepreg; the third laminate had a split bleeder/breather system for cure; the fourth laminate was cured vertically in the autoclave; and the fifth and sixth laminates were fabricated using 1076E and 3402-AS prepregs, respectively, for baseline laminate evaluation.

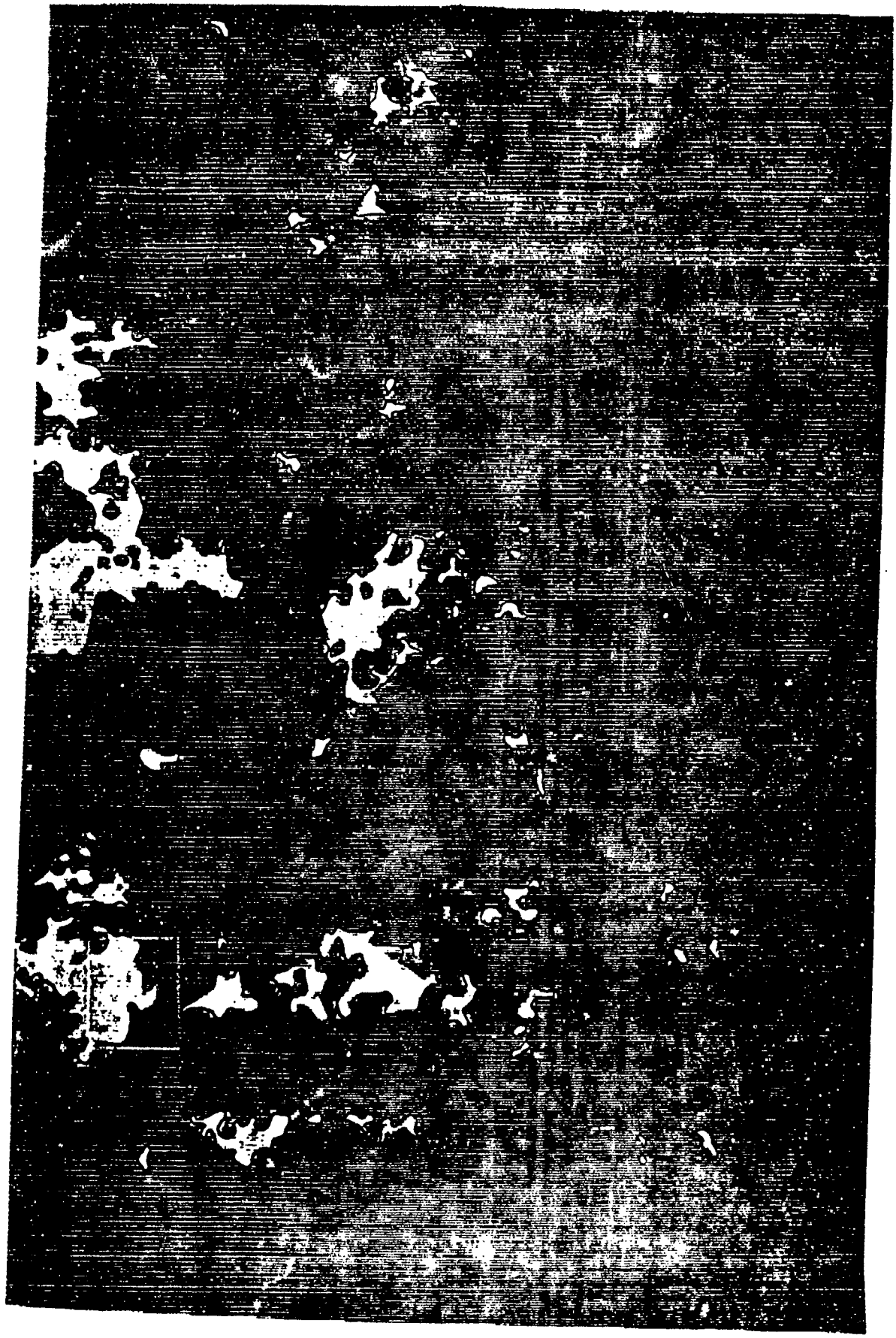

Figure 25. A Section of a Horizontally Cured Thick Laminate C-Scan

2.2.2.1 Dried Prepreg Laminate. Prepreg from batch 716 was laid up in 0.61 m by 0.61 m (2 ft by 2 ft) individual plies each separated by a ply of porous Armalon and fiberglass cloth. The separated individual plies were placed in an environmental chamber and dried in the presence of phosphorous pentoxide for six days at room temperature to remove any absorbed water. Volatile content of the prepreg prior to environmental exposure was 0.36 percent by weight, and after exposure 0.05 percent by weight. Volatiles were determined both by weight loss from heating at 177C and the Karl Fischer titration. Slight variations in volatile content between the two methods indicated that perhaps some low molecular weight resin products are being flashed off at 177C (350F), since water content was the only value determined during the Karl Fischer titration. Typically, the titration technique showed slightly lower volatile contents than the 177C (350F) heating determination.

The dried prepreg retained an acceptable level of tack during the drying exposure. The prepreg was laid up into a 64-ply 0.61 m by 0.61 m (2 ft by 2 ft) laminate and bagged and cured identically to other thick laminates produced on this program. The cure cycle used was the General Dynamics Fort Worth Division cure cycle, cure cycle #3, where the laminate was heated at 2C (3.6F)/minute to 125C (275F) and held 15 minutes prior to application of 0.586 MPa (85 psi) pressure.

The resulting cured laminate was of excellent quality as verified by both laminate C-scan and examination of a micropolished section.

2.2.2.2 Deaerated prepreg laminate. The second laminate was prepared from batch 1452, a special prepreg prepared by Narmco Corporation and processed by them in such a way that the resin was deaerated before processing. Volatile contents were determined on the material and found to be 0.35 percent by weight. A 64-ply 0.61 m by 0.61 m (2 ft by 2 ft) laminate was cured identically to other laminates on the program using cure cycle #3. Here again, an excellent

laminate was produced.

2.2.2.3 Split Bleeder Laminate. The third laminate, (from prepreg batch 1809), was also a 64-ply 0.61 m by 0.61 m (2 ft by 2 ft) laminate and was cured identically to the first two laminates. The only change was in the bleeder arrangement. A split bleeder was employed, three plies of 181 fiberglass on the top and bottom of the layup, rather than the typical six plies of 181 fiberglass on the top and bottom of the layup, rather than the typical six plies of 181 fiberglass on the top surface which was used throughout the remainder of the program. C-scans of this laminate indicated a good laminate with no apparent voids or delaminated areas.

The high quality of these three lamiantes produced from differently treated prepregs or bleeder systems strongly suggest that if either a large quantity of entrapped air or water was removed from the prepreg prior to layup and cure or an additional breather bleeder path was provided that essentially void free laminates would be the result.

2.2.2.4 Vertically Cured Laminate. As a part of the large laminate evaluation, a 0.61 m by 0.61 m (2 ft by 2 ft) pseudoiostropic laminate, 56 plies thick was laid up from the original batch of prepreg (716) and cured according to the Fort Worth Division's cure cycle. The only variation in the cure from the baseline 64-ply laminates was that the laminate was cured vertically in the autoclave. The decision to cure a laminate in this position was based in part on some of the preliminary resin migration studies which indicated a majority of the resin movement within a laminate is laterally along the fiber length.

Assuming this to be correct, a laminate placed vertically in an autoclave would allow entrapped air and moisture to be removed with greater ease than a laminate cured horizontally, which takes advantage of natural bouyancy effects.

Figure 26 is a reduction of a C-scan of PP-21, a 64-ply 0.61 m by 0.61 m (2 ft by 2 ft) laminate cured horizontally in the autoclave. Figure 27 is a

reduction of a C-scan of the 56-ply laminate cured vertically in the autoclave. Both laminates were cured from the same batch of prepreg using the same cure cycle, the only difference was the vertical or horizontal position of the laminate.

A significant difference between the two C-scans was quite obvious. Although the vertically cured laminate does have one small void area, it certainly was an improvement over the horizontally cured laminate.

A second batch of prepreg (1809) was manufactured from the same base resin and catalyst batches used to produce the first prepreg lot 716. Two psuedoisotropic laminates 9.61 m by 0.61 m (2 ft by 2 ft) by 56 plies were fabricated from this second batch of prepreg.

Both laminates were cured at the same time in the autoclave, one in a vertical position and the other was horizontal.

Both laminates had excellent C-scans with no indications of voids in either laminate. The results of these laminates and C-scans then prompted an investigation of the new batch of prepreg to determine the reason for fabricating good void-free laminates when the previous batch produced a bad, void-filled 0.61 m by 0.61 m (2 ft by 2 ft) laminate.

As discussed in Sections 2.5.1 and 2.8, the suspected culprit appears to be the method used by the prepreg manufacturer to add the diaminodiphenylsulfone (DADS) catalyst to the resin. Narmco apparently melted the catalyst at a temperature range of 193C (380F) to 227C (440F) prior to blending with the major and minor epoxies which were maintained at a temperature of 71C (160F) to 85C (185F). This technique may cause the partial resolidification (recrystallization) of the catalyst.

We have shown that this method produces a material/structure which causes the water to become more tightly bound to the catalyst. The total removal of

Figure 26. A Section of a Horizontally Cured Thick Laminate C-Scan

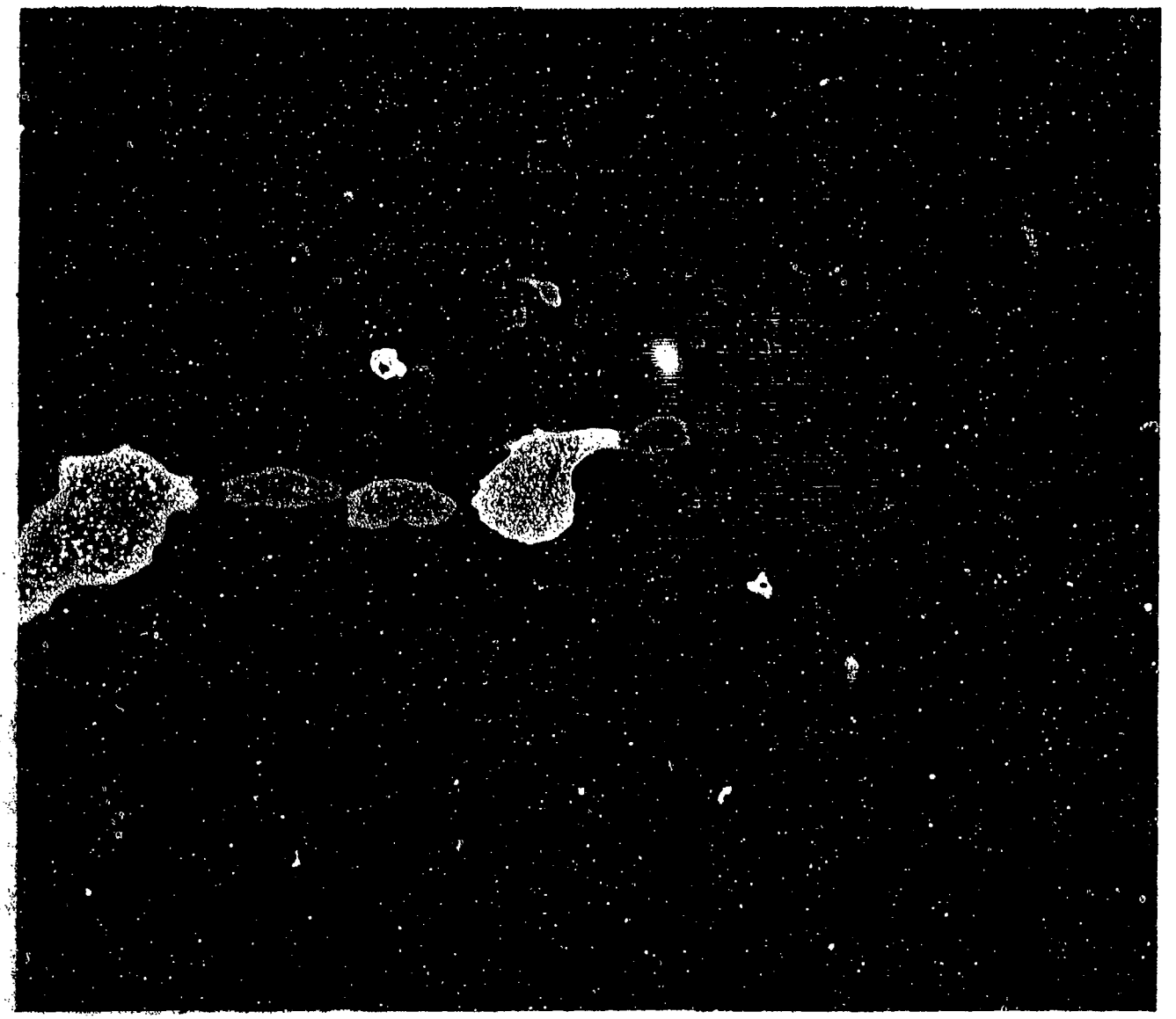

Figure 27. C-Scan of Vertically Cured Thick Laminate

water associated with recrystallized catalyst does not occur until temperatures approach 138C (280F). The melting point of pure DADS was found to be 175-177C (347-351F).

The apparent differences between the new and old prepreg lots was the absence of large catalyst crystals on the prepreg surface which were present on the first batch of prepreg which yielded the void-filled thick laminates.

2.3 DIFFUSIVITY AND SOLUBILITY CHARACTERISTICS OF DIFFERENT ADVANCEMENT LEVELS OF 5208 RESIN

Critical to the mechanical void stabilization model was the data on the diffusion rates of moisture vapor into the prepreg at various states of cure. Also critical to the model was data on the solubility of moisture vapor in the material. These critical physical characteristics are based on the statistical evidence linking laminate voids with pre-cure exposure of prepreg to high humidity environments.

Diffusion of moisture into polymeric materials follows Fick's law of diffusion. For one-dimensional diffusion, the general equation is

$$\partial c/\partial t = D\partial^2 c/\partial x^2 \qquad (1)$$

where c = concentration

t = time

D = diffusion coefficient

x = distance

The solution to this differential equation yields the following relationship for a flat plate absorbing vapor through both faces

$$F = (4/\ell)\ (Dt/\pi)^{\frac{1}{2}} \qquad (2)$$

where F = fraction of equilibrium moisture content

ℓ = plate thickness, cm

D = diffusion coefficient, cm^2/sec

t = exposure time, sec

The form of this solution shows that moisture content change in proportion to the square root of exposure time. for a given exposure time absorption is inversely proportional to plate thickness.

Increasing the exposure temperature while maintaining a constant value of relative humidity accelerates bulk moisture absorption. With continued exposure an equilibrium moisture content is reached that is independent of the exposure temperature. The equilibrium moisture is determined by the relative humidity.

The overall diffusion coefficient, D, can be expressed to show the temperature dependence of diffusion

$$D = D_o \exp(-E/RT) \qquad (3)$$

where D_o = permeability index, cm^2/S

E = activation energy for diffusion, J/gm

R = universal gas constant = 8.315 J/gm-K

T = exposure temperature, K

To obtain the diffusion coefficients and solubility data, experiments were performed which involved measurements of the weight changes of staged material at various advancement levels when exposed to different hygrothermal environments.

Six different levels of prepreg advancement were selected for study, and these represent specific points along the baseline cure cycle. This cure cycle is shown in Figure 28 with the various advancement levels identified. Advancement level 1 (AL1) represented the initial state of the laid-up prepreg prior to starting cure. The most advanced material (AL6) was exposed to all of the cure cycle up to and including the first 15 minutes exposure to 177C (350F).

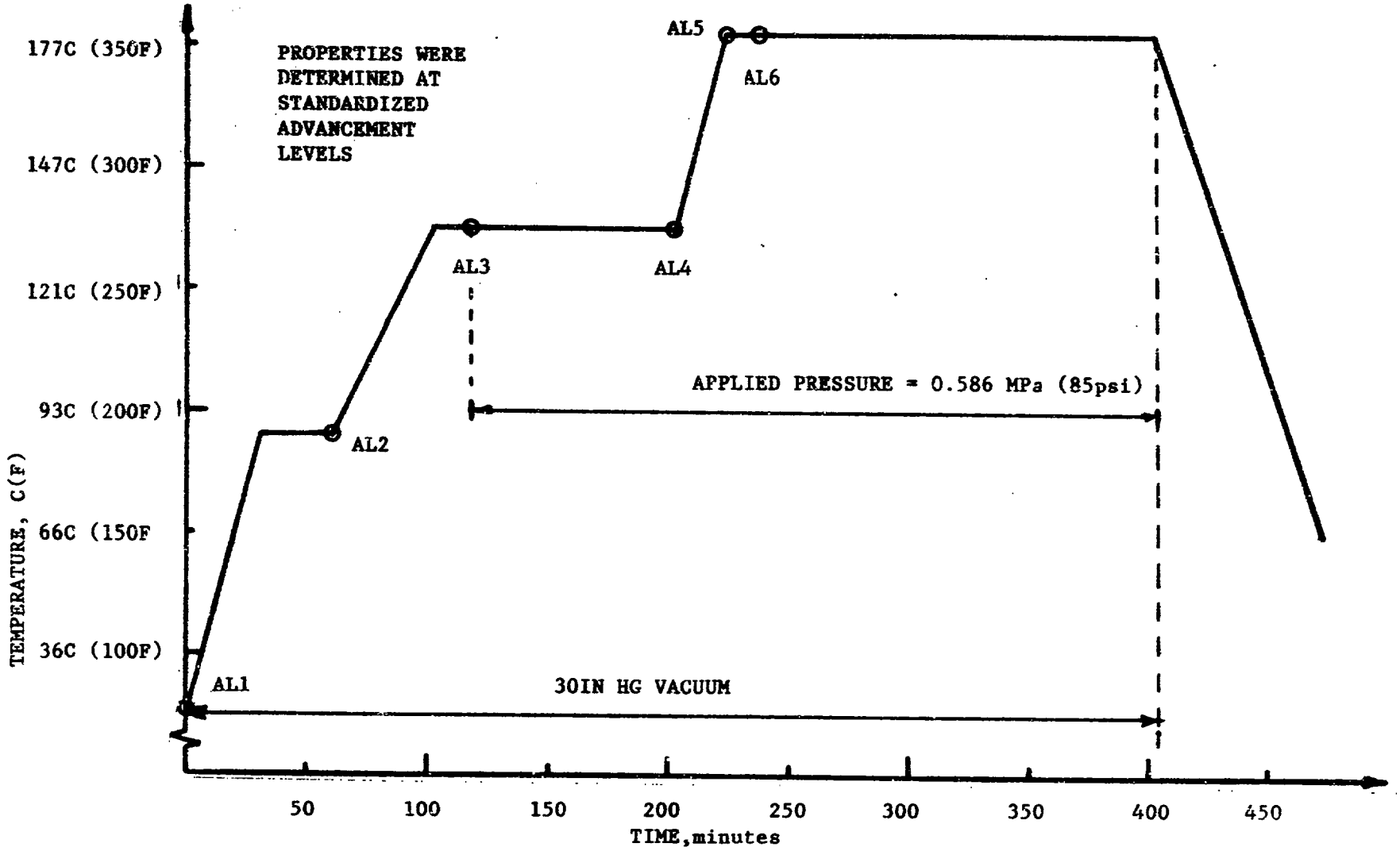

Figure 28. Baseline Cure Cycle With Specimen Advancement Levels

Prepreg specimens, 7.6 cm by 7.6 cm (3 in by 3 in), were subjected to the appropriate portion of the baseline cure cycle. Specimens for AL1 and AL2 were six ply, $(0/90/0)_s$ layups. Because diffusion rates were expected to diminish with increasing advancement, specimens for advancement levels AL3 through AL6 were thinner 3 ply (0/90/0) layups. The application of the cure cycle segments representing AL2 through AL6 was accomplished using a computer controlled cavity press that simulated an autoclave environment. Figures 29 through 33 show the cure history of specimens at these respective advancement levels. The solid line in the cure cycle graph of each figure shows the intended cure cycle; the plotted points show the conditions actually experienced by the material. In each case, conformance to the intended cycle was excellent.

The various staged specimens were sampled and tested to determine resin content. As expected, the more advanced specimens which had experienced the 0.586 MPa (85 psi) pressure had lowered resin contents. Table 5 shows the individual and averaged resin contents for the various advancement levels. The table also lists the normalization factors (the ratio of resin content for a given advancement level to that for AL6) used to normalize all weight gain data with respect to the lowest resin content specimens.

The hydrothermal environments in which specimens were exposed consisted of three humidities at each of three temperatures. Relative humidities of 45 percent, 60 percent and 75 percent were provided in jars by saturated solutions of CrO_3, $NaNO_2$, and NaCl, respectively. Temperatures of 35C and 45C were obtained by placing jars into ovens and a temperature of about 25C was provided by laboratory ambient conditions. Specimens in each jar were supported and maintained in the humidified air space by Plexiglas racks.

JOB NUMBER:	ProcSci
MATERIAL:	T300/5208
BATCH/ROLL:	1721/1B
PANEL NO.:	26-50
PANEL TYPE:	$(0/90/0)_s$
CURE CYCLE:	AL-2
TEST CONDUCTOR:	JHF
TIME STARTED:	9:37

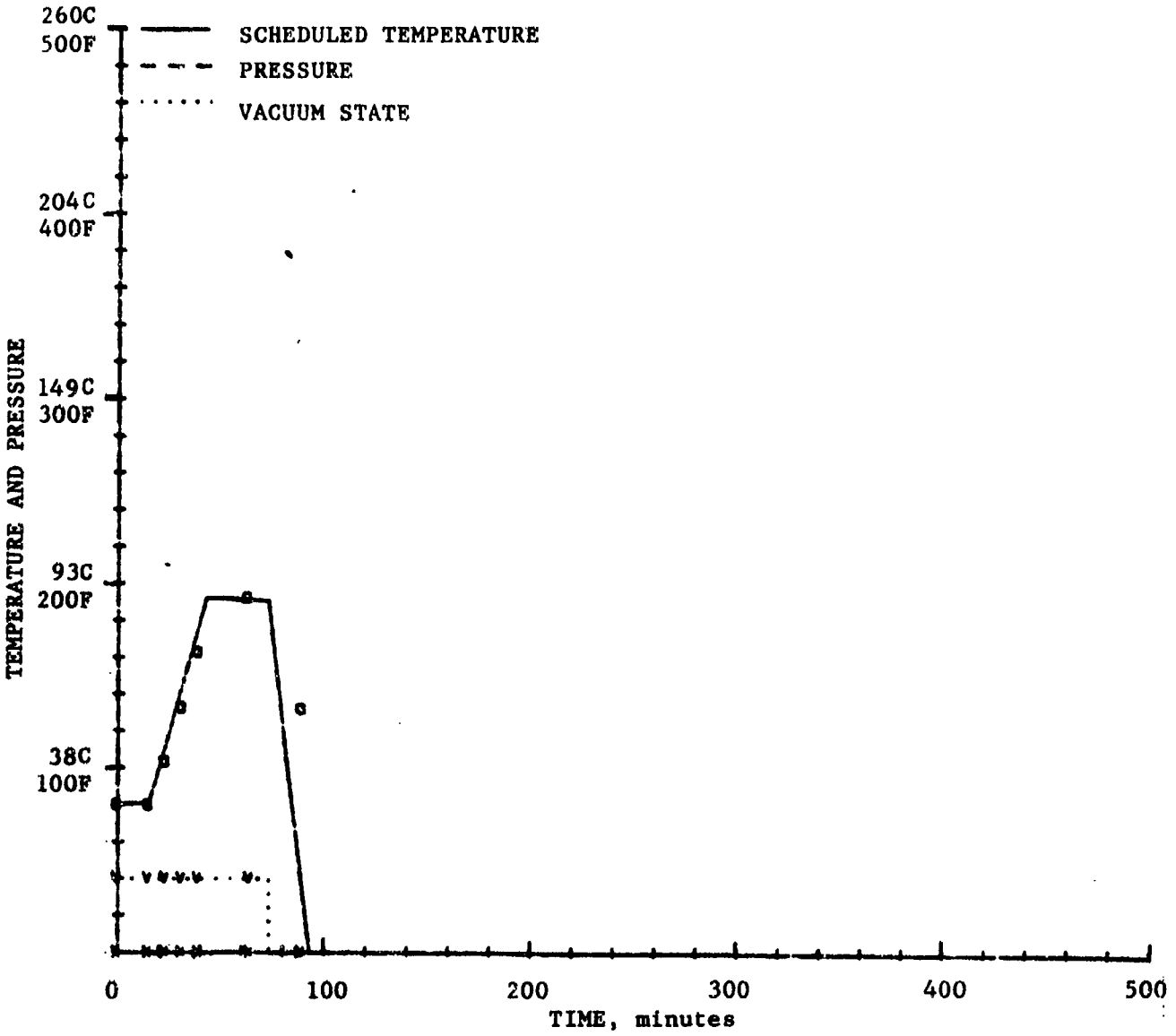

Figure 29. Composite Panel Fabrication

JOB NUMBER:	ProSci
MATERIAL:	T300/5208
BATCH/ROLL:	1721/1B
PANEL NO.:	51-75
PANEL TYPE:	(0/90/0)
CURE CYCLE:	AL-3
TEST CONDUCTOR:	JHF
TIME STARTED:	12:55

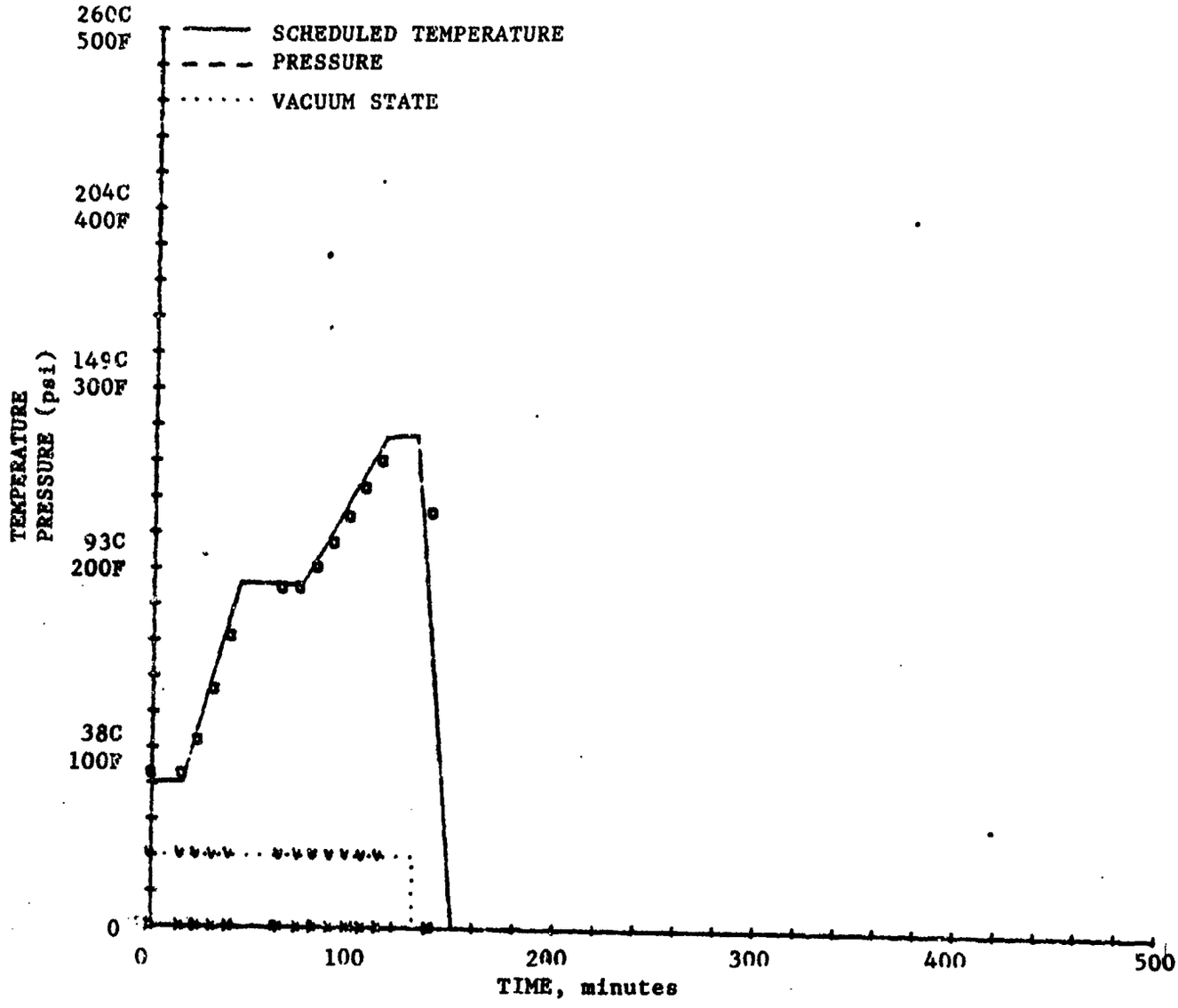

Figure 30. Composite Panel Fabrication

JOB NUMBER:	ProSci
MATERIAL:	T300/5208
BATCH/ROLL:	1721/1B
PANEL NO.:	76-100
PANEL TYPE:	(0/90/0)
CURE CYCLE:	AL-4
TEST CONDUCTOR:	JHF
TIME STARTED:	12:56

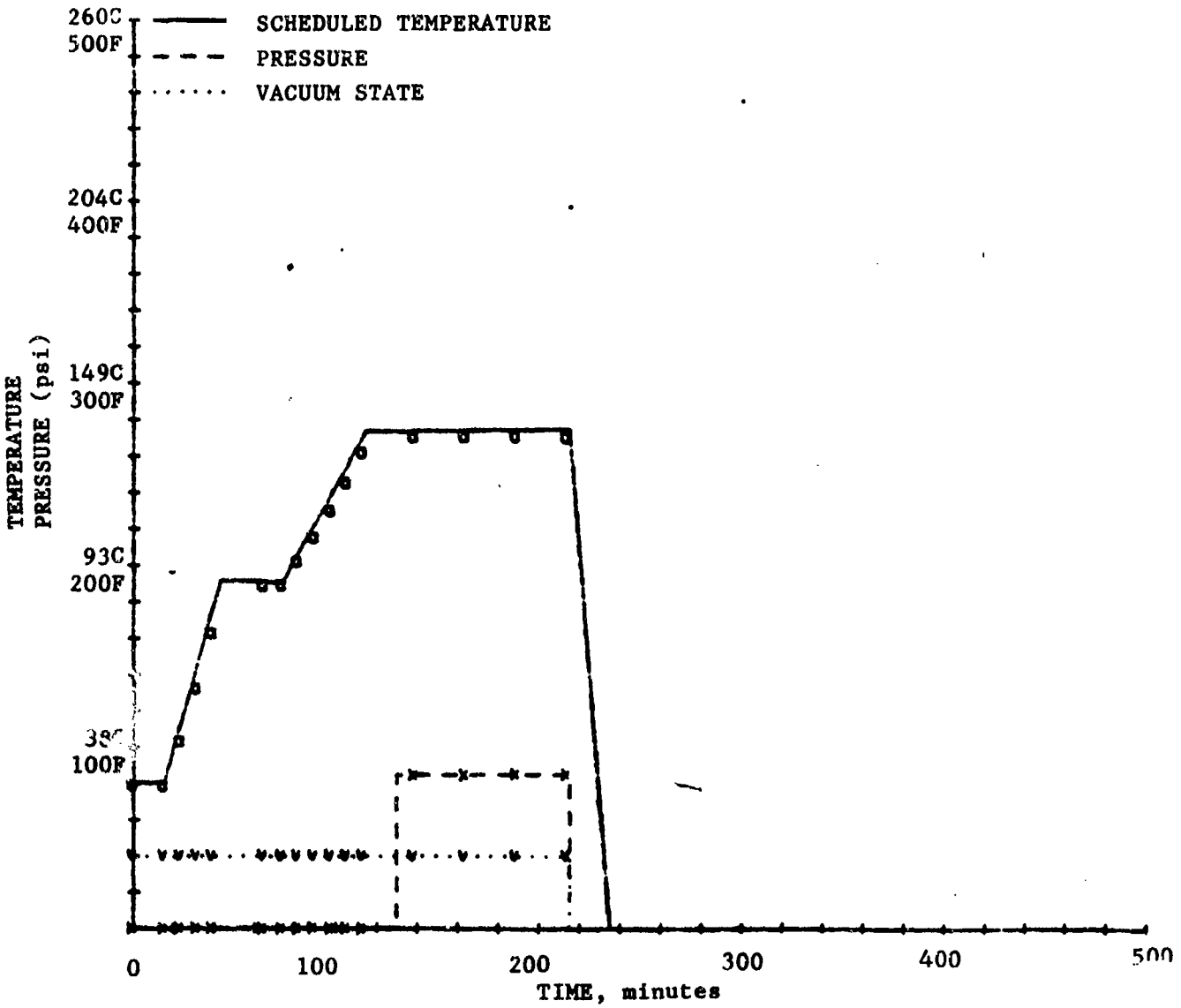

Figure 31. Composite Panel Fabrication

JOB NUMBER:	ProSci
MATERIAL:	T300/5208
BATCH/ROLL:	1721/1B
PANEL NO.:	101-125
PANEL TYPE:	(0/90/0)
CURE CYCLE:	AL-5
TEST CONDUCTOR:	JHF
TIME STARTED:	11:30

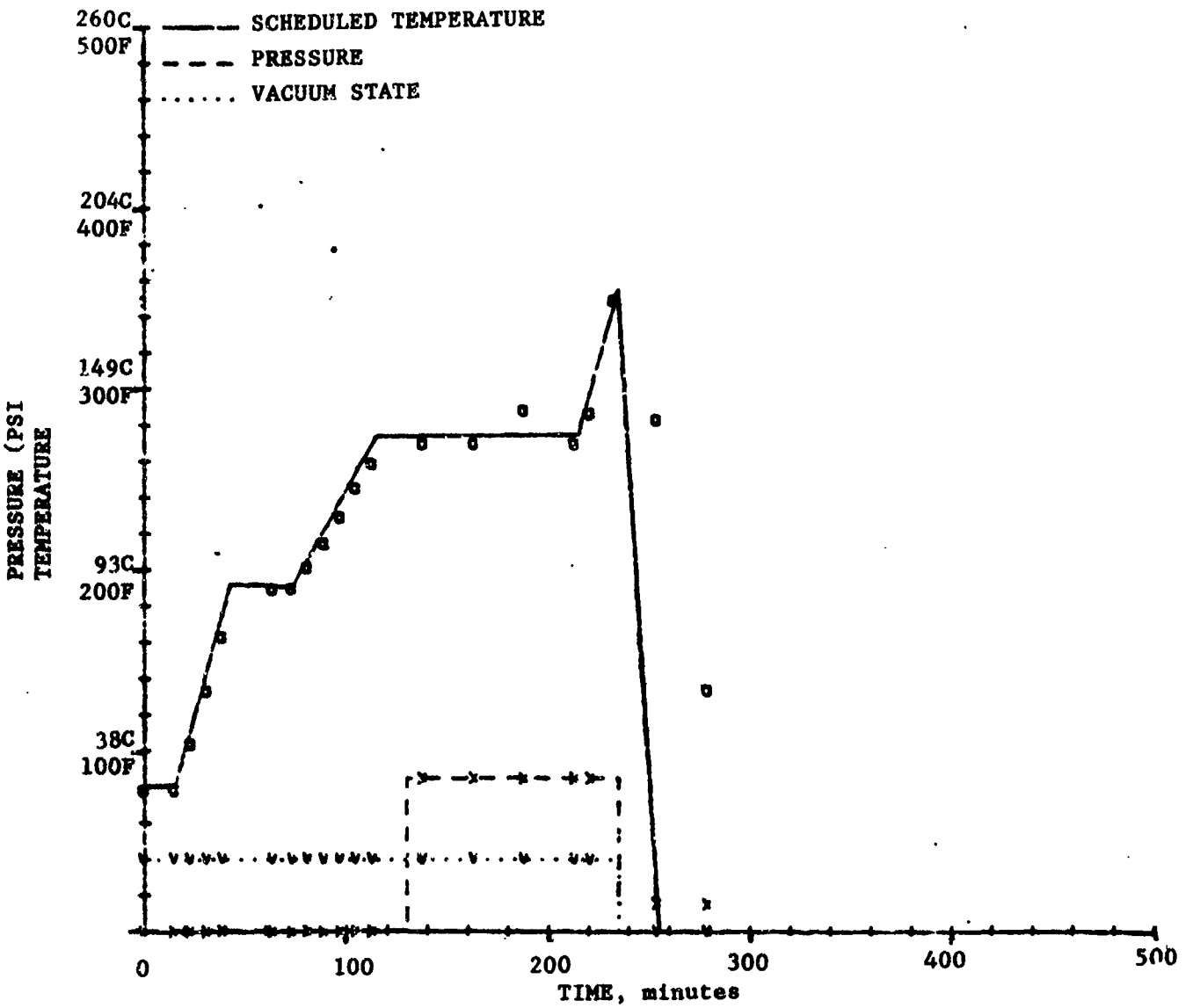

Figure 32. Composite Panel Fabrication

JOB NUMBER:	ProSci
MATERIAL:	T300/5208
BATCH/ROLL:	1721/1B
PANEL NO.:	126-150
PANEL TYPE:	(0/90/0)
CURE CYCLE:	AL-6
TEST CONDUCTOR:	JHF
time started:	10:0

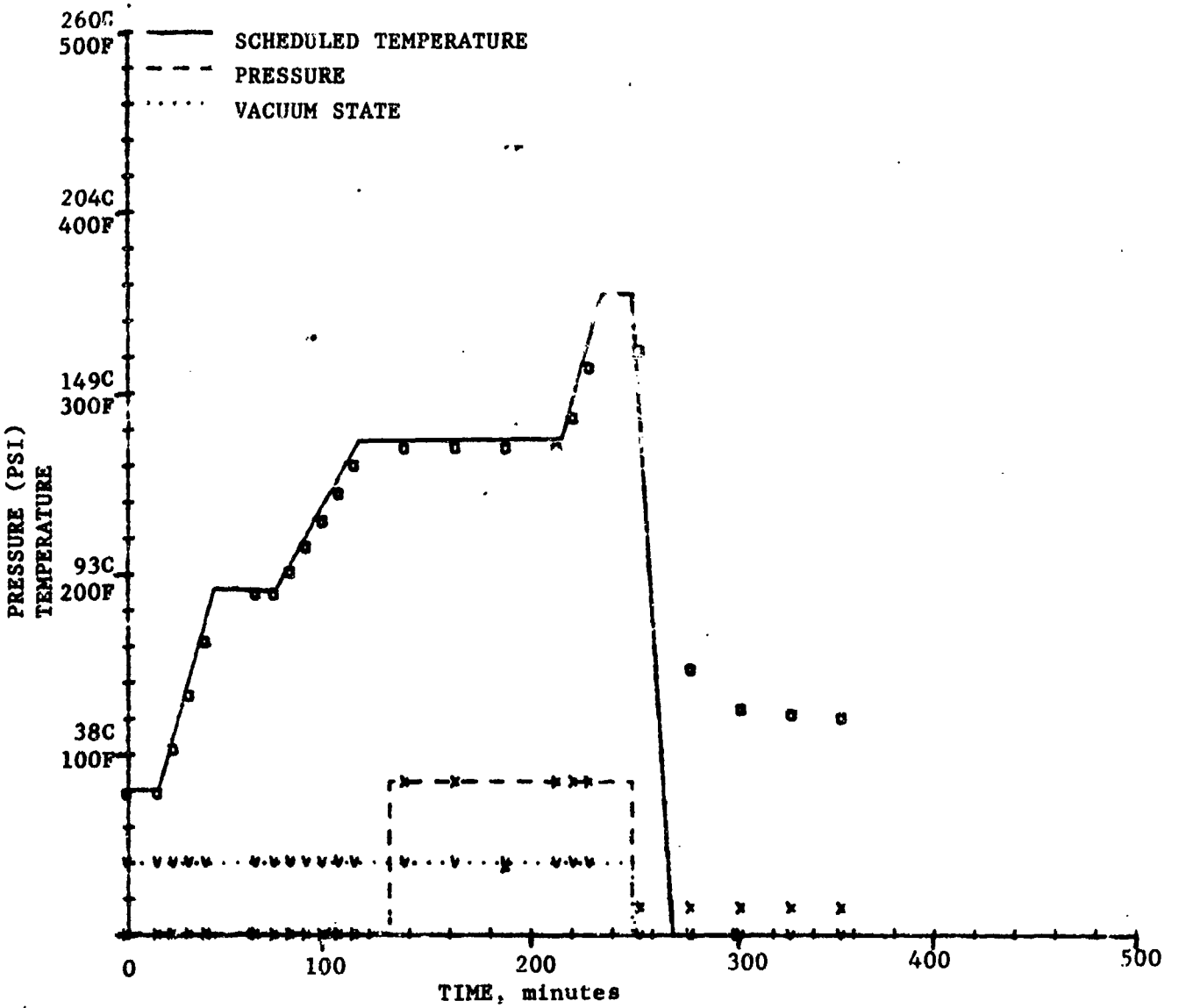

Figure 33. Composite Panel Fabrication

Table 5. Resin Contents of Advancement Level Specimens

Material	Sample	% R.C.	Avg. R.C.	$\frac{AL-i}{AL-6}$ i=1→6
5208 AR 1721/1B	AL-1A	33.16	33.87	1.3108
5208 AR 1721/1B	AL-1B	34.57		
5208 AR 1721/1B	AL-2A	29.33	29.40	1.1378
	AL-2B	29.40		
	AL-2C	29.49		
	AL-2D	29.37		
5208 AR 1721/1B	AL-3A	30.71	30.99	1.1993
	AL-3B	31.72		
	AL-3C	31.30		
	AL-3D	30.70		
	AL-3E	30.53		
5208 AR 1721/1B	AL-4A	26.30	26.08	1.0093
	AL-4B	26.01		
	AL-4C	26.59		
	AL-4D	26.20		
	AL-4E	25.30		
5208 AR 1721/1B	AL-5A	26.32	26.30	1.0178
	AL-5B	26.51		
	AL-5C	26.61		
	AL-5D	26.48		
	AL-5E	25.57		
5208 AR 1721/1B	AL-6A	26.08	25.84	1.0
	AL-6B	26.09		
	AL-6C	25.83		
	AL-6D	25.83		
	AL-6E	25.37		

All of the specimens were sequentially tested for weight change. The weight gain data for the first series of specimens was found to be erratic. This was attributed to the design of the Plexiglas racks. The racks were modified to eliminate any potential source of error before starting an additional series of exposures.

Specimens from the first modified series of exposures were placed into desiccators at each of the three temperatures, and desorption rates were measured. The water desorption studies were necessary to establish the diffusion rate constants at the different resin advancement levels. These constants were then employed in the mathematical model to determine the residual water content at any point of a proscribed cure cycle. The weight loss data, normalized with respect to the resin content of AL6, has been plotted against the square root of the measurement times as is appropriate for diffusion phenomena. Figures 34 and 35 are typical of the plots produced from the normalized weight loss behavior of the six different advancement level specimens for each of the nine hygrothermal environments used to condition the specimens. The remaining plots of this data are shown as Figure A-14 through A-19 in the Appendix. These plots show that the water solubility in the prepreg before starting cure typically is less than that in the higher advancement level materials. As expected the increase in solubility with increasing advancement is magnified with increasing relative humidity. The solubility parameter may be only important in determining the amount of moisture in a laminate at the start of a cure. This amount of solubility should correlate with the maximum amount of moisture-induced voids that could occur due to heterogeneous and homogeneous nucleating.

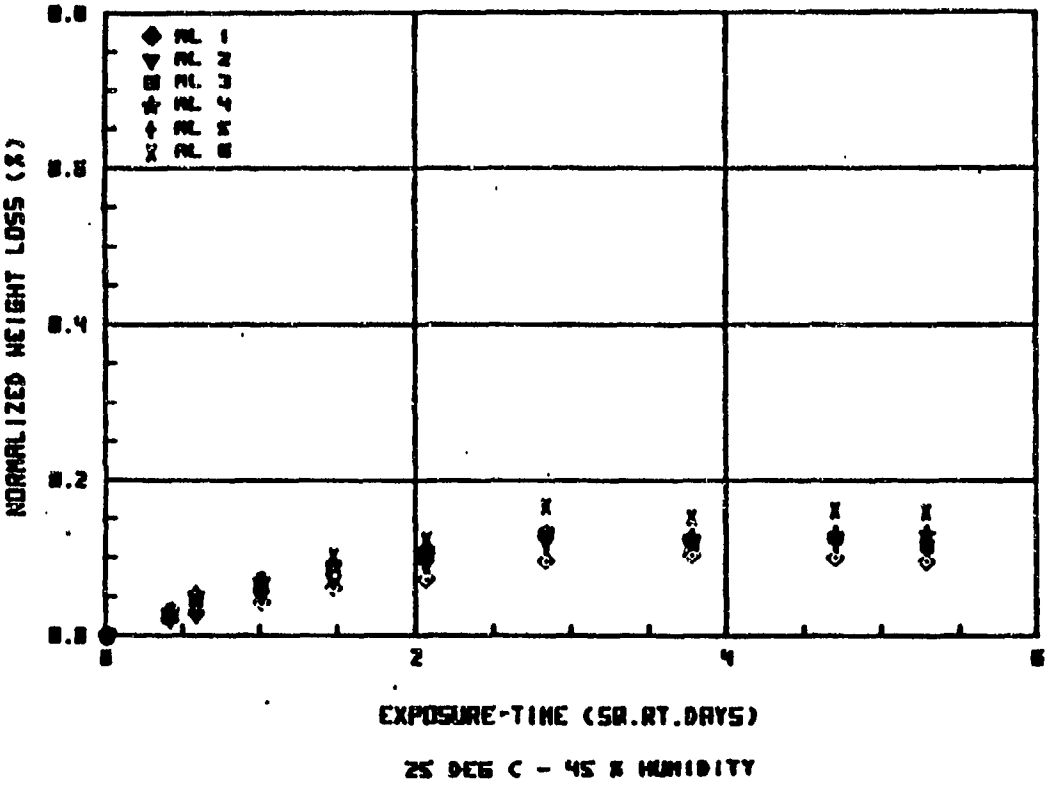

Figure 34. Weight Loss Behavior of Moisture Saturated 5208 Prepreg at 25C

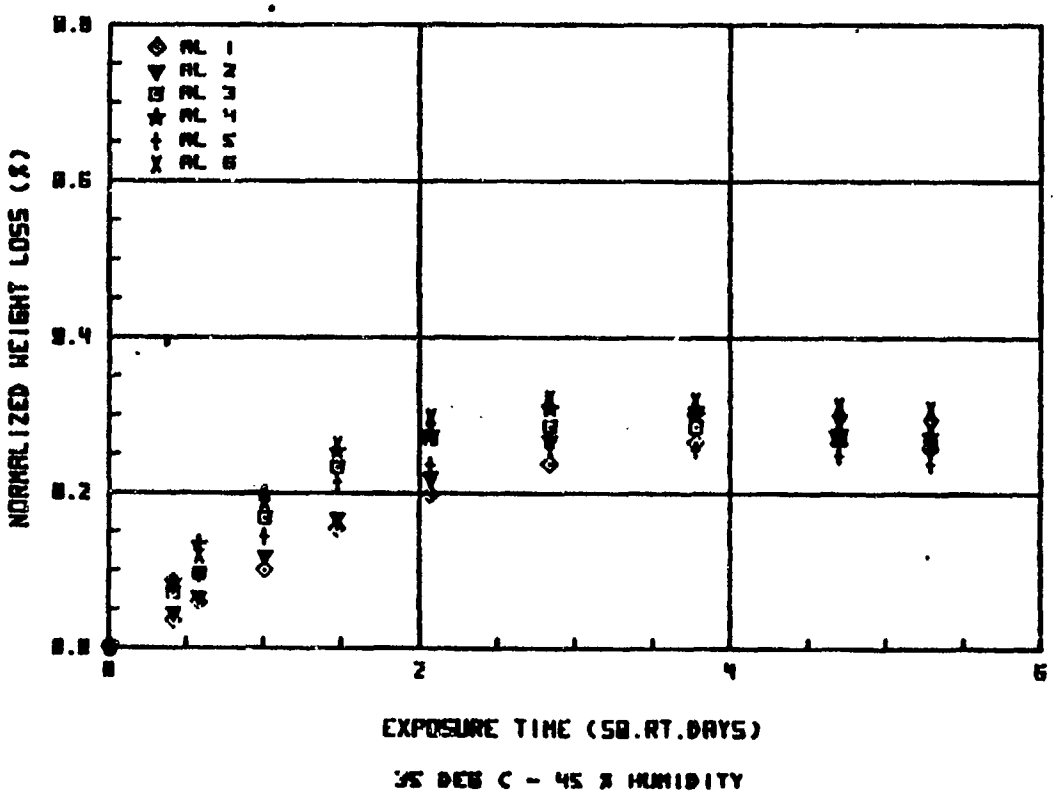

Figure 35. Weight Loss Behavior of Moisture Saturated 5208 Prepreg at 35C

The weight loss data from this first series of specimens was then plotted in two other formats to separate and help identify the effects of the temperature and humidity components of the nine hygrothermal environments. Figures A-20 through A-26 of the Appendix show drying of advancement level specimens AL1-AL6, respectively, following saturation in each of the three humidities when exposed at 25C. The results confirm that water solubility in the prepreg increases as the relative humidity increases. Figures A-27 through A-32 and Figures A-33 through A-38 of Appendix A shows similar plots for specimens originally saturated at temperatures of 35C and 45C, respectively. The other format of presentation involves a comparison of conditioning temperature effects on the drying of each advancement level specimen for each of the three humidity conditions. Figures A-39 through A-44 of the Appendix show drying of AL1-AL6, respectively, at each of the three temperatures following saturation in 45 percent relative humidity. This plotting format shows an apparent solubility increase with increasing temperature, however, as will be discussed shortly, this is in fact not the case. Figures A-45 through A-50 and A-51 through A-56 in the Appendix show similar plots for saturation in relative humidities of 60 percent and 75 percent, respectively.

Data for the second series of specimens was presented in the form of normalized (with respect to resin content of AL6) weight gain versus square root of exposure time. These data were obtained using the improved specimen rack design and improved experimental controls. Figures A-57 through A-65 of the Appendix compare the weight gain behavior of the six differently advanced specimens in each of the nine hygrothermal environments.

Although the results were not completely consistent, AL1 material's water solubility tended to be as low as or lower than that of the other materials. Again, two additional presentation formats are used to facilitate other comparisons. Figures A-66 through A-83 of the Appendix compare the effects of exposure humidity for each advancement level at each exposure temperature. These data, like those of the first series, showed that higher humidities cause higher moisture solubility. The data for the room temperature exposures seem better behaved, however, again highlighting the experimental sensitivity of these tests. Figures A-84 through A-101 of the Appendix compare the effects of temperature on the weight gain behavior of each advancement level specimen in each of the relative humidities. These data, like those of the first series of experiments, showed a significant temperature dependency of moisture solubility.

Similarly, a third series of specimens demonstrated the same anomalous temperature dependency. This apparent dependency became highly suspect and thus the relative humidities of each hygrothermal condition was measured using a Beckman humidistat. The spurious behavior of the 60 and 75 percent RH environmental chambers at 35 and 45C were verified to be attributable to unsaturated salt solutions. This of course resulted in significantly higher humidities than had been intended and for this reason these four hygrothermal conditions were not included in the moisture solubility characterization. While the $NaNO_2$ and NaCl solutions at 25C were actually 62 and 71 percent RH respectively the CrO_3 solutions at all three temperatures were indeed 45 percent RH.

Moisture solubility showed a trend to increase with both relative humidity and resin advancement. The resin advancement levels, designated A11 through AL6, represented prepreg taken to various advancement points along the cure cycle. Solubility of unheated prepreg in 45 percent relative

humidity was about 0.1 percent by weight, but for higher humidity and advancement this increased to about 0.5 percent. Table 6 contains the average solubility at the three temperature exposures at each humidity level, while Figure 36 demonstrates the relative behavior of solubility dependency on advancement and is compared with data found in the literature for postcured 5208/T300 material.

Table 6. Solubilities, Percent by Weight

Specimens	45% RH (25, 35, & 45C)	62% RH (25C)	71% RH (25C)
AL1	0.1092	0.2174	0.2864
AL2	0.1179	0.2272	0.2857
AL3	0.1201	0.2504	0.3432
AL4	0.1225	0.2283	0.2883
AL5	0.1153	0.2086	0.2701
AL6	0.1335	0.2667	0.3604

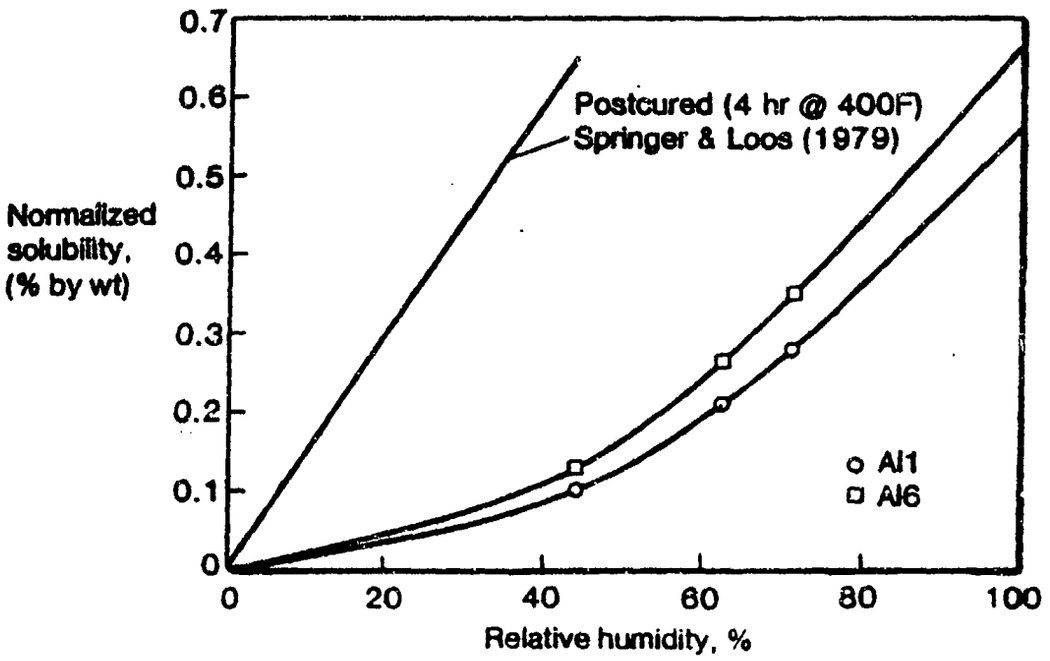

Figure 36. Solubility Dependencies

Data from the first series of tests were analyzed to determine material diffusion coefficients. The diffusion coefficients (D) were determined by extrapolating a sample's saturation level (M_∞) and measuring the initial linear slope of the weight gain (loss) versus square root time (t) plot, utilizing equation 4.

$$M_\infty \sqrt{D} = \frac{\sqrt{\pi}}{4} (2\delta) \left(\frac{\partial [m(t)]}{\partial \sqrt{t}} \right)_{T=0} \qquad (4)$$

to calculate the sample diffusivity D, where 2δ was the specimen thickness for two-sided exposure, m is the mass variable as a function of time, t.

Diffusion coefficients have been computed for the first specimen set and are shown in Table 7. Diffusivity for a given advancement level increased with temperature, as expected. For a given temperature, diffusivity decreased with increasing advancement level.

The quality of the data is naturally important. The experimental aspects of removing specimens from a hot/humid environment, weighing in a cooler/less-humid environment, and then re-establishing the original environment impose an opportunity for error. The effects of such errors could compromise the development of the overall solubility/diffusivity model. Therefore, to provide a more reliable means of spot checking the accuracy

Table 7. Diffusion Coefficients for T300/5208 in Various Subcured States

Advancement Condition	Diffusion Coefficient (10^{-4} cm^2/day)		
	25C	35C	45C
AL1	2.77	3.65	6.25
AL2	2.02	3.25	5.47
AL3	0.988	1.88	3.45
AL4	1.055	1.96	4.25
AL5	0.762	1.55	2.76
AL6	0.762	1.68	2.99

of the data, an additional test set-up was completed. This new set-up was useful for determining diffusivity at higher temperatures than 45C, where experimental difficulties would be even more pronounced with the current method. The new method involved the use of a digital microbalance interfaced with a microprocessor. The balance was mounted over an insulated environmental chamber containing a saturated salt solution. Heater tapes that are regulated by a temperature controller are wrapped around the chamber under the insulation, and they provide a constant, selectable temperature inside the chamber. A single specimen is then supported in the vapor space of the chamber by a hanger wire that passes through a small hole in the chamber lid and that is then hooked to the balance.

Once inside the chamber, the specimen's weight was continually recorded at intervals specified through the microprocessor. The specimen was never handled after placing it into the environment, eliminating the steps and conditions that introduce possible error.

Moisture diffusivity values for all 54 advancement/environment conditions are contained in Table 8. Because diffusivity is independent

Table 8. Average Diffusivities, $cm^2/day \times 10^{-4}$ (Average of Three Specimens at Each Condition

Specimens	25°C 45%	25°C 60%	25°C 75%	35°C 45%	35°C 60%	35°C 75%	45°C 45%	45°C 60%	45°C 75%
AL-1	2.2276	2.0138 2.0718	1.9742	2.5080	2.3218 2.4680	2.5742	3.9598	3.4571 3.7542	3.8457
AL-2	2.0336	2.0249 1.9713	1.8554	2.0005	2.0786 2.2064	2.5402	3.3648	2.9797 3.1490	3.1026
AL-3	1.0848	1.0933 1.0646	1.0159	1.7951	1.5703 1.7004	1.7357	2.2798	1.8905 2.2092	2.4575
AL-4	1.0501	0.9581 1.0516	1.1466	1.3499	1.5798 1.6185	1.9257	2.3301	2.7410 2.7072	3.0504
AL-5	1.0647	0.8381 0.9800	1.0371	1.7119	1.3736 1.4976	1.4073	2.1188	2.8386 2.4397	2.3617
AL-6	1.3574	0.9894 1.1331	1.0525	1.3794	1.5923 1.6158	1.8755	2.0386	2.6817 2.3756	2.4065

of relative humidity, the values for the three humidities at each advancement/temperature condition have been averaged, with the average shown below the 60 percent R.H. value. Diffusivity values increased with temperature and decreased with prepreg advancement as demonstrated in Figure 37. This competing effect resulted in an increase in diffusivity of only about 15 percent in going from as-received prepreg at room temperature to the most advanced condition (AL6) at 45C.

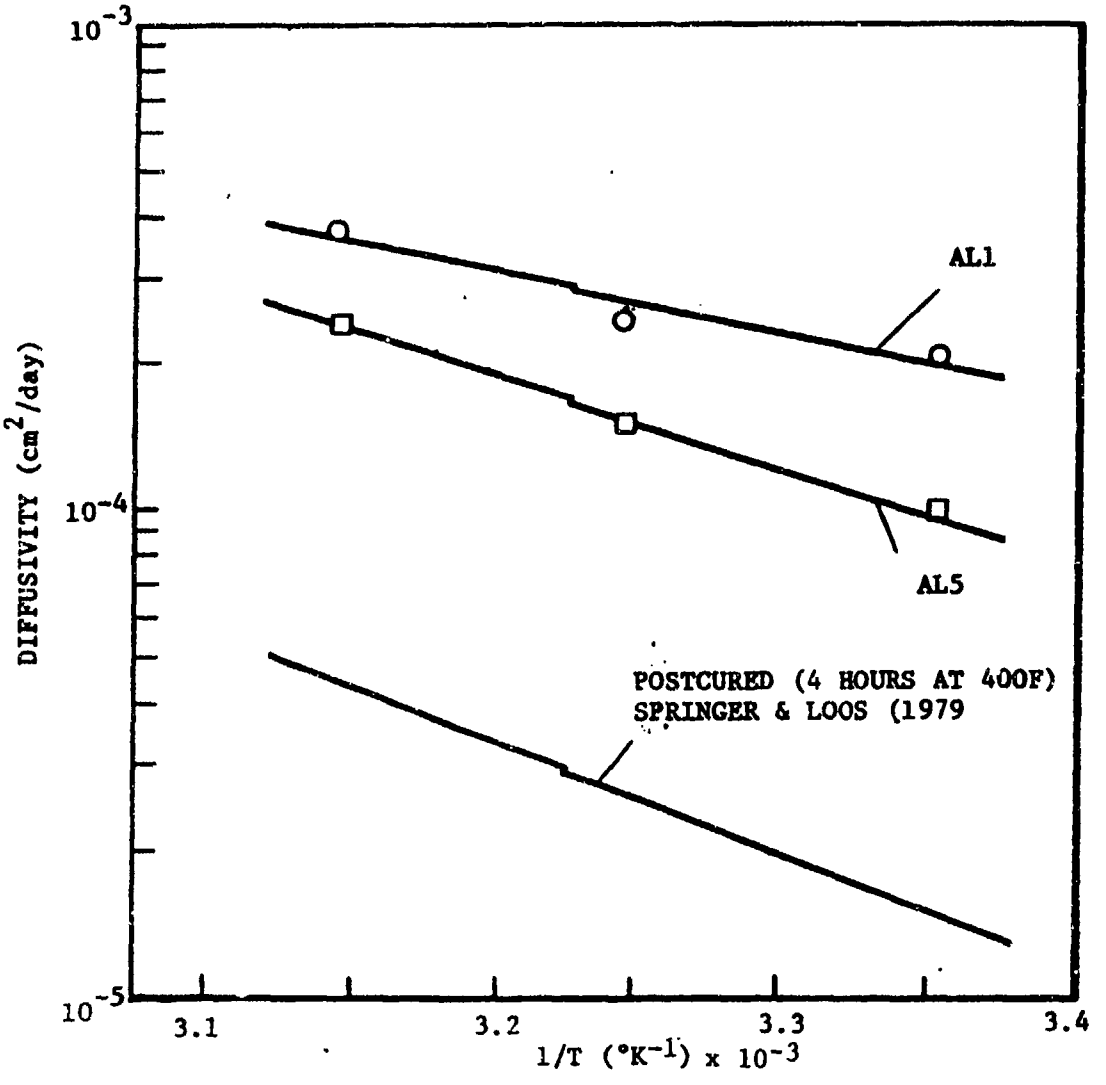

Figure 37. Diffusivity Dependencies

Surface tension measurements of 5208 resin were conducted in a heated-stage goniometer at four temperatures ranging from 85C to 155C. Surface tension decreased from an initial value of 50 dynes/cm with increases in temperature and advancement. After 50 minutes at 155C the surface tension was only half of the starting value. Figure 38 is a graph of the data and contains the governing equation that describes the data. The solid-line curves on the graph represent the description given by this equation.

2.3.1 MOISTURE DIFFUSION - MODELING AND ANALYSIS. During the laminate processing tests, the thermal cycles for cure of the vertical tail skins were modified to provide time at a low temperature for moisture leveling and desorption. Since absorptivity and diffusion tests of prepreg in different cure states has been completed, an analysis was conducted to determine how effective such leveling or desorption might be.

Values of the pre-exponential term, D_o, and of the activation energy for diffusion, E, were calculated for prepreg at advancement levels AL-3 and AL-5. These represent the cure states at the start of the 132C (270F) and 177C (350F) dwells, respectively. For AL-3 cure state $D_o = 1.25 \times 10^{-4}$ cm^2/sec and E = 6870 cal/gm, and for AL-5 cure state $D_o = 2.26 \times 10^{-3}$ cm^2/sec and E = 8580 cal/gm. Using these values and an assumed uniform moisture content of 0.35 percent in a 75-ply laminate, finite difference diffusion analyses were performed to determine the drying rate at 132C (270F) assuming two-sided desorption.

Tables 9 and 10 show the moisture at one hour increments through 10 hours. These analyses clearly indicate that the diffusion rate of moisture out of the material is so slow that the center of a 75-ply laminate will not dry prior to resin gellation. In fact, the diffusion rate is so slow that the centerline of even a 20-ply-thick laminate would experience no

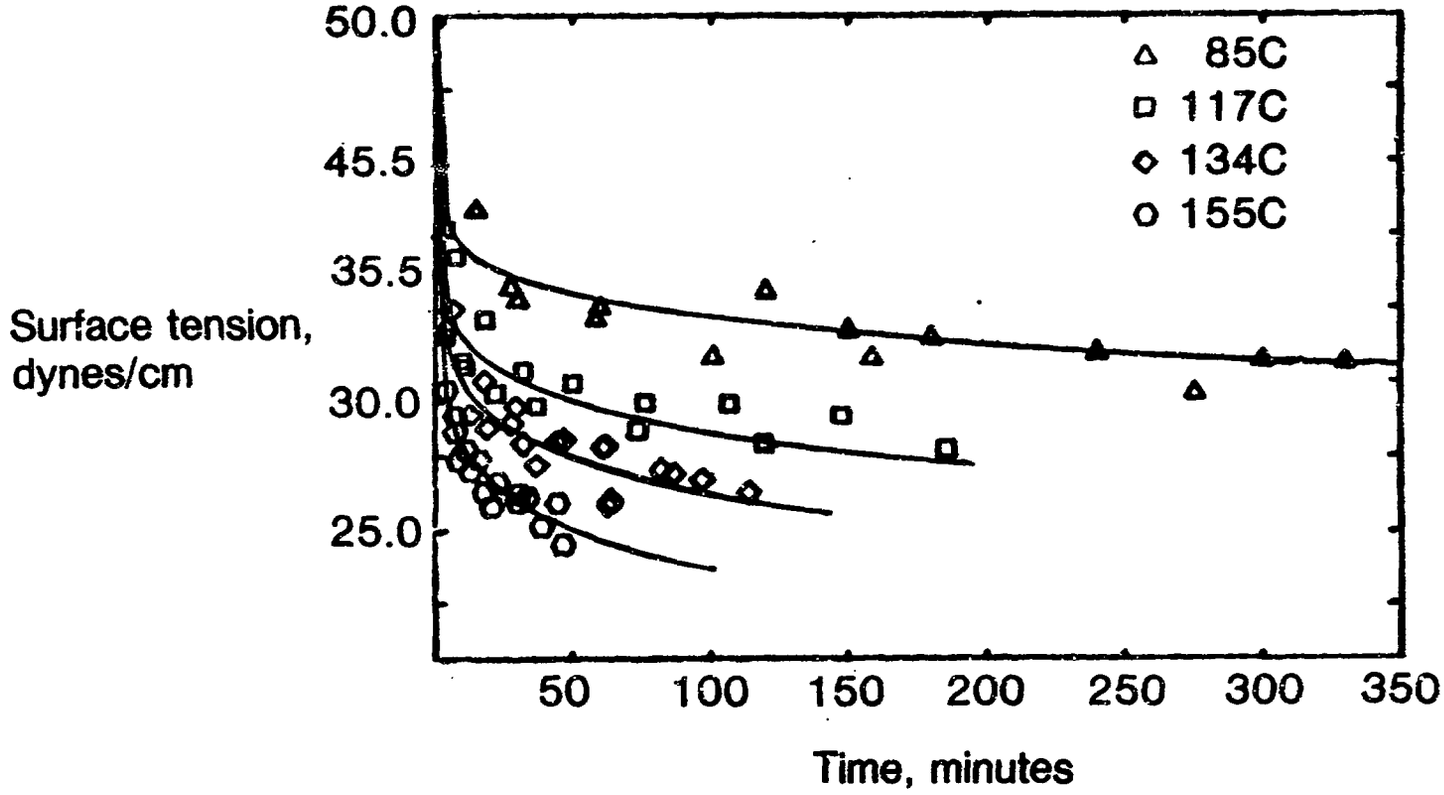

o GOVERNING EQUATION

$$\gamma_t = \gamma_0 - \Delta\gamma_1(T)\, t^n$$

WHERE: $\gamma_0 = 50$

$\Delta\gamma_1(T) = 0.07T(^\circ K) - 19.8$

$n = 0.115$

Figure 38. Parameterization of Surface Tension

TABLE 9

FINITE DIFFERENCE ROUTINE FOR MOISTURE DISTRIBUTION

DO = 0.000138Q.CM/SEC E/R = 6870.0CAL/GM A = 0.6000 PERCENT

S V = 4.85 PER INCH

COMBO	T	RH	HRS
1	270	0	1.0

SPECIMEN DATA: 75-PLY LAMINATE IN CURE AL-3 STATE

		MODE NO./DISTANCE FROM SURFACE							
		1	2	3	4	5	6	7	8
		0.00000	0.01289	0.02578	0.05156	0.07794	0.10313	0.15469	0.20625
		MOISTURE CONTENT							
HR.	0	0.350	0.350	0.350	0.350	0.350	0.350	0.350	0.350
		AVERAGE MOISTURE AT THE END OF HR. 0 = 0.350							
HR	1	0.000	0.321	0.350	0.350	0.350	0.350	0.350	0.350
		AVERAGE MOISTURE AT THE END OF HR. 1 = 0.337							
HR	2	0.000	0.297	0.348	0.350	0.350	0.350	0.350	0.350
		AVERAGE MOISTURE AT THE END OF HR. 2 = 0.336							
HR	3	0.000	0.277	0.346	0.350	0.350	0.350	0.350	0.350
		AVERAGE MOISTURE AT THE END OF HR. 3 = 0.304							
HR	4	0.000	0.259	0.342	0.350	0.350	0.350	0.350	0.350
		AVERAGE MOISTURE AT THE END OF HR. 4 = 0.333							
HR	5	0.000	0.245	0.338	0.350	0.350	0.350	0.350	0.350
		AVERAGE MOISTURE AT THE END OF HR. 5 = 0.331							
HR	6	0.000	0.232	0.333	0.349	0.350	0.350	0.350	0.350
		AVERAGE MOISTURE AT THE END OF HR. 6 = 0.330							
HR	7	0.000	0.221	0.328	0.349	0.350	0.350	0.350	0.350
		AVERAGE MOISTURE AT THE END OF HR. 7 = 0.329							
HR	8	0.000	0.212	0.322	0.349	0.350	0.350	0.350	0.350
		AVERAGE MOISTURE AT THE END OF HR. 8 = 0.328							
HR	9	0.000	0.204	0.317	0.348	0.350	0.350	0.350	0.350
		AVERAGE MOISTURE AT THE END OF HR. 9 = 0.327							
HR	10	0.000	0.196	0.312	0.348	0.350	0.350	0.350	0.350
		AVERAGE MOISTURE AT THE END OF HR. 10 = 0.325							

TABLE 10

FINITE DIFFERENCE ROUTINE FOR MOISTURE DISTRIBUTION

DO = 0.0022630.CM/SEC E/R = 8580.0 CAL/GM A = 0.6000 PERCENT

S/V = 4.85 PER INCH

COMBO	T	RH	HRS
1	350	0	1.0

SPECIMEN DATA: 75-PLY LAMINATE IN CURE AL-5 STATE

		MODE NO/DISTANCE FROM SURFACE							
		1	2	3	4	5	6	7	8
		0.00000	0.01289	0.02578	0.05156	0.07734	0.10313	0.15469	0.20028
		MOISTURE CONTENT							
HR.	0	0.350	0.350	0.350	0.350	0.350	0.350	0.350	0.350
		AVERAGE MOISTURE AT THE END OF HR. 0 = 0.350							
HR.	1	0.000	0.217	0.335	0.350	0.350	0.350	0.350	0.350
		AVERAGE MOISTURE AT THE END OF HR. 1 = 0.329							
HR.	2	0.000	0.174	0.297	0.347	0.350	0.350	0.350	0.350
		AVERAGE MOISTURE AT THE END OF HR. 2 = 0.320							
HR.	3	0.000	0.151	0.266	0.340	0.349	0.350	0.350	0.350
		AVERAGE MOISTURE AT THE END OF HR. 3 = 0.317							
HR.	4	0.000	0.134	0.241	0.332	0.340	0.350	0.350	0.350
		AVERAGE MOISTURE AT THE END OF HR. 4 = 0.313							
HR.	5	0.000	0.121	0.221	0.322	0.346	0.350	0.350	0.350
		AVERAGE MOISTURE AT THE END OF HR. 5 = 0.309							
HR.	6	0.000	0.111	0.205	0.312	0.343	0.349	0.350	0.350
		AVERAGE MOISTURE AT THE END OF HR. 6 = 0.305							
HR.	7	0.000	0.103	0.192	0.362	0.340	0.349	0.350	0.350
		AVERAGE MOISTURE AT THE END OF HR. 7 = 0.301							
HR.	8	0.000	0.096	0.181	0.293	0.336	0.048	0.350	0.350
		AVERAGE MOISTURE AT THE END OF HR. 8 = 0.298							
HR.	9	0.000	0.090	0.171	0.284	0.332	0.347	0.350	0.350
		AVERAGE MOISTURE AT THE END OF HR. 9 = 0.295							
HR.	10	0.000	0.086	0.163	0.276	0.328	0.346	0.050	0.050
		AVERAGE MOISTURE AT THE END OF HR. 10 = 0.273							

drying after 8 hours at 132C (270F). Figure 39 shows a reduction of this data to graphic form.

This data strongly suggests that a major portion of the water normally associated with prepreg is actually being cured into the laminate regardless of the cure cycle or degassing techniques employed.

2.4 MODELING STUDY

2.4.1 MODEL DEVELOPMENT. Models to describe the critical aspects of material behavior during cure were developed. Eleven models that fall into five categories were considered. All but two of these models dealt with the problem of voids or porosity in laminates. The remaining two models dealt with resin flow. The five model categories were (1) void formation, (2) void growth, (3) void dissolution, (4) void transport, and (5) resin flow.

The first priority in modeling was placed on describint the void forming process. The initial model for void formation was based on the concept of homogeneous nucleation of voids. This model considered void formation at any point within a laminate, which could occur by nucleation within the resin. This formation of homogeneous nuclei or discrete regions of a new phase requires both phase transformation and the formation of an interface between the two phases. The rate of homogeneous nucleation, I, is given by Equation 5.

$$I = \frac{P^*}{(2\pi MkT)^{1/2}} \, 4\pi r^{*2} \, n \exp - \frac{\Delta F^*}{kT} \qquad (5)$$

where

P* = water vapor pressure
M = molecular weight, water
k = Boltzmann constant
T = absolute temperature
r* = radius of critical nucleus
n = number of molecules/unit volume, water
ΔF* = maximum in free energy

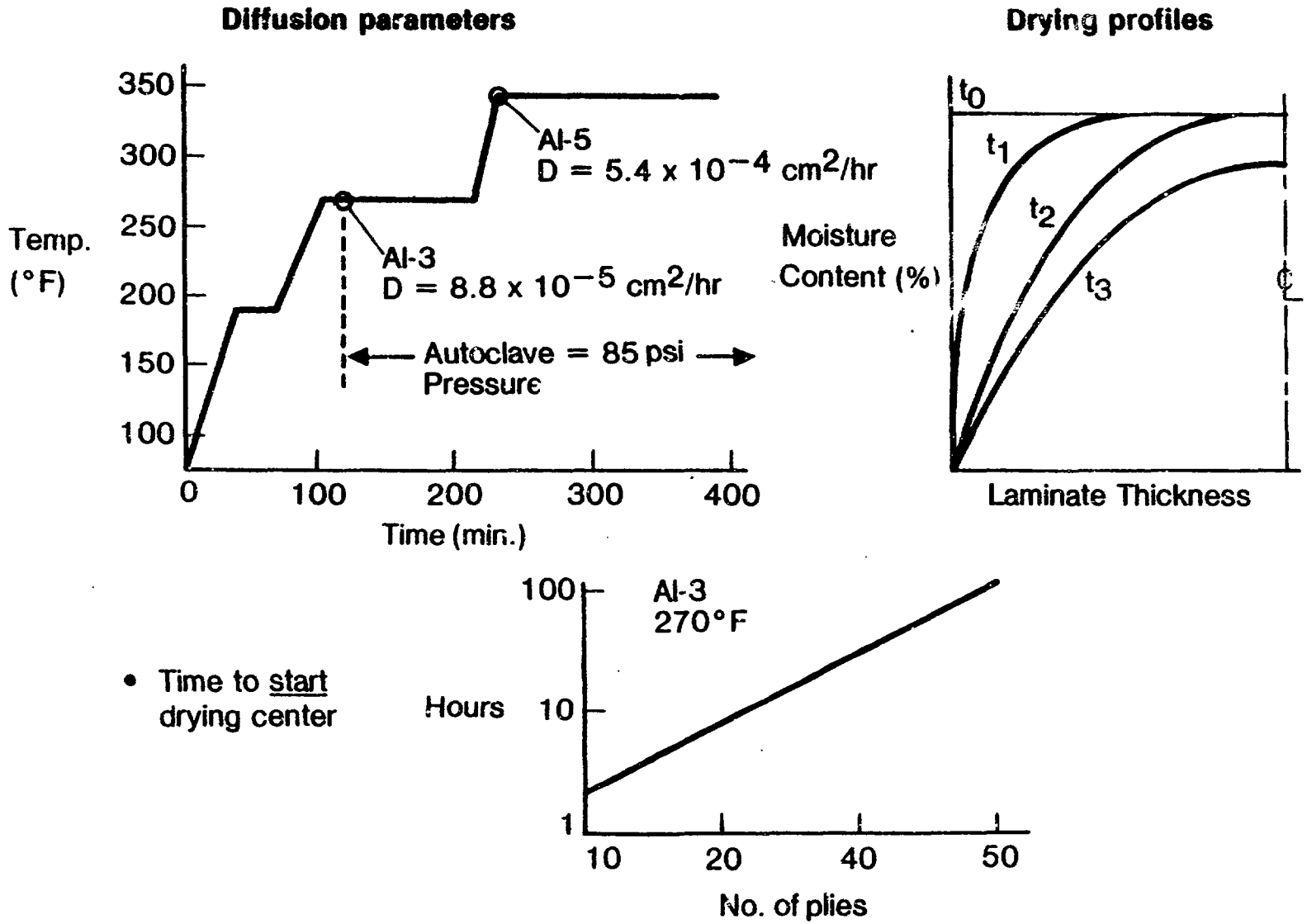

Figure 39. Cure Drying is Slow

also

$$\Delta F^* = 16 \pi (\gamma_{gl})^3 / 3 (\Delta F_v)^2 \qquad (6)$$

where

γ_{gl} = surface tension between liquid and vapor

ΔF_v = free energy change per unit volume for the phase transition

Although homogeneous nucleation within the resin is a mechanism to be considered, heterogeneous nucleation is a more likely mechanism. For this case the vapor bubble would form on some solid substrate. Potential solid substrates include the graphite fibers, dust particles or particles of DADS hardener present in uncured 5208 resin. For heterogeneous nucleation, the free energy term ΔF^* would be described by

$$\Delta F^* = \frac{16 \pi (\gamma_{sv})^3 (2 + \cos\theta) (1 - \cos\theta)^2}{3 (\Delta F_v)^2} \qquad (7)$$

where θ is the contact angle for the vapor bubble on the solid substrate and where γ_{sv} is the solid-vapor surface tension.

For either of these cases, homogeneous or heterogeneous nucleation, voids would initially be very small and would typically be formed within the body of a given ply. Photomicrographic examination of many cured laminates shows no evidence of intraply voids. All cured laminate voids are found to occur at the ply-to-ply interfaces, and these are much larger than could conceivably form within the body of a ply. Any intraply voids, therefore, would have to be vertically transported at least to the first available interface where they might coalesce, forming a larger void. In considering such vertical void transport, one would expect that intraply voids would become trapped occasionally within the body of a ply. However, no such evidence of voids has been found. Furthermore, it is common to find voids at the interface of

two identically oriented plies. This discredits the concept that vertically transported voids become trapped at an interface because the "cylindrical" spaces between fibers in a ply are reduced at the interface to small, discrete parallelogramic spaces by fibers crossing at an angle. No mechanism has been conceived by which vertically transported voids could identify and collect at the interface of two identically oriented plies.

The physically observed interfacial nature of laminate voids suggests instead that voids are formed at the ply interfaces rather than being transported to them. The physical evidence also indicates that voids occur somewhat randomly. Therefore, some randomly occurring surface condition of the prepreg might be involved. This might be contamination, either by some chemical or some particulate. Erratic or spotty transfer of backing paper release agent to the prepreg surface would be an example of such contamination. For this case the heterogeneous nucleation model would discretely apply except that the contaminant vapor surface tension would be used in Equation 6 instead of the fiber-vapor surface tension. The low surface tension and easy "wetting" of release agent contamination would produce a low value of free energy F*. This would, in turn, produce a maximum nucleation rate, as indicated by the form of Equation 5.

Another mechanism by which interfacial voids might be created involves mechanical formation. This could result from air entrapment during layup, from bridging of fibers over a thin spot in the underlying ply or over surface particulates, or from wrinkling during layup. This mechanism would require either maintenance of the mechanical condition that caused the void, e.g., bridging, or void stabilization - perhaps by diffusion of water vapor into the air pocket with subsequent pressure buildup as temperature increases.

This void stabilization mechanism seems particularly plausible in light of other information. Specifically, the occurrence of voids has been shown to have a strong statistical correlation with high relative humidity during layup. Also, photomicrographic examination typically show that voids occur in the interior of the laminate. This would correlate with a laminate losing moisture by diffusion where critical temperature-time conditions are reached before the moisture concentration gradient has been sufficiently diminished by the desorption process. A model to describe this process was developed and involved consideration of the rate of growth of the void due to diffusion of moisture vapor.

2.4.2 VOID GROWTH. There are two physical possibilities for which growth of a critical-size void may be examined. The first is the growth of a pure water vapor void by diffusion of water from the surrounding liquid resin into the gaseous water void; the second involves the same diffusion process, except that the water enters a void containing both air and water. Since we have already shown that water is the stabilizing factor in any sort of void growth, we will first concentrate on the growth of a pure water vapor void. In the treatment below, we assume that conditions are favorable for nucleation of a critical size void. For low molecular weight materials such as water, critical size nuclei are extremely small; and we may assume that the effective void diameter is essentially zero. The physical situation is shown in Figure 40. As the void grows, the boundary between resin and void moves. C_∞ is the equilibrium water concentration in the bulk liquid resin and C_{sat} is the concentration in the prepreg as a result of its prior exposure to water vapor. C_{sat} will depend on the water content in the resin and the temperature. The designation of "sat" or saturation indicates saturation in the void, not in the resin.

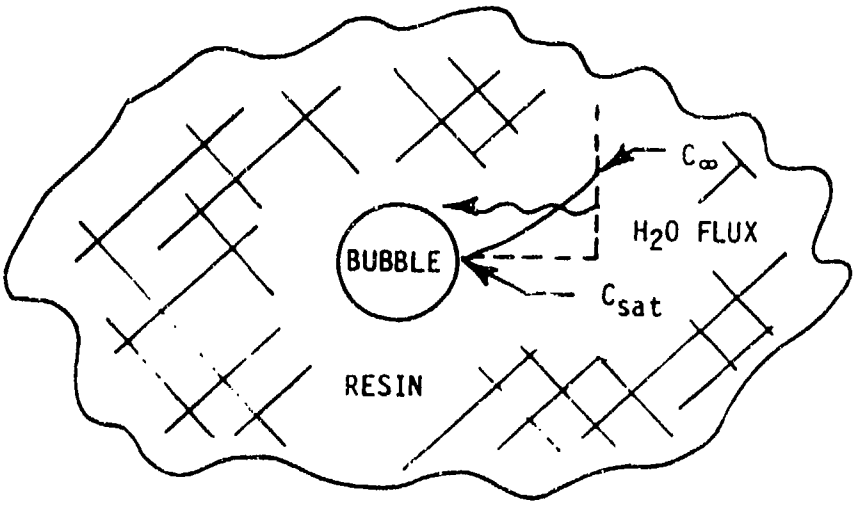

Figure 40. Void Concept for Mathematical Model

2.4.3 MAJOR ASSUMPTIONS AND DATA INPUTS

1. The void is stagnant between two plies and its center is not moving with respect to fixed coordinates in the laminate.
2. The void is spherical and its effective size is calculated based on an equivalent sphere.
3. There is no interaction between voids (no coalescence).
4. The void is considered to be in an infinite isotropic fluid medium.
5. Void nucleation is instantaneous at the reduced pressure levels in the vacuum bag.
6. At any given time, the temperature and moisture concentration in the bulk resin are uniform.
7. Fresh prepreg contains 32 percent weight resin. The resin contains 20 percent by weight of DADS.
8. The moisture content of DADS is 2.92 percent by weight. (See Appendix C-1).

9. A simple parabola fits the solubility data reasonably well (see page 57).

$$S_o = 5.58 \times 10^{-5} (RH)^2 = 1.337 \left(\frac{P_{H_2O}}{P_{H_2O*}} \right)^2 \quad (8)$$

S_o(% Wt) = water solubility (percentage in fresh prepreg of advancement level one (AL1).

RH = relative humidity at which the prepreg was saturated by water

P_{H_2O} = partial pressure of water

P_{H_2O*} = vapor pressure of water

We should note here that the revised solubility data point of 1.5 percent weight at 100 percent RH cannot be fit with a parabola and requires a higher order polynomial. The test fit of the form bn^n utilizing the new data is

$$S_o = 3.74 \times 10^{-7} (RH)^{3.25} = 1.18 \left(\frac{P_{H_2O}}{P_{H_2O*}} \right) \quad (8a)$$

However the fit of the data to this form is poor and one would have to use a polynomial with three or four terms to match all the data points well. The data accuracy does not warrant such an exercise.

10. The diffusivity of water in the prepreg can be described by the data on pages 59 and 60.

$$D_0 = 0.105 \, e^{-2817/T} \quad (9)$$

$$D_6 = 0.604 \, e^{-3508/T} \quad (9a)$$

where

D_0 (cm^2/hr) - diffusivity in fresh prepreg

D_6 (cm^2/hr) - diffusivity in cured prepreg

T(°K) - absolute temperature

11. The curing cycle is as follows:

    a. Apply vacuum (∿-0.1 atm) and heat from room temperature at a rate of 2C/min to 135C (408K).

    b. Hold the temperature constant at -0.1 atm for

        (1) 15 min (0.25 hr)

        (2) 60 min (1 hr)

        (3) 90 min (1.5 hr)

    c. Pressurize to 5.78 atm and hold for 105 min (1.75 hr).

    d. Keep pressure at 5.78 atm and heat at 1.1C/min to 179C (452K) and hold the temperature constant for 2 hours.

12. The various solid densities at room temperature are

    resin - ρ_R - 1.22 gms/cc

    fibers - ρ_f - 1.72 gms/cc

    prepreg - ρ_ρ - 1.52 gms/cc

13. If we utilize the Clausius-Clapeyron equation (7)

$$\frac{dp_{H_2O}}{dT} = \frac{\Delta H_V}{T\ (V_g - V_L)} \tag{10}$$

and assume that

a. ΔH_V, the heat of vaporization is constant,

b. the vapor phase behaves as an ideal gas,

the following dependence of vapor pressure on temperature is obtained

$$P_{H_2O^*} = \left(P_{H_2O} \quad e^{\frac{\Delta H_V}{RT_o}} \right) e^{-(\Delta H_V/RT)} \tag{11}$$

where

T_o (K) - boiling point of H_2O at 1 atm (373K)

$P_{H_2O^*}$ (atm) - water vapor pressure

P_{H_2O} (atm) - water vapor pressure at boiling point (1 atm)

ΔH_V (cal/mol) - heat of vaporization (9720 cal/mol)

$R\left(\frac{cal}{mole\text{-}K}\right)$ - ideal gas constant (1.987 ca/mole-K)

$$\therefore \quad P_{H_2O^*} = 4.962 \times 10^5 \, e^{-4892/T} \tag{12}$$

14. The diameter of a spherical bubble which grows by diffusion is described by Scriven, Chem. Eng. Sci., 10, 1 (1959).

$$d_B = 4\beta \sqrt{Dt} \tag{13}$$

The change of diameter per unit time (growth rate) is

$$\frac{dd_B}{dt} = \frac{2\beta D}{\sqrt{Dt}} = \frac{8\beta^2 D}{d_B} \tag{14}$$

assuming that at $t = 0$ $d_B \cong 0$

d_β = bubble diameter (cm)

t = time (hr)

D = diffusion coefficient (cm^2/hr)

β = constant given by the following equation

$$\frac{C_\infty - C_{sat}}{\rho_g} = 2\beta^3 \, e^{3\beta^2} \int_\beta^\infty X^{-2} \, e\left(-x^2 - \frac{2\beta^3}{x}\right) dx \tag{15}$$

where

C_∞ (gms/cc) - water concentration in the resin

C_{sat} - water concentration at the bubble (void) - resin interface (the void is assumed at saturation)

ρ_g (gms/cc) - water vapor density in the bubble

15. The pressure inside and outside the bubble (void) are effectively equal until the resin viscosity becomes so high that viscous effects become important. As the resin proceeds toward solidification, the pressure in the void can rise significantly above the resin pressure.

$$\delta_g = \frac{M_{H_2O} \cdot P}{R \cdot T} + \left[\frac{d_{B_o}}{d_B}\right]^3 \frac{P_o \cdot M_{air}}{R \cdot T_o} = \text{void gas density} \qquad (15a)$$

M_{H_2O} (gms/mol) = molecular weight of H_2O

P (atm) = total pressure in the resin

d_B (cm) = initial diameter of the pure air bubble

P_o (atm), T_o (k) = initial pressure and temperature in the resin

$$P_{H_2O} = \left[1 - \frac{P_o \cdot T}{P \cdot T_o} \left[\frac{d_{B_o}}{d_B}\right]^3\right] P \qquad (16)$$

P_{H_2O} (atm) = partial pressure of water

A check of the above assumptions shows it to be correct for bubble diameters greater than 100μ (10^{-2} cm).

16. The water concentration at the bubble (void surface) can be obtained from the measured solubility data

$$C = \left[\frac{\text{gms } H_2O}{\text{cc resin}}\right] = \frac{S}{100}\left[\frac{\text{gms } H_2O}{\text{gm prepreg}}\right] \times \frac{1}{0.32}\left[\frac{\text{gm prepreg}}{\text{gm resin}}\right] \times 1.22\left[\frac{\text{gms } H_2O}{\text{cc resin}}\right] \qquad (17)$$

$$C = 3.819 \times 10^{-2}\, S = 2.13 \times 10^{-2} \left[\frac{P_{H_2O}}{P_{H_2O^*}}\right]^2$$

$$C = 2.13 \times 10^{-6} (RH)^2 \qquad (18)$$

Utilizing equations (8) and (12)

$$C = 3.651 \times 10^{-14}\, e^{9784/T} (P_{H_2O})^2 \qquad (19)$$

17. The interface concentration, called C_{sat}, (even though the air-water mixture is not saturated) is

$$C_{sat} = 20.74 \times 10^{-14}\, e^{9784/T}\, P^2_{H_2O} \qquad (20)$$

18. At each temperature, a pseudo-steady state is established with respect to concentration profile.

2.4.4 CALCULATION SUMMARY. We will now summarize the calculations and results for two cases, prepreg initially equilibrated at 50 percent relative humidity and prepreg initially equilibrated at 100 percent relative humidity. We will follow the void volume changes through the GD processing cycle, at least until our assumptions are no longer valid, which is well into the high temperature hold.

2.4.4.1 50 Percent RH initial Exposure of Prepreg. From Equation 11, $C_\infty = 5.325 \times 10^{-3}$ gms/cc. During the vacuum part of the cycle, $T = T_{start} + 2(60)(t) = 298 + 120t$. Heating to 408K requires 0.92 hours. Thus, for the time period $0 \lesssim t \lesssim 0.92$, we have

$$D = 0.105\, e^{-2817/(298+120t)} \qquad \text{(from Equation 9)} \qquad (21)$$

for

$$P = 0.1 \text{ atm}, \; C_{sat} = 8.651 \times 10^{-16}\, e^{9784/(298+120t)} \qquad (22)$$

Calculation of C_{sat} at $t = 0$ (25C) yields $C_{sat} = 0.157$ gms/cc. However, C_∞, the resin concentration is only 5.325×10^{-3} gms/cc. Therefore, diffusion of water from the resin cannot occur at room temperature and a resin pressure of 0.1 atm. From Equation 20 it is clear that as the resin pressure decreases or the temperature increases, C_{sat} decreases. For our pressure of 0.1 atm, it is of interest to determine when C_{sat} will be equal to or less than C_∞, for it is then that the diffusion process will cause the void to grow. Another way of looking at this situation is that bubble growth via diffusion cannot occur at room temperature and a resin pressure of 0.1 atm; in fact the void would tend to collapse via diffusion in the opposite direction. Now if $C_{sat} = C_\infty$ at $t = t_c$, Equation 22 yields

$$t_o = \frac{9874/120}{\ln\,(10^{16} C_\infty / 8.651)} - \frac{298}{120} = 0.285 \text{ hours} \qquad (23)$$

Therefore, as the temperature is ramped up, only 17 minutes are required before the diffusional growth mechanism is activated. This corresponds to a temperature of 332K (59C).

As the temperature rises above 59C, the voids start to grow via diffusion. Table 11 summaries the values for the input parameters as the temperature increases to 408K (0.92 hours into the cycle).

Equation 14 must now be solved numerically. First, it is rewritten as

$$\frac{d(d_B^2)}{dt} = 16\beta^2 D \tag{24}$$

at

$$t = t_o = 0.285, \; d_B^2 = 0 \tag{25}$$

$$D = 0.105 \; e^{-2817/(298+120t)} \tag{26}$$

$$\beta^2 = \frac{C_\infty - C_{sat}}{\rho_g}^2 = \left[\frac{5.325 \times 10^{-3} - 8.651 \times 10^{-16} \; e^{9784/(298+120t)}}{18 \; (0.1)/(298+120t) \; 82.1}\right] \tag{27}$$

$$d_B^2 = 16 \int_{t=0.285}^{t=0.92} \beta^2 D dt = 16 \; (0.2674) = 4.279 \; cm^2 \tag{28}$$

Table 11. Input Parameters Needed for the Solution of Equation 5

Parameter							
t	0.3	0.4	0.5	0.6	0.7	0.8	0.92
$t-t_o$	0.015	0.115	0.215	0.315	0.415	0.515	0.635
D	2.28×10^{-5}	3.06×10^{-5}	4.02×10^{-5}	5.18×10^{-5}	6.58×10^{-5}	8.24×10^{-5}	1.06×10^{-4}
C_{sat}	4.561×10^{-3}	1.651×10^{-3}	6.4×10^{-4}	2.64×10^{-4}	1.15×10^{-4}	5.31×10^{-5}	2.20×10^{-5}
ρ_g*	6.56×10^{-5}	6.34×10^{-5}	6.12×10^{-5}	5.92×10^{-5}	5.74×10^{-5}	5.56×10^{-5}	5.37×10^{-5}
$\beta = \frac{C_\infty - C_{sat}}{\rho_g}$	11.64	57.98	76.50	85.41	90.78	94.74	98.75
T	334°K	346°K	358°K	370°K	382°K	394°K	408°K

* $\rho_g = \frac{18 \; (0.1)}{821 \; (298 + 120t)}$

The integral was computed numerically using Simpson's Rule (TI 59 Master Library Program ML-09, page 29).

Thus, at the end of the first temperature ramp during vacuum, when 135C is reached, the bubble could be as large as

$$\boxed{d_{B_1} = 2.07 \text{ cm}} \tag{29}$$

Let us now check to see whether or not this is reasonable; i.e., is there enough water in the resin to create such a bubble? The amount of water is

$$m_V = V_B \rho_g = \frac{4}{3}\left(\frac{d_{B_1}}{2}\right)^3 \frac{(13)(0.1)}{(82.1)(408)} = 2.49 \times 10^{-4} \text{ gm/bubble} \tag{30}$$

This is still an order of magnitude less than the amount of water contained per cc of resin, which is $C_\infty = 5.325 \times 10^{-3}$ gm/cc.

The use of Equations 13 and 14 is <u>strictly not correct</u> when C_{sat}, D, and T all vary with time. It is a very crude approximation of unknown accuracy, but we believe it represents an upper bound. The correct solution would involve the numerical solution of the original coupled partial differential equations [see Scriven, <u>Chem. Eng. Sci.</u>, 10, 1 (1959)], which cannot be reduced to an ordinary differential equation.

During the next part of the vacuum cycle, the temperature is held constant at 408K. Therefore, D and β are constant ($D = 1.06 \times 10^{-4}$ cm^2/hr, $\beta = 98.75$). However, Equations 13 and 14 can no longer be used because the initial bubble size is now non-zero. One of two plausible approximate solutions can be used. The first of these is due to Duda and Vrentas [AIChEJ, <u>15</u>, 351 (1969)].

$$\left(\frac{d_{B_2}}{d_{B_1}}\right)^2 = 1 - 2N_a\left[x + 0.2\sqrt{x/\pi}\right] + N_a^2\left[\frac{8}{3\pi}x^{3/2} + 2x + \frac{8}{\pi^{3/2}}x^{1/2} - 2I_1(x)\right] \tag{31}$$

where $I_1(x) = -0.68\sqrt{x}$

The second solution is due to Weinberg and Subramanian (AIChE Chicago Meeting, November 1980).

$$\frac{d_{B_2}}{d_{B_1}} = 1 - \frac{N_a}{\sqrt{\pi}} x + \left(\frac{N_a}{3\pi} - \frac{1}{4}\right) N_a x^2 + \left(\frac{5}{12} - \frac{8}{5} + \frac{N_a}{18}\right) \frac{N_a^2}{\sqrt{\pi}} x^3 \qquad (32)$$

$$N_a = \frac{C_{sat} - C_\infty}{\rho_g} = -\beta \qquad (33)$$

$$x = \frac{2\sqrt{Dt}}{R_o} = \frac{4\sqrt{Dt}}{d_{B_1}} \qquad (34)$$

Now, during the hold, $N_a = -98.75$, $d_{B_1} = 2.07$ cm, t - 0.25, 1.0, and 1.5 hours.

Thus, $x = 9.947 \times 10^{-3}$, 1.989×10^{-2} and 2.437×10^{-2} for the three hold times. At the end of the three possible hold times, the two equations predict the following results:

		t = 0.25 hr	t = 1 hr	t = 1.5 hrs
$\left(\frac{d_{B_2}}{d_{B_1}}\right)$	W-S Equation	1.649	2.448	2.840
$\left(\frac{d_{B_2}}{d_{B_1}}\right)^2$	D-V Equation	302	-	-

The D-V equation is obviously in error, whereas the W-S equation yields reasonable results. Thus, at the end of the three various possible hold times, the maximum bubble size is

$$\boxed{d_{B_2} = \begin{cases} 3.41 \text{ cm} \\ 5.07 \text{ cm} \\ 5.87 \text{ cm} \end{cases}} \qquad (35)$$

The last portion of the processing cycle consists of pressurization to 5.78 atm at T = 408K. At this pressure

$$C_{sat} = 8.651 \times 10^{-14}\, e^{9784/408}\, (5.78)^2 \tag{36}$$

$$= 7.5 \times 10^{-2} \text{ gms/cc}$$

Now $C_{sat} > C_\infty$ and void dissolution can occur. First, however, the bubble volume is instantaneously reduced due to increased total resin pressure.

$$d_{B_3} = \left(\frac{0.1}{5.78}\right)^{1/3} d_{B_2} \tag{37}$$

$$\boxed{d_{B_3} = \begin{array}{r} 0.88 \text{ cm} \\ 1.31 \text{ cm} \\ 1.52 \text{ cm} \end{array}} \tag{38}$$

Now

$$\rho_g = \frac{18\ (5.78)}{82.1\ (408)} = 3.106 \times 10^{-3} \text{ g/cc} \tag{39}$$

$$N_a = \frac{C_{sat} - C_\infty}{\rho_g} = \frac{7.507 \times 10^{-2} - 5.325 \times 10^{-3}}{3.106 \times 10^{-3}} = 22.45 \tag{40}$$

Now for T = 408K, P = 5.78 atm, t = 1.75 hours. The three bubbles now shrink

	x	(d_{B_4}/d_{B_3})	d_{B_4}
1	6.19×10^{-2}	0.399	0.35 cm
2	4.16×10^{-2}	0.560	0.74 cm
3	3.58×10^{-2}	0.608	0.92 cm

Thus, all the bubbles have shrunk considerably by the end of the temperature hold under pressure.

The temperature is now increased to 452K at 5.78 atm according to the relation, T = 408 + 66t, which requires 0.667 hours (40 minutes). The remainder of the cycle consists of a 2-hour hold at 452K and 5.78 atm. Under these conditions

$$C_{sat} = 8.651 \times 10^{-14} e^{9784/452} (5.78)^2 \quad (41)$$

$$= 7.27 \times 10^{-3} \text{ gms/cc}$$

Since $C_{sat} > C_\infty$, there is no bubble growth during this part of the cycle for this particular sample. Bubble dissolution is still possible, but not probable, because the resin viscosity has now become extremely high and void collapse would be difficult if not impossible.

2.4.4.2 100 Percent RH Initial Exposure of Prepreg. The growth and dissolution of voids is clearly sensitive to the initial prepreg water content. The calculations summarized above were repeated for prepreg equilibrated at 100 percent RH. The results are summarized below.

Stage 1: Vacuum and heating to 135C at P = 0.1 atm. Bubble growth starts at $t_o = 0.161$ hours, $C_\infty = 2.13 \times 10^{-2}$ gm/cc.

$d_{B_1} = 8.72$ cm.

Stage 2: Constant temperature hold at 135C, P = 0.1 atm

Hold Time	d_{B_2}
0.25 hrs	14.05 cm
1.0 hrs	20.59 cm
1.5 hrs	23.78 cm

Stage 3: P = 5.7 atm, T = 408K

d_{B_3}
3.63 cm
5.33 cm
6.15 cm

Stage 4: T = 408K, P = 5.78 atm, t = 1.75 hrs

d_{B_4}	
3.00 cm	$C_{sat} = 7.507 \times 10^{-2}$ gm/cc $> C_\infty = 2.15 \times 10^{-2}$
4.56 cm	gm/cc
5.32 cm	$\therefore$ dissolution occurs

Stage 5: P = 5.78 atm, T = 408 + 66t

At 452K, $C_{sat} = 7.27 \times 10^{-3}$ gm/cc $< C_\infty = 2.13 \times 10^{-2}$ gm/cc.

Therefore, growth of voids is still possible under these conditions unlike the situation for the 50 percent RH prepreg. However, we can no longer use the W-S equation because the temperature is changing and the initial bubble size (d_{B_4}) is non-zero. The temperature at which bubble growth would start (if the viscosity were not too high) is

$$T = \frac{9784}{\ell n \left(\frac{2.13 \times 10^{12}}{8.651 \ (5.78)^2} \right)} = 431K \ (158C) \qquad (42)$$

Hence, 21 minutes into the second heating ramp (under pressure) bubble growth has the potential to occur again. Only if curing has proceeded sufficiently will void expansion be prevented. A summary of the void growth for the two initial prepreg water contents is shown in Table 12.

2.4.5 SOME PERTINENT CONCLUSIONS.

1. The vacuum part of the cycle always has the potential of creating large voids.
2. The initial moisture content of the prepreg is very important. A prepreg equilibrated at 50 percent RH will have a maximum residual bubble size of 0.38 to 0.50 cm and no potential for further growth when heated under pressure, whereas a prepreg equilibrated at 100 percent RH has a maximum residual bubble size of 2.6 to 3.5 cm and a

Table 12. Bubble Diameter at End of Various Stages of Process Cycle in cm

Initial Humidity Exposure	Stage 1	Stage 2	Stage 3	Stage 4
50%	2.07	3.41	0.88	0.35
		5.07	1.31	0.74
		5.87	1.52	0.92
100%	8.72	14.05	3.63	3.00
		20.59	5.33	4.56
		23.78	6.15	5.32

Stage 1. Heating to 135C at P = 0.1 atm

Stage 2. Constant temperature hold at 135C, P = 0.1 atm for 0.25, 1.0, and 1.5 hours

Stage 3. P = 5.78 atm, T = 408K (135C)

Stage 4. P = 5.78 atm, T = 408K (135C), t = 1.75 hours

potential for further growth during the heating under pressure.

3. The approach utilized in the above calculations is approximate, but it does account for the effect of the moving bubble-resin boundary on the concentration profile and diffusion. It does not account for coalescence or for the medium (resin or bubble) geometry.

4. If the prepreg is equilibrated with moisture at a relative humidity, $(RH)_o$, then in order to prevent the potential for void growth by diffusion at all times when the temperature during the curing cycle is T(t), the pressure at all points of the prepreg P(t) must satisfy the following inequality:

$$P \geq 4.962 \times 10^3 \, e^{-4892/T} (RH)_o \qquad (43)$$

where

$(RH)_o$% = the relative humidity to which the prepreg was exposed.

P (atm) = the resin pressure in the prepreg at various times

$P = P(t)$

t (hrs) = time

T (K) = temperature during the curing cycle, T(t)

This equation was derived from the requirement that void growth by diffusion cannot occur if $C_{sat} \geq C_{\infty}$ and by using Equations 11 and 13. It is also based on the solubility relation

$$S_o = 5.58 \times 10^{-5} (RH)^2 \tag{44}$$

If we use the new data RH = 100 percent, then

$$S_o = 3.74 \times 10^{-7} (RH)^{3.25} \tag{45}$$

and

$$P \geq 2.079 \times 10^3 \, e^{-4892/T} (RH)_o^{1.624} \tag{46}$$

A plot of Equation 43 for the two relative humidities considered is shown in Figure 41. It is evident from Figure 41 that vacuum can be applied without encouraging void growth if such application is coordinated with the temperature of the system.

2.4.6 A SIMPLE QUASI-STEADY STATE APPROACH. If we relax the model requirement that the motion of the bubble surface affects the concentration profile, we have probably the simplest quasi-steady state approximation to the real problem. Physically, this amounts to saying that once the bubble starts to grow, the same concentration profile exists out in front of the bubble surface. The governing equation for this situation now becomes

$$\frac{d(d_B^2)}{dt} = \frac{4D(C_{\infty} - C_{sat})}{\rho_g} \tag{47}$$

$$@ \; t = 0 \quad d_B^2 = 0$$

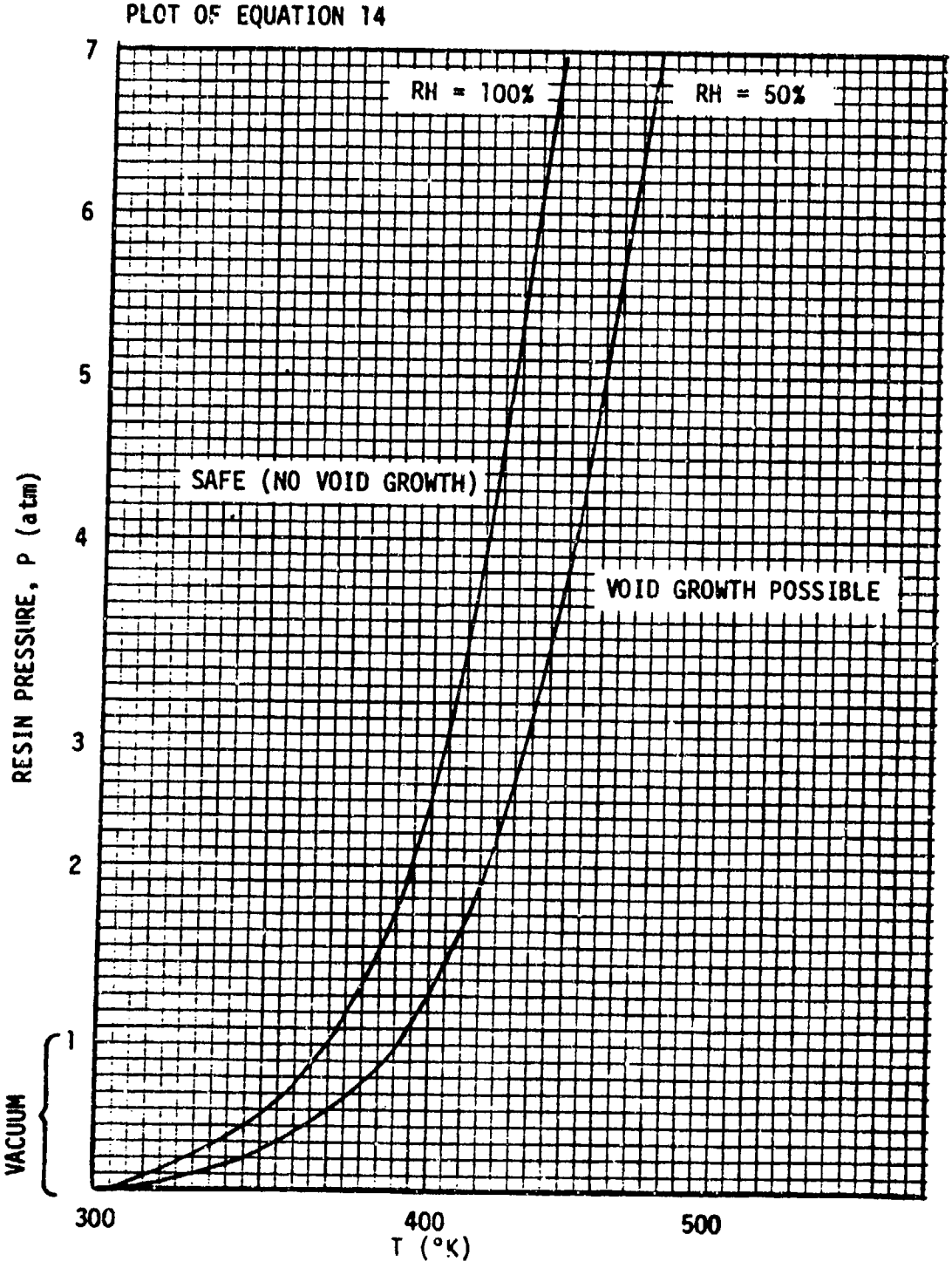

Figure 41. Plot of Equation 14 for Two Relative Humidities

which is a form the original diffusional growth equation expressed as Equation 14.

Let us reconsider the two initial prepreg equilibriums at 50 percent and 100 percent RH.

2.4.6.1 50 Percent Initial Prepreg Equilibration,

$$C_\infty = 5.325 \times 10^{-3} \text{ gm/cc} \tag{48}$$

Stage 1: Heating from 62C to 135C at P = 0.1 atm

$$D = 0.15\, e^{-2817/(298+120t)} \tag{49}$$

$$C_{sat} = 8.651 \times 10^{-6}\, e^{9784/(298+120t)} \tag{50}$$

$$\beta = \frac{C_\infty - C_{sat}}{\rho_g} = \frac{5.325 \times 10^{-3} - 8.651 \times 10^{-16}\, e^{9784/(298+120t)}}{1.8/(298+120t)\ 82.1} \tag{51}$$

$$d_{B_1}^2 = 4\int_{0.285}^{0.92} \beta D dt = 4 \times 3.02 \times 10^{-3} = 1.208 \times 10^{-2} \tag{52}$$

$$\boxed{D_{B_1} = 0.11 \text{ cm}} \tag{53}$$

Stage 2: T = 135C (constant, P = 0.1 atm, hold times are 0.25, 1.0 and 1.5 hours

$$d_{B_2}^2 = d_{B_1}^2 + 4\beta D t \tag{54}$$

$$d_{B_2}^2 = 1.208 \times 10^{-2} + 4\ (98.75)\ (1.06 \times 10^{-4})\ t \tag{55}$$

$$\boxed{D_{B_2} = \begin{cases} 0.15 \text{ cm} \\ 0.23 \text{ cm} \\ 0.27 \text{ cm} \end{cases}} \tag{56}$$

Stage 3: P = 5.78 atm, T = 208K (135C)

$$d_{B_3} = \left.\begin{matrix} 0.039 \text{ cm} \\ 0.059 \text{ cm} \\ 0.069 \text{ cm} \end{matrix}\right\} \text{ due only to pressurization}$$

Stage 4: P = 5.78 atm, T = 208K (135C), t = 1.75 hr

$$d_{B_4}^2 = \begin{matrix} 0.0015 \\ 0.0035 \\ 0.0048 \end{matrix} - 4\,(22.45)\,(1.06 \times 10^{-4})\,(1.75) \qquad (57)$$

$$\therefore\ d_{B_4} = \begin{matrix} 0.0 \\ 0.0 \\ 0.0 \end{matrix} \qquad (58)$$

All the voids would have had the potential to dissolve. This of course excludes the large bubbles which might have formed by coalescence during Stage 1 and 2. Further heating under pressure would not cause bubbles to grow.

2.4.6.2 100 Percent RH Initia' Prepreg Equilibration,

$$C_\infty = 2.13 \times 10^{-2} \text{ gm/cc} \qquad (59)$$

Stage 1: $d_{B_1} = 0.23$ cm (60)

Stage 2: $d_{B_2} = \begin{matrix} 0.31 \text{ cm} \\ 0.47 \text{ cm} \\ 0.55 \text{ cm} \end{matrix}$ (61)

Stage 3: $d_{B_3} = \begin{matrix} 0.08 \text{ cm} \\ 0.12 \text{ cm} \\ 0.14 \text{ cm} \end{matrix}$ (52)

Stage 4: $d_{B_4} = \begin{matrix} 0.0 \text{ cm} \\ 0.04 \text{ cm} \\ 0.08 \text{ cm} \end{matrix}$

Stage 5: P = 5.78 atm, heating to 452K, bubble growth could restart at 431K, but once again this growth is not describable with the current equations, nor is it likely to occur because of the very high viscosity.

2.4.7 CONCLUSIONS. Bubble growth based on diffusion and a steady-state profile approximation cannot explain formation of large bubbles unless considerable coalescence is involved. The large difference between the results and the more accurate approximation is due to motion of the bubble boundary and its iteration with the concentration profile which are accounted for in the more accurate approach.

2.4.8 MODELING ANALYSIS. An Apple Computer program has been written at Washington University for use in modeling the growth of voids during cure. The program was received at Fort Worth and was checked and used to evaluate predicted consequences of changes in cure cycles or material parameters. Some modifications of the program were devised at Fort Worth to improve the ease of operation.

The program's operation begins with input of material parameters, and these include the following:

1. Resin specific gravity
2. Weight fraction of resin in the prepreg.
3. Relative humidity to which the prepreg has been exposed
4. Moisture solubility parameters
5. Moisture diffusivity parameters

Next, the program allows input of cure cycle parameters that include up to six thermal segments and up to three pressure segments. Thus, a thermal cycle might be input that involved heating at two different, sequential rates followed by a dwell at some temperature before ramping to a final dwell tempeature. During this thermal cycle, pressure could be applied in three steps with pressure application time specified for each step.

The program also allows choices of initial void size and the choice of whether the void involves an air/water mixture or water only. After making these choices and inputs, the program determines the point in the cycle at which void nucleation can begin. For selected time increments thereafter, the program calculates void sizes that would be expected for the conditions chosen. Early studies with the model have indicated that heating rate is a critical parameter.

Conditions required for void transport have also been modeled in an effort separate from the Apple Computer model. The void transport model has been used

to calculate the pressure gradient required for vertical and lateral bubble migration. The principle of the model is that void mobilization will occur when the pressure gradient becomes sufficient to overcome the surface tension forces exerted by the resin when the resin is forced through the fiber network. In effect, the resin must have sufficient velocity in the flow direction to drag the bubble through the narrowest constriction or buoyant forces must be great enough to cause the bubble to rise through the constriction.

Using the model, calculations have been made which show that a pressure gradient of more than 10,000 psi is required to cause vertical void movement. This gradient is so large that buoyant forces cannot be expected to contribute to bubble movement. Thus, as previously suggested by experimental observations, vertical transport of voids in curing graphite/epoxy does not appear to occur. (See Appendix C-1 for a description and printout of the Apple program).

2.5 MOISTURE ABSORPTION PROBLEMS IN PREPREG

It became apparent during the initial laminate studies that different batches of 5208 prepreg behaved quite differently during identical curing or processing conditions. The material characterization(HPLC, FT-IR, moisture content and other properties), however proved identical between batches. A major finding of this program was therefore finding a minimum sized laminate to distinguish between good and bad batches of prepreg when physical and chemical methods could detect no differences. Closer examination of the prepreg that made poor laminates revealed a greater number of particles on the surface of reject material compared to good prepreg (Figure 42). The good prepreg had a much lower quantity of these crystals (which exhibited birefringence in crossed polaroids) on the prepreg surface. A series of investigations was initiated to define these physical differences and possibly detect them before use in the fabrication of major aircraft composite structures.

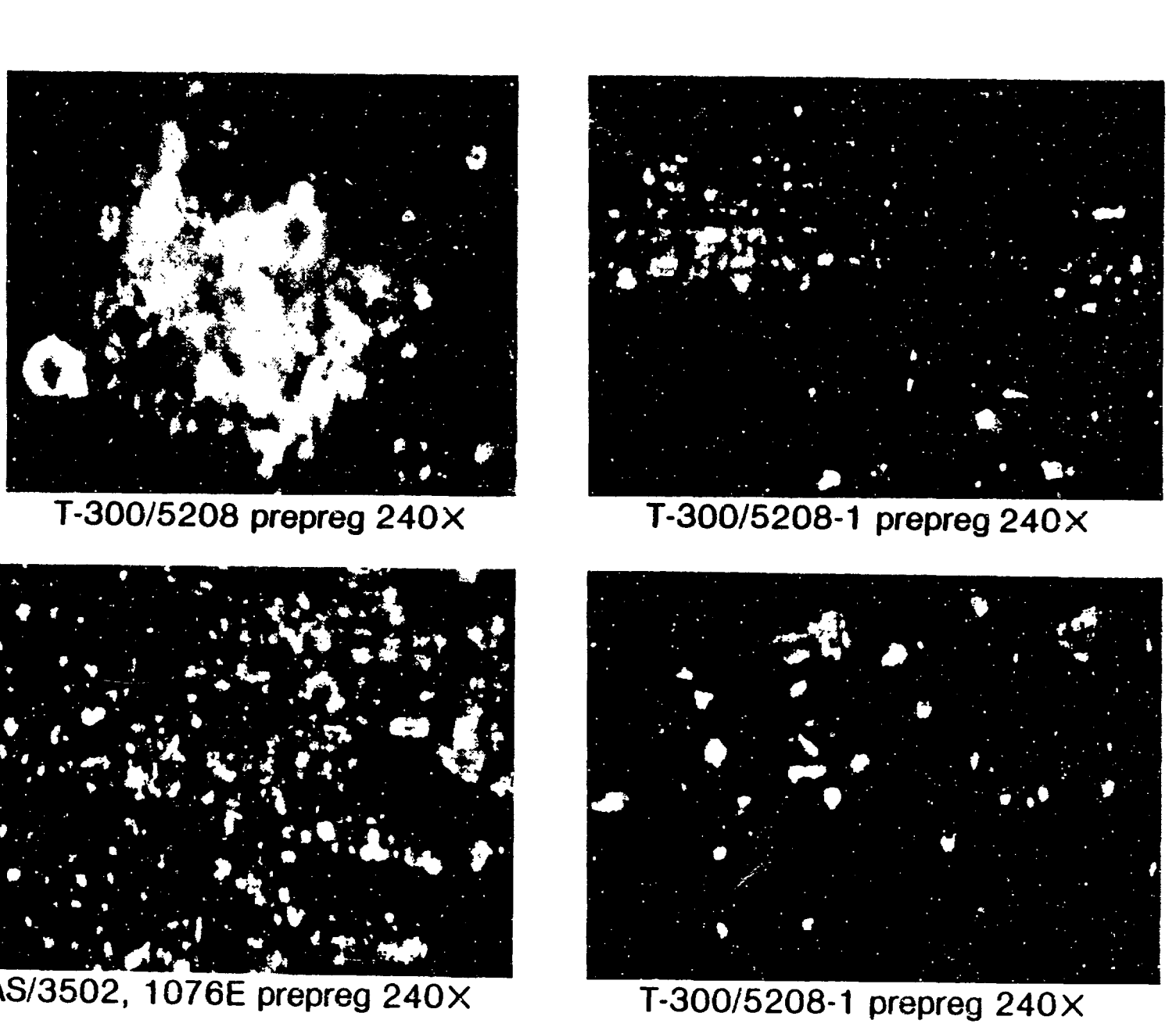

Figure 42. DADS Catalyst, Typical Size on Prepreg Surface

2.5.1 VOLATILE EVOLUTION AROUND CATALYST CRYSTALS. A sample of a bad lot of 5208/T300 prepreg (i.e., the lot which failed the large laminate discrimination test) was placed on a heated stage under a microscope. Two relatively large catalyst crystals were selected for observation during constant rate heating of a single ply of prepreg to 150C (300F). Initially there were no bubbles associated with the crystals, however, formation of bubbles started at approximately 130C (265F). These bubbles grew in size until gelation of the resin at around 155C (310F). The bubbled crystalline areas were subsequently submitted to SEM evaluation. The series of pictures identified as Figures 43 through 48 show a great deal of detail and information about the association of small catalyst crystals and related bubble formation.

The first two photographs at 60X and 120X, show the general area of investigation, including formed bubbles, fractured bubbles, and catalyst crystals. The two primary areas of interest that were examined at higher magnification are circled in all of the photos. The first area circled shows only a portion of the remains of a fractured bubble site containing a catalyst crystal. Figures 45 and 46 are photos of that site at 300X and 2300X, respectively.

The second area circled shows an unfractured bubble with small catalyst crystals attached to the surface. Figure 47 shows the same area at 600X magnification.

Additional scanning of the surface located a unique void nucleation site shown in Figure 48. In this photo we see (1) an unfractured small bubble within a fractured bubble crater, (2) the catalyst crystal associated with the fractured bubble, (3) a portion of the ruptured bubble shell, and (4) large catalyst crystals (5) not associated with the fractured bubble.

5208 Prepreg surface 60X

Figure 43. 5208 Prepreg Surface, 60X

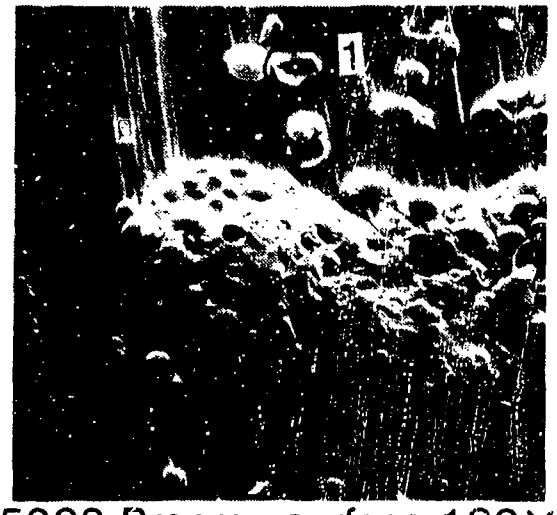

5208 Prepreg surface 120X

Figure 44. 5208 Prepreg Surface, 120X

5208 Prepreg surface 300X

Figure 45. Prepreg Surface, 300X

5208 Bubble site/crystal 2300X

Figure 46. Bubble Site/Crystal, 2300X

Figure 47. Bubble/Crystal Sites, 600X

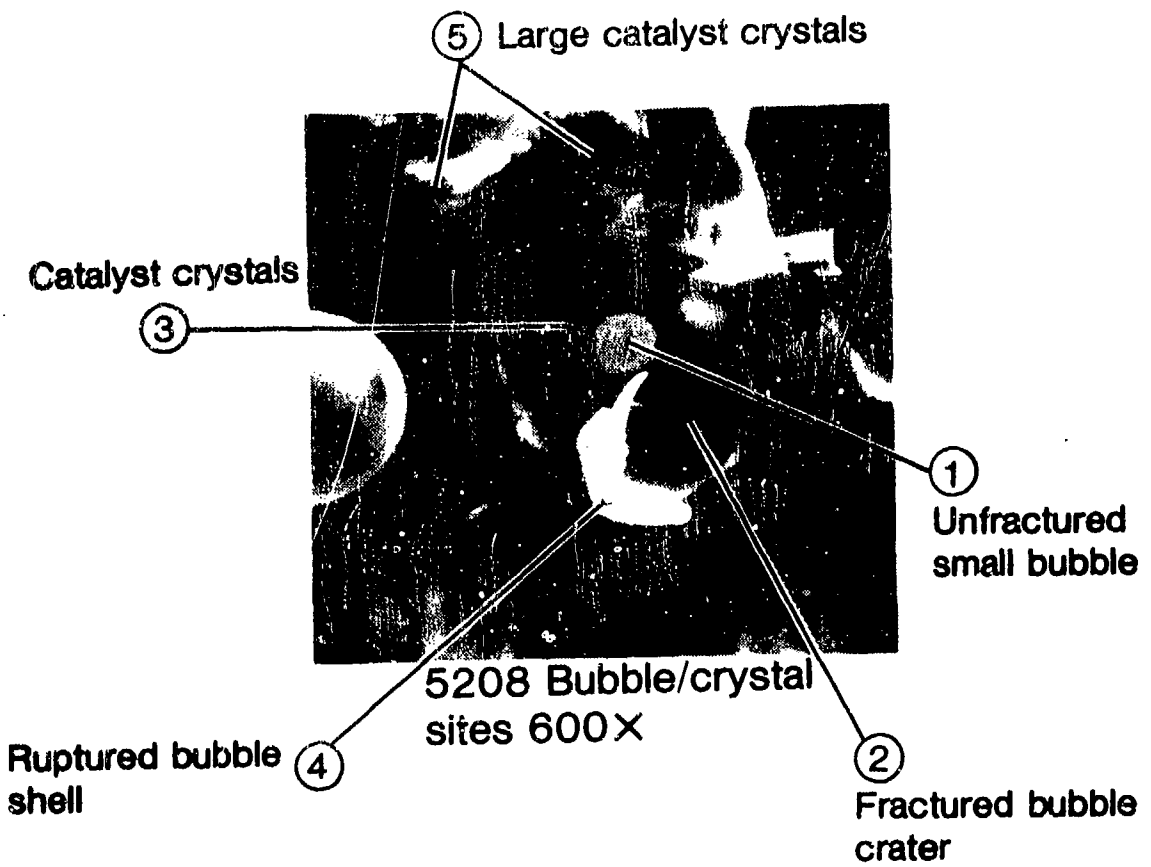

Figure 48. 5208 Bubble/Crystal Sites, 600X

There was a minimum of at least one or more catalyst crystals associated with each bubble examined. Apparently the water that was more tightly bound to these melted surface crystals was evolved during heating at 130C (265F) producing the associated bubbles, and this presumably caused voids within thick laminates due to high local concentrations of water on the ply interfaces.

2.5.2 MOISTURE ABSORPTION-5208 and 3502 PREPREG. A cursory examination of prepreg moisture pickup in relation to exposure time revealed a major difference between a specific batch (716) or 5208 prepreg and the 3502 prepreg.

Figure 49 shows the weight gain in water of pre-dried 5208 prepreg and 3502 prepreg upon exposure to 100 percent relative humidity as a function of time. Not only does the 5208 prepreg pick up water at a faster rate, but after one hour it has absorbed almost twice as much water. The figure also shows that upon heating at the critical processing temperature range of 120C to 150C (250F to 300F) the 5208 prepreg still has about twice as much water as the 3502 prepreg. Preliminary work on a second batch of 5208 prepreg (1807) showed a similar weight gain-loss curve as the 3502 prepreg. Volatile contents were determined on all of the prepregs prior to drying and moisture exposure and found to be virtually the same at 0.35 percent (weight). This initial examination then led to a comprehensive effort to determine why the large differences in moisture absorption and desorption occur between the prepregs.

The large disparity of moisture absorption between 5208 and 3502 prepreg led to the systematic, comprehensive analysis of the prepreg and the resin components. Narmco's 5208 prepreg as shown in Figure 49 absorbed almost twice the equilibrium moisture as the 3502 material.

The one component of the prepreg that was processed differently between the two resin systems was the catalyst, 4.4' diaminodiphenylsulfone (DADS).

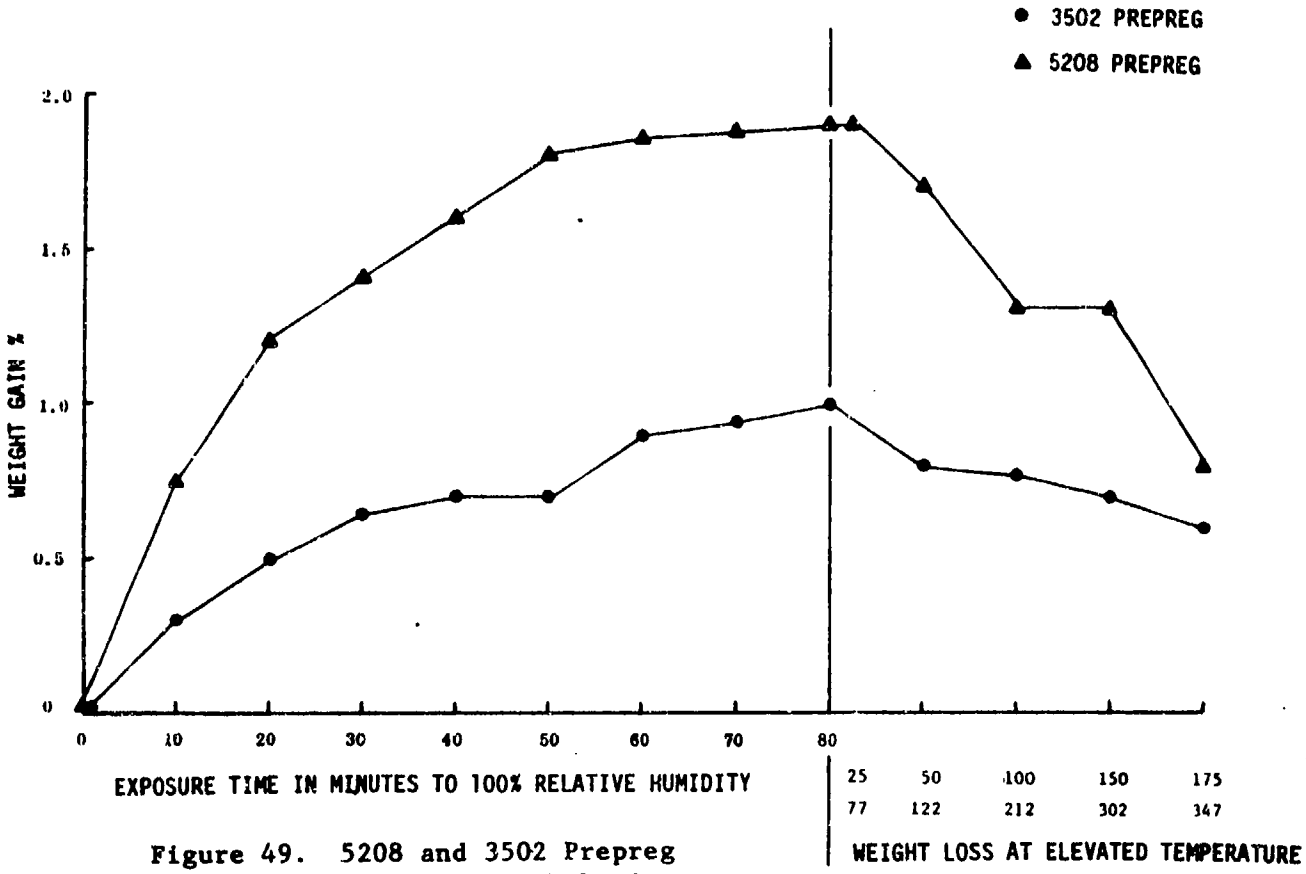

Figure 49. 5208 and 3502 Prepreg Water Pickup and Loss Behavior

Narmco melted the DADS and blended it with the base resins, whereas Hercules mixed the DADS powder into the resin. It was hypothesized that the melted DADS catalyst added to the resin via the Narmco processing procedure may in part be quenched or rapidly recrystallized by the base resin before the normally well ordered crystalline DADS structure could occur, leaving vacant polar sites capable of additional hydrogen bonding with moisture.

One of the contributing resonance structures of DADS is the dipolar compound II, as shown in Figure 50 indicating a negative charge on oxygen and a positive charge on the nitrogen. Although not a major resonance structure, it indicates that there is probably a higher negative charge on the oxygen and a higher positive charge on the nitrogen than a non-conjugated molecule.

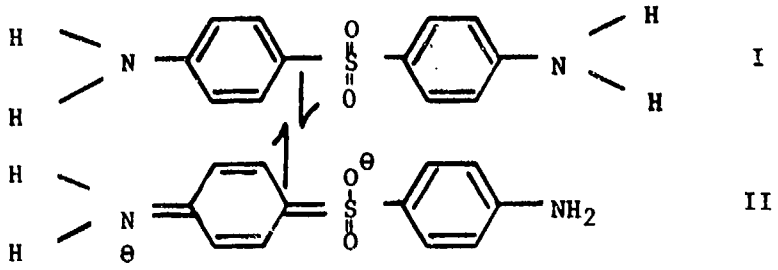

Figure 50. DADS Resonance Structure

This translates into a higher probability of a stronger hydrogen bond both available to absorb environmental water and involved in formation of the DADS crystal structure.

An examination of the melting points of DADS and its isomer 3,3'-diaminodiphenylsulfone shows higher melting points for the conjugated 4,4'-DADS.

4,4' DADS	176.5C
3,3' DADS	168C
2,2' DADS	179C

This difference is probably due to the additional charge density on the nitrogen and oxygen atoms of the 2 and 4 substituted DADS. It is well known that ortho (2,2'-isomer) resonance is stronger than para (4,4'-isomer) resonance in stabilization of charge. A higher charge density on oxygen and nitrogen would imply a stronger H bonding capability.

Experiments in the rapid quenching and partial solidification of melted DADS in water or the major epoxy resin (MY-720) led to a defect laden crystal structure where the lattices are not in the most thermodynamically stable configuration.

The hypothesis then was that there was incomplete hydrogen bond structure between DADS molecules in addition to numerous lattice defects which arise from rapid quenching and solidification which then were available for moisture absorption.

A sample of DADS was melted at 177C and poured slowly into water in a Waring blender. The particles of catalyst were separated from the water and dried. Scanning Electron Microscope examination, Figures 51 and 52 of the melted quenched powder showed that the normal macroscopic crystallinity associated with the as-received DADS, Figures 53 and 54, was apparently absent.

The melted and quenched DADS, when ground to a powder, dried over P_2O_5 and exposed to moisture, absorbs water at almost three times the rate of unquenched DADS, Figure 55. Heating the samples after attaining moisture equilibrium demonstrated that the unquenched DADS lost the same quantity of water it gained, (0.5 percent) and that the quenched DADS lost very little water (0.05 percent). This correlated quite well to the rate of moisture loss of 5208. The 5208 prepreg loses less water at higher temperatures than 3502. This fact implied a more tenaciously bound water in the resin, probably at a strong hydrogen bonding site. The normal volatiles test run on prepreg would not distinguish between loosely bound "surface" water and the strongly absorbed water. Typically, very dry 5208 prepreg absorbed 1.5 percent water as compared to 0.75 percent water for 3502 prepreg. Upon heating to 150C both prepregs lost about 0.05 percent weight. This left a considerable amount of tightly bound water (1 percent) in the 5208 (most likely associated with the imperfect DADS lattice). This water was hard to remove at low temperatures and could only be removed at higher temperatures. Additional hydrogen bonded sites appeared as the resin

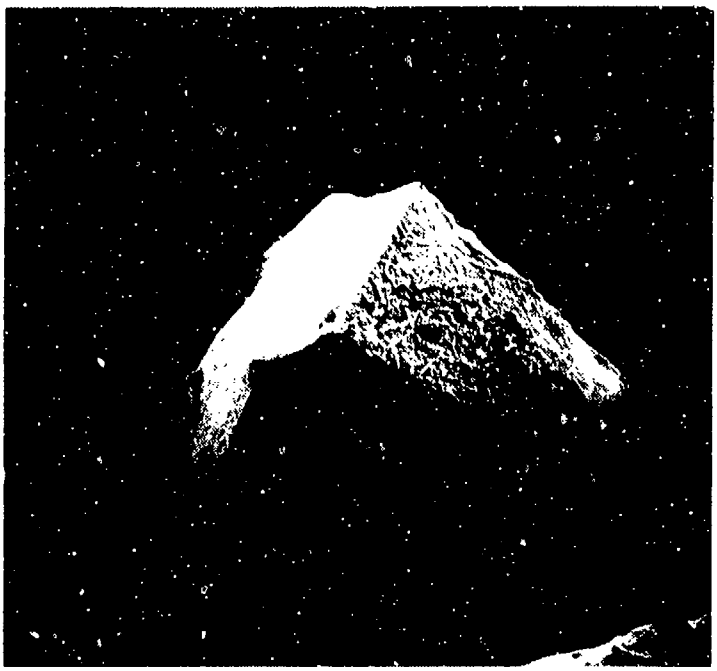

Melted quenched DADS 50X

Figure 51. Melted Quenched DADS, 50X

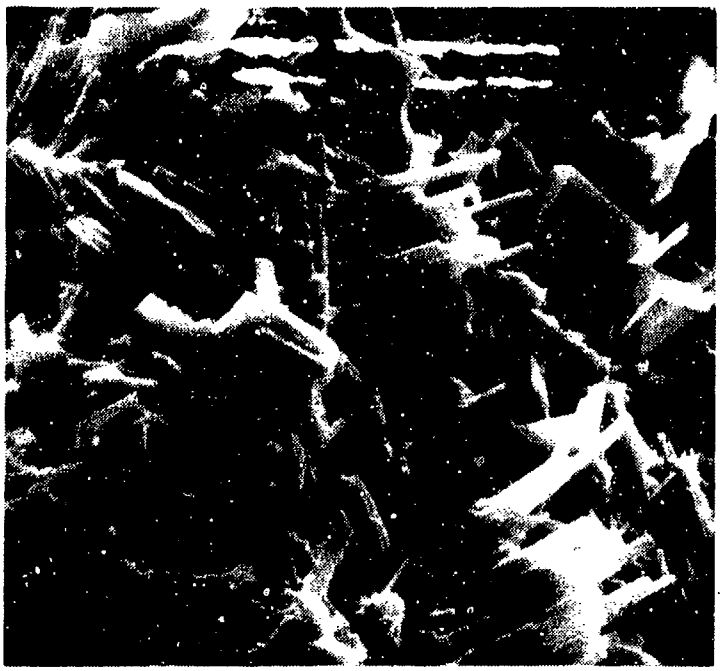

Melted quenched DADS 1,000X

Figure 52. Melted Quenched DADS, 1,000X

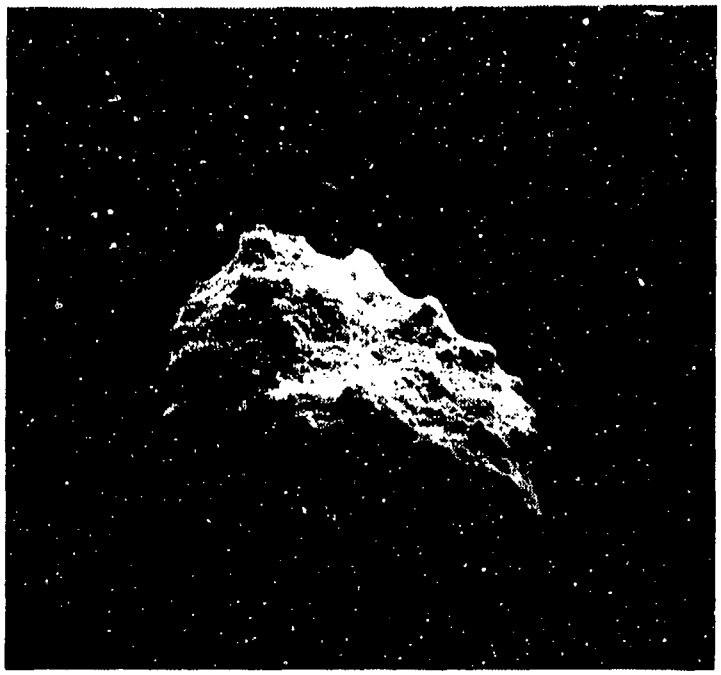

As-received DADS 50X

Figure 53. AS-Received DADS, 50X

As-Received DADS 1,000X

Figure 54. As-Received DADS, 1,000X

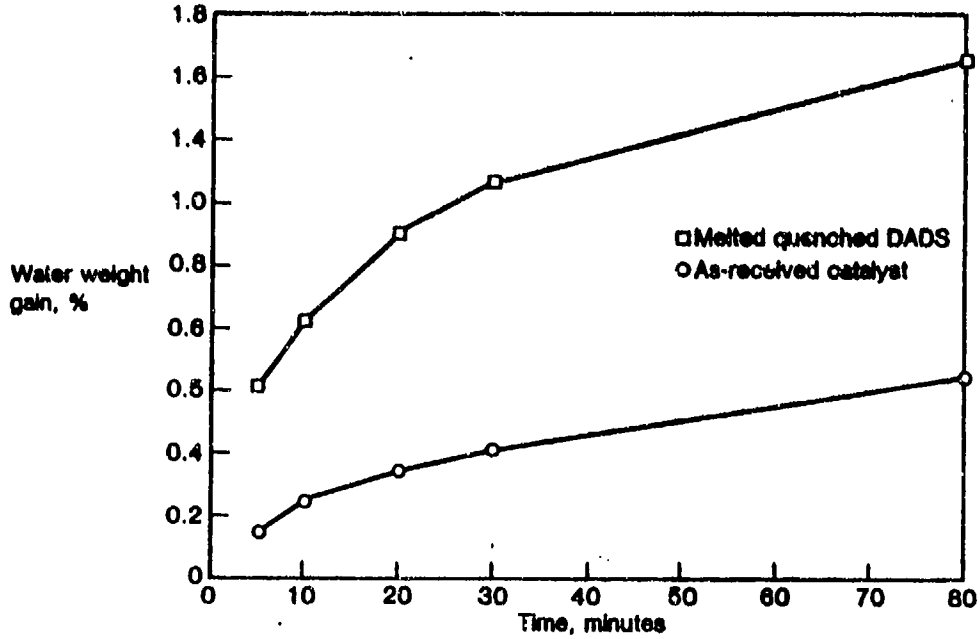

Figure 55. Water Weight Gains of DADS Catalyst Exposed to 100 Percent R.H. Via TGA

advanced (OH group formation) and the increase in the resin viscosity as the material advances would probably hinder the diffusion of the remaining water from the matrix. The potential for voids in the cured laminate was, thus, quite high. Employing typical prepreg quality control techniques, it would be almost impossible to detect this differently bound water.

Some of the DADS catalyst crystals are visible through a microscope on the surface of the 5208 and 3502 prepregs. When a polarized light was employed, the 3502 DADS crystals appear colored due to crystalline light diffraction (birefringence). The amorphous DADS catalyst on the 5208 prepreg does not diffract the light due to its amorphous (non-crystalline) nature.

Specimens of DADS melted-quenched and as-received unquenched were prepared for FT-IR analysis as KBR pellets. These pellets were each scanned twice, once after exposure to the ambient relative humidity and once after drying over P_2O_5 at almost 0 percent relative humidity for one week. The amount of DADS in the quenched pellet was a little less than the amount of DADS in the unquenched pellet, therefore the spectra had to be analyzed by relating the peak of

interest to another peak, a reference peak, in the same spectrum. This ratio could then be compared to a different spectrum.

The peak of interest in this case is the O-H stretch peak at ∿2.8μ. The appearance of this enhanced peak in an FT-IR spectra of DADS indicated the pressence of hydrogen bonding. There are two possible sources of hydrogen bonding of the DADS molecules (intramolecular) which occurs in forming the crystal structure. The second source was hydrogen bonding of water to the molecules of DADS (intermolecular) in the crystal structure. This occurred on the surface of the crystals as well as within the crystal structure of the poorly formed (defecctive) crystals. In determining the relative amounts of contribution from these two sources, one source must be experimentally eliminated while the other source must remain unchanged. This was done by drying the pellets over phosphorus pentoxide (P_2O_5) for one week, which removed the absorbed water. Any remaining water was considered tightly bound within the crystalline structure by additional hydrogen bonding.

The peak chosen as a reference peak was an aromatic peak (at ∿11.9μ), which would be unaffected by the presence or lack of hydrogen bonding and thus remain constant. The ratio to be compared was the OH peak to aromatic peak.

2.5.2.1 Comparison of Spectra.

1. Exposed to ambient humidity. The peak ratios under these conditions are shown in Figures 56 and 57.

	Quenched	Unquenched
(OH/Aromatic)	1.035/1.00	1.99/1

The spectra indicated that there was approximately twice as much hydrogen bonding in the unquenched as in the quenched DADS. This does not necessarily mean more water, but a combination of the above mentioned sources. To determine the relative contribution

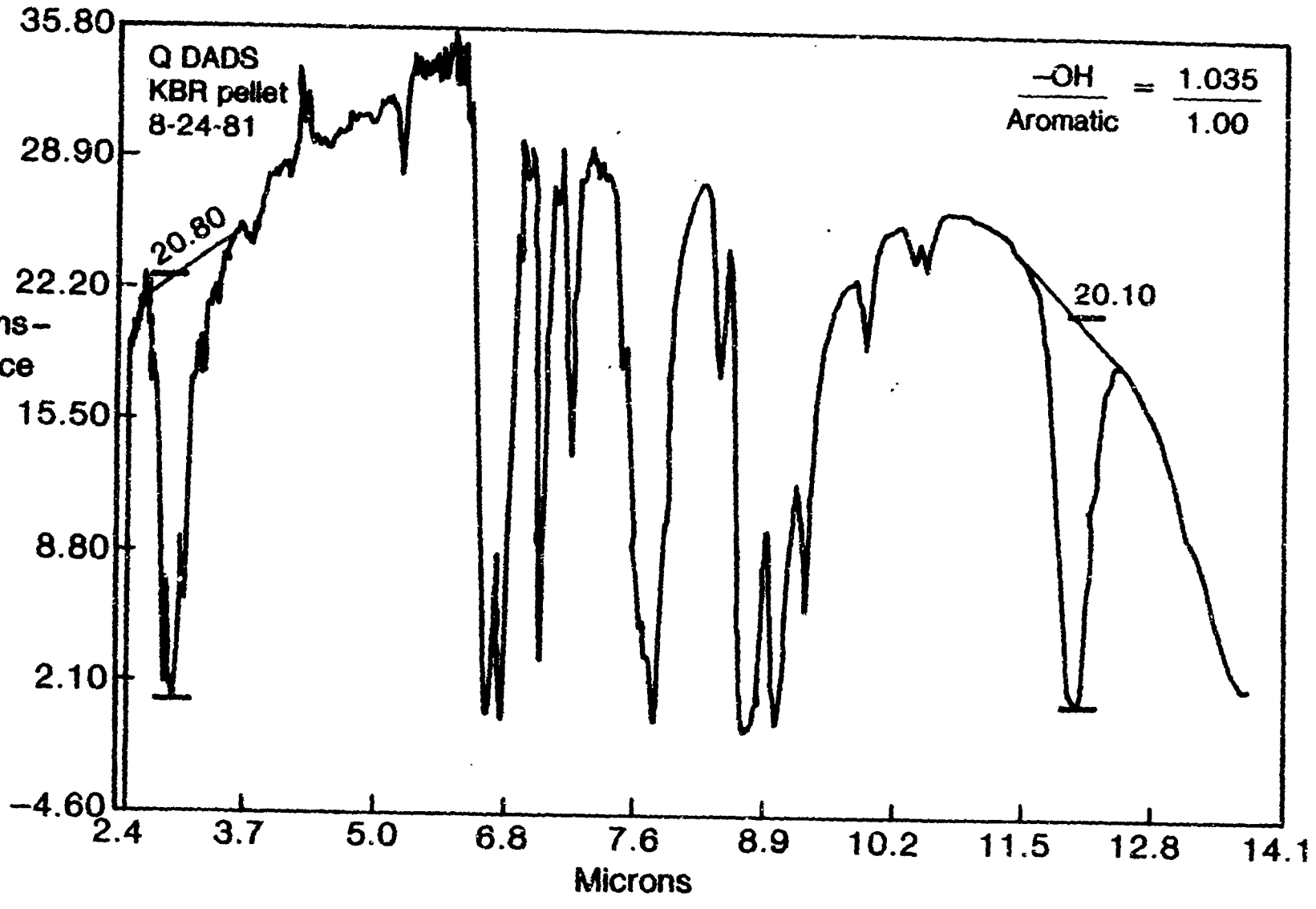

Figure 56. FT-IR Spectra of Quenched DADS - MOisture Exposed

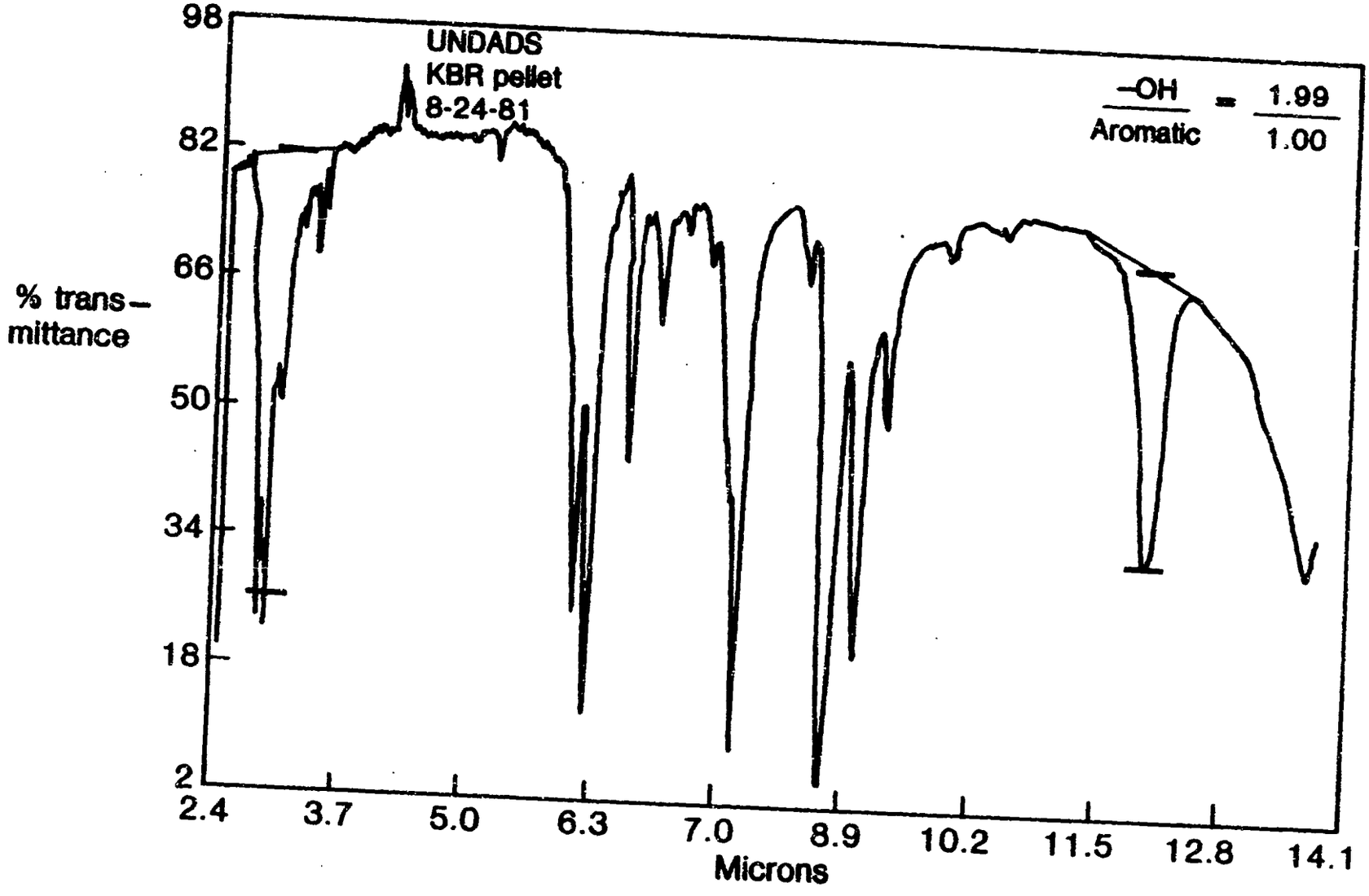

Figure 57. FT-IR Spectra of As-Received DADS - Moisture Exposed

of the absorbed water, the pellets were dried to remove the water. Drying removed the H-bonding contribution of the water from the spectrum but did not affect the intermolecular H-bonding of the DADS crystal structure.

2. Dried over P_2O_5 - 0 percent relative humidity. The peak ratios under these conditions are shown in Figure 58 and 59.

	Quenched	Unquenched
(OH/Aromatic	1.0/1.48	1.0/3.33

Under these conditions, there was approximately twice as much hydrogen bonding in the quenched as in the unquenched DADS.

In ambient humidity, the unquenched DADS has twice as much hydrogen bonding resulting from (1) hydrogen bonded water on crystal surface and (2) a more cohesive crystal structure with extensive hydrogen bonding between the DADS molecules.

Drying the pellets removed more water from the unquenched DADS than the quenched DADS, leaving essentially intermolecular hydrogen bonding in the unquenched DADS.

The quenched DADS has more hydrogen bonding as a result of water than to the intermolecular hydrogen bonding of the DADS. The hydrogen bonding that remained after the drying operation was in part intermolecular hydrogen bonding of the DADS and in part a result of water tightly held within the crystal structure. This tight holding of water implied that the quenched DADS has a poorly formed (defective) crystal structure which allowed water to become bound within the structure to a stronger degree than normal DADS crystals.

The fact that the unquenched DADS has twice as much hydrogen bonding in ambient humidity is due to the regular crystal structure having more intermolecular hydrogen bonding and some water bound on the surface of the molecule.

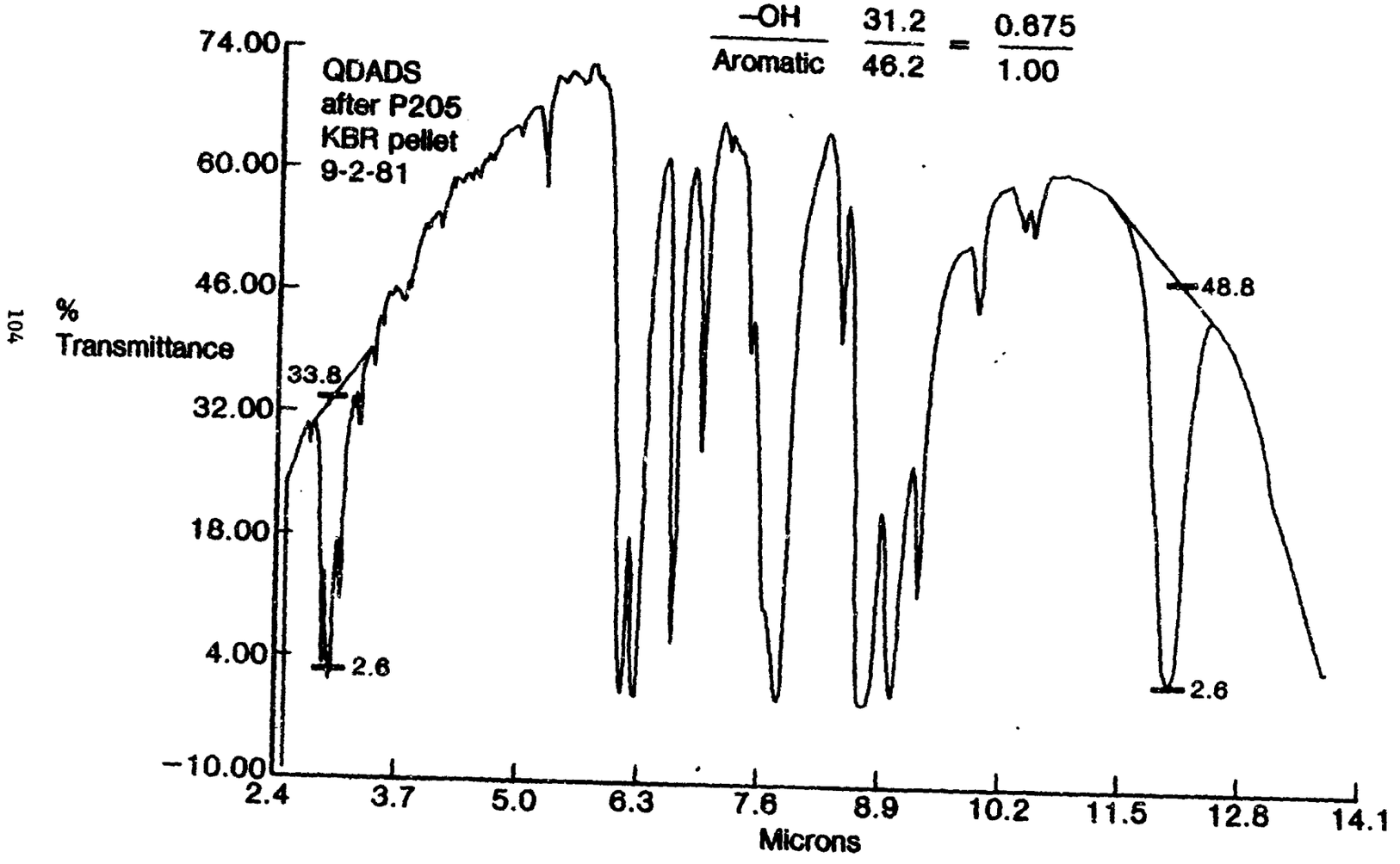

Figure 58. FT-IR Spectra of Quenched DADS - Dired

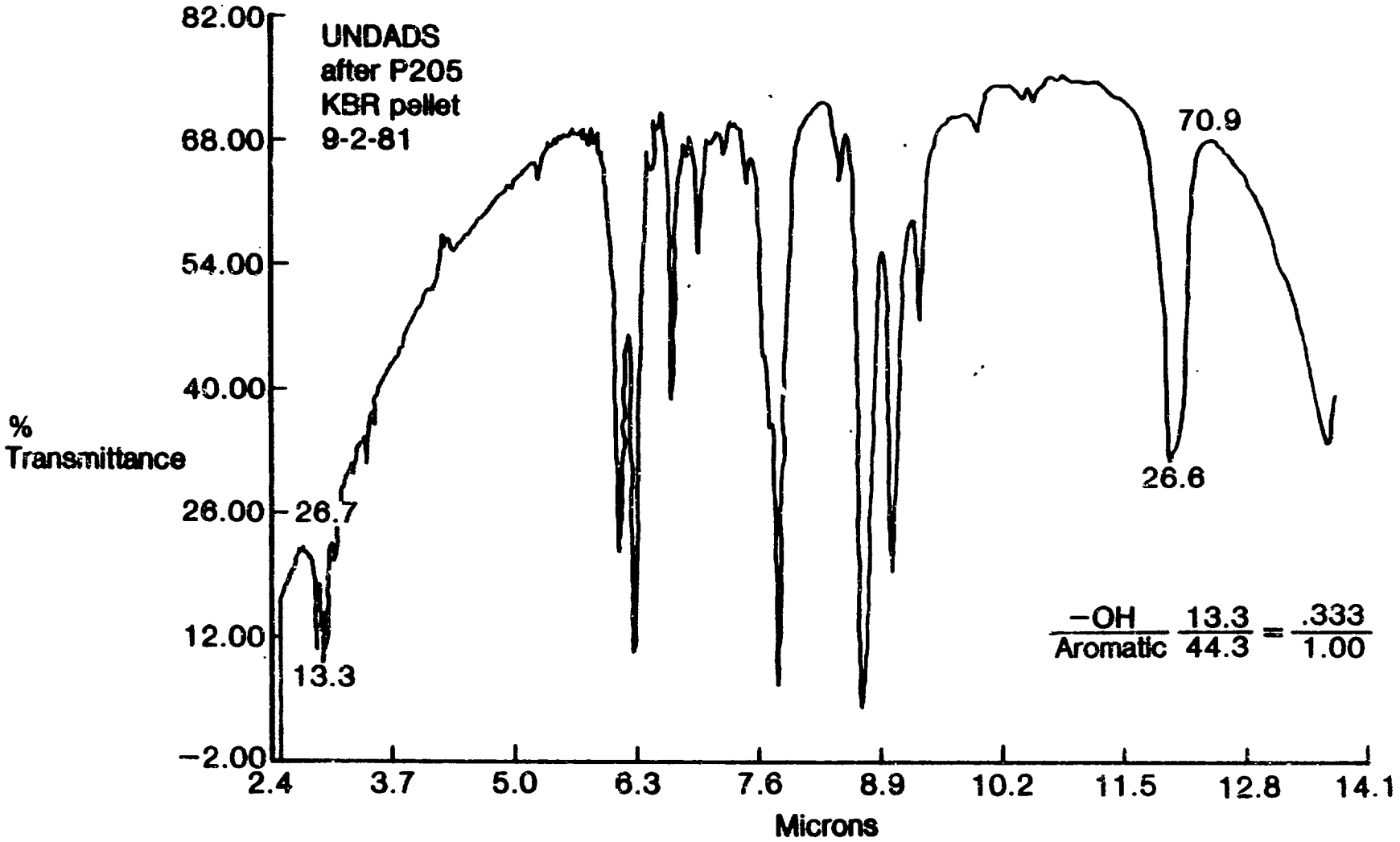

Figure 59. FT-IR Spectra of As-Received DADS - Dired

2.5.2.2 X-ray Diffraction. An investigation was initiated utilizing x-ray diffraction to determine any differences in the crystalline structure of the quenched versus the as-received DADS catalyst. The low angle x-ray patterns which are characteristic of the reflections of the heavy atoms (sulfur) and possibly nitrogen show some significant variance in some of the higher angle bands. These differences may be more representative of the nitrogen spatial arrangement and was manifested in the FTIR differences. There was also a significant and reproducible angular difference in the powder diffraction pattern of the two DADS samples, again indicating an imperfect or at least different microstructure for the melted quenched as compared to the unquenched DADS catalyst.

The possibility also existed that the DADS was not rapidly crystallized on the addition of the hardener into the epoxy resin but recrystallized during the prepregging operation and cooldowns. The DADS was known to recrystallize because of its low solubility in MY-720 at ambient temperatures under favorable conditions. Favorable conditions were nucleating sites (such as carbon fiber surfaces and mechanical shearing at lower temperature.

X-ray diffraction was also employed as a method to detect the changes in the crystalline diffraction pattern of the DADS catalyst after recrystallization in an epoxy (MY-720) matrix. X-ray diffraction patterns were measured at reflection angles of 21 through 26 degrees for melted DADS added to the major epoxy resin MY-720 at zero time after mixing and after one hour at 177C (350F). Figure 60 shows these patterns. Strong intensity of X-ray counts are noted at angles of 14, 18, 21, and 24°. The pattern produced after one hour at 177C (350F) shows the complete disappearance of these strong intensity peaks as would be expected from the dissolution of the hardener at elevated temperatures.

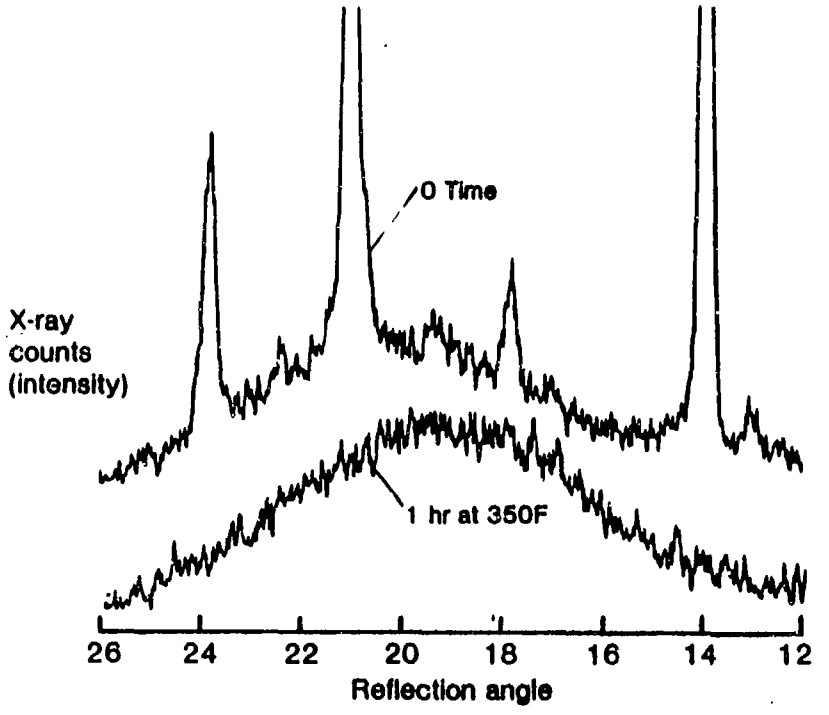

Figure 60. X-ray Diffraction Melted DADS in a Major Epoxy

The second experiment using X-ray diffraction was the monitoring of the addition of as-received dry powder DADS to the MY-720 epoxy. In Figure 61 the diffraction pattern at zero t me was significantly different than the pattern produced in Figure 60. Intensity peaks are found at many reflection angles (14, 15, 18, 19, 20, 21, 22, 23 and 25°). This difference in the fewer number of peaks in Figure 60 was believed to be the result of the recrystallization of the DADS into a completely different structure than the as-received DADS. This new epoxy/hardener material has been shown to be more absorbent to water than just the powdered DADS and MY-720.

Figure 62 compares both of the diffraction patterns, the bottom pattern is from Figure 61, the top is from Figure 60.

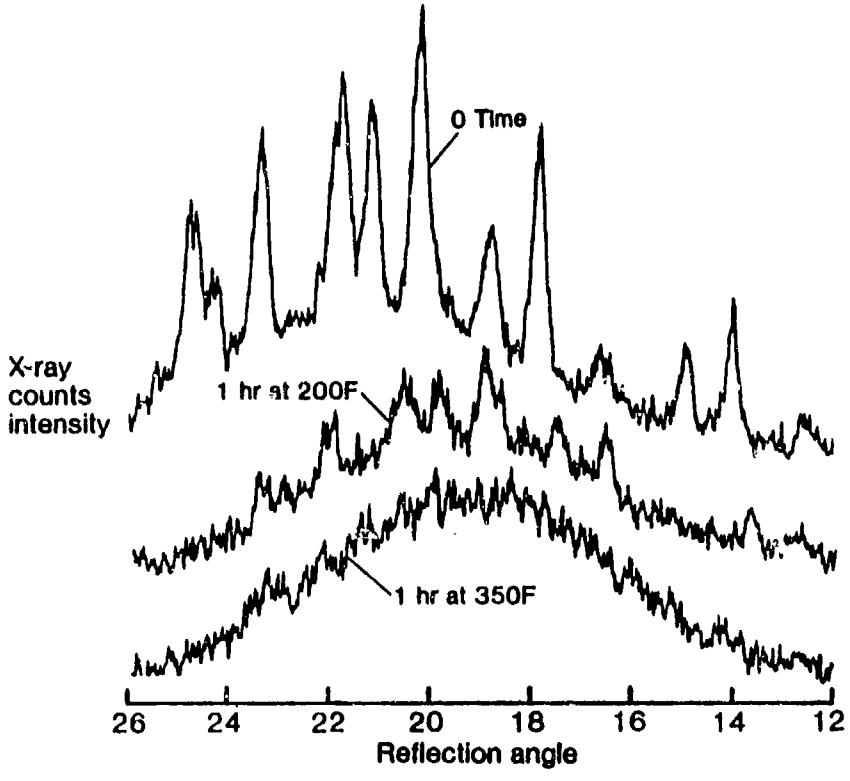

Figure 61. X-ray Diffraction Dry Powder DADS in Major Epoxy

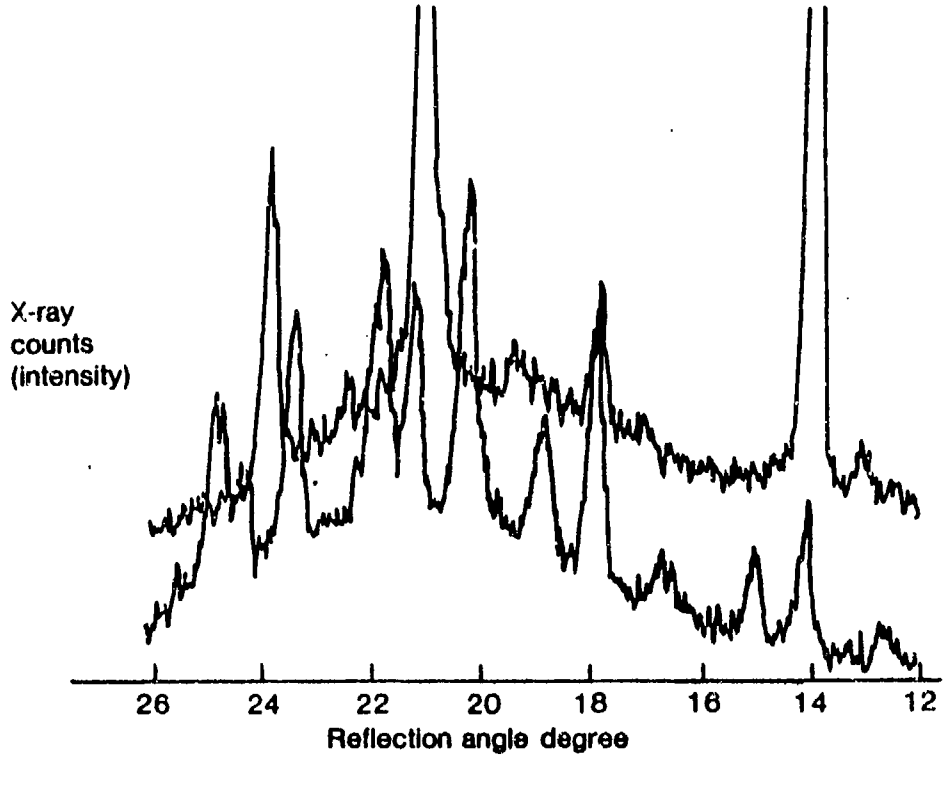

Figure 62. X-ray Diffraction Melted DADS in Major Epoxy and Dry Powder DADS in Major Epoxy

2.6 PROCESSING PARAMETERS AND TECHNIQUES

One of the original goals of this program was to define and elucidate the critical processing parameters necessary for the fabrication of high quality, void-free parts. To accomplish this goal, various processing variables were investigated including (1) thermal gradients across thick laminates which may lead to uneven resin distribution through the thickness, (2) ply thickness gradients (which resulted from processing variation) as a function of total laminate thickness, (3) resin pressure measurements and gradients resulting from applied pressure sources, (4) resin migration studies, (5) compaction studies which show the importance of ply consolidation early in the cure cycle, and (6) new curing techniques including bagless and internally pressurized bag approaches.

2.6.1 THERMAL GRADIENTS. For the determination of thermal gradients within a laminate, a pseudoisotropic, 64 ply laminate, 0.61 m by 0.61 m (ft by 1 ft) was selected for evaluation.

A total of five thermocouples were positioned 7.62 cm (3 in) in from the laminate periphery starting with the first ply nearest the tool surface and moving clockwise up through the laminate with thermocouples at the 16th, 32nd, 48th, and the 64th ply (the latter being nearest the nylon bag surface).

The laminate was cured using the Fort Worth cure cycle where the pressure was applied 15 minutes into the 135C (275F) hold. The heat-up rate was at 2C/minute (3.6F/minute). Subsequent cure heat-up rates were at 3.3, 6.7, and 7.8C/minute (5.8, 12, and 14F/minute), respectively. Figure 63 showed the maximum spread in temperatures recorded by the thermocouples at different temperatures and heat-up rates. The maximum temperature spread was between the tool side thermocouple and the nylon bag side thermocouple (T/C), the nylon bag thermocouple reading the highest temperature and the tool side thermocouple recording the lowest.

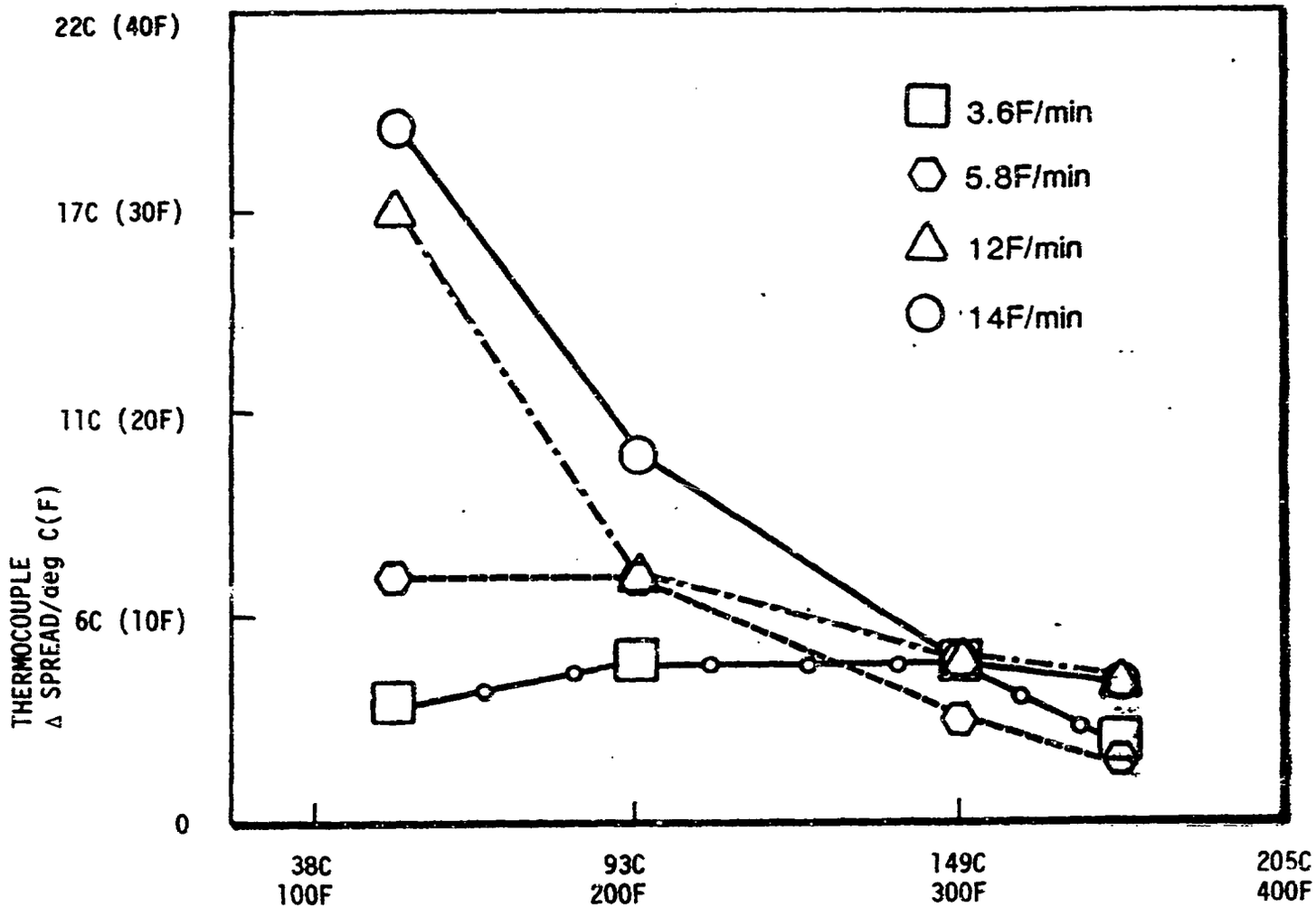

Figure 63. Thermal Gradient, 64 Ply 0.305m by 0.305m (12 In by 12 In) Laminate (5208)/T300

The greatest spread in temperature occurred with the 7.8 and 6.7C/minute (14 and 12F) heat-up rates. Both rates showed temperature deltas greater than 16.7C (30F) at 42C (125F), and greater than 7.2C (13F) at 93C (200F). However, at the more critical temperature levels of 121C (250F) and above, the thermal gradient for all heat-up rates is relatively low, 5.5C (10F) or less. A thermal gradient of up to 5.5C (10F) within a laminate could easily be tolerated by this particular resin system.

2.6.2 PLY THICKNESS GRADIENT. The change in ply thickness as a function of total laminate thickness was also investigated during this program.

A number of 32 ply laminates, four 64 ply laminates, and two 96 ply laminates were examined under the microscope to determine if a ply thikcness gradient existed through the total laminate thickness.

Figure 64 shows the number of plies per laminate and the percent variation in ply compaction for each particular laminate. For the 32 and 64 ply laminates

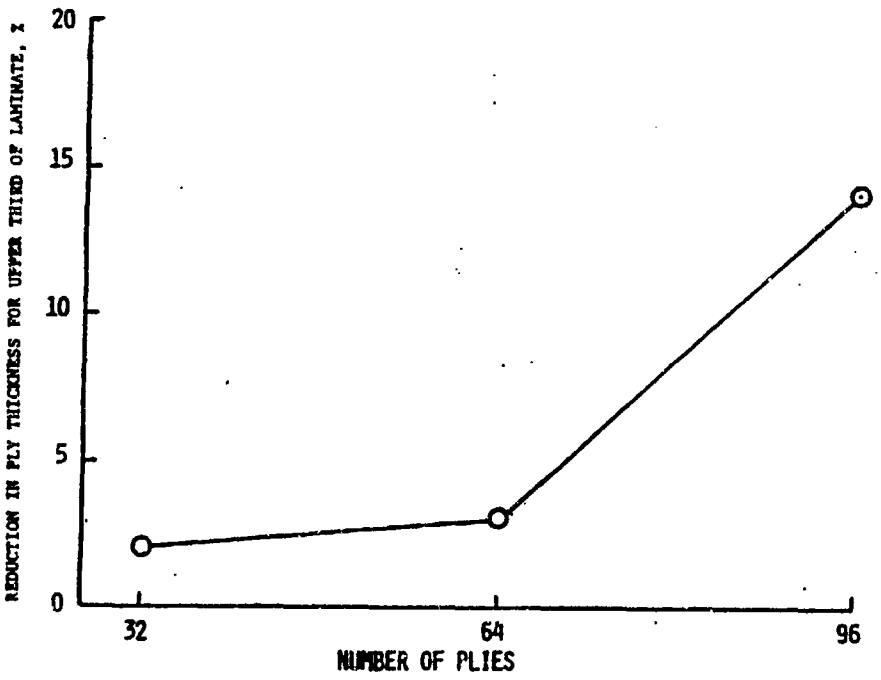

Figure 64. Ply Thickness Gradient Within 32, 64, and 96 Ply Laminates, T-300/5208

a very modest variation in ply compaction of 2 to 4 percent existed. The 96 ply laminates, however, showed a very discernable 14 percent variation in ply compaction as compared to normal cured ply thicknesses.

In all cases the variation in ply thickness for all of the laminates examined occurred in the top one third, or nylon bag side, of the laminates.

None of the laminates were subjected to debulking or pre-bleeding prior to the final cure of the laminates. If the 96 ply laminates had been pre-bled in 16 ply units there probably would not have been any noticeable variation in ply thicknesses.

The difference in ply thickness can be accounted for by knowing that there was a greater amount of bleeder on the top of the thicker laminate and the fact that most of the resin tends to migrate laterally into the bleeder system. This allowed an over-bleed situation in the top one-third of the laminate. Lateral resin migration will be discussed in detail later in Section 2.6.4. This observation implies a strong argument for net resin prepreg when constructing thick laminate parts.

2.6.3 PRESSURE GRADIENT STUDY. The pressure gradient study, initially designed by Dr. R. Hinrichs of APT, Inc., was designed to measure both the total laminate (fiber and resin) and the liquid resin pressures inside a laminate during cure processing. The basic premise of these tests was that pressurization of an autoclave or press during cure provided a constant load condition, and as the material compacts it does not change the applied load. Therefore, any pressure gradients which might be generated are strictly a function of the flow stress-relaxation pathways within the laminate. Since laminates were fabricated with bleeder/breather pathways there was always resin flow. It was this flow which allowed laminate compaction to occur. Without these pathways, a hydraulic cell effect would prevent compaction and elimination of interply voids.

Based on this premise, the question was whether or not a significant amount of restriction or blockage of these pathways could occur to hinder resin flow and thus generate a pressure gradient with different laminate thicknesses. If this were true, then the applied pressure would be translated directly to the liquid resin. A transducer was designed which measured the liquid resin environment without the fiber network in contact with the sensitive measurement membrane of the transducer. A miniature transducer was built with a guard ring raised slightly above the measurement surface. The cavity formed by this ring was then filled with the liquid resin to provide a fluid couple to the laminate and the prepreg stack was placed on top. The ring acted as a bridge to the high modulus fibers but allowed the resin to be in direct contact with both the measuring plate and prepreg. As pressure was applied, the resin was compressed against the transducer plate until flow could occur to lower the pressure. A second type of transducer was built without the guard ring to measure total area pressure. The combination of the two sensors placed side-by-side during these tests allowed measurement of the two different types of pressure simultaneously. A tool surface was machined to accommodate the transducers upon which laminates of varying thicknesses (10, 30, and 64 plies) were arranged. This allowed the transducers to measure pressure as a function of depth or plies within the composite during cure. The laminates themselves were constructed in such a way as to maintain a minimum of 4 inches of spacing between the transducers and any edge of the panel. Both autoclave and hydraulic press evaluations were performed to verify results as a function of applied external pressure. Both methods utilized the General Dynamics' cure cycle of heating from room temperature to 132C (270F), and apply 0.586 MPa (85 psi) pressure after 20 minutes of hold at 132C (270F). The transducers were coupled with an Applied

Polymer Technology CAPS cure controller-monitor system for data acquisition and thermal monitoring of the actual cure cycle. The sensors were calibrated for 0 to 0.589 MPa (0 to 100 psi) and temperature compensated to 150C (300F).

Hydraulic press cured laminates were used to confirm the transducer operations and define preliminary techniques. It was evident that the total pressure sensors responded immediately to the applied pressure. The applied pressure was translated rapidly to the entire depth of the laminate. It should be noted that during the press experiments continual adjustment of the press was necessary to maintain the desired 0.586 MPa (85 psi) pressure. This procedure was consistent with compaction and flow concepts discussed previously. Thus, a constant load was maintained while the laminate was compacting.

The test results are summarized in Figures 65 and 66. As might be expected, the thin 10 ply laminate which should flow readily, had essentially

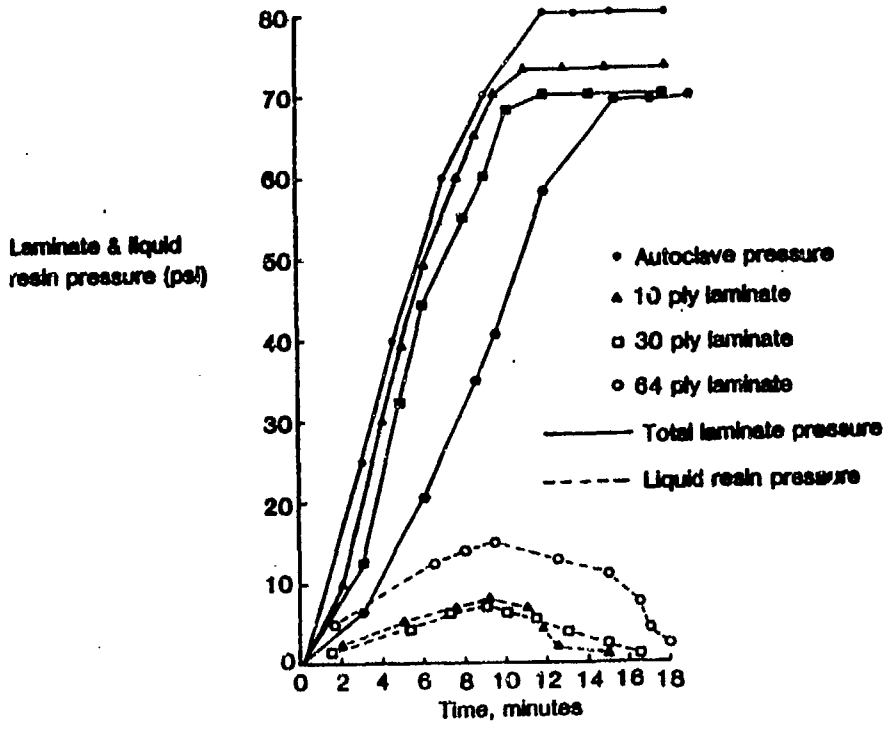

Figure 65. Laminate Pressure Gradient Study

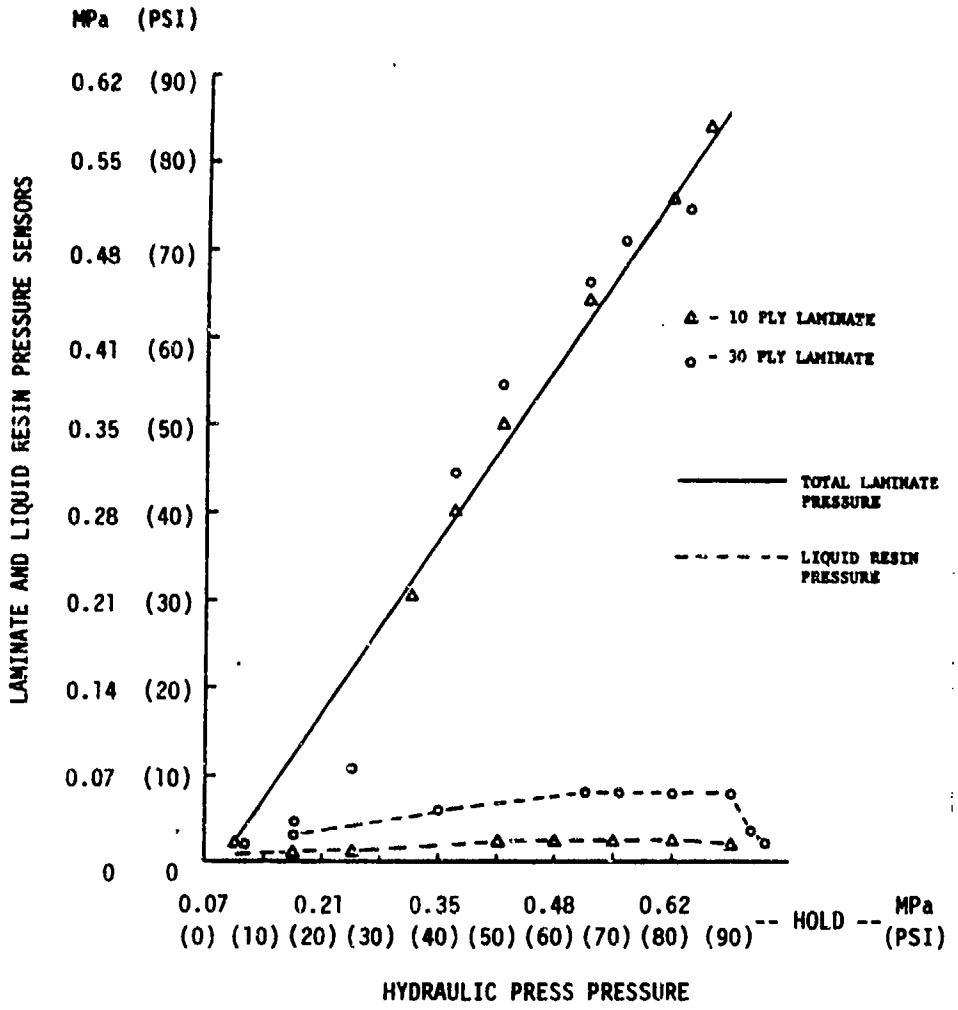

Figure 66. Laminate Pressure Gradient Study

no resin pressure across the entire 0.586 MPa (85 psi) range. The 30 ply laminate showed an initial pressure rise, but then the resin pressure diminished very rapidly once total constant pressure was achieved. In fact, within a few minutes of reaching full pressurization, the liquid resin seemed to have achieved the full flow-relaxation and the pressure dropped to 0.007 to 0.014 MPa (1 to 2 psi). It was interesting to note that the liquid pressure did not increase appreciably throughout the test indicating easy access to resin flow pathways. Low resin pressure combined with dissolved moisture at high temperatures provide conditions conducive to void generation in the resin.

The autoclave test panels were layed up to achieve as close an approximation to a perfectly dammed tool as possible. Besides the Coroprene dam, bagging

sealing compound was also used around the dam perimeter to prevent resin leakage. A bleed ratio of one bleeder for ten plies of prepreg was employed on all of the laminates. In Figure 65 it was clear that the thicker the laminate, the greater the pressure translation to the resin occurred before the pressure dropped off due to bleeding.

Even though the autoclave pressure was 0.586 MPa (85 psi), all three panels only achieved 0.483 MPa (70 psi) total pressure. This suggested that resin movement was still occurring. Since the 10 ply laminate tracked directly with the autoclave, it suggested that the time lag for the thicker laminates was due to the easy flow of the resin from the top layers first, into the bleeder before compaction and translation of pressure occurred in the lower plies. Even though an obvious pressure delay appeared to exist, it readily dissipated within a few minutes after full pressurization was reached. The translation to the total 64 ply laminate layers occurred readily and therefore did not indicate a true pressure gradient effect.

Differences in the liquid resin and total laminate pressure profiles were more dramatic for the thicker laminates. It was interesting to note that the liquid resin pressure did not exceed 0.103 MPa (15 psi) in the 64 ply panel and 0.055 MPa (8 psi) in both the 30 and 10 ply panels. This again indicated that the resin can easily find a pathway of escape and flow under these pressure application conditions.

Examination of the ringed sensors at the conclusion of the experiments showed them to still contain full resin cavities and no evidence of fiber infringement in the transducer cavity. Figure 67 displays the type of test apparatus used for the pressure gradient study.

2.6.4 ADDITIONAL RESIN PRESSURE EXPERIMENTS. Early data in the Processing Science program generated by Dr. R. J. Hinrichs indicated that during a

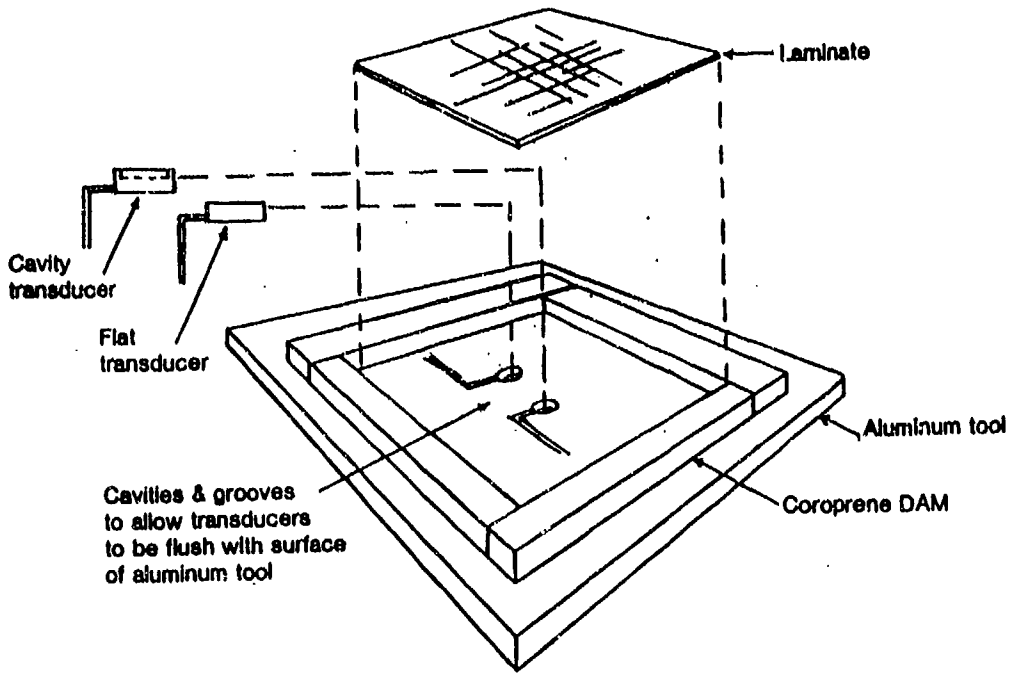

Figure 67. Pressure Gradient Test Fixture

simulated cure of 5208 the actual pressure of the resin never exceeded 0.103 MPa (15 psi) during an applied pressure of 0.586 MPa (85 psi). Apparently, the fluid resin (test temperature of 132C (270F), minimum 5208 resin viscosity) did not reach any pressure maximum until its movement into the bleeder system was halted or gelation occurred. These experiments have been repeated with a different type of transducer than employed earlier (an absolute psi transducer requiring no atmospheric compensation tube). The transducer was calibrated in the autoclave prior to the cure.

A caul plate with a cavity was filled with degassed Epon 828 resin (uncatalyzed) which provided a fluid couple to the transducer. The transducer electrical leads were routed through the autoclave to a constant voltage source and a voltage actuated strip chart recorder to obtain a continuous pressure reading as a function of time. It was critical that no air be trapped in the resin coupling system and meticulous care was taken to

devolatilize the coupling resin. A slight excess of resin at the cavity allowed good coupling to the laminate during heat-up and pressure application. Standard bleeder systems for 10, 30 and 64 ply 5208 layups were utilized. The laminates were bagged, vacuum was applied, and the laminates heated to 132C (270F). At 132C (270F), 0.586 MPa (85 psi) pressure was applied and held for 15 minutes. After 15 minutes the pressure was released and the autoclave cooled. The short test time was designed to prevent significant advancement of the couplant by the curing agent in the 5208. Table 13 summarized the results of the pressure studies during a simulated heating and pressure application.

Table 13. Resin Pressure Drop-off Results

Test Conditions: Heat Laminate to 132C (270F) Under Vacuum, Apply 0.586 MPa (85 psi) at 132C (270F) and Hold for 15 Minutes

	Laminate					
	[0] Plies			[0, 90] Plies		
	10	30	64	10	30	64
Vacuum Felt [Near 132C (270F)]	0.069 MPa (10 psi)	0.035 MPa (5 psi)	0.017 MPa (2.5 psi)	0.048 MPa (7 psi)	0.069 MPa (10 psi)	0.017 MPa (2.5 psi)
Maximum Pressure	0.172 MPa (25 psi)	0.228 MPa (33 psi)	0.552 MPa (80 psi)	0.234 MPa (34 psi)	0.200 MPa (29 psi)	0.159 MPa (23 psi)
Pressure Drop	Not in test	Yes	Yes	Yes	Yes	No
Time to Max. Press.	12.5 min	5 min	4 min	3 min	5 min	17.5 min
Time to Min. Press.	-	10 min/ test stopped, still dropping	15 min/ test stopped, still dropping	10 min stable @28	12.5 min	-
Bleeder No. (Plies of 181 Glass)	2	6	12	2	6	12

The following generalizations were made:

1. The results basically confirmed R. Hinrich's earlier work.
2. The maximum average pressure reached in most of the runs was 0.207 MPa (30 psi).
3. Vacuum was measured in the resin in all of the runs, ranging from 0.084 to 0.032 MPa absolute (12.2 to 4.7 psia).

A typical pressure readout chart is shown in Figure 68. The only test that deviated from the others was the 64 ply unidirectional lay-up whose pressure peaked at 0.552 MPa (80 psi) momentarily before bleeding off. If one extrapolated the decay of pressure, as a function of time, a resin pressure of less than 0.207 MPa (30 psi) would be obtained in less than one hour. This assumption was based on minimal viscosity changes at 132C (270F).

Another pressure test was run on a 64 ply lay-up of U.S. Polymeric's E767/T-300. The 0.586 MPa (85 psi) was applied at 93C (200F) which was recorded as 0.586 MPa (85 psi) on the pressure transducer. As the temperature increased to 132C (270F), the resin viscosity apparently dropped rapidly and started to flow into the standard bleeder system. As a result, the pressure in the resin decreased over a period of 15 minutes to 0.163 MPa absolute (0 psig, 15 psia) with the pressure decreasing commencing at about 132C (270F). Again, this experiment showed the general trend that once the resin viscosity becomes low enough and space for bleeding is provided, then resin pressures drop relative to the applied pressure. If sufficient moisture was present in the resin and was vaporized, voids will form (if the water vapor pressure exceeds the resin pressure in the resin).

2.6.5 LATERAL PRESSURE GRADIENT STUDY. One of the objectives of the resin pressure study was to determine not only the pressure within the resin of a curing laminate at a single central location within the laminate, but to

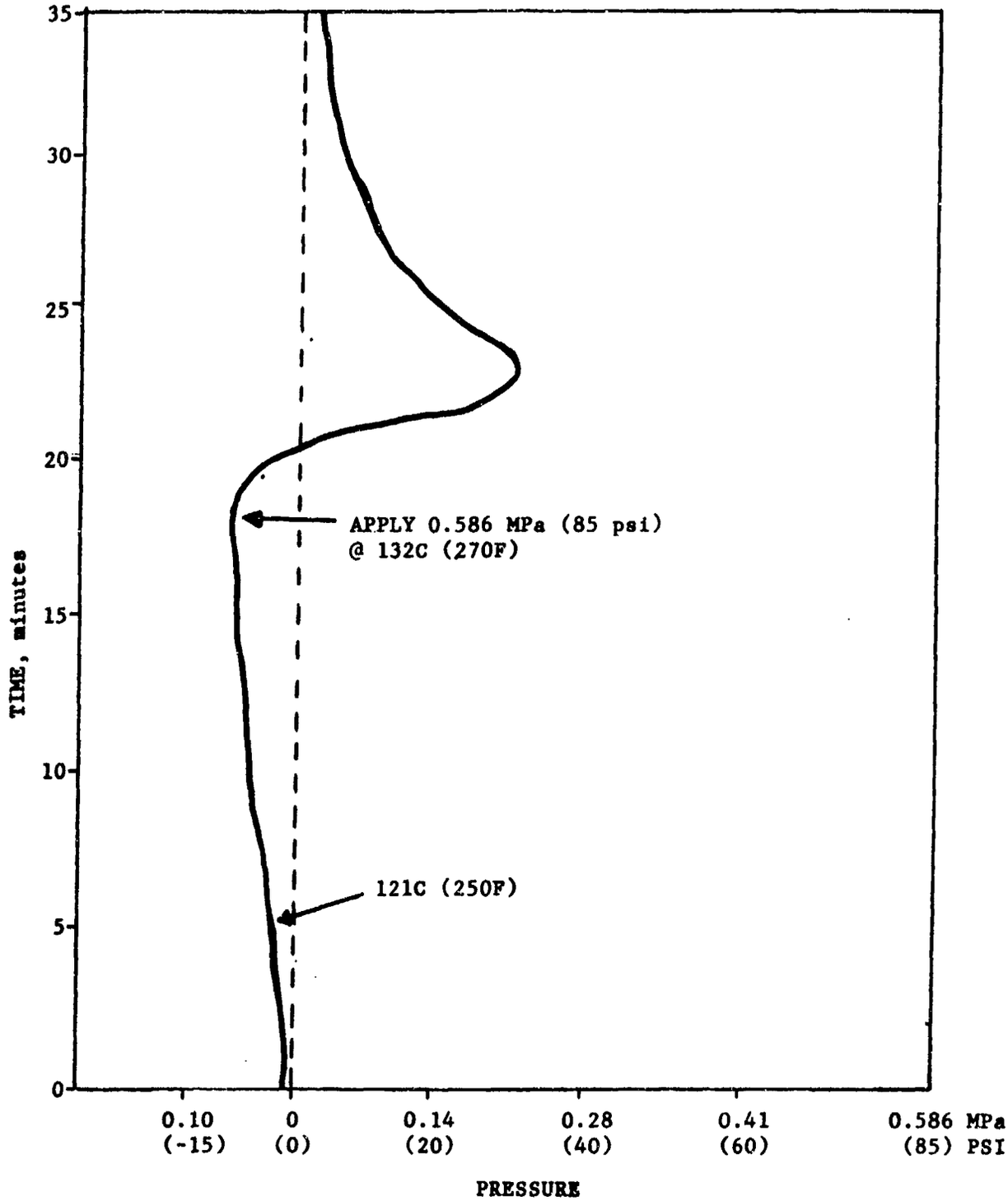

Figure 68. Typical Pressure Readout for Transducer Experiment

also determine if a lateral pressure gradient existed within a curing laminate. To answer this question, a series of three cavity pressure transducers were positioned diagonally from the center of a laminate every 10.16 cm (4 in) to within 7.62 cm (3 in) of the laminate edge. An 0.46 m by 0.46 m (18 in by 18 in) by 30 ply laminate was positioned over the cavity pressure transducers and vacuum bagged in position. The laminate was heated at 3C/minute (5F/minute) to 116C (240F) at which time 0.689 MPa (100 psi) autoclave pressure was applied. Figure 69 shows the laminate schematic and transducer location as well as the pressure within the resin at the different transducer locations as a function of temperature. In reviewing the transducer pressure table, an 0.083 to 0.103 MPa (12 to 15 psi) pressure delta was evident between 121C (250F) to 132C (270F) from the center of the laminate to the edge.

2.6.6 RESIN MIGRATION STUDIES. As a part of the overall program objective, one of the subtasks was to determine the direction of resin flow during the normal curing process. To accurately determine the direction of resin

	TRANSDUCER			
C	0.614 MPa 89 psi	0.600 MPa 87 psi	0.558 MPa 81 psi	0.524 MPa 76 psi
+4	0.614 MPa 89 psi	0.600 MPa 87 psi	0.558 MPa 81 psi	0.524 MPa 76 psi
+8	0.586 MPa 85 psi	0.517 MPa 75 psi	0.455 MPa 66 psi	0.427 MPa 62 psi
	240F 116C	250F 121C	260F 127C	270F 132C

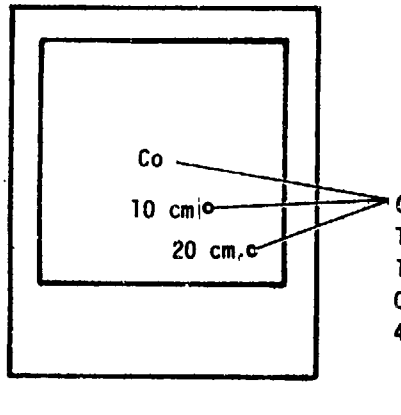

Figure 69. Lateral Resin Pressure Gradient Study

migration a scanning electron microscope (SEM) equipped with an x-ray analyzer was used to detect the presence and dispersion of bromine which was added as the brominated minor epoxy of a 5208 formulation. Additions of brominated minor epoxy of 1, 3, and 5 percent by weight were added to the formulation. These blends were then used to impregnate 3-inch wide single plies of dry T-300 graphite tows. The impregnated graphite samples with 1, 3, and 5 percent by weight of bromine were subjected to SEM/x-ray detection. It was determined that the 3 percent by weight brominate epoxy provided a good detectable level of bromine by the SEM,and this material was then used for inserted plugs within a 32 ply laminate for the resin migration study.

The laminate employed for the resin migration study was a 0.15 m by 0.15 m (6 in by 6 in) by 32 ply pseudoisotropic laminate with a ply sequence of $(0°, +45°, 90°, +135°)_s$ typical of all laminates fabricated on the program. Three 2.5 cm (1 in) diameter, 1 ply plugs of 3 percent by weight of brominated epoxy resin prepreg were positioned in the center of the 0.15 m by 0.15 m (6 in by 6 in) laminate. Plies 15, 16, and 17 of the laminate had a 2.5 cm (1 in) diameter hole cut in the center of each ply. The brominated epoxy plugs were then positioned in the holes with the fiber direction of the plug common to the fiber direction of each respective ply.

The laminate was then cured using the Fort Worth Division's cure cycle. The bleeder / breather sequence used on this laminate was identical to those used on all 32 ply laminates fabricated for the program. The cured laminate was sectioned through the center of the 1 inch plug and scanned with the SEM. Figure 70 shows the counts of bromine and sulfur detected as a function of the specimen length. Also shown by dashed lines is the location of the 1 inch diameter brominated epoxy plug within the length of the laminate. The presence of sulfur comes from 5208 hardener and in general is inversely

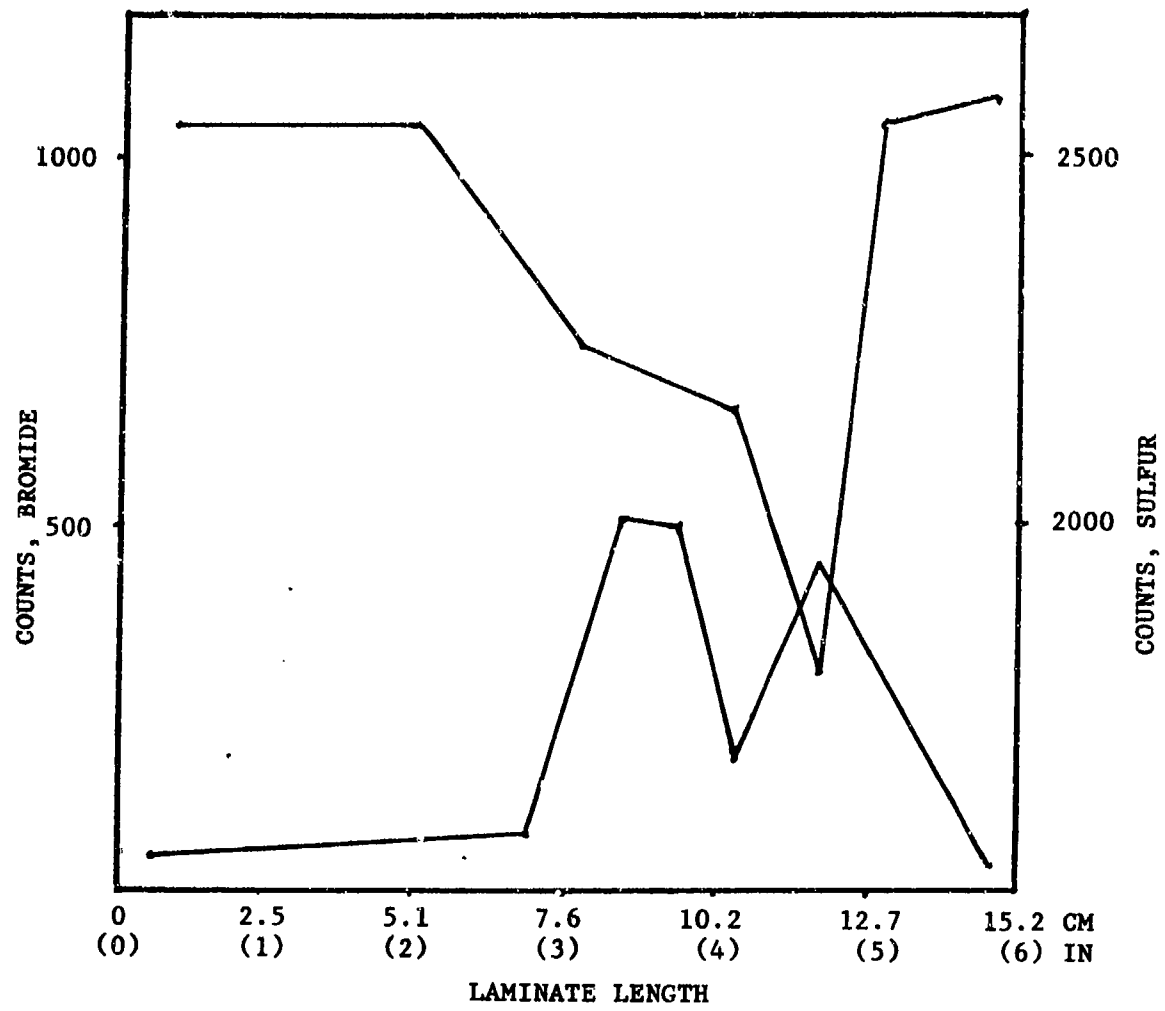

Figure 70. Resin Migration Study

proportional to the presence of the bromine. The highest concentration of bromine occurred above and below the plug, with migration of bromine moving laterally out to the extremities of the laminate.

Figure 71 displays visually where the migration of brominated resin was detected by the SEM. Of particular interest in viewing these two figures, is the evidence that resin migration moves laterally 7.62 cm (3 in) from the plug but only approximately 0.080 of an inch to the top and bottom plies of the laminate. It is quite clear then, that the resin will preferentially move laterally within a laminate rather than vertically toward the bleeder/breather

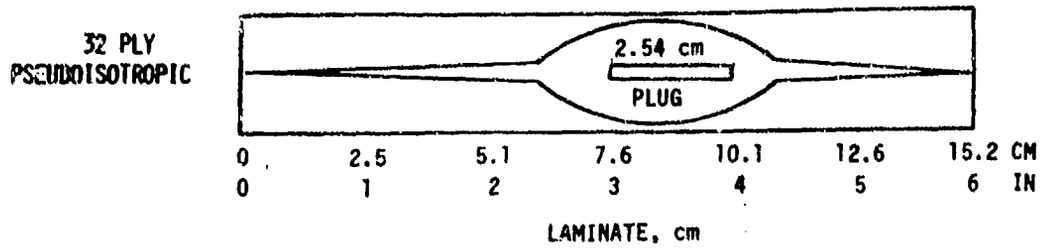

Figure 71. Resin Migration Study

system. This information also suggests that entrapped air or water bubbles will also move laterally with the primary direction of flow of the resin.

2.7 COMPACTION STUDIES

Two compaction studies were accomplished on this program. The initial study was originally done to determine the point in terms of temperature and pressure at which a prepreg stack consolidated. Consolidation means the loss of individual ply integrity which occurs when all of the mechanical voids introduced during lay-up are eliminated and the interfaces between two plies disappears.

2.7.1 FIRST COMPACTION STUDY. The first compaction study began as an attempt to determine where during a typical processing cycle does consolidation of the laminate stack or lay up occur. A series of 48 ply lay-ups ($[0,90]_s$) were prepared from Fiberite 976/T-300 and subjected to vacuum bag and thermal conditions. The uncured laminates were then ultrasonically C-scanned for voids. Figure 72 shows the mildest conditions tested; two minutes at room temperature in a vacuum bag, and illustrates the large amount of interlaminar voids.

After one hour at 66C (150F) under a vacuum bag, compaction was evident (Figure 73) but voids still remained. When the same laminate was heated to 121C (250F) (Figure 74) under a vacuum bag, better compaction occurred. However, new voids are apparently being generated in the center of the laminate, presumably by the vacuum bag conditions. At this point,

C-SCAN OF UNCURED 48 PLY, 0/90°
15 CM X 15 CM (6 IN X 6 IN)
LAMINATE 976/T-300

2.25 MHz, 3.0 x 10.0
2 Min., RT, Vac. Bag

After 2 Minutes under vacuum bag at RT, a considerable amount of entrapped air still remains.

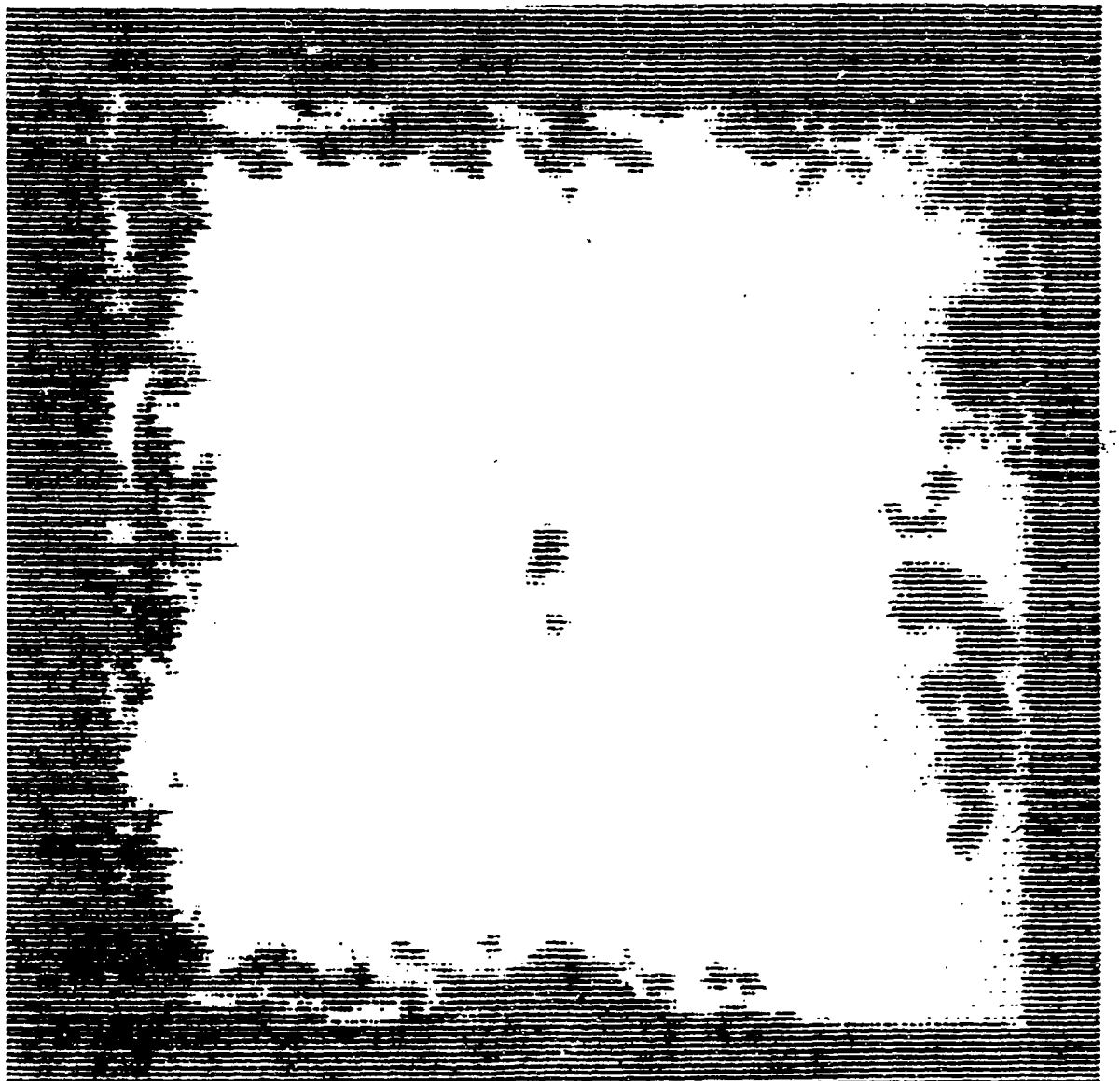

Figure 72. Laminate Compaction Study - Typical Debulking Cycle

C-SCAN OF UNCURED 48 PLY, 0/90°
15 CM X 15 CM (6 IN X 6 IN)
LAMINATE 976/T-300

2.25 MHz, 5.0 x 1.0

150F, 1 HR, VAC. BAG

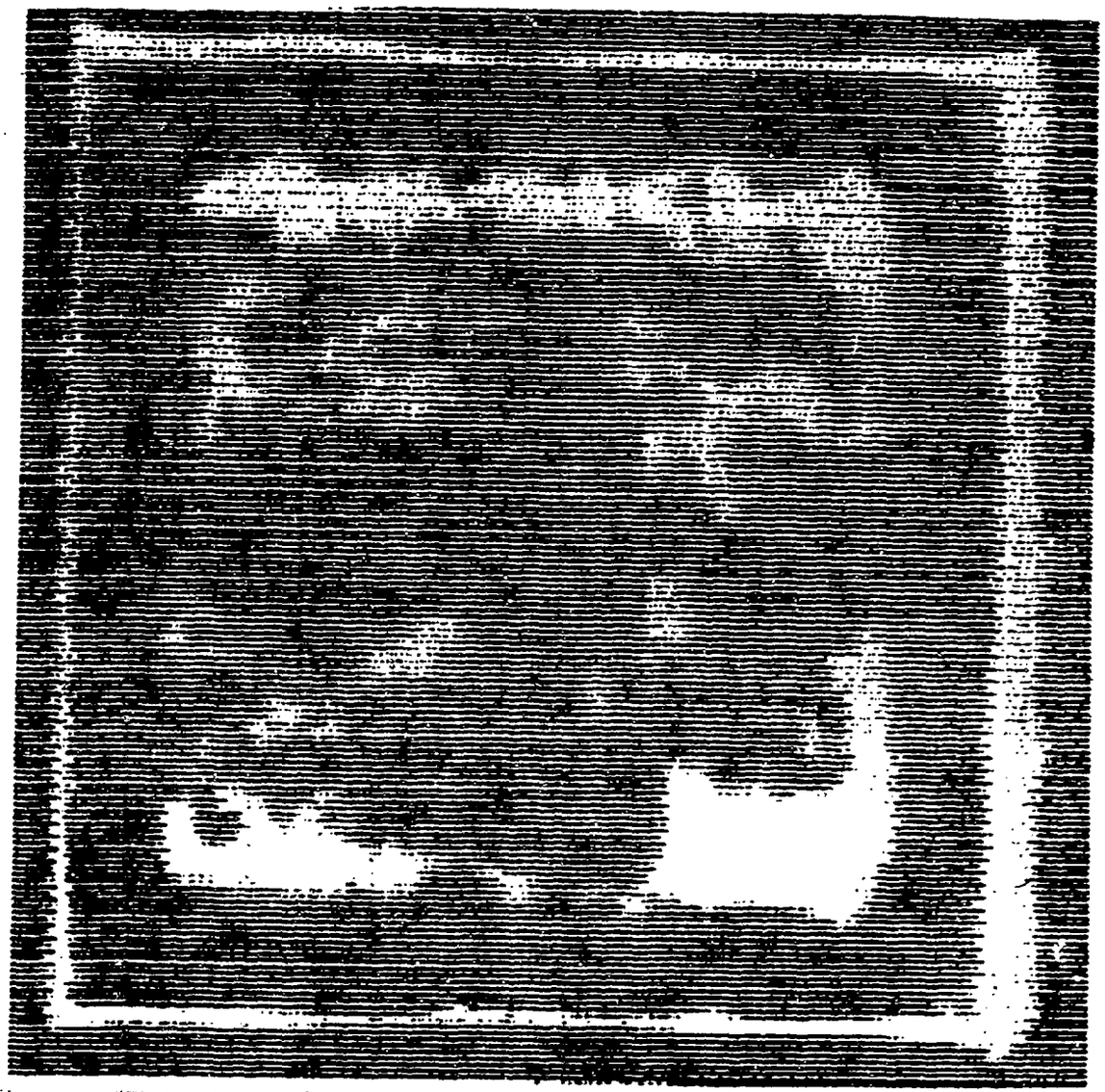

After 1 Hr. under Vacuum Bag at 150°F, compaction of the prepreg plies is evident. Still some apparent void areas

Figure 73. Laminate Compaction Study - Typical - Vacuum Bag Compaction

C-SCAN OF UNCURED 48 PLY, 0/90°
15 CM X 15 CM (6 IN X 6 IN)
LAMINATE 976/T-300

2.25 MHz 5.0 x 1.0

250F, 1 HR, VAC. BAG

After 1 Hr. under Vacuum Bag at a higher temperature of 250°F, better compaction, but still void areas are present

Figure 74. Laminate Compaction Study - Typical Vacuum Bag Compaction

the vacuum bag approach was abandoned in favor of only pressure. Figure 75 shows the result of a 60 minute compaction at ambient temperature and 0.689 MPa (100 psi) of pressure. As the temperature is allowed to increase to 66C (150F) the quality of the compaction is seen to improve; i.e., the sensitivity of the C-scan increases, Figure 76.

The conclusions reached in the first series of compaction laminates are that the best conditions for high quality consolidation of prepreg layups are primarily pressure and temperature dependent with vacuum definitely hindering void elimination. In fact, vacuum appeared to generate voids during the consolidation portion of the curing process. Woven prepreg required higher temperatures and pressure [80C (175F) and 1.03 MPa (150 psi)] to consolidate well.

The value of knowing when and at what conditions consolidation occurs is apparent when the typical cure schedule is examined. Most cure schedules put the pressure on later in the cycle. The Fort Worth Division, for example, puts the pressure on after the 132C (270F) hold is entered. At this point, voids could have actually been generated if sufficient moisture is in the prepreg. Gelation of the resin occurs fairly rapidly at this temperature, so void removal is competitive with resin advancement. The ideal situation is to consolidate the laminate early in the processing cycle and create conditions to inhibit void growth during the remainder of the cycle.

Voids are either present during cure or generate during cure. Bubbles which are present can be stabilized or grow by moisture diffusion and volume expansion caused by heating. Generated voids result when an sufficient amount of dissolved water (or solvent) in the resin at a high enough temperature and low pressure vaporizes at some nucleation site. Once

C-SCAN OF UNCURED 48 PLY 0°/90°,
15 CM X 15 CM (6 IN X 6 IN)
LAMINATE 976/T-300

2.25 MHz, 3.0 x 10

0.689 MPa
100 PSI, RT, 1 HR.

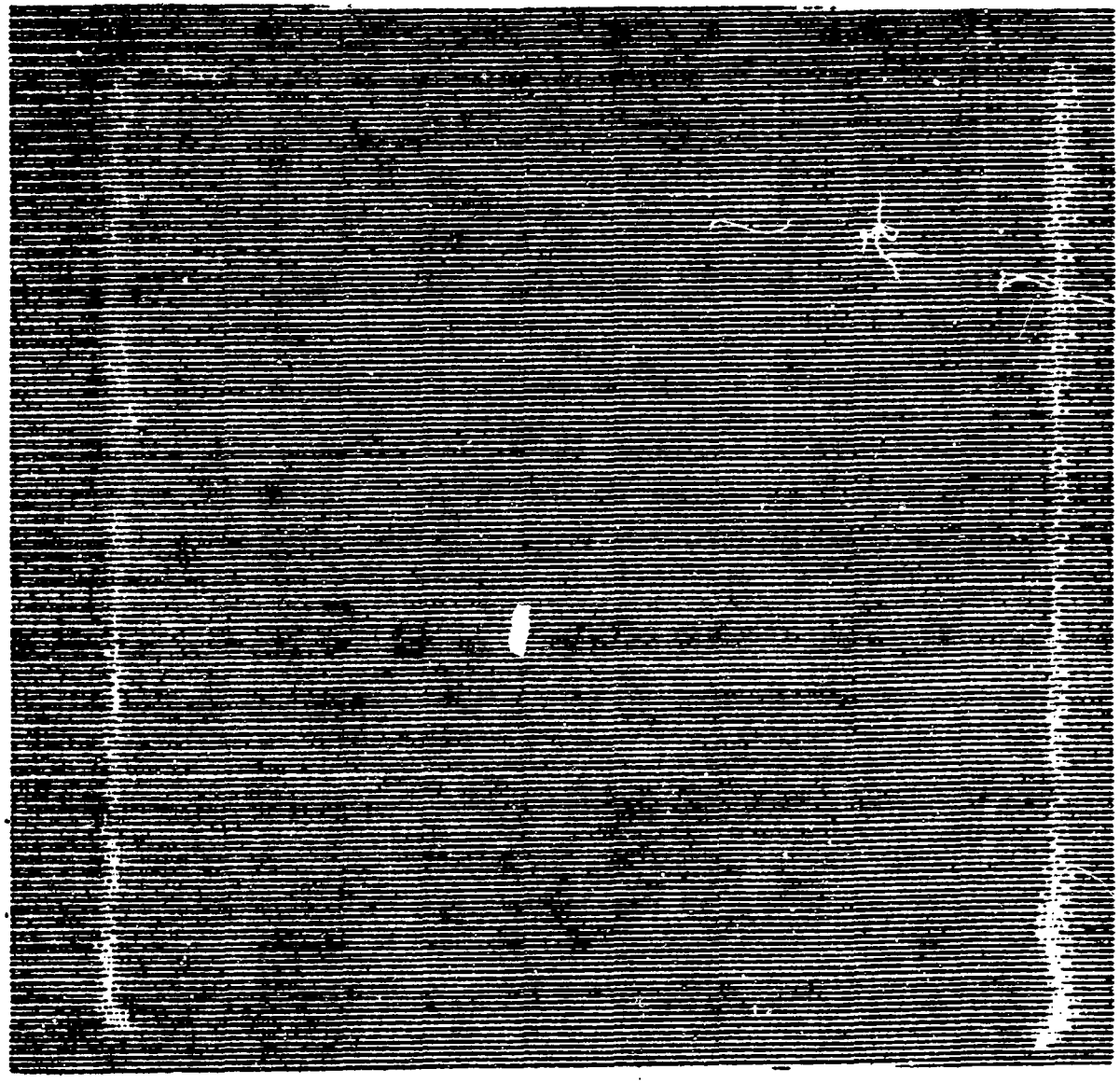

No Vacuum used for this compaction cycle of 1 Hr at RT and 100 PSI. Good clear C-SCAN of Prepreg as compared to compactions using Vacuum.

Figure 75. Laminate Compaction Study - No Vacuum and High Pressure

C-SCAN OF UNCURED 48 PLY 0°/90°
15 CM X 15 CM (6 IN X 6 IN)
LAMINATE 976/T-300

2.25 MHz, 1.0 x 5.0

0.689 MPa
100 PSI, 1 HR, 150F

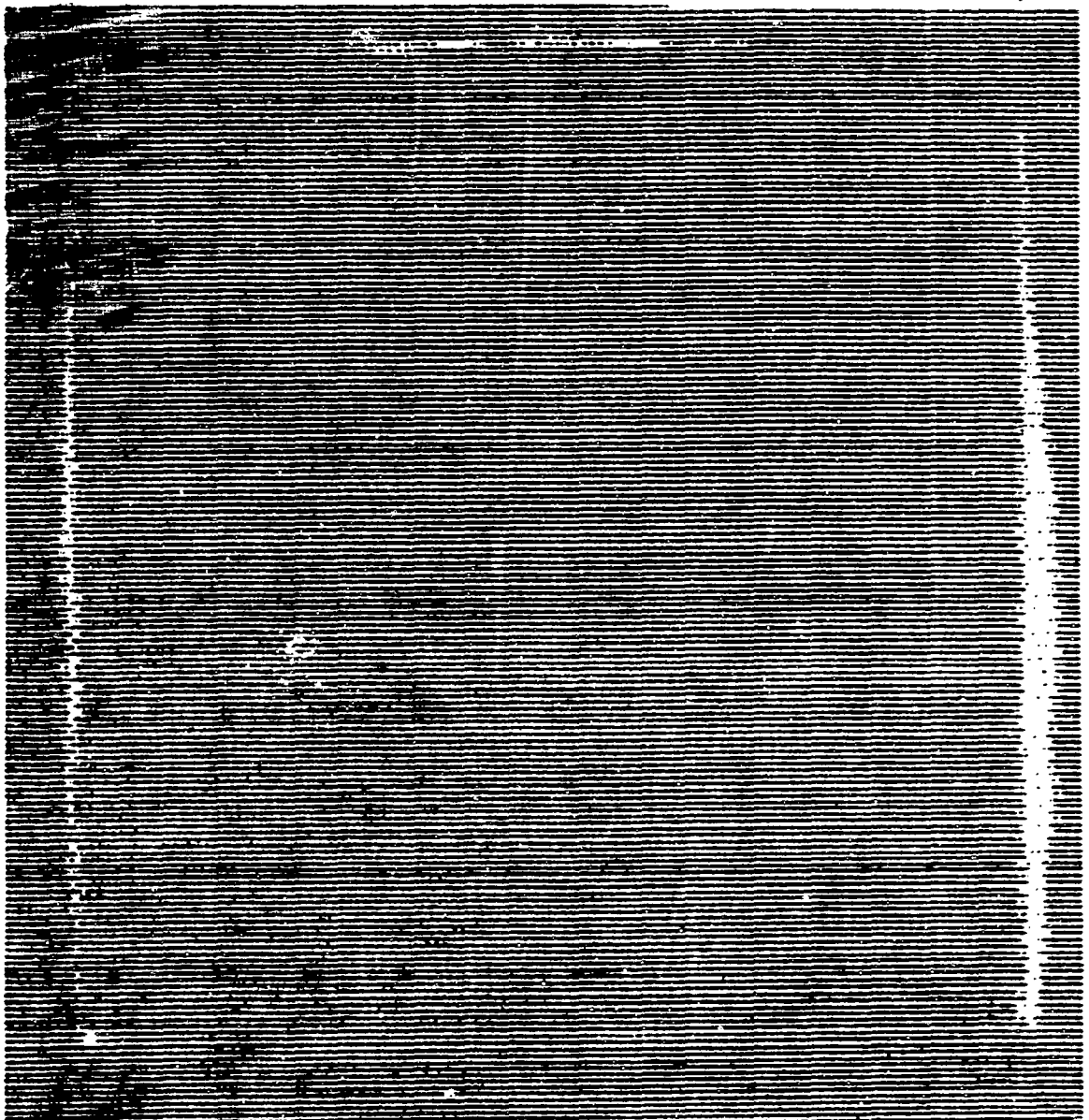

An increase in temperature to 150°F for the Non-Vacuum, 100 PSI compaction also provides a well compacted Prepreg Billet.

Figure 76. Laminate Compaction Study - No Vacuum and High Pressure

generated, this steam bubble can only collapse by increasing the resin pressure or by lowering the temperature.

Situations like over-bleeding are eliminated because the resin viscosity is moderately high at the consolidation temperature of 70-100C (160-210F). Resin advancement also proceeds at a very slow rate, so if the laminate has a large area and more time is required to accomplish the consolidation, time is available without adverse effects on the remaining cure cycle.

2.7.2 SECOND COMPACTION STUDY. The effective consolidation of the laid-up stack of prepreg during cure is the first critical step to procuring good, void-free composites. Two major sources have been identified as causing the majority of composite voids during processing. The first source is merely mechanical voids, air pockets trapped between plies during the lay-up operation. These air pockets are literally squeezed out of the laminate when the viscosity of the resin drops during heating and pressure is applied. The second source and probably the worst culprit in processing appears to be absorbed water which is evolved later in the cure cycle when the resin viscosity is too high to allow lateral transport to edge of the laminate. It is particularly troublesome because even though the overall concentration of water in the prepreg is not that high, local concentrations, however, do get high. These local concentrations can manifest themselves as generated voids. The Fort Worth Division has done preliminary work with the consolidation of prepreg which correlates well with the results generated at the Convair Division. They have shown that consolidation takes place early in the cure cycle if sufficient pressure is applied and voids are generated (presumably by water vapor evolution) at higher temperatures in the cure schedule.

These empirical observations are corroborated by work done at Rockwell, where investigators found that degassing of the prepreg prior to consolidation and cure allows the production of void-free parts. Our own studies concerning the drying of 5208/T-300 prepreg with chemical desiccants also confirm these results.

Apparantly, there are two routes to take to obtain good composites. One is to degas (remove all the volatiles prior to compaction) the prepreg and then cure without the requirement of high pressure and the second method is to impart effective pressure into the resin during the cure process such that volatiles are never allowed to vaporize and form voids.

General Dynamics has developed several methods to introduce into the resin during cure thus avoiding generated voids. The next logical investigation was to quantify the time, temperature, and pressure that must be applied to a layup of given dimensions to assure that all of the mechanically entrapped voids have been removed.

The objective of the compaction study investigation was to establish an optimum pre-cure thermal/pressure cycle for consolidating thick composites. The criteria for selecting the best compaction profile would depend on effectively debulking the laminate at the lowest possible temperature (thus precluding any significant resin advancement) as well as demonstrating the capability to yield a minimal void content.

The composite panels used in this study were prepared by hand-layup using 50 plies of Fiberite's T-300/976 graphite/epoxy prepreg; bagged in order to pull vacuum, and compacted within an air cavity press. Full vacuum, then a pressure of 85 psi were applied at room temperature followed by ramping up to a specified temperature at 3 C/min (5F/min), and holding

for the desired amount of time. At the end of the dwell, the pressure was released, vacuum vented, and the panel removed and allowed to cool in an ambient environment.

Assessment of the quality of the laminate compaction was accomplished using the In-Service Inspection System (NDI technique) developed at General Dynamics Fort Worth Division under Air Force Contract F33615-78C-5152 entitled "In-Service Inspection System Producibility." This system offers the user the choice of three software packages for NDI of honeycomb laminates, or adhesively bonded structures. During this investigation, the latter two programs were utilized. Although the two types of scan incorporate the same hardware, there are fundamental differences. The LAMINATE scan has the time gates set between the front and back surfaces and can discriminate and locate flaws having diameters greater than 0.1 inches through the thickness of the composite. On the other hand, an ADHESIVE BOND scan, having the time gate set only at the back surface, in essence measures the attenuation of the transmitted signal lost between the front and back surfaces. Thus, the LAMINATE scan can yield information from which the macroscopic void content can be determined while the ADHESIVE BOND scan is indicative of the microscopic void content or how well a panel is consolidated. Generally, for the LAMINATE scan, the higher the gain setting required to idenfity macroporosity the better the panel in that respect. Since, however, this parameter is normally kept constant for a given thickness, the primary indicator is the amount of data (voids) shown within the boundaries of the panel. For the ADHESIVE BOND scans, on the other hand, the gain setting is adjusted until the amplitude level returning from the back surface over the entire panel remains primarily

between 0 and full scale of the CRT screen displaying the wave form. If possible, the mean amplitude level should be at 50 percent of full scale. Here the gain level setting is the most sensitive indicator as a change of 1 dB equates to approximately a 25 percent change in the amplitude level. A lower gain level corresponds to better consolidation since less transmitted power is required to receive a signal from the back surface. It is important to note and understand the differences between the LAMINATE and ADHESIVE BOND scans regarding the interpretation of gain level prior to proceeding with this test. In all, six different laminate compaction profiles were examined and are listed below:

1. 0° undirectional, consolidated for 15 minutes at 160F.
2. 0/90 crossply, consolidated for 15 minutes at 160F.
3. 0/90 crossply, consolidated for 15 minutes at 180F.
4. 0/90 crossply, consolidated for 15 minutes at 200F.
5. 0/90 crossply, consolidated for 60 minutes at 160F.
6. 0/90 crossply, no consolidation.

Although a LAMINATE scan was performed on the unidirectional panel, the results were so superior to the crossply panels that the gains had to be adjusted to 90 dB before any substantial data could be recorded. At this level, however, data is more apt to represent artifacts such as ply splices, resin rich pockets, and multiple reflections. It is evident from the LAMINATE scan that the consolidated unidirectional panel contained no macroscopic voids. Furthermore, the ADHESIVE BOND scan demonstrates that its compaction state is also superior having a gain setting of only 50 which is at least 10 dB better than any crossply panel examined. These results are, of course, related to the fact that for a unidirectional composite

the fibers between plies are capable of nesting. The propitious compaction state for this panel made it apparent that further examination of unidirectional composites would be unproductive.

Another case for which recorded data is lacking involves the unconsolidated crossply (#6). This panel was so bulky that a signal from the back surface could not be received. In fact, in an attempt to employ the ADHESIVE BOND program on this laminate compaction state, the gain was adjusted up to 106 dB at 5 MHz without success. In light of what follows, this exemplifies the benefit which can be achieved by applying an appropriate compaction cycle.

The following discussion will be confined to data collected from the ADHESIVE BOND scans of the 0/90 crossplied specimens (#2-5). The manner by which this data was assessed will need some explanation. Data sheet "a" for each compaction state (previously identified by the laminate profile number) is in essence an information sheet listing all of the scan parameters, the most important being the gain level obtained by adding items 20 and 21. In some cases, after initiation of a scan, the determination would be made that the fine gain setting required readjusting. This is identifiable by checking post comments. For example, on D. S. 3a, item 31 (Figure 77) indicates that the fine gain was actually 4 dB, thus the gain level during this scan was 64 dB rather than 63 dB. Data sheet "b" (Figure 78) represents the area scan map. The white blocks are indicative of no return from the back surface. Data sheet "c" (Figure 79) (discrimination limits set at none) is a record displaying the data, denoted by the dark blocks having amplitudes above a bias setting which is internal to the program. Data sheets "d" through "k" (Figures 80 through 87) separate the amplitudes

1. LOCATION GD FT WORTH
2. INSPECTOR BELL
3. DATE/TIMER READING 5 20-83
4. ACFT TYPE/TAIL NO. 0 90 DEG, 180 F
5. PART NAME/SERIAL NO. 15 MIN. VAC, 85 PSI
6. UNIT # - SKIN # 10
7. TAPE RECORD # 1
8. CELL SIZE SQ = .2

9. CALIBRATION LIST #2 ADHESIVE BOND
10. REF STD.NO. N/A
11. TRANSDUCER TYPE .5 ANAMETRIC
12. TRANSDUCER FREQ (MHZ 5
13. BUFFER DELAY .75" AC YLIC
14. REP RATE (KHZ) 3
15. P/R FREQ (MHZ) BB
16. PULSE LENGTH (DAMPIN) 1
17. VIDEO REJECT 7
18. FILTER LO
19. DIFFERENTIAL ON
20. GAIN COARSE 60
21. GAIN FINE 3
22. DEC START LEFT OF CR
23. DEC SLOPE (%) 18
24. RANGE 2
25. MATL VEL 0.0
26. DELAY COARSE 0-4
27. DELAY FINE 2.7
28. FRONT SURF GATE (.1 SEC UNITS) 7
29. LOST COUPLING VALUE .1 USEC UNITS) 90
30. MAX STEP (PLIES) 0

COMMENTS:
31. FINE GAIN = 4DB. POS LOGIC
32. REJ =3, GAIN= 84 DB OR WAVE FORMS
33.
34.

Figure 77. Data Sheet for Scan Parameters of Compaction State #3

1. LOCATION GD FT WORTH
2. INSPECTOR BELL
3. DATE/TIMER READING 5 20-83
4. ACFT TYPE/TAIL NO. 0 90 DEG, 180 F
5. PART NAME/SERIAL NO. 15 MIN. VAC, 85 PSI
6. UNIT # - SKIN # 10
7. TAPE RECORD # 1
8. CELL SIZE SQ = .2

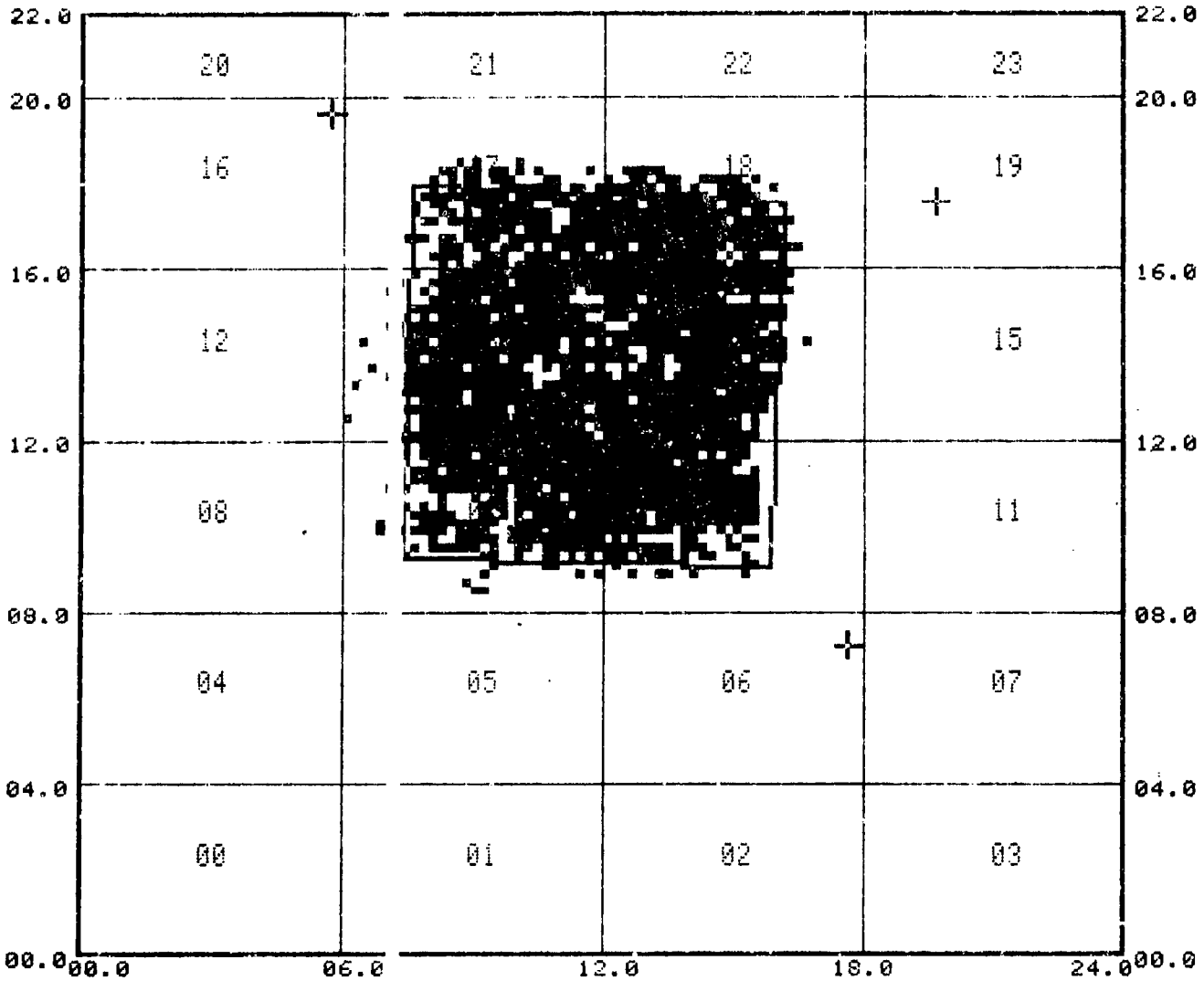

Figure 73. Area Scan Map of Compaction State #3

1. LOCATION GD FT WORTH
2. INSPECTOR BELL
3. DATE/TIMER READING 5 20-83
4. ACFT TYPE/TAIL NO. 0 90 DEG, 180 F
5. PART NAME/SERIAL NO. 15 MIN. VAC, 85 PSI
6. UNIT # - SKIN # 10
7. TAPE RECORD # 1
8. CELL SIZE SQ = .2

DISCRIMINATION L MITS
NONE

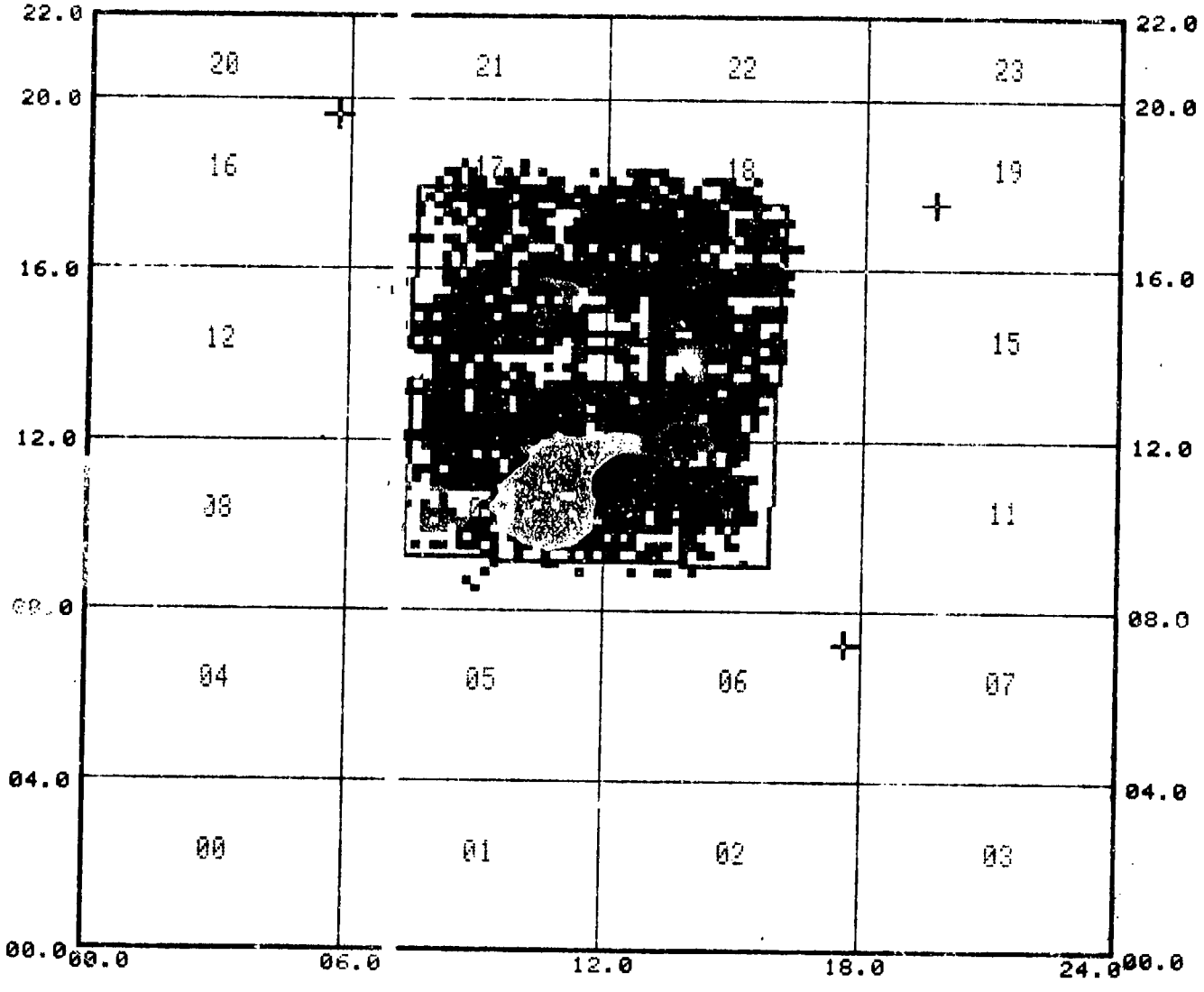

TARGET POINTS
X = 17.6, Y = 07.2
X = 19.6, Y = 17.5
X = 05.7, Y = 19.6

Figure 79. Data Display of Compaction State #3 With Discrimination Limits Set at None

1. LOCATION GD FT WORTH
2. INSPECTOR BELL
3. DATE/TIMER READING 5 20-83
4. ACFT TYPE/TAIL NO. 0 90 DEG, 180 F
5. PART NAME/SERIAL NO. 15 MIN. VAC, 85 PSI
6. UNIT # - SKIN # 10
7. TAPE RECORD # 1
8. CELL SIZE SQ = .2

DISCRIMINATION L MITS
1ST GATE AMP. ABOVE
080 PER ENT

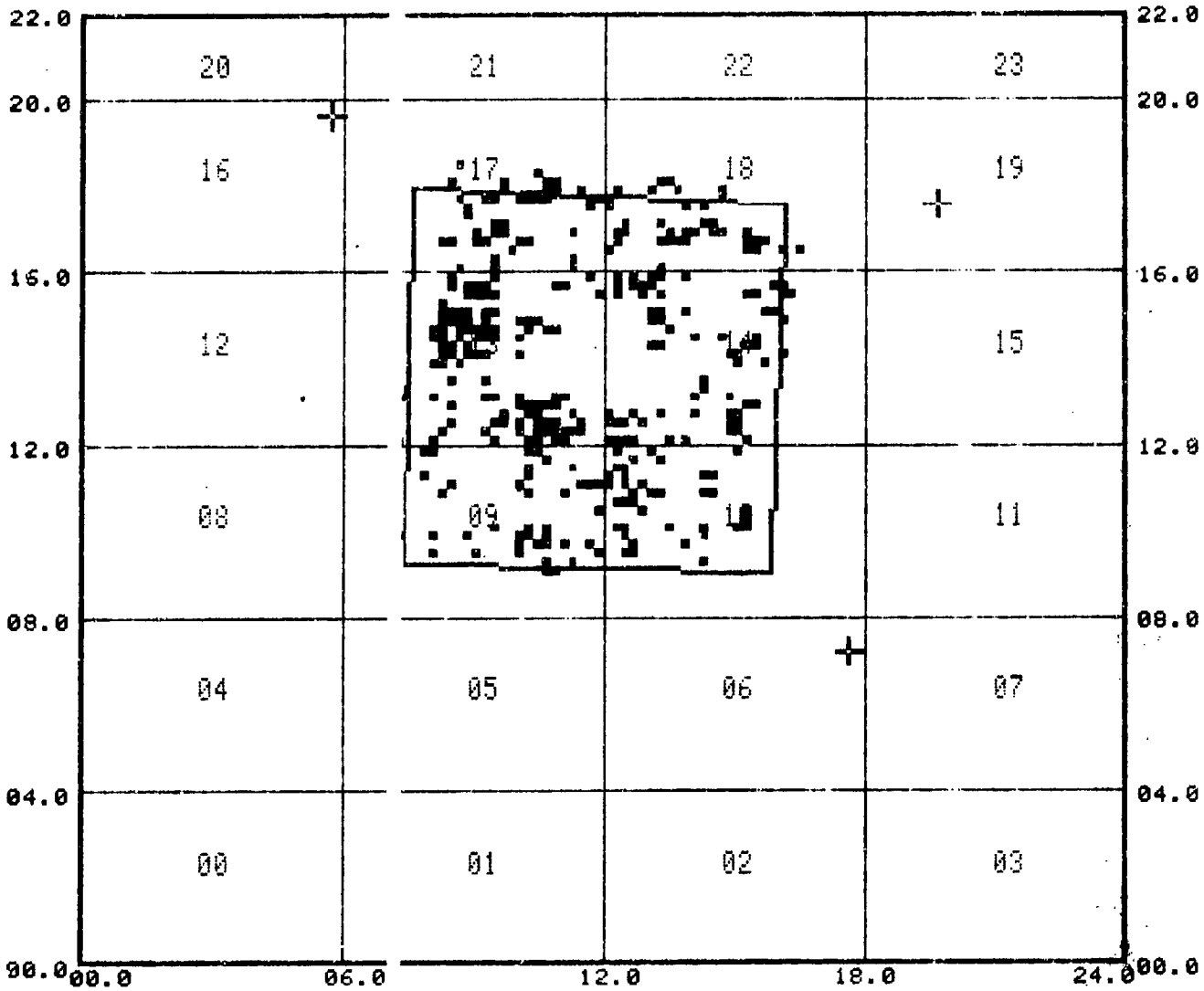

TARGET POINTS
X = 17.6, Y = 07.2
X = 19.6, Y = 17.5
X = 05.7, Y = 19.6

Figure 80. Data Display of Compaction State #3 With 80 Percent or Greater Amplitude Discrimination

1. LOCATION GD FT WORTH
2. INSPECTOR BELL
3. DATE/TIMER READING 5 20-83
4. ACFT TYPE/TAIL NO. 0 90 DEG, 180 F
5. PART NAME/SERIAL NO. 15 MIN. VAC, 85 PSI
6. UNIT # - SKIN # 10
7. TAPE RECORD # 1
8. CELL SIZE SQ = .2

DISCRIMINATION L MITS
1ST GATE AMP. BELOW
000 PER ENT

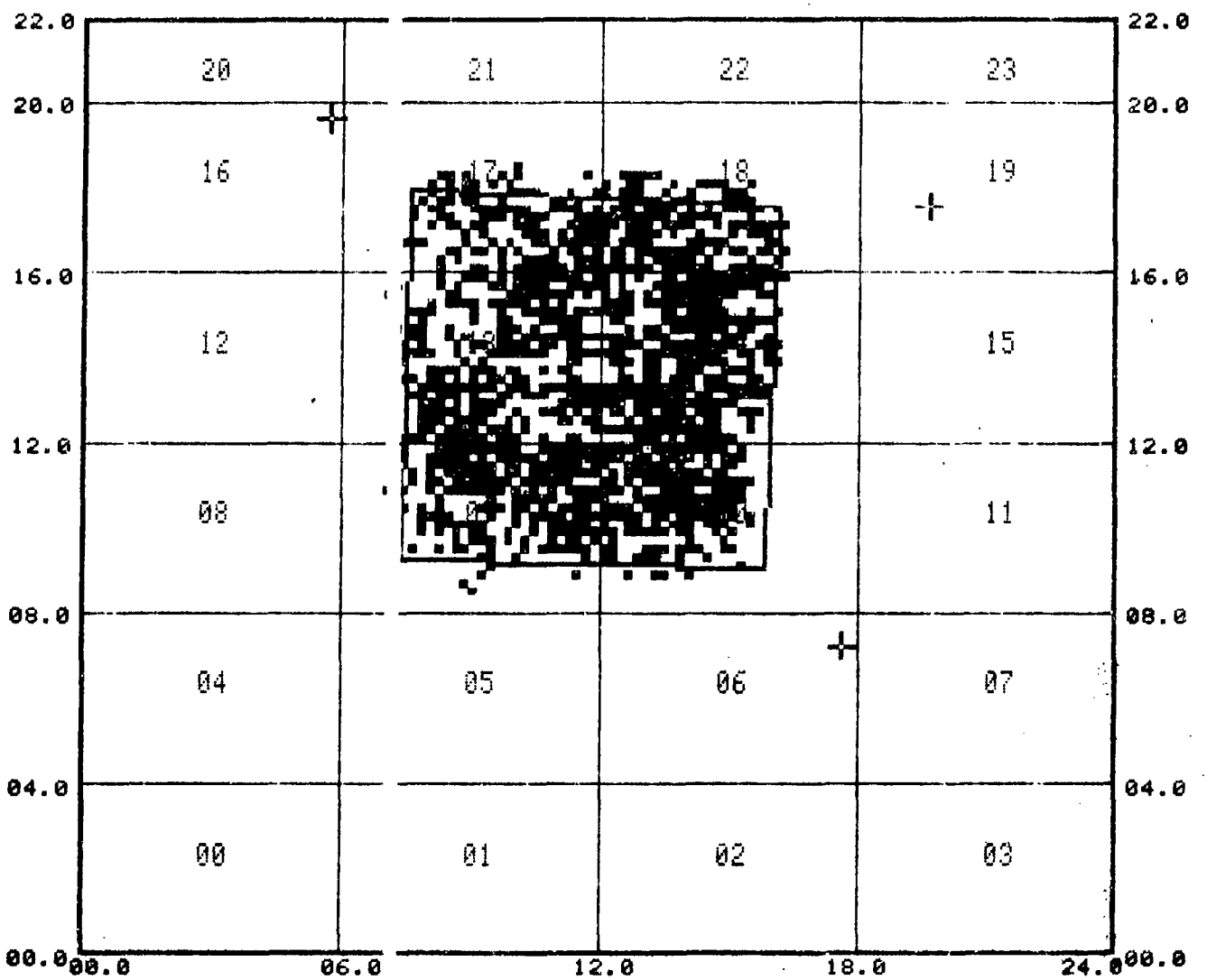

TARGET POINTS
X = 17.6, Y = 07.2
X = 19.6, Y = 17.5
X = 05.7, Y = 19.6

Figure 81. Data Display of Compaction State #3 With Less Than 80 Percent Amplitude Discrimination

1. LOCATION GD FT WORTH
2. INSPECTOR BELL
3. DATE/TIMER READING 5 20-83
4. ACFT TYPE/TAIL NO. 0 90 DEG, 180 F
5. PART NAME/SERIAL NO. 15 MIN. VAC, 85 PSI
6. UNIT # - SKIN # 10
7. TAPE RECORD # 1
8. CELL SIZE SQ = .2

DISCRIMINATION L MITS
1ST GATE AMP. ABOVE
060 PER ENT

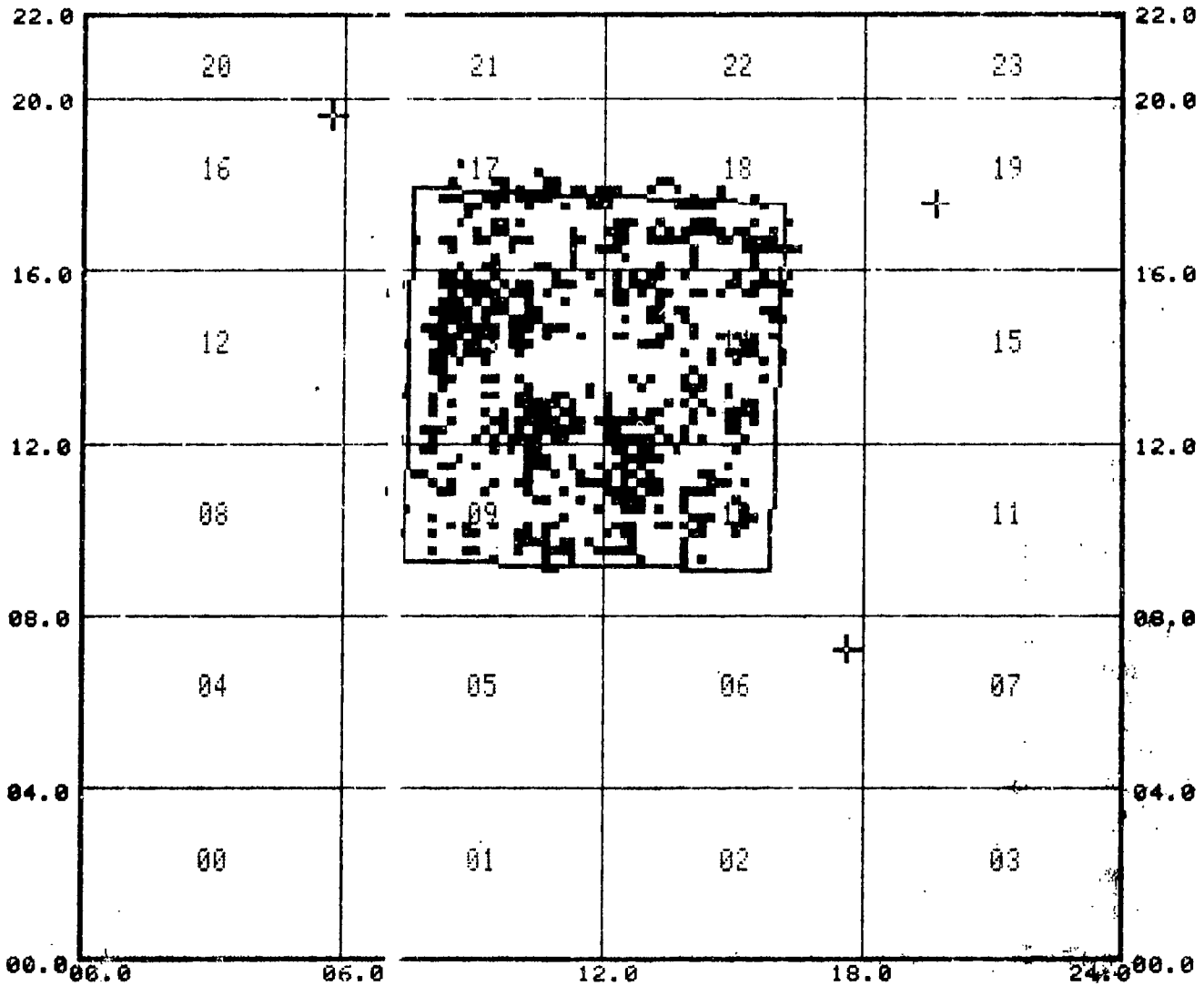

TARGET POINTS
X = 17.6, Y = 07.2
X = 19.6, Y = 17.5
X = 05.7, Y = 19.6

Figure 82. Data Display of Compaction State #3 With 60 Percent or Greater Amplitude Discrimination

1. LOCATION GD FT WORTH
2. INSPECTOR BELL
3. DATE/TIMER READING 5 20-83
4. ACFT TYPE/TAIL NO. 0 90 DEG, 180 F
5. PART NAME/SERIAL NO. 15 MIN. VAC, 85 PSI
6. UNIT # - SKIN # 10
7. TAPE RECORD # 1
8. CELL SIZE SQ = .2

DISCRIMINATION L MITS
1ST GATE AMP. BELOW
060 PER ENT

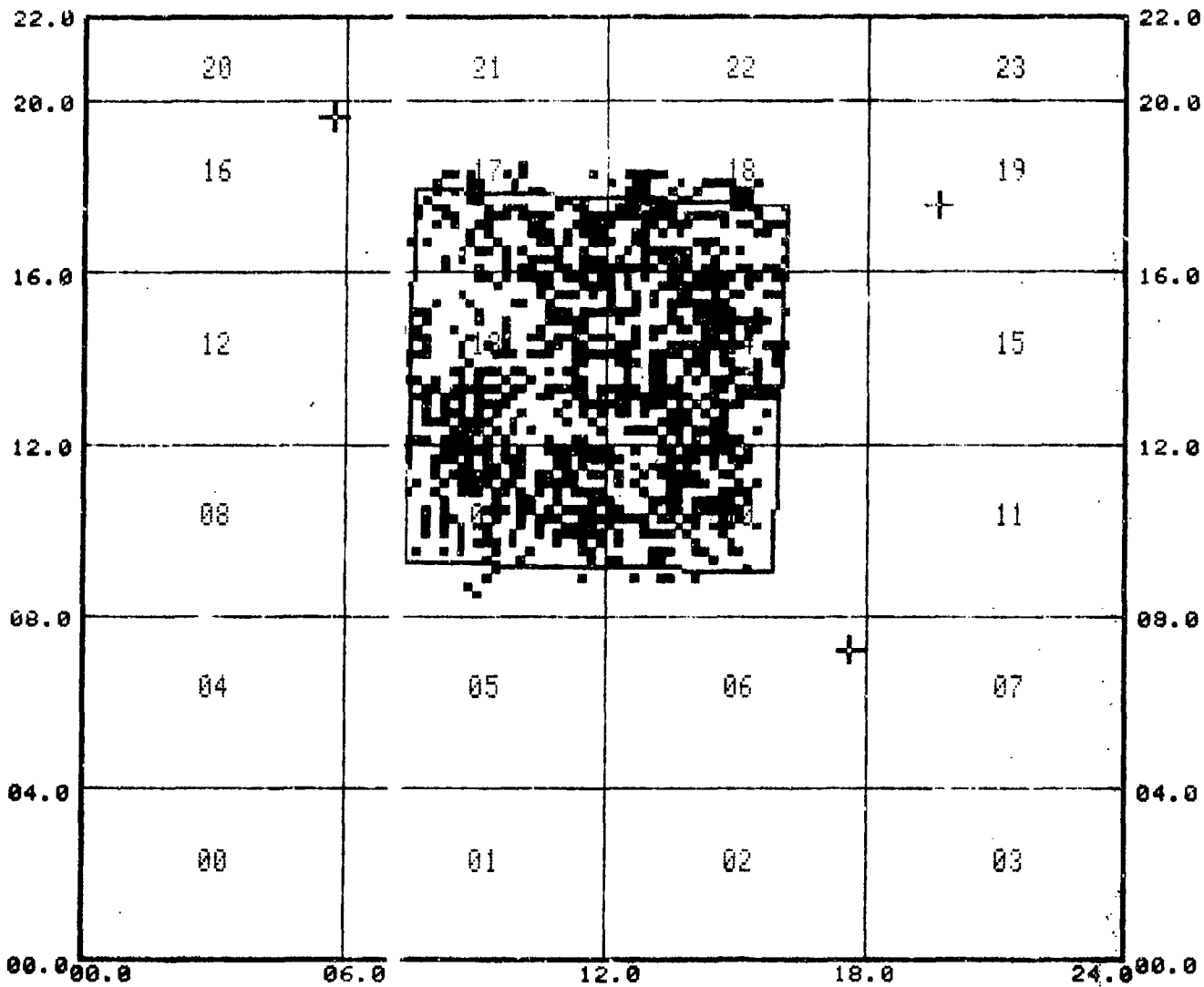

TARGET POINTS
X = 17.6, Y = 07.2
X = 19.6, Y = 17.5
X = 05.7, Y = 19.6

Figure 83. Data Display of Compaction State #3 With Less Than 60 Percent Amplitude Discrimination

1. LOCATION GD FT WORTH
2. INSPECTOR BELL
3. DATE/TIMER READING 5 20-83
4. ACFT TYPE/TAIL NO. 0 90 DEG, 180 F
5. PART NAME/SERIAL NO. 15 MIN. VAC, 85 PSI
6. UNIT # - SKIN # 10
7. TAPE RECORD # 1
8. CELL SIZE SQ = .2

DISCRIMINATION L MITS
1ST GATE AMP. ABOVE
040 PER ENT

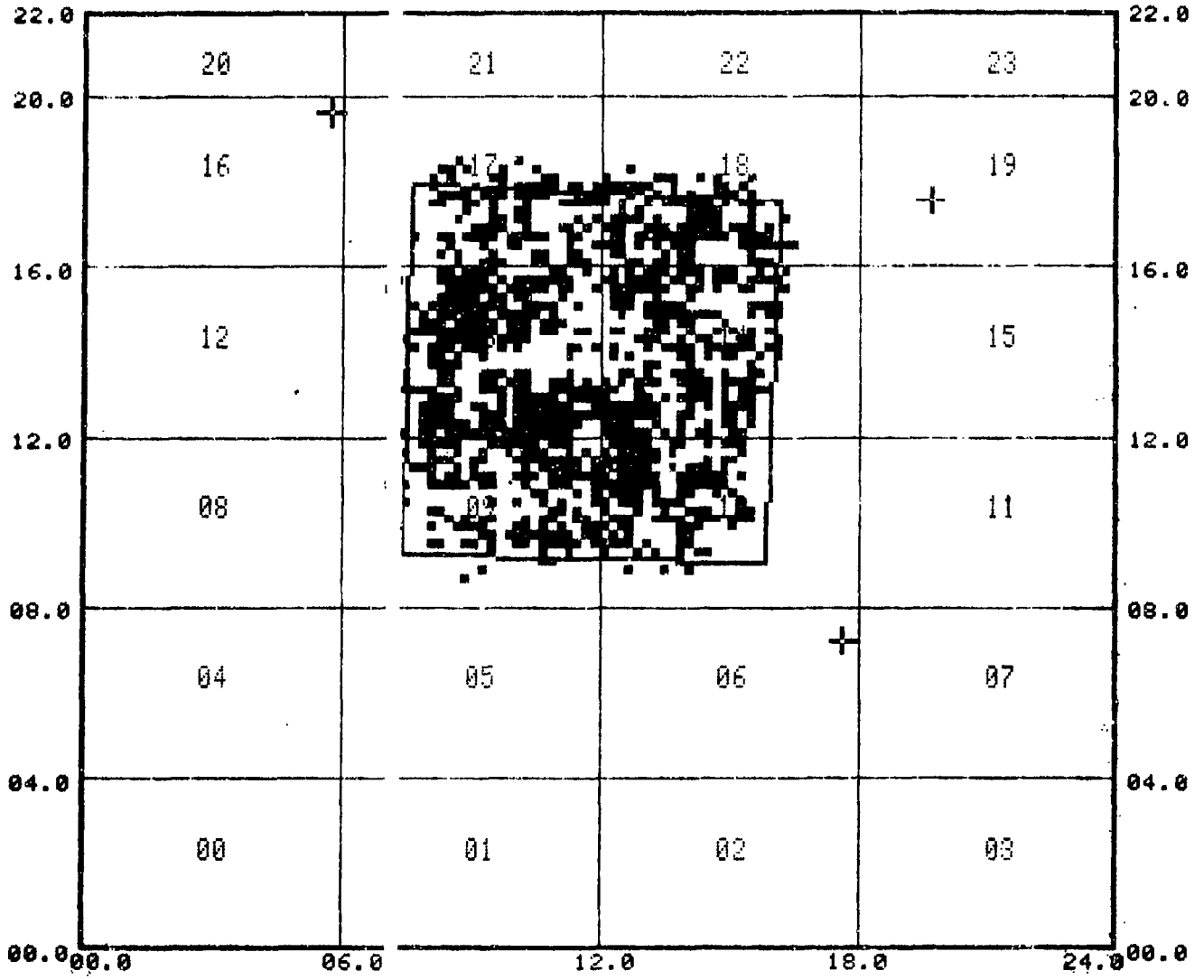

TARGET POINTS
X = 17.6, Y = 07.2
X = 19.6, Y = 17.5
X = 05.7, Y = 19.6

Figure 84. Data Display of Compaction State #3 With 40 Percent or Greater Amplitude Discrimination

1. LOCATION GD FT WORTH
2. INSPECTOR BELL
3. DATE/TIMER READING 5 20-83
4. ACFT TYPE/TAIL NO. 0 90 DEG, 180 F
5. PART NAME/SERIAL NO. 15 MIN. VAC, 85 PSI
6. UNIT # - SKIN # 10
7. TAPE RECORD # 1
8. CELL SIZE SQ = .2

DISCRIMINATION L MITS
1ST GATE AMP. BELOW
040 PER ENT

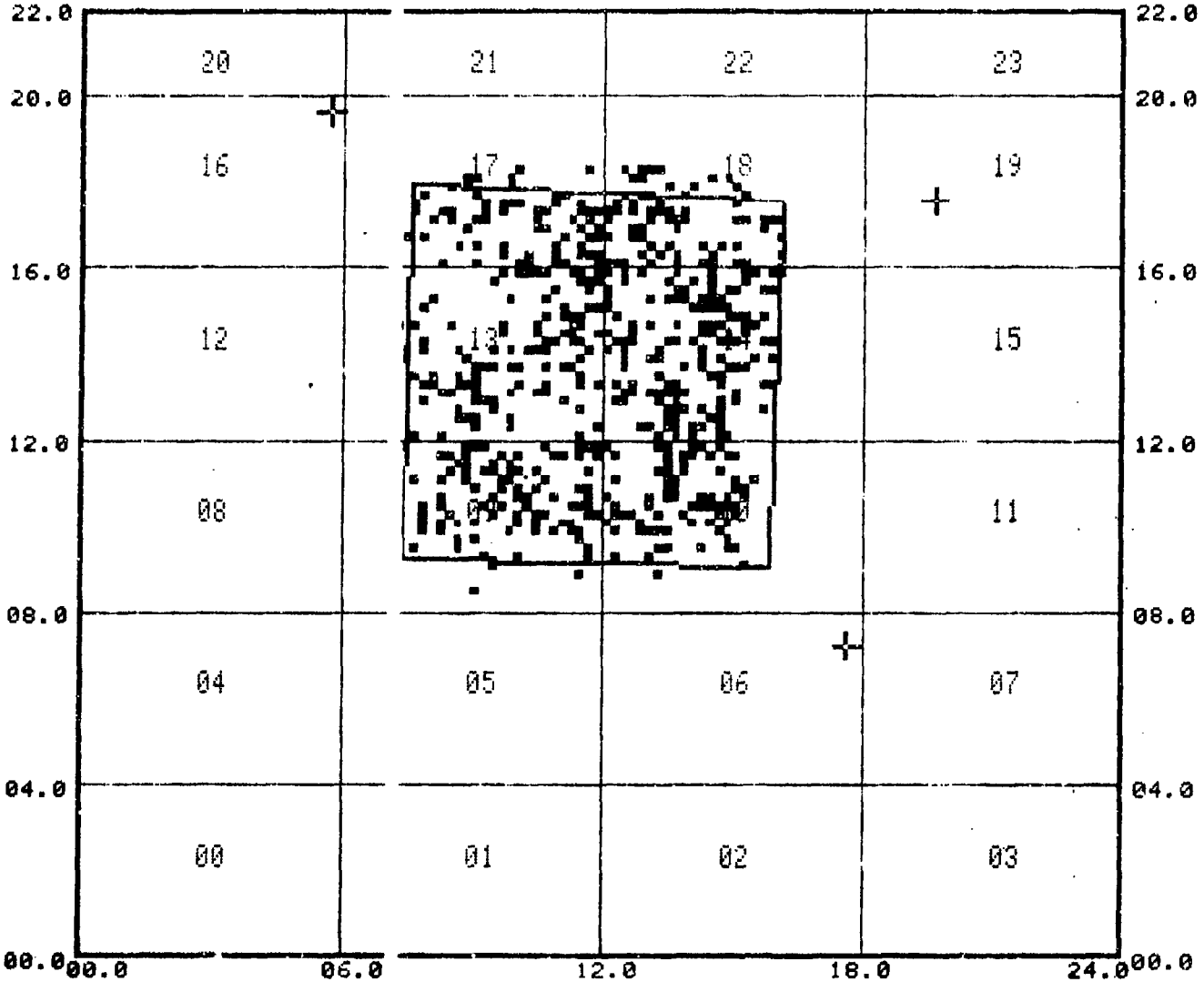

TARGET POINTS
X = 17.6, Y = 07.2
X = 19.6, Y = 17.5
X = 05.7, Y = 19.6

Figure 85. Data Display of Compaction State #3 With Less Than 40 Percent Amplitude Discrimination

1. LOCATION GD FT NORTH
2. INSPECTOR BELL
3. DATE/TIMER READING 5 20-83
4. ACFT TYPE/TAIL NO. 0 90 DEG, 180 F
5. PART NAME/SERIAL NO. 15 MIN. VAC, 85 PSI
6. UNIT # - SKIN # 10
7. TAPE RECORD # 1
8. CELL SIZE SQ = .2

DISCRIMINATION L MITS
1ST GATE AMP. ABOVE
020 PER ENT

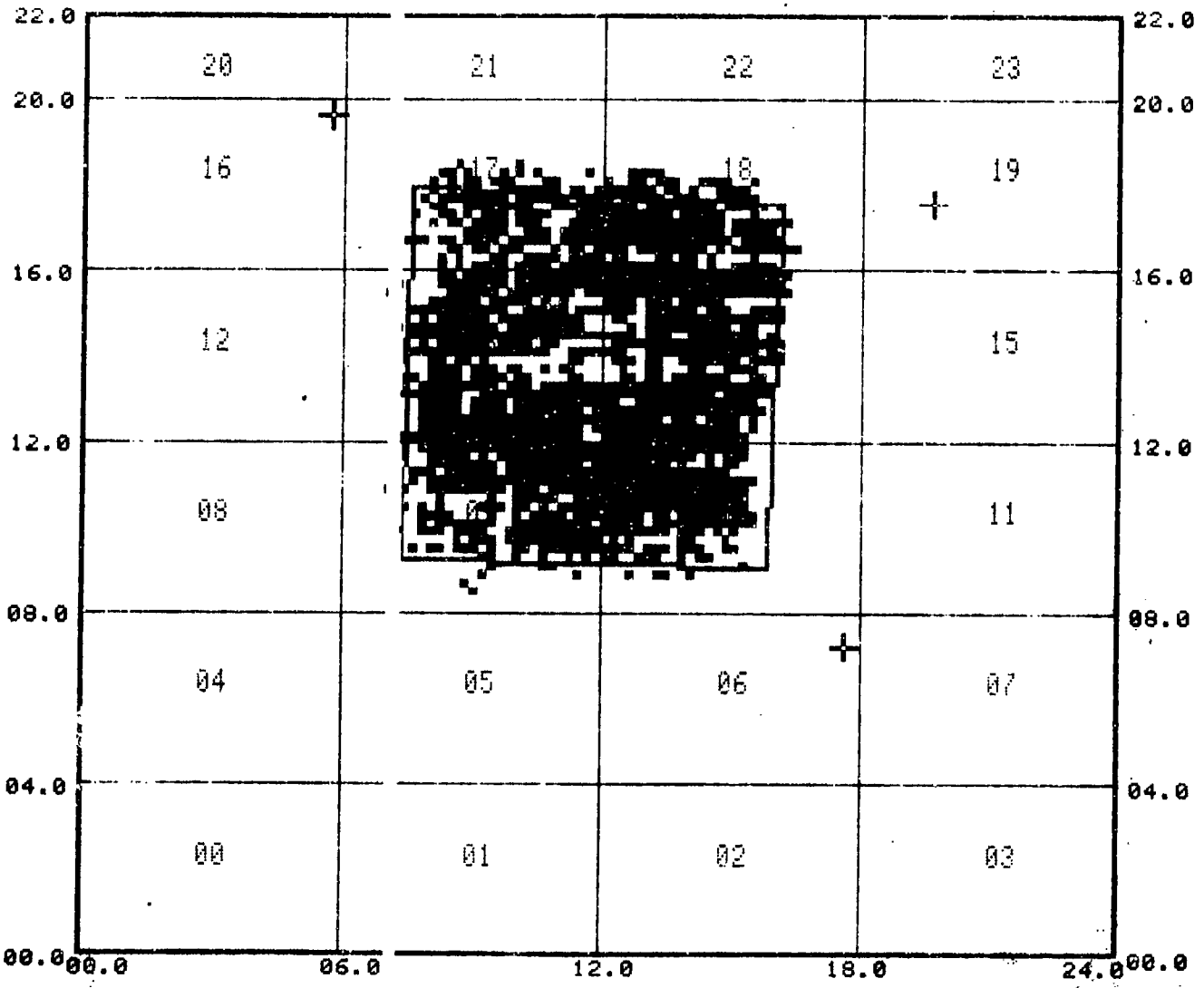

TARGET POINTS
X = 17.6, Y = 07.2
X = 19.6, Y = 17.5
X = 05.7, Y = 19.6

Figure 86. Data Display of Compaction State #3 With 20 Percent or Greater Amplitude Discrimination

1. LOCATION GD FT WORTH
2. INSPECTOR BELL
3. DATE/TIMER READING 5 20-83
4. ACFT TYPE/TAIL NO. 0 90 DEG, 180 F
5. PART NAME/SERIAL NO. 15 MIN. VAC, 85 PSI
6. UNIT # - SKIN # 10
7. TAPE RECORD # 1
8. CELL SIZE SQ = .2

DISCRIMINATION L MITS
1ST GATE AMP. BELOW
020 PER ENT

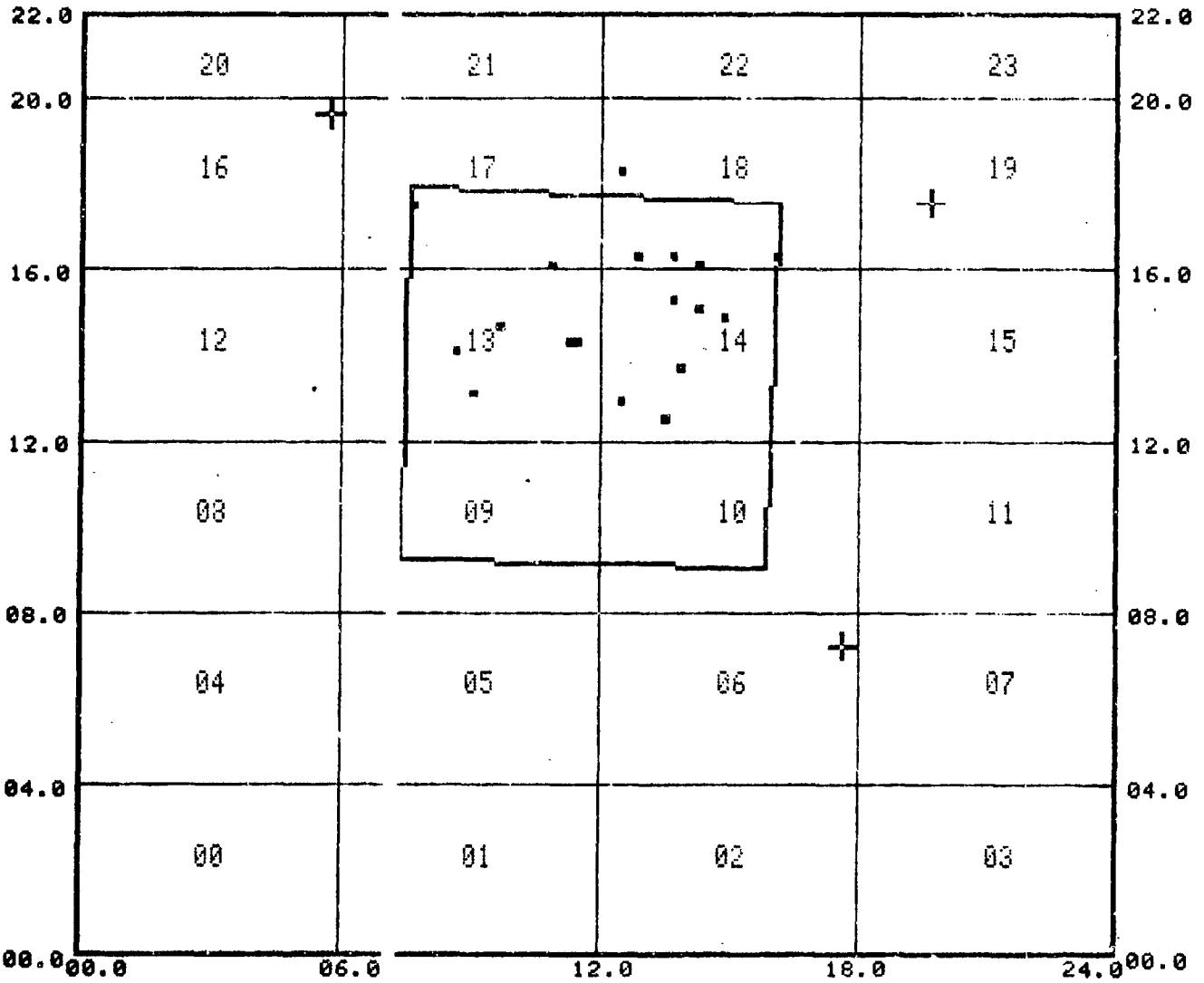

TARGET POINTS
X = 17.6, Y = 07.2
X = 19.6, Y = 17.5
X = 05.7, Y = 19.6

Figure 87. Data Display of Compaction State #3 With Less Than 20% Amplitude Discrimination

returning from the back surface into percentages of full scale. For instance, D. S. 3d (Figure 80) shows the amount of data whose returning amplitudes were in excess of 80 percent full scale for a gain setting of 67 dB while D. S. 3e (Figure 81) shows the data having amplitudes beneath 80 percent. In presenting the data in this form, one can assess what percentage of full scale is representative of the average amplitude. For example, in compaction state 2 we find the average amplitude lies at approximately 55 percent of full scale for a gain level of 67 dB. For the sake of comparison, we can convert the percentile corresponding to the average amplitude to dB and adjust the gain levels accordingly. Recalling that a 1 dB change in gain equates approximately to a 5 percent change in amplitude, the normalized gain levels for compaction states 2, 3, 4, and 5 would be 64.8, 62.0, 61.8 and 59.7 dB, respectively. Let's examine this information more closely. Compaction states 2, 3, and 4 all have a 15 minute dwell for their respective temperatures of 71C, 82C, and 93C (160, 180, and 200F). The normalized gain levels suggest that consolidation is enhanced as the dwell temperature in increased. However, it does so asymptotically such that there is little compaction benefit in a 93C (200F) over a 82C (180F) dwell temperature especially since a higher temperature would also lead a higher matrix advancement state. On the other hand, by extending the dwell period to 1 hour at a temperature of 71C (160F) as was the case for compaction profile 5, we see a significantly

augmented consolidation state.

The LAMINATE scans for compaction profile 2, 3, 4, and 5 are found in Figures 88 through 94, respectively). Data sheet Figure 88, represents the apparent void content (real and artifact) throughout the entire thickness of the laminate while the sequential sheets contain the flaw data for specified thickness modules found under the heating "discrimination limits." We have found that a majority of the data shown on data sheet "m" for each compaction state is primarily artifact. Due to surface irregularity and tackiness and their interaction with the scanning transducer, anomalies (historically) appear within module 0-13 (first 1.3 μsec or 10 plies) and module 55-63 (5.3-6.3 μsec or bottom six plies). For this reason an additional data sheet ("r") has been included and contains the same flaw information as "m" with the exception of the two anomalous modules, which have been eliminated. Inspection of what is known to be the true macroscopic void state unequivocally demonstrates that the panels exposed to the lower temperature of 71C (160F) contain none or significantly fewer voids than the panels subjected to the higher dwell temperatures.

In conclusion, we have found that for a unidirectional thick laminate, compaction profile 1 [15 minutes at 71C (160F)] under vacuum plus 0.586 MPa (85 psi) not only consolidates well but will also result in a near void-free pre-cured laminate.

A cured panel of 5208/T300 (PP-21) was sectioned and inspected with ISIS to compare to the Convair through C-scan. The ISIS scan matched very well with the through C-scan and gave additional evidence of void distribution through the thickness. Figures 95 through 99 show the total C-scan and sections through the thickness. Note that the majority of the voids are in the bottom third of the panel (nearest the tooling surface). This observation

1. LOCATION GD FT WORTH
2. INSPECTOR BELL
3. DATE/TIMER READING 5 20-83
4. ACFT TYPE/TAIL NO. 0 90 DEG, 180 F
5. PART NAME/SERIAL NO. 15 MIN. VAC, 85 PSI
6. UNIT # - SKIN # 10
7. TAPE RECORD # 002
8. CELL SIZE SQ = .2

9. CALIBRATION LIST #1 LAMINATE
10. REF STD.NO. N/A
11. TRANSDUCER TYPE .5 ANAMETRIC
12. TRANSDUCER FREQ (MHZ 5
13. BUFFER DELAY .75" AC YLIC
14. REP RATE (KHZ) 3
15. P/R FREQ (MHZ) BB
16. PULSE LENGTH (DAMPIN) 1
17. VIDEO REJECT 3
18. FILTER LO
19. DIFFERENTIAL ON
20. GAIN COARSE 70
21. GAIN FINE 0
22. DEC START LEFT OF CR
23. DEC SLOPE (%) 18
24. RANGE 2
25. MATL VEL 0.0
26. DELAY COARSE 0-4
27. DELAY FINE 2.7
28. FRONT SURF GATE (.1 SEC UNITS) 7
29. LOST COUPLING VALUE .1 USEC UNITS) 70
30. MAX STEP (PLIES) 6

COMMENTS:
31. NONE
32. REJ =3, GAIN= 84 DB OR WAVE FORMS
33.
34.

Figure 88. Data Sheet for Laminate Scan Parameters of Compaction State #3

1. LOCATION GD FT WORTH
2. INSPECTOR BELL
3. DATE/TIMER READING 5 20-83
4. ACFT TYPE/TAIL NO. 0 90 DEG, 180 F
5. PART NAME/SERIAL NO. 15 MIN. VAC, 85 PSI
6. UNIT # - SKIN # 10
7. TAPE RECORD # 002
8. CELL SIZE SQ = .2

DISCRIMINATION L MITS
NONE

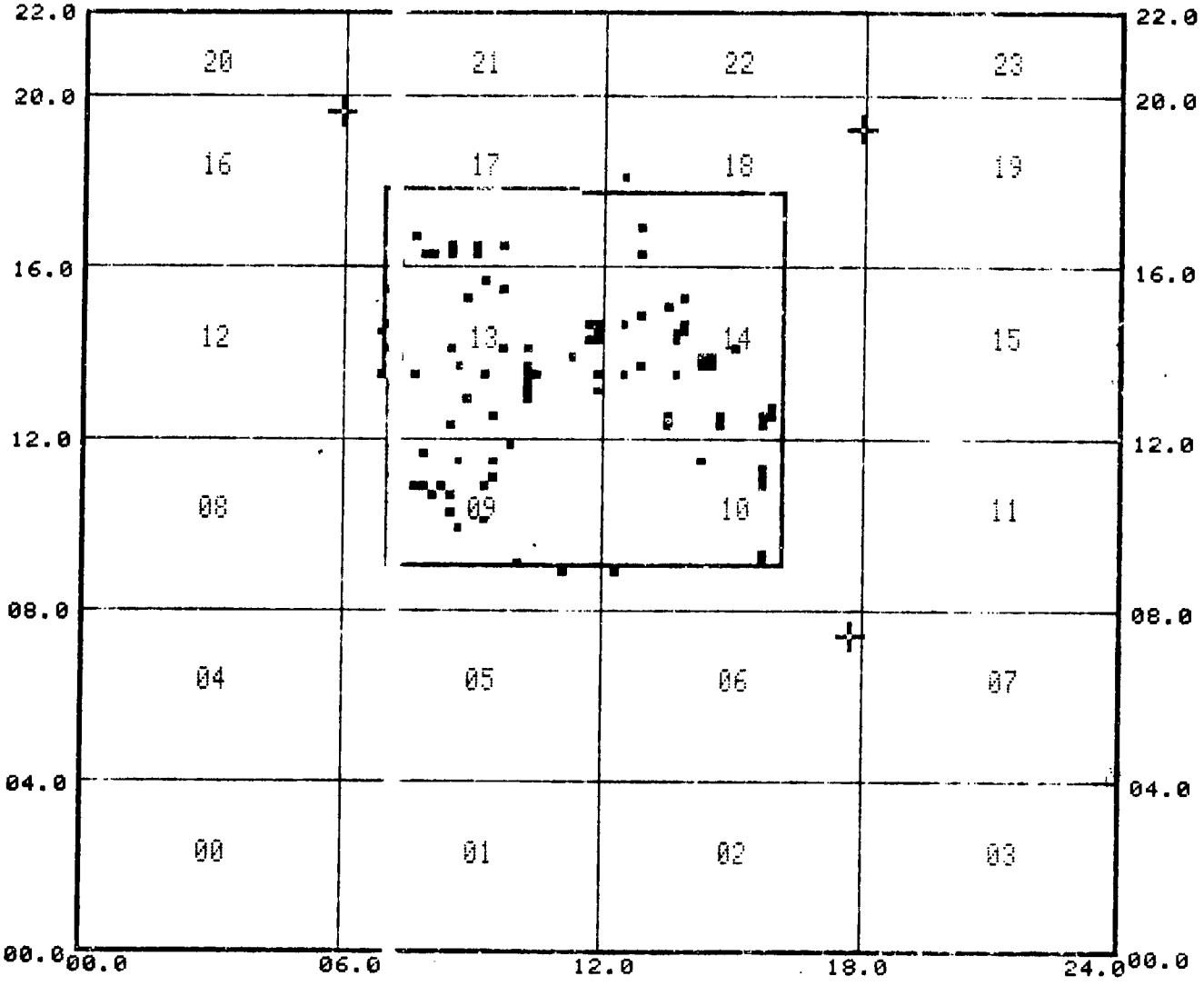

TARGET POINTS
X = 17.7, Y = 07.4
X = 17.9, Y = 19.2
X = 05.9, Y = 19.6

Figure 89. Apparent Void Content of Compaction State #3 - (Laminate Scan Mode - Discrimination None)

1. LOCATION GD FT WORTH
2. INSPECTOR BELL
3. DATE/TIMER READING 5 20-83
4. ACFT TYPE/TAIL NO. 0 90 DEG, 180 F
5. PART NAME/SERIAL NO. 15 MIN. VAC, 85 PSI
6. UNIT # - SKIN # 10
7. TAPE RECORD # 002
8. CELL SIZE SQ = .2

DISCRIMINATION L MITS
2ND GATE DPTH RANGE
014 TO 23

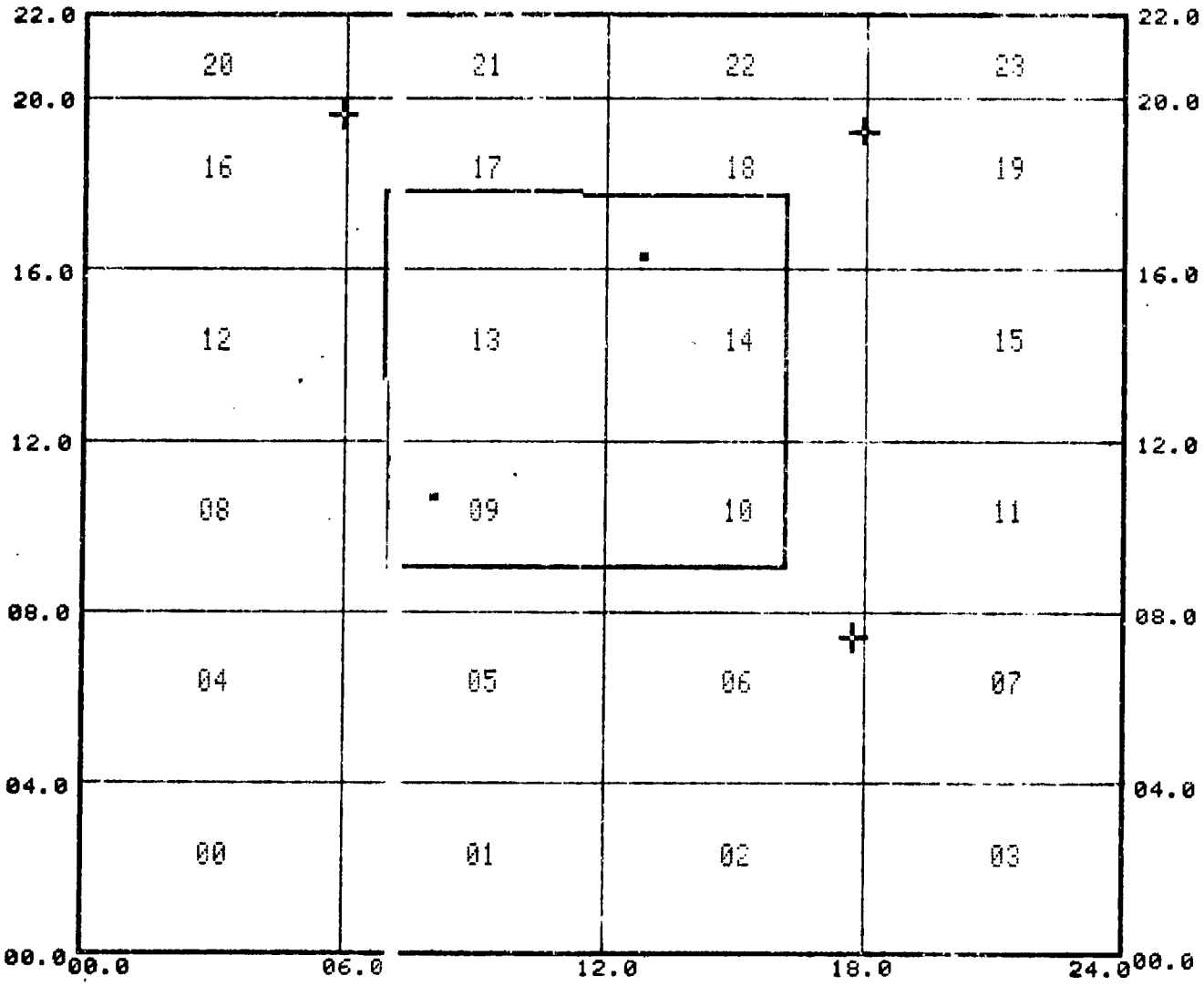

TARGET POINTS
X = 17.7, Y = 07.4
X = 17.9, Y = 19.2
X = 05.9, Y = 19.6

Figure 90. Apparent Void Content of Compaction State #3 Discrimination Depth of 14 to 23 μsec (Laminate Scan)

1. LOCATION GD FT WORTH
2. INSPECTOR BELL
3. DATE/TIMER READING 5 20-83
4. ACFT TYPE/TAIL NO. 0 90 DEG, 180 F
5. PART NAME/SERIAL NO. 15 MIN. VAC, 85 PSI
6. UNIT # - SKIN # 10
7. TAPE RECORD # 002
8. CELL SIZE SQ = .2

DISCRIMINATION L MITS
2ND GATE DPTH RANGE
024 TO 33

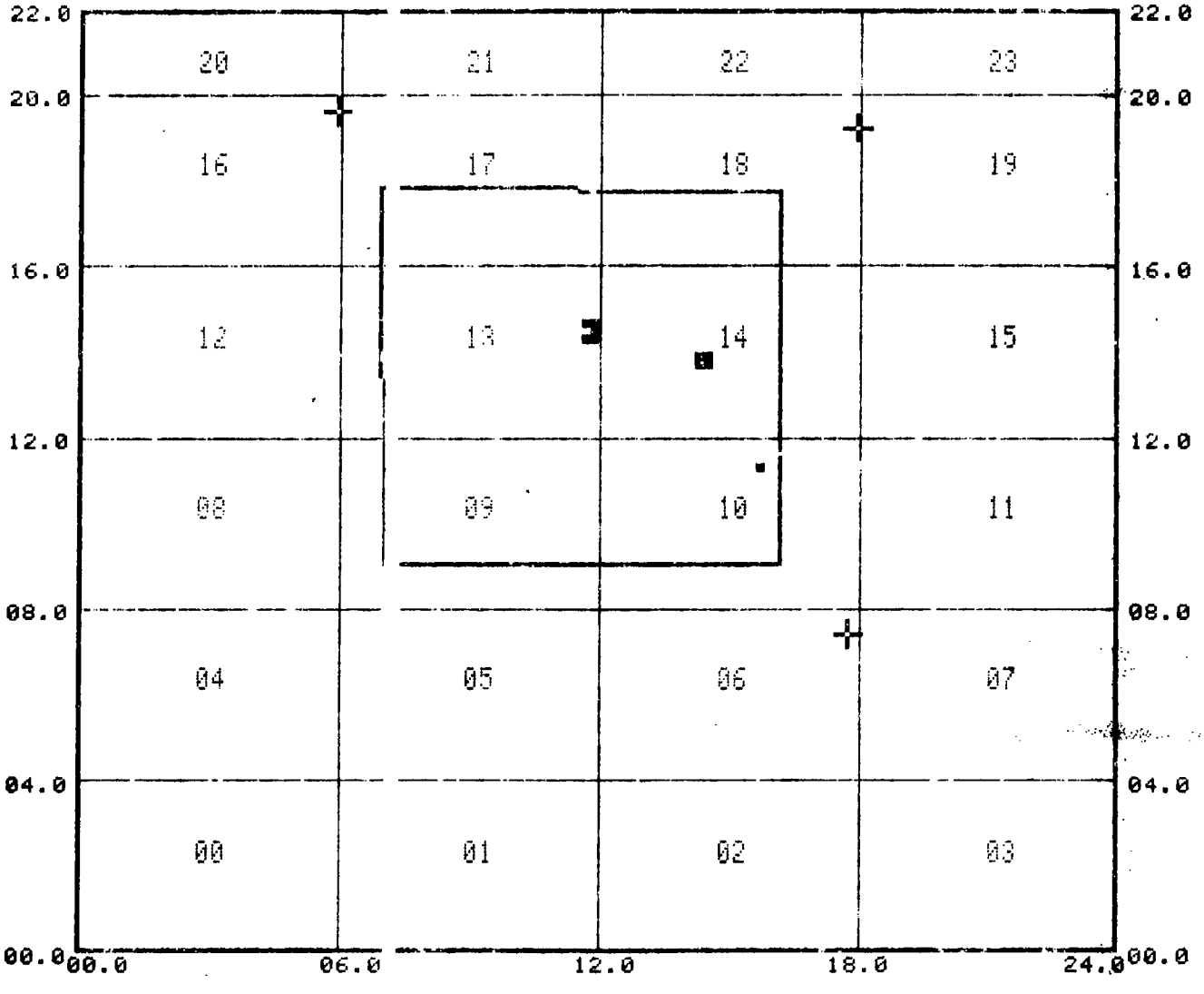

TARGET POINTS
X = 17.7, Y = 07.4
X = 17.9, Y = 19.2
X = 05.9, Y = 19.6

Figure 91. Apparent Void Content of Compaction State #3 Discrimination Depth of 24 to 33 μsec (Laminate Scan)

1. LOCATION GD FT WORTH
2. INSPECTOR BELL
3. DATE/TIMER READING 5 20-83
4. ACFT TYPE/TAIL NO. 0 90 DEG, 180 F
5. PART NAME/SERIAL NO. 15 MIN. VAC, 85 PSI
6. UNIT # - SKIN # 10
7. TAPE RECORD # 002
8. CELL SIZE SQ = .2

DISCRIMINATION L MITS
2ND GATE DPTH RANGE
034 TO 43

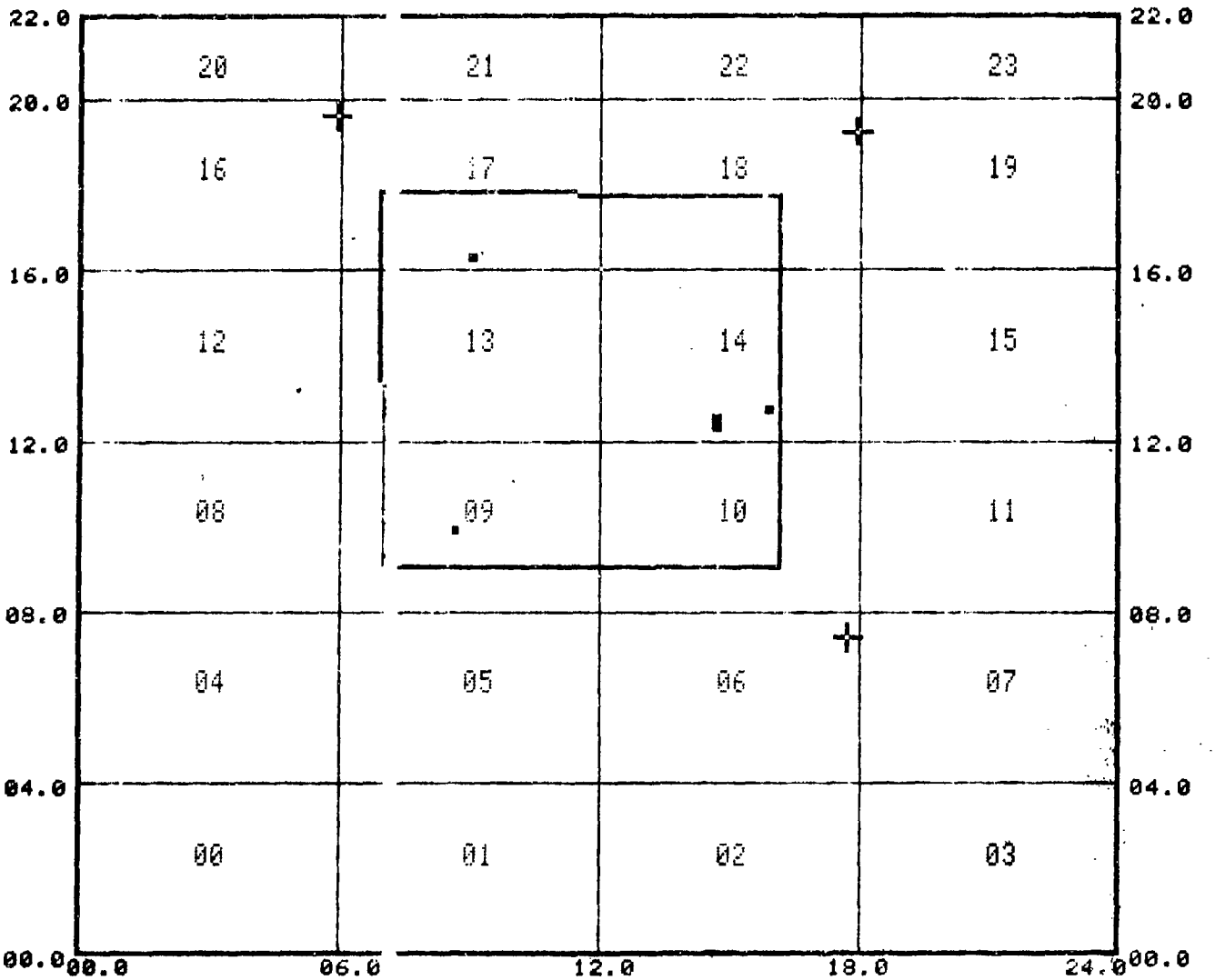

TARGET POINTS
X = 17.7, Y = 07.4
X = 17.9, Y = 19.2
X = 05.9, Y = 19.6

Figure 92. Apparent Void Content of Compaction State #3
Discrimination Depth of 34 to 43 μsec

1. LOCATION GD FT WORTH
2. INSPECTOR BELL
3. DATE/TIMER READING 5 20-83
4. ACFT TYPE/TAIL NO. 0 90 DEG, 180 F
5. PART NAME/SERIAL NO. 15 MIN. VAC, 85 PSI
6. UNIT # - SKIN # 10
7. TAPE RECORD # 002
8. CELL SIZE SQ = .2

DISCRIMINATION L MITS
2ND GATE DPTH RANGE
044 TO 53

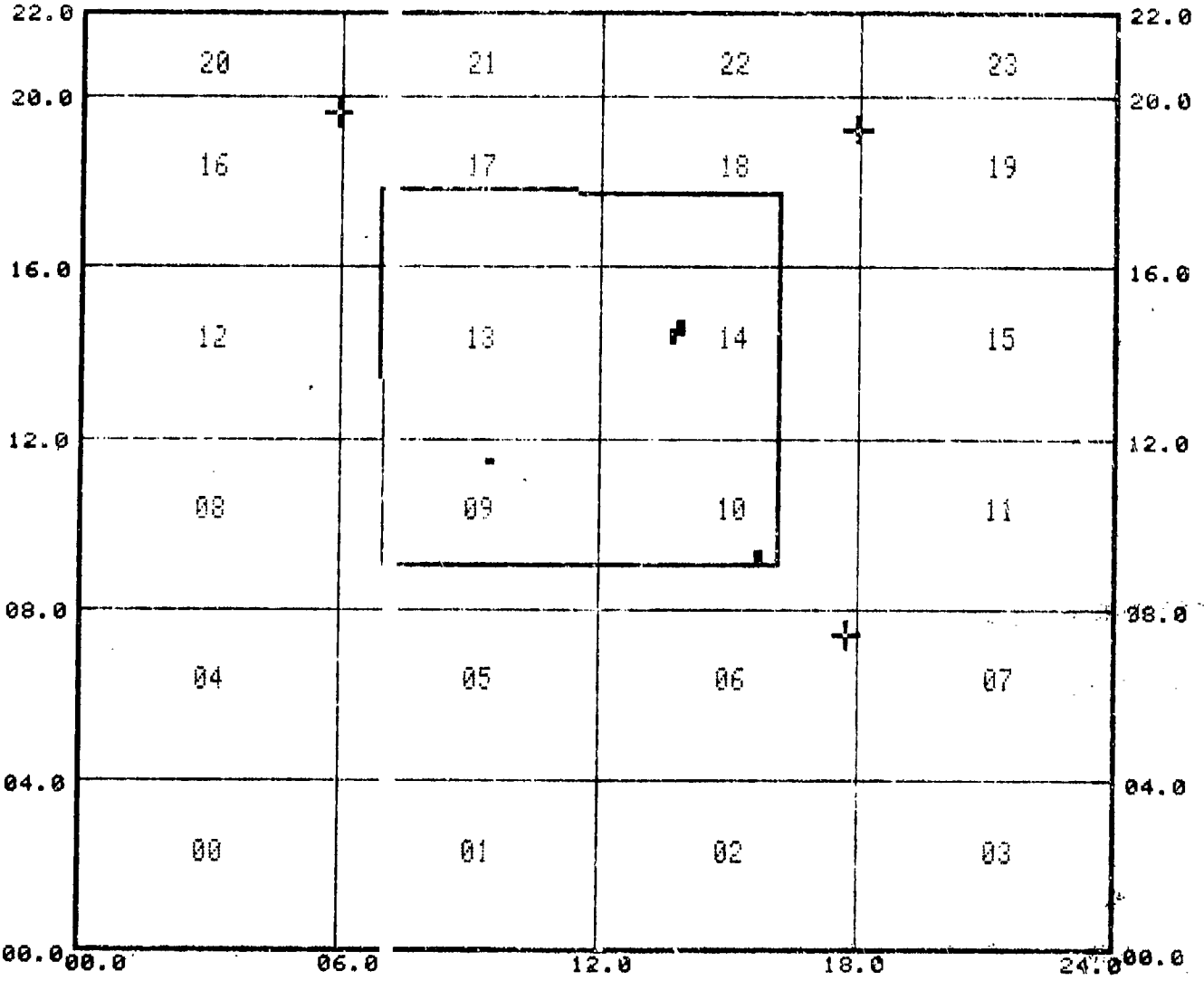

TARGET POINTS
X = 17.7, Y = 07.4
X = 17.9, Y = 19.2
X = 05.9, Y = 19.6

Figure 93. Apparent Void Content of Compaction State #3
Discrimination Depth of 44 to 53 μsec (Laminate Scan)

1. LOCATION GD FT WORTH
2. INSPECTOR BELL
3. DATE/TIMER READING 5 20-83
4. ACFT TYPE/TAIL NO. 0 90 DEG, 180 F
5. PART NAME/SERIAL NO. 15 MIN. VAC, 85 PSI
6. UNIT # - SKIN # 10
7. TAPE RECORD # 002
8. CELL SIZE SQ = .2

DISCRIMINATION L MITS
2ND GATE DPTH RANGE
014 TO 54

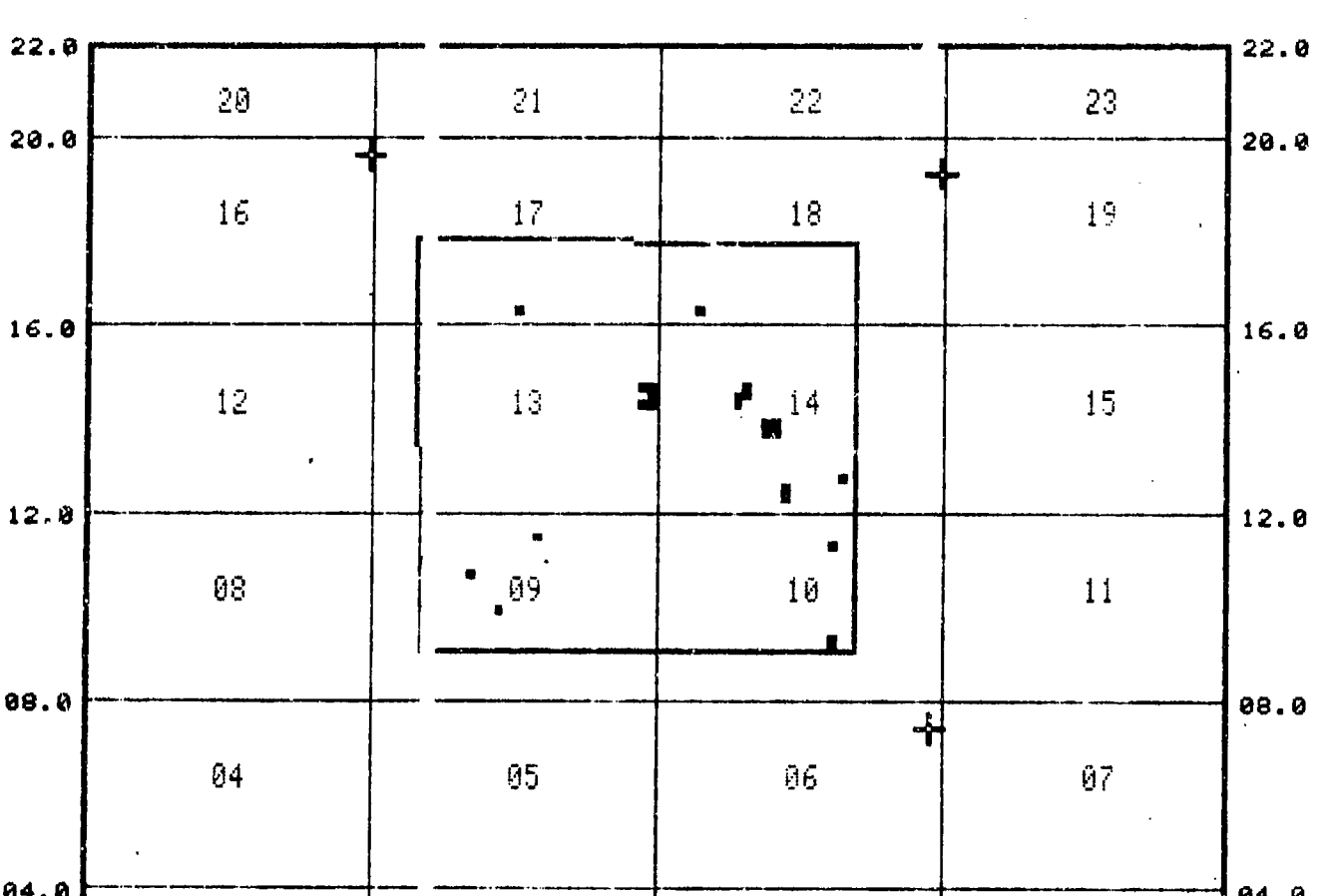

TARGET POINTS
X = 17.7, Y = 07.4
X = 17.9, Y = 19.2
X = 05.9, Y = 19.6

Figure 94. Apparent Void Content of Compaction State #3, Discrimination Depth of 14 to 54 μsec

1. LOCATION GD/FT WORTH
2. INSPECTOR BELL
3. DATE/TIMER READING 4 29/83
4. ACFT TYPE/TAIL NO. 6 PLY LAMINATE
5. PART NAME/SERIAL NO. PP-21
6. UNIT # - SKIN #
7. TAPE RECORD # 2
8. CELL SIZE SQ = .2

DISCRIMINATION L MITS
NONE

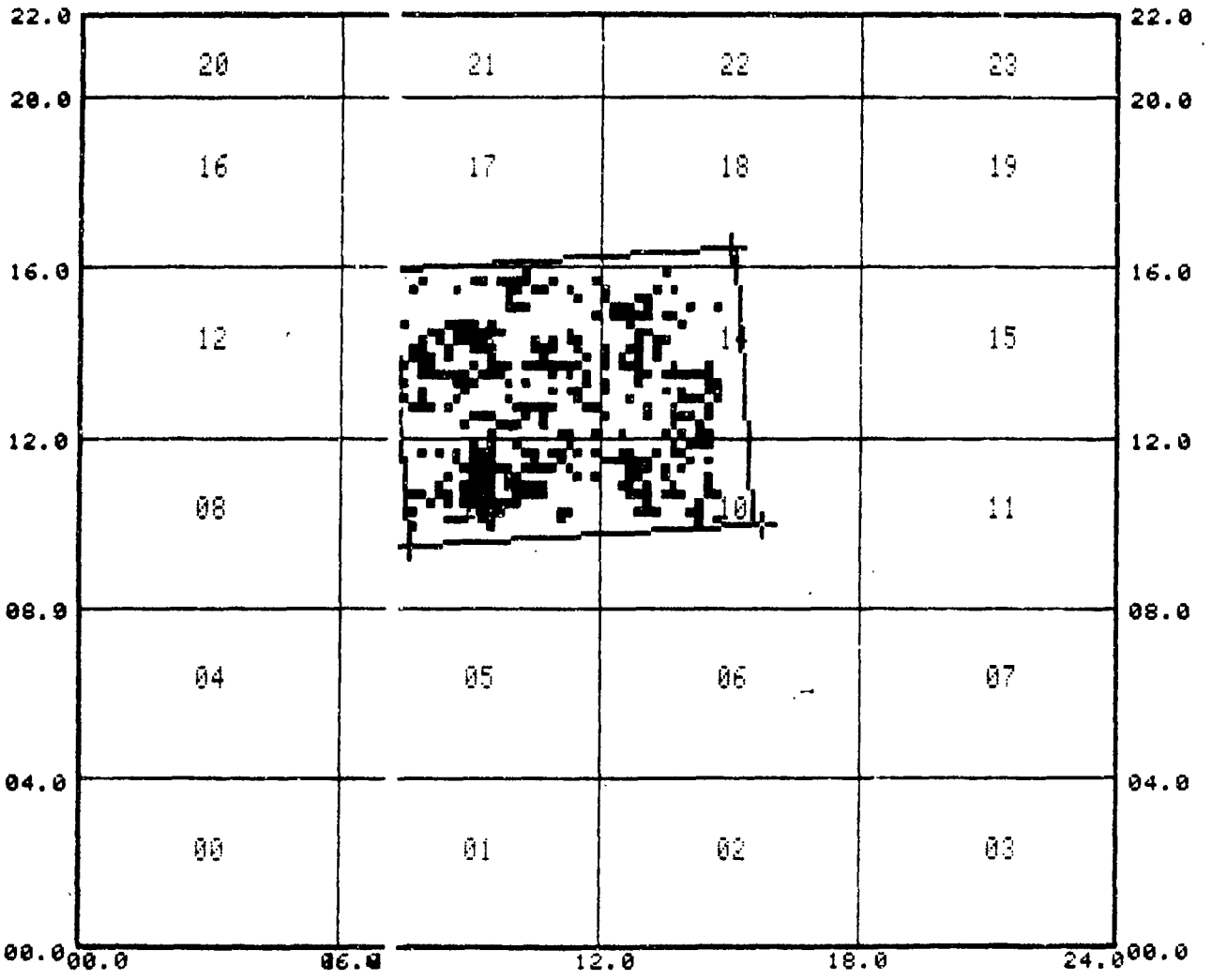

TARGET POINTS
X = 15.7, Y = 09.4
X = 07.6, Y = 09.4
X = 15.0, Y = 16.4

Figure 95. 5208 Laminate (PP-21) ISIS Pulse Echo C-Scan

1. LOCATION GD/FT WORTH
2. INSPECTOR BELL
3. DATE/TIMER READING 4 29/83
4. ACFT TYPE/TAIL NO. 6 PLY LAMINATE
5. PART NAME/SERIAL NO. PP-21
6. UNIT # - SKIN #
7. TAPE RECORD # 2
8. CELL SIZE SQ = .2

DISCRIMINATION LIMITS
2ND GATE DPTH RANGE
009 TO 12

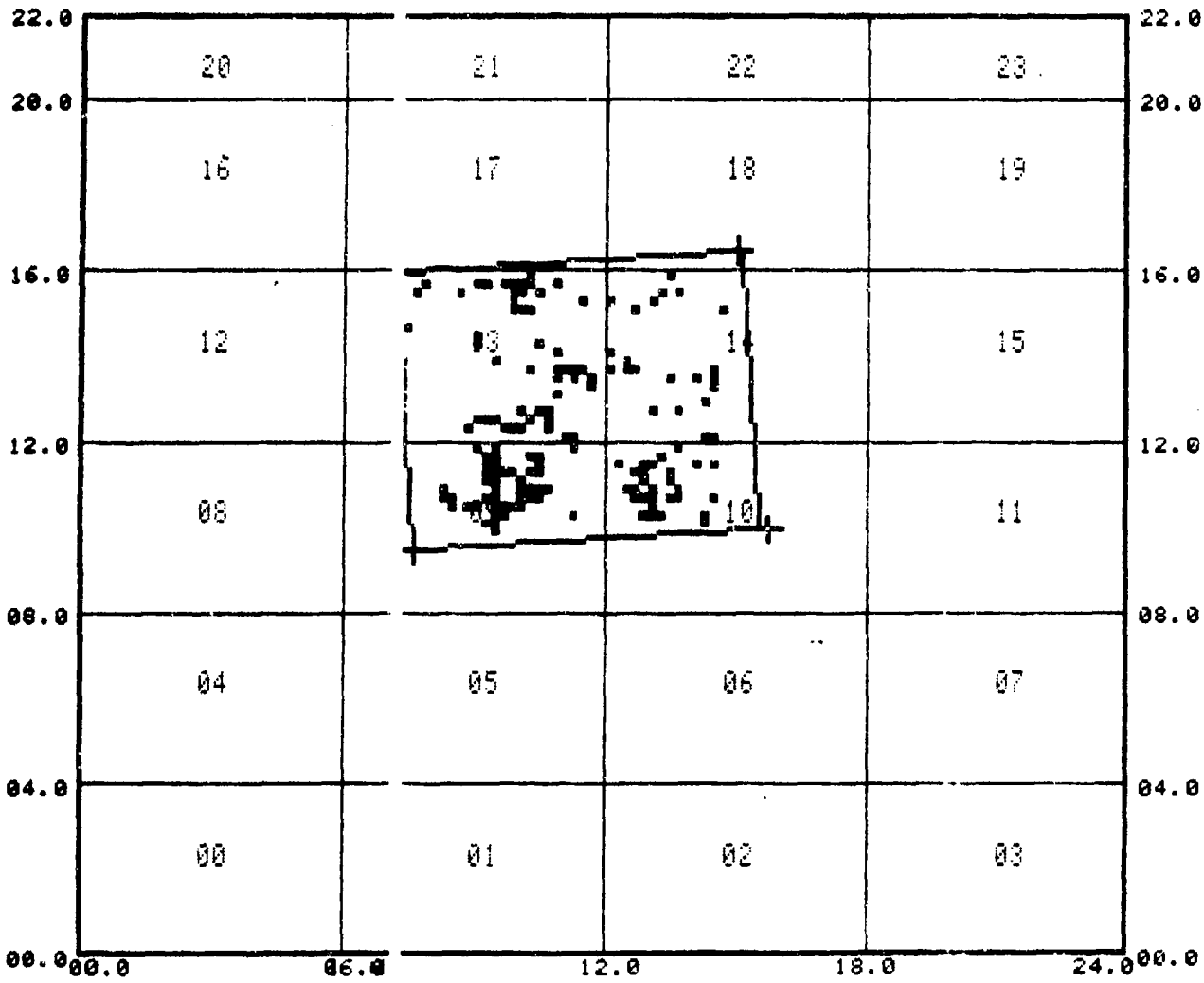

TARGET POINTS
X = 15.7, Y = 09.3
X = 07.6, Y = 09.4
X = 15.0, Y = 16.4

Figure 96. 5208 Laminate (PP-21) ISIS Pulse Echo Scan Discrimination Depth of 9 to 12 µsec

1. LOCATION GD/FT WORTH
2. INSPECTOR BELL
3. DATE/TIMER READING 4 29/83
4. ACFT TYPE/TAIL NO. 6 PLY LAMINATE
5. PART NAME/SERIAL NO. PP-21
6. UNIT # - SKIN #
7. TAPE RECORD # 2
8. CELL SIZE SQ = .2

DISCRIMINATION L MITS
2ND GATE DPTH RANGE
013 TO 23

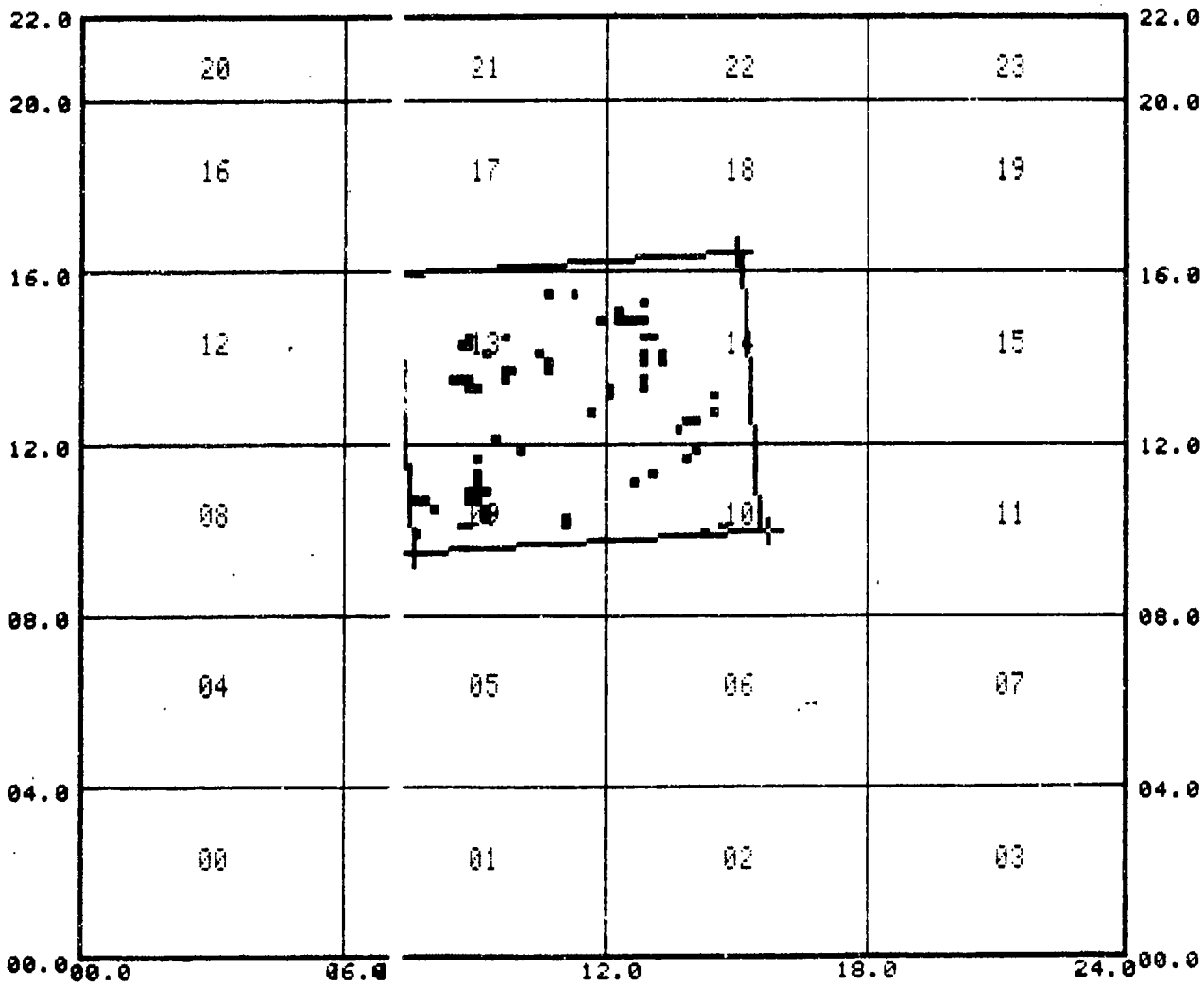

TARGET POINTS
X = 15.7, Y = 09.9
X = 07.6, Y = 09.4
X = 15.0, Y = 16.4

Figure 97. 5208 Laminate (PP-21) ISIS Pulse Echo Scan Discrimination Depth of 13 to 24 µsec

1. LOCATION GD/FT WORTH
2. INSPECTOR BELL
3. DATE/TIMER READING 4 29/83
4. ACFT TYPE/TAIL NO. 6 PLY LAMINATE
5. PART NAME/SERIAL NO. PP-21
6. UNIT # - SKIN #
7. TAPE RECORD # 2
8. CELL SIZE SQ = .2

DISCRIMINATION L MITS
2ND GATE DPTH RANGE
024 TO 34

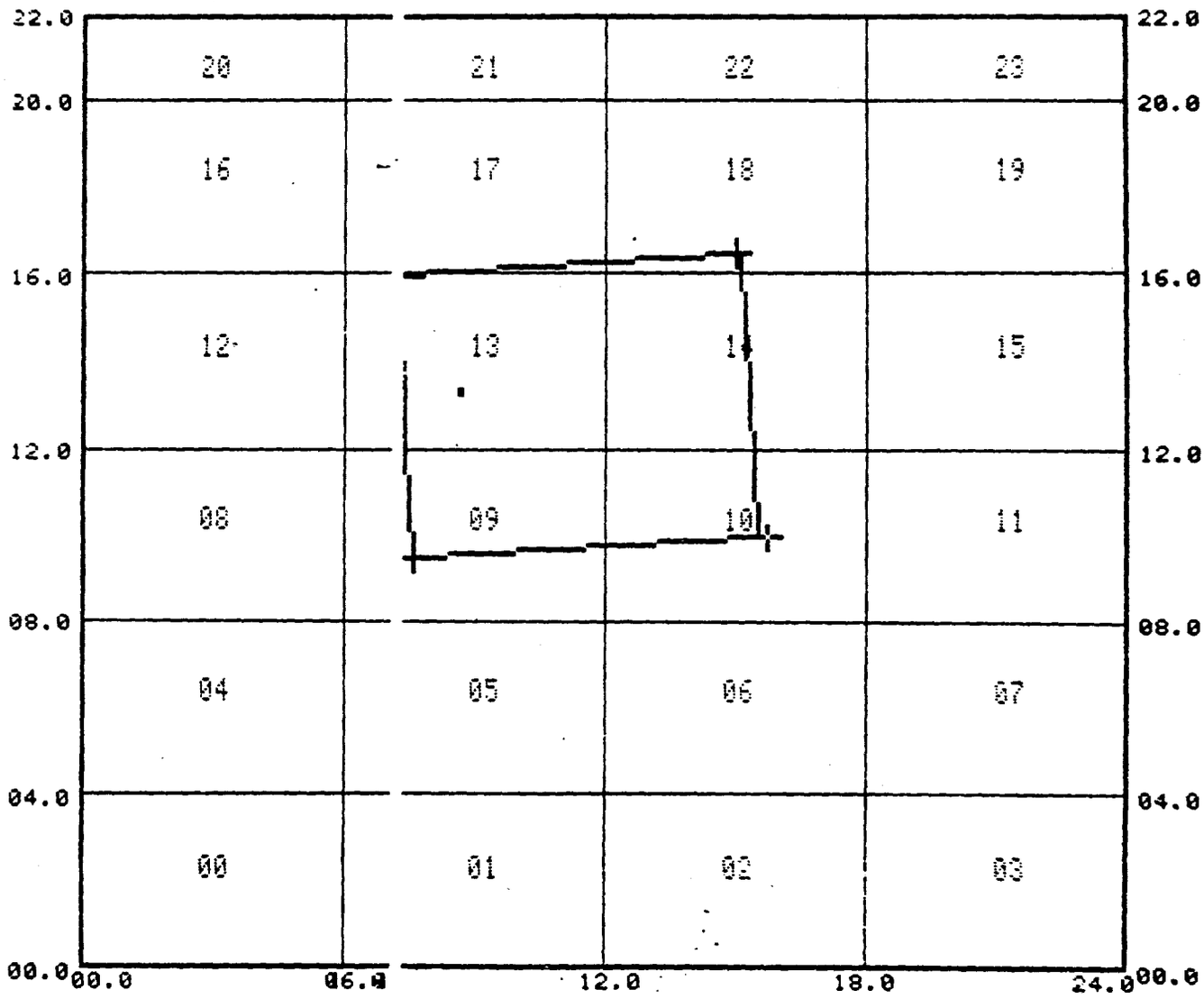

TARGET POINTS
X = 15.7, Y = 09.9
X = 07.6, Y = 09.4
X = 15.0, Y = 16.4

Figure 98. 5208 Laminate (PP-21) ISIS Pulse Echo Scan Discrimination Depth of 24 to 34 µsec

1. LOCATION GD FT WORTH
2. INSPECTOR BELL
3. DATE/TIMER READING 4 29/83
4. ACFT TYPE/TAIL NO. 6 PLY LAMINATE
5. PART NAME/SERIAL NO. PP-21
6. UNIT # - SKIN #
7. TAPE RECORD # 2
8. CELL SIZE SQ = .2

DISCRIMINATION L MITS
2ND GATE DPTH RANGE
035 TO 52

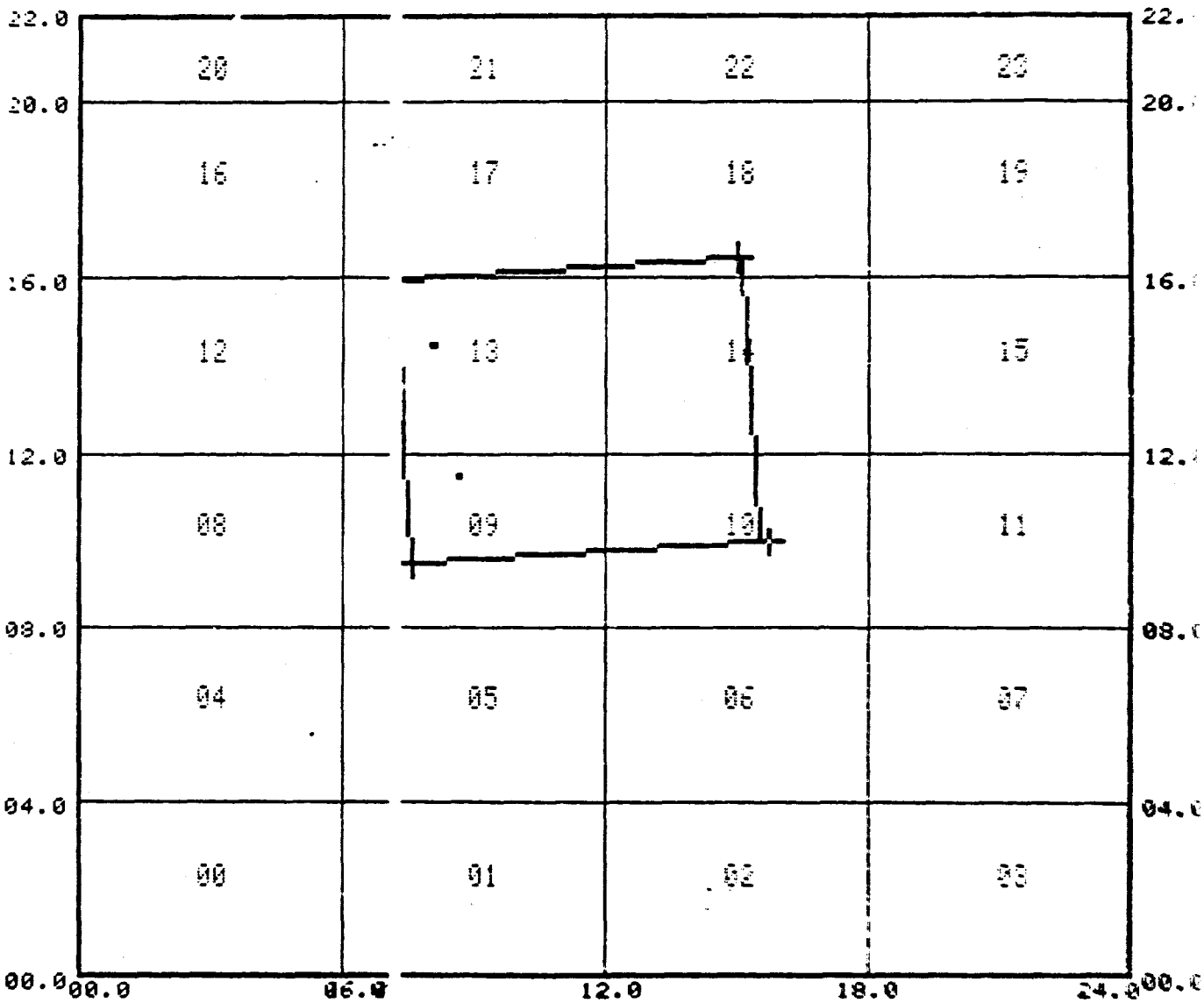

TARGET POINTS
= 15.7, = 04.3
= 07.6, = 03.4
= 17.0, = 16.1

Figure 99. 5208 Laminate (PP-21) ISIS Pulse Echo Scan Discrimination Depth of 35 to 52 µsec From Bottom

appears to be general with all the microsections of 0.61 m by 0.61 m (24 by 24 in), 64 ply T-300/5208 laminates.

2.7.3 TACK TENSION TESTING. It became apparent during the process development phase of this program that there appeared to be significant differences in tack between Narmco's 5208/T-300 and Fiberite's 1076E prepreg. It was hypothesized that the increased tack of the 5208 made it difficult to remove mechnically entrapped air pockets established during the lay up operations.

A method was devised whereby we could get a relative idea of the level of prepreg tack. Two 10 ply, 0°, 90° stacks of prepreg were placed between two flatwise tension blocks and loads of 0.103 and 0.689 MPa (15 and 100 psi, respectively) were applied to each set of blocks for a period of 5 minutes at room temperature. The blocks were removed from the press and immediately subjected to tension testing. A significant difference in tack tension was noted between 5208/T-300 prepreg and 3502/AS and 1076E prepreg.

Figure 100 shows the flatwise tension blocks used and data associated with loading at 0.103 MPa and 0.596 MPa (15 and 100 psi, respectively). The data shows a difference of 2 to 6 times higher tack tension for 5208/T-300 at ambient temperature than for the other two materials tested.

2.8 VOID ETIOLOGY

To accurately model cure behavior and improve laminate quality, it is crucial to understand void etiology.

Review of photomicrographs of laminate cross-sections from this program and from the F-16 Production Program indicated that voids and porosity occurred between the ply interfaces of the laminates. This suggested that some kind of a surface condition of the prepreg was involved in the void forming

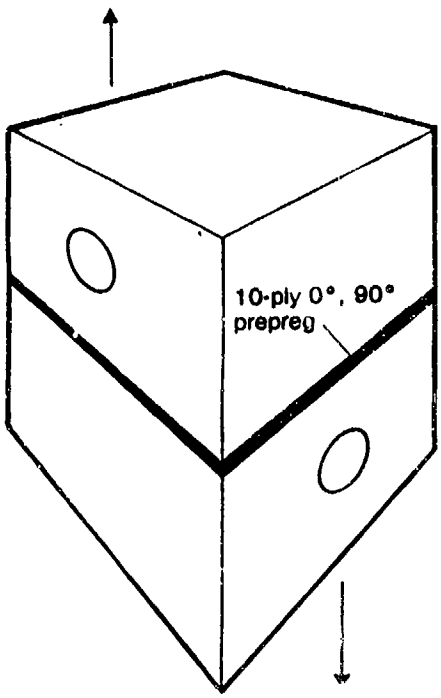

Material	0.103 MPa (15 psi) Load Applied		0.586 MPa (100 psi) Load Applied	
	MPa (psi) at Separation		MPa (psi) at Separation	
5208/T-300 Batch 1864	0.159	(23)	0.496	(72)
3502/AS H-1957	0.050	(7.2)	0.097	(14)
1076E C2-347	0.024	(3.5)	0.303	(44)

Figure 100. Prepreg Flatwise Tack Tension Data

process. Although the initial model for void formation involved heterogeneous nucleation about fibers, the photomicrographic records support a different process. Accordingly, alternate models were considered.

One of the candidate models involved moisture diffusion into a mechanically formed void or pocket. It was hypothesized that during cure the moisture in the void created a pressure that inhibited the flow of resin into the void. This mechanism required maintenance of the mechanical condition that originally formed the void. Such conditions could be wrinkles in a ply formed during layup, uneven thickness in the preceeding ply, or ply bridging over surface particulate contamination.

Using this concept, we attempted to purposely create voids in a laminate using 5208/T-300 prepreg. A 30.5 cm by 30.5 cm (12 in by 12 in) by 52-ply panel was laid up in a 50 percent relative humidity environment. In plies 20 through 26, small irregularities in ply thickness were created by grinding the surface

of a ply with a 0.159 cm (0.626 in) wide abrasive wheel. This removed material was a "footprint" about 0.152 cm by 0.635 cm (0.06 in by 0.25 in) to a depth of about 0.002 cm (0.001 in). Several such pockets were created, and ply gaps were formed by laying tape so that the edges did not completely touch. In addition, cured neat resin was ground up, passed through a 325-mesh screen, and sprinkled on a ply surface at locations that were 2.5, 5.1, and 7.6 cm (1, 2, and 3 inches) from a panel corner. After cure, the panel was ultrasonically inspected, sectioned, and photomicrographed. Some voids were found in the panel, but not at locations where attempts had been made to create voids. All such locations apparently filled with resin without creating a void. Figure 101 shows the voids which were found and also shows some ply gaps which were filled with resin.

Another candidate model to explain interfacial void formation involved prepreg surface contamination with release agent from the release paper. In the case of release agent contamination creating voids, the surface tensions should be very low. A low surface tension should cause the void nucleation rate to assume its highest value.

To evaluate this possibility, tests were conducted to attempt formation of interfacial voids in a laminate by purposeful contamination of ply faces with silicone. A 0.305 m by 0.305 m (12 in by 12 in) by 52 ply laminate of T-300/5208 was laid up and cured with various means of incorporating silicone. This included hot rolling of release paper onto prepreg, addition of release agent shavings from release paper, and spot contamination with silicone fluid. Layup was performed in a 50 percent relative humidity environment with each ply exposed to the air for about an hour. NDI of the cured laminate did not reveal any voids at the contamination sites. Two factors could contribute to this result. First, the panel size could have been too small to reliably

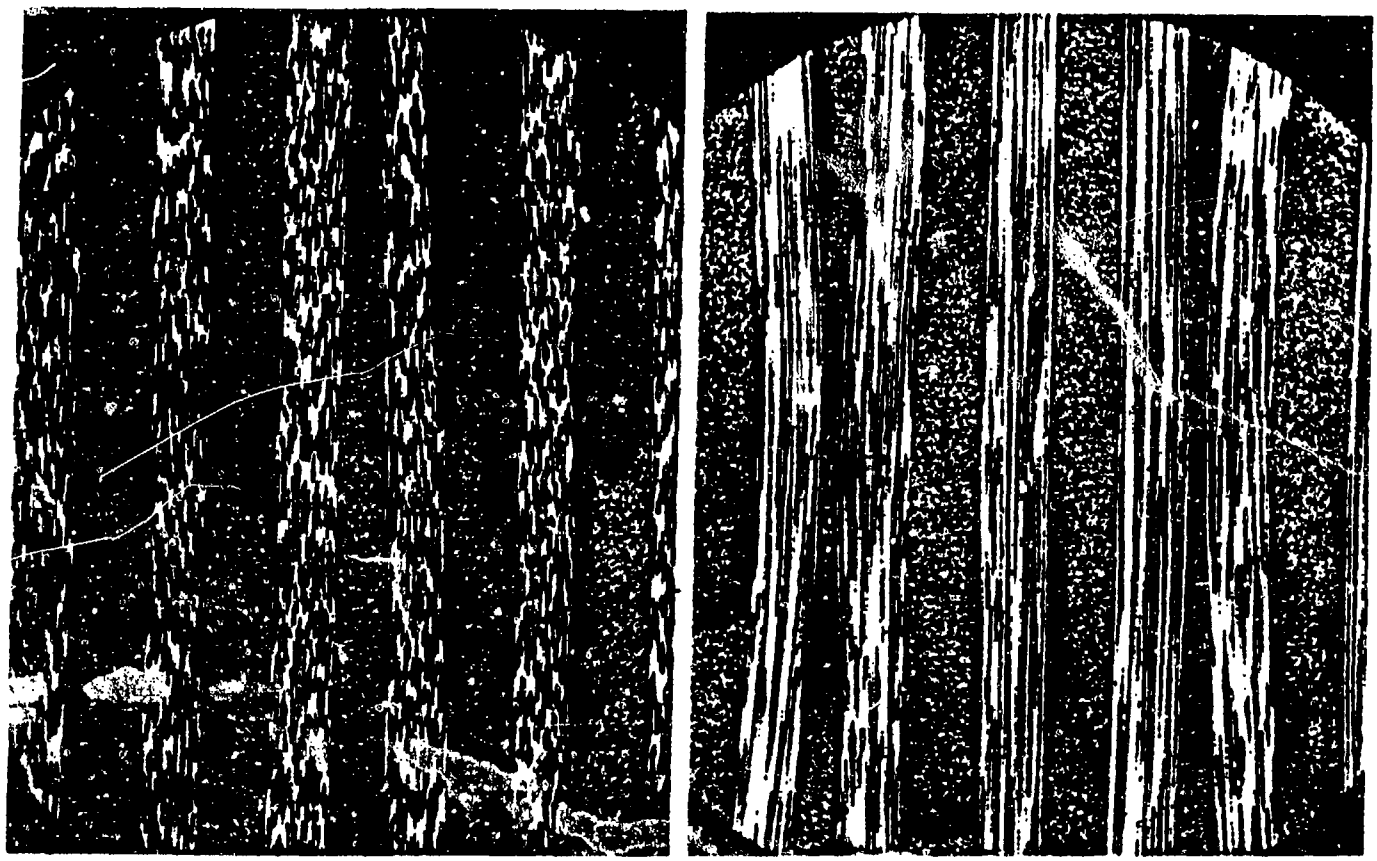

VOIDS AT PLIES 9,15,&17

60X

LARGE RESIN FILLED PLY GAPS

Figure 101. 52 Ply Narmco T-300/5208 Batch 1721

result in voids. Secondly, no particulates, such as airborne dust, were purposely added. Such particulates may be required, in combination with release agent contamination, to achieve void formation by serving as initiation sites with void growth occurring at the interface of the release agent and the particulates.

A laminate in which interfacial voids occurred for unknown reasons has been examined for evidence of silicone contamination. The laminate was cleaved open in the plane of the void and subjected to scanning electron microscopy (SEM) examination. No significant evidence of silicone was detected. The SEM method, however, is probably not sufficiently sensitive to detect very thin layers of silicone contamination.

Tests have selectively examined the possible involvement of three different factors. One factor was release agent contamination of the prepreg surfaces. Laminates have been made with purposeful release agent contamination or prepreg plies, and with prepreg specially made on release-free, clean Mylar. Neither showed significant effects on voids. A second factor that was examined involved DADS curing agent concentrations. Tests of special resin mixtures with different concentrations of DADS showed no significant difference in amount or rate of volatile evolution. Laminates cured with resin that involved no particulate type curing agent also produced interlaminar voids. These results indicate that DADS particles screened toward the surface of the prepreg are not the cause of interlaminar voids. The third factor that has been examined involves surface contamination by dust particles, which could serve as nucleation sites for voids. These investigations also have proved to be negative and do not explain the interlaminar character of voids.

Tests of the silicone treated release paper used with T-300/5208 were conducted to determine if there are conditions that favor loss of some

release agent. Thermomechanical analysis (TMA) using the penetration mode were run to look for evidence of softening. Figure 102 is a plot of probe deflection versus temperature which shows some kind of softening or thickness reduction in the as-received paper. Thinking that this might be the result of moisture loss during test, paper samples were dried at room temperature and at 132C (270F) (see Figures 103 and 104, respectively). Both show an apparent softening at about 38C (100F) showing that the effect was not a result of moisture. It has not been determined whether this was a result of behavior of the silicone or the paper, but the silicone was suspected.

All of the current physical evidence suggest that voids are only formed at ply interfaces, presumably as a result of entrapped air, nucleation of water vapor voids, or combinations of these phenomena. Attempts to purposely cause voids by contaminating prepreg ply faces with silicone release agent were unsuccessful. Attempts to purposely create voids by mechanically introducing air pockets were also unsuccessful.

Because of the nature of the dependence of water vapor pressure on temperature (an exponential relationship), it might be possible that air voids can be stabilized by the introduction of water vapor. This could account for the observations that exposure of air-free prepreg to high humidity does not necessarily result in voids, and that purposely introduced air without high humidity exposure also does not yield voids.

Earlier in this program it was observed that panel size and thickness are related to the probablility of void formation when 0.586 MPa (85 psi) cure pressure is used. An area of at least 0.61 m by 0.61 m (2 ft by 2 ft) and a thickness of at least 60 plies were found to be necessary for occurrence of voids. Because this size panel was expensive to make, the relationship of lower cure pressure and panel size was investigated. Vacuum bag cure was

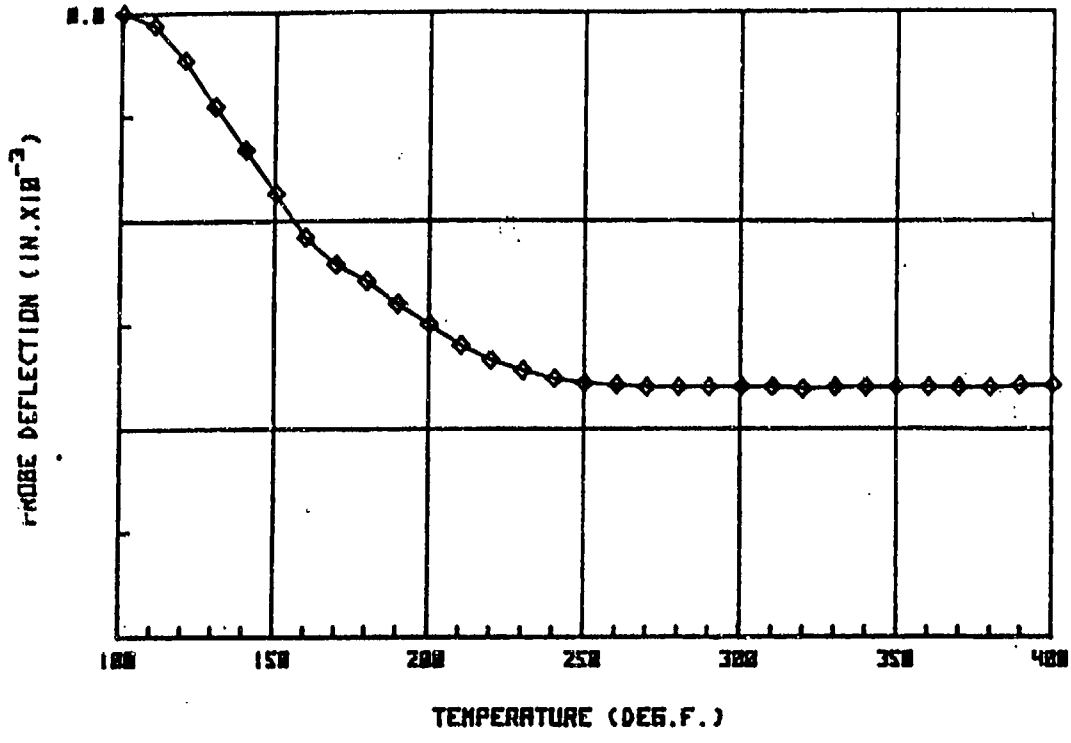

Figure 102. TMA Penetration of T-300/5208 Release Paper, 4 GM, Load #1

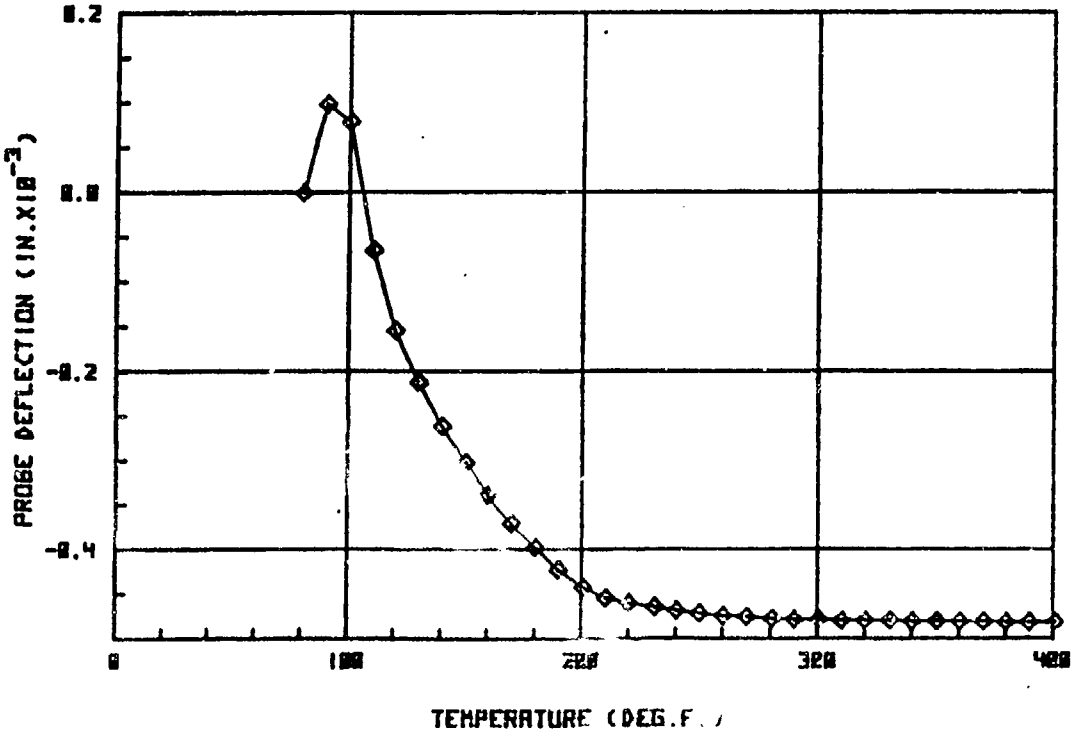

Figure 103. TMA Penetration of T-300/5208 Release Paper Dried 24 Hours at RT, #1

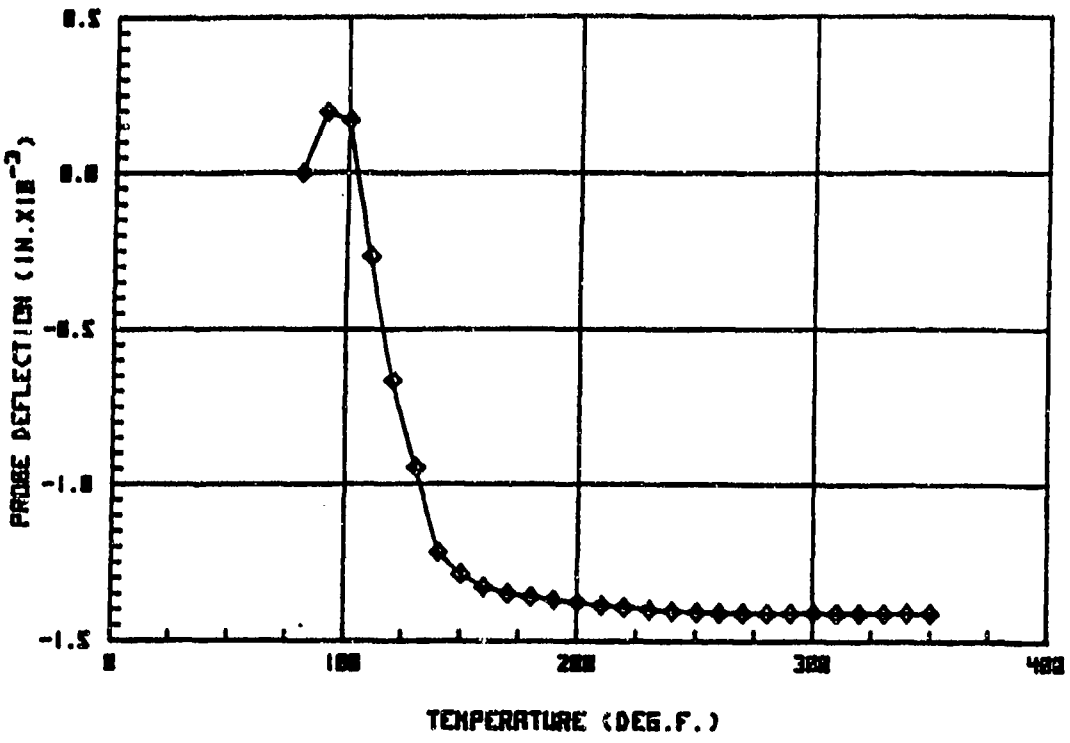

Figure 104. TMA Penetration of T-300/5208 Release Paper Dried 5 Hours at 132C (270F)

found to produce interlaminar voids in unidirectional panels as small as 7.6 cm by 76 cm (3 in by 3 in) by 15 plies. These voids were found to be of the same character as voids occurring in much larger and thicker laminates. The economy of such a small panel, therefore, made it the preferred size and vacuum bag curing the preferred method for studying the cause of interlaminar voids. Fiberite's T-300-976 graphite/epoxy prepreg was selected for all tests because it was found to produce interlaminar voids when vacuum bag cured, even though it was one of the better materials for void-free large laminates when cured at 0.586 MPa (85 psi). The cure cycle used for the vacuum bag cure of all such panels involved heating to 132C (270F) at 1-2C/min. (2-4F/min.), dwelling at 132C (270F) for 90-100 min., heating to 79C (355F) at 1-2C/min. (2-4F/min.), and dwelling at 179C (355F) for 4 hours. Vacuum was maintained throughout the cure.

One of the objectives of these experiments was to determine whether voids form at the ply-to-ply interfaces or whether they form within plies and then migrate to an interface. To make this determination, laminates were cured in both the customary flat position and in a vertical position, i.e., turned on edge. For the vertical position, a void that might form within a ply would have to move horizontally to get to an interface, a direction for which no buoyancy forces would exist. Two 7.6 cm by 7.6 cm (3 in. by 3 in.) by 15-ply unidirectional laminates were vacuum bag cured in the vertical position. In one laminate, the fibers were perpendicular to the floor, but in the other they were parallel. Because earlier vacuum exposures of prepreg immersed in oil had shown that bubbles traveled along fibers, it was thought that perpendicularly oriented fibers in a vertical panel might favor buoyant void removal from the top edge of the panel. However, photomicrographic examinations showed no significant void differences between horizontally and vertically cured panels or between the two vertically cured panels with the different fiber orientation. In the vertically cured panels, there was no difference in void distribution from the bottom to the top edge. This indicated that there was no buoyantly induced void movement. Altogether, the interfacial voids in the vertically cured panels indicated that the voids form at the interfaces rather than forming inside a ply and then migrating to an interface.

Because all photomicrographic evidence indicated that voids form and remain at the ply-to-ply interfaces, a series of experiments were initiated to identify the factor(s) that cause interfacial voids. One of the first candidate causes examined was air entrapped between the plies during layup. It was hypothesized that such air pockets could become stabilized against collapse by the autoclave cure pressure through the process of moisture diffusion into the air pockets.

The first attempt to evaluate layup entrapped air involved a "belljar" de-aeration cycle. A laminate with a vacuum bag over it was covered with a belljar, as indicated by Figure 105, and vacuum was drawn above and below the bag. Vacuum above the bag was drawn at a slightly faster rate so that the bag "floated" and exerted no compacting force on the laminate. The laminate was heated for 45 minutes at 82C (180F) in this condition. Then the vacuum above the bag was vented, the tool was placed in a cavity press, and 0.586 MPa (85 psi) compacting pressure was applied at 82C (180F). Then the pressure was removed and the laminate was vacuum bag cured. Photomicrographs showed extensive interlaminar voids, as shown by Figure 106.

Post-mortem explanations suggested that tack of the prepreg had locked entrapped air between the plies and that a vacuum environment was not adequate to pull this air out of the layup. Therefore, it was considered that layup and bagging of a laminate in a vacuum environment would be necessary to prove the role of entrapped air. This was accomplished using the belljar setup indicated in Figure 107. The 15 plies of the laminate were placed in a fanned arrangement with a layer of TX-1040 release coated fabric between each ply. A belljar was placed over the fan of material, and a vacuum was drawn so that there could be no air between the plies. Then a remote manipulator rod was used to withdraw the TX-1040 layers and to tamp down the plies. Remote rods were then used to position a vacuum bag over the layup and to seal it in place. Then the belljar was vented, and a leak-check indicated no leaks. The laminate was vacuum bag cured then. Photomicrographs showed that this panel also contained interlaminar voids. The experiment was repeated except that an 0.586 MPa (85 psi) compaction step was added just prior to vacuum-bag cure. The thought was that any void could be stabilized by diffused moisture, whether it was filled with air or not. The compaction

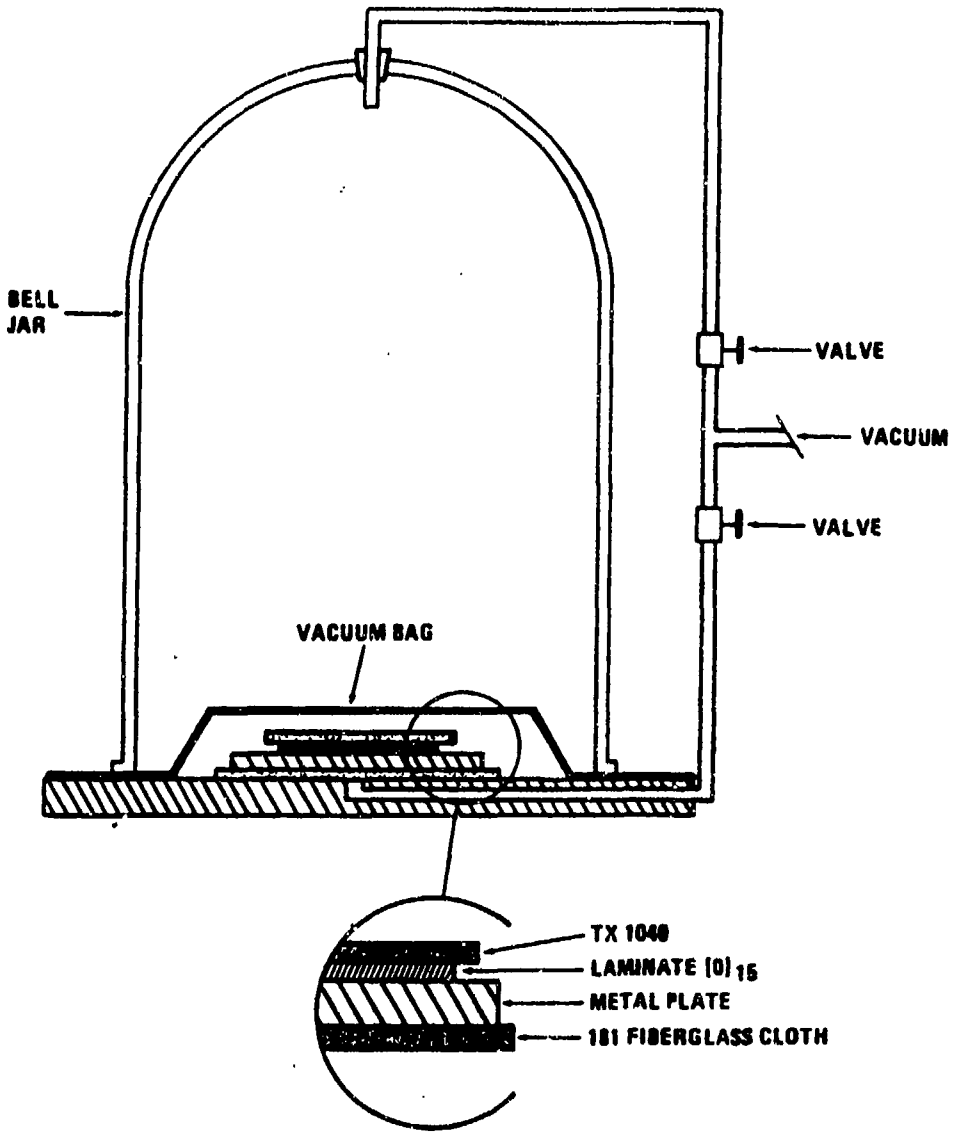

PROCESS STEPS:

(1) VACUUM PULLED ABOVE AND BELOW BAG

(2) LAMINATE HELD AT 180°F FOR 45 MINUTES

(3) VACUUM ABOVE BAG VENTED, THEN HELD FOR 45 MINUTES

(4) LAMINATE COMPACTED AT 85 PSI 180°F FOR 45 MINUTES

(5) LAMINATE VACUUM BAG CURED AT 350°F

Figure 105. Vacuum Jar Deaeration Cycle

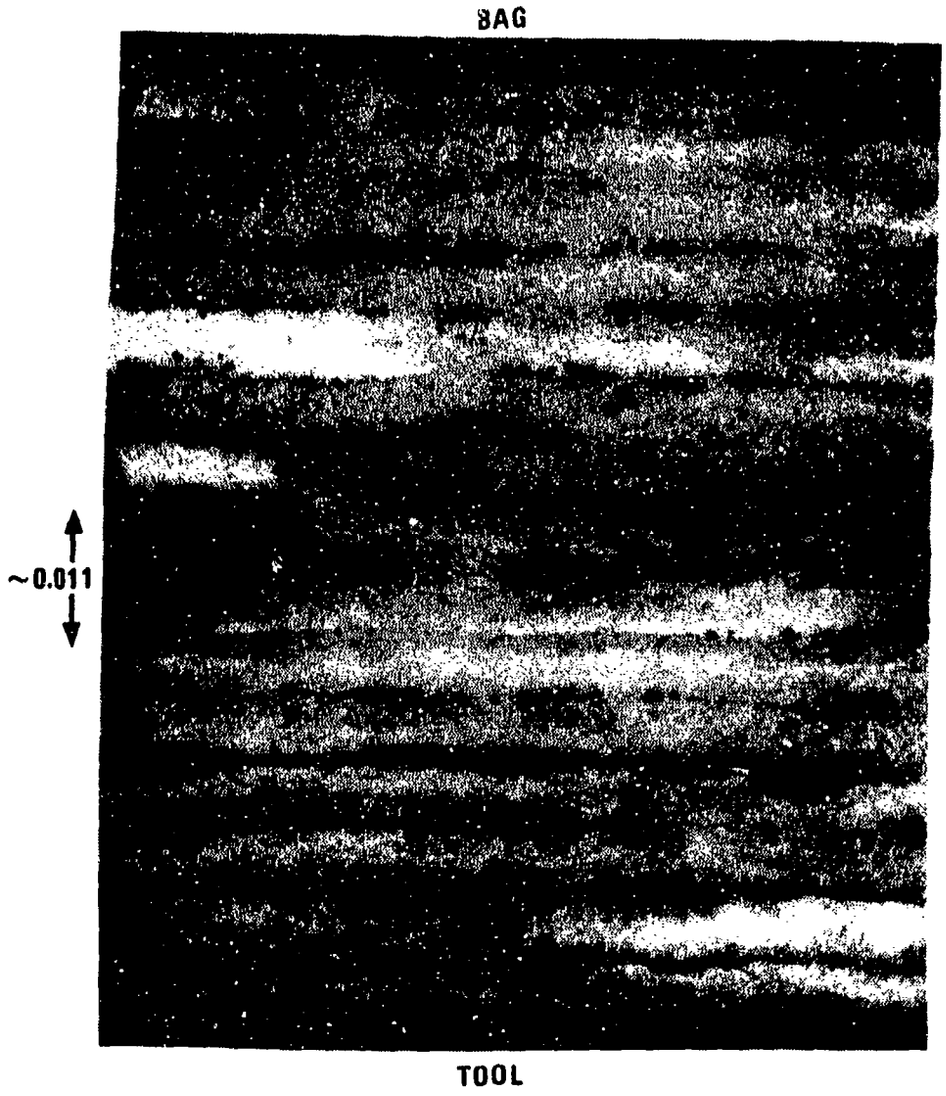

PROCESS STEPS:

(1) VACUUM PULLED ABOVE AND BELOW BAG

(2) LAMINATE HELD AT 180°F FOR 45 MINUTES

(3) VACUUM ABOVE BAG VENTED, THEN HELD FOR 45 MINUTES

(4) LAMINATE COMPACTED AT 85 PSI AND 180°F FOR 45 MINUTES

(5) LAMINATE VACUUM BAG CURED AT 350°F

Figure 106. Photomicrograph of Interlaminar Voids After Vacuum Bag Deaeration

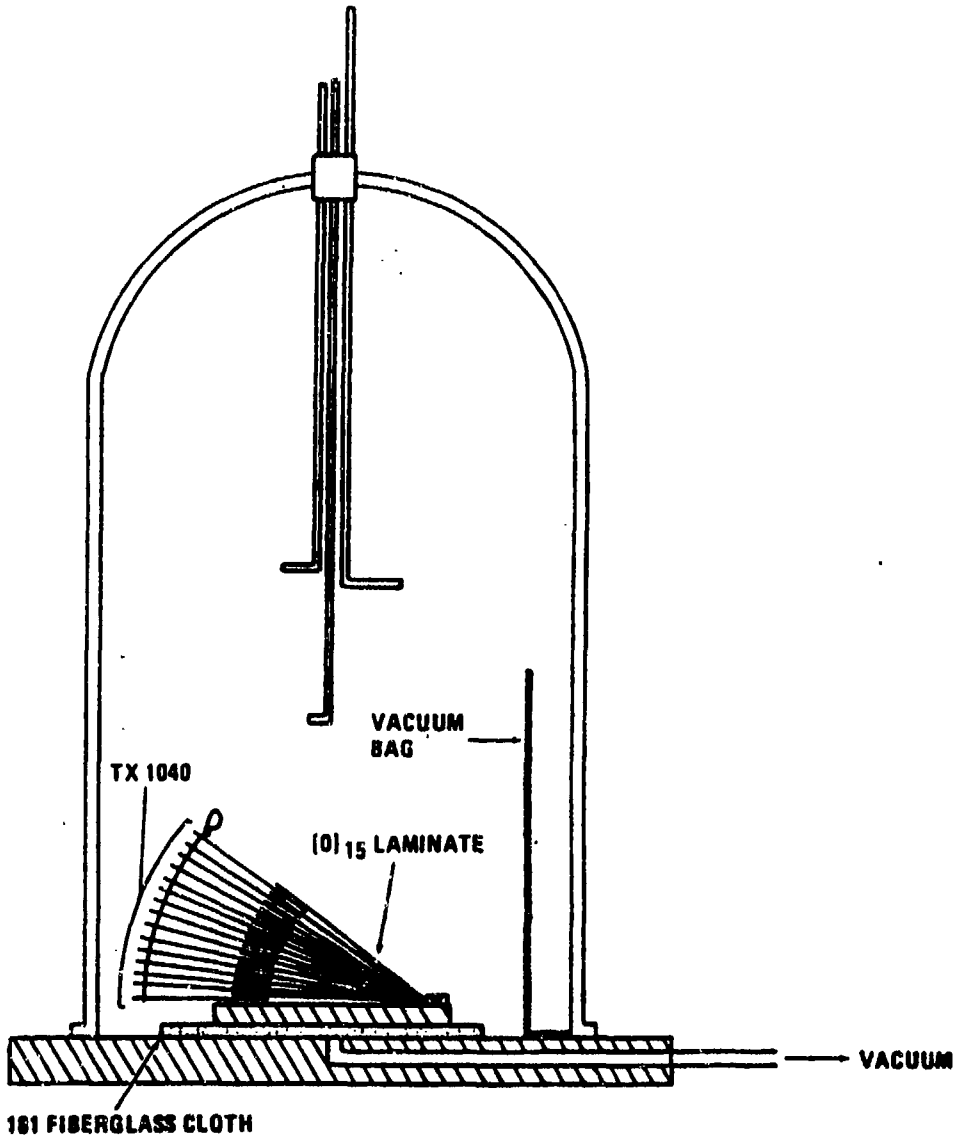

PROCESS STEPS:

(1) VACUUM DRAWN IN BELLJAR

(2) SEPARATORS PULLED FROM BETWEEN PLIES

(3) PLIES TAMPED DOWN

(4) VACUUM BAG REMOTELY PUT IN PLACE, SEALED

(5) BELLJAR VENTED

(6) LAMINATE VACUUM BAG CURED TO 350°F

Figure 107. In Vacuo Lay-up Technique

step involved 0.586 MPa (85 psi) for 30 minutes at 54C (130F). This temperature was used because it would aid compaction by softening the resin without causing a terribly high diffusion rate. However, the resulting laminate also had interlaminar voids. Thus, it was concluded that layup entrapped air or voids are not a significant factor in causing interfacial voids when doing a vacuum bag cure.

By inference, then, it appears that the voids form at the ply interfaces because of some surface chemical condition that either favors void nucleation or that causes the release of gases at the interface. The following candidate factors have been or are under consideration.

a. Moisture is absorbed on the surfaces of the plies, as well as absorbed within the plies, and is released at the interface as a vapor at some temperature below resin gelation.

b. Carbon dioxide is released from the DADS curing agent as the reversible part of a CO_2-amine reaction.

c. Some other reaction results from having DADS screened to the ply surfaces during prepregging.

d. Release agent from the carrier paper contaminates the prepreg with a film that is either volatilizable or that favors void nucleation by reduction of surface tension.

Tests have been completed which sought to remove any moisture that might be absorbed on the surface of the prepreg prior to layup. Plies were flash heated to 176C (350F) with a heat lamp in a dry argon atmosphere and held at 176C (350F) for 20-30 seconds. These are conditions that are normally adequate to flash water off of most surfaces. Figure 108 shows the experimental setup. The flash heated plies were cooled and then laid up and bagged in a dry argon atmosphere to prevent re-absorption of moisture. After vacuum bag curing, photomicrographs showed that interlaminar voids still resulted.

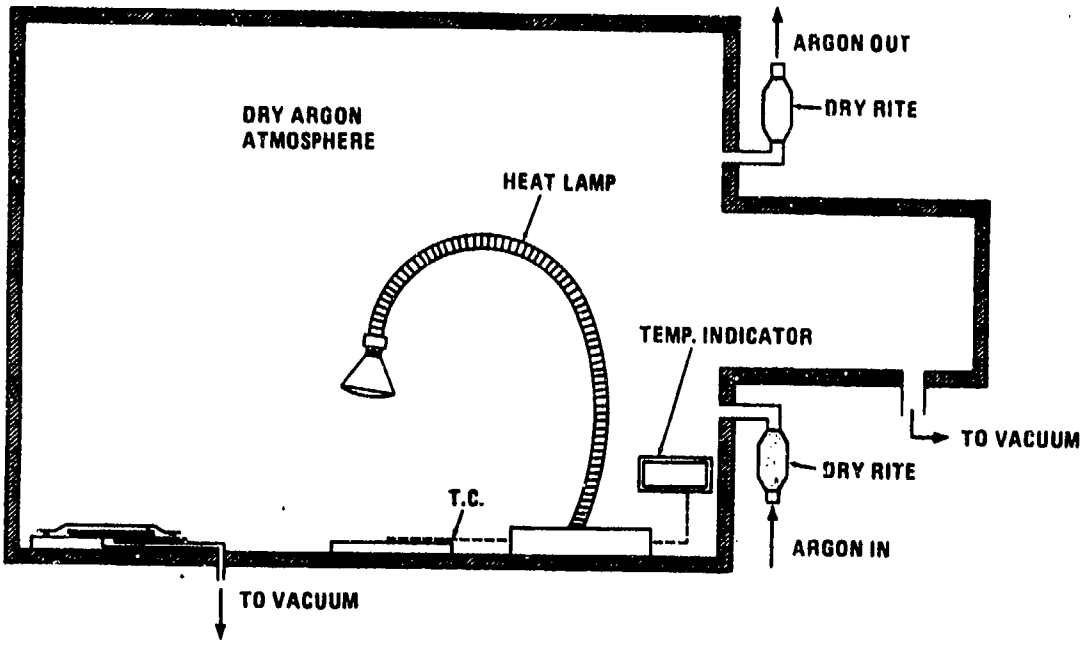

Figure 108. Flash Heating and Lay up Apparatus

Results of a Rockwell cure (Section 2.10.6) have indicated that a degassing step of the prepreg or the lay up at 132C (270F) for 75 minutes was adequate to remove the volatiles prior to the cure step. The volatile removal step in the void etiology study apparently was not adequate to completely remove the volatiles prior to cure.

It appears from the digestion of all of the data obtained on this program that the main source of voids are either mechanical or generated in nature. Mechanical void elimination is dependent on adequate pressure/time/temperature conditions. Generated voids result when the volatiles contained in the prepreg or layup boil at a critical temperature and pressure. The water absorption studies indicated that as water is absorbed, a concentration gradient across the thickness of the laminate exists (unless equilibration has been allowed to occur) with the highest concentration at or near the ply surfaces.

2.9 NEW CURING TECHNIQUES

As a result of the pressure transducer studies, it became apparent that a critical processing parameter of graphite/epoxy laminates had been discovered. During processing, the resin pressure was always quite low with regard to the applied pressure. If the uncured laminate had absorbed sufficient moisture during the cooking, prepregging or layup operations, this moisture could be evolved at temperatures greater than 100C (212F) dependent directly on the resin pressure. A main criteria for the prevention of void generation from volatile evolution within the resin was the control of the resin pressure during the cure process.

Two techniques were developed which have been shown to introduce and maintain pressure into the epoxy resin during cure and thereby inhibit the formation of voids due to volatile evolution. The high pressure in the liquid resin, in essence, raises the boiling point of the water sufficiently to minimize the volatile evolution at the cure temperature. The first technique was termed the "bagless" cure because it was based simply on the cure of a consolidated, void-free prepreg stack in an autoclave without the mechanical contrivance of a bag to introduce pressure into the resin. The hydrostatic pressure introduced into the autoclave was the pressure felt by the resin. Experiments have been accomplished to confirm these statements and are presented later in this report. The bagless cure began as an academic exercise employed to demonstrate how pressure can simply be introduced into the resin during cure.

The second approach was termed the "internally pressurized bag" technique. It was a variation of the bagless cure in that the layup and cure process was essentially conventional, employing a nylon bag, however, the interior of the bag was pressurized with nitrogen to establish a minimum pressure into the resin to guarantee that moisture voids would not be allowed to occur. The pressure in the bag was obviously less than the autoclave pressure and the pressure differential was used to maintain the laminate geometry on the tooling surface.

To demonstrate these new processing approaches, several laminates were prepared and analyzed. The first technique, the bagless cure, showed that a thick-section laminate (greater than 2.60 cm thick) can be cured into a void-free part by only employing a consolidation step and a hyperbaric cure.

2.9.1 BAGLESS CURING OF A 3.05 CM (1.2 IN) THICK COMPOSITE. For the 201 ply (0°, 90°) 3.05 cm (1.2 in) thick laminate, a pressure compaction for one hour at room temperature with 0.689 MPa (100 psi) was employed for consolidation of the prepreg stack (Fiberite 1076E net resin prepreg). This is a critical step necessary for the removal of entrapped air pockets incorporated into the stack during the normal layup operation.

After compaction of the 201 ply prepreg stack, the nylon bag, fiberglass bleeder and porous Teflon coated glass separator film were removed from the compacted prepreg layup. The simple removal of the nylon bag allowed complete pressure to be imparted into the resin during pressurization of the autoclave. The unbagged layup was placed in an autoclave and 0.689 MPa (100 psi) pressure applied. Since net resin prepreg was employed, low flow compaction cycle, any change to higher resin content material would necessitate a prebleeding procedure to reduce the resin content prior to a bagless cure.

Experiments were conducted where cavity pressure transducers were positioned on the bottom of prepreg stacks and embedded within the thickness of the stack. In both cases, the cavity transducers recorded the same pressure as the autoclave gauges, thus demonstrating that indeed the resin was seeing the full pressurization of the autoclave and not the normally low pressure seen in vacuum bagged/bleeder system cures. These pressure experiments were run over a temperature range from room temperature to 135C (275F).

The diffusivity and solubility studies conducted on this program showed that (regardless of the advancement level of the prepreg) water was easily diffused

and solubilized in the resin in a rather short period of time at elevated temperature. The quantity of water readily solubilized was as high as 0.4 percent by weight, usually more water than that normally present in the a received prepreg.

Rather than develop a cure cycle that provided sufficient time at a temperature for complete lateral migration of the entrapped water, which, course, would be dependent upon laminate area, enough time was allowed at (190F) for the entrapped water to diffuse uniformally into the resin and thus eliminate local concentrations. Depending upon the quantity of water present, usually 2 to 2.5 hours was an adequate time at 88C (190F) to completely solubilize the water into the resin.

After the dwell cycle at 88C (190F) of 2.5 hours with 0.689 MPa (100 psi) pressure applied to the unbagged laminate, the temperature was increased to 177C (350F) and cured for two hours under pressure at that temperature. The laminate was cooled under pressure to 66C (150F) and removed from the autoclave.

The resulting laminate cured and precompacted as described, provided excellent C-scans at highly sensitive scan parameters. Figures 109 and 110 are reductions of C-scans of the thick laminate.

The laminate was sectioned and polished for examination under the microscope. Examined sections of the laminate showed no evidence of void presence, confirming the C-scans indication of a void-free laminate. Figures 111 and 112 are photographs of the laminate's polished surface at 50X and 100X magnifications.

Physical properties were determined on the laminate as follows:

Cure ply thickness	0.0147 cm/ply (0.0058 in/ply)
Fiber volume	62 percent

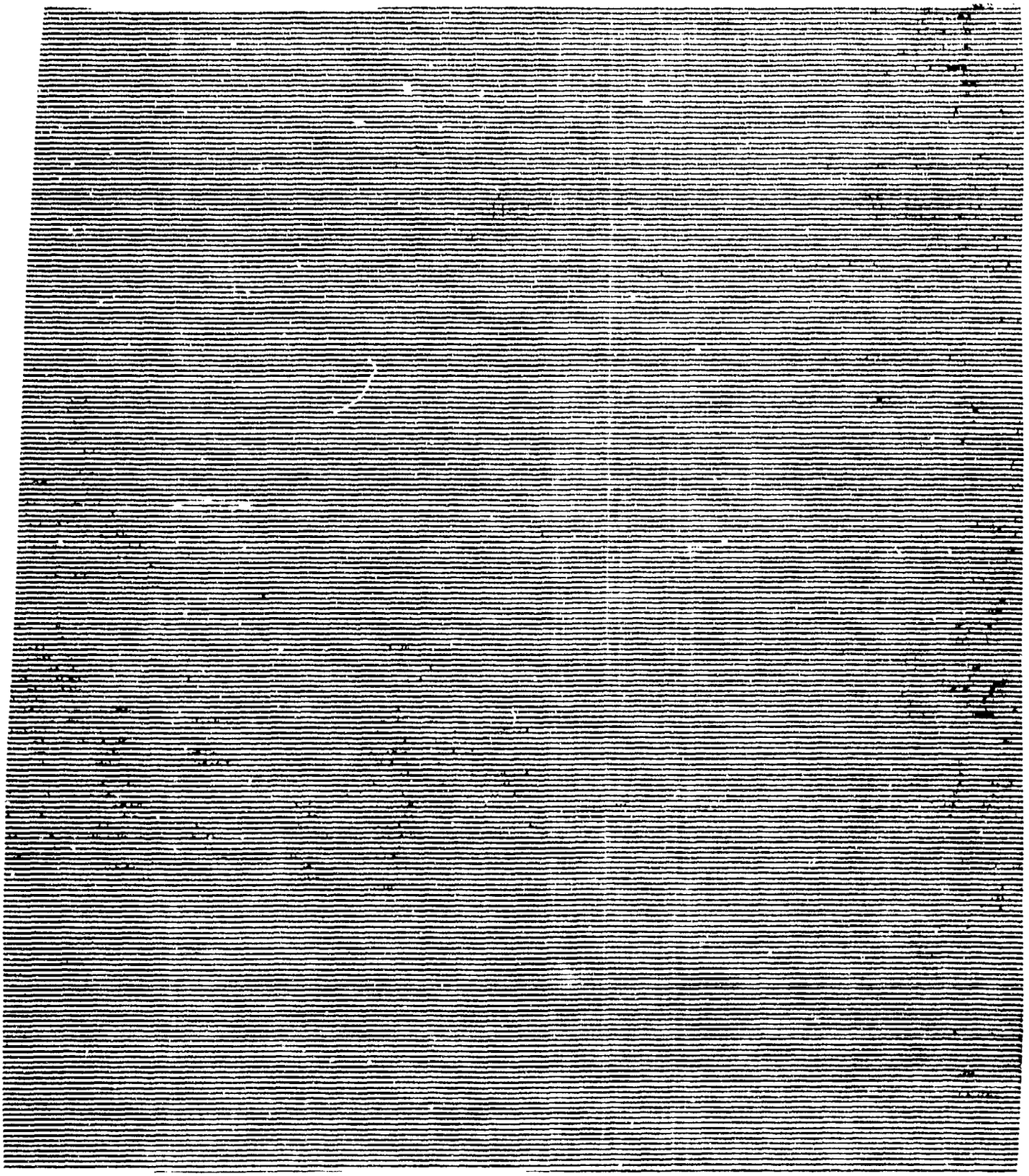

Figure 109. C-Scan of Thick Laminate 3.0 x 1.0 Gain at 5 MHZ

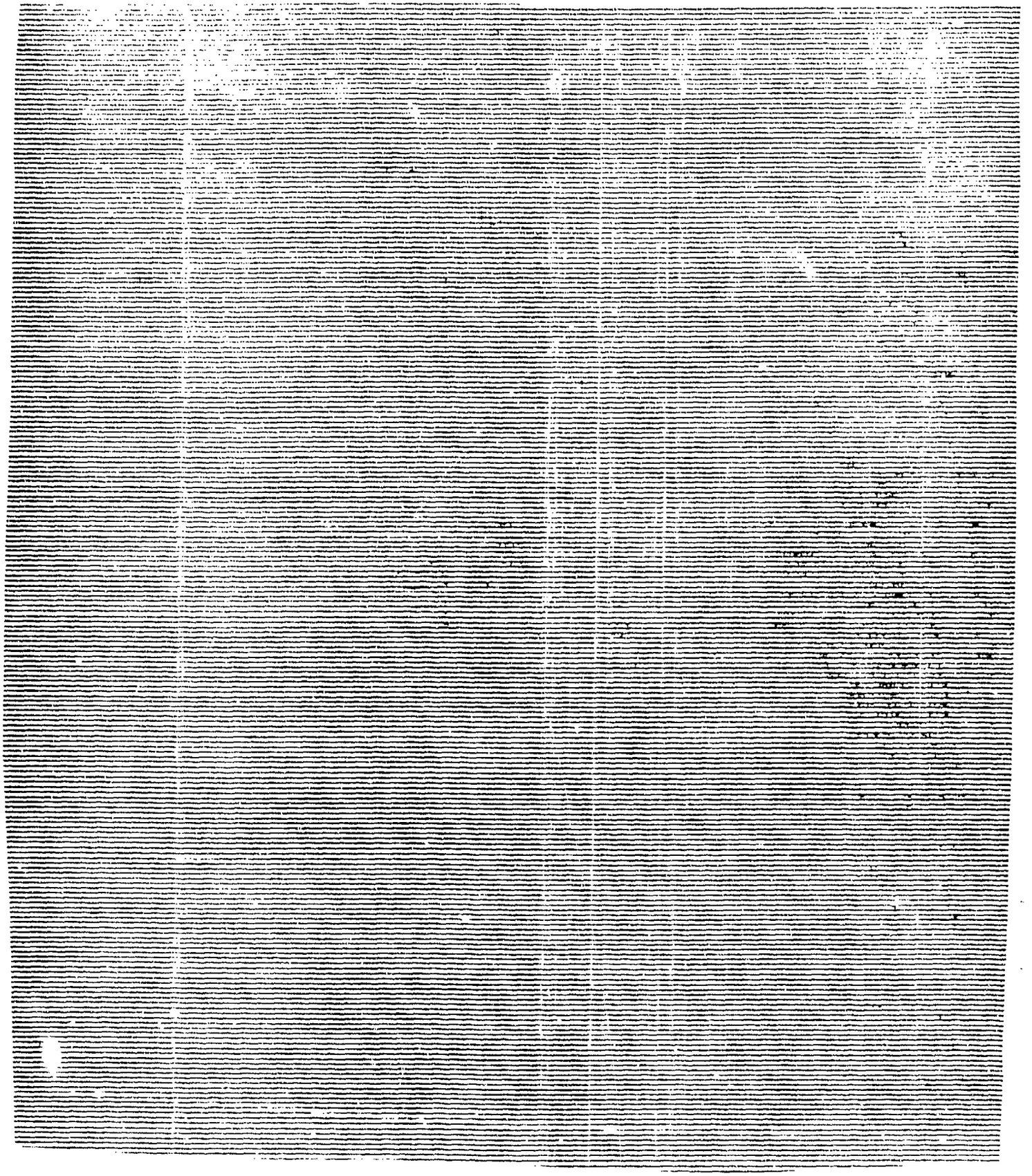

Figure 110. C-Scan of Thick Laminate 1.0 x 1.0 Gain at 5 MHZ

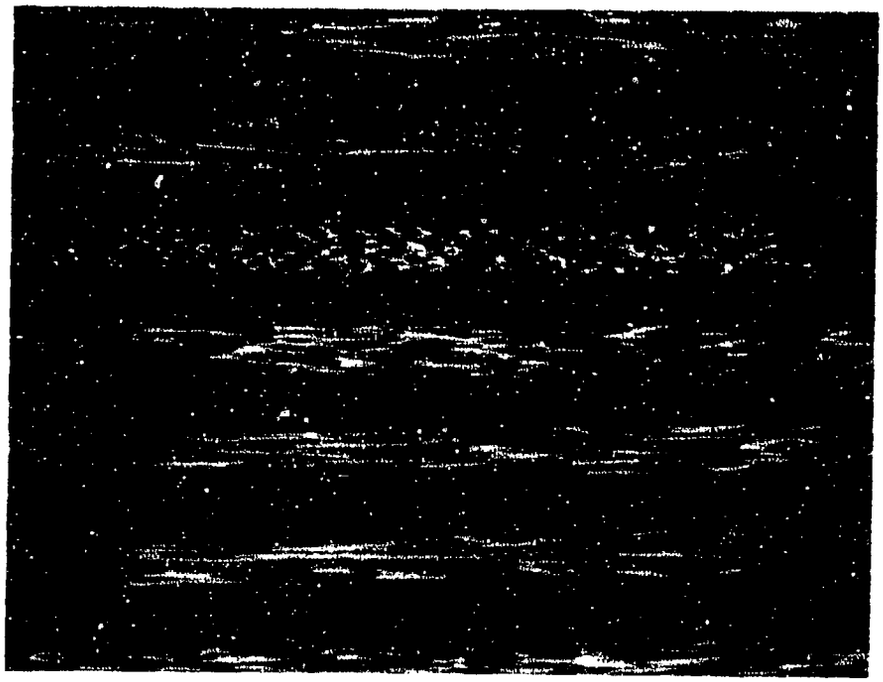

Figure 111. Micropolished Section of Thick Laminate, 50X

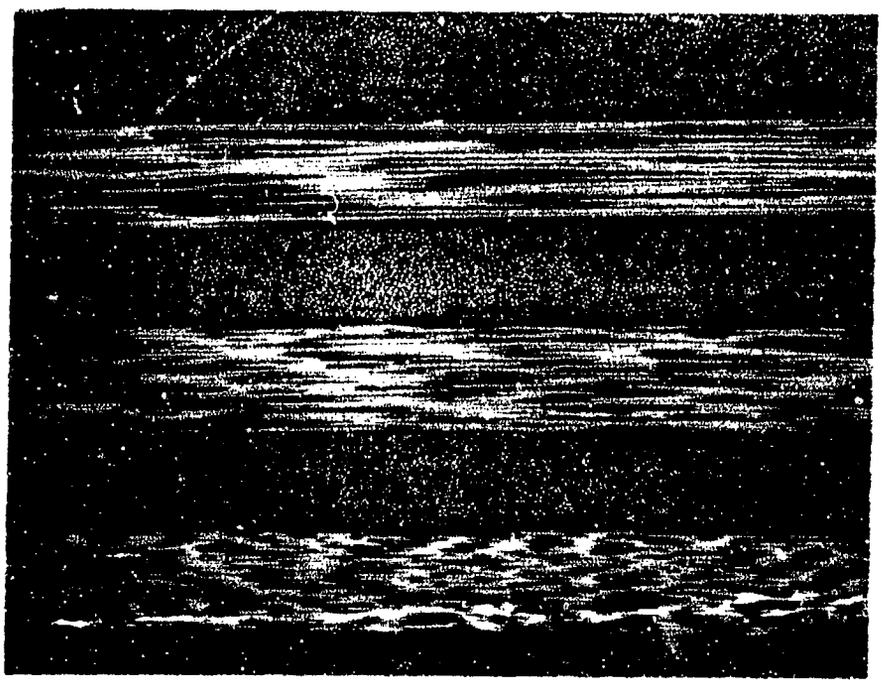

Figure 112. Micropolished Section of Thick Laminate Laminate, 100X

Specific gravity	1.574 gm/cc
Calculated void volume	0.2 percent
Resin content	31 percent by weight

Mechanical properties were determined on thinner unidirectional and pseudoisotropic laminates fabricated and cured identically to the thick laminate. The short beam shear strength of the unidirectional laminate ranged between 110 MPa to 113.8 MPa (16,000 to 16,500 psi). Flexural strengths determined on the pseudoisotropic 50 ply laminate were 517 to 552 MPa (75 to 80 ksi) with 25 percent of the zero plies in the test direction. Both of these test values were well within anticipated ranges for laminates with a 62 percent fiber volume.

2.9.2 DEVELOPMENT OF BAGLESS CURED TUBES AND HAT SECTIONS. The first, more complex geometric structure to be investigated for its application to the bagless curing technique was a 7 cm (2.75 in) diameter tube approximately 35.6 cm (14 in) in length. The tube was precompacted at 0.103 MPa (15 psi) vacuum bag type pressure for 1 hour at 54C (130F). The vacuum bag and non-porous Teflon film were removed from the compacted tube surface and the tube was cured without a bag in an autoclave.

The bagless cure cycle which provided void- and wrinkle-free tubes consisted of a direct heatup at 2-4C/minute (3-4F/minute) to 177C (350F) followed by a hold for 2 hours at 177C (350F).

A variety of tube diameters, thicknesses, and lengths were fabricated and cured with the bagless technique using Fiberite's 1076E prepreg tape. Diameters of 7, 8, and 33 cm (2.75, 3.5, and 13 in), respectively were fabricated. Number of plies varied from 4 to 20 plies, and the lengths of the tubes varied from 30.5 to 76.2 cm (12 to 30 in).

An indication of some non-uniform resin distribution was evident on some of the tube surfaces. Excess resin merely tended to flow unimpeded on the surface due to gravity. This problem was overcome by simply wrapping porous Armalon tightly on a bias around the outer tube surface. The porous Armalon allows for the excess surface resin to be wicked into the Armalon by capillary action and provides a textured Armalon surface. Experiments with graphite fibers in low viscosity resin systems such as Epon 828/Versamid 125 indicate that the graphite fibers behave somewhat as a thixotrop. Small quantities (2-5 percent) of graphite fibers in the resin will inhibit or even prevent resin flow and a large shear force is required to induce flow. It is possible that the 177C (350F) curing resin interacts with the graphite fibers when it goes through the viscosity minima in the precompacted shape. This prevents or minimizes normal resin flow and thus maintains part shape even under the influence of gravity. Surface resin does not appear to be held as tenacously and flows somewhat on cure. The Armalon wrap prevents this from occurring. The tubes were sectioned and polished for examination to determine the presence of voids. No voids were found in any of the tubes sectioned. In addition to producing void free tubes, the tubes were wrinkle free. The cured thicknesses of the tubes were also correct. Unlike conventional curing methods where vacuum bags are used and pressure sometimes distributes unevenly over the part because of the bagging configuration, bagless curing applies pressure evenly to the resin/graphite surface. With high pressure transmitted to the resin, any remaining void sites are reduced in volume to an insignificant level. At 0.689 MPa (100 psig), the void volume would decrease approximately 85 percent. Figure 113 illustrates the relationship between pressure and void volume. At atmospheric conditions (MPa = 0) the void volume is assumed to be 100 percent, and as the external resin pressure

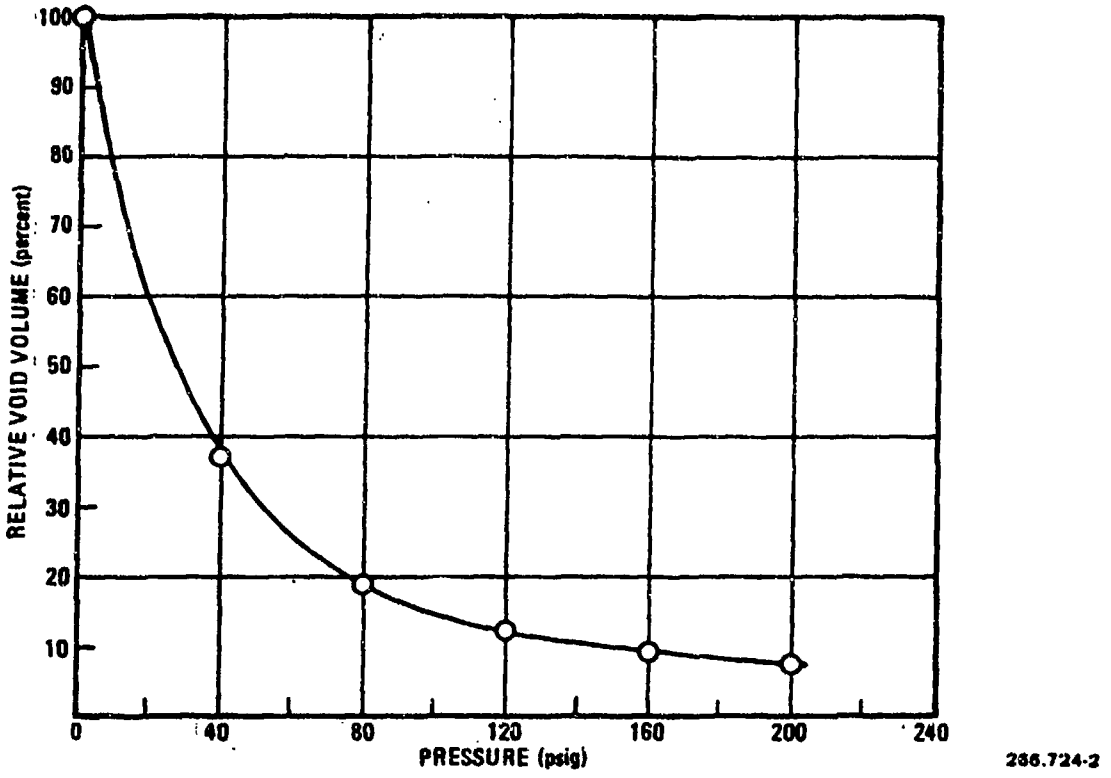

Figure 113. Void Volume as a Function of Resin Pressure at Constant Temperature

increases the void volume decreases as shown. A pressure of 0.689 MPa (100 psig) which is a typical autoclave capability and condition for laminate curing decreases void sizes by about 85 percent. A pressure of 138 MPa (200 psig) would reduce the void sizes by 92.5 percent.

An ideal resin system for the bagless curing technique might therefore consist of (1) a low viscosity resin to aid in precompaction of the prepreg layup and (2) an internal thixotrop (such as Cab-O-Sil) to prevent sagging or flow of the surface resin on complex geometries when shear is removed. Being thixotropic, the resin system would flow under the shear forces of the pre-compaction step. More research into this area is necessary to optimize the bagless cure approach to composite fabrication.

The second complex structure investigated for the bagless curing techniques was a hat section 61 cm (2 ft) long with a 5.08 cm (2 in) high by 5.08 cm (2 in) wide hat having 3.81 cm (1.5 in) flanges. The hat section was made from 16 plies of Fiberite's 1076E and consisted of a $(\pm 45^{\circ}_{2}, 0^{\circ}_{8})_{s}$ layup. The same compaction and cure cycle used for the tubes was also used in making the hat section.

The hat section, like the tubes, were also essentially void free parts without wrinkles.

The bagless curing technique demonstrated a significant reduction in manhours and ancillary materials when compared to conventional curing methods.

2.9.3 DEVELOPMENT OF A SILICONE VACUUM BAG PRESS TECHNIQUE. The bagless cure technique requires an initial bagging of the composite layup for precompaction. The precompaction step may include resin bleeding into a bleeder ply if the prepreg is not net resin. The next logical developmental step in optimizing the bagless cure technique is to eliminate the bag and bleeder/breather required for the precompaction step and consolidate the previous two step bagless cure fabrication process to a single step technique. To accomplish this, a clamshell press configuration was developed that employed a high elongation silicone rubber diaphragm as the reusable "bag" for the precompaction step.

Figure 114 illustrates the press configuration with the graphite/epoxy net resin layup on the aluminum hat section. When pressure was applied to the upper chamber, the silicone diaphragm (A) expanded downward onto the tooling surface of the mold conforming precisely to the geometry of the layup and exerting a pressure equal to the pressure differential of the upper and lower halves of the clam shell press (B). The press was heated and held at 66C (150F) for one hour to afford consolidation of all the plies. After consolidation the

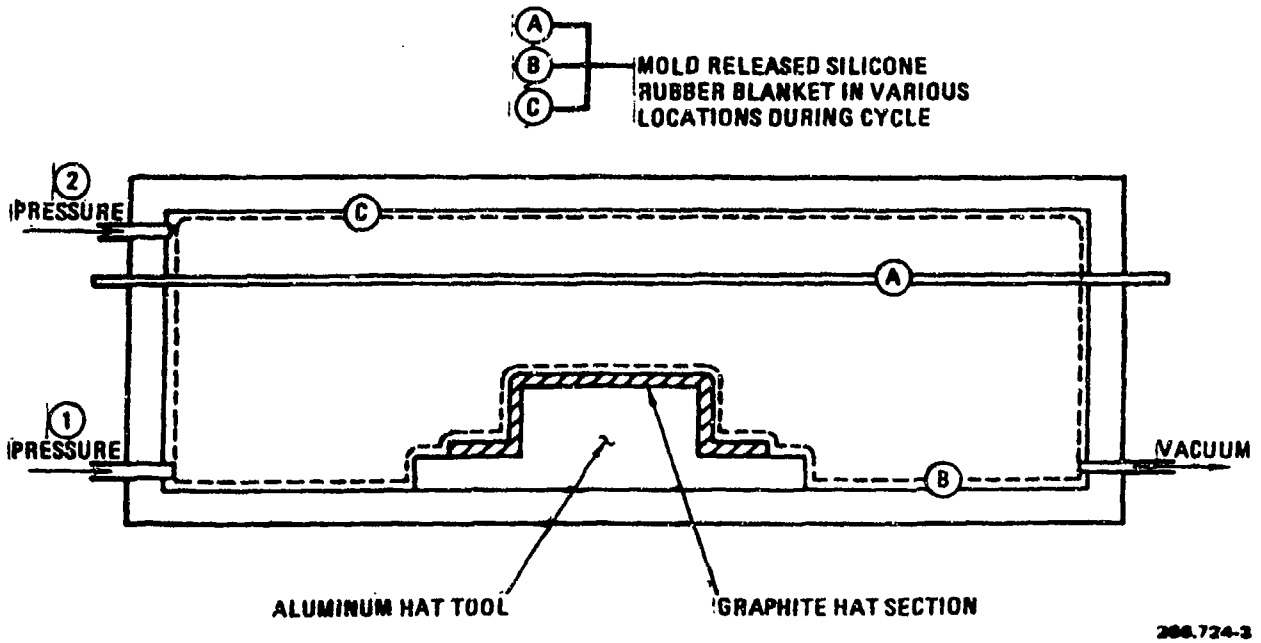

Figure 114. Press Configuration for the Silicone Vacuum Bag Curing Technique

the vacuum is released and the pressure in the upper chamber is bled off. The bottom chamber was then pressurized. The diaphragm is pulled away from the layup due to the pressure and was forced to conform to the geometry of the top chamber (C). The pressure was then increased to the desired level, say 0.689 MPa (100 psig), and the temperature increased to the cure temperature at 1 to 2C/min (2 to 4F/min) and held until cure is complete.

This method allowed the net resin part to be consolidated (precompacted) into the desired geometry and cured without the material requirements of bleeder/breather systems or manhour intensive bagging and debagging operations.

This operation was adaptable to press cures or autoclave configurations with only slight modifications.

Figure 114 illustrates the press configuration and Figure 115 illustrates an autoclave configuration.

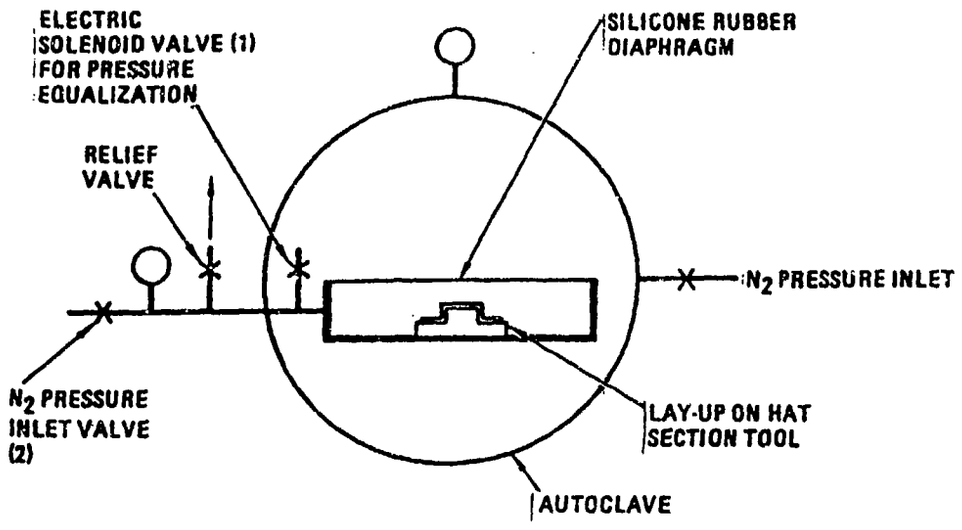

Figure 115. Autoclave Configuration for the Silicone Vacuum Bag Curing Technique

An additional remote controlled electric solenoid valve (1) was introduced to equalize the pressure inside the tool fixture with the autoclave pressure after the consolidation has occurred. A slightly higher positive pressure 0.014-0.021 MPa (2-3 psi) was introduced through valve 2 to ensure the removal of the silicone blanket from the tooling surface prior to cure. The silicone diaphragm is treated with mold release and is capable of multiple cures before replacement becomes necessary.

The simple hat section illustrated in Figure 113 was cured employing the press variation of this technique. The hat section fabricated was void free.

2.9.4 INTERNALLY PRESSURIZED BAG TECHNIQUE. The internally pressurized bag curing process was developed to enable effective pressure translation into the resin of the conventionally cured laminate systems. Basically, the approach was to provide a back pressure into the nylon bag with concommittant autoclave pressure. The pressure differential provided the mechanical force against the laminate to enable conformation to a tooling surface. The process consisted of:

a. A high pressure 0.586 MPa to 0.689 MPa (85 to 100 psi) hold at a low temperature (82C, 180F) to consolidate the prepreg lay-up.

b. Application of a back pressure (0.345 to 0.517 MPa - 75 to 76 psia) into the bag to prevent volatile evolution and void generation.

c. An intermediate hold at 120C (250F) to encourage water redistribution from ply interface concentrations to uniform distribution throughout the resin.

d. A high temperature 177C (350F) hold for curing.

A schematic of the system is illustrated in Figure 116. The diagram also indicates a pressure transducer location which was included in the early experiments to measure the actual pressure of the resin during a processing cycle.

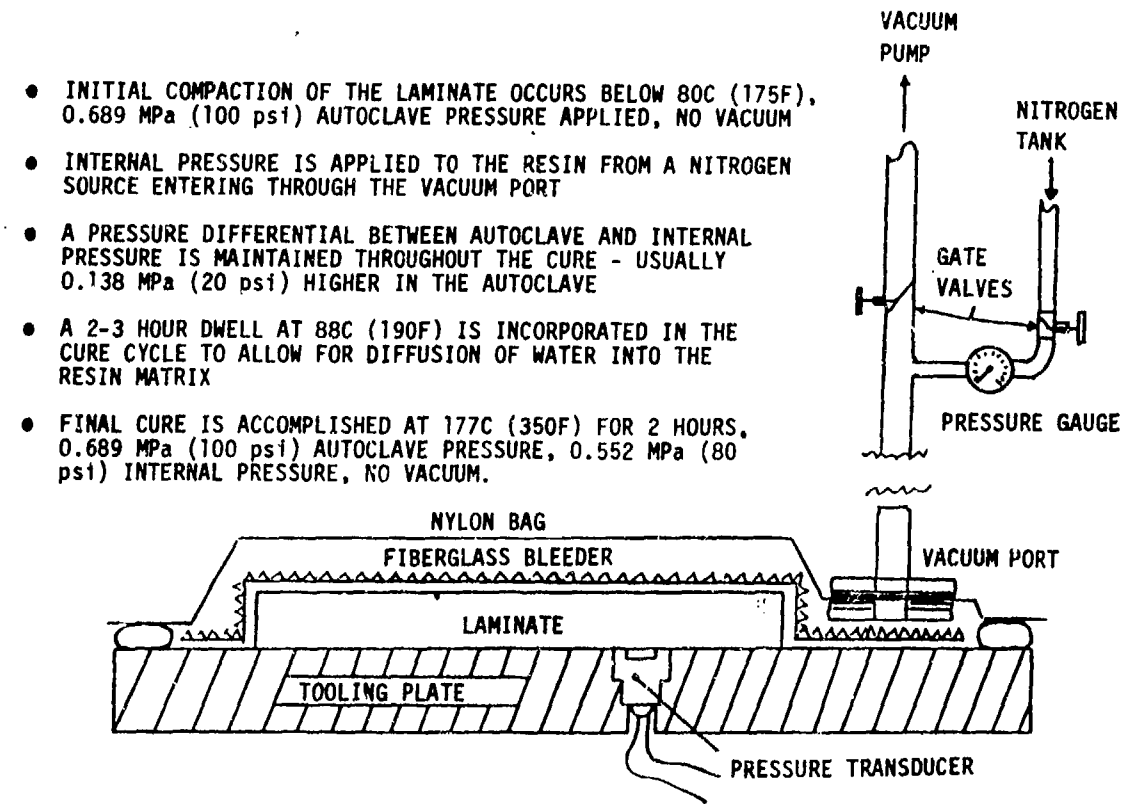

Figure 116. Internally Pressurized Bag Cure Concept for Providing High Pressure Into the Resin During Cure

Figure 117 shows the results of a 5208/T-300 lay-up and conventional bleeder/breather system which was heated to 121C (250F) and which had 0.517 MPa (75 psi) pressure applied. The pressure of the resin started dropping immediately to about 0.069 MPa (10 psi). At about twelve minutes into the cycle the bag was pressurized to 0.483 MPa (70 psi). The transducer responded precisely to the applied internal pressure as shown on the pressure diagram. When the internal pressure was released, the resin pressure again dropped to a low level.

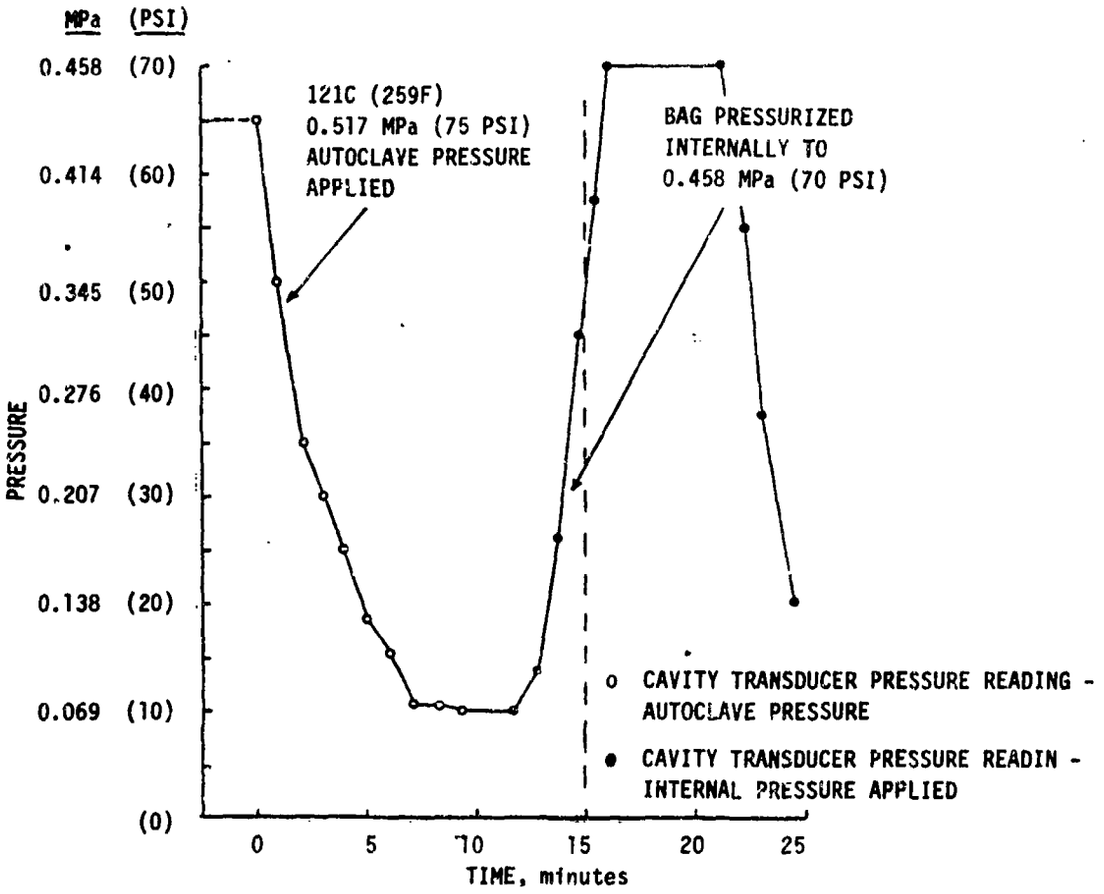

- AUTOCLAVE PRESSURE APPLIED AT 121C (250F) SHOWS A DECAY IN RESIN PRESSURE DOWN TO 0.069 MPa (10 PSI) WITHIN 6 MINUTES.
- INTERNAL PRESSURE APPLIED SHOWS AN IMMEDIATE INCREASE IN RESIN PRESSURE TO 0.458 MPa (70 PSI) WITHIN 6 MINUTES.

Figure 117. Internally Pressurized Bag Resin Pressure

The pressure that the resin must maintain to prevent the generation of water voids is depicted in Figure 118 and is a function of the amount of moisture at the potential void site. If the resin pressure drops below a minimum value established by the gas laws, conditions exist for void generation. As can be seen from the chart, at 137C (275F) at a 2 percent moisture level (locally) a bubble pressure of about 0.172 MPa (25 psi) could be present. If the resin pressure is less than 0.172 MPa (25 psi), a bubble will form. Therefore, it is critical to maintain adequate resin pressure during processing.

A series of 16-ply unidirectional composites were fabricated from Fiberite's 1076E prepreg to determine whether any differences in mechanical properties existed between conventional curing techniques and the internally pressurized bag approach. Figure 119 summarized the results. The flexural and interlaminar shear strengths are equivalent within experimental error.

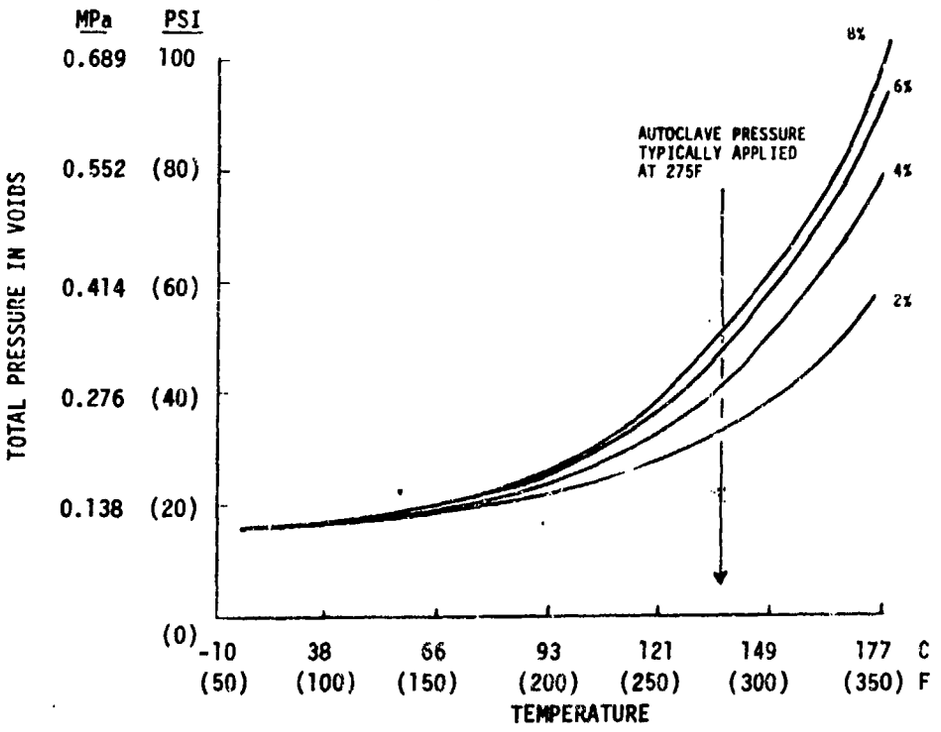

Figure 118. Effect of Temperature on Void Pressure as a Function of Initial Resin Water Content Assuming Uniform Distribution of Water Within Laminate

MECHANICAL TEST DATA

	FLEXURAL STRENGTH		SHORT BEAM SHEAR	
	ROOM TEMP.	177C (350F)	ROOM TEMP.	177C (350F)
• INTERNALLY PRESSURIZED BAG CURE				
UNIDIRECTIONAL 16 PLY FIBERITE - 1076E	1703 MPa (247 ksi)	1317 MPa (191 ksi)	958 MPa (13.9 ksi)	64.1 MPa (9.3 ksi)
• CONVENTIONAL VACUUM BAG AUTOCLAVE CURE				
UNIDIRECTIONAL 16 PLY FIBERITE - 1976E	1744 MPa (253 ksi)	1324 MPa (192 ksi)	102.7 MPa (14.9 ksi)	59.3 MPa (8.6 ksi)

ALL DATA, AVERAGE OF FIVE TEST SPECIMENS

• NO DIFFERENCE IS NOTED IN ELEVATED TEMPERATURE TEST DATA BETWEEN THE TWO DIFFERENT CURE CONCEPTS. INTERNAL PRESSURIZED CURE ALLOWS FOR THE DIFFUSION OF WATER INTO THE MATRIX.

Figure 119. Comparison of the Mechanical Properties of Internally Pressure Cured Laminates to Conventional Autoclave Cured Laminates

A 0.61 m by 0.61 m (2 ft by 2 ft) by 64 ply pseudoisotropic laminate was made with rejected Ft. Worth 5208/T-300 prepreg in a conventional cure process. The same material and laminate configuration was also made employing the internally pressurized bag technique. Ultrasonic C-scans of the two panels are shown in Figures 120 and 121. The conventional curing process shows voids located in the center of the laminate. Presumably, these voids were formed by water evolution when the resin pressure was low. The C-scan of the internally pressurized bag cure shows a void-free panel. This technique can therefore be applied to yield void-free parts from reject material.

2.10 VALIDATION ARTICLES

The validation task of the Processing Science Program was planned to be the integration of all of the processing parameters investigated to develop methodologies which would accurately predict the critical processing parameters and variables associated with material behavior to ultimately provide a procedure to reproducibly process high quality composite parts. The methodologies were validated by the fabrication of F-16 vertical stabilizer skins.

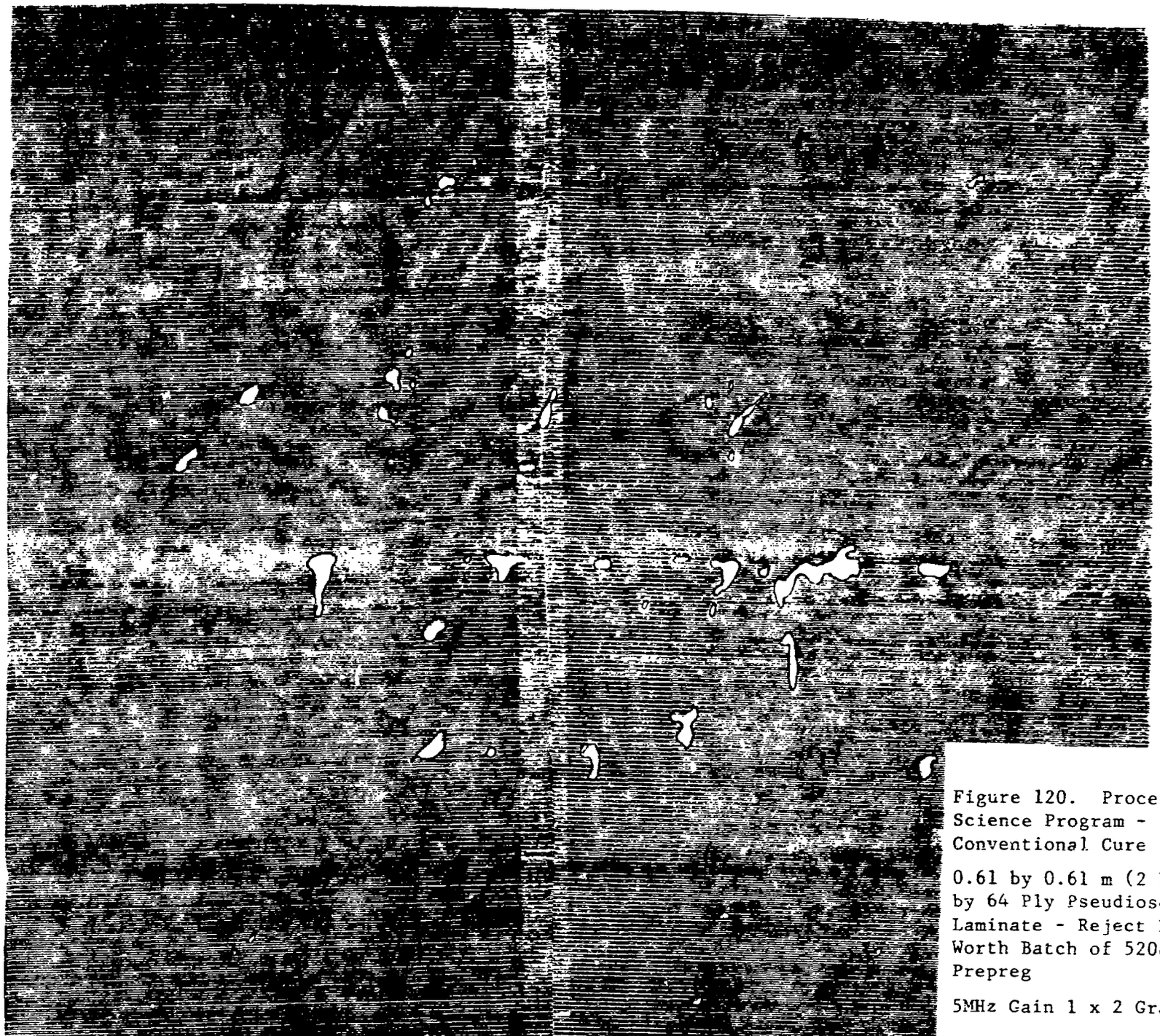

Figure 120. Processing Science Program - Conventional Cure

0.61 by 0.61 m (2 by 2 ft) by 64 Ply Pseudiosotropic Laminate - Reject Fort Worth Batch of 5208-T300 Prepreg

5MHz Gain 1 x 2 Gray Scale

5-11-81

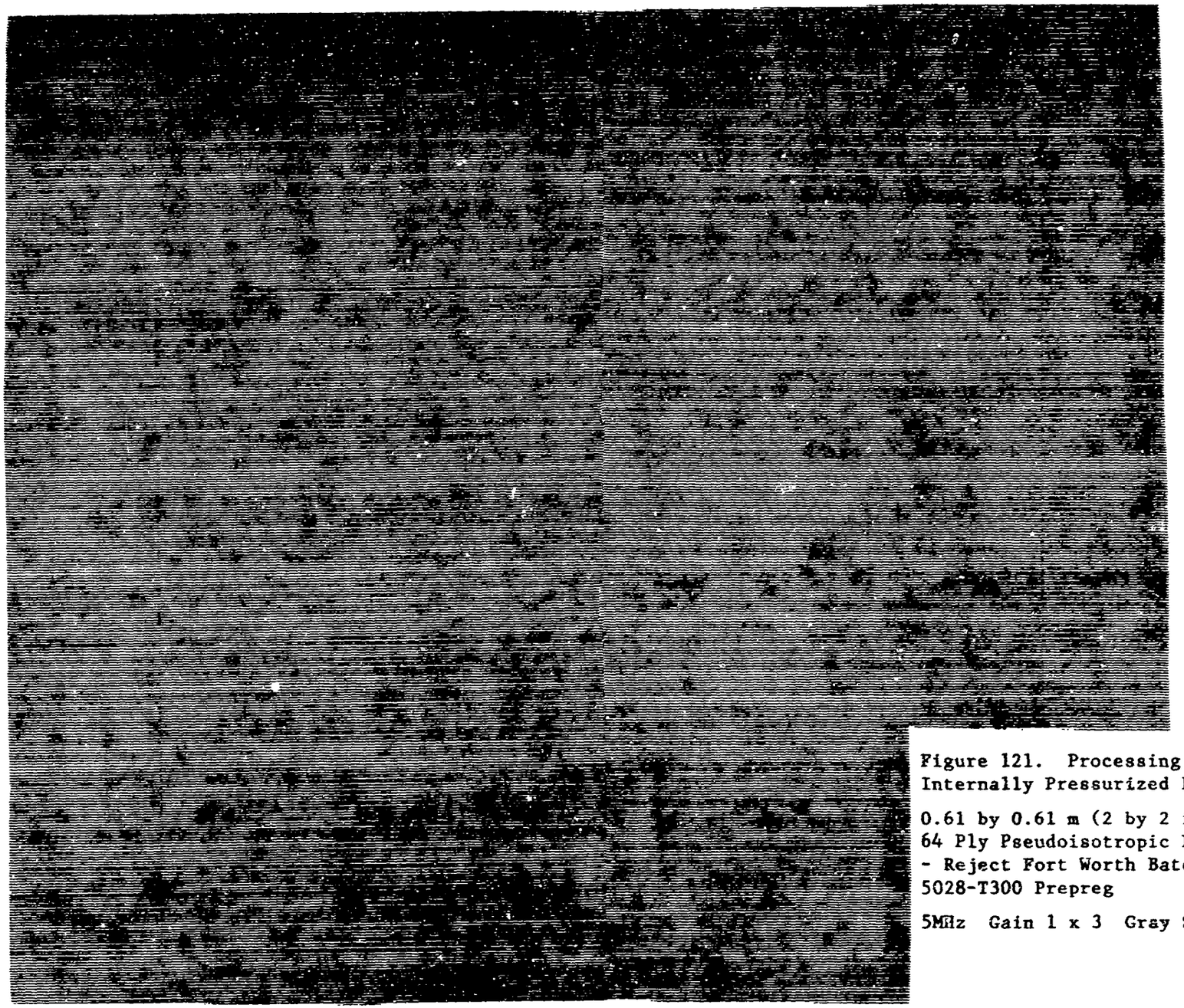

Figure 121. Processing Science Internally Pressurized Bag Cure

0.61 by 0.61 m (2 by 2 ft) by 64 Ply Pseudoisotropic Laminate - Reject Fort Worth Batch of 5028-T300 Prepreg

5MHz Gain 1 x 3 Gray Scale

2.10.1 F-16 VERTICAL TAIL SKIN - BAGLESS CURE TECHNIQUE. Bagless cure of 0.61 m by 0.61 m (2 ft by 2 ft) laminates with internal ply drop-offs, 60 to 80 plies thick, fabricated earlier on this program showed the presence of puckered areas associated with the top ply of the laminates. The probable cause for this condition was attributed to the fact that the ply or top plies were not "balanced" by a corresponding facing. The situation was resolved by placing one or two plies of 120 bleeder (woven and reasonably balanced plies) on top of the Armalon. During consolidation the bleeder wets out with resin and during cure the fiberglass cloth prevents the anisotropic graphite top ply from moving or shifting due to a strain imbalance, the glass providing an isotropic facing.

An alternate method was consolidation with a non-porous Teflon film over the top surface.

A number of flat panels, L angles, and tubes were then precompacted and bagless cured without excessive bleeding or resin loss from the top plies. All of the parts showed excellent C-scans and evidenced no voids under microscopic examination of polished sections.

Actual fabrication of the vertical tail skin was accomplished at the Fort Worth Division of General Dynamics and followed these preliminary experiments. The tail skin was laid up via a machine layup operation typically used in production. The net resin (29-32 percent/weight) prepreg unidirectional tape used in the skin layup was Fiberite's 1076E graphite/epoxy and was 15.24 cm (6 in) wide.

Bagging of the skin was accomplished as follows:

a. One ply of thin, non-porous Teflon was smoothed over the skin surface.

b. Two plies of 181 fiberglass breather was placed on top of the non-porous Teflon and extended to the breather ports.

c. A silicone rubber bag, which also acts as a seal, was used for clam-shell press.

The skin, tool and layup were placed in a clamshell type press and compacted and cured according to the following schedule.

a. Evacuate fiberglass breather for 30 minutes.

b. Initial compaction under silicone rubber bag at 54C (130F), 0.586 MPa (85 psi) for 1 hour.

c. Remove bag, fiberglass breather, and non-porous Teflon film from part surface.

d. Close clamshell press.

e. Apply 0.586 MPa (85 psi) to laminate surface.

f. Heat to 88C (190F) and hold for 1 hour.

g. Heat to 177C (350F) and hold for 2 hours.

h. Cool to 66C (150F) under pressure.

Figure 122 shows a diagram of a vertical tail skin and the location of internal ply drop-offs. The bagless cured vertical tail skin was not void free, however, it was determined to be an acceptable skin based upon Fort Worth's void-accept/reject criteria. The location of small void areas

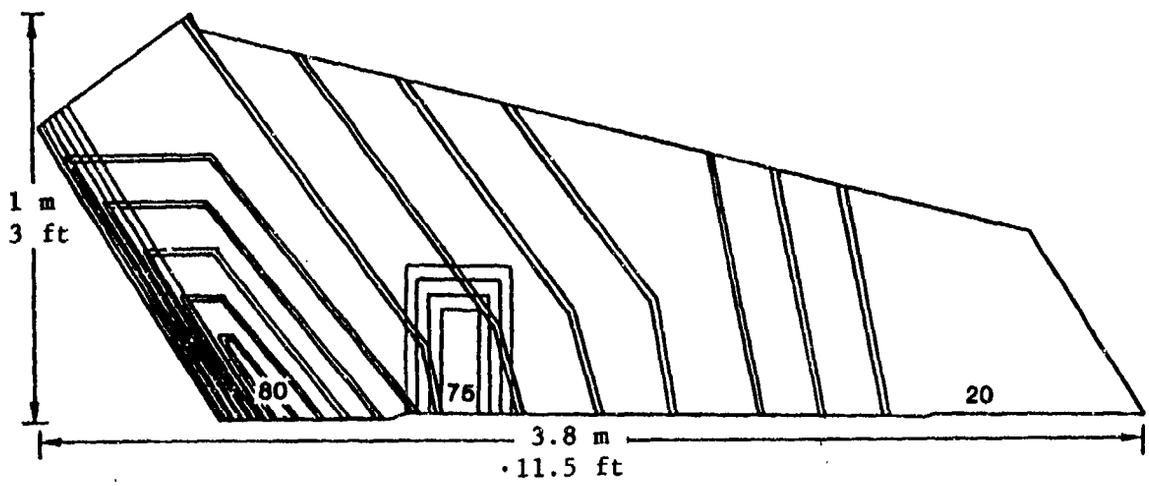

Figure 122. F-16 Vertical Tail Skin Showing Location of Internal Ply Drop-Offs

determined by C-scan and sectioning were in the ply drop-off areas in the thickest sections of the skin, near the 80 and 75 ply thickness as indicated in Figure 122.

The tool surface of the skin was quite good and replicated the tool finish. The bagless side of the skin showed distinct ply drop off locations and a less smooth, more textured surface than the tool side of the skin.

A considerable reduction in the amount of ancillary breather/bleeder materials was noted for the bagless cure concept; roughly 70 percent less fiberglass bleeder and breather was used in the bagless cure. Labor hours associated with this type of cure were also reduced from the normal time required for the fabrication and cure of F-16 tail skins.

The test data on flat laminates with a 0/90° ply orientation cured by the bagless process in the same way as the vertical tail skin, yielded short beam shear values between 12-14 ksi.

2.10.2 F-16 VERTICAL TAIL SKINS - INTERNAL PRESSURIZATION TECHNIQUE. It was decided, with the concurrence of the AFML technical monitor, that additional validation articles be fabricated from 5208-1/T-300 prepreg that was determined to be of poor quality and had been previously rejected by the Fort Worth Division for producing void filled tail skins.

The method to be used in curing the validation article was the internally pressurized, (IP) cure concept. This concept has been described in detail in the "Process Techniques" section of this report. The method for the introduction of pressure into the resin was simply to allow regulated nitrogen pressure to be applied back through the vacuum/vent port in the bag layup. The rationale for employing the internally pressurized (IP) cure cycle was based on producing an acceptable vertical tail skin from reject prepreg.

Three F-16 vertical tail skins and a thick laminate screening panel were fabricated using Narmco's 5208-1/T-300 Batch 9 prepreg. This material was previously identified at Fort Worth as being prone to produce planar voids and porosity in cured tail skins. The batch of prepreg had a moisture content variation of 0.099 percent to 0.32 percent depending upon the roll of prepreg tested. Water content was determined by DuPont 902 moisture analyzer, Karl Fisher titration, and water weight loss by heating to 177C (350F) and holding for 15 minutes. Test results from all three methods of analysis showed basically the same quantity of water or weight loss.

The vertical tail skin, shown in Figure 122, is approximately 0.91 m (3 ft) at its widest point by 3.41 m (11-1/2 ft) in length. The numbers 20, 75, and 80 shown on the figure indicate the number of plies of prepreg in each of the respective areas. The diagonal lines indicated on the tail skin show the areas where two and three internal ply drop-offs occur. The location of voids within rejected tail skins generally occur in the thicker root section of the tail in close proximity to the internal ply drop-offs. The first tail skin that was fabricated served as the control part and was cured using Fort Worth Division's standard production process. Ultrasonic C-scan examination of the tail skin revealed definite patterns of voids and porosity around internal ply drop-offs in the thick root section of the skin.

The second vertical tail skin was also bagged for cure using the standard Fort Worth procedure, which included placement of a Teflon film, perforated on 10.2 cm (4 inch) centers, between the fiberglass bleeder and the breather materials. The second skin was cured with the internal pressure cure cycle.

2.10.2.1 Internally Pressurized Cure Cycle. Vacuum was applied to the bagged part for approximately 30 minutes, 0.586 MPa (85 psi) autoclate pressure was applied prior to heating and the vacuum removed. The bag was vented to the atmosphere.

The skin was heated at approximately 1C/min (2F/min) to 66C (150F) and remained under those conditions for 30 minutes. The 0.586 MPa (85 psi) and 66C (150F) conditions allowed for the initial compaction of the skin. An internal pressure of 0.448 MPa (65 psi) was introduced through the vacuum port under the vacuum bag and held through the cure cycle. Cure of the skin continued by heating to 104C (220F) and dwelling one hour then to 177C (350F) for two hours. Ultrasonic examination of the skin showed it to be of poor quality, with porosity indicated even in the thin 20 ply sections. It has been theorized, (a) that early venting of the vacuum would help prevent void growth, (b) that the low temperature dwells at 66C (150F) and 104C (220F) would enable moisture concentrations to diffuse into the resin, and (c) that application of internal pressure would hydrostatically pressurize the resin within the laminate so as to inhibit void growth. The internal pressure apparently was not translated to the resin through the Teflon perforations. This led to the fabrication of the third skin with an alternate method used to introduce effective pressure.

A third vertical tail skin was laid up with a non-perforated film over the bleeder. Autoclave pressure again was applied at room temperature. The thermal cycle, however, was modified to provide two hours at 104C (220F) in lieu of a short time at 66C (150F) but internal pressure of 0.448 MPa (65 psi) was applied at 66C (150F). After the dwell at 104C (220F), heating resumed to 132C (270F) where the skin was held for four hours instead of one hour and thirty minutes. The objective was to get the resin to gel at that temperature instead of at some higher temperature that would possibly promote higher void pressures. After this dwell, heating to 177C (350F) progressed at half the rate previously used to further assure that the gel state would resist void formation. This required a ten minute dwell at each 5C (10F) increment. C-scanning of this third tail skin also indicated a poor quality, voidy skin.

In retrospect, several critical errors were made with the 5208/T-300

validation articles. The compaction studies done early in the program indicated that consolidation of Narmco's 5208/T-300 was more difficult to attain than Fiberite's 1076E system. Tack tests in tension also supported the contention that 5208, at least at room temperature, had much more tack than the 1976E material. The higher the tack, the more difficult it was to remove the mechanically trapped voids. Examination of the cure schedules showed inadequate time at a temperature and pressure necessary to produce a good consolidation of the layup. The differential pressure was too low to be capable of effective consolidation. The internally pressurized bag technique prevents voids (from moisture in the resin) from generating but only shrinks existing voids. Therefore, it is critical to have the layup consolidated prior to internally pressurizing the bag.

Up to this time on the program, internal ply drop-off areas in laminates and their influence on the formation of air pockets and areas of localized water concentration had not been considered.

We feel, as a result of our successful fabrication of the large laminates with our internal pressurization process from reject Fort Worth material, that we could produce an acceptable F-16 vertical tail skin from reject material.

Based upon the test results of the vertical tail skins that were fabricated and the location of void areas around internal ply drop-offs within the skins, we then began an investigation of the influence of ply drop-offs on laminate quality.

2.10.3 VACUUM AND PRESSURE LEVELS WITHIN PLY DROP OFF VOID AREAS. It was theorized that the pressure that could be generated within a trapped void area within a laminate, such as occurs around internal ply drop-off areas could easily exceed 0.172 to 0.207 MPa (25 to 30 psi) during a curing operation if water were present at the void site. There was also some question as to what effect vacuum had on trapped void areas. To determine the affects of vacuum on, and pressure generated at a trapped void site, a relatively simple test was developed which simulated an internal ply drop-off within a laminate. As shown in Figure 123, we utilized a cavity pressure

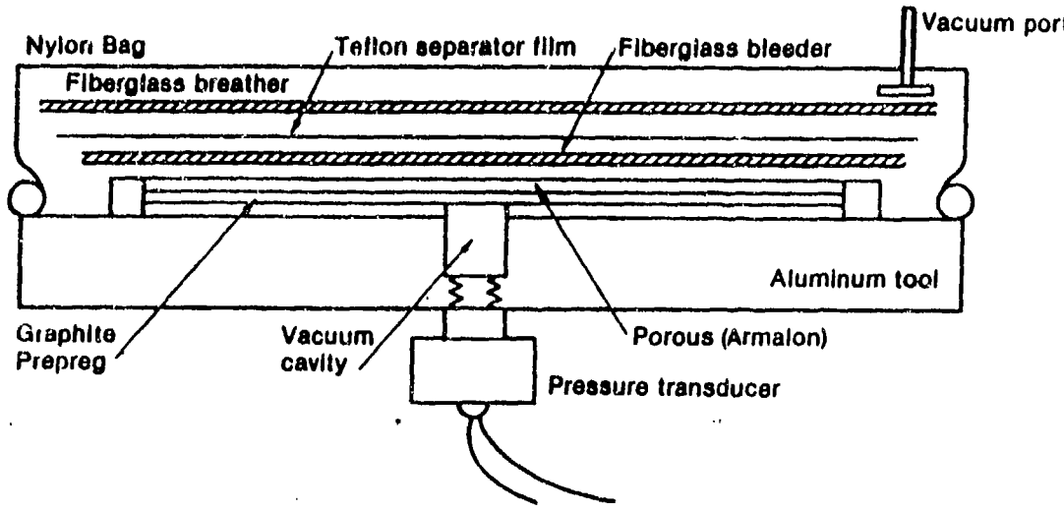

Figure 123. Ply Drop-Off, Cavity Pressure Transducer Test Setup

transducer inside a grooved aluminum tool. Graphite/epoxy prepreg was layed up over the groove and certain plies terminated at the groove's edge. In this configuration moisture and entrapped gas can migrate laterally between plies and concentrate in the groove, which simulated an uncompacted internal ply drop-off within a laminate.

A series of experiments were performed with this test configuration using different graphite/epoxy prepregs and test conditions. The cavity pressure transducer was subjected to heating to 163C (325F) to determine if temperature had an effect on the transducer millivolt readings. No change in readings were recorded as a function of heating to elevated temperature.

Figures 124 and 125 plot test results from the cavity pressure transducer experiments, the solid circle or square indicated no vacuum being applied. The hollow circle or square indicated vacuum being applied. The semifilled symbol indicates where the pressure transducer and cavity have been sealed off to the external vacuum source.

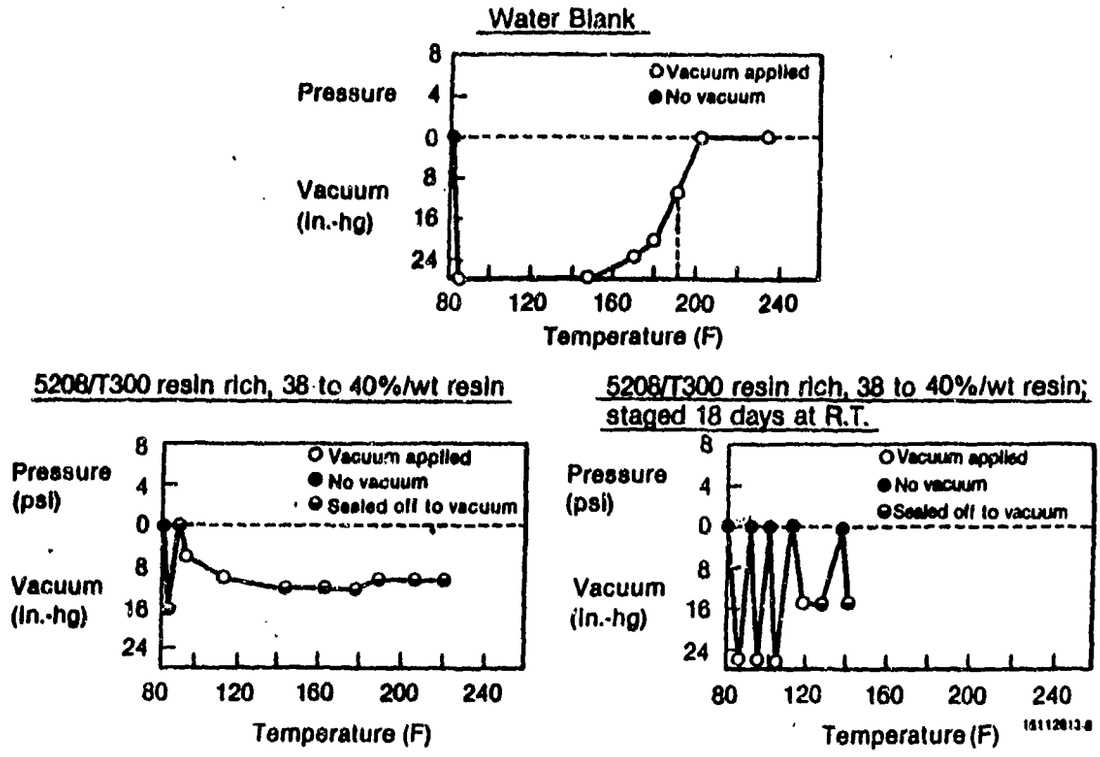

Figure 124. Ply Drop-Off, Cavity Pressure Transducer Experiment

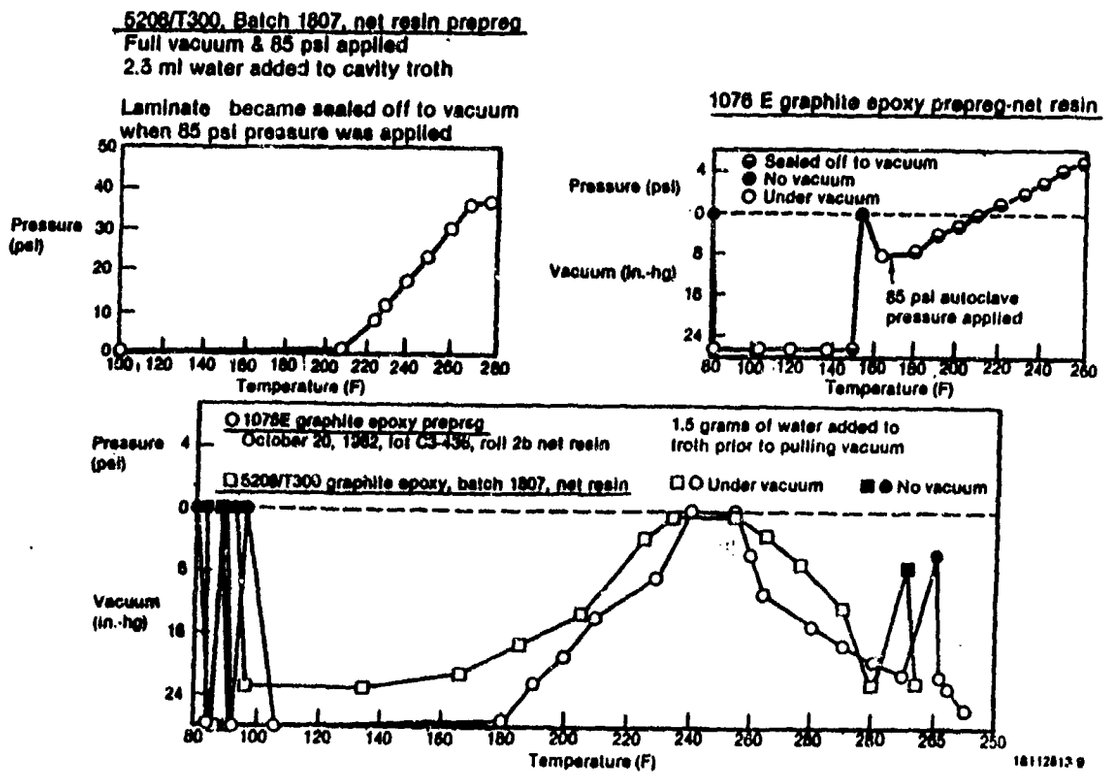

Figure 125. Ply Drop-Off, Cavity Pressure Transducer Experiment

In Figure 124 the top plot is a water blank. Two millimeters of water were added to the cavity and a thick layer of Mylar film positioned over the cavity. A typical vacuum bag was placed over the Mylar film and cavity. Vacuum was applied to the bag, and immediately the pressure transducer indicated a millivolt reading equal to 0.090 MPa (26 in) of vacuum. Subsequent heating to 110C (230F) generated steam pressure from the water present, resulting in a pressure increase or vacuum decrease.

The pressure change started around 77C (170F) and became equal to ambient pressure (14.7 psia) near 100C (212F).

The lower left plot in Figure 124 utilized 5208/T-300, 38 to 40 percent/ weight resin prepreg for the subject test. As can be seen in this plot, immediate application of vacuum caused a sealing of the cavity at 0.055 MPa (16 in) of vacuum. The pressure transducer was vented to atmosphere and then was measured at the cavity. At this point, the cavity was sealed from the vacuum source.

In the third plot, lower right of Figure 124, the same prepreg was staged for 18 days at room temperature and then subjected to identically the same vacuum-heat application. From this plot we see that the measured vacuum in the cavity remains high for a considerably longer period of time, thus enabling the removal of moisture or gas from a void pocket. It was apparent then that the level of resin tack was playing a part in the removal of moisture and air in a laminate.

Tacky fresh prepreg has a tendency to seal off void pockets, while staged, lower tack prepreg allowed for the removal of volatile products by not completely sealing off void areas in the initial part of the cure cycle.

Figure 125 shows additional cavity pressure experiments using different materials and test parameters. The data plotted in the upper left of this figure utilized 5208/T-300 net resin prepreg, 2.5 milliliters of water was added to the cavity and 0.586 MPa (85 psi) pressure and vacuum were applied immediately. This plot showed only pressure generated from steam and no vacuum. The cavity sealed off to external vacuum immediately with the application of 0.586 MPa (85 psi). This plot shows however, that localized concentrations of water trapped in a void area can generate in excess of 0.241 MPa (35 psi) internal pressure at 127C to 132C (260 to 270F). This data also followed predictable pressure levels from the steam tables over the temperature range investigated.

The upper right plot in Figure 125 was data generated on 1076E graphite/epoxy net resin prepreg. As shown by this plot, a full vacuum can be measured in the cavity for a considerable period of time. When the temperature increased up to 66C (150F), the resin softened and sealed off the cavity to the vacuum source. The vacuum was then released and reapplied. Autoclave pressure of 0.586 MPa (85 psi) was then applied to the laminate. Continued heating to 127C (260F) showed the pressure within the cavity going to the positive pressure side to about 0.034 MPa (5 psi). The pressure increase was a result of water and air migration between plies into the evacuated cavity negating the established vacuum.

The bottom plot in Figure 125 showed a comparison of vacuum profiles of 5208/T-300 and 1076E net resin prepregs. Water had been added to the cavity, and as shown before, pressure from the generation of steam started around 82C to 88C (180F to 190F). Both of these net resin systems remained open to vacuum throughout the temperature profile indicated.

Several conclusions were reached in this study:

a. Resin rich prepreg plies can consolidate under vacuum to prevent evacuation of potential void sites.

b. Net resin prepreg void sites remain open to the influence of vacuum for a longer period of time than resin rich prepreg.

c. Degree of resin tack can affect the way prepreg plies consolidate under a vacuum bag.

d. Application of additional pressure at any temperature level immediately seals off laminate void sites to external vacuum.

e. Moisture trapped in a void site can generate internal pressure in excess of 0.241 MPa (35 psi) at 132C (270F).

2.10.4 FABRICATION OF A QUALIFICATION LAMINATE. A qualification laminate, 0.61 m by 0.91 m (2 by 3 ft) by 80 plies with internal ply drop-offs was fabricated from the same batch of material used in the fabrication of the three vertical tail skins, Batch 9, 5208/T-300. The water content of the roll of prepreg used to fabricate the qualification laminate was determined to be 0.098 percent/weight as compared to water contents of prepreg used for vertical tail fabrication of 0.25 to 0.35 percent by weight. (A considerably lower water content prepreg was used to make the qualification laminate). The laminate was bagged and cured identically with Production F-16 vertical tail skins. The resulting qualification laminate was examined both using ultrasonic C-scan and micro-sectioning to determine the laminate quality. Both examinations showed a void-free laminate, i.e., no voids around ply drop-off areas. The results from this laminate were certainly different than those attained with the vertical tail skins.

Either the general geometry of the qualification laminate was not representative of a vertical tail skin, or a much lower water content in the prepreg used

for the qualification laminate played a significant part in achieving a void-free quality laminate.

A relatively simple internal ply drop-off laminate was constructed using both 5208/T-300 and 1076E net resin prepreg. The laminate configuration as shown in Figure 126 was 0.46 m by 0.46 m (18 in by 18 in), 0°, 90° ply orientation and incorporated three and four ply internal drop-offs.

The 5208/T-300 laminate was precompacted for one hour with no vacuum at 82C (180F) with 0.689 MPa (100 psi) applied to the laminate surface via autoclave processing. The 1076E laminate was compacted with no vacuum for one hour under 0.689 MPa (100 psi) at room temperature.

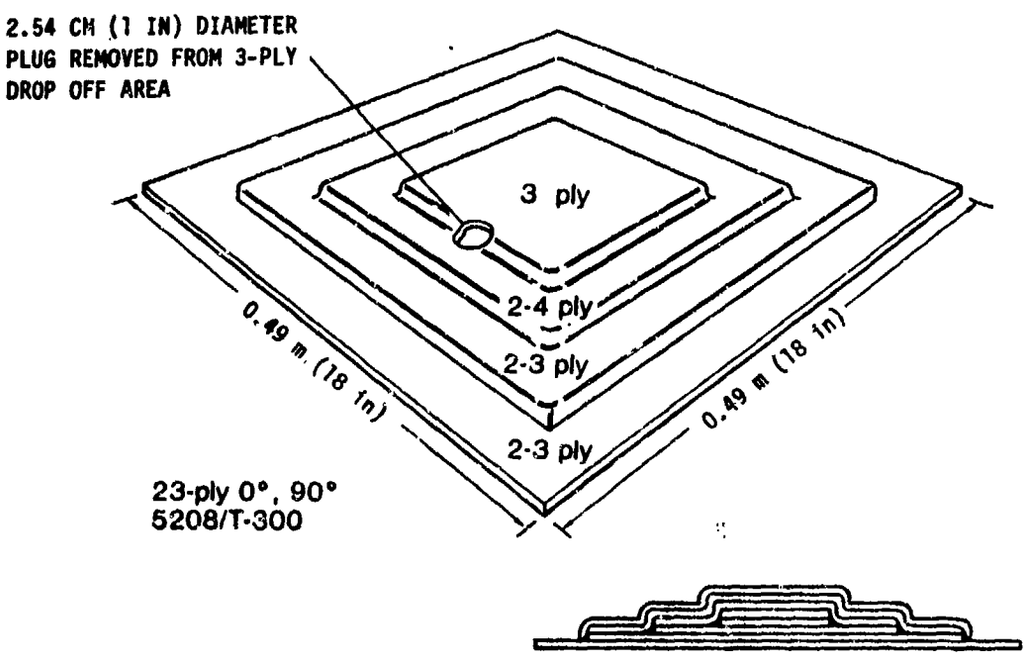

Figure 126. Compaction Study Internal Ply Drop-Off Laminate

Figure 127 shows C-scans of these two compacted laminate billets. The appearance of apparent void areas are easily seen in the 5208/T-300 laminate, while void areas are not seen in the 1076E laminate compaction.

Two 2.54 cm (1 in.) diameter plugs were cored from each compacted laminate in the areas shown as dark circles on the C-scans in Figure 127. The cored sections were then inspected for the presence of voids around internal ply drop-off areas. The 1076E laminate had no void areas associated with its internal ply drop-offs, however, the 5208/T-300 laminate had distinct void areas located precisely at the internal ply drop-off area. As shown in Figure 128, the size of the voids were 0.038 to 0.508 cm by 0.33 to 0.533 cm (0.015 in. to 0.020 in. by 0.13 in. to 0.21 in.) wide. Additional inspection of selected void areas around the ply drop-off revealed voids as wide as 1.9 cm (0.75 in.) by 0.038 cm (0.015 in) to 0.635 cm (0.025 in) high. Considering the level at which compaction was attempted on the 5208 system, the quality of the compaction was quite poor. This confirmed previous compaction studies on 5208. At 82C (180F) the viscosity of the 5208 resin is nearly at its lowest level of between 2 to 5 poises. At that viscosity level, it had been previously assumed that resin flow would have easily filled any void areas.

2.10.5 BAGLESS CURED INTERNAL PLY DROP-OFF LAMINATE. Internal ply drop-offs were incorporated into a laminate for bagless curing. The material selected for this experiment was Fiberite's 1076E prepreg, the same material that produced a good C-scan of compacted prepreg in Figure 127. The actual laminate size for this experiment as shown in Figure 129, was a 0.61 m by 0.61 m (2 ft by 2 ft) by 80 plies maximum dropping-off to a minimum of 20 plies in the thinnest area.

Compaction of this laminate was attained after just one hour at 0.689 MPa (100 psi) at room temperature. The nylon bag, two plies of 181 bleeder and

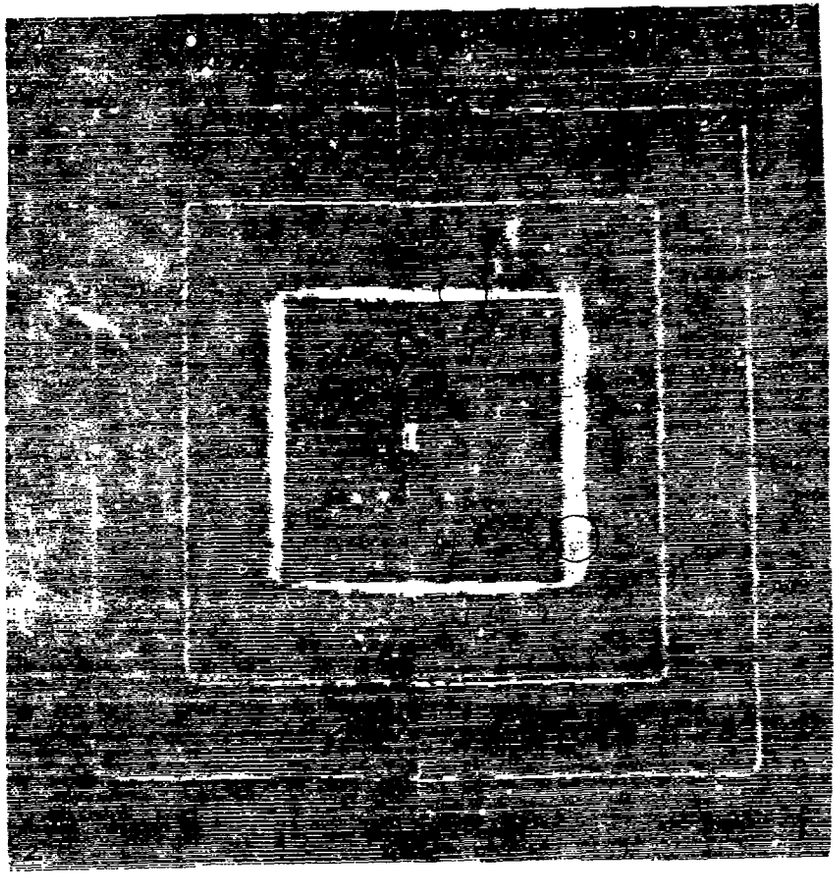

5208/T-300 Narmco
Compacted 1 Hour,
0.689 MPa (100 psi) at 82C (180F)
2.25 MHz, 1 x 2.5

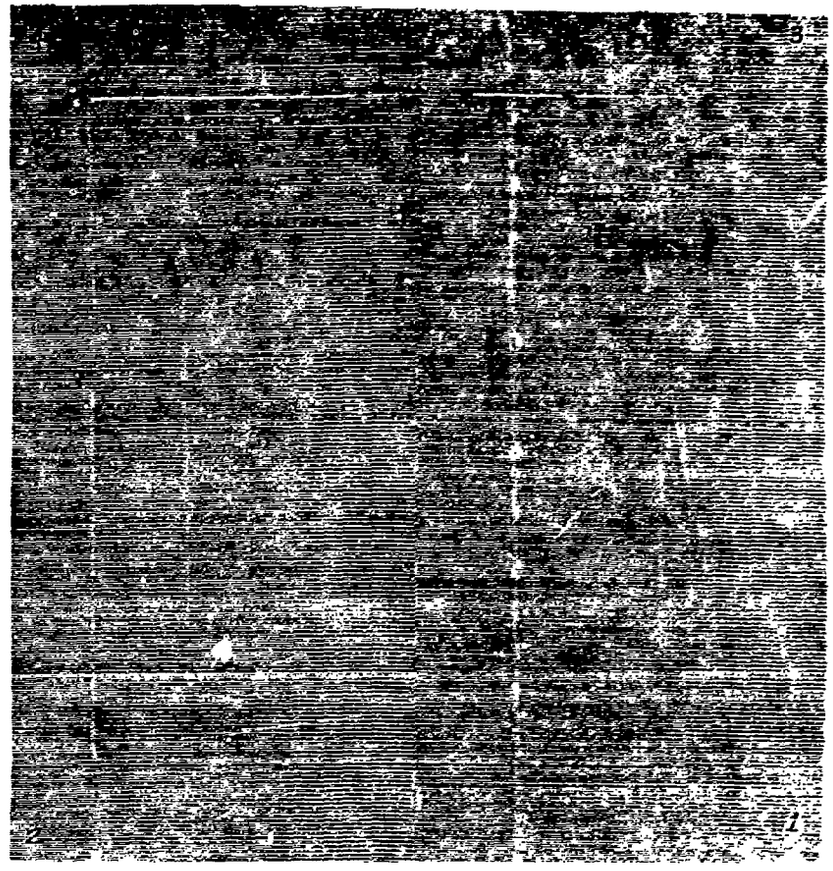

1076E Fiberite
Compacted 1 Hour,
0.689 MPa (100 psi) at RT
2.25 MHz 1 x 2.5

DARK CIRCLES in 5208 LAMINATE INDICATE AREAS CORED FROM PREPREG LAYUP FOR INSPECTION

Figure 127. C-Scans of Internal Ply Drop-off Compacted Prepreg Lamiantes (23 Ply, 45 cm by 45 cm)

6X

0.038 cm X 0.33 Cm
(0.015 in X 0.13 in)

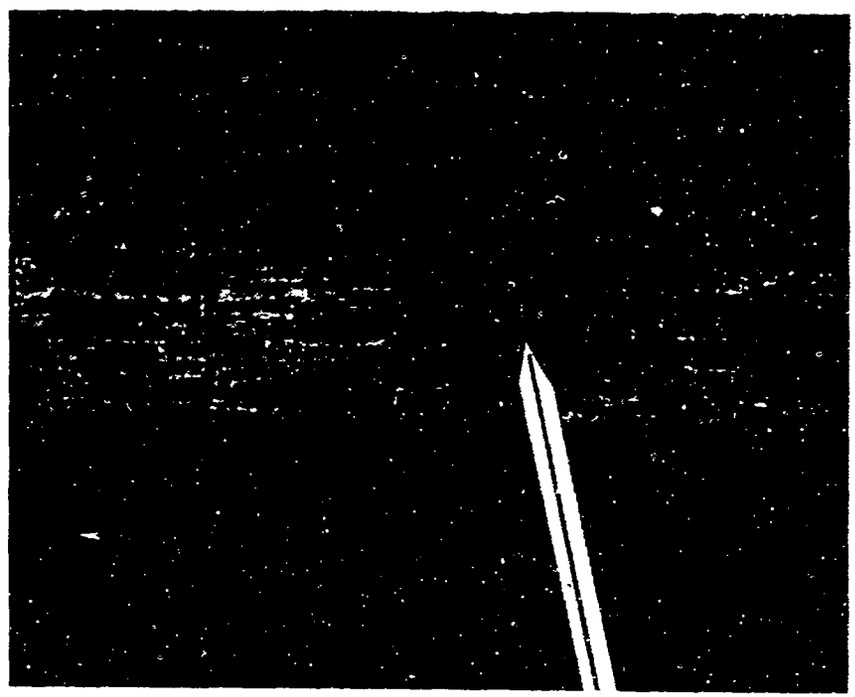

6X

0.051 cm X 0.53 cm
(0.020 in X 0.21 in)

LAMINATE COMPACTED FOR 1 HOUR, 0.689 MPa (100 PSI) AT 82C (180F)

Figure 128. Void Sites, 5208/T-300 Ply Drop-Off Laminates

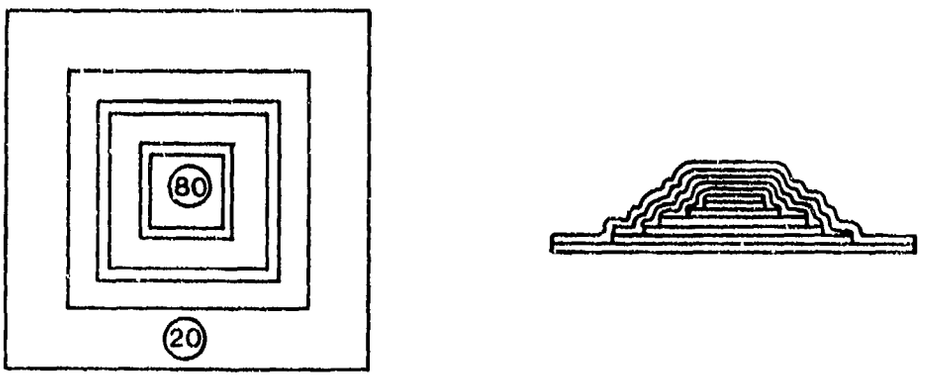

61 CM X 61 CM (24 IN X 24 IN)
80-PLY TOTAL INTERNAL PLY
DROP-OFF LAMINATE

Figure 129. Bagless Cured Internal Ply Drop-Off Laminate 1076E Prepreg

porous Armalon were removed from the laminate surface. The laminate was then cured under 0.689 MPa (100 psi) through a stepped temperature cure up to 177C (350F) for two hours.

The resulting cured laminate was subjected to C-scan and sectioning for micro-polish examination. C-scans showed a void free laminate, and Figure 130 shows a void-free 6 ply internal drop-off at 11X and at 50X.

2.10.6 ROCKWELL CURE EXPERIMENTS. In the previous section, ply drop-off experiments were described in which a machined groove in a caul plate functioned as a simulated ply drop-off. The groove was attached to a pressure transducer which monitored the air pressure in the groove during various cure schedules. It was shown that the groove (ply drop-off) can easily be sealed off from the vacuum source before a high vacuum is attained in the groove. This means that although the layup is in a vacuum environment, the actual pressure in the simulated ply drop-off region can be as high as atmospheric pressure depending on the history of the pre-plying in the vicinity of the ply drop-off. Resin viscosity, resin content, tack, and pre-ply history (how well the individual

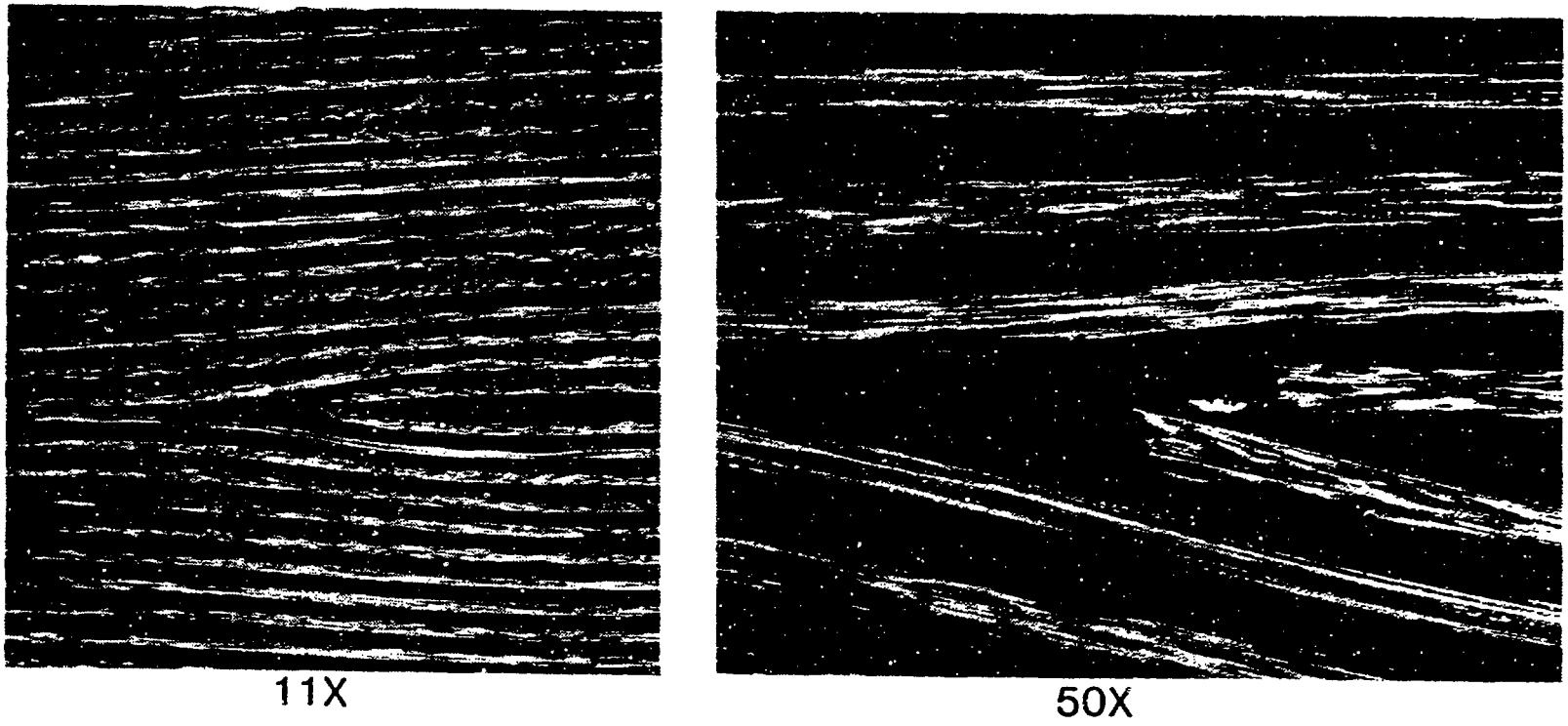

Figure 130. Polished Cross-Section of Internal Ply Drop-Off Laminate, Bagless Cured

plies are mated to the lay up stack) of the prepreg are all important factors which affect the pressure (vacuum) that a ply drop-off region experiences.

The effect of the measurement technology of the ply drop-off region was extended to the Rockwell nonautoclave (double vacuum bag) cure process to determine the pressure in a simulated ply drop-off. The Rockwell cure schedule is shown in Figure 131. The layup configuration for the Rockwell cure is shown in Figure 132. Two vacuum bags are employed during the cure. The first is the vacuum bag normally assembled next to the composite layup on the tooling surface. The second vacuum bag covers the first but outside of a "hard cover" which prevents the collapse of the second bag onto the part when the vacuum is applied thereby eliminating any compaction pressure. The transducer was attached to the groove and the wiring led to a continuous readout strip recorder which measured the voltage output of the transducer (a linear function of the pressure). The input voltage was controlled by a stable 10 volt power supply. The gain and offset of the recorder were adjusted to maximize the pen response to a pressure change of ambient to a nominal 711 cm (28 in) of mercury vacuum. This technique gave the best pressure measurement accuracy.

A 50 ply, 0.305 m by 0.305 m (12 in by 12 in) crossplied layup [0, 90°], of U.S. Polymeric's E767 low flow resin system on T-300 carbon fiber was positioned on the grooved caul plate so that the first ply ran orthogonal to the groove. The layup was covered with Armalon and a Teflon barrier film. Four plies of 181 glass fabric over the stack served as the breather for the system. The vacuum bag was assembled and checked for leaks. A steel and plywood frame was constructed over the first bag, complete with breather and vacuum ports. It was also tested for leaks prior to starting the Rockwell cure schedule. A second pressure transducer was inserted between the inner and outer vacuum bag. The second transducer served as an applied pressure (vacuum) check and since it tracked the pressure at the same rate as the groove transducer, would indicate

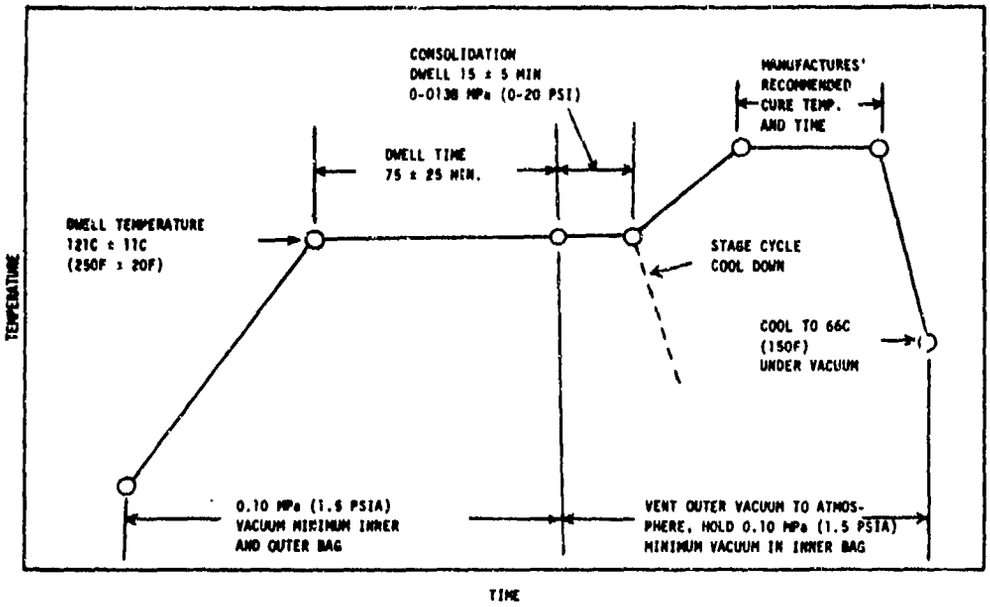

Figure 131. Rockwell Cure Schedule

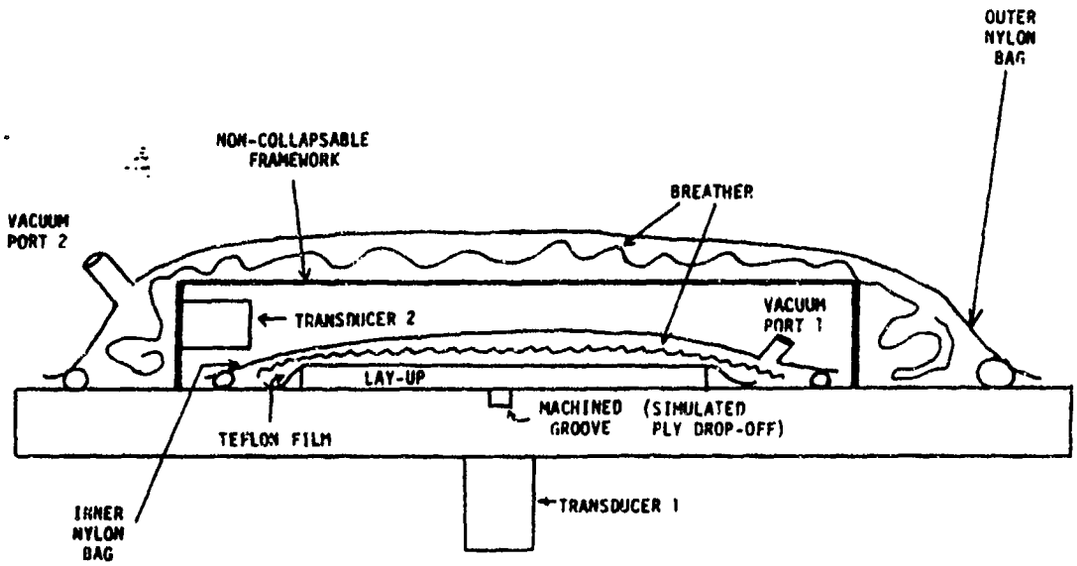

Figure 132 Lay-up Configuration for Rockwell Cure

lag any times of the vacuums measured between the inner and outer bags and in the groove below the laminate.

The Rockwell cure is essentially a vacuum degassing operation followed by a consolidation step. The first vacuum bag doesn't exert any force on the layup since the pressure in the inner and outer bags are equal. This allows the layup to expand and degas on heating during the first part of the cure schedule (Figure 131). The cure schedule is a simple heat-up to 121C (250F) followed by a 75 minute hold, after which the vacuum between the inner and outer bags is vented to atmosphere. The venting allows 0.101 MPa (14.7 psia) absolute to be applied to the degassed lay up and consolidation occurs during an additional 15 minute dwell at 121C (250F). After consolidation, the cure can either proceed or the laminate can be cooled for storage and later use.

The first step in the Rockwell schedule is the application of vacuum to both the inner and outer bags. The pressure in the simulated ply drop-off was at ambient before vacuum application. As the inner and outer bags were evacuated, the pressure in the groove followed the applied vacuum (between the inner and outer vacuum bags) to the maximum applied. Heat was started and the pressure monitored continuously through the schedule. After 75 minutes of hold at 121C (250F), the vacuum between the inner and outer bags was vented to consolidate the prepreg stack. The vacuum in the groove was maintained (see Figure 133) through the consolidation step and cooldown.

The laminate was removed from the caul plate, and it was observed that the laminate had been forced partially into the groove by the vacuum pressure. The portion of the laminate in the groove was observed to have a resin rich surface. Presumably the vacuum started to draw the resin into the vacuum void area. Figures 134 and 135 are microsection photographs which illustrate the resin rich area and small voids in the laminate. No significant

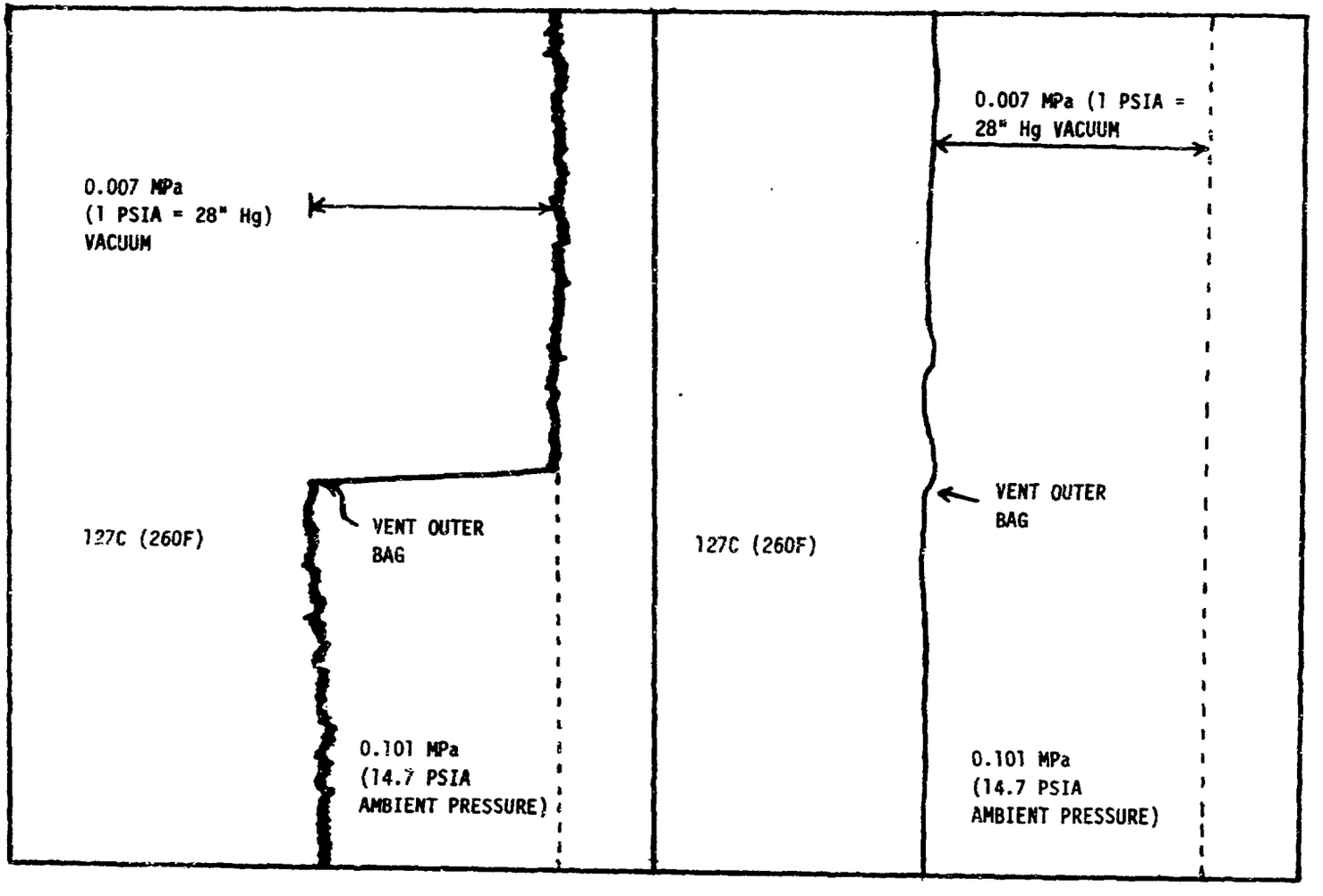

Figure 133. Trasnducer Read-Outs of Rockwell Cure

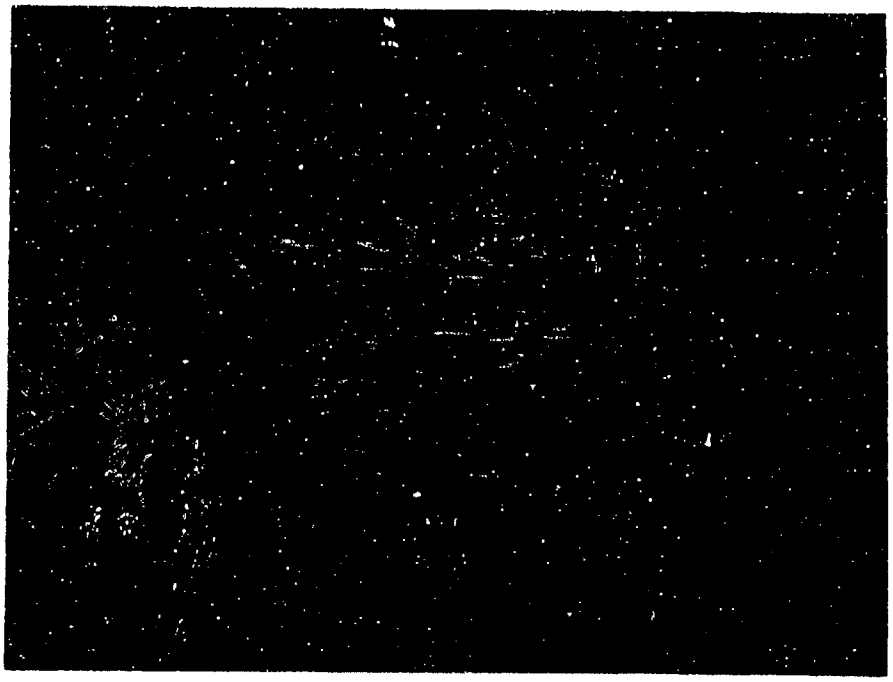

Figure 134. 18X Magnification of Unidirectional E767 Laminate Cured by Rockwell Technique

Figure 135. 100X Magnification of Unidirectional E767 Laminate Cured by Rockwell Technique

voids were observed in the cross-section micropolish. The small voids are probably remnants of incomplete degassing of the very viscous resin employed in the system. A lower viscosity resin system (e.g. 976) should fill (collapse) the vacuum void with resin.

2.10.7 FINAL THICK LAMINATE SCREENING PANEL. Prior to completing the final F-16 vertical stabilizer validation article, a thick laminate screening panel was fabricated. The screening panel serves as a prepreg lot acceptance test for incoming material at the Fort Worth Division. It is a 0.61 m by 0.91 m (2 ft by 3 ft) by 72-ply panel with numerous internal ply drop-offs. The panel geometry is similar to the panel in Figure 127. The panel was laid up according to Fort Worth drawing MED 82001 in a layup sequence illustrated in Figures 136 and 137. In this particular panel, a 0.32 cm by 15.24 cm (0.125 in by 6 in) groove was carefully cut into the internal 25 plies from the middle of the longest side of the layup. A steel tube with appropriate fittings to a transducer was filled with degassed MY-720 (uncatalyzed) to act as a fluid couple to the transducer. The groove was also filled with degassed MY-720 and the tube carefully embedded in the resin to eliminate any air bubbles. The panel was laid up with Fiberite's 1076E (lot C3-442) which was a net resin system. Armalon and a Teflon barrier film covered both surfaces of the panel. Two plies of 181 fiberglass served as a vacuum port breather. When the panel was started, a sample of the prepreg was left out in the 50 percent relative humidity layup area. The sample of prepreg was later tested for volatiles and compared to the as-received prepreg volatiles. The as-received material contained 0.40 percent by weight volatiles. The prepreg left out under ambient conditions during the layup time (approximately two days) absorbed moisture from the air and had a volatile content of about 0.4 percent. The laminate would not be expected to contain this latter quantity but some figure between the two, probably nearer to 0.40 percent because of the very

PLY NO.	ORIENT.
NYLON PEEL PLY	
P5362-1	
72	+45
71	-45
70	0
69	+45
68	-45
67	0
66	+45
65	-45
64	0
63	+45
62	-45
61	0
60	+45
59	-45
58	0
57	+45
56	-45
55	0
54	+45
53	-45
52	0
51	+45
50	-45
49	+45
48	-45
47	+45
46	0
45	-45
44	0
43	+45
42	0
41	0
40	-45
39	0
38	+45
37	0
36	0
35	+45
34	0
33	-45
32	0
31	0
30	+45
29	0
28	-45
27	0
26	+45
25	-45
24	+45
23	-45
22	+45
21	0
20	-45
19	+45
18	0
17	-45
16	+45
15	0
14	-45
13	+45
12	0
11	-45
10	+45
9	0
8	-45
7	+45
6	0
5	-45
4	+45
3	0
2	-45
1	+45
P5284-3	
NYLON PEEL PLY	
CURING TOOL	

Figure 136. Thick Laminate Screening Panel Layup Sequence

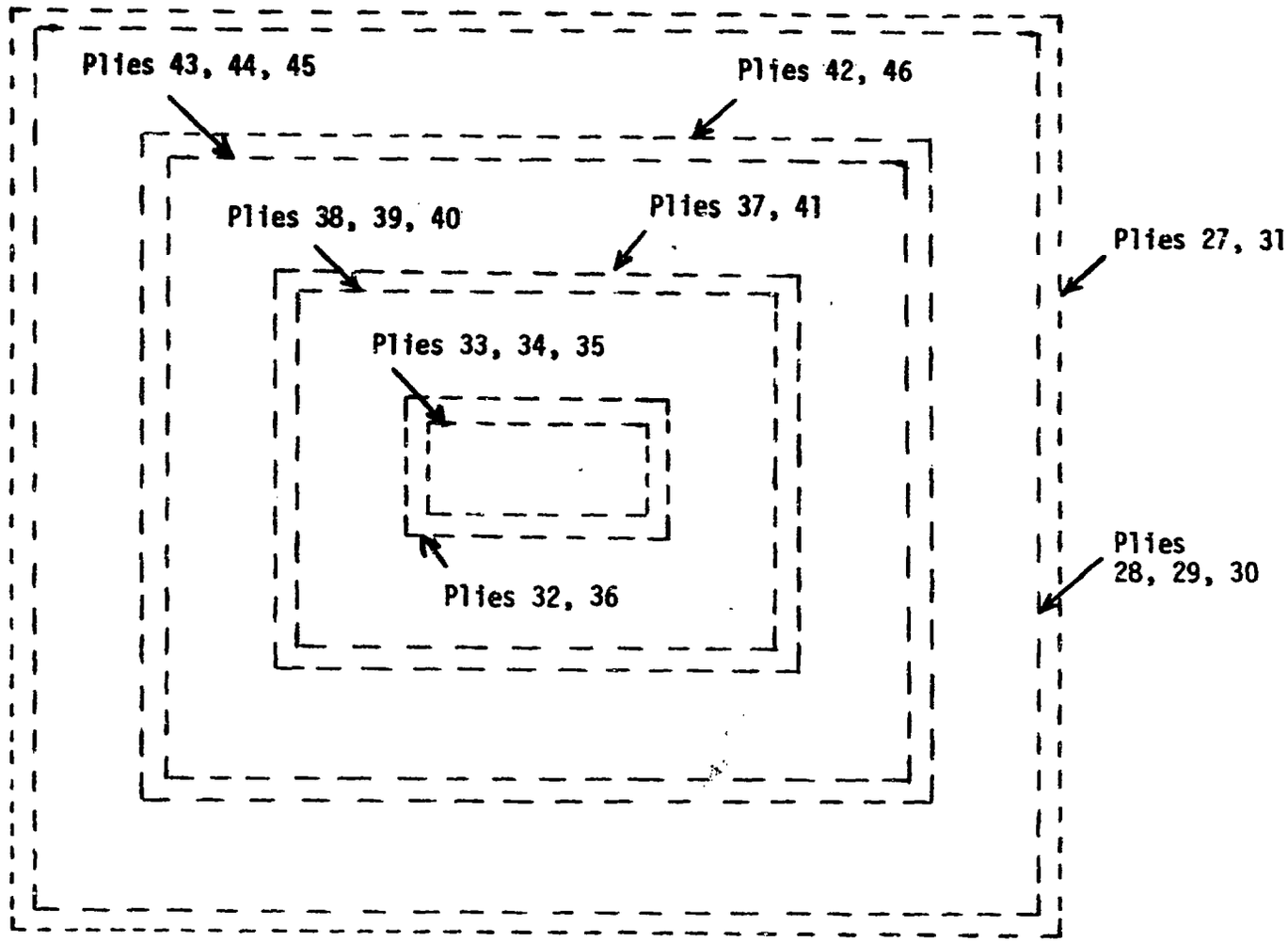

Figure 137. Thick Laminate Screening Panel Drawing

short actual exposure time to the atmosphere during the lay-up operation. The resin content of the prepreg was determined to be 30.3 percent. The laminate was bagged and an internally-pressurized-bag cure run according to the following cure schedule.

a. Heat to 93C (200F) and hold under 0.689 MPa (100 psi) for two hours, vacuum port vented to atmosphere.

b. Heat to 121C (250F) and hold for one hour.

c. Apply 0.345 MPa (50 psi) via pressurized nitrogen tank into the bag at start of heat-up to 121C (250F).

d. Heat at 2C/min (4F/min) to 177C (350F) and hold for two hours.

e. Cool down under pressure.

During this cure schedule, the resin pressure inside of the laminate was continuously monitored. At the beginning of the cycle, the applied pressure, 0.689 MPa (100 psi) was translated to the same pressure inside the laminate at low temperatures. As the temperature increased to 93C (200F) the pressure bled off to 0.517 MPa (75 psi). The pressure remained stable until a further heat-up to 121C (250F) commenced. The pressure gradually dropped to 0.386 MPa (56 psi) and then began to rise. At this point the viscosity of the resin increased and more applied pressure was translated into the laminate resin. The transducer readings were terminated after this point. The net resin prepreg laminates have been shown to have higher resin pressures than the high resin content 5208 prepregs which required considerable bleeding (or pre-bleeding) during the cure cycle. The internally applied pressure was not picked up by the transducers since only 0.345 MPa (50 psi) was applied and the resin never dropped below 0.386 MPa (56 psi). The internal pressurized bag technique provides good insurance against a low resin pressure which

in turn is a candidate for void generation. The resin in the laminate near the edge may very well have been less than 0.345 MPa (50 psi) as shown by the pressure gradient studies. The technique is required for high bleed systems to assure adequate resin pressure.

Ultrasonic C-scans of the panel indicated that the panel had no porosity at high sensitivity. The ply drop-offs could be seen in the C-scan but were probably due to a material discontinuity (a slightly resin rich area) in the thickness. Micropolishes indicated that no major voids existed at the ply drop-offs, Figures 138 to 143.

The specific gravity of the panel was an average of 1.61 g/cc. The resin content was determined to be 25 percent.

2.10.8 F-16 VERTICAL TAIL SKIN VALIDATION ARTICLE. Following the fabrication of the 0.61 m by 0.91 m (2 ft by 3 ft) Fort Worth qualification laminate, an F-16 vertical tail stabilizer skin was made at the Fort Worth facility employing the internal pressurization technique. The prepreg was machined layed up to the vertical tail dimensions. The layup was placed directly against the released tooling surface with Armalon fabric on the top extending beyond the boundary and breather chain. Bleeder (mat) was placed just over the part followed by perforated Teflon Film. One ply of 181 breather also extended beyond the breather chain. The bag was then placed into position.

The tool was placed into the clamshell tooling press and a vacuum applied internal to the bag. A pressure of 0.586 MPa (85 psi) was applied external to the bag and the vacuum vented to atmosphere. Steam pressure (about 0.041 MPa - 6 psi) was introduced into the press to heat the tool to 82C (180F). The part tended to heat from one end (steam source end) to the other. After about one hour, the part was up to temperature and was held for 60 minutes at 82C (180F). We had planned to maintain a longer hold time at 82C (180F), but because of a

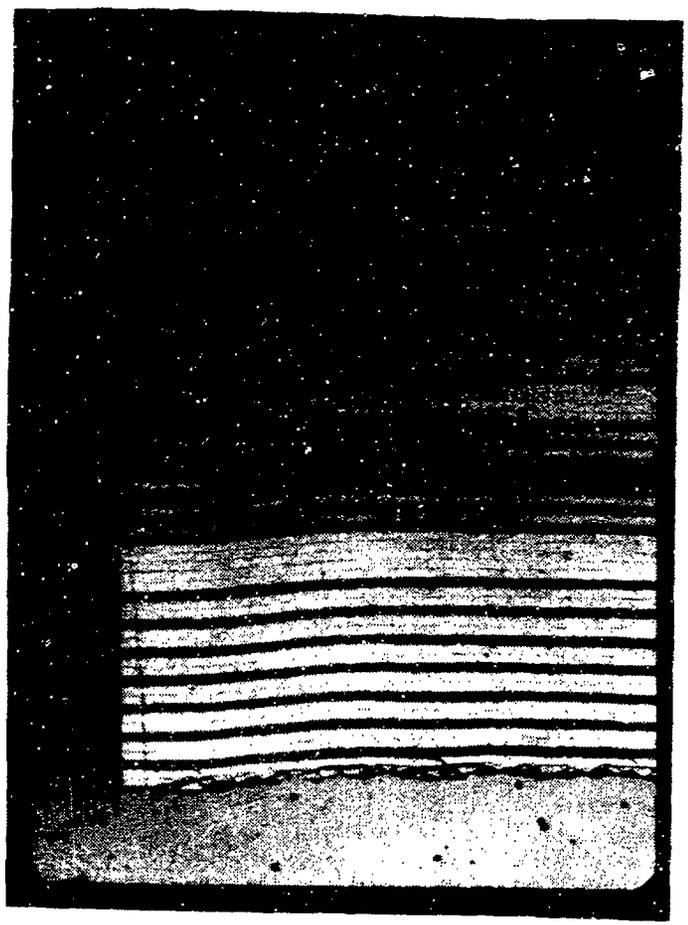

Figure 138. Ply Drop Off No. 1
Micropolish 9X

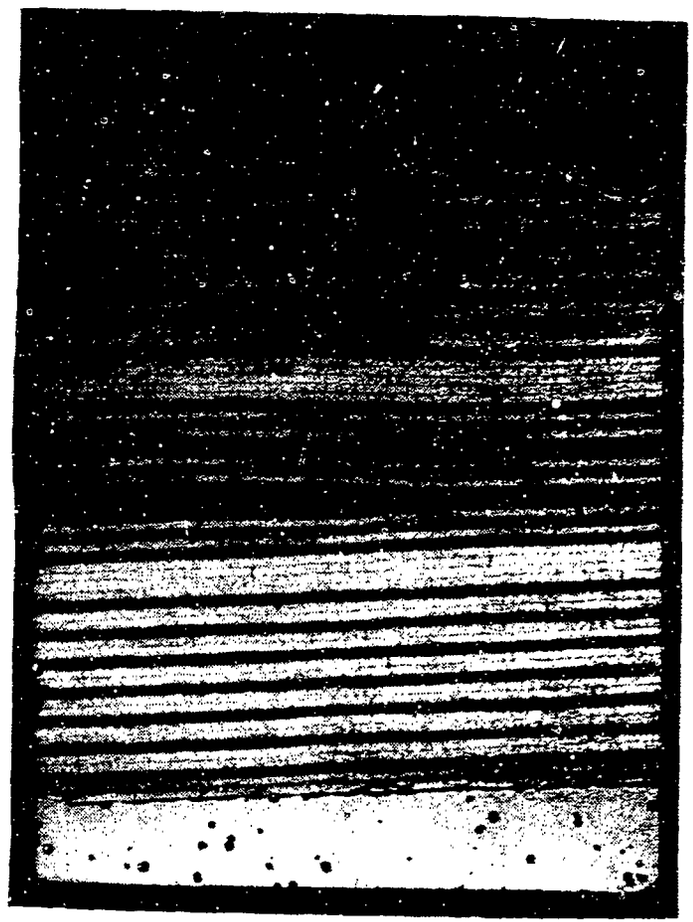

Figure 139. Ply Drop Off No. 2
Micropolish 9X

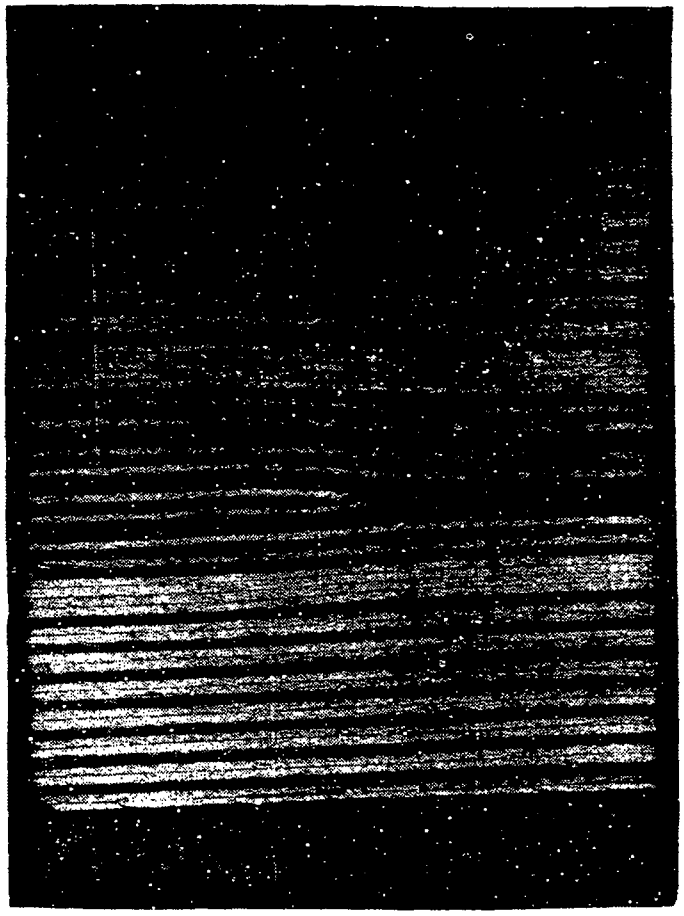

Figure 140. Ply Drop Off No. 3
Micropolish 9X

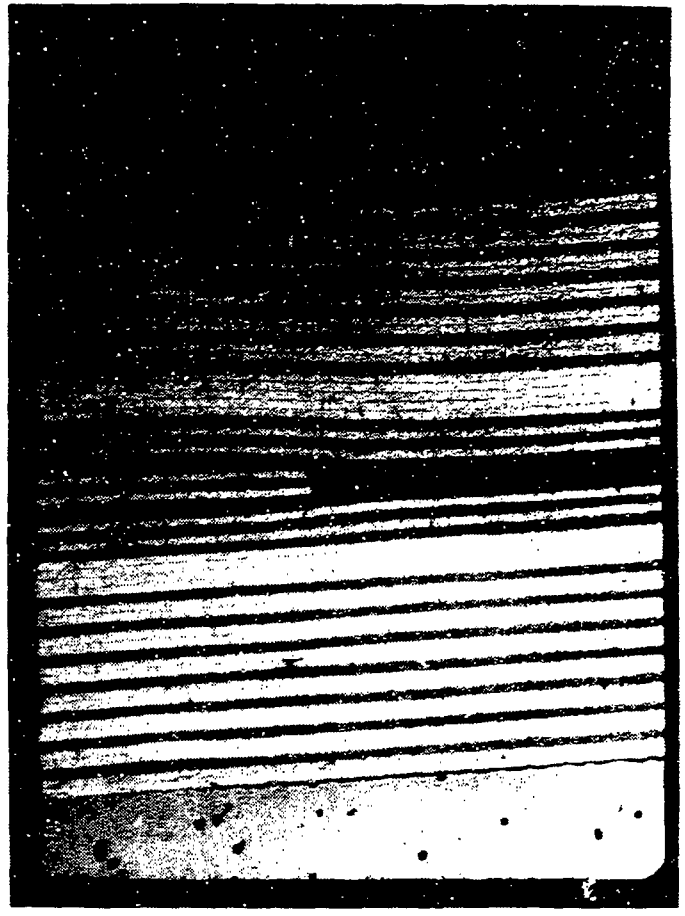

Figure 141. Ply Drop Off No. 4
Micropolish 9X

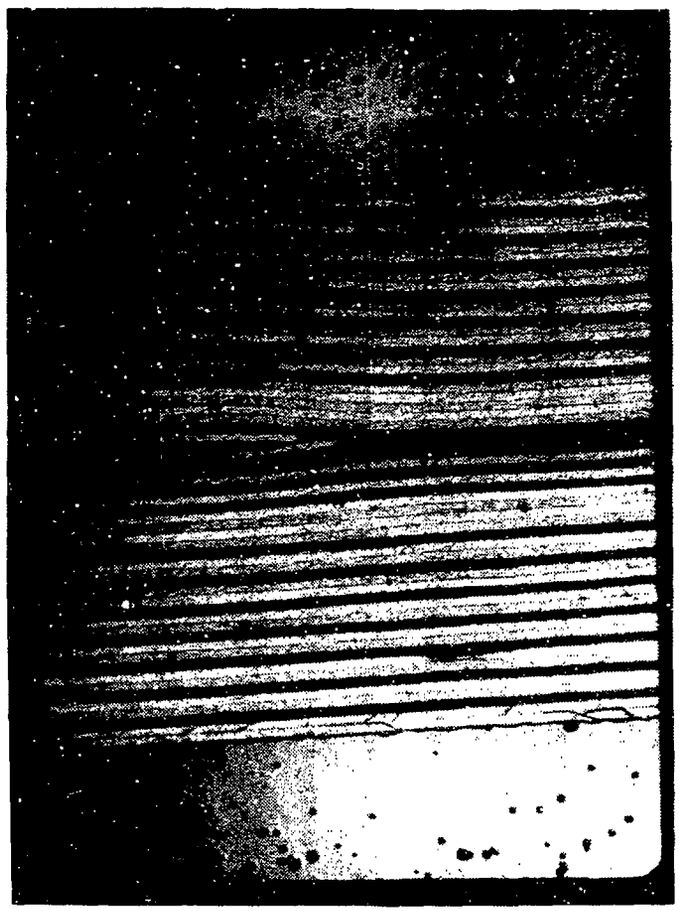

Figure 142. Ply Drop Off No. 5
Micropolish 9X

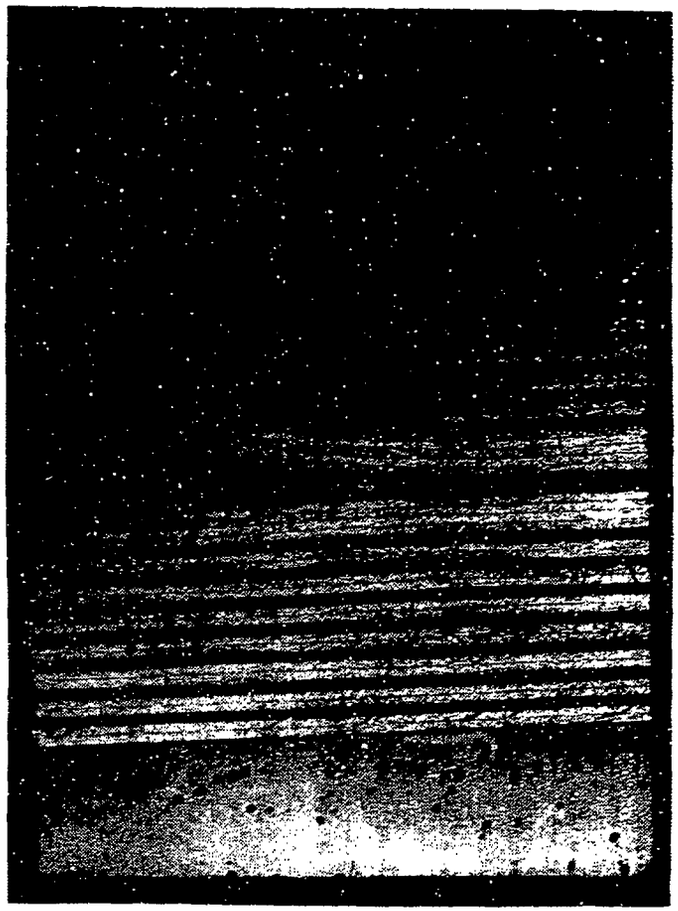

Figure 143. Ply Drop Off No. 6
Micropolish 9X

shift change, a shorter time was accepted. A transducer had been previously calculated and was inserted into the edge of the laminate. During the hold the pressure dropped from 0.414 MPa to 0.310 MPa (60 to 45 psi). This pressure corresponded quite well with the 0.61 m by 0.91 m (2 ft by 3 ft) laminate internal pressure measurements 0.379 Mpa (55 psi). After the one hour hold, the internal pressure was raised to 0.379 MPa (60 psi) (a differential of 0.172 MPa - 25 psi) and held at this value through the cure. The transducer readings tracked the internal pressure increase. The laminate skin was then heated to 177C (350F) and held for two hours for cure completion.

The bleeder/breather exhibited uniform resin distribution which appears to be different from the conventional Fort Worth cure. The Fort Worth cure usually produced a spotty bleeding into the breather ply through the porous Teflon separator film. This observation implies that a denser composite (higher carbon fiber volume) was produced with the internal pressure cure.

The ultrasonic C-scan results conducted at the Fort Worth facility indicated that the vertical stabilizer was of acceptable quality to be employed on the F-16. The only areas which indicated small void regions were at the internal ply drop-off areas. The voids were traced with a pulse echo transducer and the void were at the internal ply drop-off areas. The voids were traced with a pulse echo transducer and the void locations generally followed the build-up location and depth. Allowing an additional hour of compaction (as initially planned) may have decreased the amount of voids found by the secondary C-scan inspection technique.

APPENDIX A

VISCOSITY AND DIFFUSION DATA

SR 5208 batch 718

AUTOCLAVE CURE CYCLE VARIATION AC-2

3.6°F/min ramp to 190°F - Hold 30 minutes

3.6°F/min ramp to 260°F - Hold 140 minutes

3.6°F/min ramp to run termination

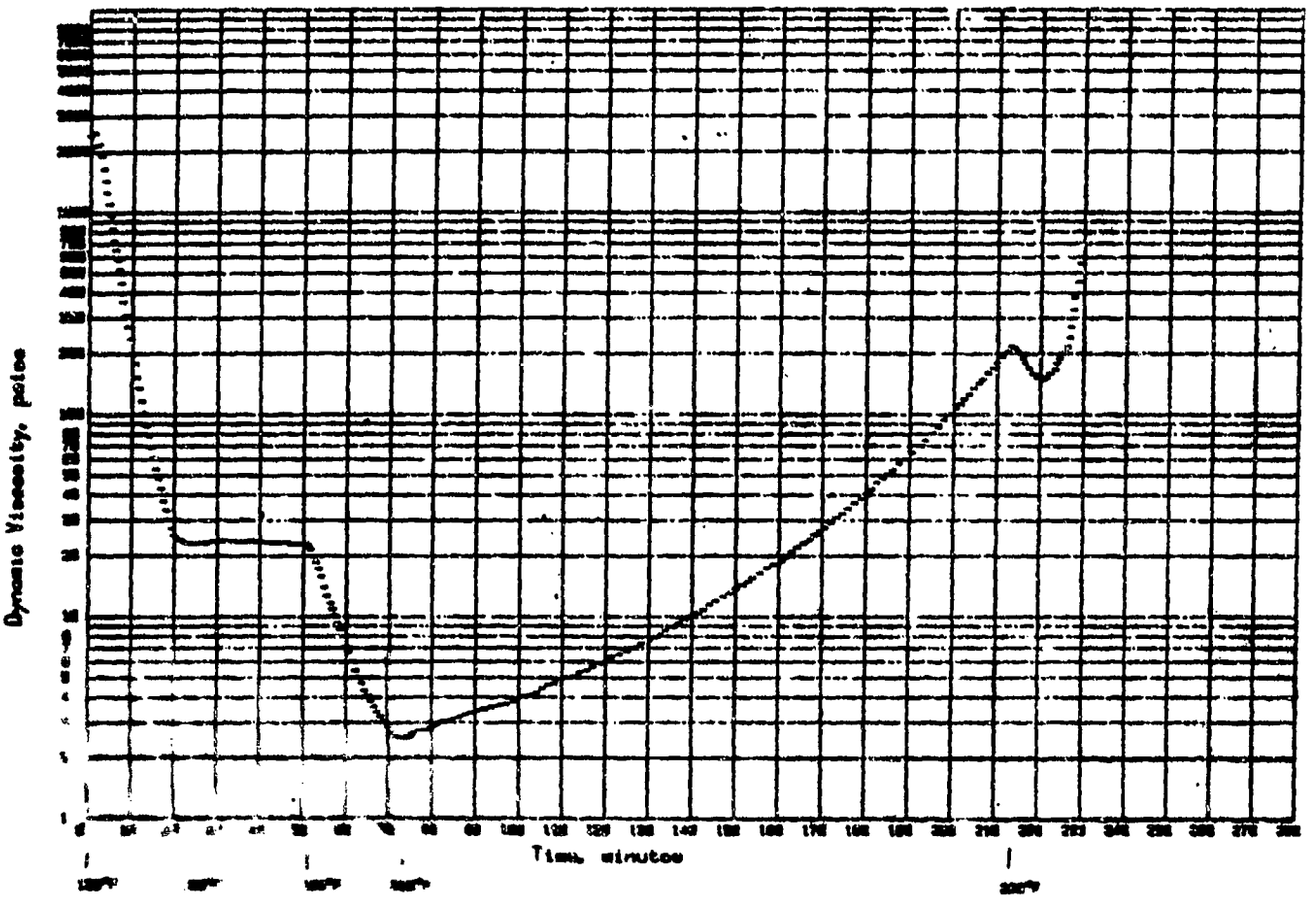

FIGURE A-1

Rheometric Visco-Elastic Tester
March 31, 1981

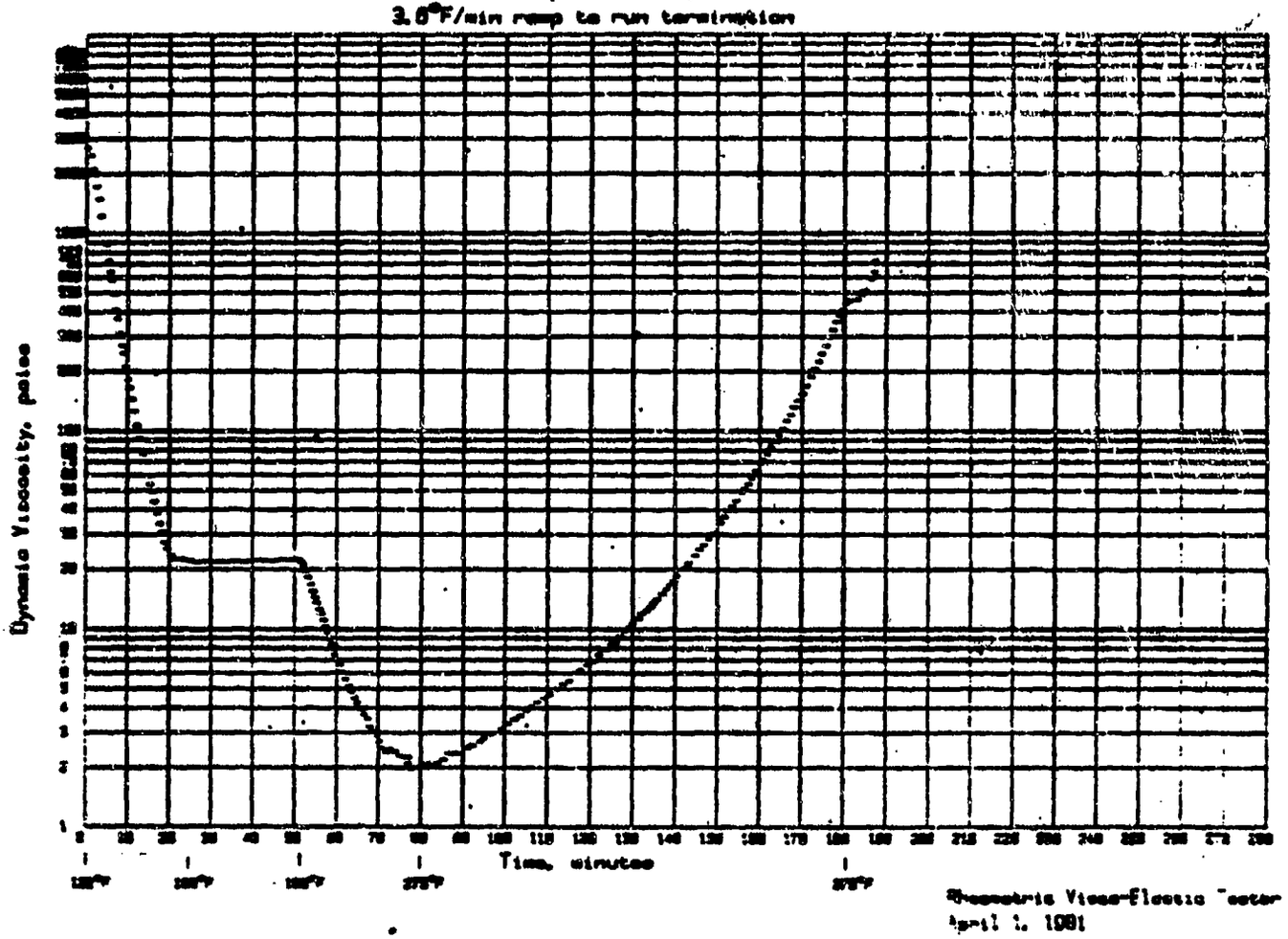
SR 5208 batch 718
AUTOCLAVE CURE CYCLE VARIATION AC-3
3.0°F/min ramp to 190°F - Hold 30 minutes
3.0°F/min ramp to 275°F - Hold 180 minutes
3.0°F/min ramp to run termination
Dynamic Viscosity, poise
Time, minutes

FIGURE A-2

SR 5208 batch 716

AUTOCLAVE CURE CYCLE VARIATION AC-4

2.8°F/min ramp to 180°F - Hold 30 minutes

3.6°F/min ramp to 275°F - Hold until run termination

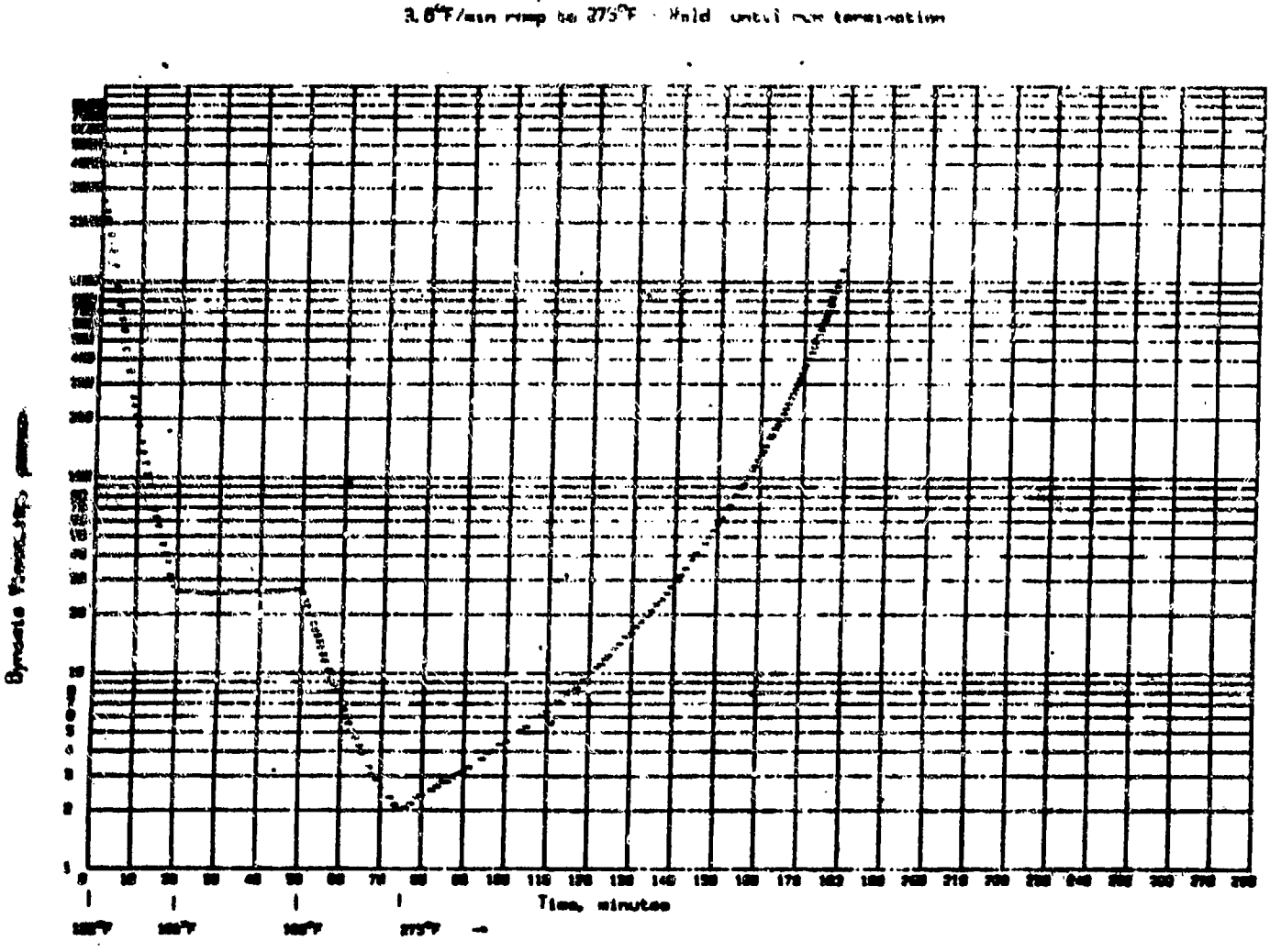

Rheometric Visco-Elastic Tester
April 22, 1981

Figure A-3

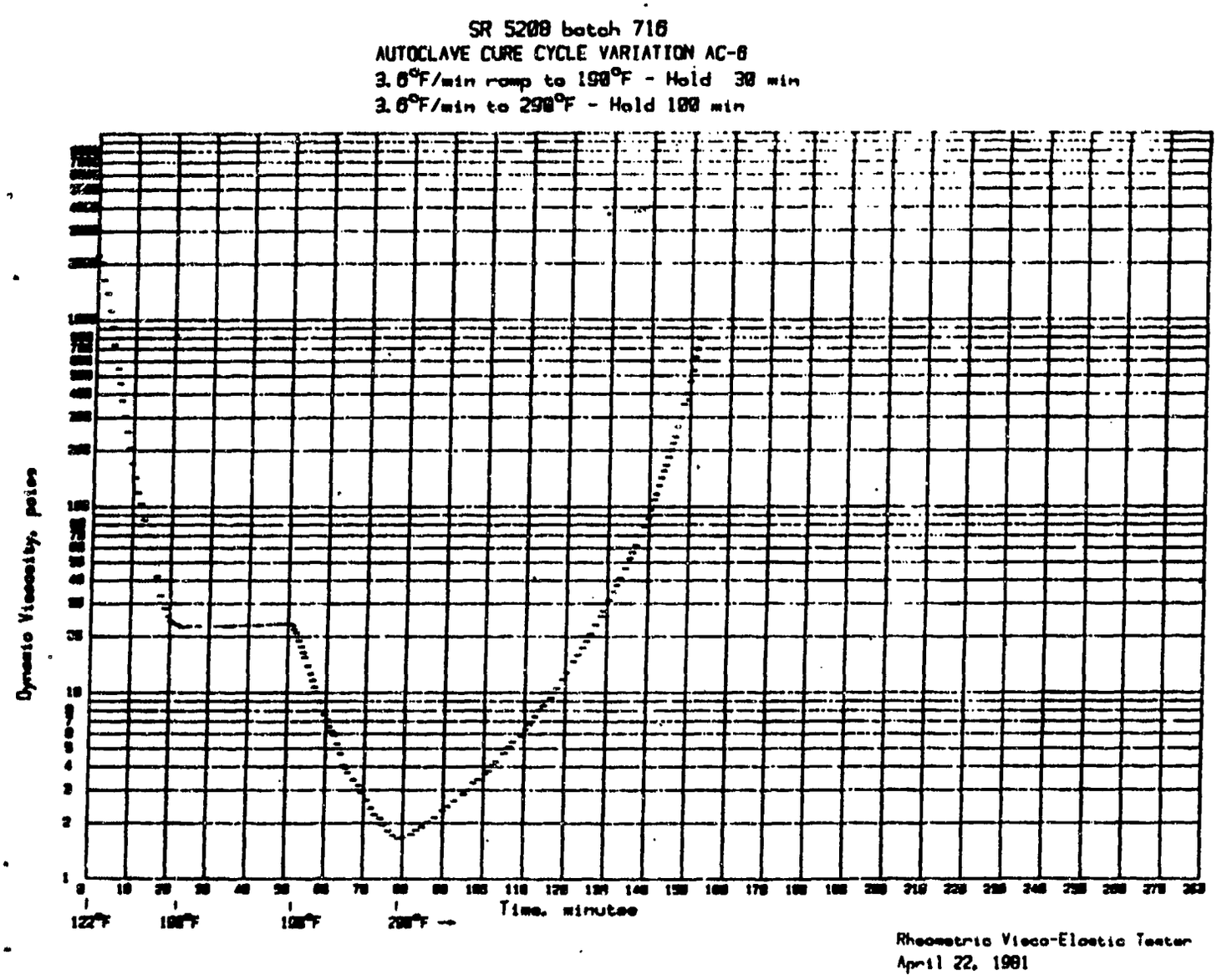
SR 5208 batch 716
AUTOCLAVE CURE CYCLE VARIATION AC-6
3.6°F/min ramp to 190°F - Hold 30 min
3.6°F/min to 290°F - Hold 100 min
Dynamic Viscosity, poise
Time, minutes
122°F
190°F
290°F →
Rheometric Visco-Elastic Tester
April 22, 1981

Figure A-4

SR 5208 batch 716

AUTOCLAVE CURE CYCLE VARIATION AC-7

1.8°F/min ramp to 190°F - Hold 30 minutes
1.8°F/min ramp to 260°F - Hold 100 minutes
1.8°F/min ramp to 317°F - run terminated

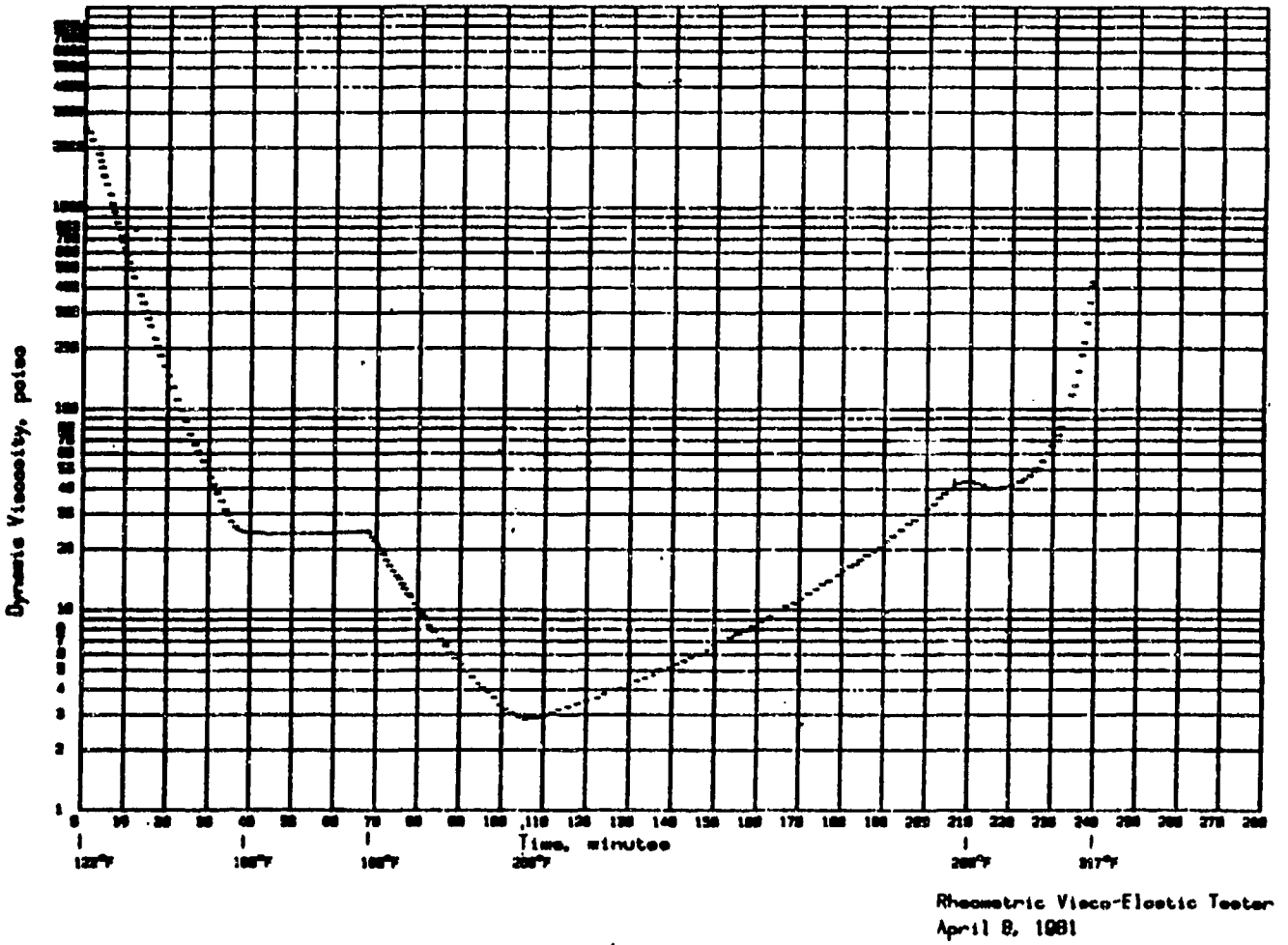

Rheometric Visco-Elastic Tester
April 8, 1981

FIGURE A-5

SR 5200 batch 716

AUTOCLAVE CURE CYCLE VARIATION AC-8

1.8°F/min ramp to 195°F - Hold 30 minutes

1.8°F/min ramp to 250°F - Hold 140 minutes

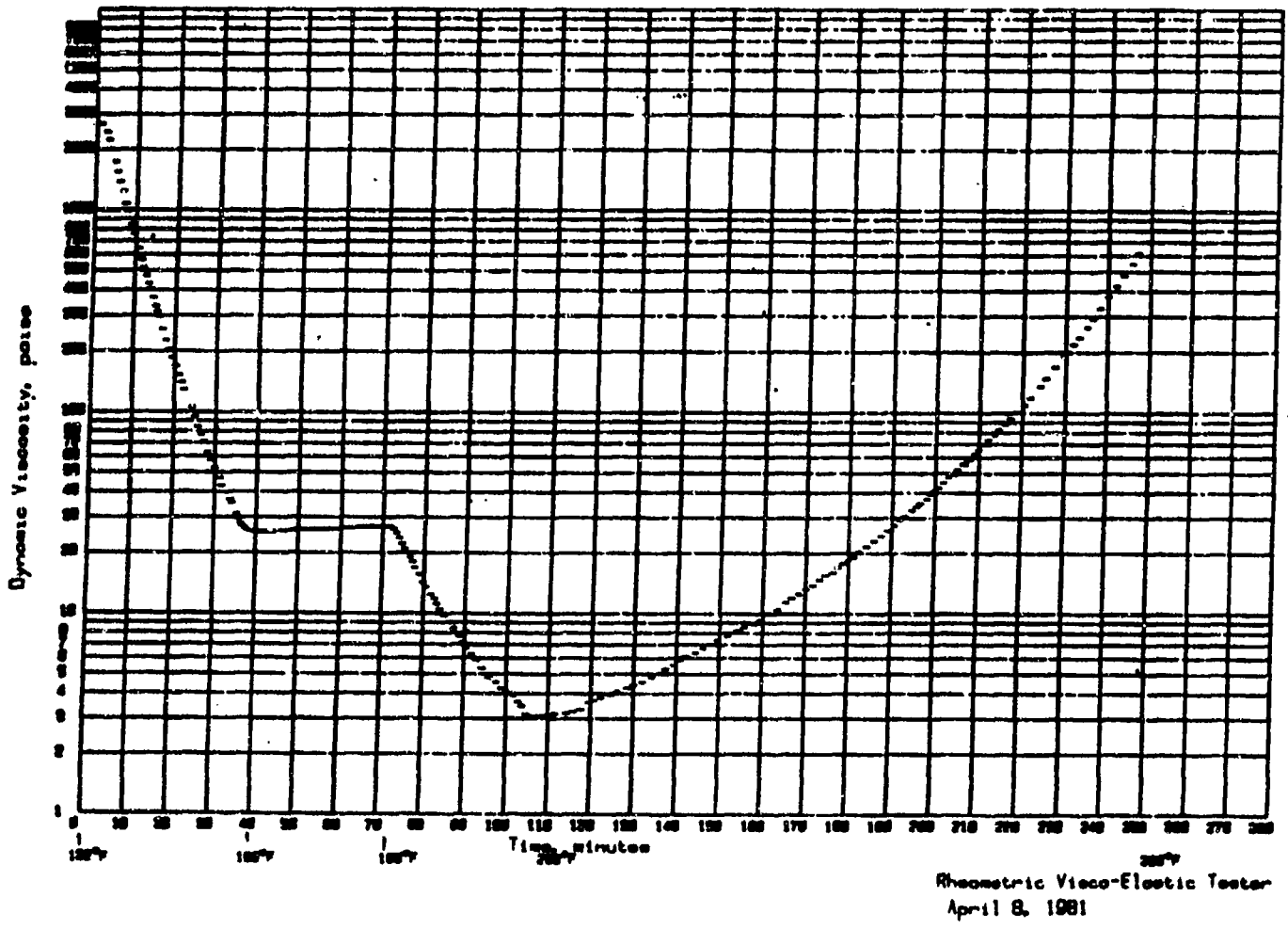

Figure A-6

SR 5200 batch 716

AUTOCLAVE CURE CYCLE VARIATION AC-9

1.8°F/min ramp to 190°F - Hold 30 minutes

1.8°F/min ramp to 275°F - Hold until run termination

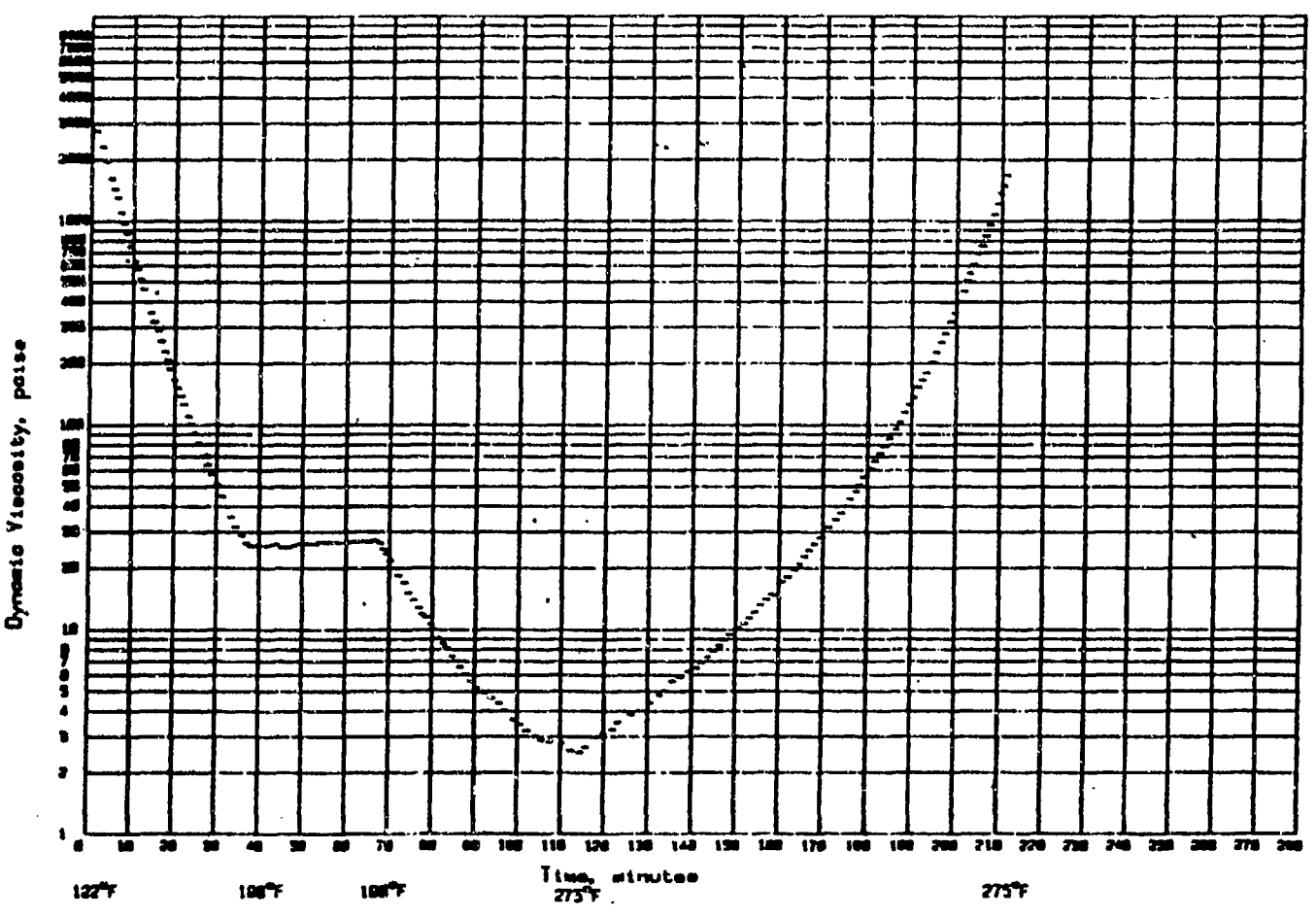

FIGURE A-7

SR 5208 batch 718

AUTOCLAVE CURE CYCLE VARIATION AC-11

1.8°F/min ramp to 190°F - Hold 30 minutes

1.8°F/min ramp to 290°F - Hold 180 minutes

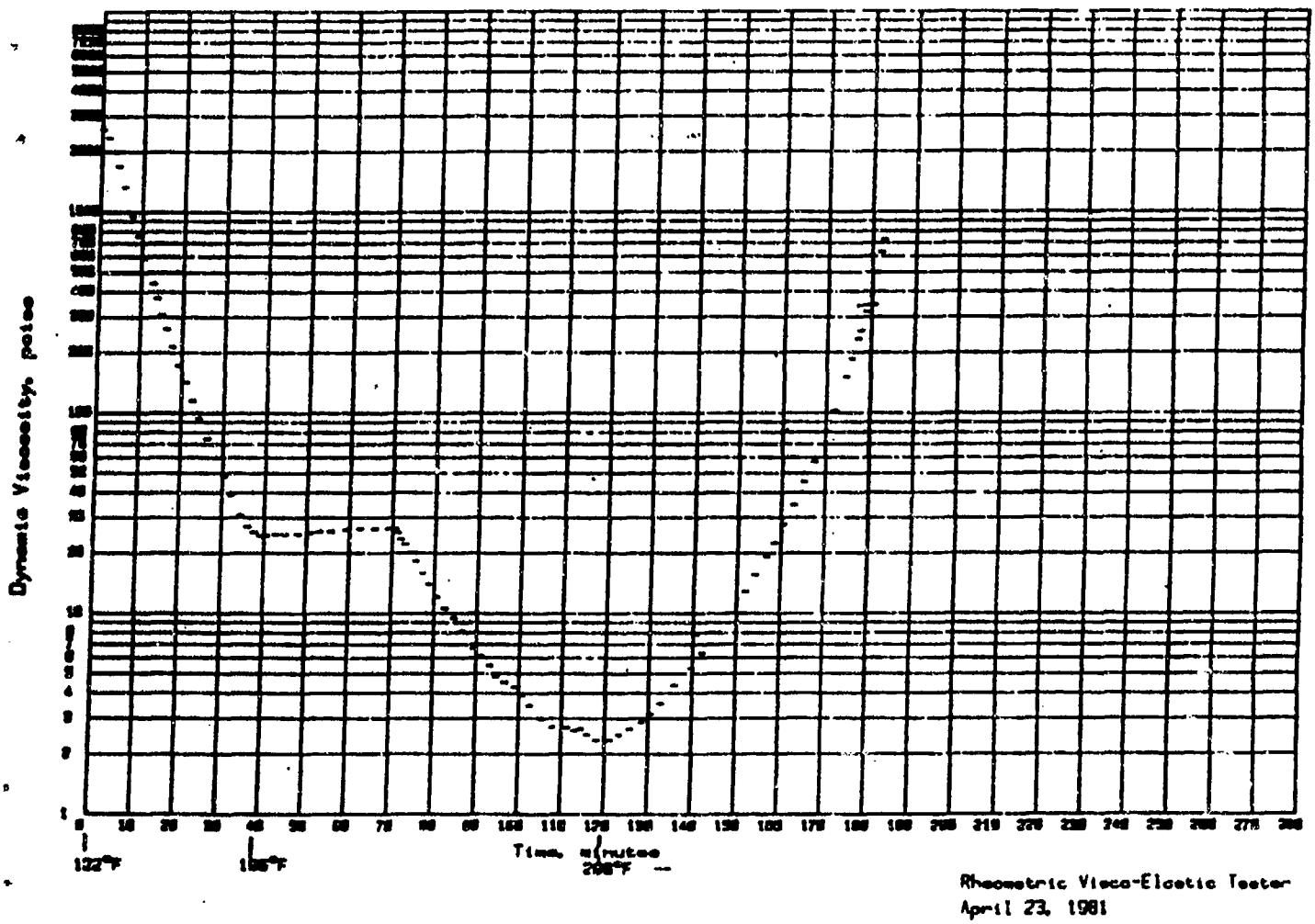

Figure A-8

SR 5208 batch 718

AUTOCLAVE CURE CYCLE VARIATION ACR-13

3.6°F/min ramp to 190°F - Hold 30 minutes
1.8°F/min ramp to 275°F - Hold 185 minutes
1.8°F/min ramp to run termination

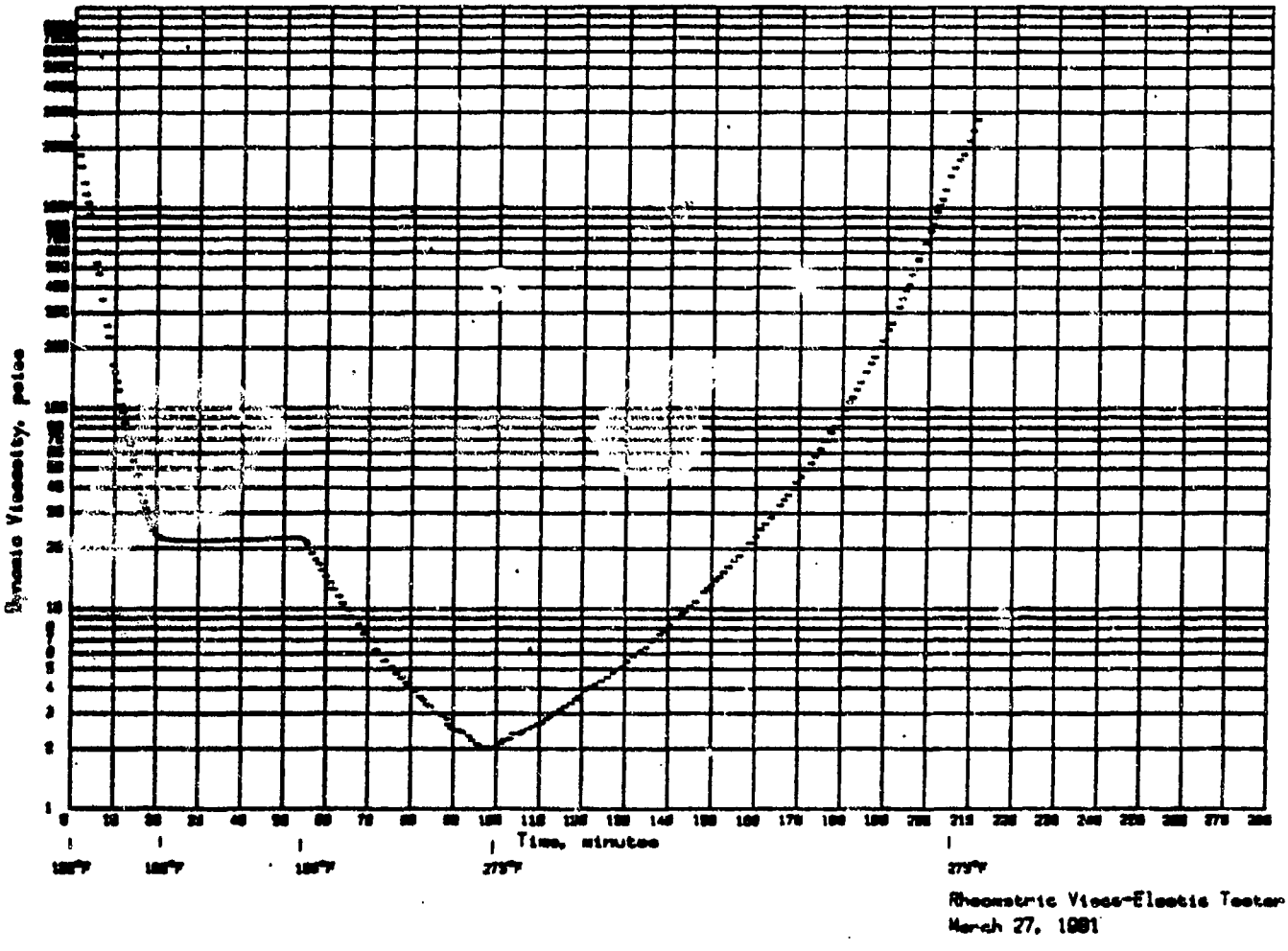

FIGURE A-9

SR 5208 batch 716

AUTOCLAVE CURE CYCLE VARIATION ACR-14

3.6°F/min ramp to 225°F - Hold 0 minutes

1.8°F/min ramp to 275°F - Hold 105 minutes

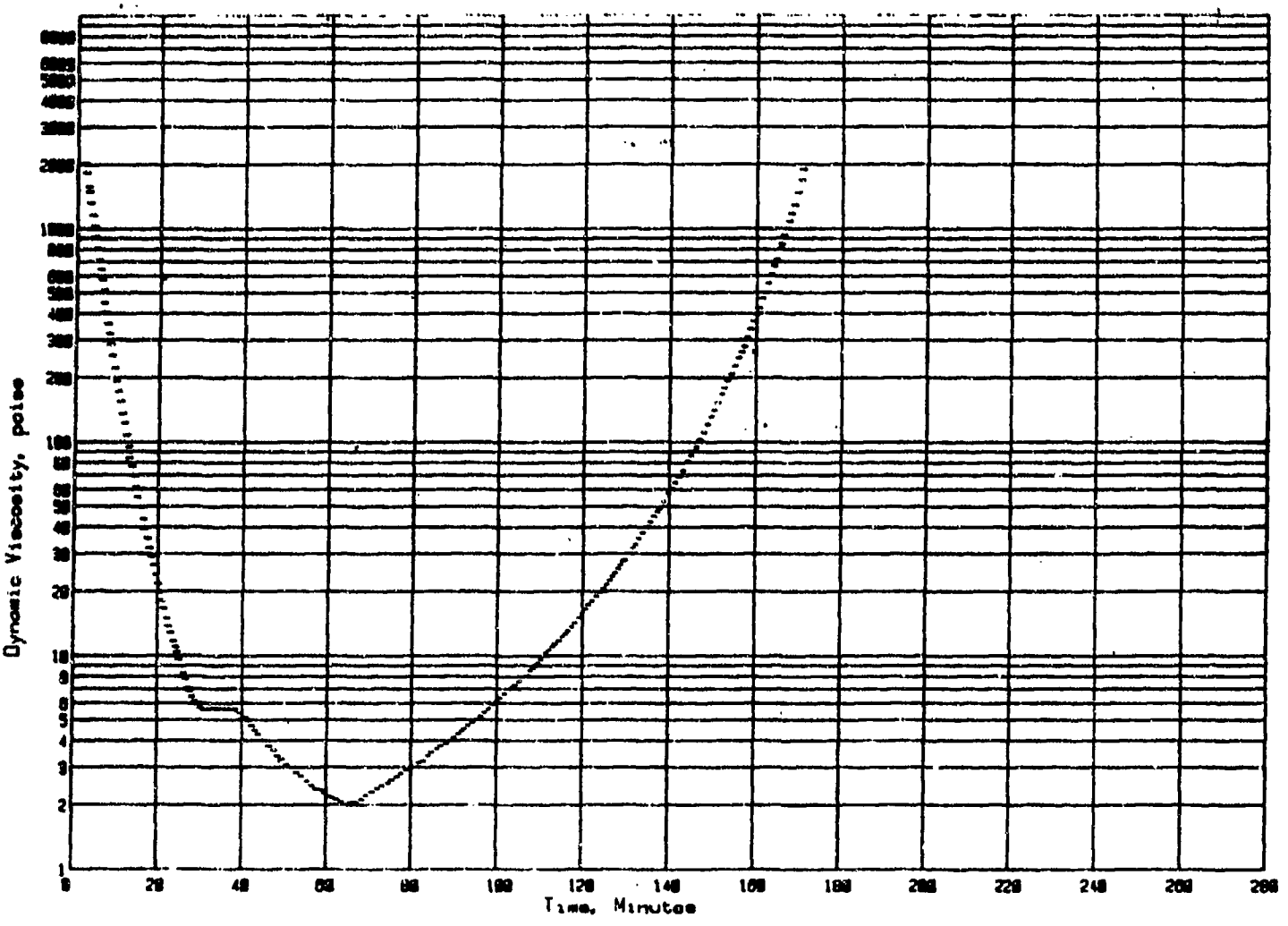

Rheometric Visco-Elastic Tester

May 11, 1981

FIGURE A-10

SR 5208 batch 716
AUTOCLAVE CURE CYCLE VARIATION ACR-16
3.8°F/min ramp to 225°F - no hold
1.8°F/min ramp to 275°F - Hold 105 minutes

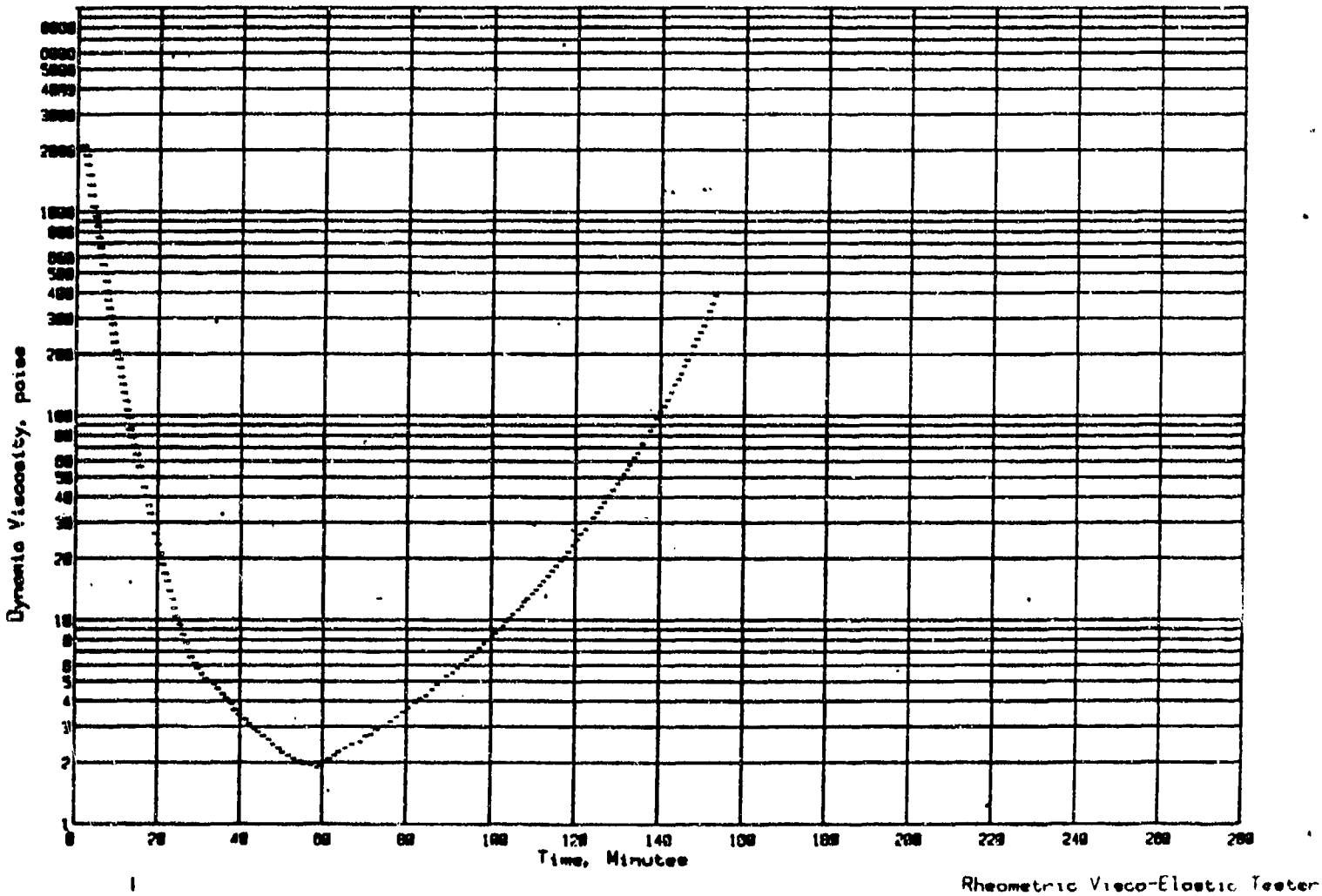

Rheometric Visco-Elastic Tester
May 12, 1981

FIGURE A-11

SR 5208 batch 716

AUTOCLAVE CURE CYCLE VARIATION ACR-18

7.2°F/min ramp to 175°F - Hold 30 minutes

7.2°F/min ramp to 275°F - Hold to run termination

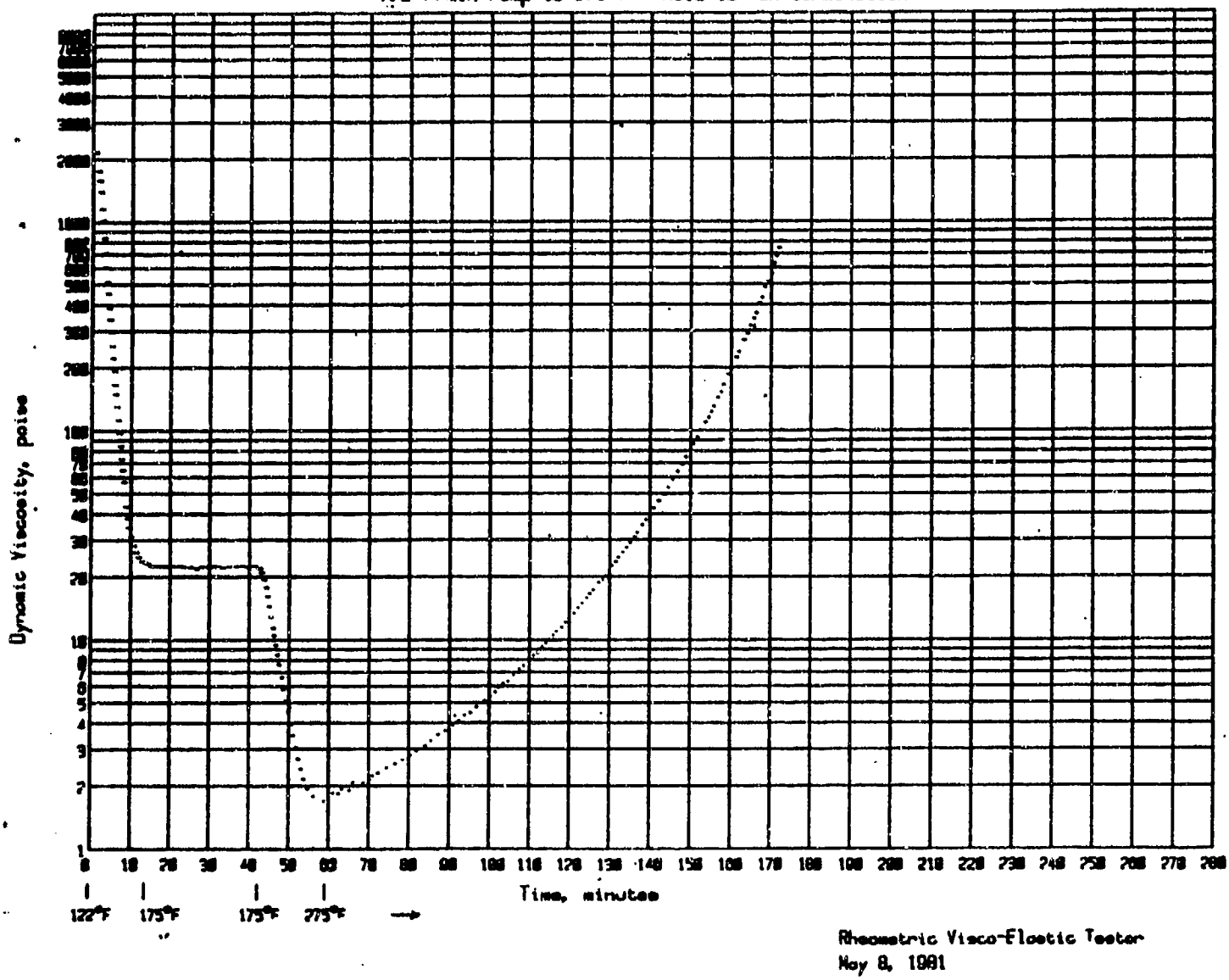

FIGURE A-12

SR 5208 batch 716

AUTOCLAVE CURE CYCLE VARIATION ACR-19

11°F/min ramp to run termination

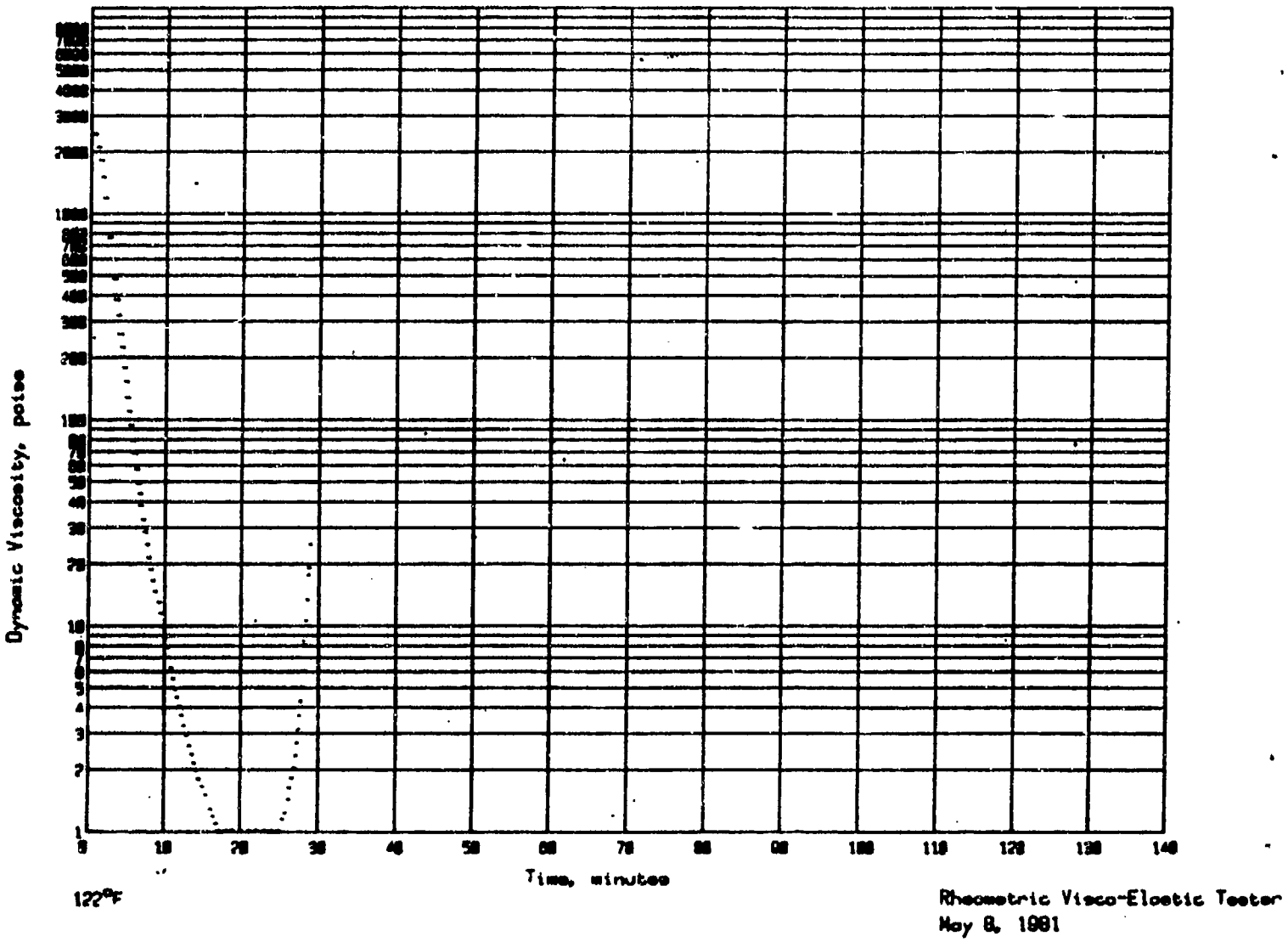

FIGURE A-13

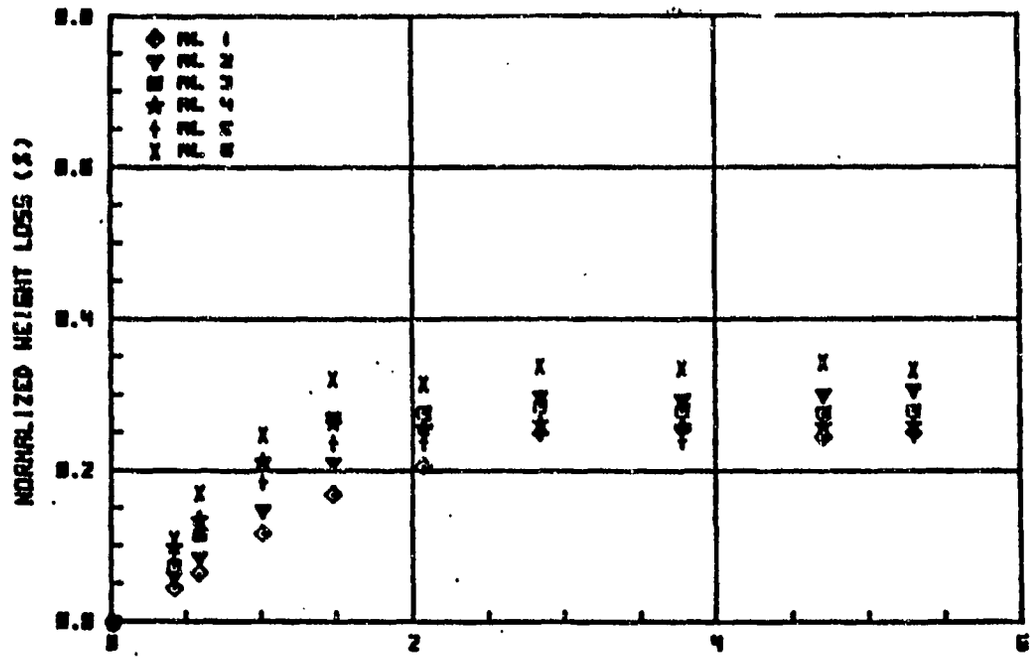

45 DEG C - 45 % HUMIDITY

FIGURE A-14

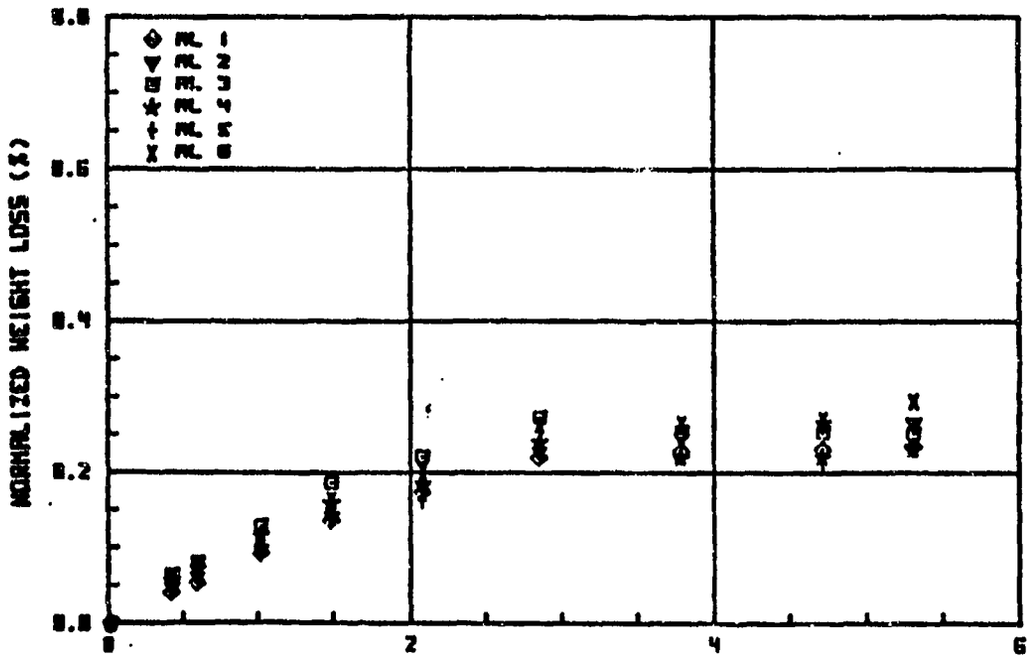

25 DEG C - 60 % HUMIDITY

FIGURE A-15

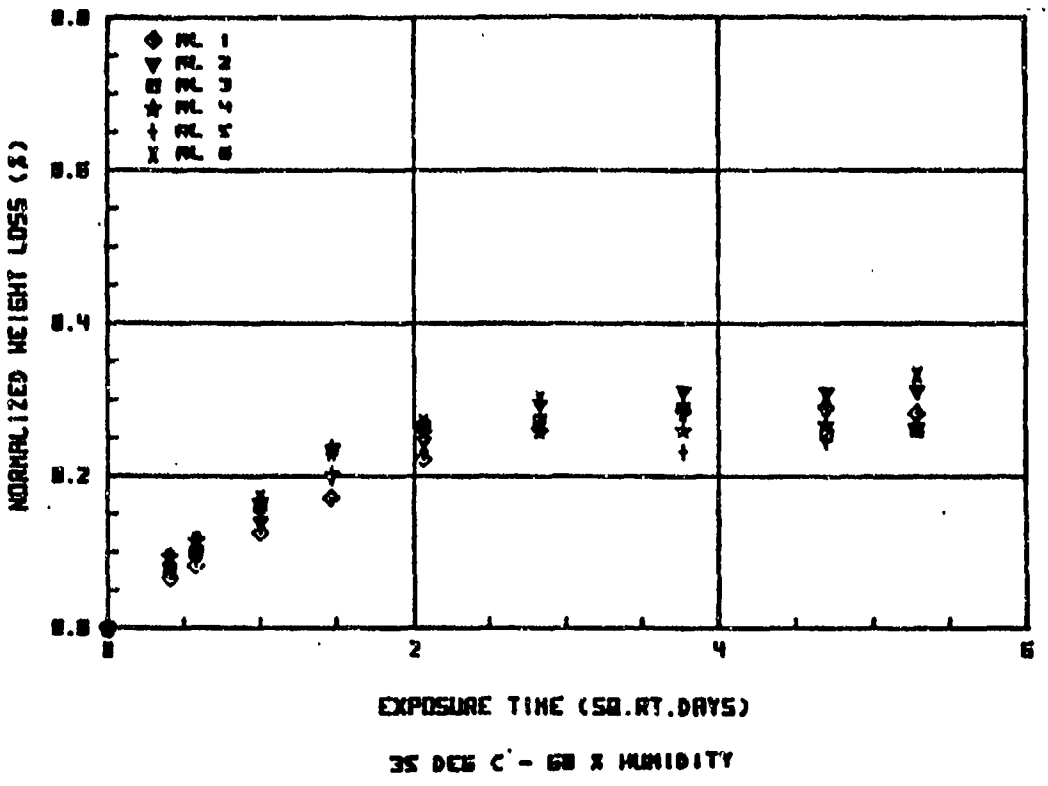

FIGURE A-16

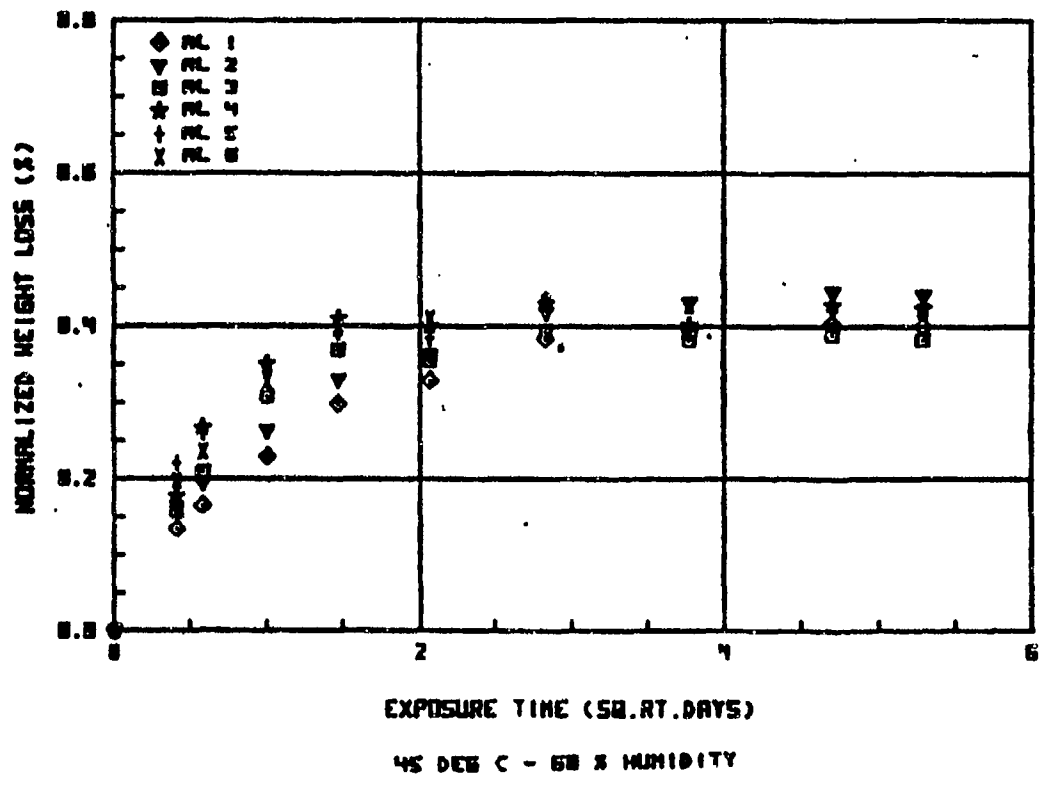

FIGURE A-17

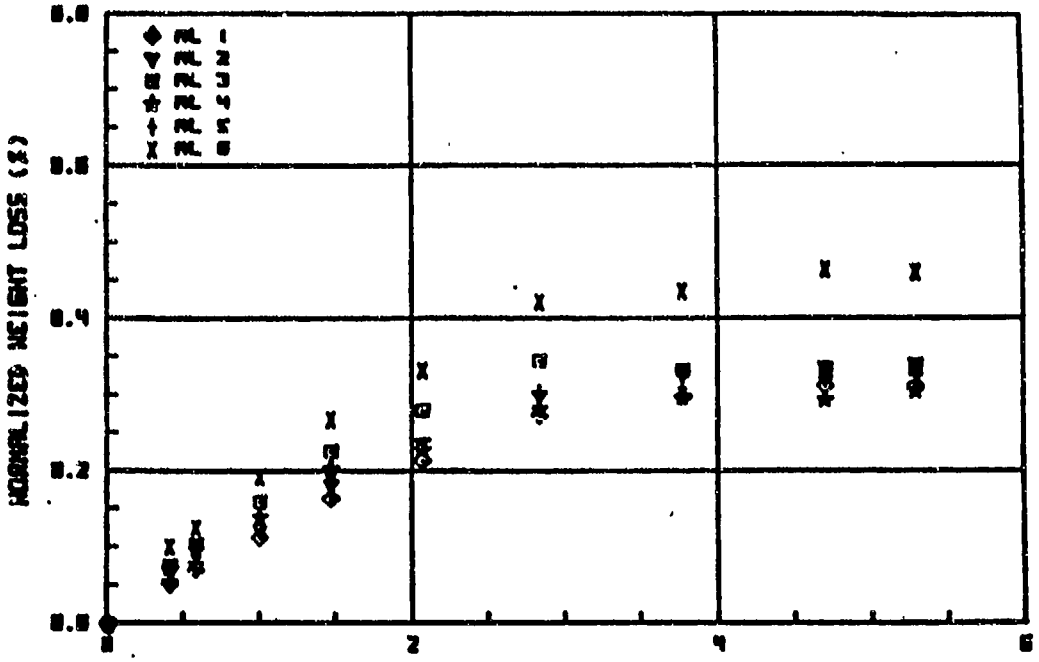

25 DEG C - 75 % HUMIDITY

FIGURE A-18

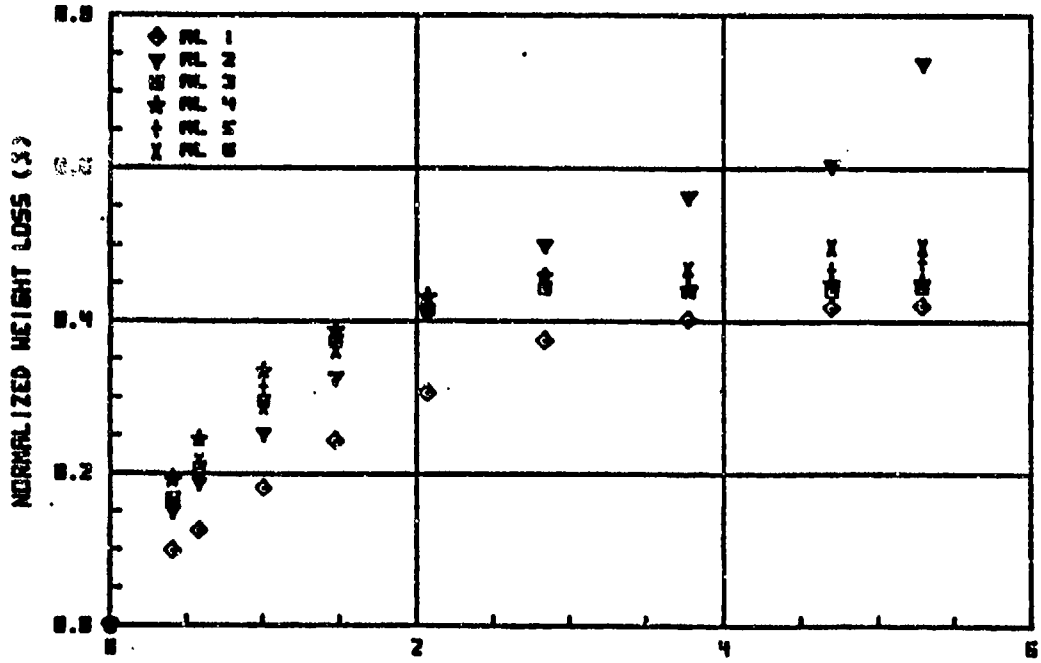

35 DEG C - 75 % HUMIDITY

FIGURE A-19

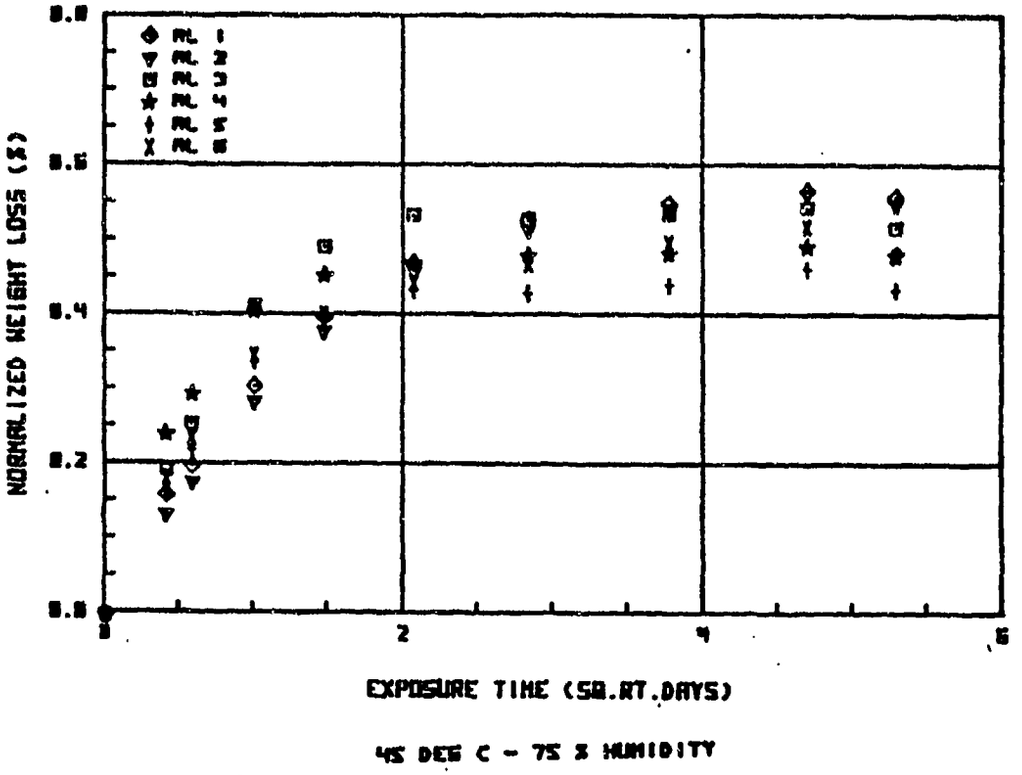

FIGURE A-20

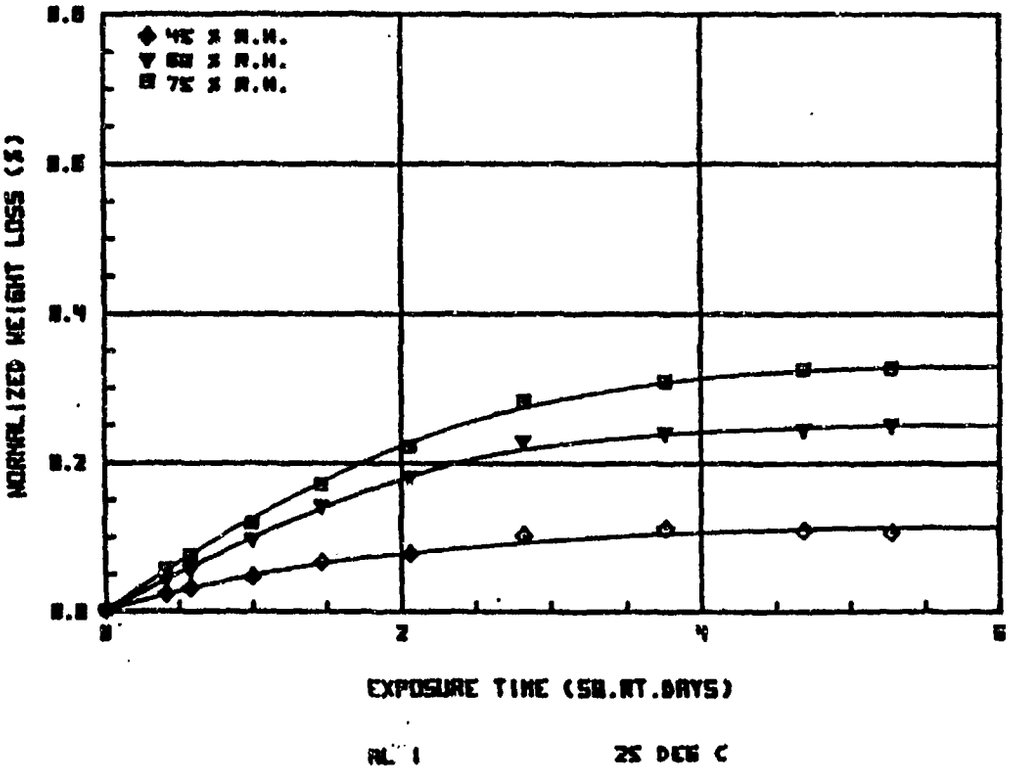

FIGURE A-21

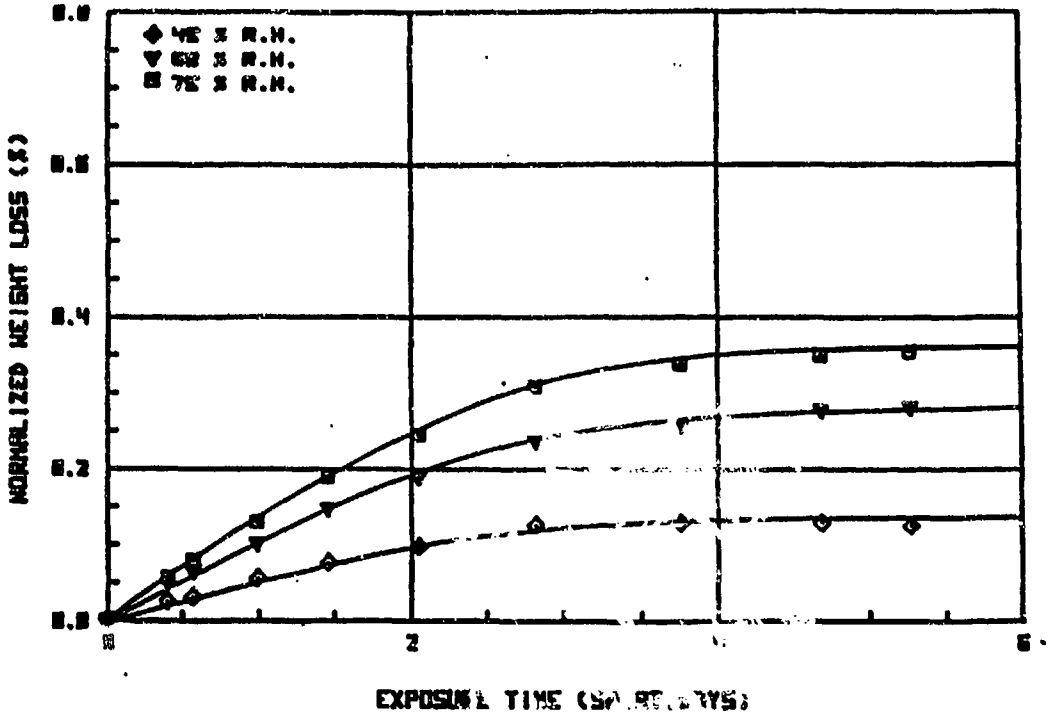

NL 2 25 DEG C

FIGURE A-22

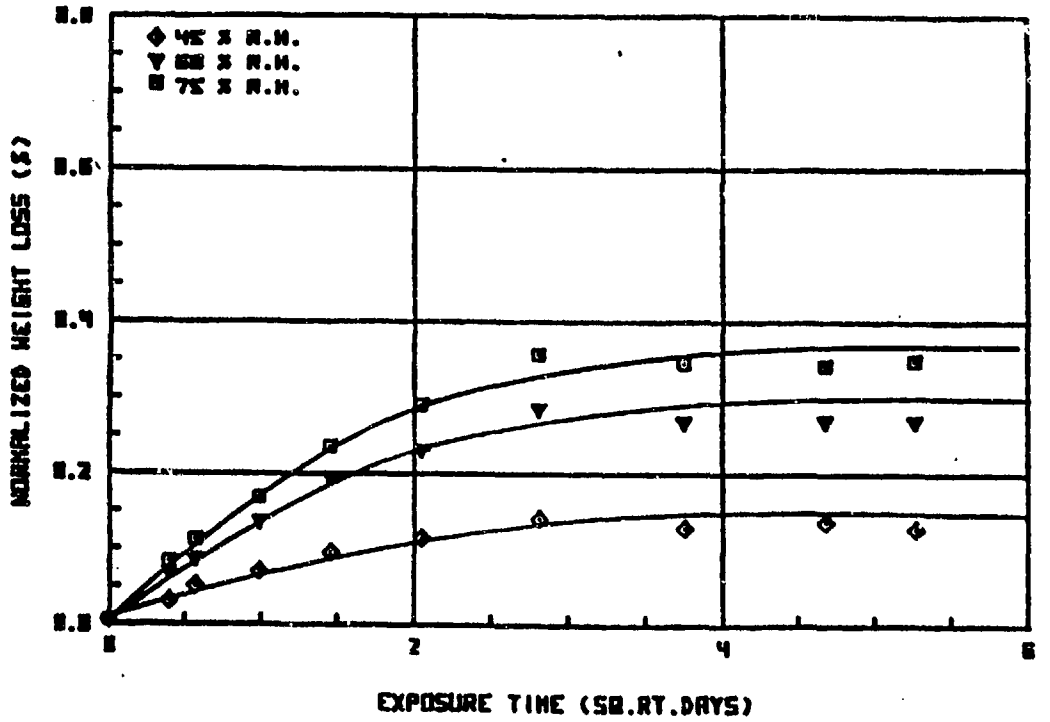

NL 3 25 DEG C

FIGURE A-23

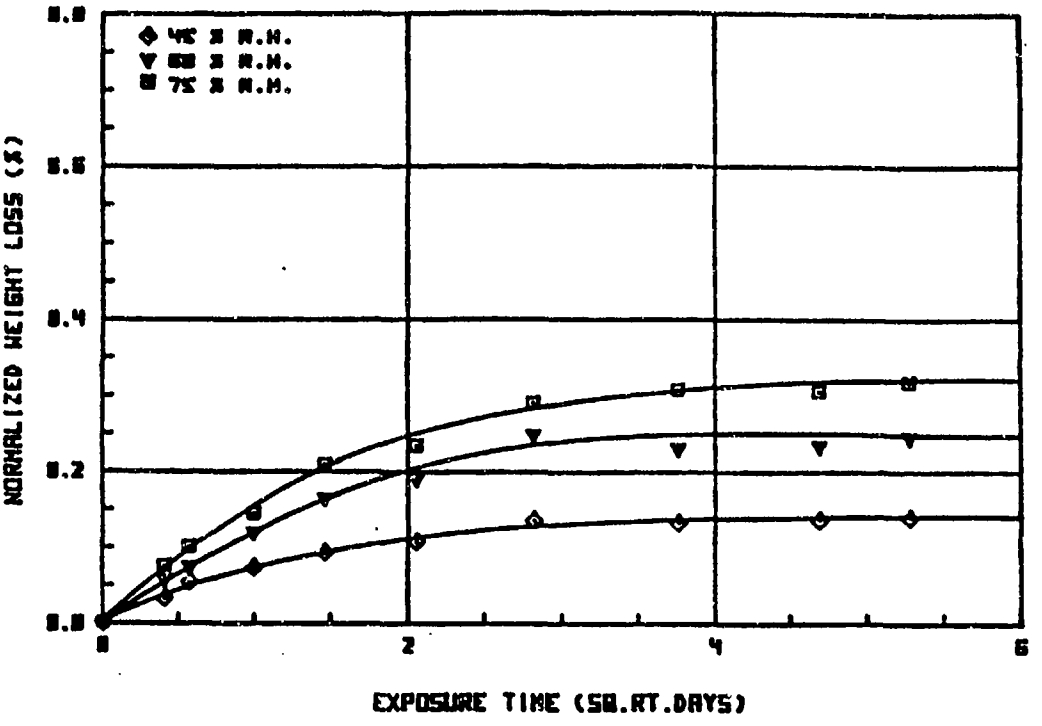

FIGURE A-24

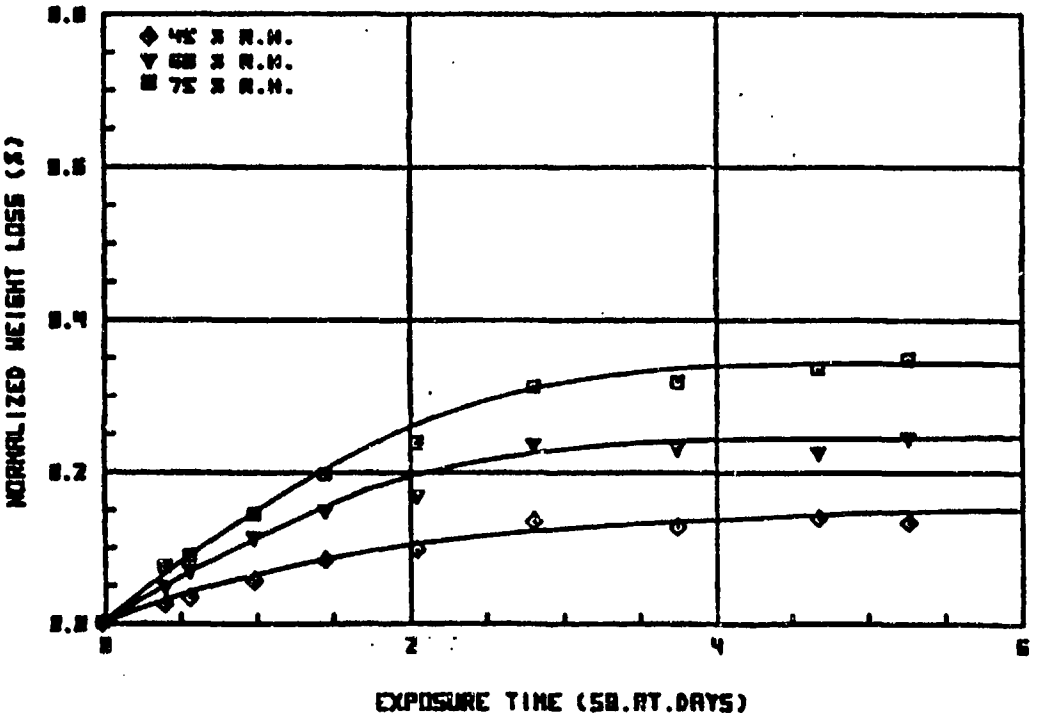

FIGURE A-25

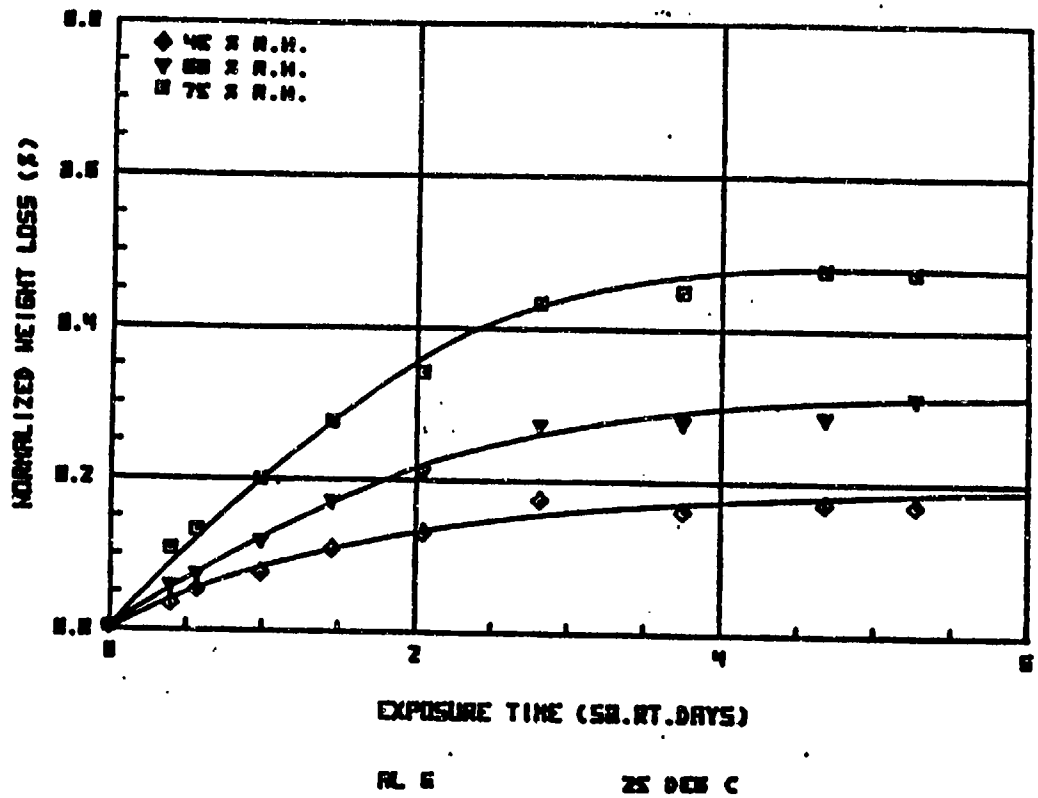
NORMALIZED WEIGHT LOSS (%)
0.0
0.2
0.4
0.6
0.8
0
2
4
6
EXPOSURE TIME (SH.RT.DAYS)

FIGURE A-26

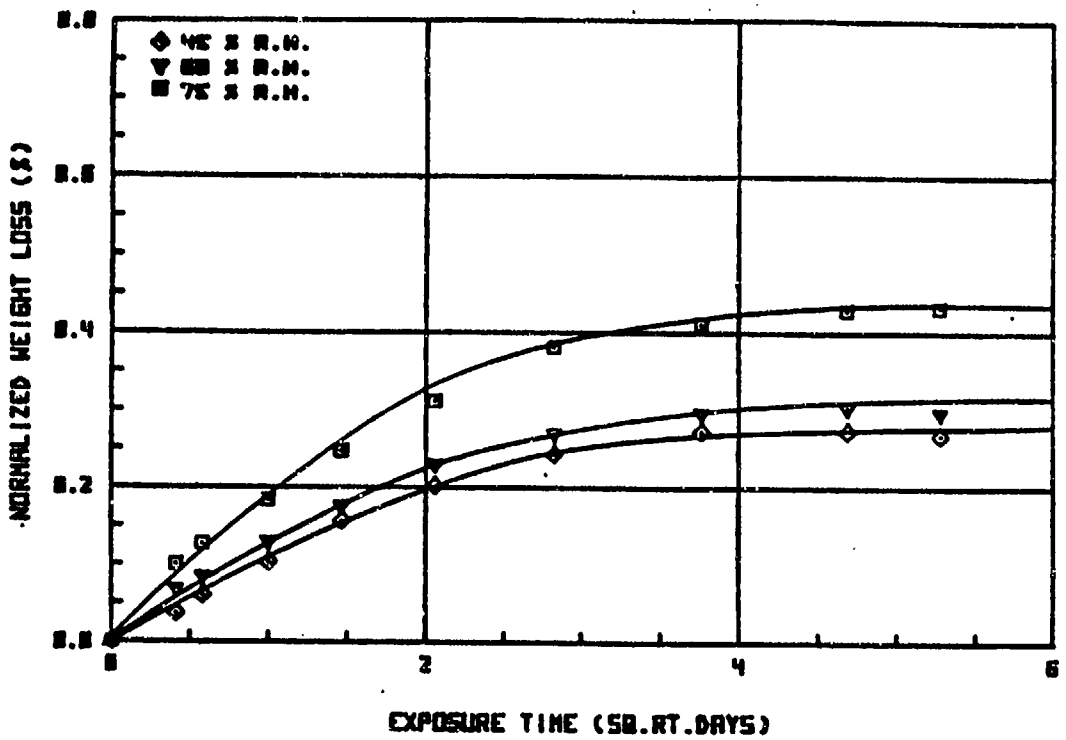

AL 1 35 DEG C

FIGURE A-27

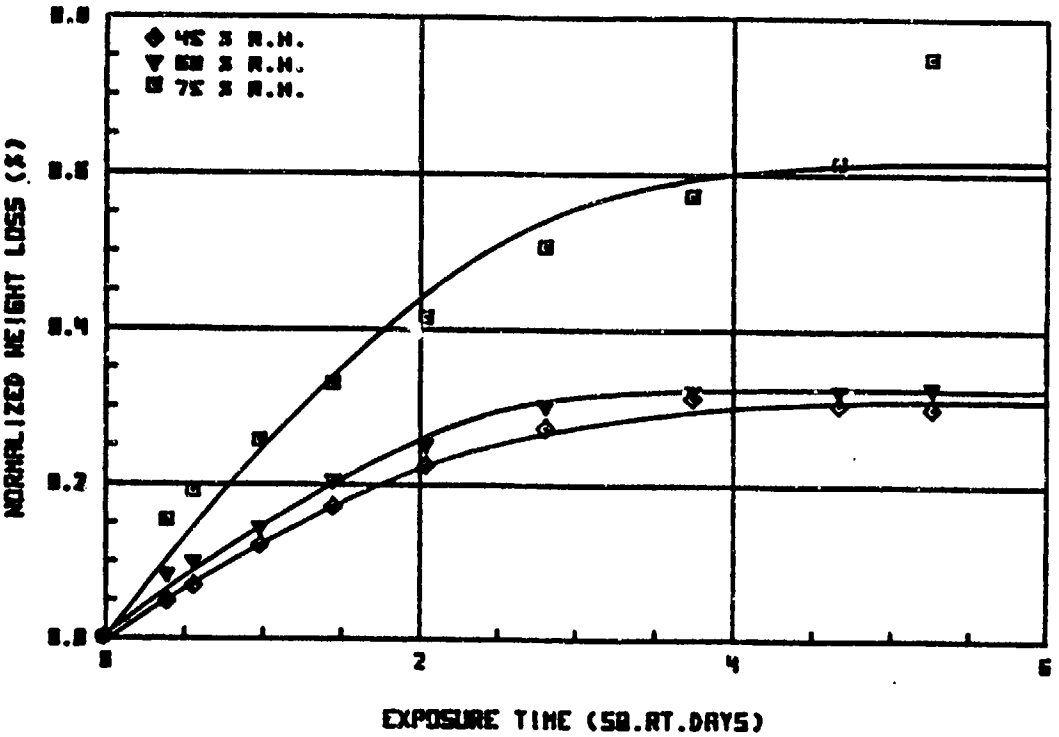

AL 2 35 DEG C

FIGURE A-28

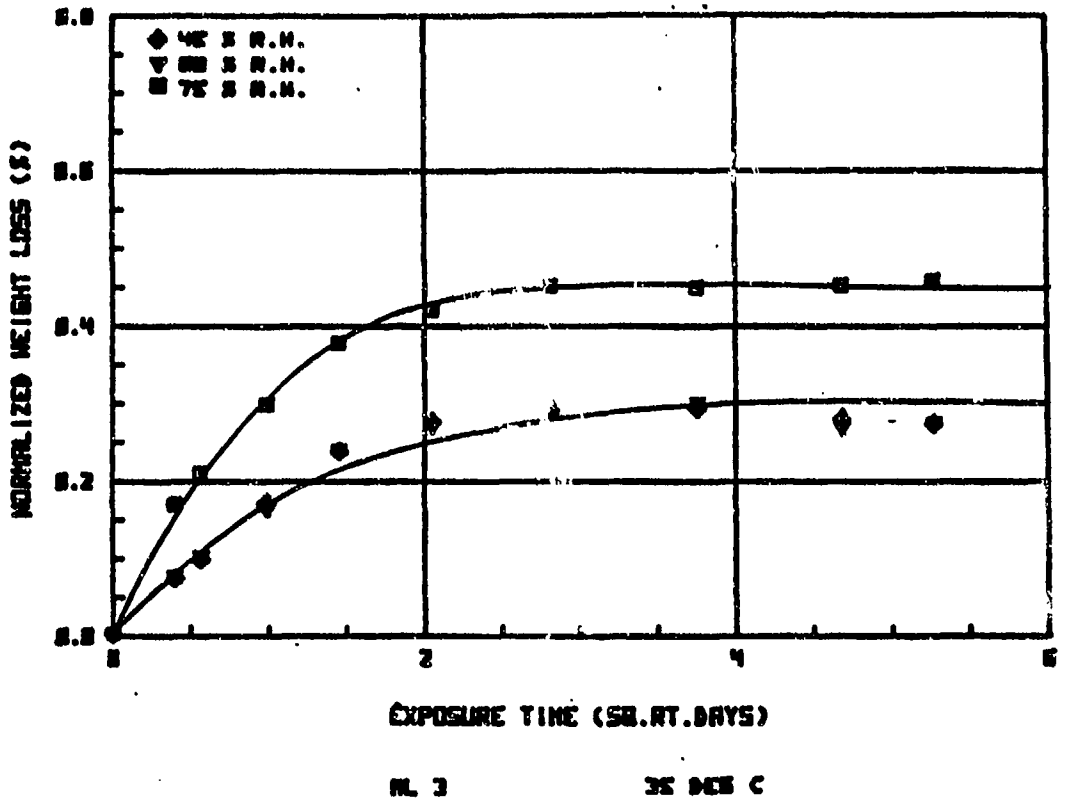

FIGURE A-29

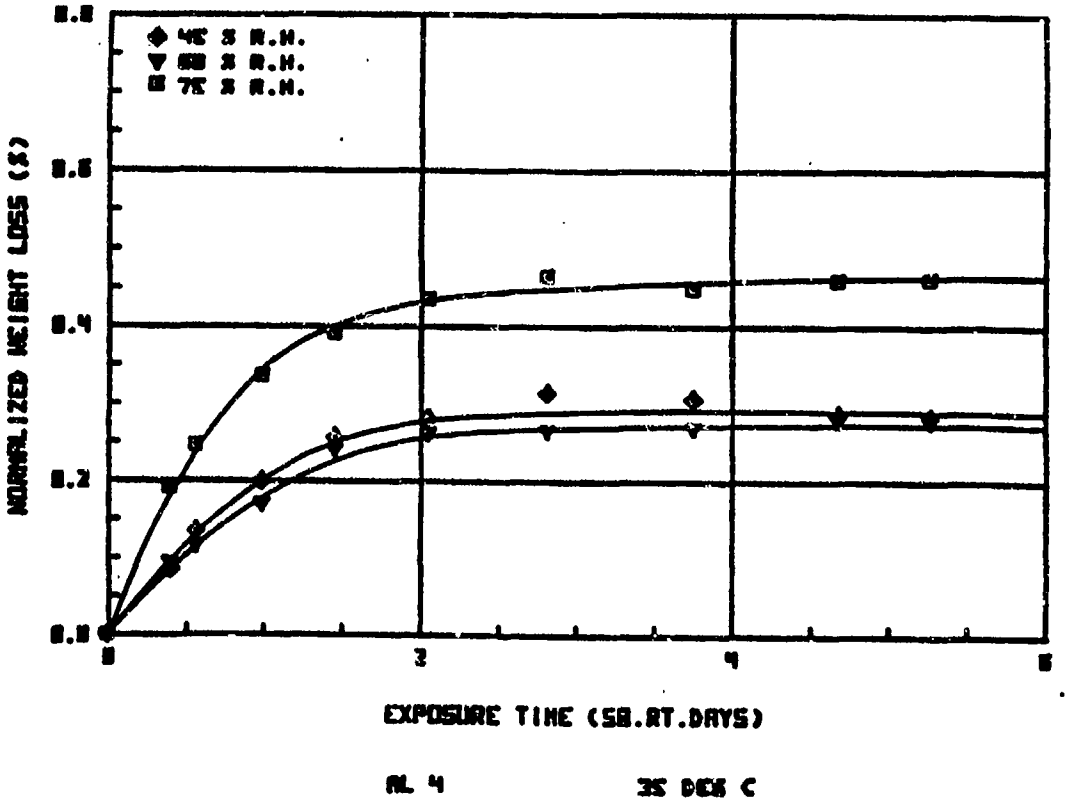

FIGURE A-30

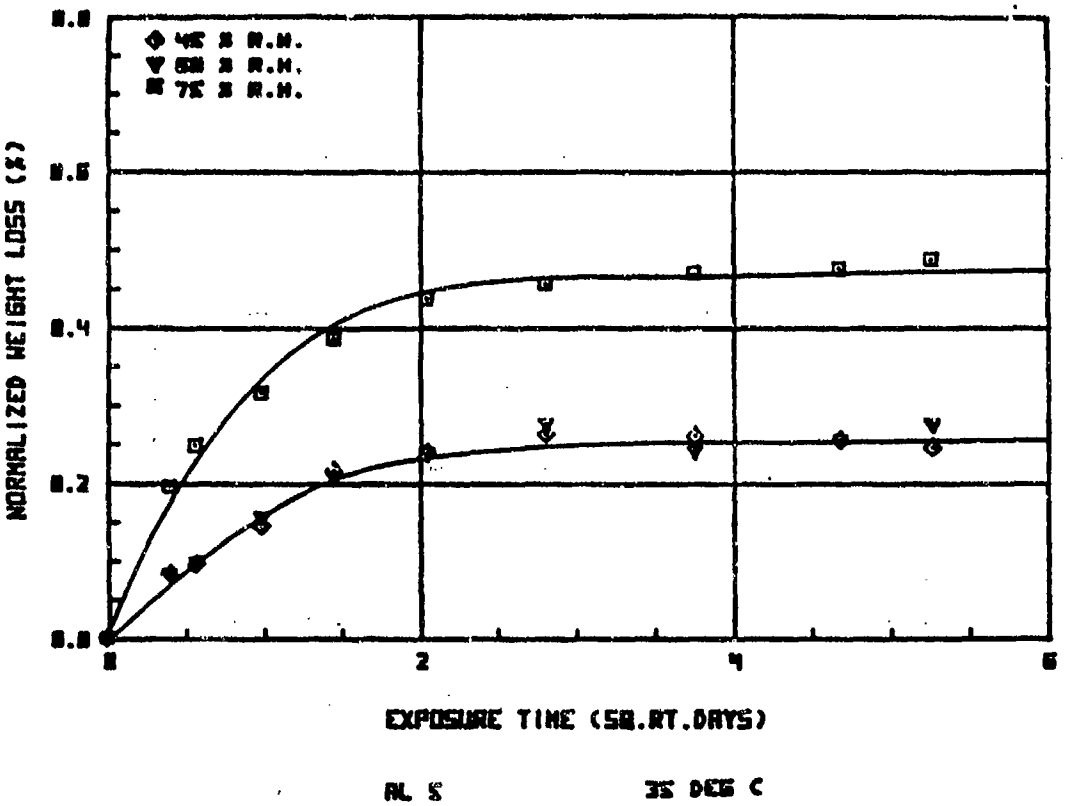

FIGURE A-31

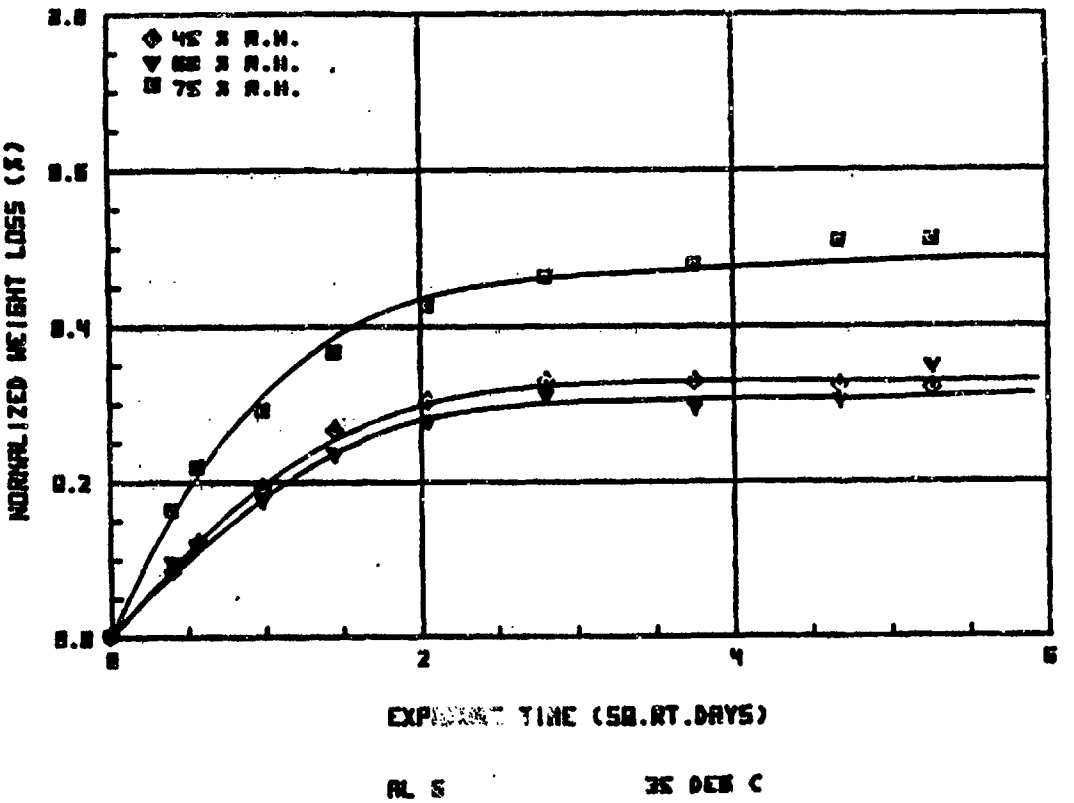

FIGURE A-32

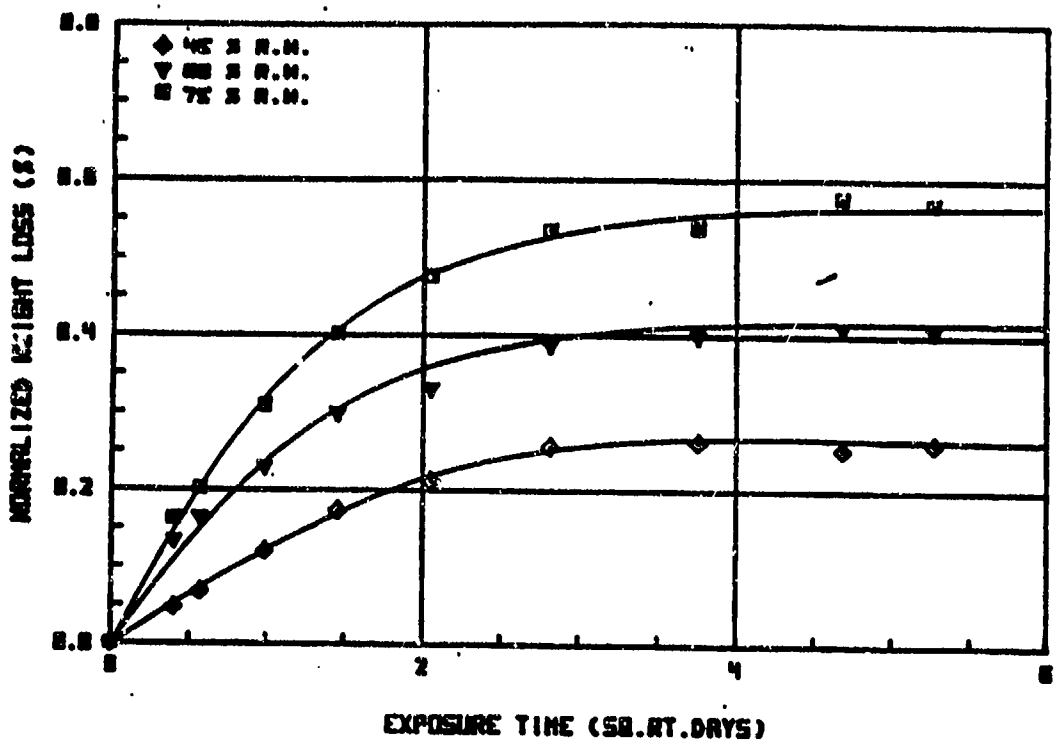

RL 1 45 DEG C

FIGURE A-33

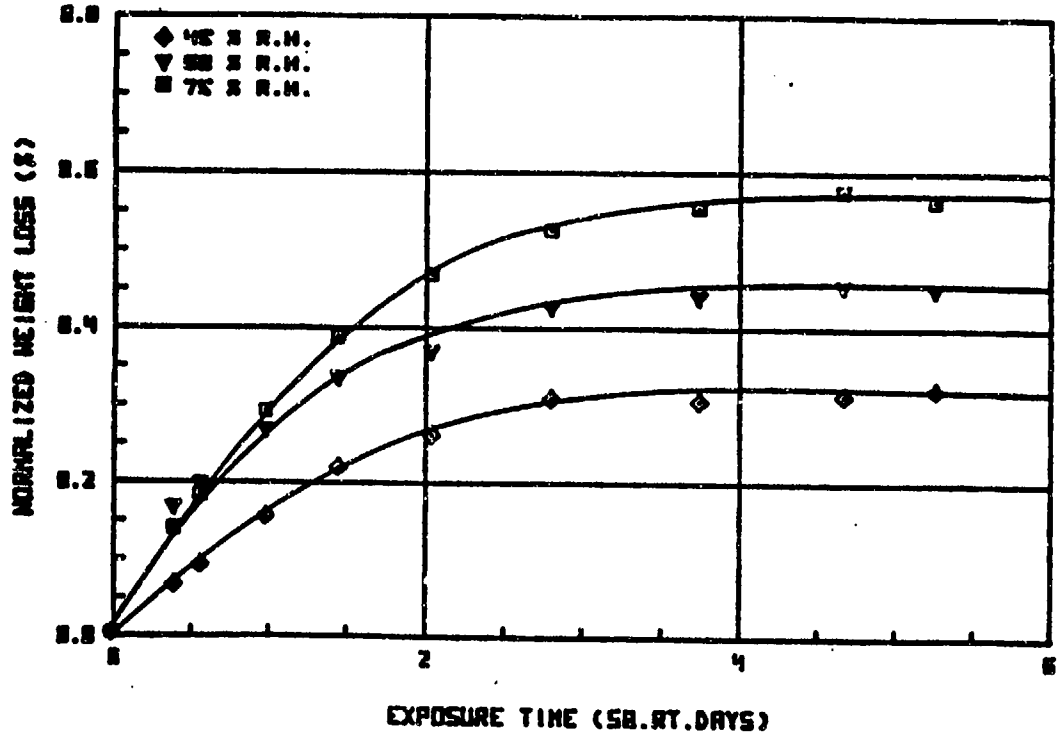

RL 2 45 DEG C

FIGURE A-34

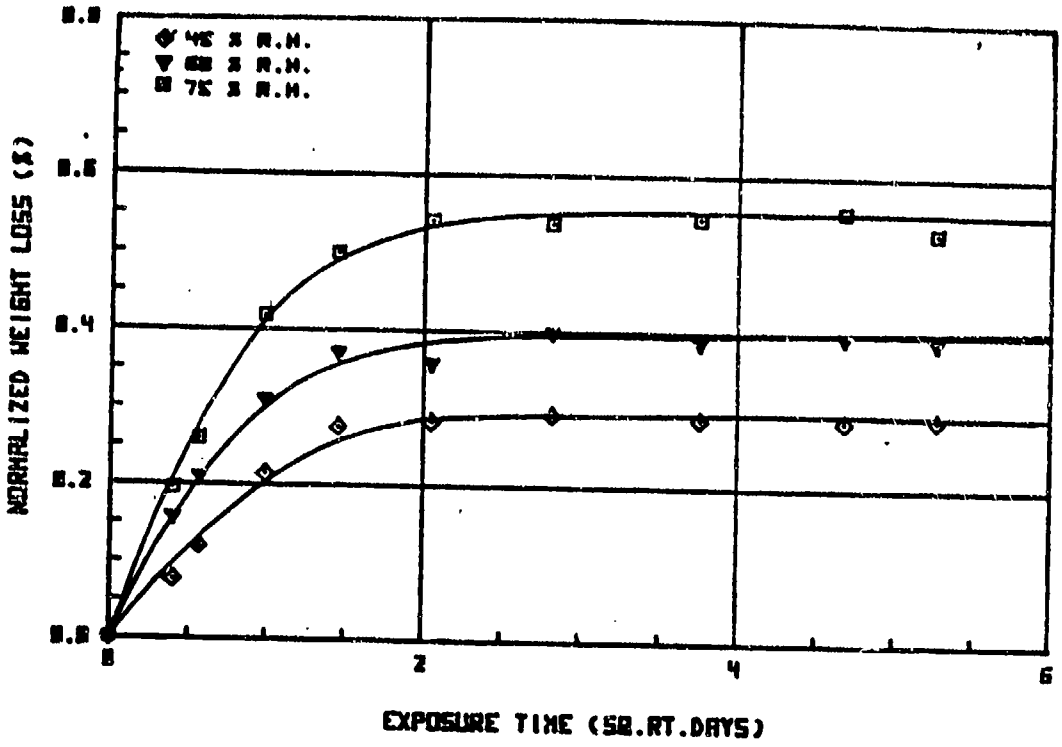

RL 3 45 DEG C

FIGURE A-35

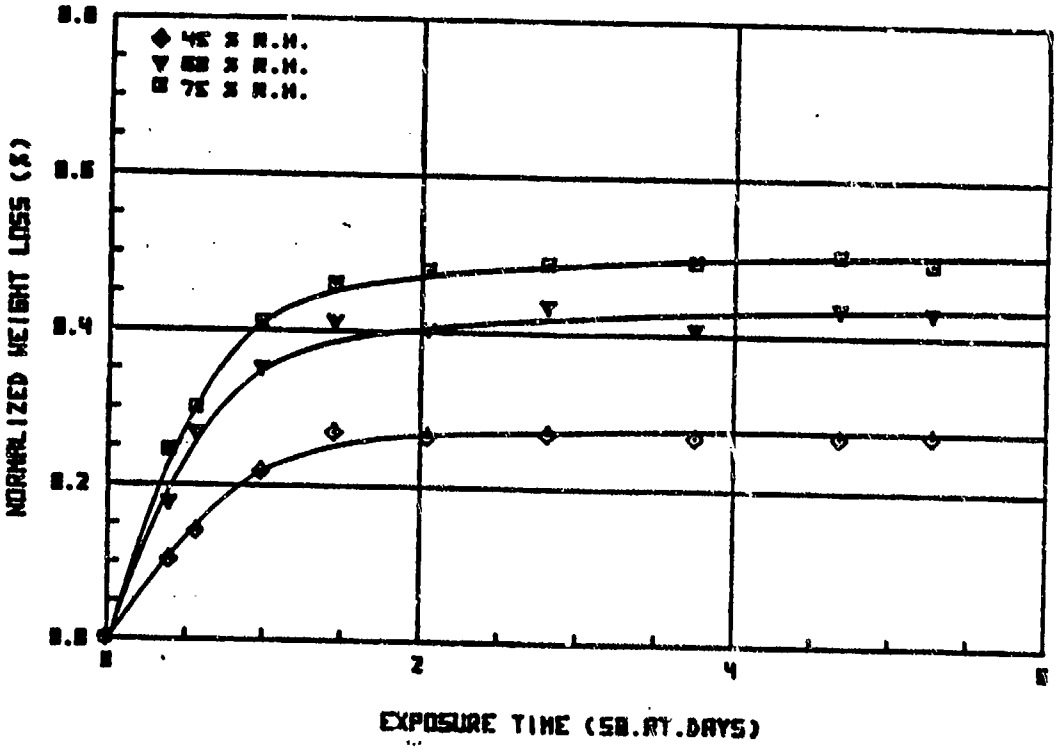

RL 4 45 DEG C

FIGURE A-36

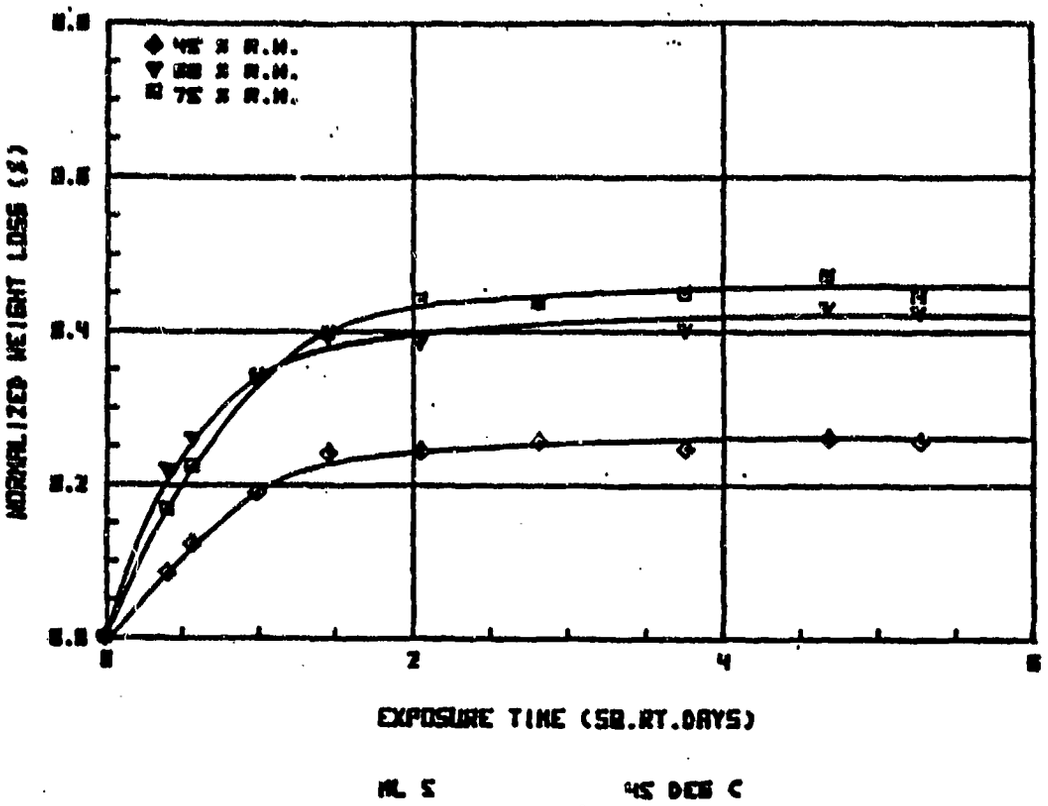

AL 5 45 DEG C

FIGURE A-37

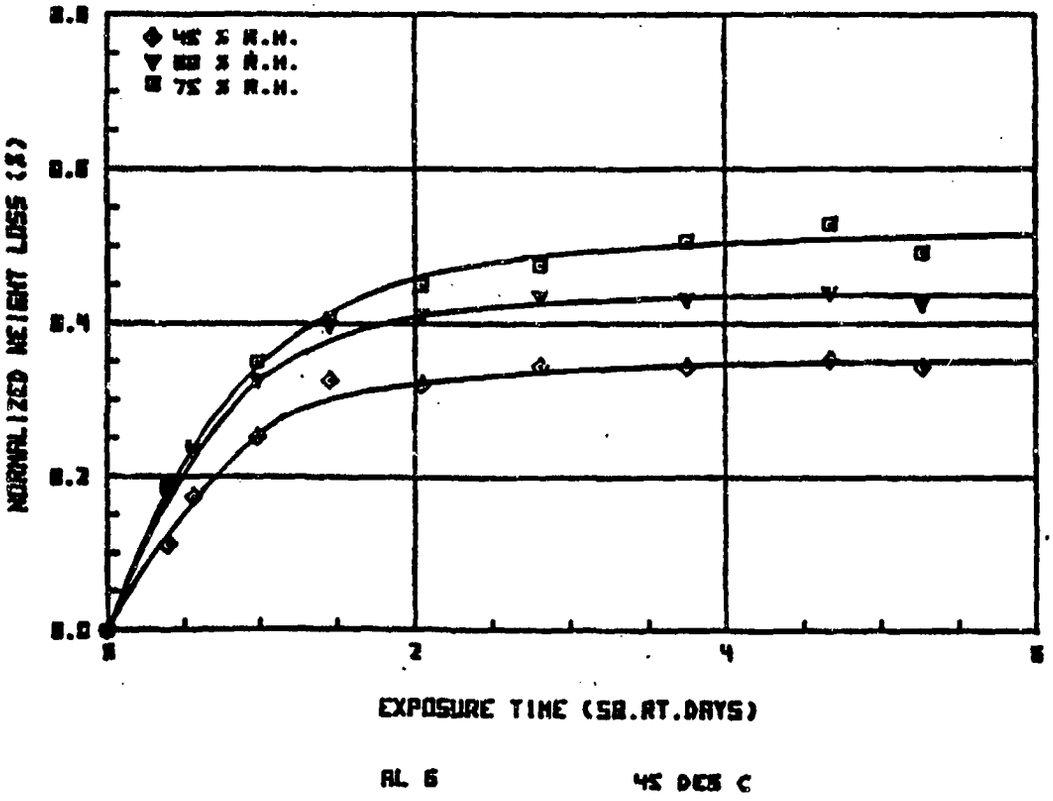

AL 6 45 DEG C

FIGURE A-38

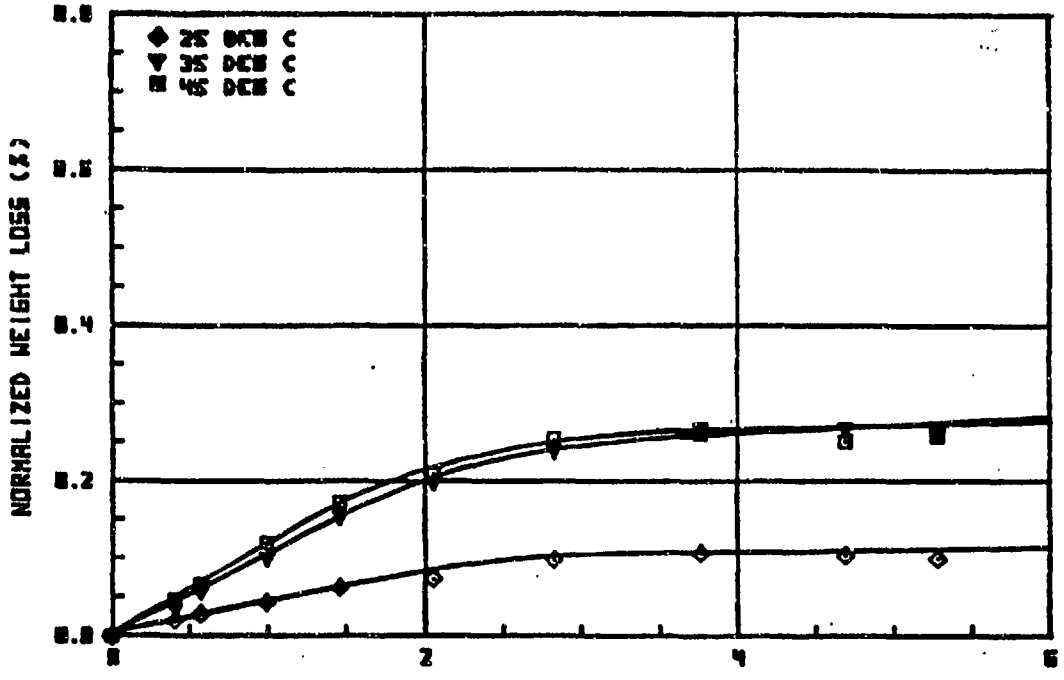

FIGURE A-39

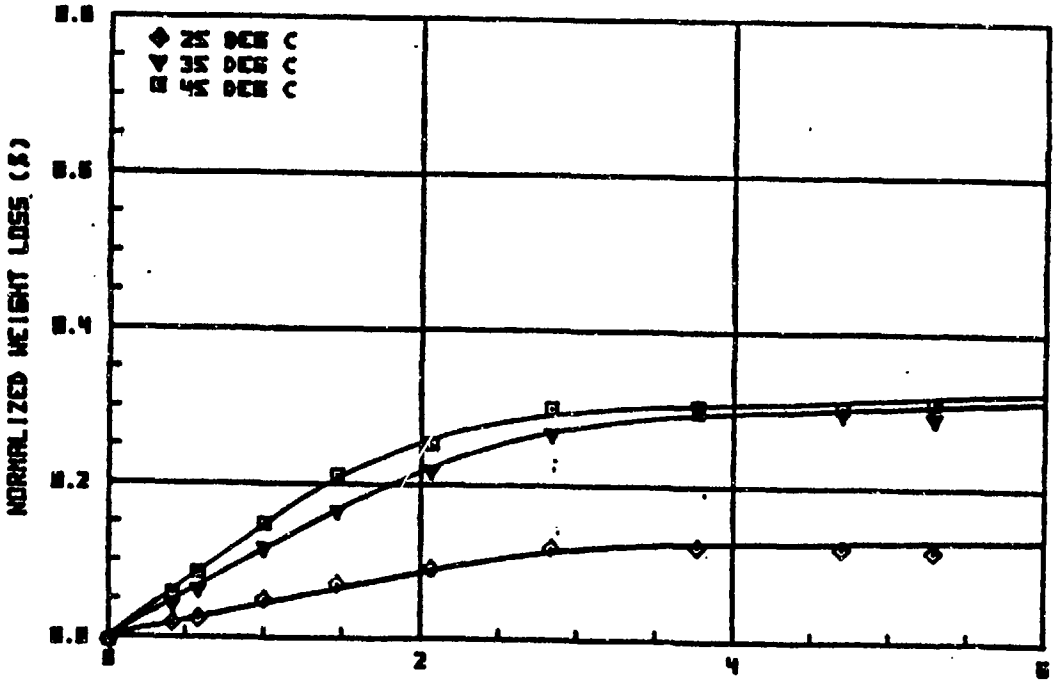

FIGURE A-40

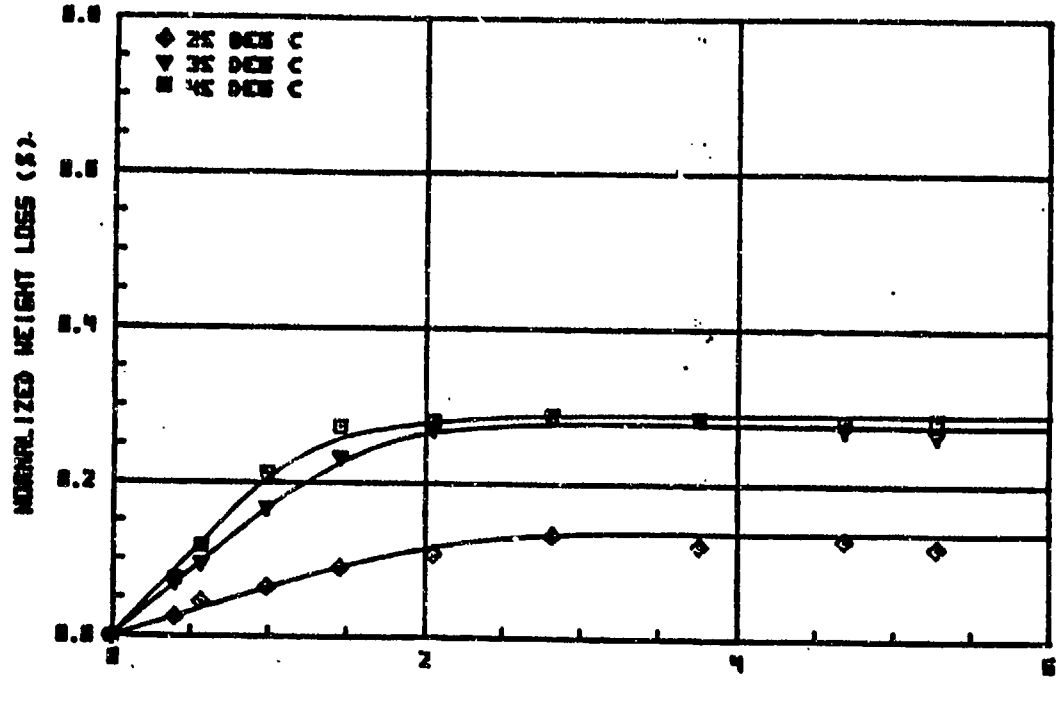

RL 3 45 % HUMIDITY

FIGURE A-41

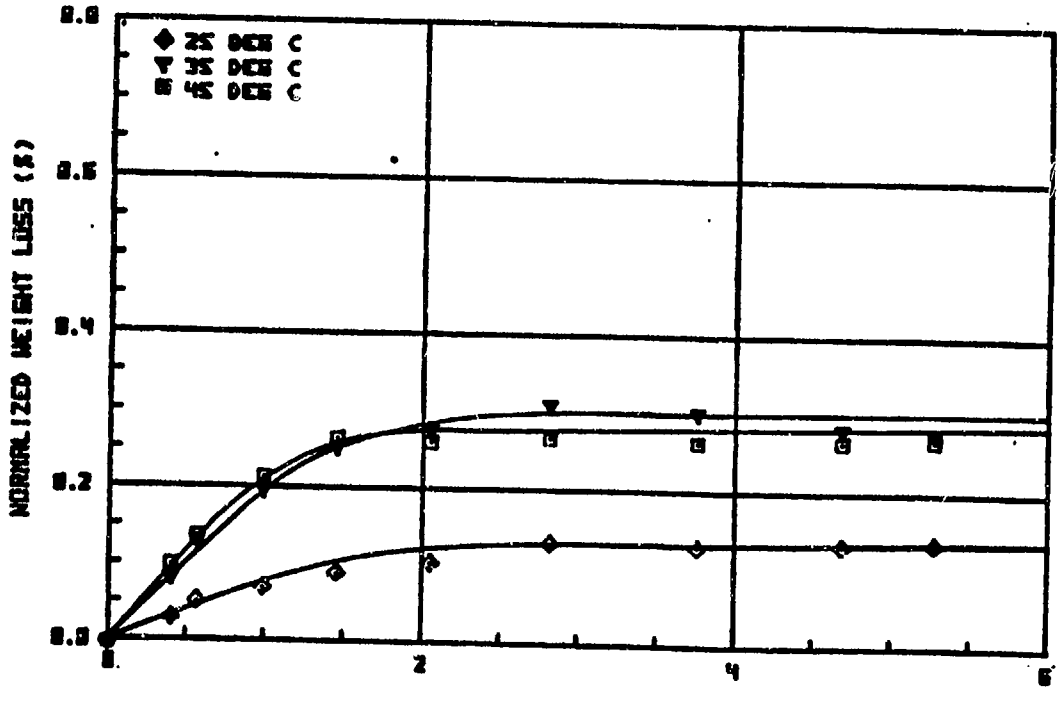

RL 4 45 % HUMIDITY

FIGURE A-42

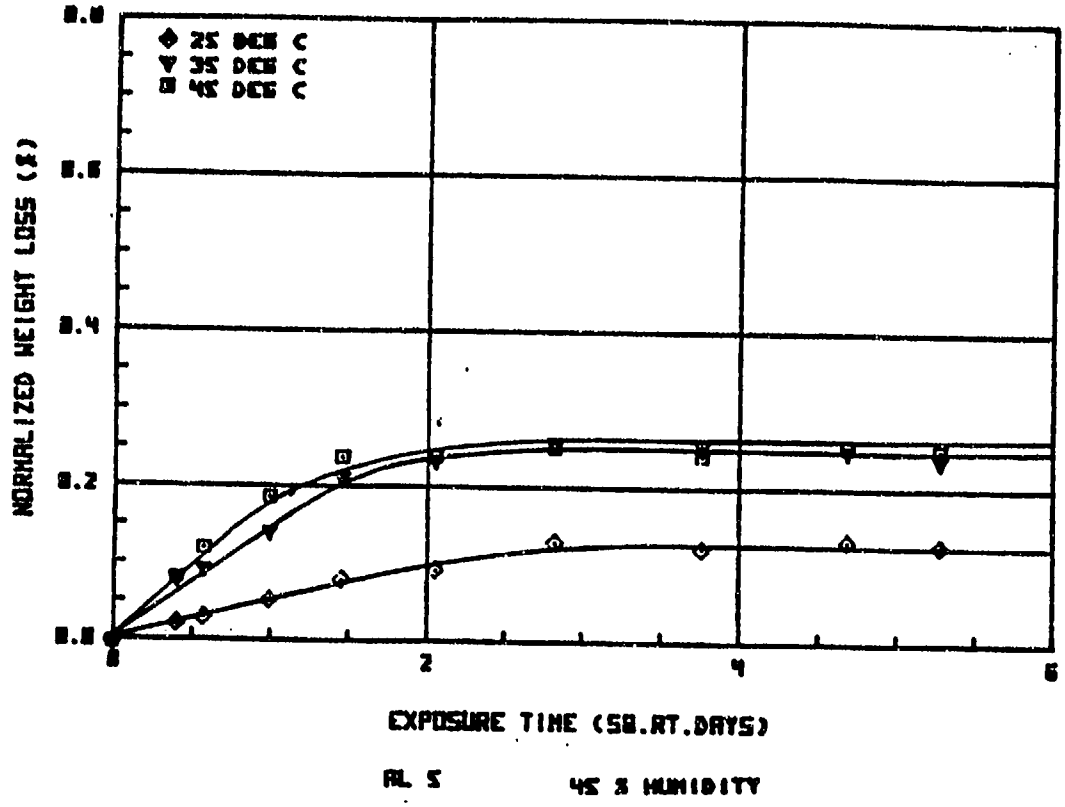

FIGURE A-43

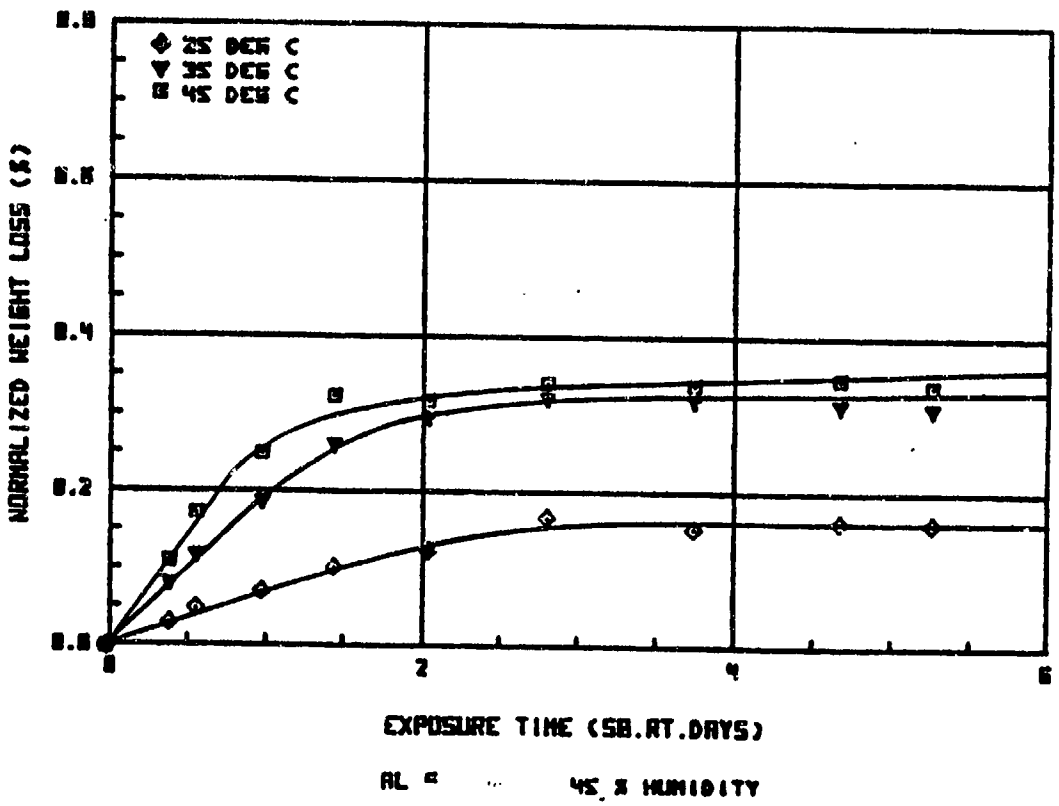

FIGURE A-44

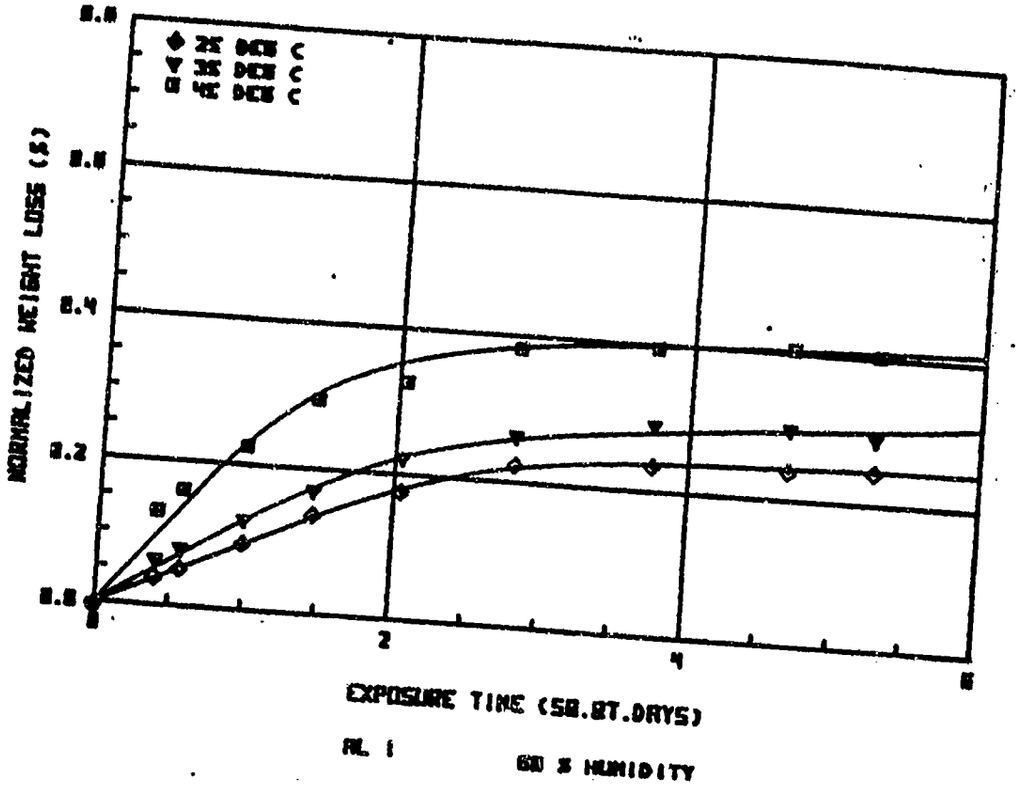

FIGURE A-45

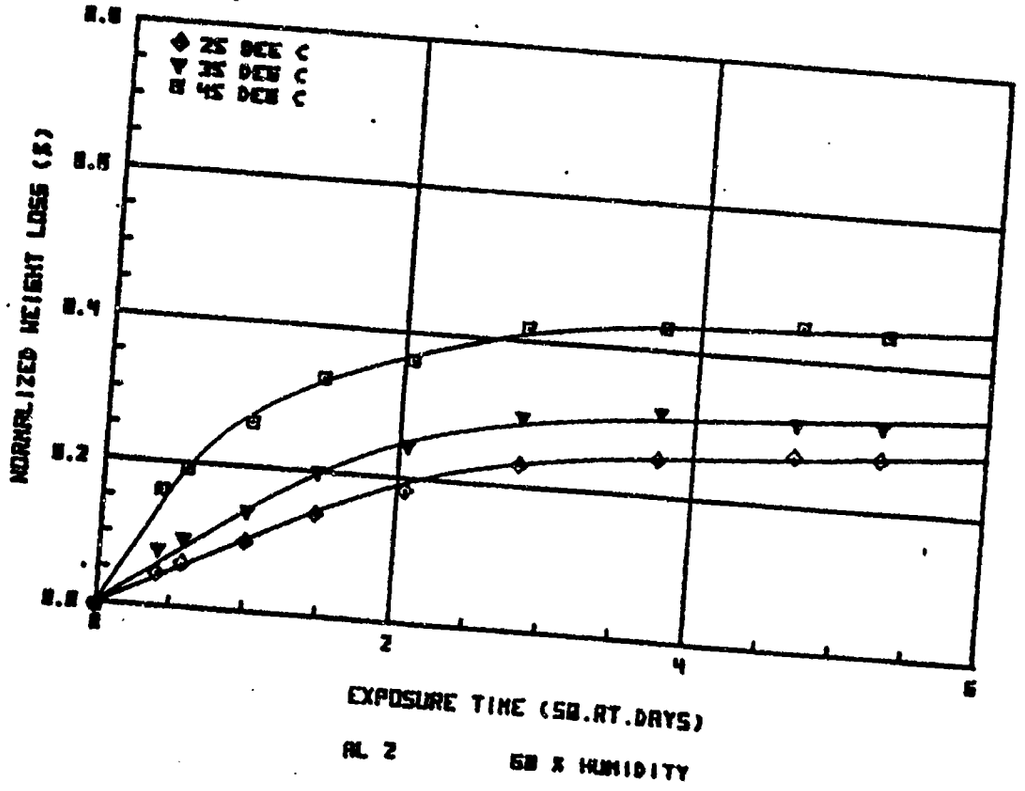

FIGURE A-46

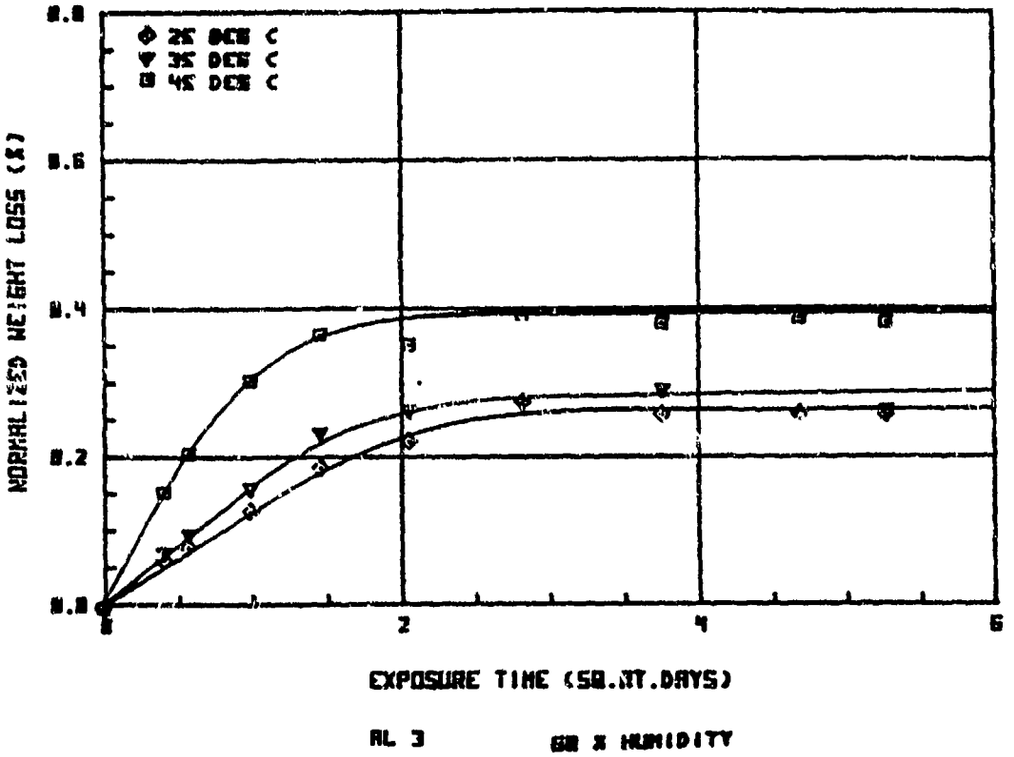

FIGURE A-47

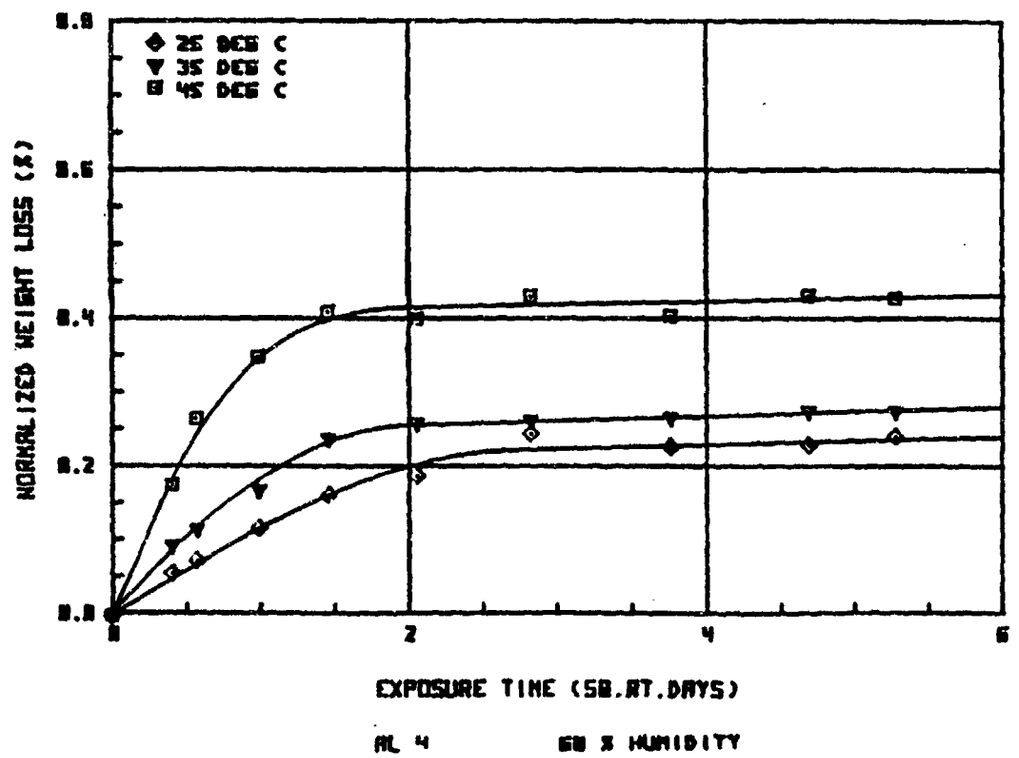

FIGURE A-48

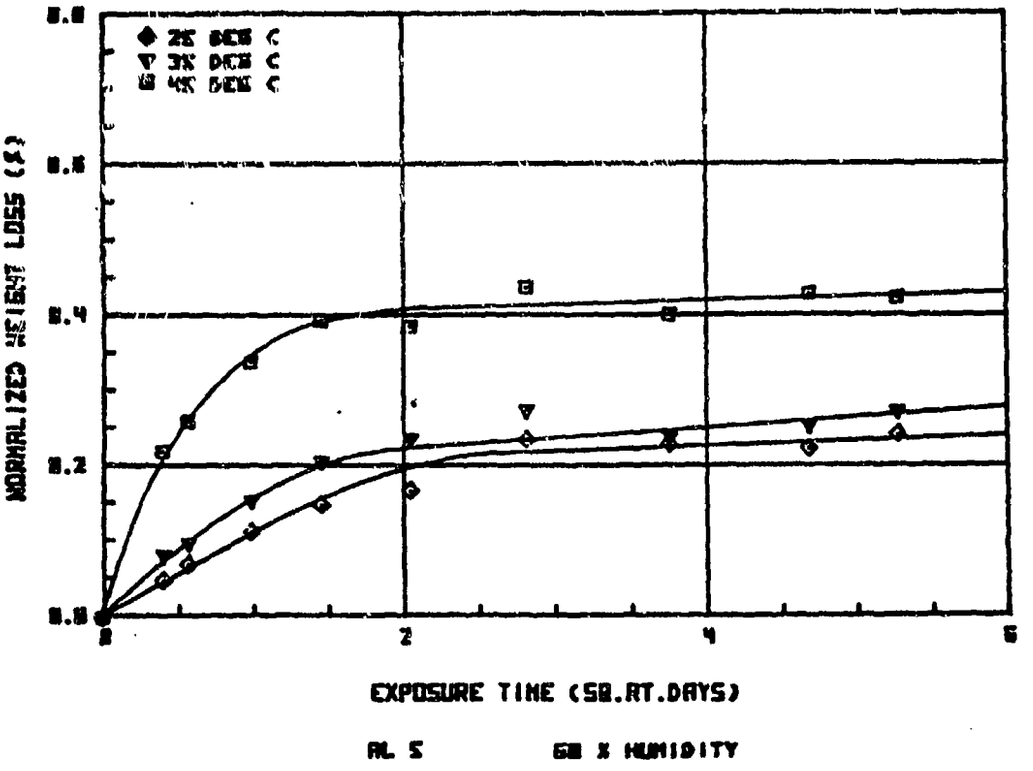

FIGURE A-49

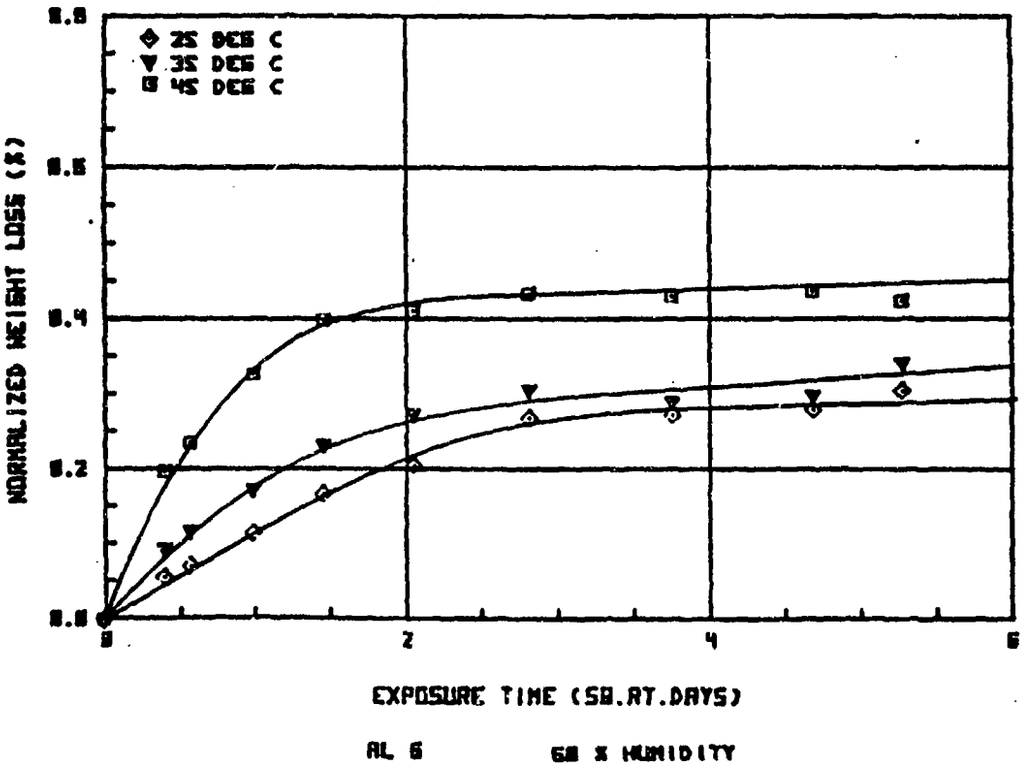

FIGURE A-50

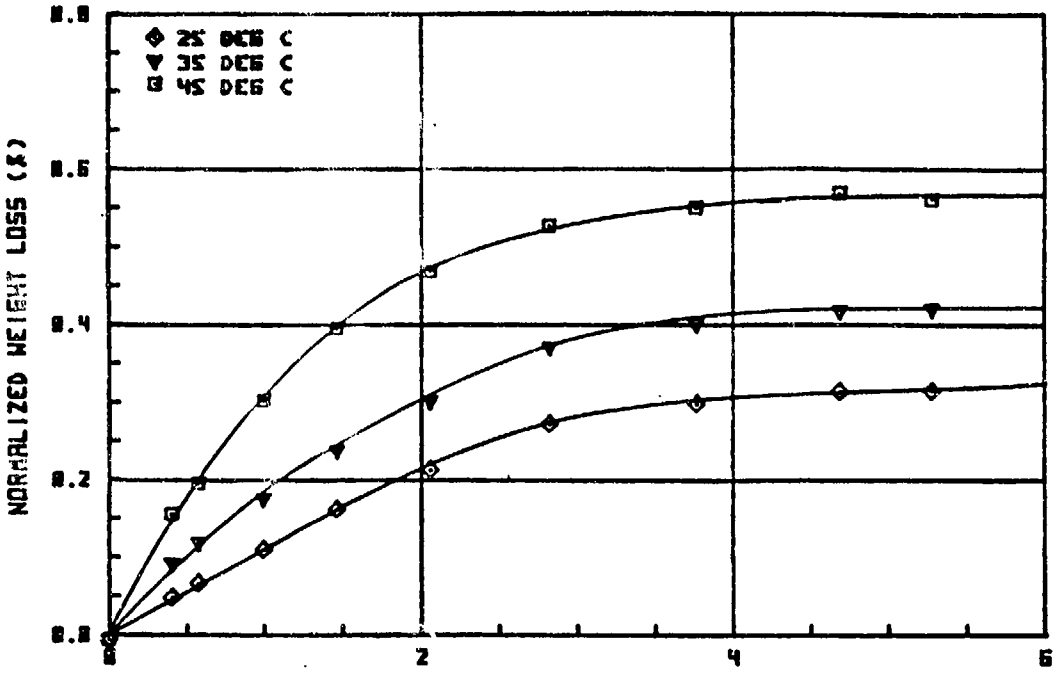

FIGURE A-51

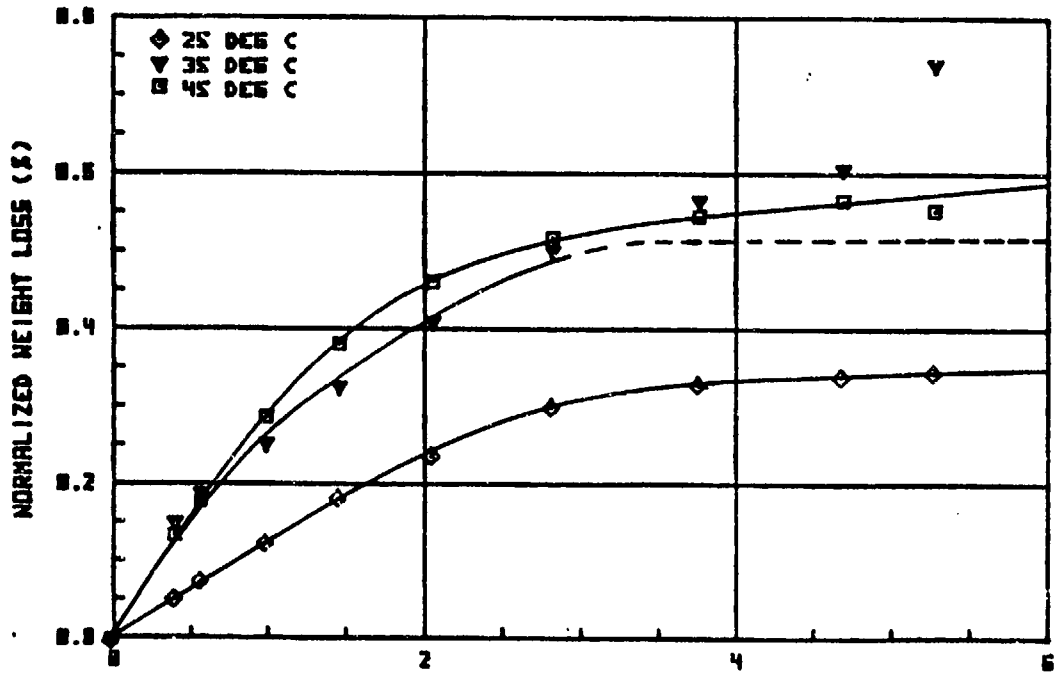

FIGURE A-52

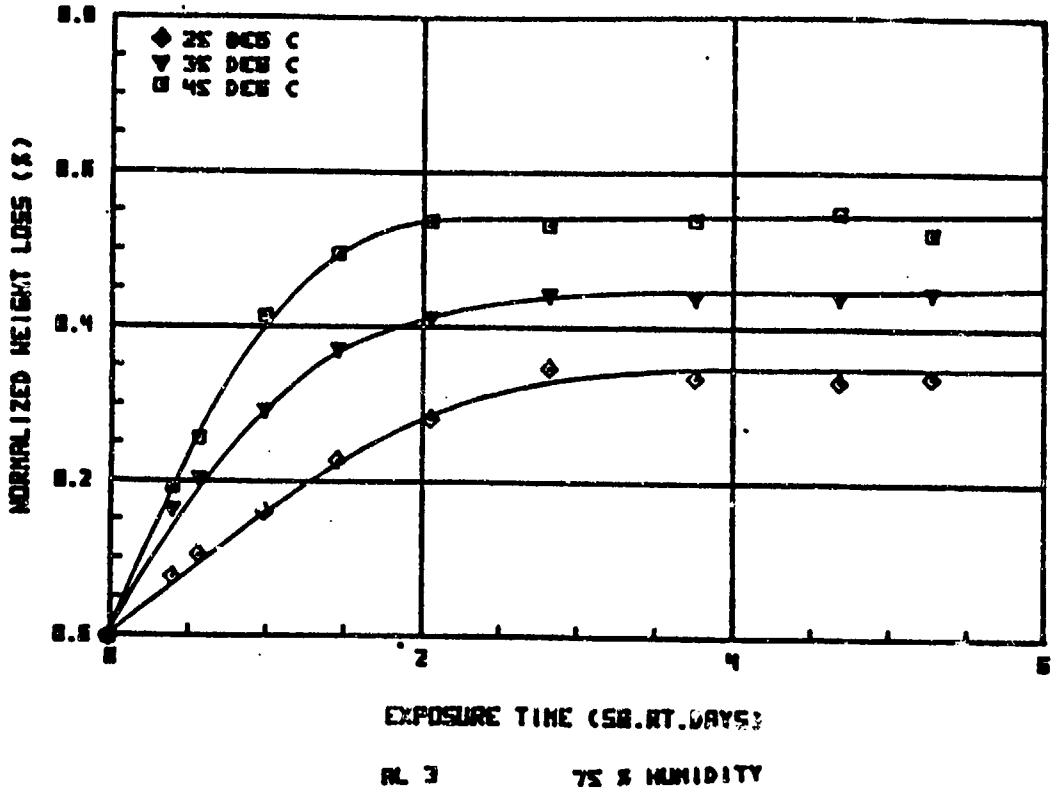

FIGURE A-53

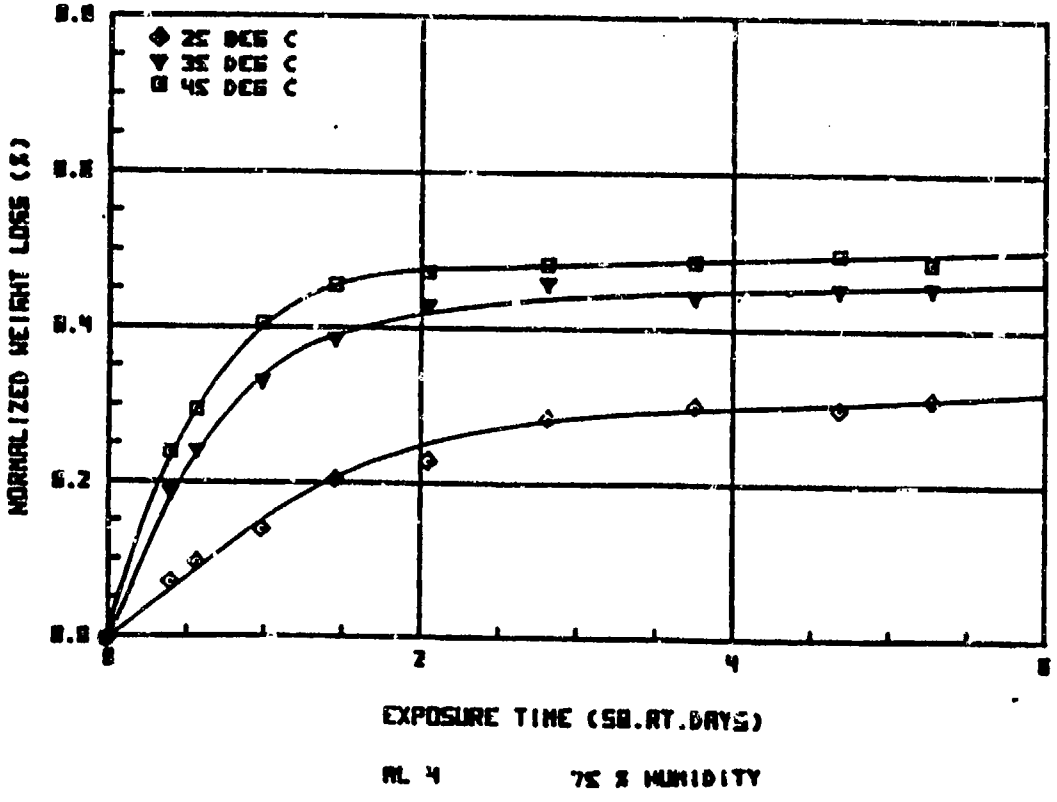

FIGURE A-54

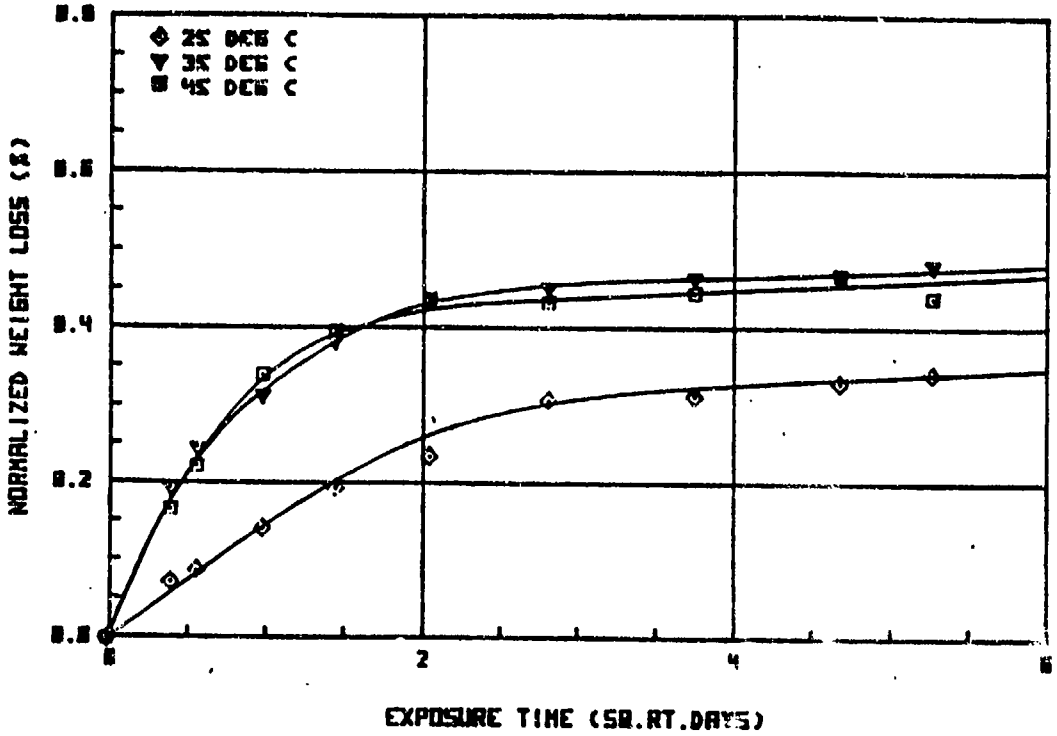

FIGURE A-55

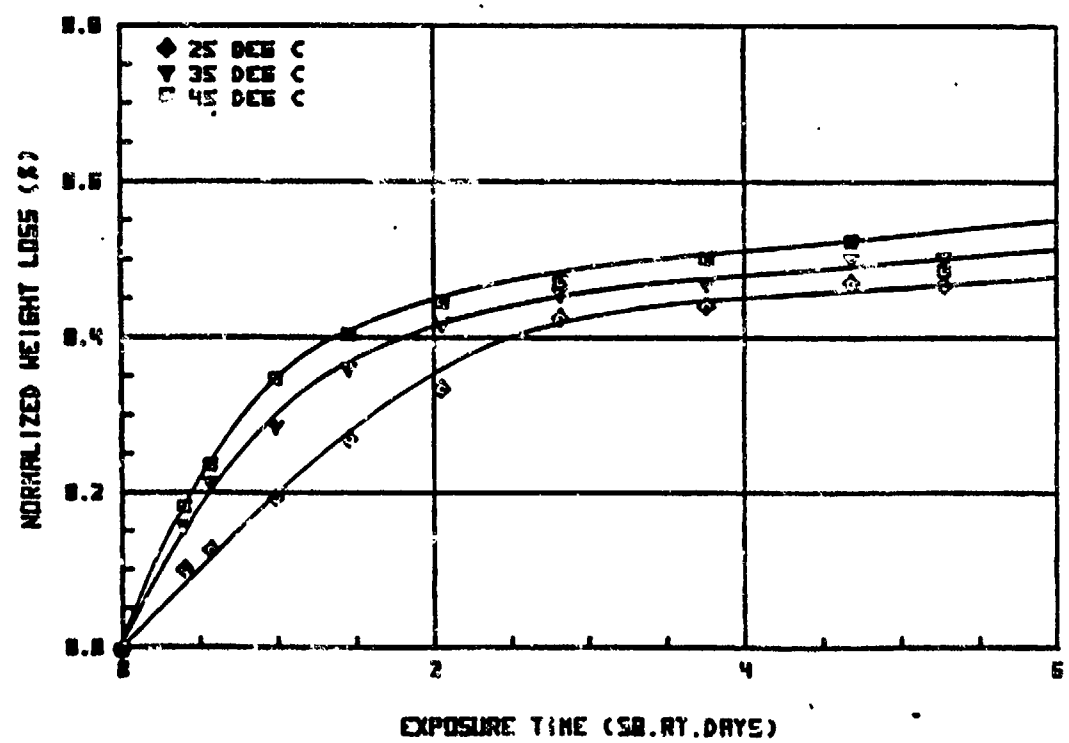

FIGURE A-56

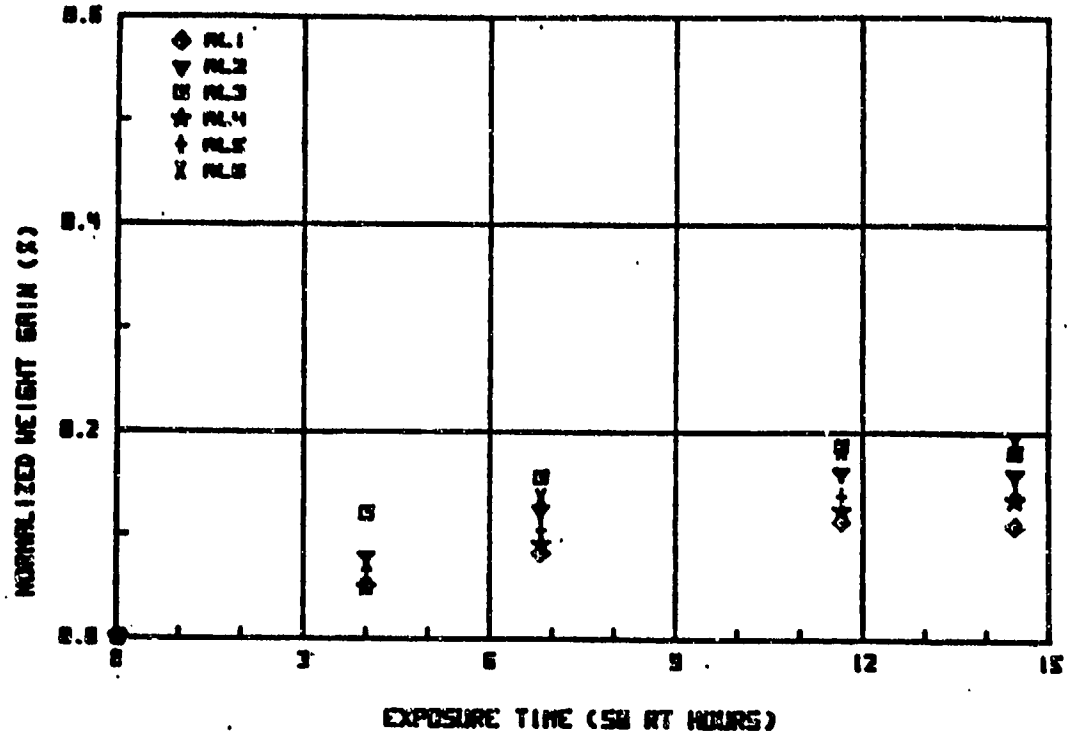

25 DEG C - 45 % HUMIDITY

FIGURE A-57

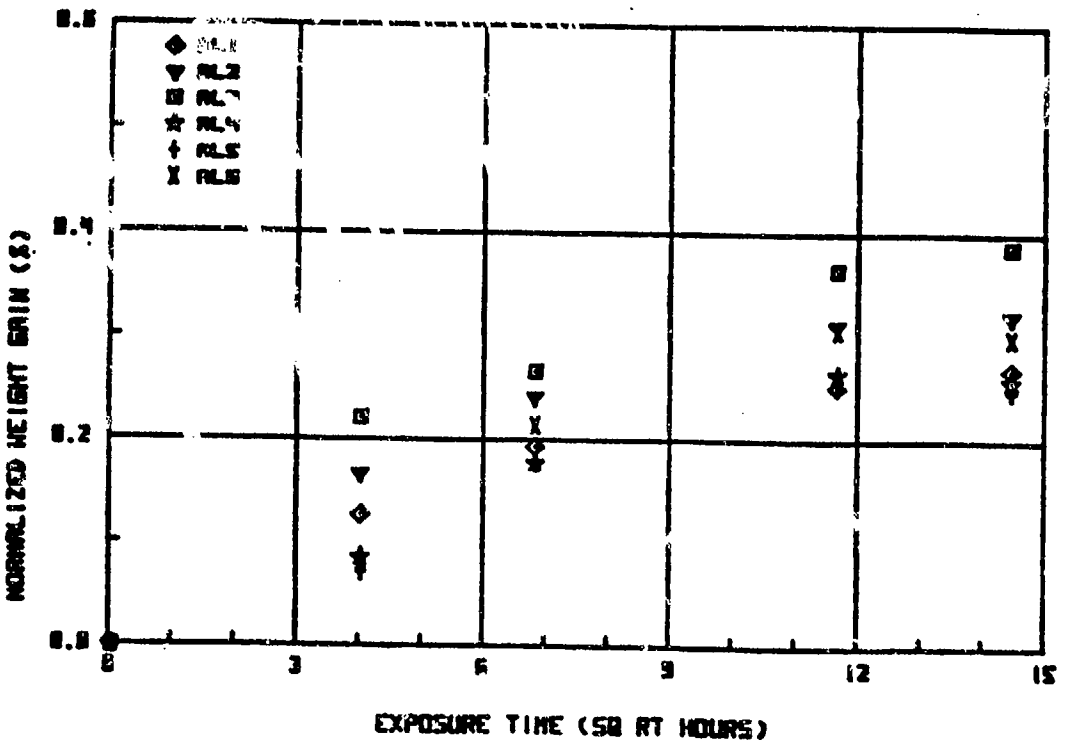

25 DEG C - 95 % HUMIDITY

FIGURE A-58

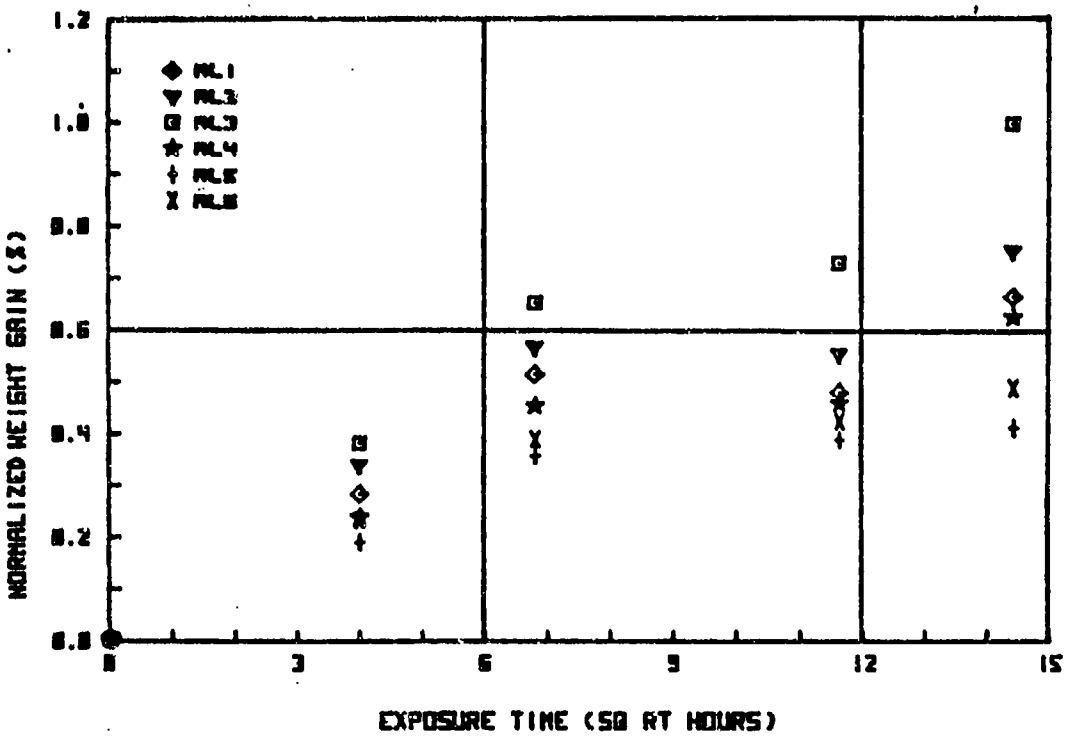

45 DEG C - 45 % HUMIDITY

FIGURE A-59

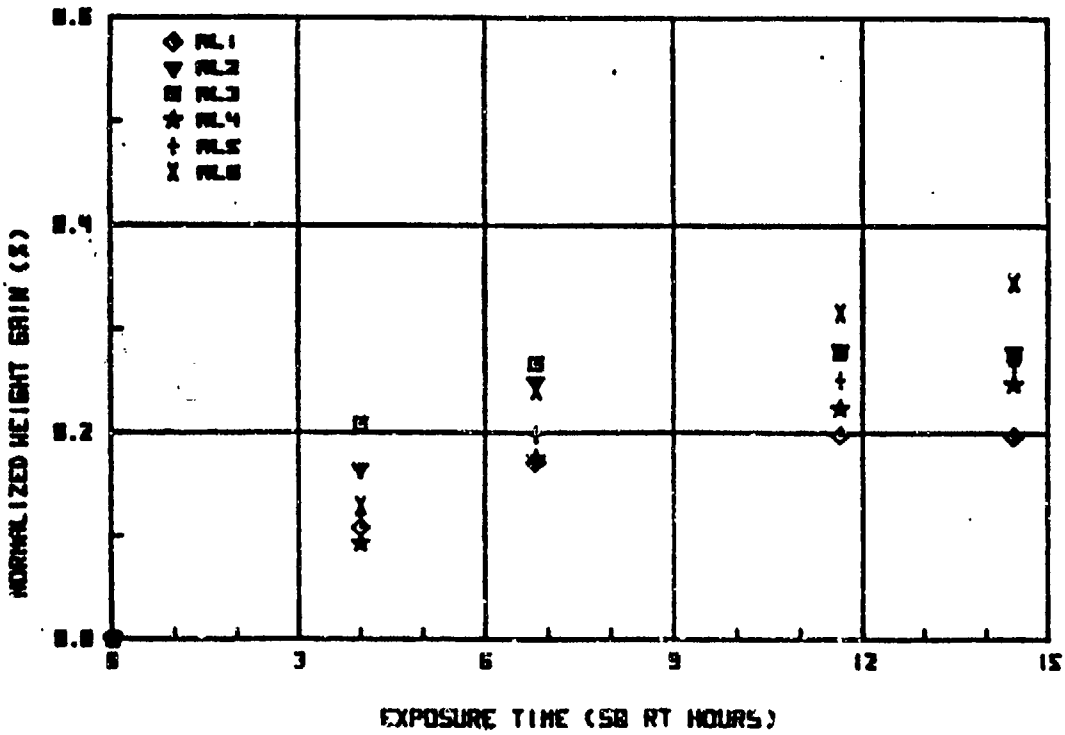

25 DEG C - 88 % HUMIDITY

FIGURE A-60

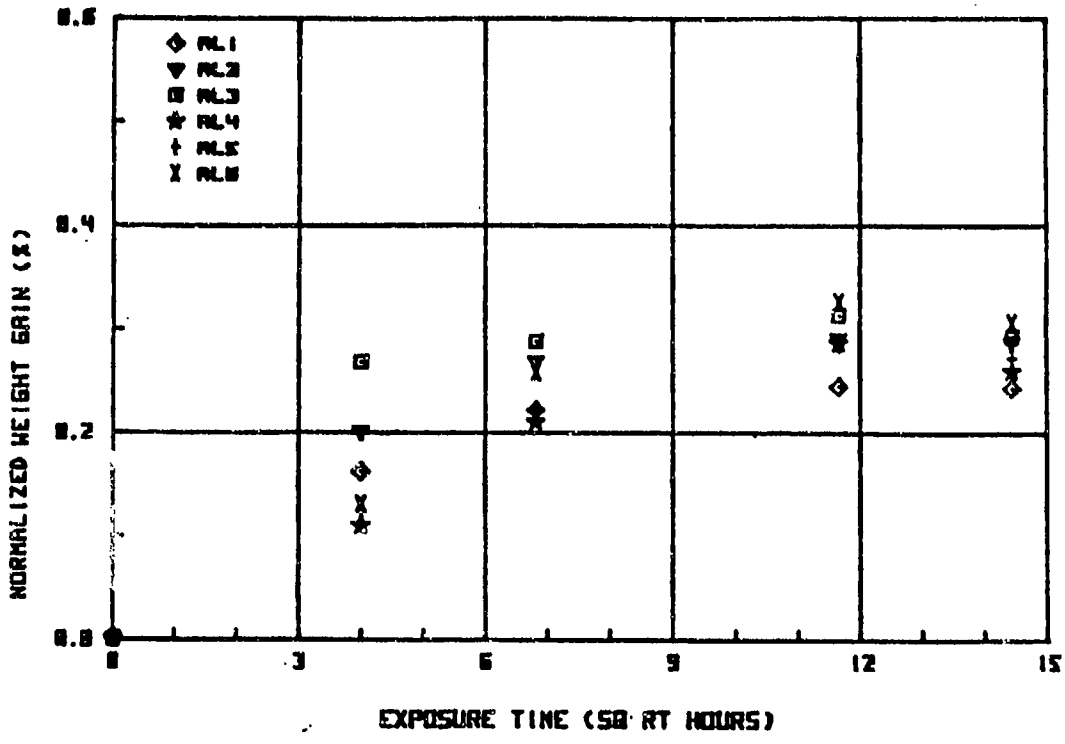

FIGURE A-61

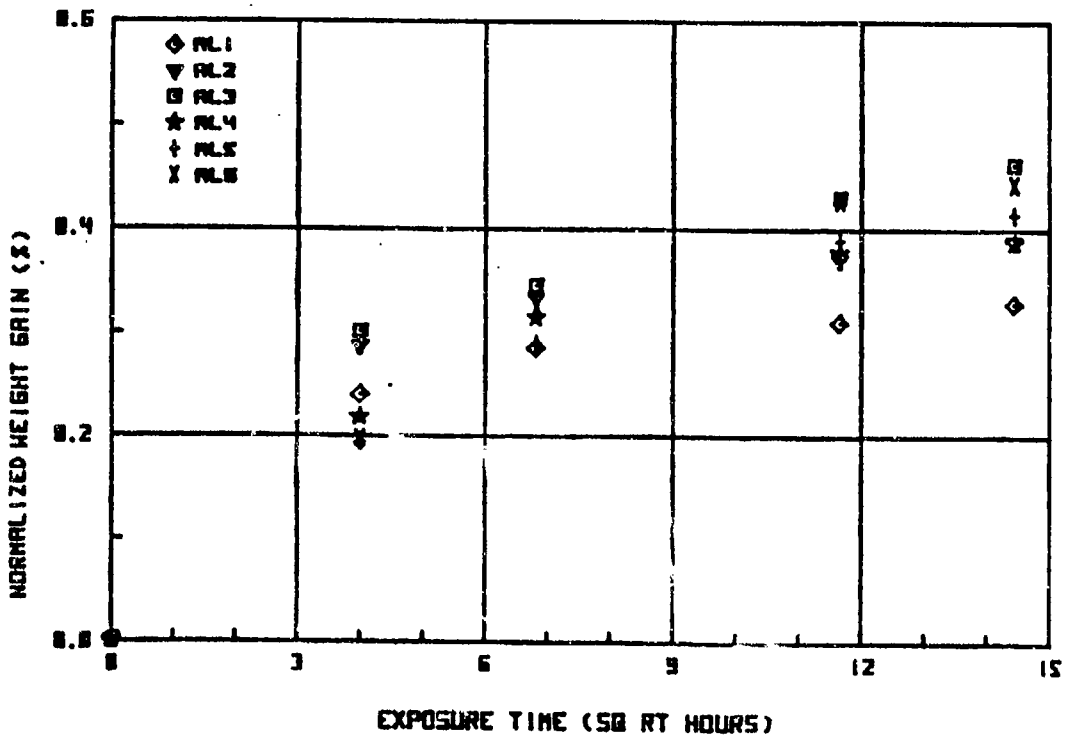

FIGURE A-62

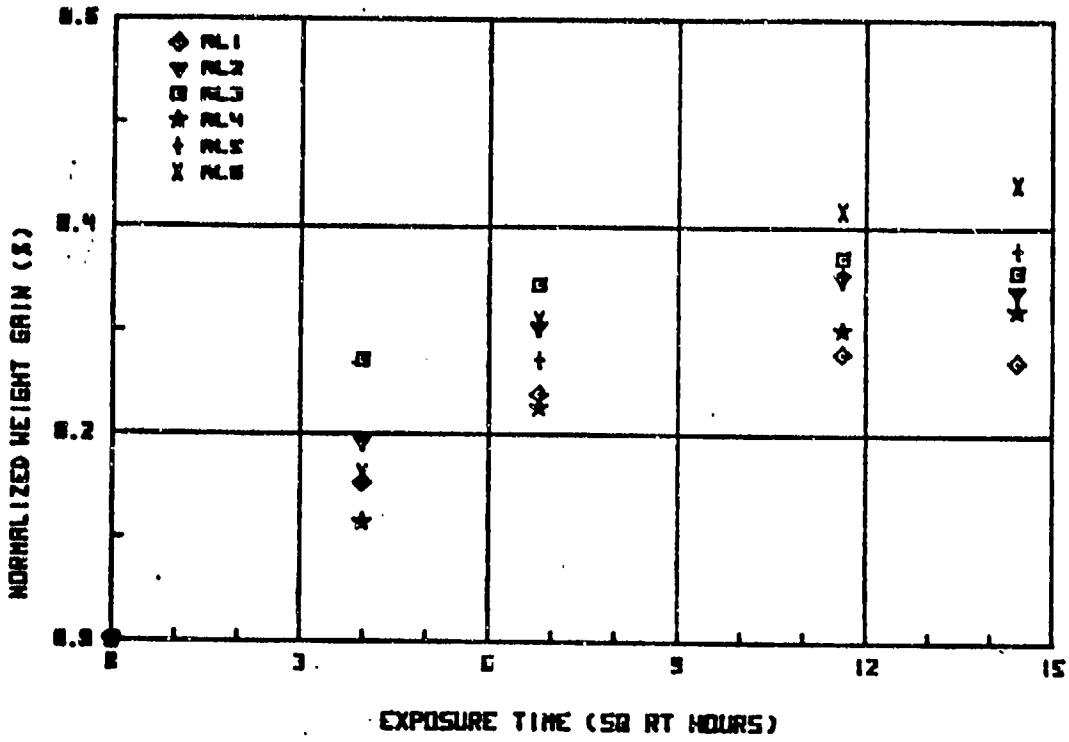

FIGURE A-63

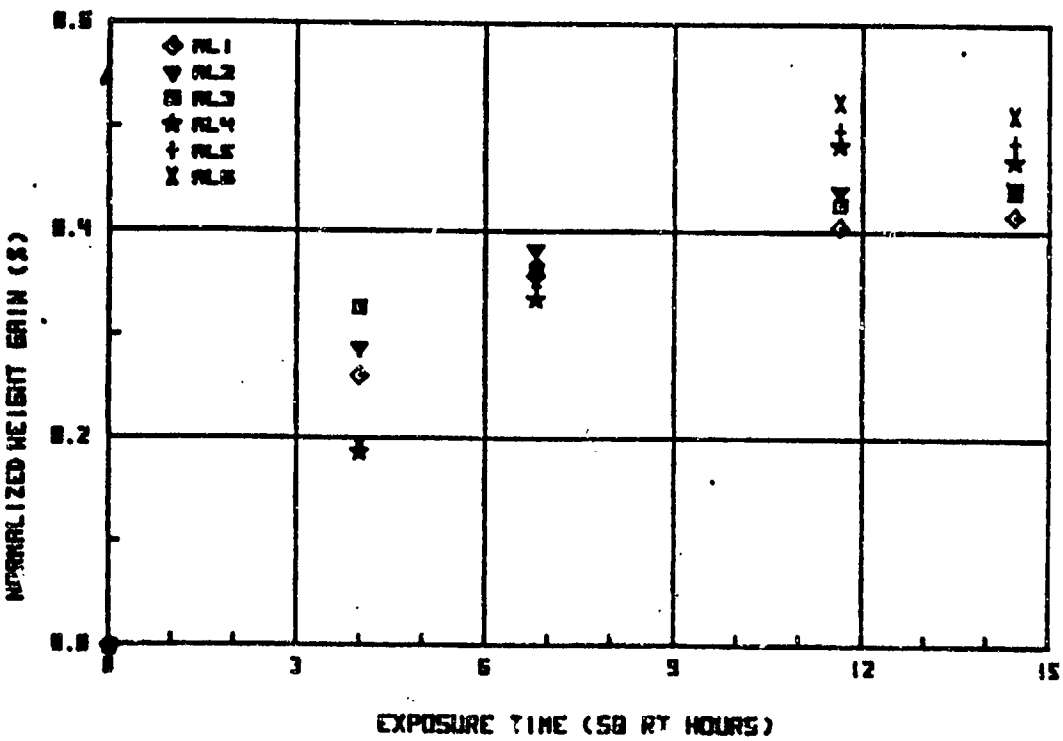

Figure A-64

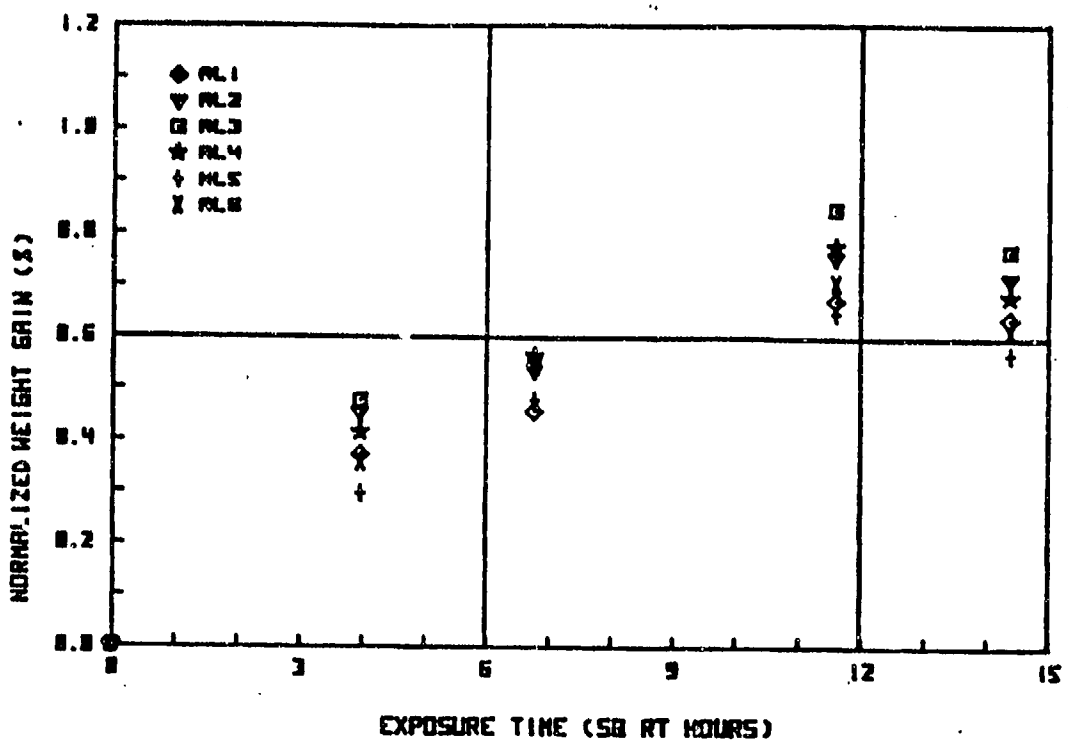

45 DEG C - 75 % HUMIDITY

FIGURE A-65

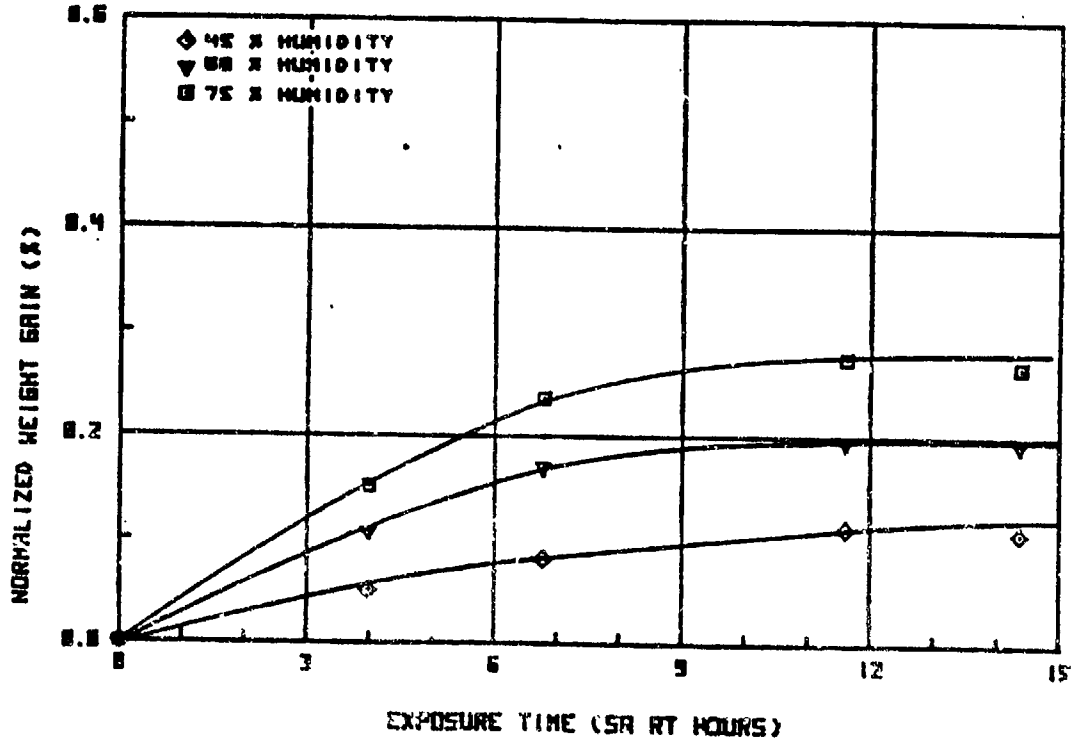

RL 1 25° DEG C

FIGURE A-66

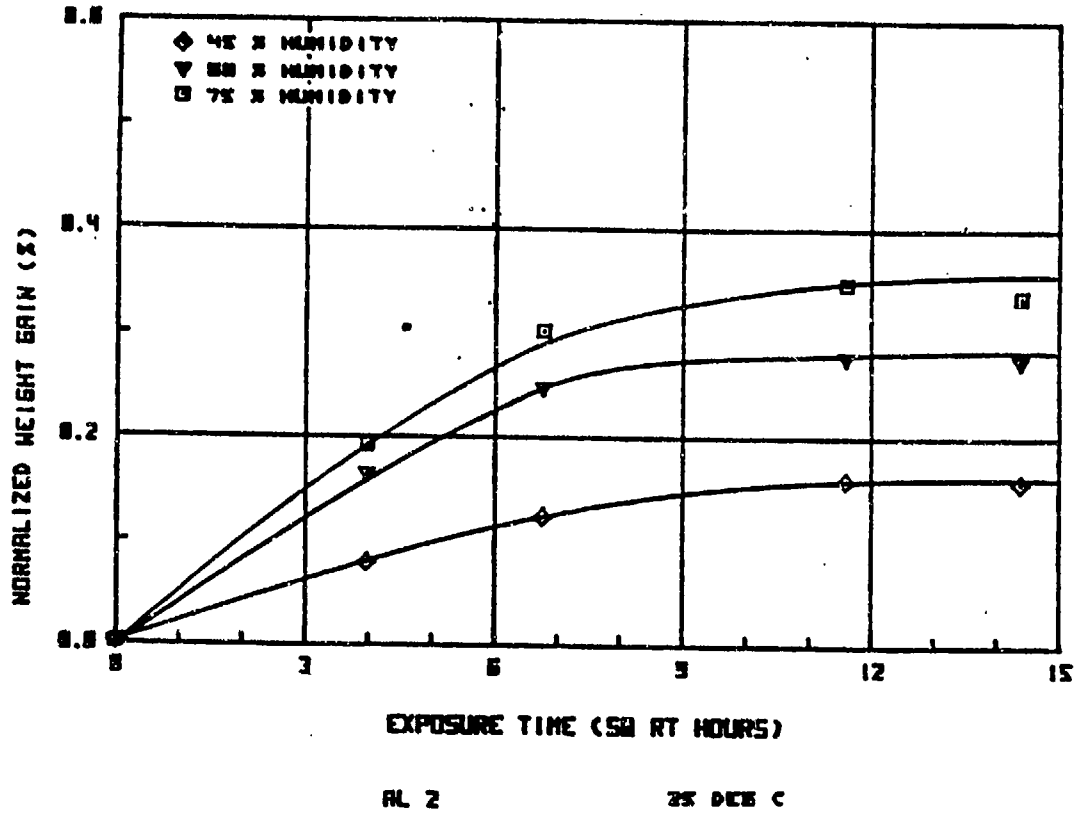

FIGURE A-67

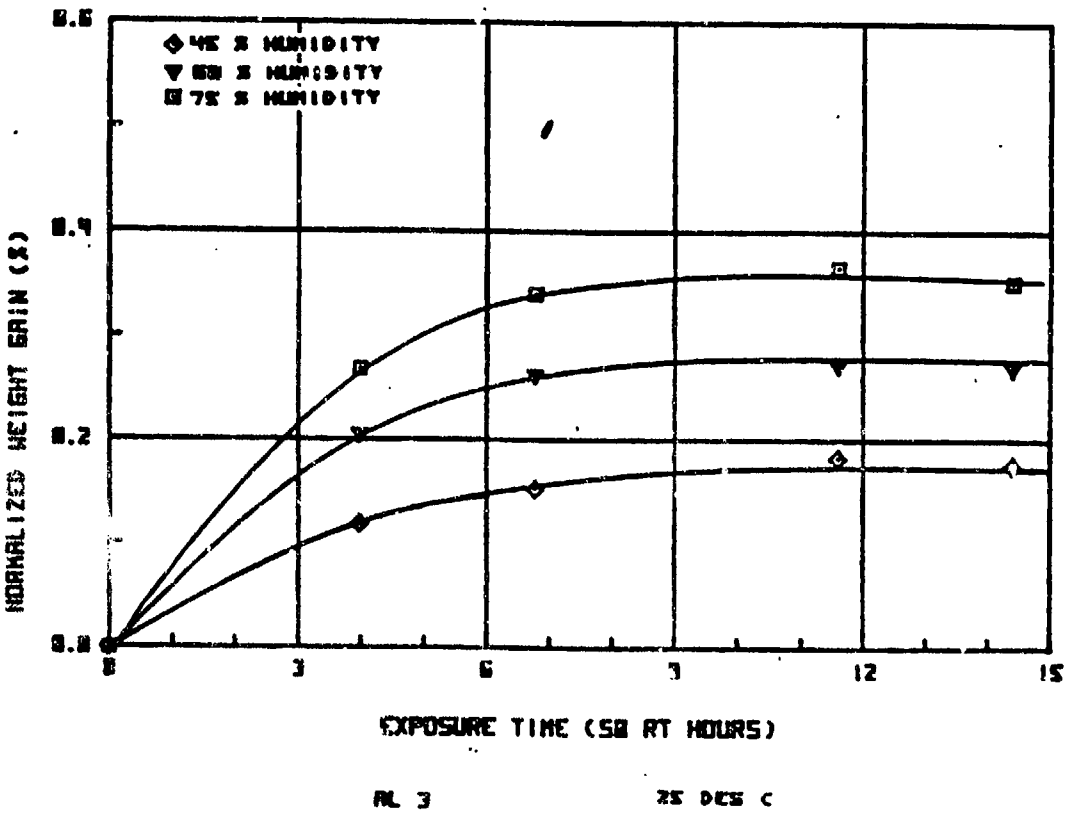

FIGURE A-68

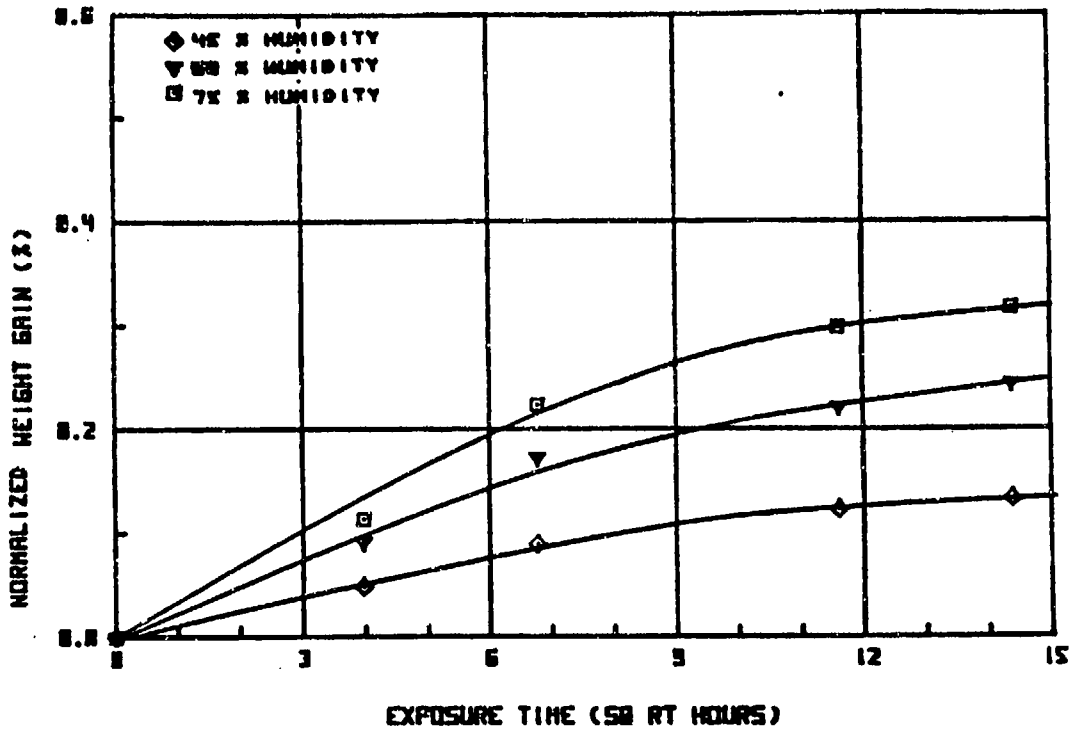

FIGURE A-69

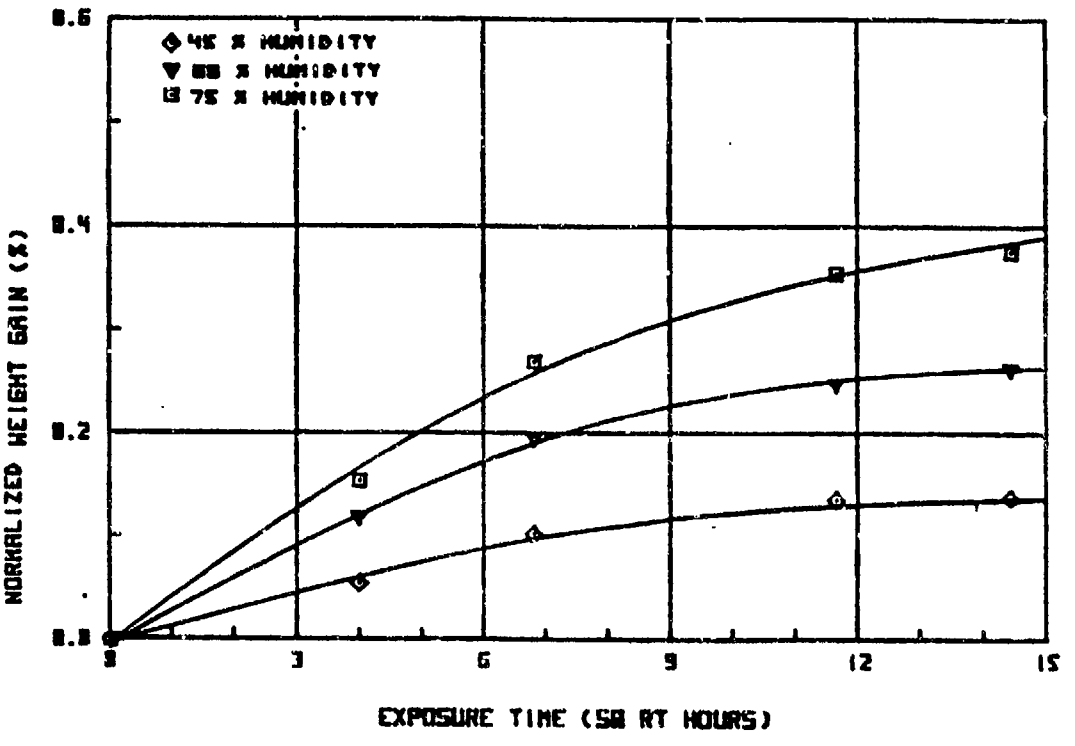

FIGURE A-70

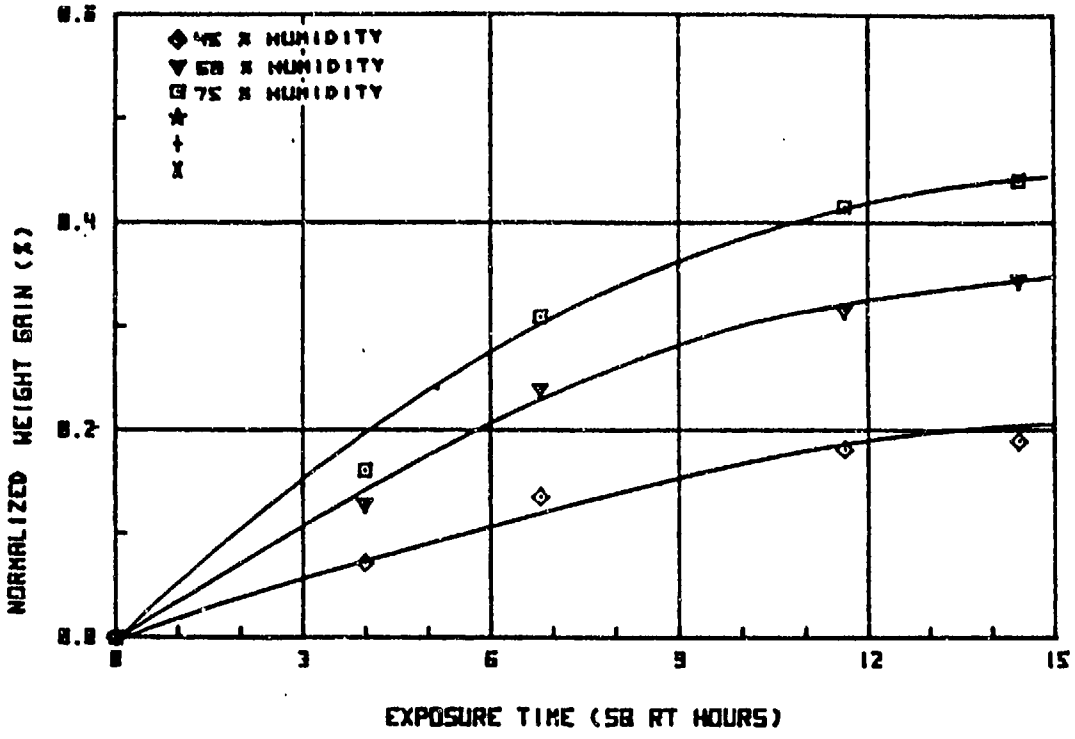

- FIGURE A-71

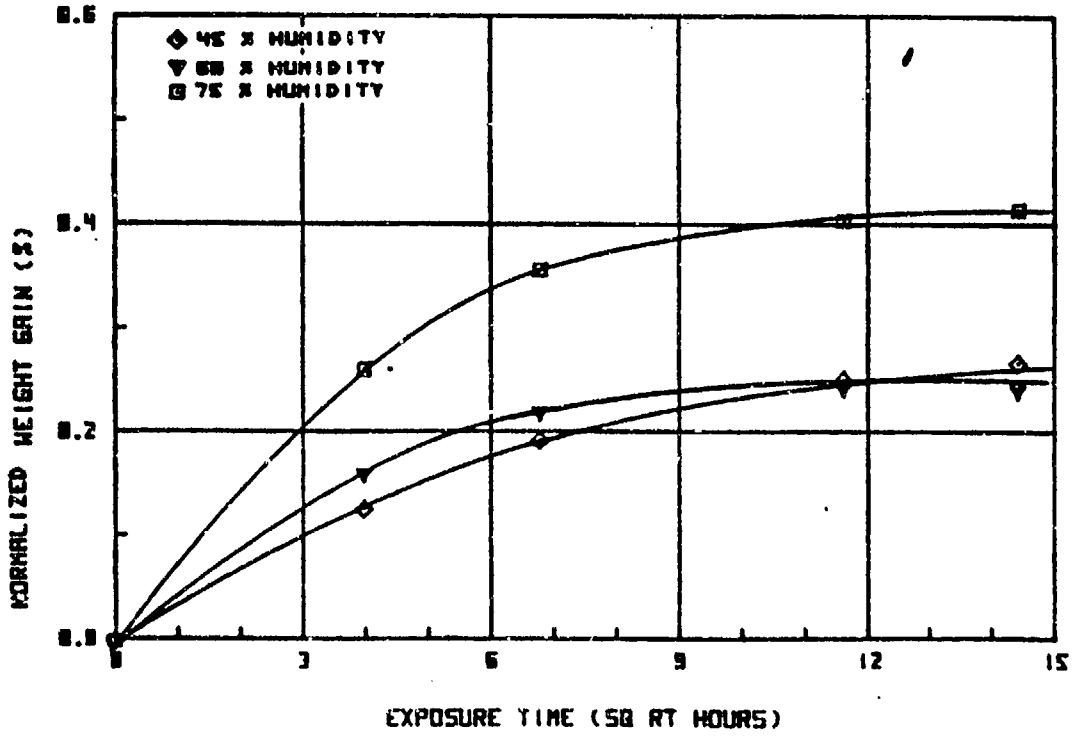

Figure A-72

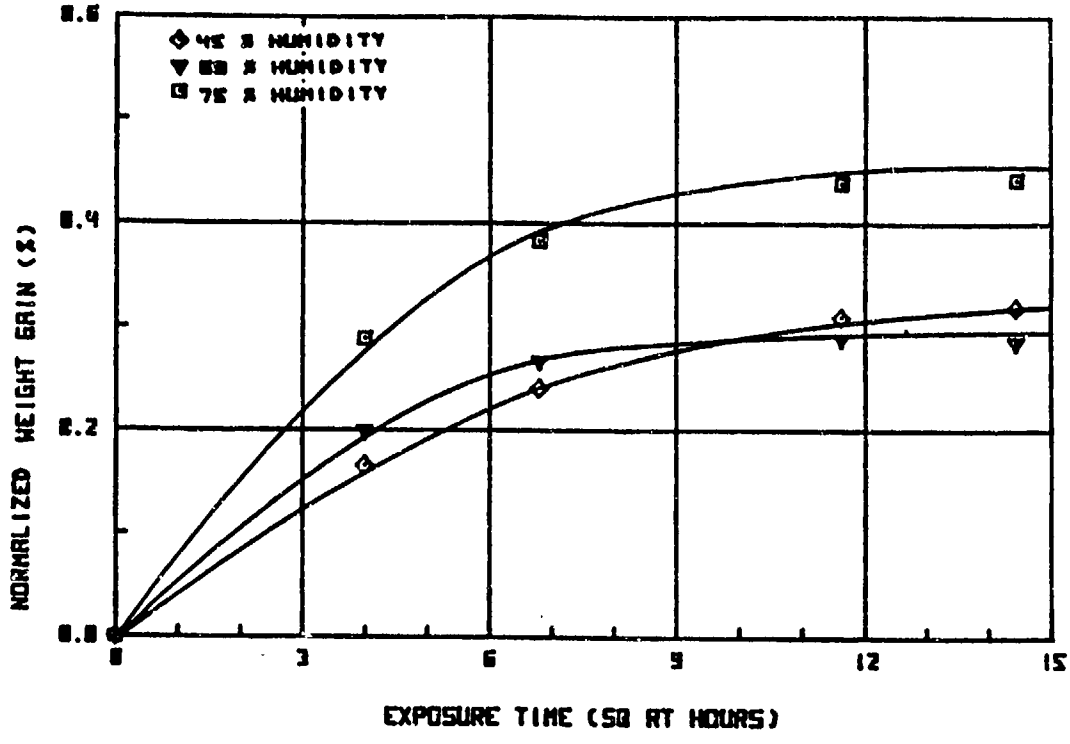

RL 2 35 DEG C

FIGURE A-73

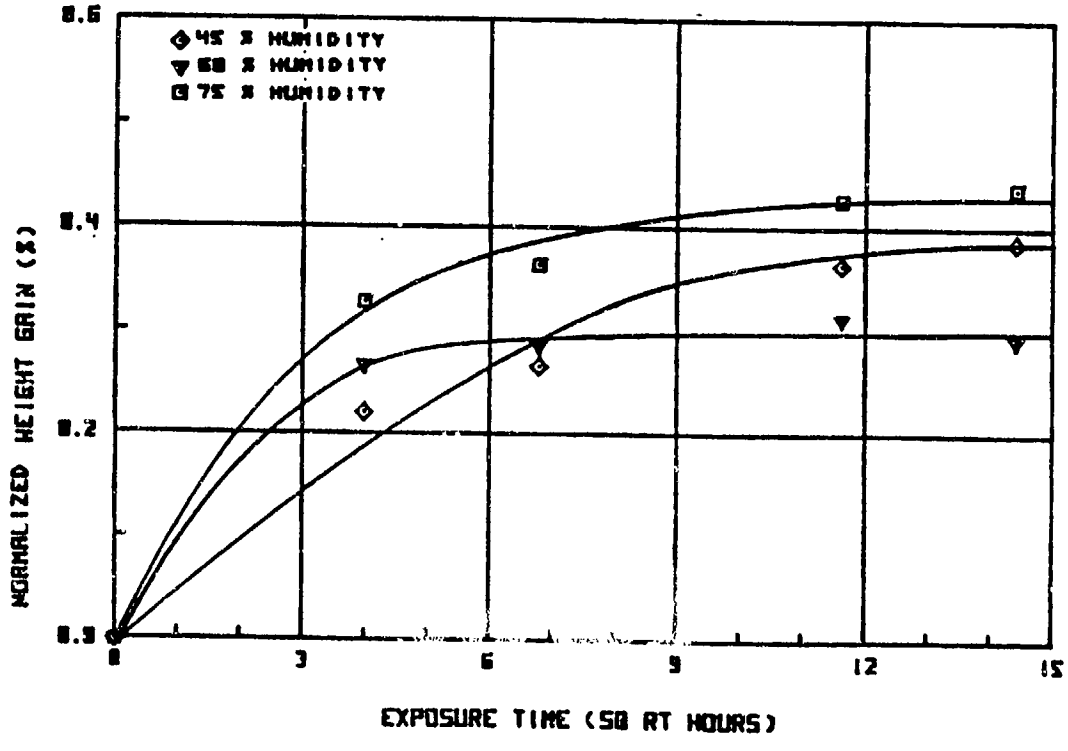

RL 3 35 DEG C

FIGURE A-74

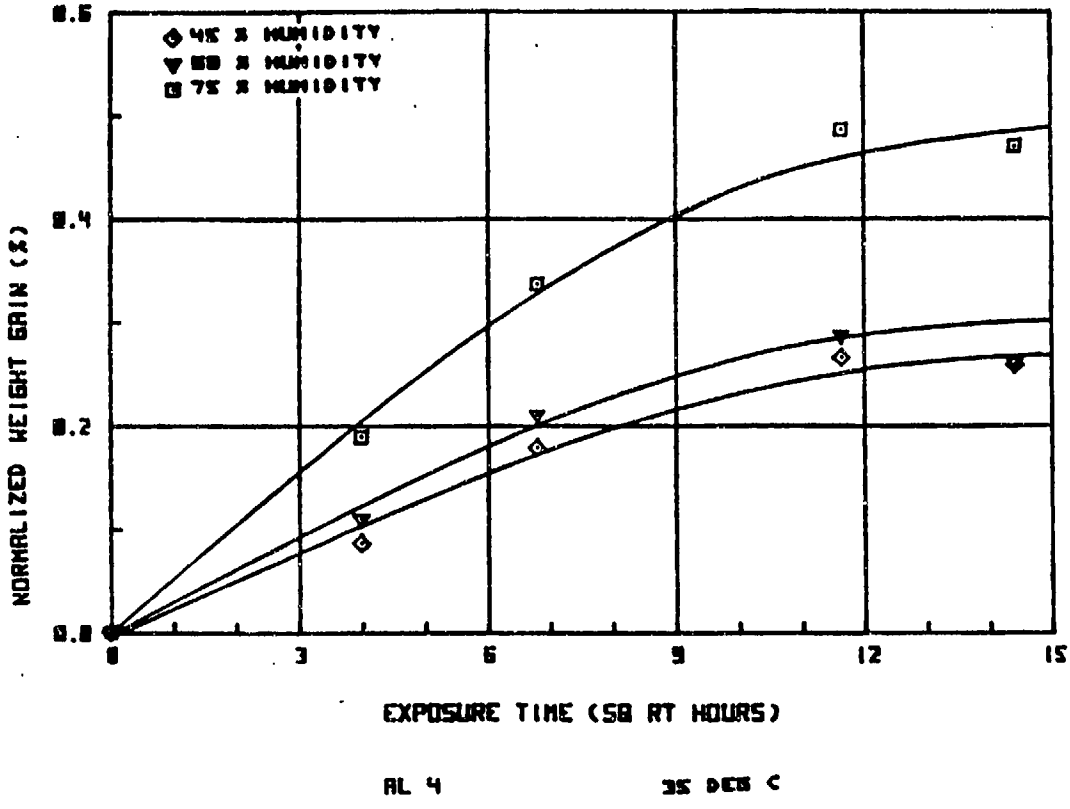

FIGURE A-75

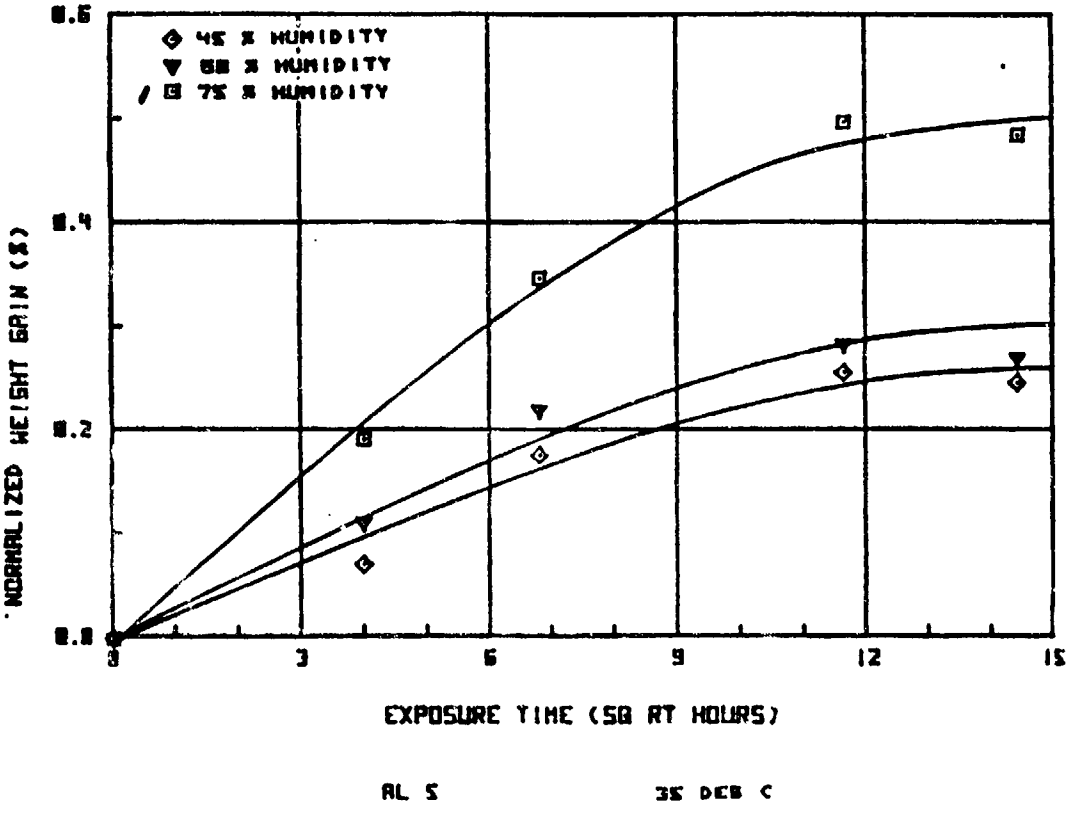

FIGURE A-76

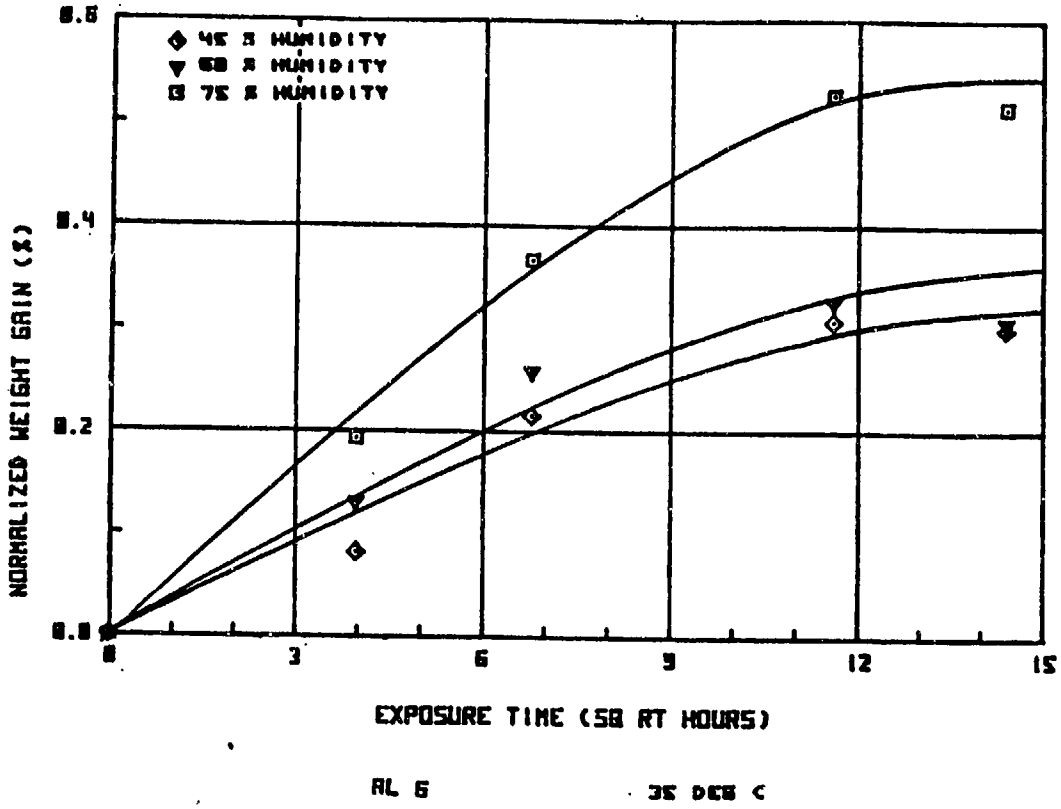

FIGURE A-77

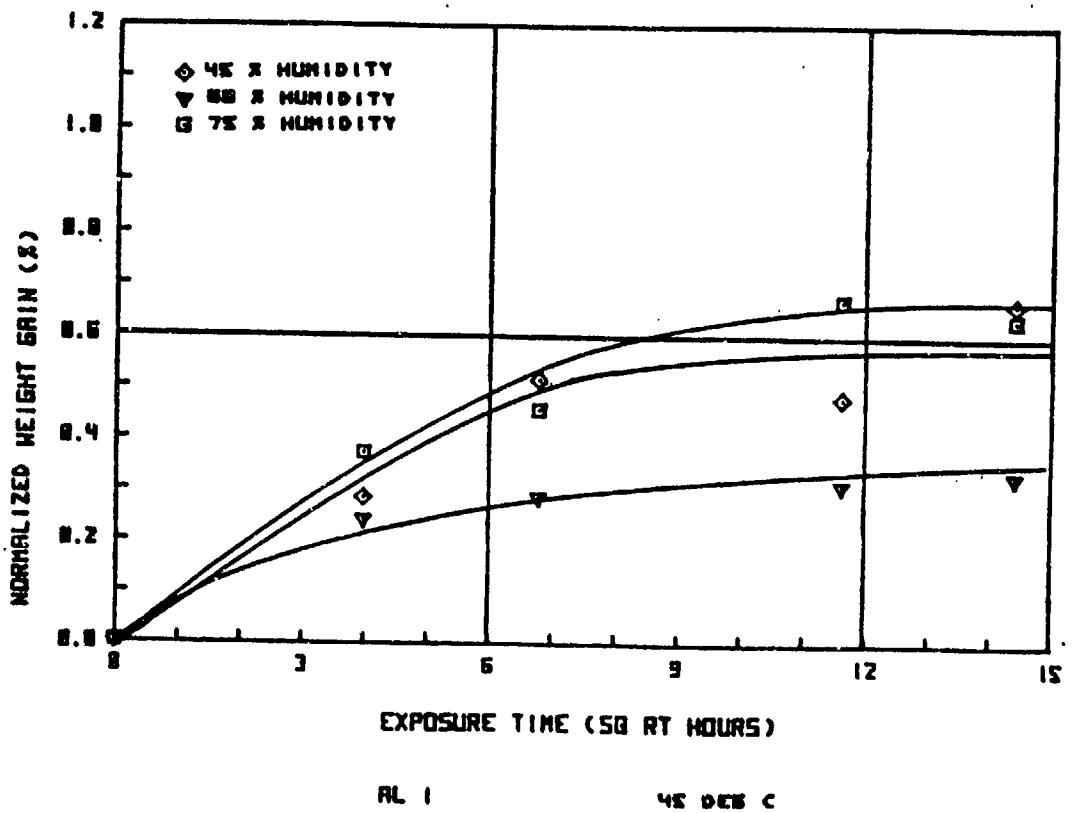

FIGURE A-78

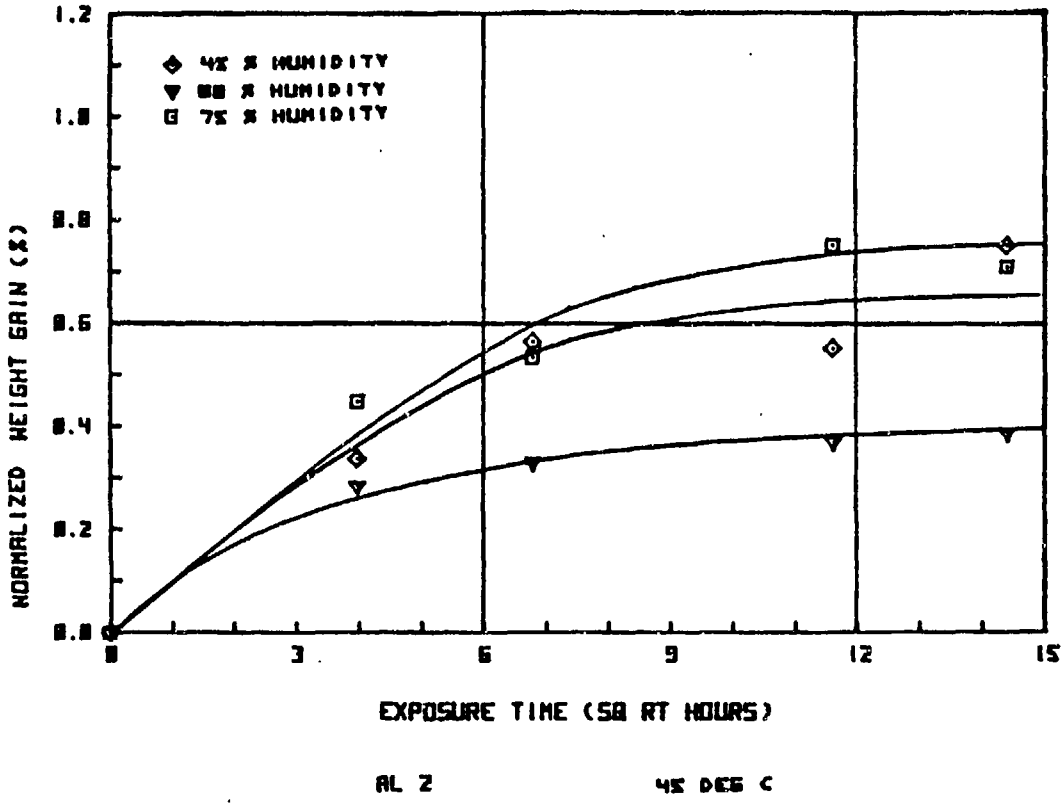

FIGURE A-79

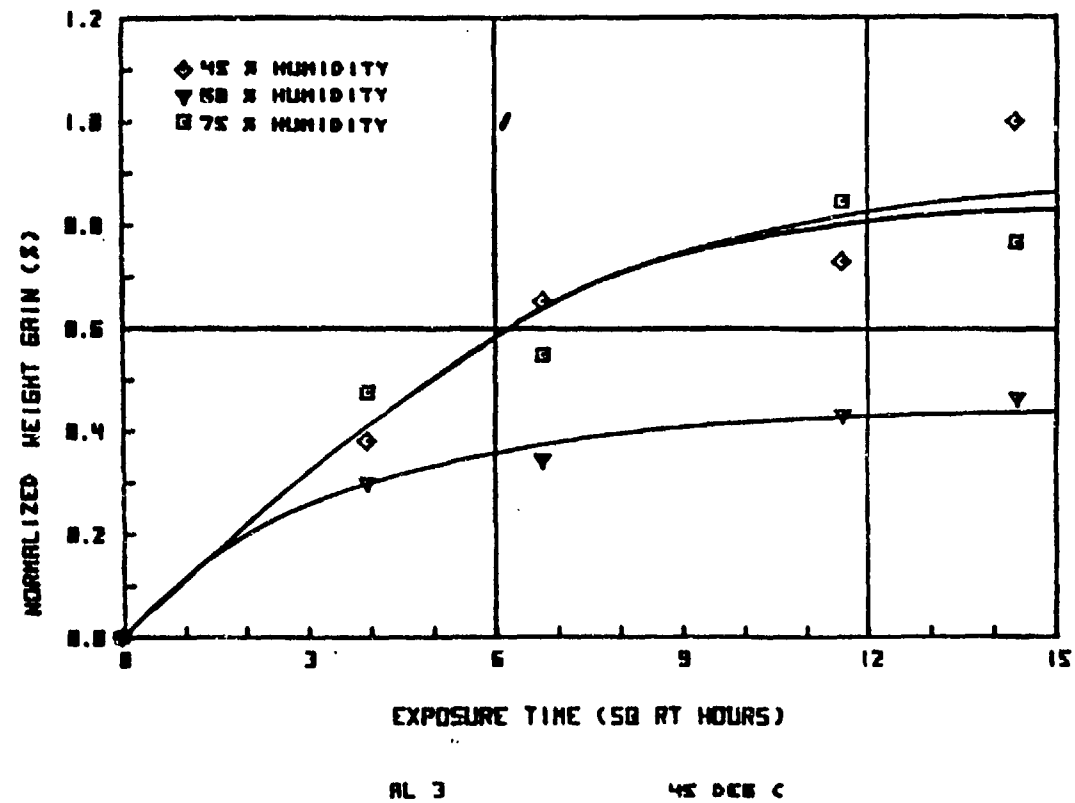

FIGURE A-80

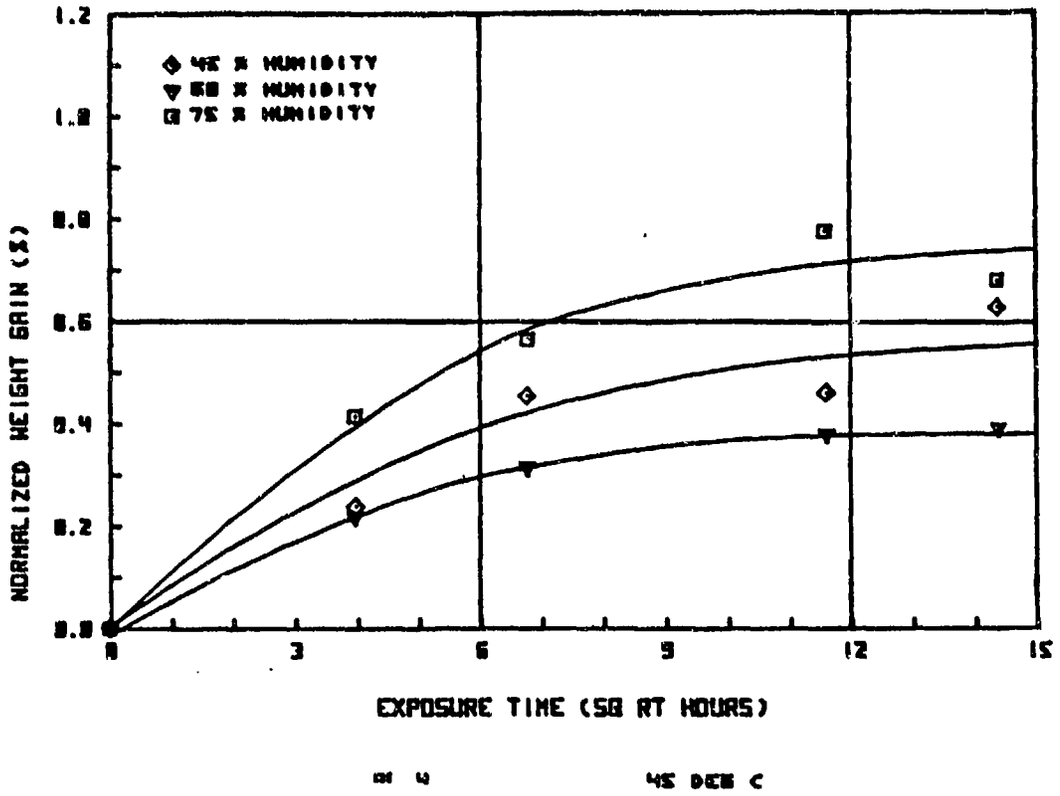

FIGURE A-81

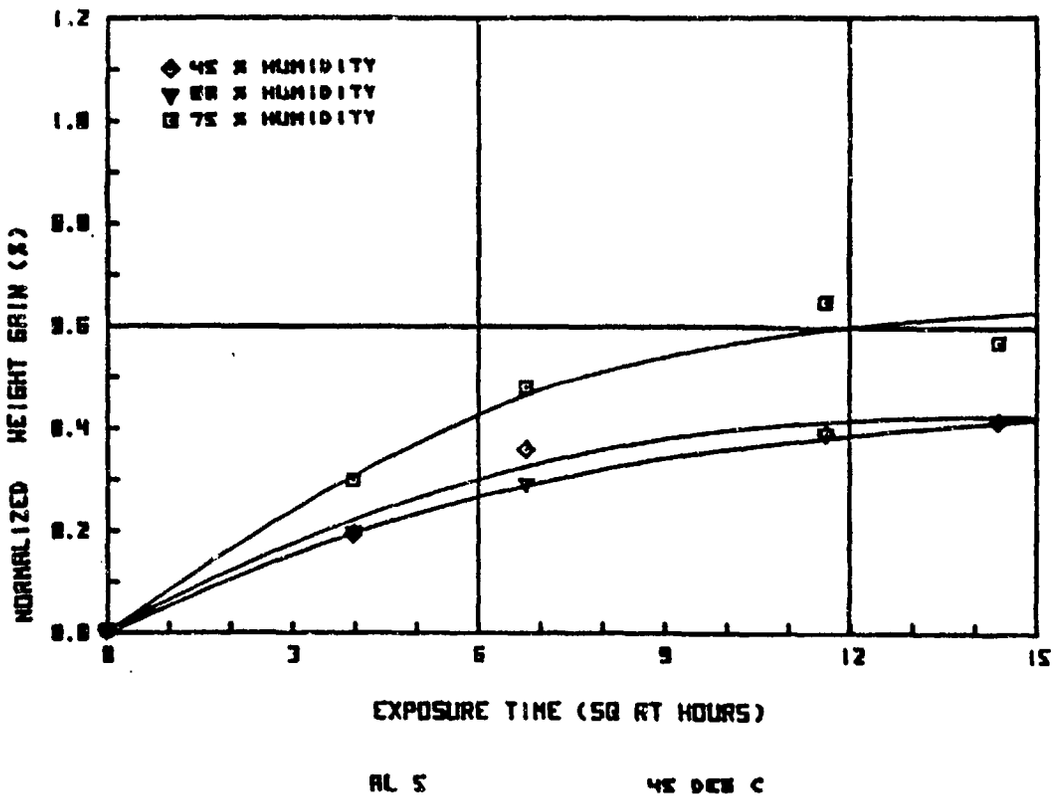

FIGURE A-82

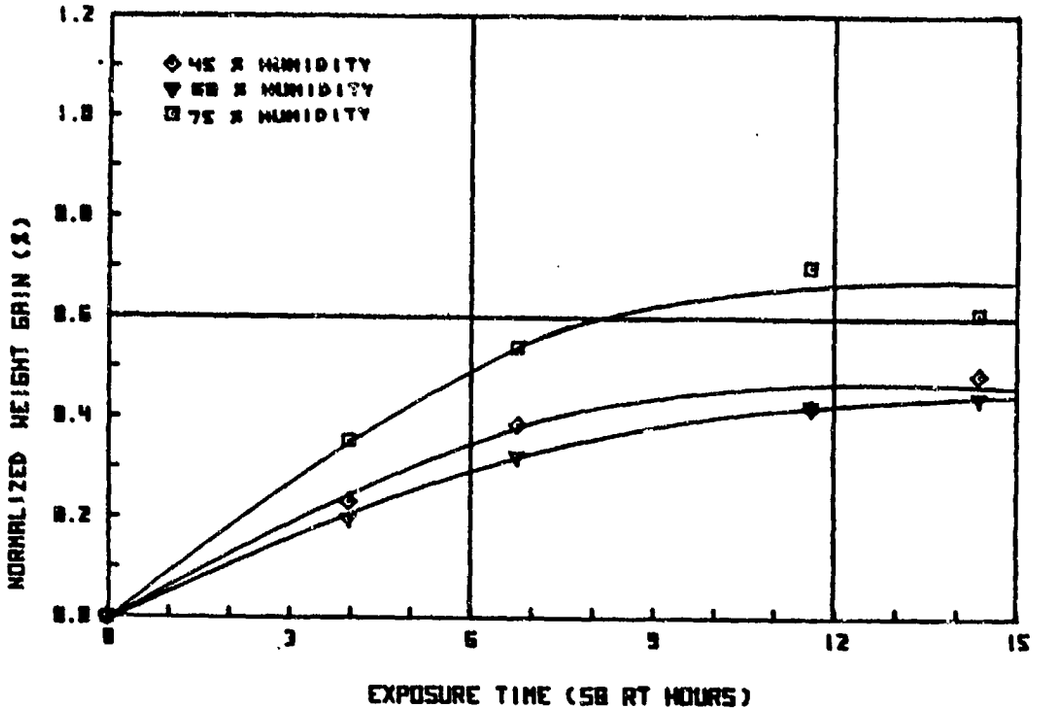

FIGURE A-83

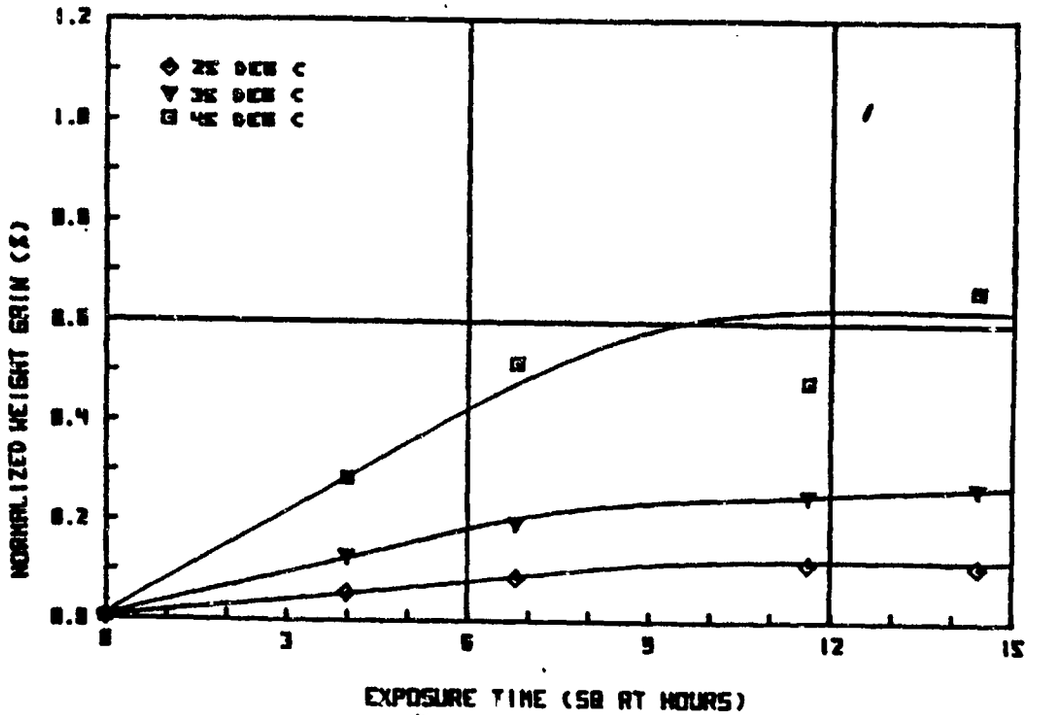

FIGURE A-84

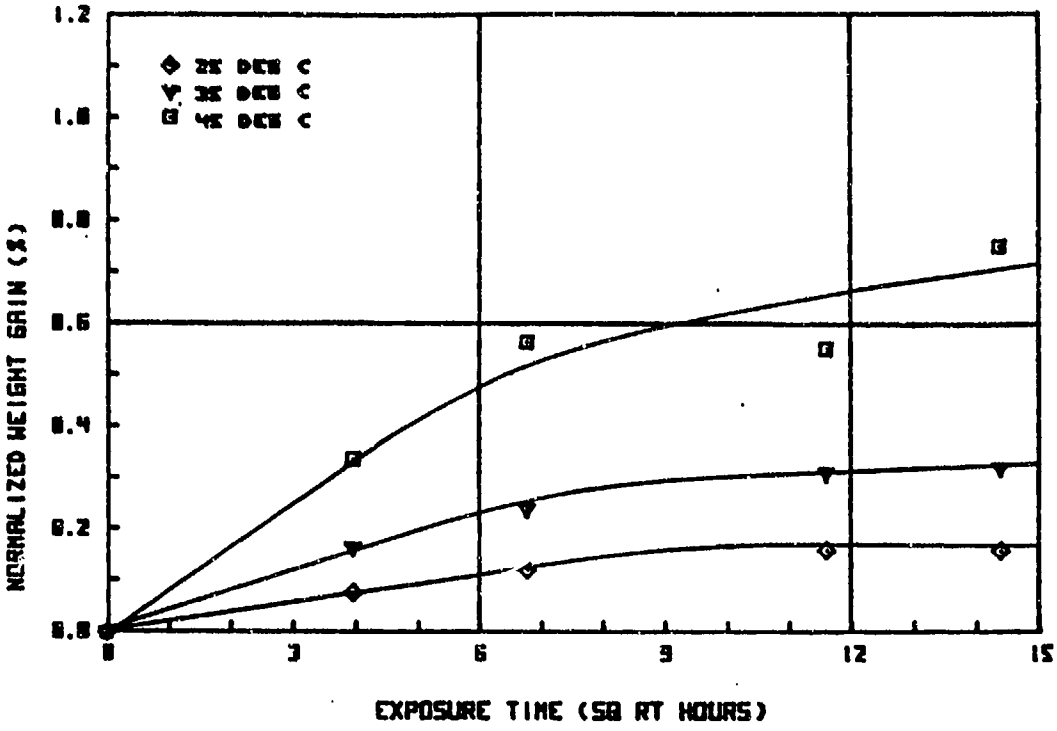

FIGURE A-85

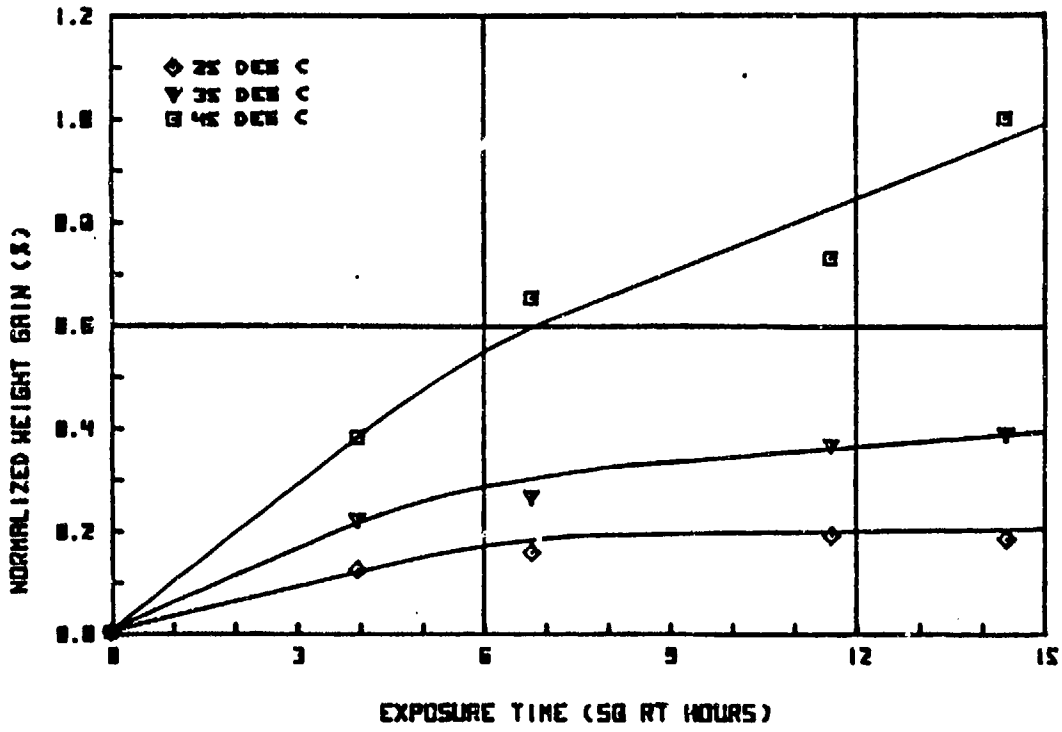

FIGURE A-86

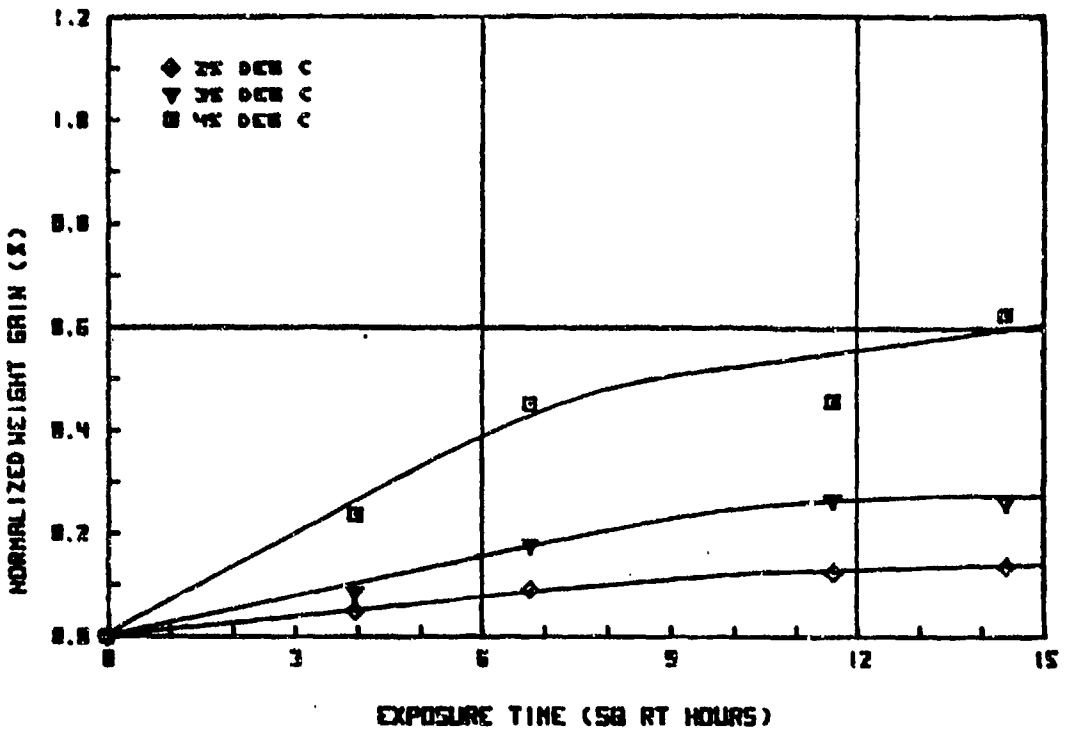

AL 4 45 % HUMIDITY

FIGURE A-87

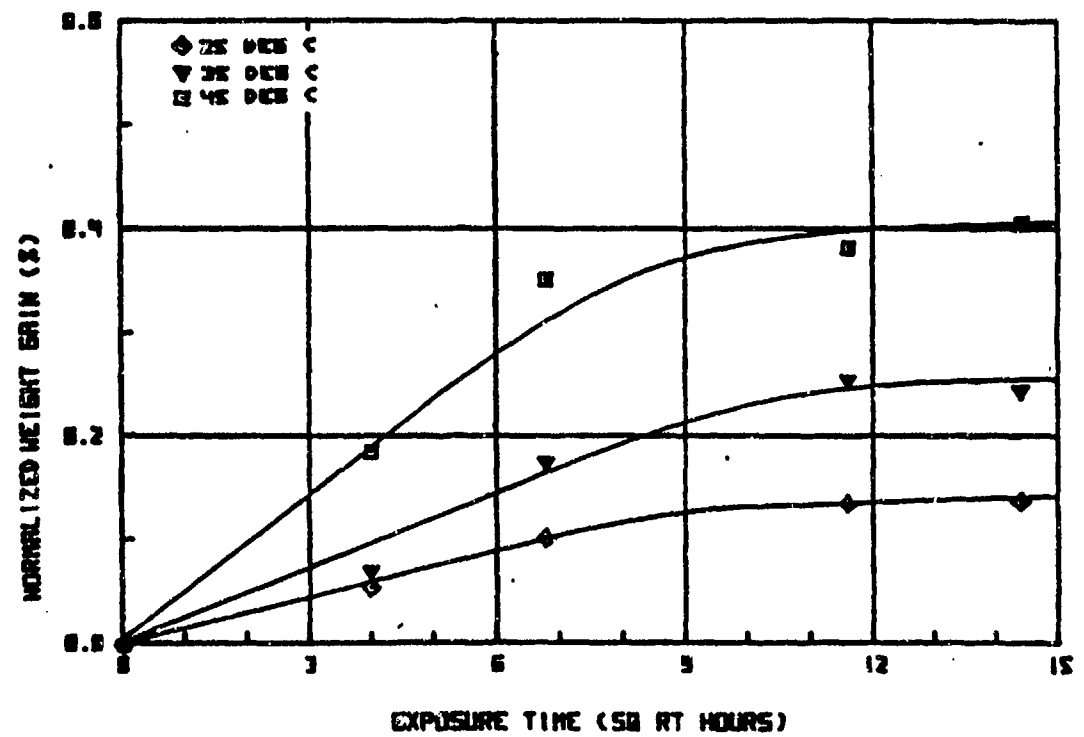

AL 5 45 % HUMIDITY

FIGURE A-88

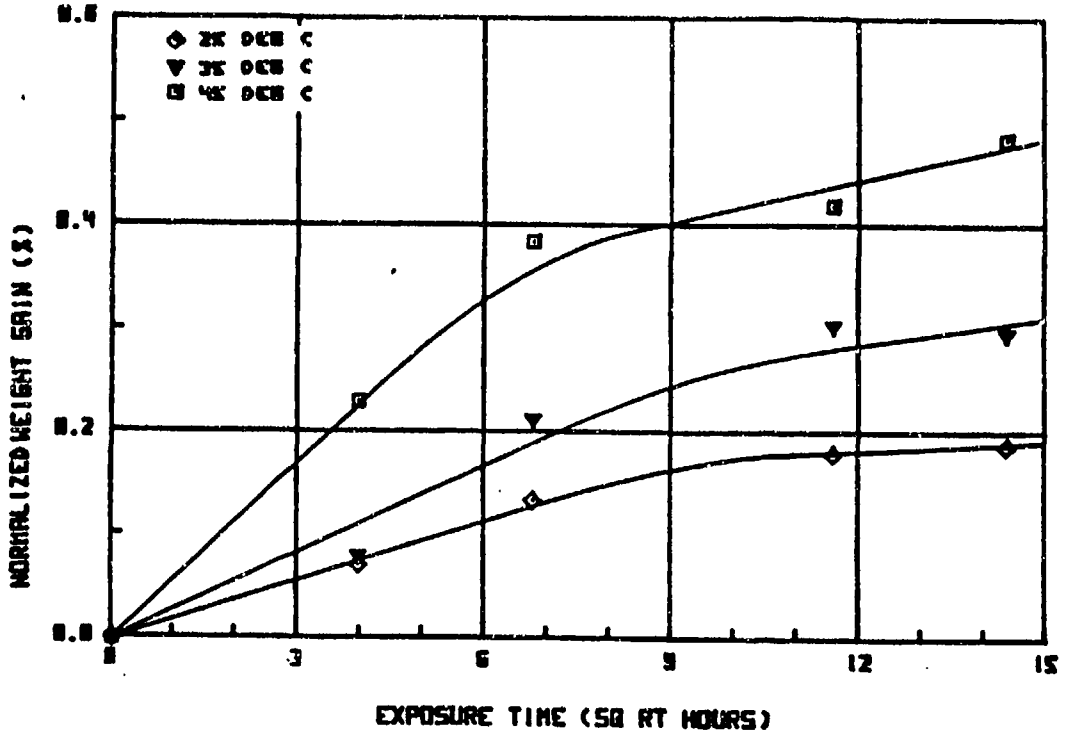

AL 6 HUMIDITY

FIGURE A-89

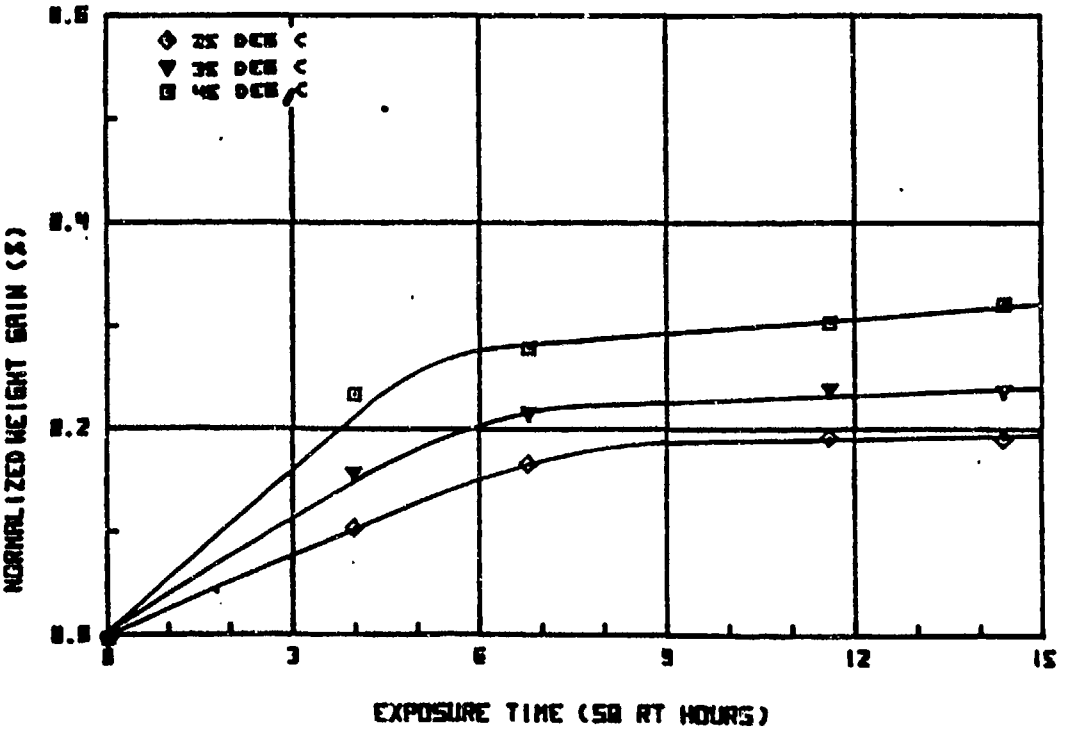

AL 1 HUMIDITY

FIGURE A-90

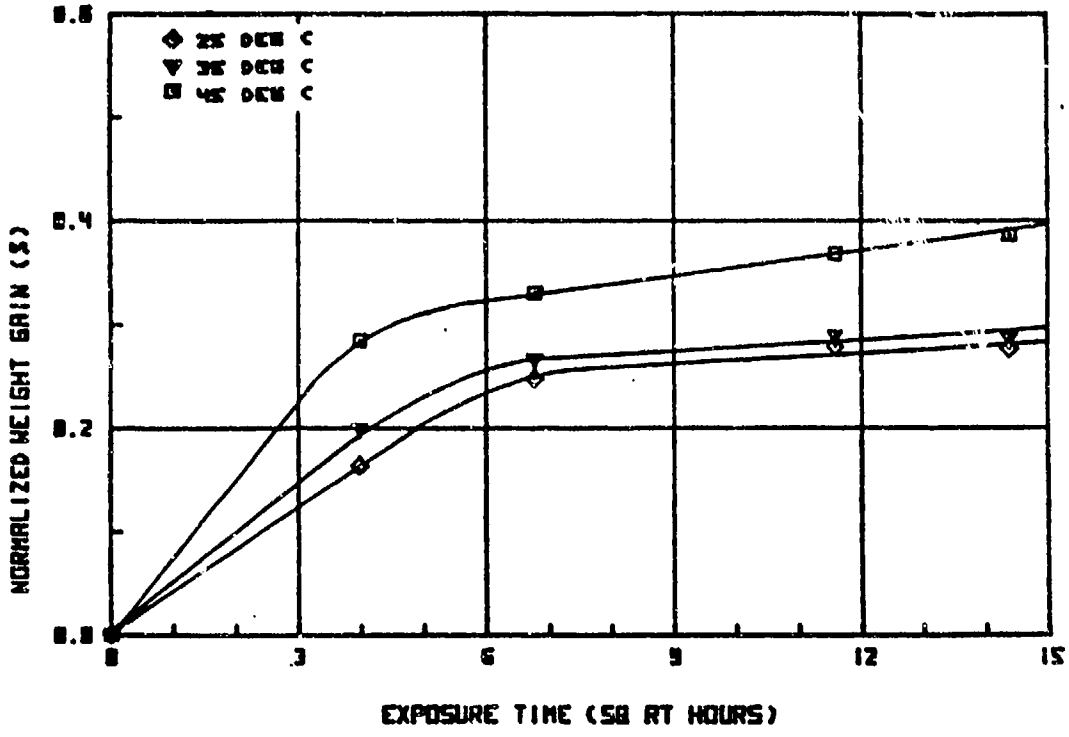

FIGURE A-91

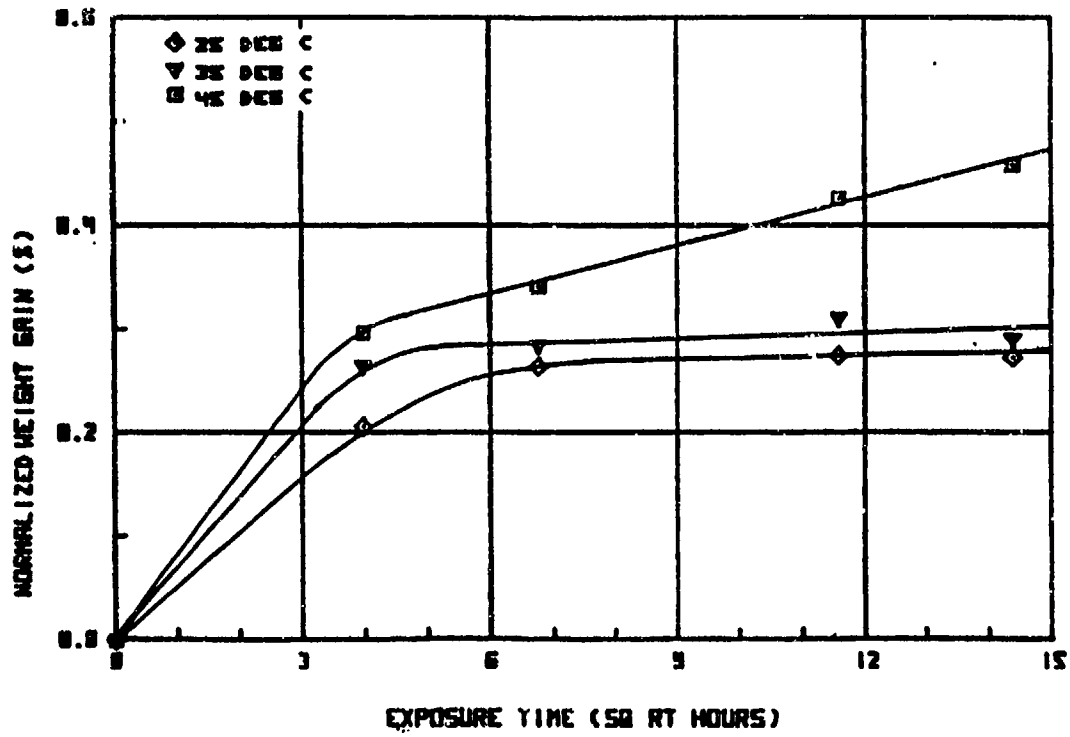

FIGURE A-92

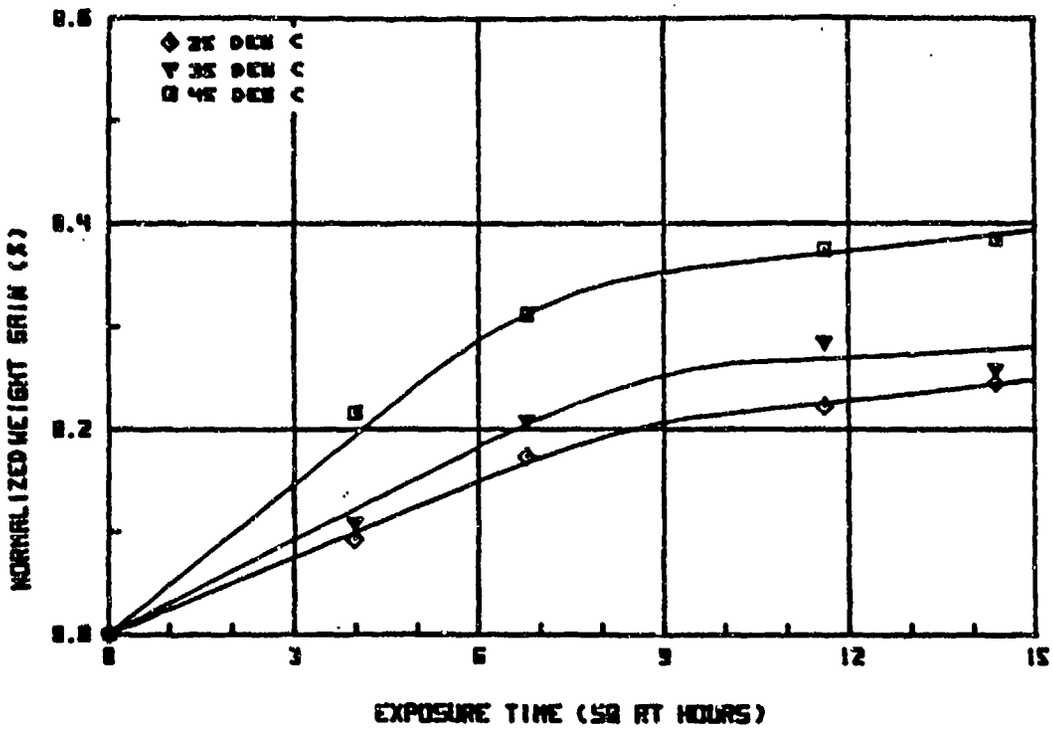

AL 4 60.% HUMIDITY

FIGURE A-93

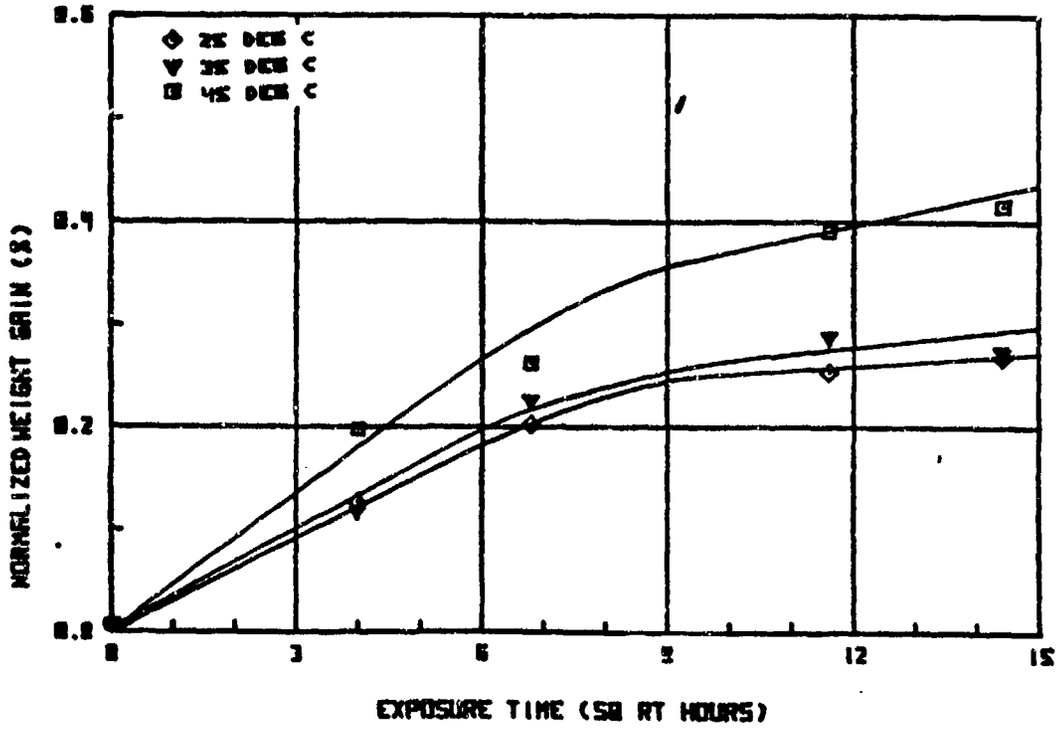

AL 5 80 % HUMIDITY

FIGURE A-94

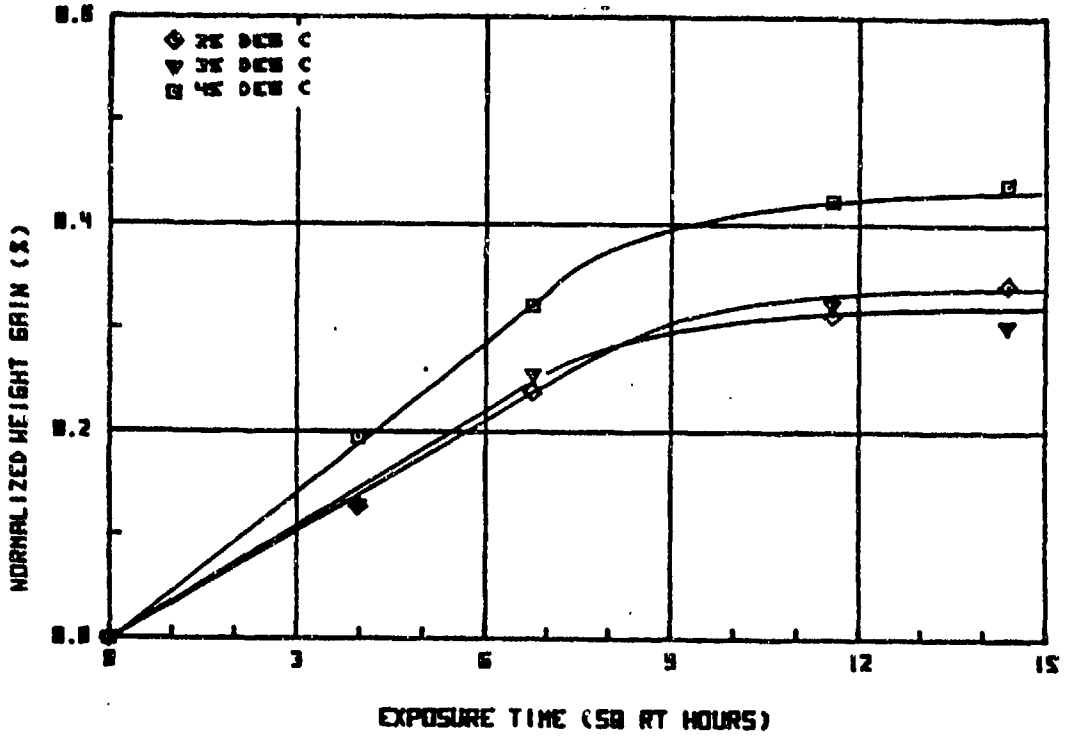

FIGURE A-95

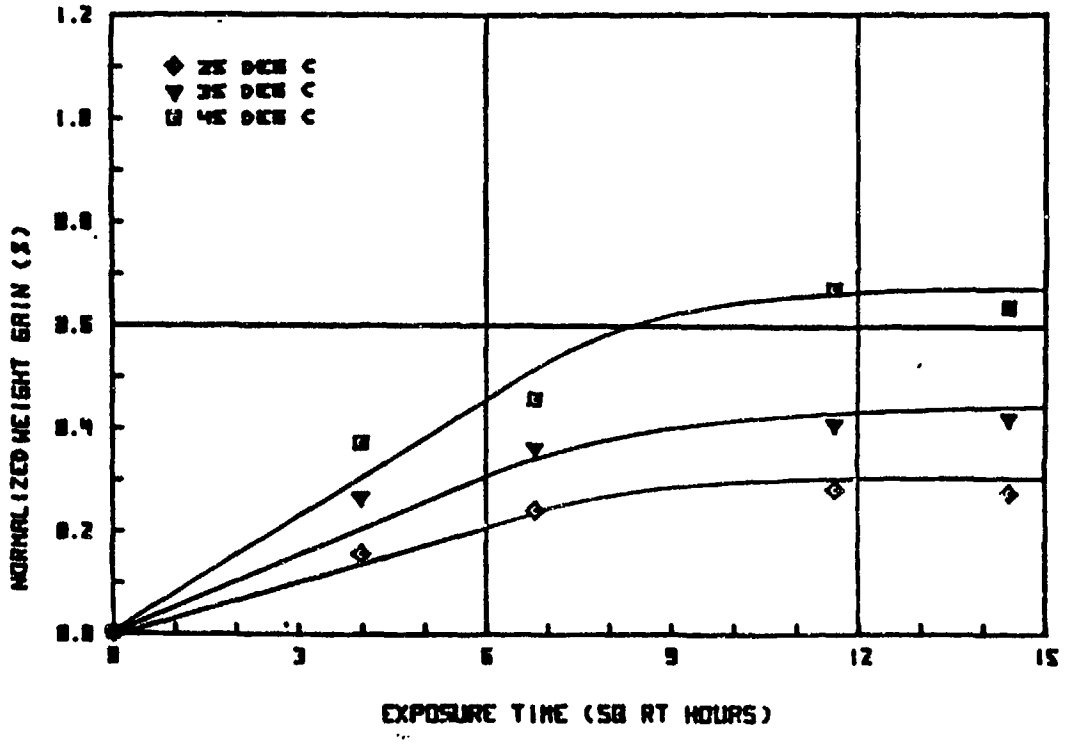

FIGURE A-96

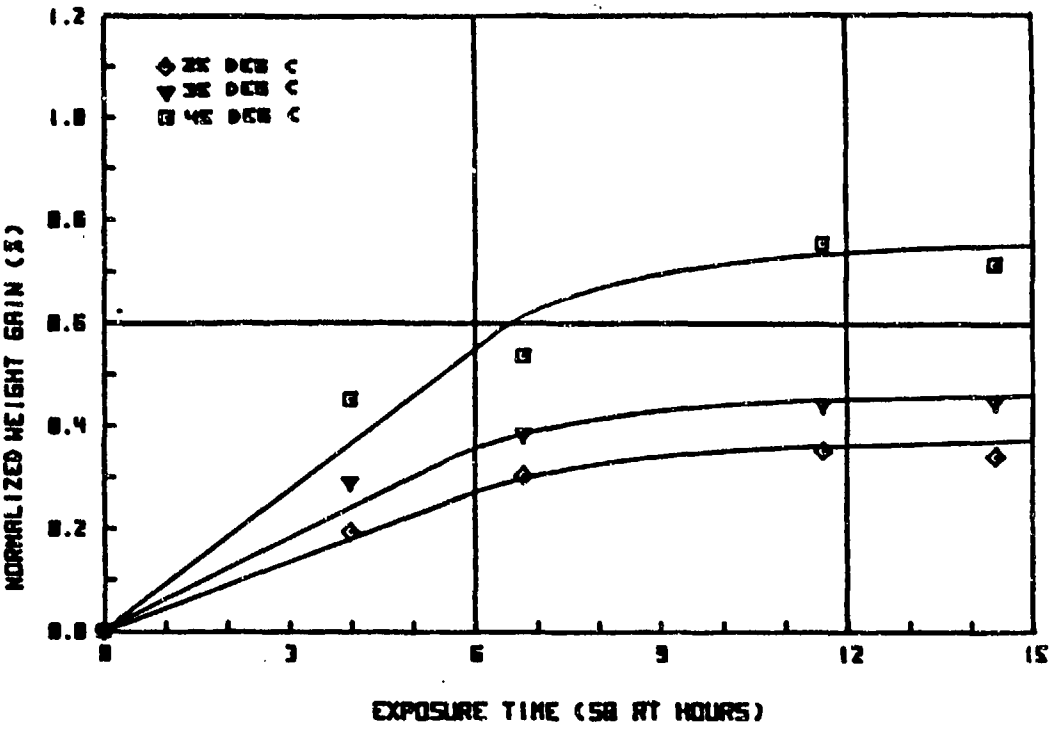

FIGURE A-97

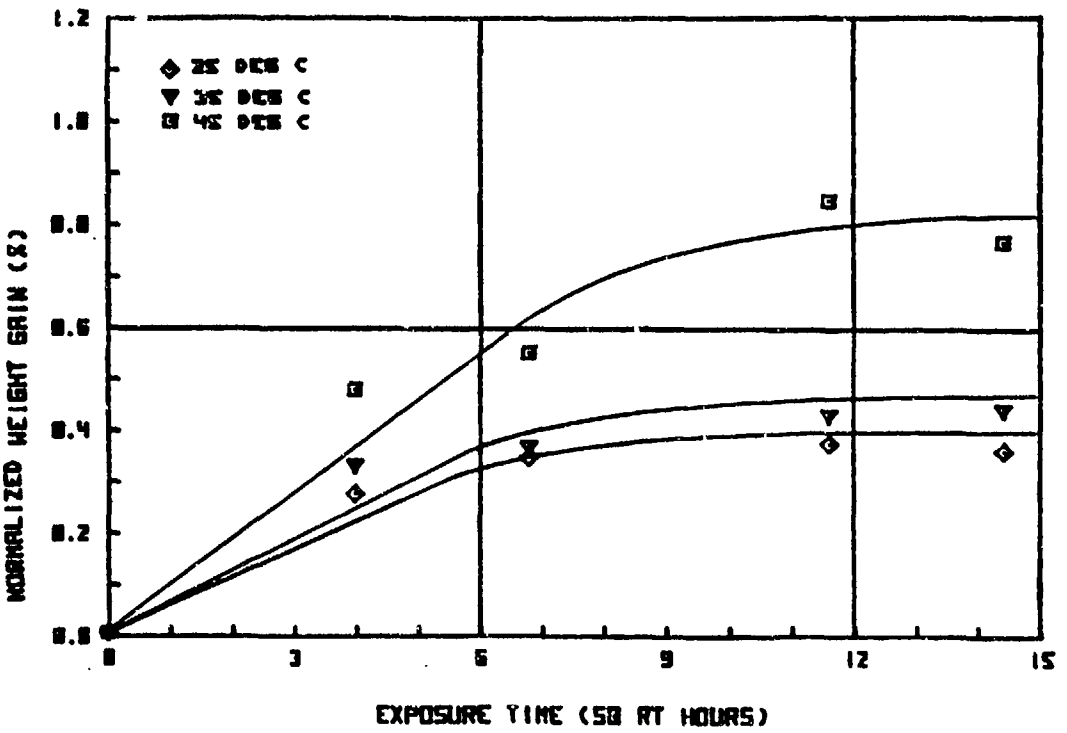

FIGURE A-98

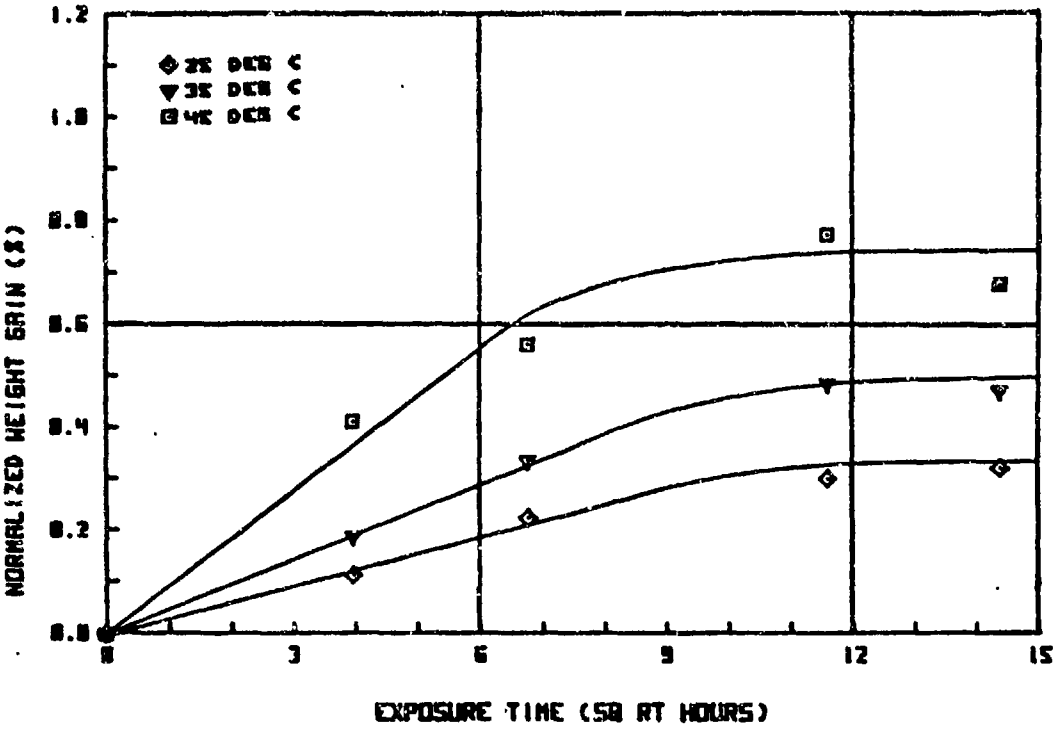

AL 4 75 % HUMIDITY

FIGURE A-99

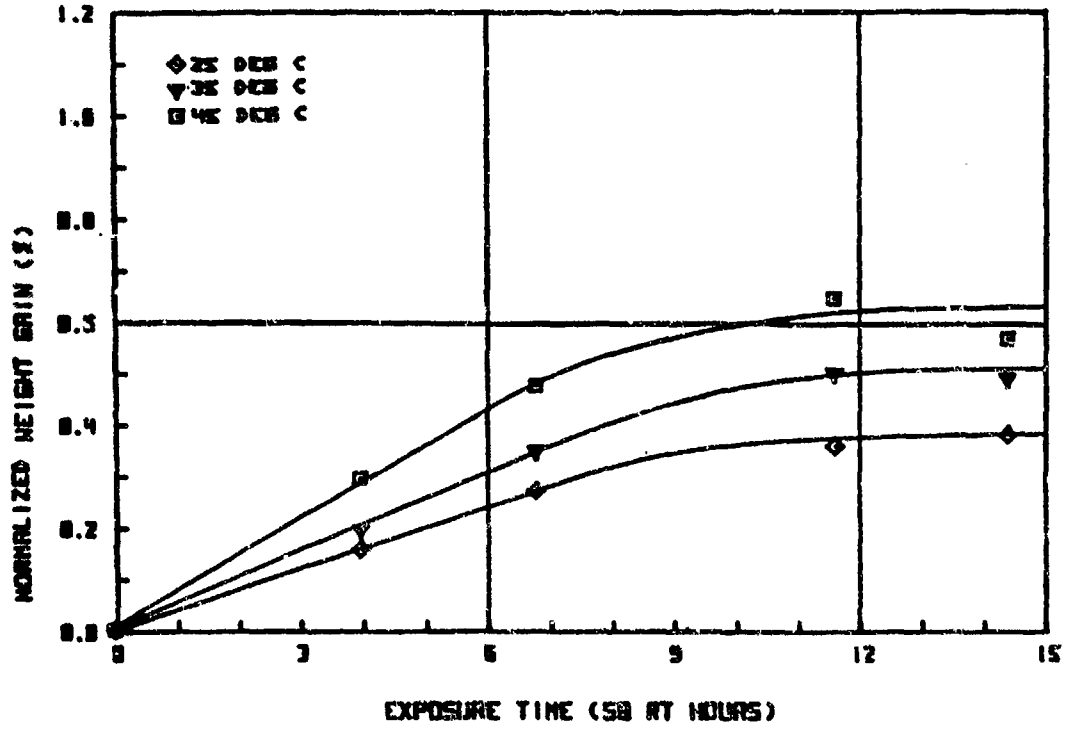

AL 5 75 % HUMIDITY

FIGURE A-100

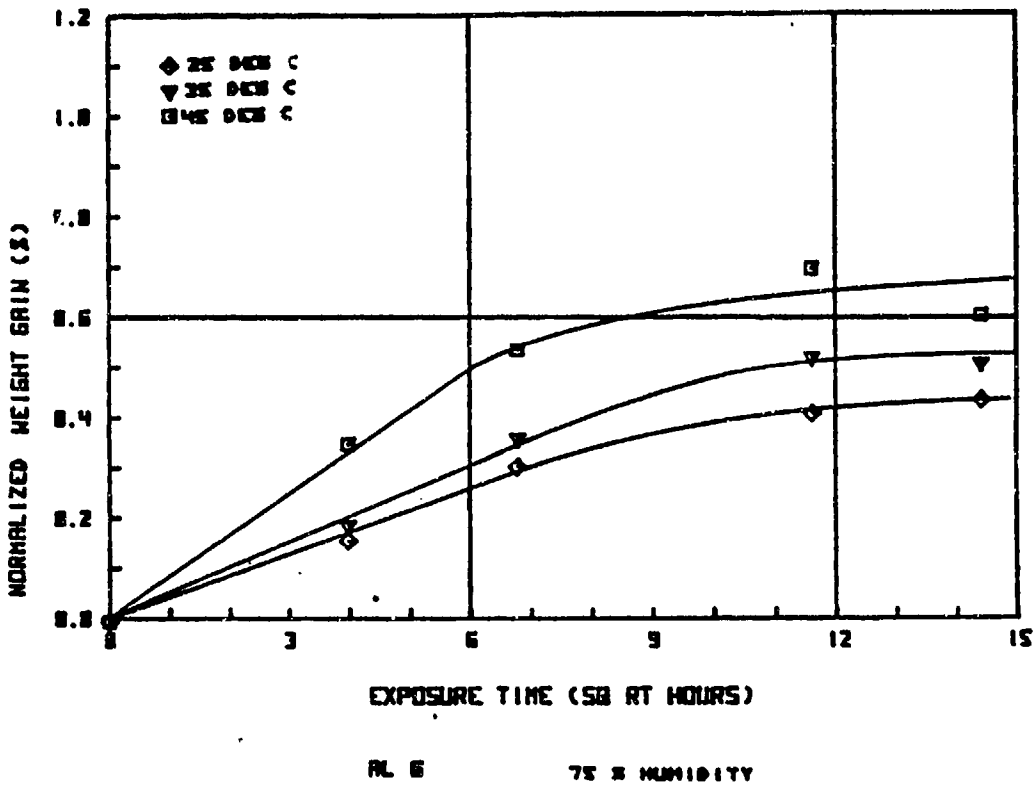
1.2
1.0
0.8
0.6
0.4
0.2
0.0
NORMALIZED WEIGHT GAIN (%)
0
3
6
9
12
15
EXPOSURE TIME (50 RT HOURS)
RL 6
75 % HUMIDITY

FIGURE A-101

APPENDIX B

OPERATING PROCEDURES

OPERATING PROCEDURES

The development of a set of general operating procedures which define the process, material, behavioral characteristics and their interrelationships was the initial goal of the Processing Science program. As the program developed, it became apparent that the initial goals of the program, i.e., the integration of specific material and process data into a generic operating procedure designed to produce a high quality, void-free laminate structure were overshadowed by the discovery of critical material and processing parameters. By exercising judicious control over the critical material and processing parameters, obtaining a quality part is virtually guaranteed.

The critical material and process parameters are:

(1) volatile content of the resin during cure

(2) dynamic viscosity (rheology) of the resin during the cure cycle

(3) initial laminate compaction early in the cure

(4) controlling resin pressure during cure

(5) lateral resin and volatile migration

The volatile content of the resin or prepreg is the ultimate indicator for potential void generation during cure. It has been shown that when the volatile content approaches zero, voids in laminates disappear (under identical material/processing conditions). Since the control of moisture to a near zero level is almost an impossible practical procedure, alternative methods to deal with volatiles in the resin were developed. Two approaches are feasible. The first is to layup the part and run it through a de gas cycle to remove all volatiles prior to cure. This is an approach Rockwell has taken. The alternative approach is to insure that the resin pressure is

high enough during cure so that the pressure dependent boiling point of the volatiles is never exceeded.

The rheology of the resin, and to a lesser extent its self-adhesion, determines the ease and effectiveness of consolidation of a prepreg layup. Compaction of the layup is a critical parameter to obtain a good laminate. The degree of advancement, and the temperature of the resin define the resulting rheology of a 177C (350F) curing epoxy resin system. If the resin viscosity is too high (temperature too low or the material advanced), flow does not occur easily and compaction does not occur. The knowledge of the state of advancement of the resin and the part geometry (area and complexity) will determine the time at a specific temperature necessary to consolidate the prepreg part. One of the major sources of voids in a laminate are mechanically entrapped air pockets which occur during layup operations. The consolidation step eliminates these pockets as shown by the experimental results of this program.

The consolidation step is intimately related to the basic resin rheology and is a critical step in composite fabrication. The Processing Science program has amply illustrated that voids or air pockets tend to move laterally between plies and exit at the laminate perimeter. The lateral migration is a function of applied pressure, resin viscosity and laminate area and geometry. Ply tack (as tested by a flatwise tension technique) has also been implicated as a factor in ease of lateral bubble removal.

Assuming that all of the mechanical bubbles/pockets have been removed during a consolidation step, any voids that appear during the cure necessarily arise due to volatilization of low boiling materials in the resin (usually

water). The voids occur because the resin pressure was not high enough to prevent boiling. Resin pressure can easily be controlled by back-pressure techniques discovered on this program. They consist of pressurizing the bag at a pressure high enough to prevent volatiles from boiling (bubble formation) yet below the applied autoclave pressure to yield a pressure delta or differential to adequately hold the layup to a tooling surface or perform a designed bleeding operation.

In summary, the two basic steps in fabricating a high quality laminate are:

- Layup consolidation
- Guaranteeing minimum resin pressure during cure

The other critical parameters listed are primarily concerned with obtaining these results.

It should be obvious that any process for curing a laminate should be specific for the structure in question. The structure's size (area and thickness), geometry, layup design (utilization of internal and external ply drop-offs), resin rheology as a function of temperature, resin curing kinetics, volatile content and moisture absorption characteristics must all be taken into consideration to developing a cure procedure and schedule.

The first step in developing a successful cure process is to characterize the resin that is being employed. Each batch of material should be accompanied by a neat resin sample for testing purposes or the certified results of the vendor if facilities are unavailable to accomplish the characterization. The characterization should minimally include a high pressure liquid chromatogram of the resin to establish advancement, purity, and so on. The chromatograms

also build up a quality control data base. Next, the rheology of the resin should be investigated at various heat-up rates and holds to develop enough data to enable the engineer to know or predict the resin rheology (dynamic viscosity) at any point in the cure. If the resin kinetics are known, they too can be correlated to the rheology of the resin so that at any advancement level the viscosity is known. The knowledge of the reaction kinetics coupled with the corresponding resin rheology is a powerful tool in designing cure schedules for specific part configurations.

Volatile measurement of prepreg on receipt of material should be standard procedure. Additionally, a piece of material should be exposed to layup conditions as a worst case example of moisture up-take during the layup operation and the volatiles measured at the completion of the layup. The actual volatile content of the layup will be somewhere between the as-received and the exposed prepreg volatile values, probably weighted more towards the as-received value (dependent on the procedure used to layup the laminate).

At this point, a good basis of understanding of the resin and prepreg has been acquired. Consolidation studies show the amount of pressure, the time, and the temperature a given laminate must see in order to effectively compact or consolidate the material. It is highly recommended that consolidation occur at the lower temperatures to inhibit advancement and allow longer consolidation times (if dictated by part size). Typical conventional cure schedules apply the pressure after the resin attains minimum viscosity, and if a large part is involved, consolidation is unlikely to occur to the quality desired. As the resin advances, the viscosity increases and this actually slows the consolidation process. A balance must therefore be maintained

between consolidation time and temperature and the resin reaction kinetics.

Before investing in a large amount of material, manpower and time to produce the prototype composite parts for testing and inspection purposes, it is recommended that a large laminate of minimum dimensions (61 cm X 61 cm, 2 ft X 2 ft) be fabricated with ply drop-offs or any configurations which replicates problem areas in the actual size part. The qualification laminate is employed to fine tune the curing process and screen material lots.

Internal ply drop-offs are employed extensively in the design and fabrication of graphite/epoxy composites. Ply drop-offs are regions of potential void accumulation and care must be taken to avoid void concentrations in these areas. The tack of the material determines to a large extent the ease of lateral interply removal of bubbles. Prepregs exhibiting high values in tack tension tests have been correlated with large amounts of voids in ply drop-off regions. If composites are to be fabricated which employ ply drop-offs, it is recommended that prepreg with low tack tension be used.

After consolidation is completed, several possible curing options exist. The first option is to proceed directly to the curing temperature and hold until the material is cured. The second option is to proceed to an intermediate temperature for a hold to allow moisture which is localized on the prepreg surfaces to diffuse into general distribution in the resin. This step is dependent on the quantity of water in the layup and the method employed for maintaining pressure in the resin during cure. If the moisture/resin pressure data indicate that a back pressure will prevent intraply void generation, then this step is unnecessary. If there is some question

whether adequate pressure can be introduced into the laminate, the hold may help prevent the generation of voids.

The internal pressure is typically introduced into the bag after the consolidation step. The actual point of application may vary somwhat dependent on whether a net resin system or a resin rich prepreg is employed. The magnitude of the internal pressure will depend on the volatile content of the laminate. The higher the internal pressure, the smaller the volume of any microvoids still entrained in the resin will become. Typical values of 0.586 to 0.689 MPa (85 to 100 psi) have been used as the autoclave pressure with 0.345 to 0.448 MPa (50 to 65 psi) internal bag pressure.

It is also a prudent policy to maintain the pressure on the part until cooling to a temperature well below the glass transition temperature (Tg) of the resin.

Another procedure which has been successful in the curing of graphite/epoxy composites was the bagless cure approach. The bagless cure essentially follows the consolidation procedure to eliminate mechanical voids. The bag was removed (or vented to the internal pressure of the autoclave) and the cure was allowed to proceed. Several precautions were followed, however. To improve the surface finish, a porous Armalon barrier was used next to the laminate surface followed by one or two plies of a balanced weave glass fabric. The glass prevented the top ply from misaligning on resin cure. This misalignment was observed when no balance ply was employed. The balance ply also served as a mild bleeder ply during consolidation. A variety of structures have been fabricated on various tooling surfaces and all have been quite successful, having minimum-void laminates.

CALCULATION OF C_∞ IN REGION OF DADS PARTICLES

From data provided by M. Lehmann on 26 April 1982.

Water concentration in resin with powdered DADS = 0.475%

Water concentration in resin with quenched DADS = 0.965%

Water concentration in regions of DADS = ω_∞

Basis: 1 gram wet resin plus DADS (20 w%)

$$H_2O \text{ Balance: } 0.8 \text{ gm resin} \frac{0.00475 \text{ gms } H_2O}{\text{gm resin}} + 0.2 \text{ gms DADS } (\omega_\infty) = 1 \text{ gm } (0.00965)$$

$$\omega_\infty = \frac{0.00965 - 0.8\ (0.00475)}{0.2} = 0.02925$$

$$\therefore \omega_\infty = 0.0292 \frac{\text{gm } H_2O}{\text{gm DADS } H_2O} = 2.92\%$$

Check of surface tension effect on bubble growth; i.e. can we say that $P_{resin} = P_{void}$?

For r = 10 microns = 10^{-3} cm, $\frac{2\gamma_{LV}}{r} = 1.45$ psi for $\gamma = 50 \frac{\text{dynes}}{\text{cm}^2}$

r = 100 microns = 10^{-2} cm, $\frac{2\gamma_{LL}}{r} = 0.145$ psi

Thus, for voids larger than 100μ $P_V \approx P_R$

Void Transport

Void mobilization will occur when the pressure gradient becomes sufficient to overcome the surface tension forces exerted by the resin when the bubble is forced through the fiber network.

$$\left| \frac{dp}{dx} \right| > \left| \frac{dp}{dx} \right|_c = \frac{4\,\gamma_{LV}\cos\theta}{d_c L_V} \tag{1}$$

$\frac{dp}{dx}$ = pressure gradient in the direction of flow

γ_{LV} = resin-void surface tension

θ = apparent contact angle

d_c = diameter of the narrowest constriction in the network perpendicular to flow

L_V = void length projected on the main flow direction

In effect, the resin must have sufficient velocity in the flow direction to drag the bubble through the narrowest constriction.

Let us now assume that the resin flow through the fiber network follows Darcy's Law

$$V_L = -\frac{K_e}{\mu_L}\left(\frac{dp}{dx}\right) \tag{2}$$

where V_L is the resin velocity

K_e = effective permeability

μ_L = resin viscosity

The critical conditions for void movement may also be expressed in terms of a critical capillary number

$$Ca \geq Ca_c = \frac{\mu_L V_L}{\gamma_{LV}} = -\frac{dp}{dx}\frac{K_e}{\mu_L}\frac{\mu_c}{\gamma_{LV}} = -\frac{dp}{dx}\frac{K_e}{\gamma_{LV}} \tag{3}$$

From equation (1),

$$Ca \geq Ca_c = \frac{4\,\gamma_{LV}\cos\theta}{d_c L_V}\frac{K_e}{\gamma_{LV}} = \frac{4\,K_e\cos\theta}{d_c L_V} \qquad (4)$$

The physical situation is shown schematically below

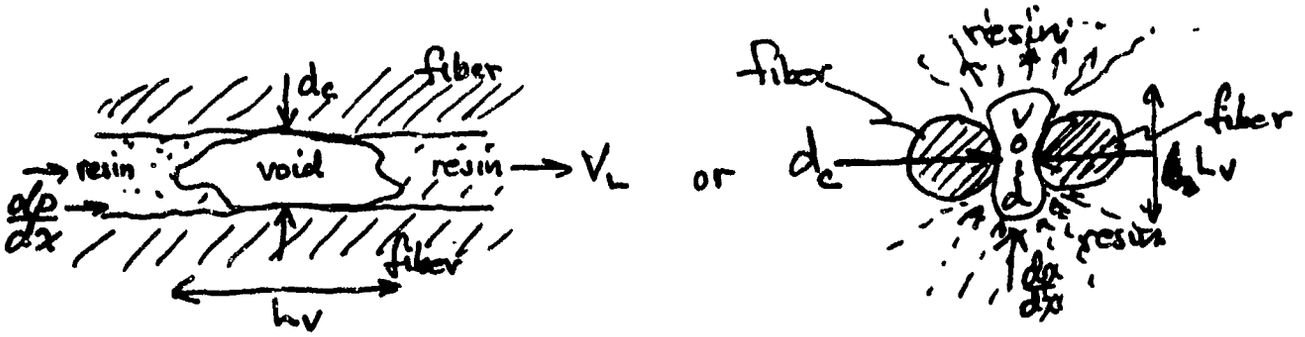

It is instructive to first estimate the critical pressure gradient in the laminate thickness direction

θ = 46° for epoxy on graphite in air

γ_{LV} = 50 dynes/cm^2

d_c = 1/2 fiber diameter

L_V = one fiber diameter = 1μ

$$\left(\frac{dp}{dx}\right)_c = \frac{4\,(50)\,(0.69)\ \text{dynes/cm}}{0.0001\ \text{cm}\ (0.0000.5\ \text{cm})} = 2.76 \times 10^{10}\ \frac{\text{dynes}}{\text{cm}^3}$$

$$= 2.76 \times 10^{10}\ \frac{\text{dynes}}{\text{cm}^2 - \text{cm}}\ \left(\frac{1.45 \times 10^{-5}\ \text{psi}}{\text{dynes/cm}^2}\right) = 4.0 \times 10^5\ \frac{\text{psi}}{\text{cm}} \cdot \frac{2.54\ \text{cm}}{\text{inch}}$$

$$= 1.02 \times 10^6\ \text{psi/inch}$$

Actual dp/dx:

$$\frac{dp}{dx} = \frac{10\ \text{psi}}{.064\ \text{inches}} = 156\ \text{psi/inch}$$

At this point the buoyant force due to gravity has been neglected. In order to move the void through the thickness with the available pressure gradient

$$156 \frac{\text{psi}}{\text{inch}} \cdot \frac{1 \text{ inch}}{2.54 \text{ cm}} \left(\frac{1 \text{ dynes cm}^2}{1.45 \times 10^{-5} \text{ psi}}\right) = 4.23 \times 10^6 \frac{\text{dynes/cm}^2}{\text{cm}}$$

$$d_c L_V = \frac{4\,(50)(0.69)}{4.23 \times 10^6} = 32.6 \times 10^{-6} \text{ cm}^2$$

If $L_V = 10^{-4}$ cm

$\therefore d_c = 32.6 \times 10^{-2}$ cm $= 0.326$ cm

Examine possibility of lateral flow

$$\frac{dp}{dx} = \frac{27 \text{ psi}}{8 \text{ in}} = 3.38 \frac{\text{psi}}{\text{in}} \left(\frac{1 \text{ in}}{2.54 \text{ cm}}\right) \left(\frac{1 \text{ dynes/cm}^2}{1.45 \times 10^{-5} \text{ psi}}\right) = 0.92 \times 10^5 \frac{\text{dynes/cm}^2}{\text{cm}}$$

$$d_c L_V = \frac{4\,(50)\,(0.69)}{0.92 \times 10^5} = 315 \times 10^{-5} = 3.15 \times 10^{-3} \text{ cm}^2$$

If $L_V = 1$ cm

$$d_c = 3.15 \times 10^{-3} \text{ cm} \left(\frac{1 \text{ inch}}{2.54 \text{ cm}}\right) = 1.24 \times 10^{-3} \text{ inch} = 1 \text{ mil}$$

$= 31.5\ \mu$

It is obvious from the above calculations that any voids growing between the plies will not be able to move vertically under the pressure gradients actually found in the laminates.

On the other hand, lateral motion is indeed possible. Pore diameters on the order of one mil or less would allow void transport. Thus, the degree of ply compaction is important with regard to void transport.

Further advances on the void transport part of the model will depend on an estimate of the permeability, K_e, of the fiber network in the laminate. This will have to come from experimentation.

PRESSURE GRADIENT VS PORE DIAMETER FOR VOID TRANSPORT

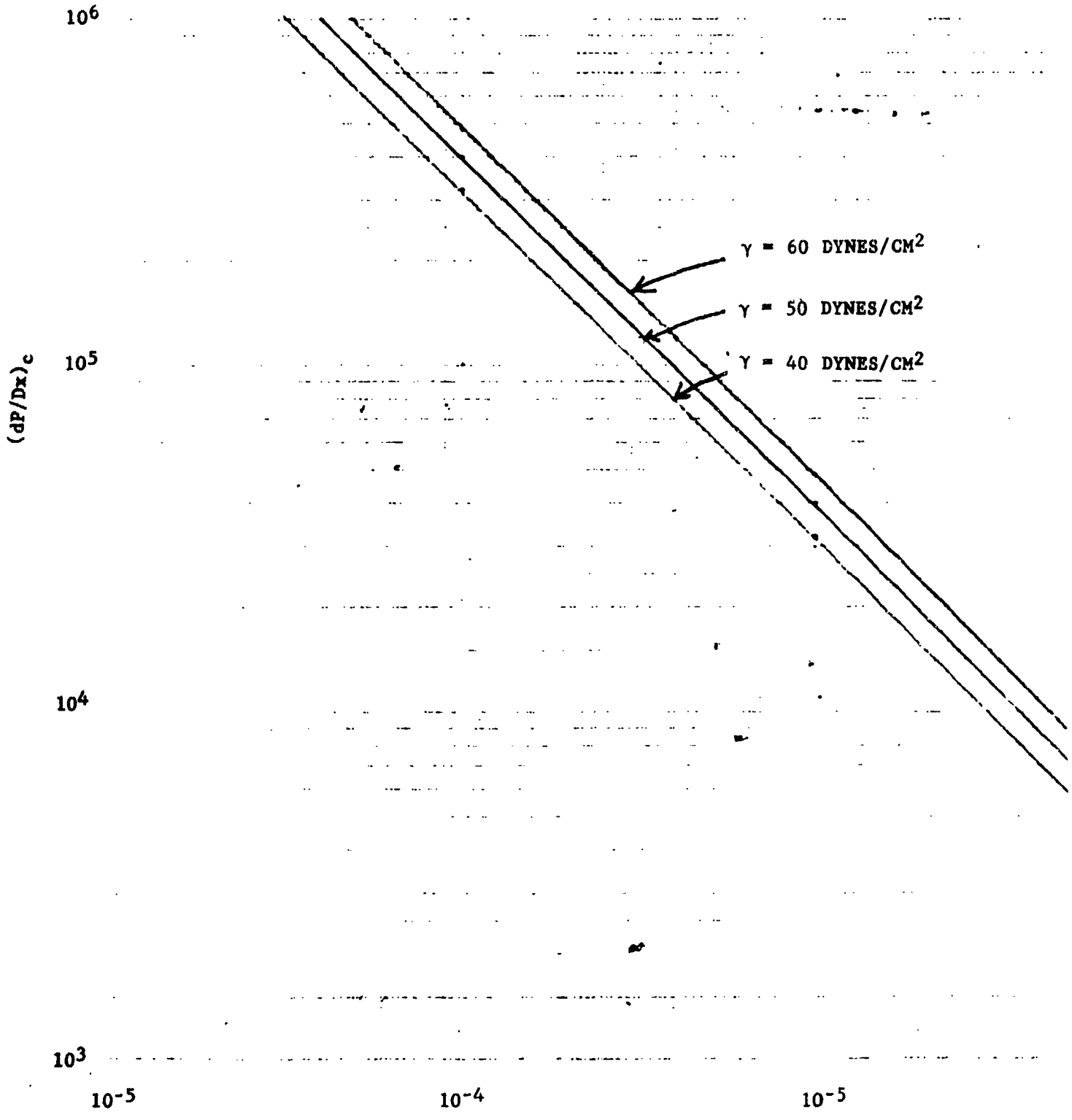

Description of General Dynamics Apple Program for Void Size

The program consists of an

a) Input Subroutine,

b) Calculational Subroutine,

c) Output Subroutine

Input Subroutine

User specifies

- resin density, DENR
- resin mass fraction in fresh prepreg, WR
- describes water solubility SO in prepreg by:

a) either a power law expression (Form 1)

$$SO = AP \left(\frac{RH}{100}\right)^{N}$$

b) or by an exponential

$$SO = AE \cdot e^{B \times RH/100} \quad \text{(Form 2)}$$

where

AP, N or AE & B are constants selected by the user based on his solubility data and RH is relative humidity in %.

- describes water diffusivity by

$$D1 = DO \exp^{-ED/T}$$

where ED and DO are user-selected constants

The user also specifies

- the duration and temperature and pressure settings of the cure cycle

- the relative humidity at which prepreg is prepared

- initial temperature

- resin gelation temperature

Default options are provided for all above quantities.

There are two options

1. void growth by water vapor nucleation and diffusion

2. void growth by water vapor diffusion into an existing air bubble

An initial bubble diameter must be specified by the user for option 2 and may be specified for option 1 (i.e. in a water only system bubble may either nucleate or be assumed to exist)

Calculational Subroutine

Option 1 (water only)

Same as in our report:

a) Calculates water concentration in saturated prepreg prepared at relative humidity HO

$$CINF = \frac{SO\ (HO)}{100} \times \frac{DENR}{WR}$$

b) Calculates saturation concentration at void-resin interface

$$CSAT = \frac{AP \cdot (100^{N}) \cdot (P/PV)^{N}}{100} \cdot \frac{DENR}{WR}$$

for Form 1 †

$$CSAT = \frac{AE \cdot EXP\ (B \cdot 100 \cdot P/PV)}{100} \times \frac{DENR}{WR}$$

for Form 2 †

where PV is the vapor pressure of water

$$PV = 4.962 \times 10^{5}\ e^{-4892/T}$$

T is temperature in Kelvin everywhere

If zero initial bubble diameter is assumed, the program calculates the time for bubble nucleation

$$\text{TBEGIN} = \frac{\text{TCRITICAL} - \text{T}}{\text{RT} \times 60}$$

where T is the temperature at that time

RT is the slope of the temperature time line (if non zero) RT (°K/min) and

TCRITICAL is the temperature at which CSAT < CINF.

Note that temperature increases in time as

$$\text{T} = \text{TINITIAL} + \text{RT} \times \text{time}$$

when the bubble is nucleated, Scriber's equation (our eq. 5) is used to calculate growth until bubble diameter, BD

$$(*) \qquad \frac{dBD}{dt} = \frac{8 \cdot (\text{BETA})^2 \times \text{D1}}{\text{BD}} \qquad \text{Scriven's equation}$$

BD - bubble diameter (cm) reaches 0.01 cm. At that point Subramanian-Weinberg equation is used.

$$\text{BETA} = \frac{\text{DINF} - \text{CSAT}}{\text{ROG}}$$

where ROG is gas density

$$\text{ROG} = \left[\frac{M_{H_2O} \cdot P}{RT} \right] \begin{array}{l} \leftarrow \text{molecular weight} \\ \leftarrow \text{pressure} \\ \leftarrow \text{gas constant} \\ \leftarrow \text{molecular weight} \end{array}$$

$$(**) \qquad \frac{dBD}{dt} = \frac{2 \cdot BETA}{\sqrt{\pi}} \quad \frac{D1}{t - t_1} + 16 \cdot \left[\frac{(BETA)^2}{3\pi} + \frac{BETA}{4}\right] \cdot \frac{D1}{1D} \qquad \text{Weinberg-Subramanian}$$

t - time, t_1 - time at which bubble diameter was 0.01 cm and a switch from Scriven's to Weinberg-Subramanian formula is made.

ID = initial bubble diameter for growth by this equation

When initial bubble diameter is specified as nonzero (even for water-only mixture), the routine starts with Scriven's eq. (*) until 0.01 cm is reached, then switches to (**) if the bubble grows or shows bubble collapse. If initial diameter > 0.01 cm (**) is immediately used for consistency of results.

Option 2

For air-water mixture an initial bubble diameter BOD must be assigned and it is assumed to consist of air only.

Gas density is now given by

$$ROG = \frac{18.P}{82.1 \cdot T} + \left(\frac{BOD}{BD}\right)^3 \frac{P_o \cdot 28.8}{82.1 \cdot T_o}$$

Partial pressure of water is:

$$PP = \left[1 - \frac{P_o \cdot T}{PT_o} \left(\frac{BOD}{BD}\right)^3\right] P$$

P - pressure, T - temperature

P_o, T_o = Initial values of P and T

$$CSAT = AP \cdot 100^{N-1} \left(\frac{PP}{PV}\right)^N \cdot \frac{DENR}{WR}$$

or

$$CSAT = \frac{AE}{100} \cdot e^{100 \cdot B \cdot \frac{PP}{PV}}$$

Bubble growth or shrinkage is now calculated by eq. (**) if initial diameter BOD > 0.01 cm. If BOD < 0.01 cm, Scriven's equation is used.

The effect of the change of pressure for both pure water and water/air mixture is accounted for by the ideal gas law i.e.

$$\frac{BD_{new}}{BD_{old}} = \left(\frac{P_{old}}{P_{new}}\right)^{1/3}$$

unless the temperature has reached resin gelatin temperature in which case there is no effect of pressure on bubble size.

Output Subroutine

time, temperature, β, and bubble diameter can be printed

a) at equal time increments selected by the user

b) at times when either heating rate RT or pressure are changed.

APPENDIX C

FINAL VOIDS - PROGRAM LISTING FOR APPLE II COMPUTER

FINAL VOIDS - PROGRAM LISTING FOR APPLE II COMPUTER

```
1  REM    FILE NAME IS FINAL VOIDS: DATE OF LAST CHANGE IS 10/14/83.
2  REM   VOID GROWTH MODEL PROGRAM
3  REM   PROCESSING SCIENCE OF EPOXY MATRIX COMPOSITES PROGRAM, CONTRACT
     #F33615-80-C-5021
4  REM   PROGRAM WRITTEN BY WASHINGTON UNIVERSITY (M. P. DUDUKOVIC AND J
     . L. KARDOS)
5  REM   PROGRAM FORMAT AND INPUT MODIFICATIONS BY GENERAL DYNAMICS/FT.
     WORTH (J. T. SCHUELER AND E. L. MCKAGUE, JR.)
6  REM   AIR FORCE PROGRAM MONITOR, DR. C. E. BROWNING, AFWAL/MLBC, PHON
     E (513) 255-2201.
7  REM    FOR INFORMATION ON PROGRAM, PHONE (1) DR. JOHN KARDOS, (314) 8
     89-6062 OR  (2) LEE MCKAGUE, (817) 777-2126.
8  REM
9  PRINT "DO YOU WANT A PROGRAM LISTING?"
10  INPUT "ENTER Y OR N/";L$
11  IF L$ = "N" THEN 18
12 :
13 I$ =  CHR$ (9)
14  PR# 1: PRINT I$"80N"
15  LIST
16  PR# 0
18  REM       GET INPUT FROM INPUT SUB.
20  GOTO 3010
25  REM   INITIALIZE
26 HFE = 5.
27 TIME = 0.
28 MPD = 1.
30 RH = H0: REM  RELATIVE HUMIDITY AT PREPREG PREPARATION
35 BD = DSTART: REM  CURRENT BUBBLE DIAMETER
40 PRES = P(1): REM  CURRENT PRESSURE IN ATMOSPHERES
45 TEMP = T7 + 273.15: REM  CURRENT TEMPERATURE IN DEGREES K
46 XITEMP = TEMP
49  IF ((N2TI = NT) AND (N1PI = NP)) THEN  GOTO 275
50 TBEGIN = 0: REM  START TIME OF CURRENT CYCLE STEP
55 N2TI = 1: REM  CURRENT INDEX OF TT/RT ARRAYS
60 N1PI = 1: REM  CURRENT INDEX OF TP/P  ARRAYS
62  GOSUB 335
65  GOSUB 300:CINF = CONC: REM  TOTAL WATER CONC. IN BULK RESIN
70 TCRITICAL = 4892. /  LOG ((4.962E3 * H0) / PRES): REM  CRITICAL TEMP.
     FOR NUCLEATION
75  IF (TCRITICAL > TEMP) THEN  GOTO 90
80 TBEGIN = 0: GOTO 150: REM  PROCESS STARTED AT OR ABOVE TCRITICAL
90  GOSUB 335: REM  TEMC NOT REACHED IN STEP,NEXT STEP
91  REM :TLIMIT=TEMP+(TSTP-TBEGIN)*RT(N2TI):REM NEXT STEP MAX. TEMP.
92 TLIMIT = (TEMP(N2TI + 1) - 32) * 5 / 9 + 273.15
94  IF ((N1PI >  = NP) AND (N2TI >  = NT) AND (TCRITICAL > TLIMIT)) THEN
     GOSUB 1066
95  IF ((N1PI >  = NP) AND (N2TI >  = NT) AND (TCRITICAL > TLIMIT)) THEN
     GOTO 275
100  IF (TLIMIT < TCRITICAL) THEN  GOTO 120: REM    PASS TEST IF TCRITIC
    AL NOT IN STEP
105 TBEGIN = (TCRITICAL - TEMP) / RT(N2TI) + TBEGIN: REM  TIME FOR NUCLE
    ATION IN STEP
110 TEMP = TCRITICAL
112 XITEMP = TEMP
113 TOUT = TBEGIN
115  GOTO 150: REM   SCRIVEN APPROX. OF BUBBLE GROWTH
120  GOSUB 410: REM   BUMP TO NEXT  STEP,SET PRES/TEMP
125  GOTO 70: REM  PRES CHANGE MAY CHANGE TEMC
```

```
130  REM
135  REM  INTEGRATE SCRIVEN EQUATION UNTIL WE REACH END OF CURRENT STEP
140  REM
150 TIME = TBEGIN: GOSUB 695: REM
151  GOSUB 335: REM  SET TSTP
155  IF (IPRT = 0) THEN TOUT = (1 +  INT (TBEGIN / TRI)) * TRI: REM    F
     IND OUTPUT TIME PRINT OPTION 0
160  IF (BD > 0.) THEN  GOTO 212: REM  DON'T NEED SCRIVEN APPROX.
164 KAR =  INT ((TSTP - TBEGIN) / MPD)
165 INC = (TSTP - TBEGIN) / KAR
170 D2 = BD * BD
180  FOR ICNT = 1 TO KAR
182  INVERSE : VTAB 16: HTAB 15: PRINT "  WORKING  ": HTAB 15: PRINT "PL
     EASE WAIT": NORMAL
185  GOSUB 545: REM  SCRIVEN APPROX. INTEGRATED WITH 4 TH ORDER RUNGE-KU
     TTA-GILL
190  IF (IPRT = 1) THEN  GOTO 205
195  IF  NOT ((TOUT <  = TIME) AND (TOUT > (TIME - INC))) THEN  GOTO 205

200  GOSUB 690: REM  PRINT RESULTS
205  IF (BD > .1) THEN  GOTO 212
210  NEXT ICNT
211  GOTO 215
212 ID = BD:TD = TIME
213 TEMP = TEMP + (TIME - TBEGIN) * RT(N2TI):TBEGIN = TIME
214  IF (TIME < TSTP) THEN  GOTO 218
215 ID = BD: REM .SUBRAMANIAN AND WEINBERG PARAMETER
216 TD = TIME
217  GOSUB 625: REM  GET NEXT CYCLE STEP
218  IF (IPRT = 1) THEN  GOSUB 695: REM  PRINT OUTPUT FOR OPTION 1
225  IF (IQUIT = 1) THEN  GOTO 275: REM   INTEGRATED TO TMAX WE'RE FINIS
     HED
230 TIME = TBEGIN: REM   INITIALIZE TIME FOR INTEGRATION STEP
232 KAR =  INT ((TSTP - TBEGIN) / HFE)
233 KAR = 25: REM   OVERIDES 232 AND FIXES NUMBER OF INTEGRATION STEPS (
     CANCELED IN 1.2 7/15/83 HFE)
235 INC = (TSTP - TBEGIN) / KAR
236  IF (IPRT = 0) THEN NITER = (TOUT - TIME) / INC
237  IF (IPRT = 1) THEN NITER = KAR
238 IKOUNT = 0.
240  FOR ICNT = 1 TO KAR
241  INVERSE : VTAB 16: HTAB 15: PRINT "  WORKING  ": HTAB 15: PRINT "PL
     EASE WAIT": PRINT : HTAB 30: PRINT "NEXT  ": HTAB 30: PRINT "OUTPUT
     ": HTAB 30: PRINT "VVVVVV": PRINT
242 IKOUNT = IKOUNT + 1.: IF ( ABS (NITER) <  = 1.E - 3) THEN NITER = 1.
     E - 3
243 IV =  INT ((IKOUNT / NITER) * 34.): IF (IV >  = 34) THEN IV = 35
244  FOR IW = 1 TO IV: VTAB 22: HTAB IW: PRINT " ": VTAB 23: HTAB IW: PRINT
     " ": NEXT IW
245  NORMAL
246  GOSUB 890: REM  SUBRAMANIAN AND WEINBERG 4 TH ORDER RUNGE-KUTTA-GIL
     L
247  IF (BD > 0.) THEN  GOTO 251
248  GOSUB 1016: REM    BUBBLE HAS  COLLAPSED WE MUST FIND NUCLEATION TI
     ME AGAIN
249  IF (TCRITICAL > TLIMIT) THEN  PR# 1: PRINT : PRINT "NUCLEATION CANN
     OT OCCUR ANYMORE": PRINT "DURING THIS CYCLE.": PR# 0: GOTO 275
250  GOTO 150
251  IF (IPRT = 1) THEN  GOTO 265
255  IF  NOT ( ABS (TOUT - TIME) < INC) THEN  GOTO 265
260  GOSUB 695: REM  OUTPUT RESULTS FOR OPTION 0
261 IKOUNT = 0.
262 NITER = (TOUT - TIME) / INC
263 NITER =  ABS (NITER)
264  IF (NITER <  = 1.E - 3) THEN NITER = 1.E - 3
265  NEXT ICNT
```

```
270  GOTO 217
275  FOR ICNT = 1 TO 2000: NEXT ICNT
278  INVERSE
277  PRINT "                                                    "
278  PRINT "                THE  END                            "
279  PRINT "                                                    "
280  NORMAL
281  PRINT  CHR$ (20)
282  END
285  REM
290  REM  SUBROUTINE WATER CONC. IN RESIN
295  REM
300  IF (SOLO = 1) THEN S0 = AP * ((RH / 100.) ^ N)
305  IF (SOLO = 2) THEN S0 = AE *  EXP (B * (RH / 100.)): REM  GET S0 FO
     R EXPONENTIAL
306  IF (OPTN = 2) THEN JUNK = ((DSTART / BD) ^ 3) * P(1) * X1TEMP / (PR
     ES * (T7 + 273.15))
307  IF ((OPTN = 2) AND (JUNK >  = 1)) THEN CONC = CINF
310 CONC = (S0 * DENR) / (100. * WR)
315  RETURN
320  REM
325  REM  SUBROUTINE CYCLE SEQUENCE TIMER
326  REM    - DECIDES IF HEATING RATE OR PRESSURE CHANGE IS NEXT
330  REM
335 N4TN = 0: REM    FLAG SET TO 1 IF HEATING RATE CHANGE IS NEXT
340 N3PN = 0: REM    FLAG SET TO 1 IF PRESSURE CHANGE IS NEXT
345 I1 = N2TI + 1
350 T1 = TMAX: IF (I1 <  = NT) THEN T1 = TT(I1): REM  TIME FOR NEXT HEAT
     RATE CHANGE
355 I2 = N1PI + 1
360 T2 = TMAX: IF (I2 <  = NP) THEN T2 = TP(I2): REM  TIME FOR NEXT PRES
     SURE CHANGE
361  IF  NOT ((T1 = T2) AND (T1 = TMAX)) THEN  GOTO 365
362 N1PI = NP:N2TI = NT:TSTP = TMAX: RETURN
365  IF (T1 = T2) THEN  GOTO 385: REM   BOTH CHANGE AT SAME TIME
370  IF (T1 > T2) THEN  GOTO 380
375 TSTP = T1:N4TN = 1: RETURN : REM  HEAT RATE CHANGES NEXT
380 TSTP = T2:N3PN = 1: RETURN : REM  PRESSURE CHANGES NEXT
385 TSTP = T1:N4TN = 1:N3PN = 1: RETURN : REM  BOTH CHANGE NEXT
390  REM
395  REM  SUBROUTINE CYCLE STEP PARAMETER SETTER
400  REM    - SETS PRESSURE AND TEMPERATURE FOR NEXT STEP IN CURING CYCL
     E
405  REM
410 N1PI = N1PI + N3PN: REM    INCREMENT N1PI IF IT CHANGES (N3PN SET TO
     1 BUMPS IT)
415 PRES = P(N1PI): REM   SET NEW PRESURE IF N1PI IS BUMPED
420 TEMP = TEMP + (TSTP - TBEGIN) * RT(N2TI): REM     BRING TEMP UP TO D
     ATE
425 N2TI = N2TI + N4TN: REM    INCREMENT  N2TI IF IT CHANGES (N4TN SET T
     O 1 BUMPS IT)
430 TBEGIN = TSTP: REM      SET NEW START TIME
431 CP = N3PN: REM  REMEMBER IF PRESSURE WAS CHANGED HERE
435  GOSUB 335: REM  CALL SUBROUTINE CYCLE SEQUENCE TIMER TO RESET NTN A
     ND NPN FOR NEXT STEP
440  RETURN
445  REM
450  REM  SUBROUTINE GET CSAT, ROG, AND BETA
451  REM     - NOTE X1TEMP IS TEMP AT GIVEN TIME
455  REM
460 PV = 4.942E5 *  EXP ( - 4892. / X1TEMP): REM   VAPOR PRESSURE OF WAT
     ER AT TEMPERATURE
461 PP = PRES
462  IF (OPTN = 2) THEN PP = (1. - ((P(1) * X1TEMP) / (PRES * (T7 + 273.
     15)) * ((DSTART / BD) ^ 3))) * PRES
465 RH = 100. * (PP / PV): REM  DEFINE PSEUDO RELATIVE HUMIDITY OF RESIN
```

```
470  GOSUB 300:CS = CONC: REM  GET CSAT FROM SUBROUITNE WATER CONC. IN R
     ESIN
475 ROG = (18. * PRES) / (82.1 * X1TEMP): REM    RHO (GREEK) SUB G  I.E.
      GAS DENSITY
477  IF (OPTN = 2) THEN ROG = ROG + (((DSTART / BD) ^ 3) * P(1) * 28.8 /
     (82.1 * (T7 + 273.15)))
480 BETA = (CINF - CS) / ROG: REM   DEFINE THE BETA PARAMETER BY CAUTIOU
     S ASSUMPTIONS
485  RETURN
490  REM
495  REM  SUBROUTINE SCRIVEN EQUATION EVALUATION
500  REM
505 X1TEMP = TEMP + (X2TIME - TBEGIN) * RT(N2TI): REM  FIND OPERATING TE
     MPERATURE
510 DI = D0 *  EXP ( - ED / X1TEMP) / 60.: REM  DIFFUSIVITY (CM^2/MIN)
515  GOSUB 460: REM  GET BETA
520 FUNC = 16. * BETA * BETA * DI: REM  TIME DERIVATIVE OF BD SQUARED
525  RETURN
530  REM
535  REM  SUBROUTINE SCRIVEN EQUATION FOURTH ORDER RUNGE-KUTTA-GILL INTE
     GRATION
540  REM
545 X2TIME = TIME: REM  SET TEMPORARY TIME
550  GOSUB 505: REM  EVALUATE RHS OF TIME DERIVATIVE OF SCRIVEN APPROX.
555 K1 = INC * FUNC
560 X2TIME = TIME + INC / 2.
565  GOSUB 505
570 K2 = INC * FUNC
572 K3 = K2
575 X2TIME = TIME + INC
578  GOSUB 505
580 K4 = INC * FUNC
585 D2 = D2 + (K1 + 2. * K2 + 2. * K3 + K4) / 6.: REM  INTEGRATION STEP

590 TIME = TIME + INC
595 BD =  SQR (D2)
600  RETURN
605  REM
610  REM  SUBROUTINE NEXT CYCLE STEP
615  REM    - RESETS PRESSURE / TEMPERATURE AND CHANGES BUBBLE DIAMETER
     IF NECESSARY
620  REM
625 IQUIT = 0: REM .FLAG SET TO 1 IF TIME REACHES TMAX
635  IF ((N3PN = 1) AND (N1PI + 1 <  = NP)) THEN TIME = TP(N1PI + 1)
640  IF ((N4TN = 1) AND (N2TI + 1 <  = NT)) THEN TIME = TT(N2TI + 1)
645  GOSUB 410: REM  SUBROUTINE CYCLE PARAMETER SETTER
650  IF (CP = 0) THEN  GOTO 665
651  IF (TEMP >  = GEL) THEN  HOME : PRINT CD$;"PR#";IZ: PRINT : PRINT "
     TEMPERATURE ABOVE ";GEL;" NO FURTHER PRESSURE EFFECT ON BUBBLE SIZE
     "
652  PRINT CD$;"PR#0"
653  FOR ICNT = 1 TO 5000: NEXT ICNT
655  IF (TEMP >  = GEL) THEN  GOTO 665: REM     HERE WE ASSUME RESIN HAS
      GELLED
657  IF ( ABS ((P(N1PI - 1) / P(N1PI)) - 1) <  = 1.E - 3) THEN  GOTO 665

660 BD = BD * (P(N1PI - 1) / P(N1PI)) ^ (1. / 3.): REM  BUBBLE DIAMETER
     CHANGE VIA PRES. CHANGE
661 ID = BD: REM  RESET SUBRAMANIAN AND WEINBERG INITIAL BUBBLE DIAMETER

662 TD = TIME
665  IF ( ABS (TIME - TMAX) <  = 1.E - 3) THEN IQUIT = 1: REM        WE
     ARE FINISHED IF THIS HAPPENS
666  IF ((IPRT = 0) AND (IQUIT = 1)) THEN TOUT = TMAX
667  IF ((IPRT = 0) AND (IQUIT = 1)) THEN  GOSUB 695
```

```
675  RETURN
680  REM
685  REM  SUBROUTINE PRINT RESULTS
690  REM
695  NORMAL
696 CD$ =  CHR$ (4): REM  CHR$(4) IS ^D (CNTRL-D)
698  HOME
700 B7D = BD
701 X2TIME = TIME
704  PRINT CD$;"PR#";IZ: PRINT  CHR$ (20): REM   ^D PR# (PORT NMBER) THE
     N ^T TO TOGGLE ECHO/NO ECHO TO ECHO
705  IF (IPRT = 1) THEN  GOTO 710
706  IF ((IPRT = 0) AND (TIME = TOUT)) THEN  GOTO 710
707 X2TIME = TOUT
708 B7D = B7D - (TIME - TOUT) * FUNC: IF B7D < 0 THEN B7D = 0
709 X1TEMP = X1TEMP - (TIME - TOUT) * RT(N2TI)
710  GOSUB 460
715  PRINT
720  PRINT "TIME             = "; LEFT$ ( STR$ (X2TIME * 1.0000001),5);"
     MINUTES"
721  PRINT
724 JUNK = PRES * 14.7
725  PRINT "PRESSURE         = "; LEFT$ ( STR$ (JUNK * 1.0000001),5);" PS
     I"
726  PRINT
729 JUNK = (X1TEMP - 273.15) * 1.8 + 32
730  PRINT "TEMPERATURE      = "; LEFT$ ( STR$ (JUNK * 1.0000001),5);" DE
     G FAHRENHEIT"
731  PRINT
732 B1ETA = BETA
734  IF ( ABS (B1ETA) <  = 1.E - 2) THEN  PRINT "BETA              = ";B1E
     TA
735  IF ( ABS (B1ETA) > 1.E - 2) THEN  PRINT "BETA             = "; LEFT$
     ( STR$ (B1ETA * 1.0000001),8)
738  PRINT
740 C$ =  STR$ (B7D / 2.54):A$ =  RIGHT$ (C$,4):B$ =  LEFT$ (A$,1): IF B
     $ = "E" THEN  GOSUB 0500: GOTO 745
     [illegible] / 2.54 = 0) THEN  PRINT "BUBBLE DIAMETER = 0      INCHES": GOTO
     [illegible]
742  IF (B7D / 2.54 > 1.E - 2) THEN  PRINT "BUBBLE DIAMETER = "; LEFT$ (
     [illegible]
745  PRINT "BUBBLE DIAMETER = "C$" INCHES"
750  PRINT : PRINT
755  PRINT CD$;"PR#0": REM  PRINT ^D PR#0 TOO DEENERGIIZE THE PRINTER IN
     TERFACE
760  IF (IPRT = 0) THEN TOUT = TOUT + TRI
765  RETURN
770  REM
775  REM  SUBROUTINE SUBRAMANIAN AND WEINBERG EQUATION EVALUATION
780  REM
785 PI = 3.141592654
790  GOSUB 505: REM  GO TO SCRIVEN FUNCTION TO GET DI
795  GOSUB 460: REM  GET CSAT , ROG , AND BETA
800 P2 = 1.7724538
810 FUNC = 16. * ((BETA / (3. * PI)) + 0.25) * BETA * DI / ID
815  IF ((X2TIME - TD) <  = 1.E - 3) THEN  GOTO 870
820 FINK = 2. * BETA *  SQR (DI /  ABS (X2TIME - TD)) / P2
821  IF ((BETA < 0.) AND ( ABS (FUNC) > .8 *  ABS (FINK))) THEN FUNC = 0
822 FUNC = FUNC + FINK
870  RETURN
875  REM
880  REM  SUBROUTINE SUBRAMANIAN AND WEINBERG FOURTH ORDER RUNGE-KUTTA-G
     ILL INTEGRATION
885  REM
890 X2TIME = TIME
```

```
895  GOSUB 785: REM  EVALUATE TIME DIFFERENTIATED S AND W APPROXIMATION
900 K1 = INC * FUNC
905 X2TIME = TIME + INC / 2.
910  GOSUB 785
915 K2 = INC * FUNC
917 K3 = K2
920 X2TIME = TIME + INC
925  GOSUB 785
930 K4 = INC * FUNC
935 BD = BD + (K1 + 2. * K2 + 2. * K3 + K4) / 6.
936  IF (BD < 0.) THEN BD = 0.
940 TIME = TIME + INC
945  RETURN
1000  REM
1010  REM  SUBROUTINE BUBBLE COLLAPSE
1015  REM
1016  PRINT  CHR$ (4);"PR#";IZ: HOME
1017  INVERSE : VTAB 7: PRINT "                                        ": PRINT
     "          BUBBLE COLLAPSES          ": PRINT "
                    ": NORMAL
1018 BD = DSTART * ((P(1) * X1TEMP / (PRES * (T7 + 273.15))) ^ (1. / 3.)
     )
1019 ID = BD
1020  IF (OPTN = 2) THEN  PRINT "BUBBLE DIAMETER IS REDUCED TO"
1021  IF (OPTN = 2) THEN C$ =  STR$ (BD / 2.54):A$ =  RIGHT$ (C$,4):B$ =
     LEFT$ (A$,1): IF B$ = "E" THEN  GOSUB 8500: PRINT C$" INCHES"
1023 TEMP = TEMP + (TIME - TBEGIN) * RT(N2TI)
1024 TBEGIN = TIME
1025  PRINT "TIME = "; LEFT$ ( STR$ (TIME),5);" MINUTES"
1026  PRINT  CHR$ (4);"PR#0"
1027  REM :PR# 1: PRINT TCRITICAL,TBEGIN,N2TI,RT(N2TI),TT(N2TI): PR# 0
1030 TCRITICAL = 4892. /  LOG ((4.962E3 * H0) / PRES): REM    CRITICAL T
     EMP. FOR NUCLEATION
1040  IF (TCRITICAL > TEMP) THEN  GOTO 1060
1050  RETURN
1060  GOSUB 335: REM    TEMC NOT REACHED IN STEP,NEXT STEP
1065  IF ((N2TI < NT) OR (N1PI < NP)) THEN  GOTO 1070
1066  PRINT CD$;"PR#";IZ: PRINT  CHR$ (20)
1067  PRINT : PRINT "NUCLEATION CAN NOT OCCUR ANYMORE ": PRINT "DURING T
     HIS CURING CYCLE"
1068  PRINT  CHR$ (4);"PR#0"
1069  RETURN
1070  REM :TLIMIT=TEMP+(TSTP-TBEGIN)*RT(N2TI):REM NEXT STEP MAX. TEMP.
1075 TLIMIT = (TEMP(N2TI + 1) - 32) * 5 / 9 + 273.15
1080  IF (TLIMIT < TCRITICAL) THEN  GOTO 1140: REM     PASS TEST IF TCRI
     TICAL NOT IN STEP
1090 TBEGIN = (TCRITICAL - TEMP) / RT(N2TI) + TT(N2TI): PRINT TCRITICAL,
     TBEGIN,N2TI,RT(N2TI),TT(N2TI): REM   TIME FOR NUCLEATION IN STEP
1091  IF TBEGIN < TIME THEN TBEGIN = TIME
1100 TEMP = TCRITICAL
1110 X1TEMP = TEMP
1120 TOUT = TBEGIN
1130  RETURN
1140  GOSUB 410: REM    BUMP TO NEXT  STEP,SET PRES/TEMP
1150  GOTO 1030
1160  REM  END OF SUBROUTINE
1170  REM  NO OUT HERE
2000  REM
2010  CLEAR : HOME
2011  VTAB 6: PRINT "PLEASE ENTER THE SLOT NUMBER"
2012  PRINT "FOR THE PRINTER.  ENTER 0 FOR NO"
2013  PRINT "PRINTER, SLOT NUMBER (1 TO 6) FOR": PRINT "PRINTER, OR <RET
     URN> FOR THE DEFAULT"
2014  INPUT "OF 1 : ";IZ$:IZ =  INT ( VAL (IZ$))
2015  IF ( LEN (IZ$) = 0) THEN IZ = 1
2016  IF (IZ < 0) OR (IZ > 6) THEN  GOTO 2011
```

```
2010  HOME
2020  REM  INPUT SUBROUTINE FOR VOIDS
2030  REM
2040  REM  FIRST DISPLAY INTRODUCTION
2050  REM
2060  PRINT "THIS PROGRAM CALCULATES THE EFFECT OF"
2070  PRINT "CURING CYCLE ON VOID FORMATION AND"
2080  PRINT "ULTIMATE VOID SIZE.  VOID (BUBBLE)"
2090  PRINT "GROWTH IS BASED ON THE ASSUMPTIONS:     "
2100  PRINT
2110  PRINT "    - PSEUDOHOMOGENOUS,ISOTROPIC MEDIA"
2120  PRINT "    - SPHERICAL VOID (BUBBLE)"
2130  PRINT "    - STAGNANT MEDIUM (RESIN)"
2140  PRINT "    - NO INTERACTION (COALESCENCE)"
2150  PRINT "          BETWEEN VOIDS
2160  PRINT "    - UNIFORM TEMPERATURE AND PRESSURE"
2170  PRINT "          AT ANY TIME THROUGHOUT THE"
2180  PRINT "          MEDIUM AS GIVEN BY THE "
2190  PRINT "          TEMPERATURE AND PRESSURE OF"
2200  PRINT "          THE CURING CYCLE AT THAT TIME"
2210  PRINT
2220  PRINT "THE ASYMPTOTIC SOLUTION OF SCRIVEN,"
2230  PRINT "CHEM. ENG. SCI., 10, 1, (1959) AND THE"
2240  PRINT "PETURBATION SOLUTION OF SUBRAMANIAN "
2250  PRINT "AND WEINBERG, AICHE J., 27 (4), 739"
2260  PRINT "(1981) ARE USED TO CALCULATE BUBBLE"
2270  PRINT "GROWTH."
2280  PRINT
2290  INVERSE
2300  INPUT "  PRESS <RETURN> TO CONTINUE";JUNK$
2310  NORMAL
2320  HOME
2330  PRINT "THE PROGRAM HAS TWO OPTIONS."
2340  PRINT
2350  PRINT "    - OPTION 1 CALCULATES VOID GROWTH"
2360  PRINT "          WHEN THE VOID CONTAINS ONLY"
2370  PRINT "          WATER VAPOR"
2380  PRINT "    - OPTION 2 CALCULATES VOID GROWTH"
2390  PRINT "          WHEN WATER VAPOR DIFFUSES "
2400  PRINT "          INTO AN EXISTING AIR BUBBLE."
2410  PRINT
2420  PRINT "THE USER MUST SUPPLY INFORMATION ON:"
2430  PRINT
2440  PRINT "    - WATER SOLUBILITY DATA"
2450  PRINT "    - WATER DIFFUSIVITY IN THE PREPREG"
2460  PRINT "    - CURING CYCLE INFORMATION"
2461  PRINT
2470  INVERSE
2480  INPUT "  PRESS <RETURN> TO CONTINUE";JUNK$
2490  NORMAL
2500  HOME
2510  REM
2520  REM  INPUT OPTION, RESIN DENSITY, RESIN MASS FRACTION
2530  REM  INPUT WATER-SOLUBILITY-IN-RESIN EXPRESSION AND ITS PARAMETERS

2540  REM
2550  PRINT
2560  PRINT
2570  PRINT "DO YOU WISH TO CALCULATE VOID GROWTH"
2580  PRINT "CONTAINING : "
2590  PRINT
2600  PRINT "    - 1. PURE WATER VAPOR"
2610  PRINT "    - 2. AIR AND WATER VAPOR"
2620  PRINT
2630  INPUT "  TYPE 1 OR 2 : ";OPTN
2640  NORMAL
```

```
2650 OPTN =  INT (OPTN)
2660  IF (OPTN = 1) OR (OPTN = 2) THEN  GOTO 2730
2670  PRINT
2680  INVERSE
2690  PRINT "INVALID OPTION.  ONLY 1 OR 2 ALLOWED."
2700  PRINT "TRY AGAIN PLEASE                      "
2710  NORMAL : PRINT "": REM  5 ^G (BELL)
2720  GOTO 2590
2730  PRINT
2740  PRINT "ENTER RESIN SPECIFIC GRAVITY OR"
2750  INPUT "<RETURN> FOR DEFAULT OF 1.27 : ";DENR$
2760 DENR =  VAL (DENR$)
2770  IF (DENR <  = 0.) THEN DENR = 1.27
2780  PRINT
2790  PRINT "ENTER RESIN MASS FRACTION (0 < MF < 1)"
2800  PRINT "OR <RETURN> FOR DEFAULT OF "
2810  INPUT " 0.32 : ";WR$
2820 WR =  VAL (WR$)
2830  IF (WR = 0.) THEN WR = 0.32
2840  IF (WR > 0.) AND (WR < 1.) THEN  GOTO 2910
2850  INVERSE
2860  PRINT
2870  PRINT "MASS FRACTION MUST BE BETWEEN 0. AND 1."
2880  PRINT "TRY AGAIN PLEASE                      "
2890  NORMAL : PRINT "": REM   5 ^G (BELL)
2900  GOTO 2780
2910  HOME
2920  PRINT
2930  PRINT
2940  PRINT "SPECIFY EXPRESSION USED FOR WATER"
2950  PRINT "SOLUBILITY (WT. %) OF PREPREG"
2960  PRINT
2970  PRINT "   - 1 FOR POWER LAW"
2980  PRINT "       S0 = AP*((RH/100.)^N)"
2990  PRINT "   - 2 FOR EXPONENTIAL"
3000  PRINT "       S0 = AE*((EXP(B*RH/100.)))"
3010  PRINT
3020  INPUT "ENTER 1 OR 2 : ";SOLO
3030 SOLO =  INT (SOLO)
3040  IF (SOLO = 1) OR (SOLO = 2) THEN  GOTO 3100
3050  INVERSE
3060  PRINT "YOU CAN ONLY ENTER 1 OR 2            "
3070  PRINT " TRY AGAIN PLEASE                     "
3080  NORMAL : PRINT "": REM  5 ^G (BELL)
3090  GOTO 2960
3100  HOME
3110  IF (SOLO = 2) THEN  GOTO 3340
3120  REM
3130  REM  SOLUBILITY OPTION 1 POWER LAW
3140  VTAB 6
3150  PRINT "WATER SOLUBILITY IN FRESH PREPREG"
3160  PRINT "IS GIVEN BY S0 = AP*(RH/100)^N, WITH"
3170  PRINT "RH REPRESENTING RELATIVE HUMIDITY"
3180  PRINT "DURING PREPREG PREPARATION.  CONSTANTS"
3190  PRINT "AP AND N MUST BE ENTERED"
3200  PRINT
3210  PRINT "ENTER THE AP CONSTANT OR <RETURN>"
3220  INPUT "FOR DEFAULT VALUE OF 0.558 : ";AP$
3230 AP =  VAL (AP$)
3240  IF (AP = 0.) THEN AP = 0.558
3250  PRINT
3260  PRINT "ENTER THE N CONSTANT OR <RETURN>"
3270  INPUT "FOR DEFAULT VALUE OF 2. : ";N$
3280 N =  VAL (N$)
3290  IF (N = 0.) THEN N = 2
3300  GOTO 3490
```

```
3310  REM
3320  REM  SOLUBILITY OPTION 2 EXP. LAW
3330  VTAB 6
3340  PRINT "WATER SOLUBILITY IN FRESH PREPREG"
3350  PRINT "IS GIVEN BY S0 = AE*XP(B*RH/100)), WITH"
3360  PRINT "RH REPRESENTING RELATIVE AIR HUMIDITY"
3370  PRINT "DURING PREPREG PREPARATION.  THE"
3380  PRINT "CONSTANTS AE AND B MUST BE ENTERED"
3390  PRINT
3400  PRINT "ENTER THE AE CONSTANT OR <RETURN>"
3410  INPUT "FOR DEFAULT VALUE 0.011 : ";AE$
3420 AE =  VAL (AE$)
3430  IF (AE <  = 0.) THEN AE = 0.011
3440  PRINT
3450  PRINT "ENTER THE B CONSTANT OR <RETURN>"
3460  INPUT "FOR DEFAULT VALUE 4.8 : ";B$
3470 B =  VAL (B$)
3480  IF (B = 0.) THEN B = 4.8
3490  HOME : VTAB 6
3500  PRINT "WATER DIFFUSIVITY, DI (IN**2/HR) , IN"
3510  PRINT "THE PREPREG IS GIVEN BY "
3520  PRINT "    DI = D0*(E**(-ED/TEMP)),"
3530  PRINT "WHERE TEMP IS THE TEMPERATURE IN"
3540  PRINT "DEGREES RANKINE.  THE CONSTANTS"
3550  PRINT "D0 (IN**2/HR) AND ED (DEG. R) MUST BE"
3560  PRINT "ENTERED.  "
3570  PRINT
3580  PRINT "ENTER THE D0 CONSTANT OR <RETURN>"
3590  INPUT "FOR DEFAULT VALUE 0.01628 : ";D0$
3600 D0 =  INT (( VAL (D0$) / .155 * 1000) + .5) / 1000
3610  IF (D0 = 0.) THEN D0 = 0.105
3620  PRINT
3630  PRINT "ENTER THE ED CONSTANT OR <RETURN>"
3640  INPUT "FOR DEFAULT VALUE 5070.0 : ";ED$
3650 ED =  INT (( VAL (ED$) - 491.7) * 5 / 9 + 273.2)
3655  IF (ED <  = 0.) THEN ED = 2817.
3660  HOME
3670  VTAB 6
3680  PRINT "ENTER THE RELATIVE HUMIDITY AT WHICH"
3690  PRINT "PREPREG WAS PREPARED (THIS NUMBER"
3700  PRINT "MUST BE BETWEEN 0. AND 100.) "
3710  INPUT "OR <RETURN> FOR DEFAULT 50. : ";H0$
3720 H0 =  VAL (H0$)
3730  IF (H0 = 0.) THEN H0 = 50.
3740  IF (H0 > 0.) AND (H0 <  = 100.) THEN  GOTO 3825
3750  INVERSE
3760  PRINT "RELATIVE HUMIDITY MUST BE BETWEEN"
3770  PRINT "0. AND 100.  TRY AGAIN PLEASE    "
3780  NORMAL : PRINT "": REM  5 ^G (BELL)
3790  GOTO 3660
3800  REM
3810  REM  INPUT CURING CYCLE INFO. TEMPERATURE/HEATING RATES/TIMES FIRS
    T
3820  REM
3825  HOME : VTAB 6
3830  REM   PRINT "ENTER THE DURATION OF THE CURING"
3831  REM   PRINT "CYCLE IN MIN. OR <RETURN> FOR DEFAULT"
3832  REM   INPUT "VALUE OF 215 MINUTES : ";TMAX$
3833  REM   TMAX =  VAL (TMAX$)
3834  REM   IF (TMAX = 0.) THEN TMAX = 215.
3850  HOME
3860  VTAB 6: PRINT "ENTER THE INITIAL TEMPERATURE (DEGREES"
3870  PRINT "FAHRENHEIT) AT THE START OF THE "
3880  PRINT "CURING CYCLE OR <RETURN> FOR DEFAULT"
3890  INPUT "OF 75.0 : ";T$
3900 T7 = (( VAL (T$) - 32) * 5 / 9)
```

```
3920  IF (T7 <  = 0.) THEN T7 = 23.9
3930  HOME : VTAB 6
4070  PRINT "ENTER THE NUMBER OF HEATING RATE"
4080  PRINT "CHANGES INCLUDING PERIODS OF CONSTANT"
4090  PRINT "TEMPERATURE (0 HEATING RATE) UP TO A"
4100  PRINT "LIMIT OF 6, OR <RETURN> FOR DEFAULT"
4110  INPUT "VALUE OF 3 : ";NT$
4120 NT =  INT ( VAL (NT$))
4130  IF (NT = 0) THEN NT = 3
4140  IF (NT > 0) AND (NT <  = 6) THEN  GOTO 4210
4150  INVERSE
4160  PRINT "THE TOTAL NUMBER OF HEATING RATE  "
4170  PRINT "CHANGES MUST BE AN INTEGER BETWEEN"
4180  PRINT "1 AND 6.  TRY AGAIN PLEASE        "
4190  NORMAL : PRINT "": REM  5 ^G (BELL)
4200  GOTO 3930
4210  FOR ICNT = 1 TO NT
4250  HOME : GOSUB 7500: PRINT : PRINT : GOSUB 8000: HOME : NEXT ICNT
4260 ICNT = NT:FLAG = 1: GOSUB 8000: HOME
4300  FOR ICNT = 1 TO NT
4310  IF (RT(ICNT) = 0) THEN 4325
4320  GOTO 4380
4325  VTAB 6
4330  IF (ICNT = 1) THEN  PRINT "FOR THE "ICNT"ST TEMPERATURE PERIOD"
4340  IF (ICNT = 2) THEN  PRINT "FOR THE "ICNT"ND TEMPERATURE PERIOD"
4350  IF (ICNT = 3) THEN  PRINT "FOR THE "ICNT"RD TEMPERATURE PERIOD"
4360  IF (ICNT > 3) THEN  PRINT "FOR THE "ICNT"TH TEMPERATURE PERIOD"
4370  PRINT : PRINT "THE CURE CYCLE IS ON A CONSTANT          TEMPERATURE
      PLATEAU AT "TEMP(ICNT)" DEGREES.      PLEASE ENTER THE DURATION OF
     THE         PLATEAU IN MINUTES OR <RETURN> FOR": INPUT "DEFAULT VALU
     E OF 120 MINUTES. ";P$(ICNT).
4374 P(ICNT) =  VAL (P$(ICNT))
4375  IF (P(ICNT) <  = 0) THEN P$(ICNT) = "120"
4380  HOME : NEXT ICNT
4382 TT(1) = 0.
4385  FOR I = 2 TO NT:JUNK(I) = RT(I - 1):PS$(I) = P$(I - 1): NEXT I
4390  FOR ICNT = 2 TO NT
4395  IF JUNK(ICNT) = 0 THEN TT(ICNT) = TT(ICNT - 1) +  VAL (PS$(ICNT)):
      GOTO 4406
4400 TT(ICNT) = TT(ICNT - 1) + (TEMP(ICNT) - TEMP(ICNT - 1)) / JUNK(ICNT
     )
4406 TT(ICNT) =  INT (TT(ICNT))
4410  NEXT ICNT
4412  FOR I = 1 TO NT:RT(I) = RT(I) * 5 / 9: NEXT I
4415  FOR ICNT = 1 TO (NT - 1)
4420  IF (TT(ICNT) < TT(ICNT + 1)) THEN 4430
4425  PRINT : PRINT : INVERSE : PRINT "TIMES AT WHICH HEATING RATE CHANG
     ES     ARE NOT SEQUENTIALLY INCREASING.       PLEASE ENTER HEATING
      RATE AND            TEMPERATURE DATA AGAIN.                    ": NORMAL
     : FOR I = 1 TO 5000: NEXT I: GOTO 3825
4430  NEXT ICNT
4690 TMAX =  VAL (P$(NT)) + TT(NT)
4700  HOME
4720  VTAB 6
4730  PRINT "CURING CYCLE PRESSURE/TEMPERATURE"
4740  PRINT "DATA MUST BE ENTERED."
4750  PRINT
4820  PRINT
4830  PRINT "ENTER INITIAL PRESSURE (PSI"
4840  PRINT "APPLIED OR <RETURN> FOR DEFAULT"
4850  INPUT "OF 14.70 PSI : ";P1$
4870 P(1) =  VAL (P1$) / 14.7
4880  IF (P(1) <  = 0.) THEN P(1) = 1.0
4890 TP(1) = 0.0
4900  HOME
4910  VTAB 6
```

```
4920  PRINT "ENTER THE NUMBER OF PRESSURE SETTINGS"
4930  PRINT "THAT ARE USED DURING THE CURING CYCLE"
4940  PRINT "UP TO A LIMIT OF 6, OR <RETURN>"
4950  INPUT "FOR DEFAULT VALUE OF 2 : ";NP$
4960 NP =  INT ( VAL (NP$))
4970  IF (NP <  = 0) THEN NP = 2
4980  IF (NP > 0) AND (NP <  = 6) THEN  GOTO 5050
4990  INVERSE
5000  PRINT "THE TOTAL NUMBER OF SETTINGS MUST BE"
5010  PRINT "AN INTEGER BETWEEN 1 AND 6          "
5020  PRINT "TRY AGAIN PLEASE                    "
5030  NORMAL : PRINT "": REM  5 ^G (BELL)
5040  GOTO 4910
5050  HOME
5060  IF (NP = 1) THEN  GOTO 5540
5070  PRINT
5080  FOR ICNT = 2 TO NP
5090  VTAB 6
5100  IF (ICNT = 2) THEN  PRINT "FOR THE ";ICNT;" ND PRESSURE SETTING"
5110  IF (ICNT = 3) THEN  PRINT "FOR THE ";ICNT;" RD PRESSURE SETTING"
5120  IF (ICNT > 3) THEN  PRINT "FOR THE ";ICNT;" TH PRESSURE SETTING"
5130  IF  NOT (NP = 2) THEN  GOTO 5270
5140  PRINT
5150  PRINT "ENTER THE TIME (MINUTES) FROM START OF "
5160  PRINT "CYCLE AT WHICH THE SETTING IS MADE OR "
5170  INPUT "<RETURN> FOR DEFAULT OF 70 MIN. : ";T$
5180 TP(2) =  VAL (T$)
5190  IF (TP(2) <  = 0.) THEN TP(2) = 70.
5200  PRINT
5210  PRINT "ENTER THE PRESSURE SETTING IN PSI OR"
5220  INPUT "<RETURN> FOR DEFAULT OF 85 PSI: ";P1$
5240 P(2) =  VAL (P1$) / 14.7
5250  IF (P(2) <  = 0.) THEN P(2) = 5.78
5260  GOTO 5540
5270  PRINT
5280  PRINT "ENTER THE TIME (MIN.) FROM START OF"
5290  INPUT "CYCLE AT WHICH THE SETTING IS MADE : ";T$
5300 TP(ICNT) =  VAL (T$)
5310  IF (TP(ICNT) =  - 999.) THEN  GOTO 4830
5320  IF (TP(ICNT) >  = TMAX) THEN  GOTO 5350
5330 IK = 1
5340  IF (TP(ICNT) > TP(IK)) THEN  GOTO 5420
5350  INVERSE
5360  PRINT "PRESSURE SETTING TIMES ARE NOT      "
5370  PRINT "SEQUENTIALLY INCREASING.  TRY AGAIN,"
5380  PRINT "OR ENTER -999. TO START OVER        "
5390  PRINT "ENTERING PRESSURE/TIME SETTING DATA "
5400  NORMAL : PRINT "": REM  5 ^G (BELL)
5410  GOTO 5270
5420 IK = IK + 1
5430  IF (IK < ICNT) THEN  GOTO 5340
5440  PRINT
5450  INPUT "ENTER THE PRESSURE SETTING IN PSI : ";P1$
5460 P1$ = P1$ / 14.7
5470 P(ICNT) =  VAL (P1$)
5480  IF (P(ICNT) > 0.) THEN  GOTO 5530
5490  INVERSE
5500  PRINT "PRESSURE MUST BE GREATER THAN 0.    "
5510  PRINT "TRY AGAIN PLEASE                    "
5520  NORMAL : PRINT "": REM  5 ^G (BELL)
5530  NEXT ICNT
5540  HOME : VTAB 6
6000  PRINT "ENTER THE INITIAL BUBBLE DIAMETER IN"
6010  INPUT "INCHES OR <RETURN> FOR DEFAULT OF 0. : ";DSTART$
6020 DSTART = ( VAL (DSTART$)) * 2.54
6030  IF (DSTART < 0.) THEN DSTART = 0.
```

```
6040  IF (OPTN = 2) AND (DSTART > 0.) THEN  GOTO 6230
6050  IF (OPTN = 1) AND (DSTART >  = 0.) THEN  GOTO 6230
6060  REM
6070  REM  ERROR IN INPUT -CAN'T HAVE OPTION 2 (AIR/WATER) WITH NO INITI
    AL BUBBLES
6080  REM
6090  INVERSE
6100  PRINT "FOR OPTION 2 YOU MUST SPECIFY "
6110  PRINT "A BUBBLE SIZE.  TRY AGAIN      "
6120  NORMAL : PRINT "": REM  5 ^G (BELL)
6130  GOTO 6000
6140  REM
6150  REM  ERROR IN INPUT - CAN'T HAVE OPTION 1 (WATER ALONE) WITH NONZE
    RO INITIAL BUBBLE SIZE
6160  REM
6170  INVERSE
6180  PRINT "OPTION 1 IS SELECTED AND INITIAL "
6190  PRINT "BUBBLE SIZE MUST BE ZERO.        "
6200  PRINT "PLEASE TRY AGAIN                 "
6210  NORMAL : PRINT "": REM  5 ^G (BELL)
6220 GO TO 6000
6230  HOME
6240  VTAB 6
6250  PRINT "DO YOU WANT BUBBLE DIAMETER PRINTED"
6260  PRINT "ONLY AT TIMES WHEN PRESSURE AND "
6270  PRINT "HEATING RATE CHANGE. ENTER 1 FOR    "
6280  PRINT "YES, OR (RETURN) FOR BUBBLE    "
6290  PRINT "DIAMETER PRINTED AT EVEN TIME       "
6300  INPUT "INTERVALS : ";T$
6310 IPRT =  INT ( VAL (T$))
6320  IF (IPRT < 0) THEN IPRT = 0
6330  IF (IPRT > 1) THEN IPRT = 1
6340  IF (IPRT = 1) THEN  GOTO 6460
6350  PRINT
6360  PRINT "ENTER THE TIME INTERVAL (MINUTES)"
6370  PRINT "FOR WHICH YOU WISH TO SEE BUBBLE "
6380  INPUT "DIAMETER PRINTED : ";T$
6390 TRI =  VAL (T$)
6395  GOTO 6460
6400  IF (TRI > 0.) AND (TRI <  = TMAX) THEN  GOTO 6460
6410  INVERSE
6420  PRINT "PRINT TIME INTERVAL MUST LIE BETWEEN"
6430  PRINT "0. AND ";TMAX;"  TRY AGAIN PLEASE       "
6440  NORMAL : PRINT "": REM   5 ^G (BELL)
6450  GOTO 6350
6460  HOME : VTAB 6
6470  PRINT "ENTER THE TEMPERATURE AT WHICH THE"
6480  PRINT "RESIN SETS (GELATION TEMPERATURE)"
6490  INPUT "IN DEG. F, OR (RETURN) FOR 350. : ";T$
6500  IF  VAL (T$) <  = 0 THEN GEL = 450: GOTO 6530
6510 T$ =  STR$ ((( VAL (T$) - 32) * 5 / 9) + 273.15)
6520 GEL =  VAL (T$)
6530  HOME
6540  INVERSE
6550  PRINT
6560  PRINT
6570  PRINT "*****************************************"
6580  PRINT "***                                   ***"
6590  PRINT "***          INPUT COMPLETED          ***"
6600  PRINT "***                                   ***"
6610  PRINT "*****************************************"
6620  NORMAL
6630  REM
6640  REM  NOW PRINTOUT THE INPUT INFORMATION
6650  REM
6660 CD$ =  CHR$ (4): REM     ^D (CNTRL-D)
```

```
6670 CL$ =  CHR$ (12): REM      ^L (CNTRL-L)
6680  FOR ICNT = 1 TO 750: NEXT ICNT: REM     I/O PAUSE
6690  HOME
6700  REM
6710  REM  ENERGIZE PRINTER AND PRINT THE INPUT INFORMATION
6720  REM
6730  PRINT CD$;"PR#";IZ: PRINT  CHR$ (20): REM  ^D PR# THEN ^T TO TOGGL
     E ECHO/NO ECHO TO ECHO
6740  INVERSE : PRINT CL$
6750  PRINT : PRINT : PRINT
6760  PRINT "                                                "
6761  PRINT "          PROCESSING SCIENCE OF                 ": PRINT "     EPOXY
     MATRIX COMPOSITES PROGRAM     "
6762  PRINT "                                                "
6763  PRINT " CONTRACT  AFWAL/MLBC F33615-80-C-5021 ": PRINT "
                                    "
6764  PRINT "     PROGRAM BY WASHINGTON UNIVERSITY    ": PRINT " WITH MODI
     FICATION BY GENERAL DYNAMICS "
6765  PRINT "                                               ": PRINT "
                                    "
6780  PRINT '                                               "
6800  PRINT "                                               ": PRINT "
       PROGRAM VOIDS                ": PRINT "
                "
6810  NORMAL
6820  PRINT : PRINT
6830  FOR ICNT = 1 TO 5000: NEXT ICNT
6840  HOME
6850  PRINT : PRINT "PROGRAM OPTION = ";OPTN
6860  PRINT
6870  IF (OPTN = 1) THEN  PRINT "      VOID CONTAINS ONLY WATER VAPOR"
6880  IF (OPTN = 2) THEN  PRINT "      VOID CONTAINS BOTH AIR AND WATER"
6890  PRINT
6900  PRINT "PREPREG RESIN SPECIFIC GRAVITY = ";DENR
6910  PRINT
6920  PRINT "PREPREG RESIN MASS FRACTION = ";WR
6930  PRINT
6935  PRINT "RELATIVE HUMIDITY AT WHICH PREPREG WAS"
6936  PRINT "PREPARED IS ";H0;" (PERCENT)"
6937  PRINT
6940  PRINT "SOLUBILITY OPTION ";SOLO;" SELECTED"
6950  PRINT
6960  IF (SOLO = 1) THEN  PRINT "      S0 = ";AP;" * (";H0 / 100;") ^ ";N
     ;" (WT %)"
6970  IF (SOLO = 2) THEN  PRINT "      S0 = ";AE;" * EXP( ";B;" * (";H0 /
     100;")) (WT %)"
6980  FOR ICNT = 1 TO 6000: NEXT ICNT
6990  HOME
7000  PRINT
7010  PRINT "WATER DIFFUSIVITY IN PREPREG IS"
7020  PRINT "GIVEN BY DI (IN^2/HR),WHERE"
7030  PRINT "      DI = ";D0;" * EXP( -"; INT (((ED - 273.15) * 9 / 5 + 4
     92));" / T)"
7040  PRINT
7080  PRINT "THE INITIAL BUBBLE DIAMETER AT ROOM"
7090  PRINT "TEMPERATU  AND 14.7 PSI PRESSURE IS"
7100 C$ =  STR$ (DSTAR / 2.54):A$ =  RIGHT$ (C$,4):B$ =  LEFT$ (A$,1): IF
     B$ = "E" THEN  GOSUB 8500
7105  PRINT C$" INCHES"
7110 DSTART = DSTART / (P(1) ^ (1. / 3.))
7120  FOR ICNT = 1 TO 3000: NEXT ICNT
7130  HOME
7140  PRINT : PRINT
7150  PRINT "DURATION OF CURING CYCLE IS ";TMAX;" MIN."
7160  PRINT
7170  PRINT "TOTAL NUMBER OF PRESSURE SETTINGS = ";NP
```

```
7180  PRINT
7190  PRINT "TIME (MIN.)      PRESSURE (PSI)"
7200  PRINT
7210  FOR ICNT = 1 TO NP: PRINT  TAB( 7 -  LEN ( STR$ (TP(ICNT)))); LEFT$
       STR$ (TP(ICNT)),5); TAB( 27 -  LEN ( STR$ (P(ICNT)))); LEFT$ ( STR$
     ((P(ICNT)) * 14.7),5): NEXT ICNT
7220  FOR ICNT = 1 TO 7000: NEXT ICNT
7230  HOME : PRINT : PRINT
7240  PRINT "TOTAL NUMBER OF HEATING RATES = ";NT
7250  PRINT
7260  PRINT "TIME (MIN.)      HEATING RATES (F / MIN)"
7270  PRINT
7280  FOR ICNT = 1 TO NT:JUNK = RT(ICNT) * 1.8: PRINT  TAB( 7 -  LEN ( STR$
     (TT(ICNT))); LEFT$ ( STR$ (TT(ICNT)),5); TAB( 27 -  LEN ( STR$ (JU
     NK))); LEFT$ ( STR$ (JUNK),5): NEXT ICNT
7290  FOR ICNT = 1 TO 6000: NEXT ICNT
7300  HOME : PRINT : PRINT
7310 T9 =  INT (T7 * 1.8 + 32): PRINT "INITAL TEMPERATURE IS ";T9;" F": PRINT
     : PRINT
7320  PRINT "RESIN GELATION TEMPERATURE IS "; INT ((GEL - 273) * 1.8 + 3
     2);" F"
7330  FOR ICNT = 1 TO 3000: NEXT ICNT
7340  PRINT
7350  FOR ICNT = 1 TO 1000: NEXT ICNT
7360  PRINT  CHR$ (4);"PR#0"
7370  GOTO 26
7500  REM  SUBROUTINE HEAT RATE
7505  VTAB 6
7510  IF (ICNT = 1) THEN  PRINT "FOR THE "ICNT"ST TEMPERATURE PERIOD"
7520  IF (ICNT = 2) THEN  PRINT "FOR THE "ICNT"ND TEMPERATURE PERIOD"
7530  IF (ICNT = 3) THEN  PRINT "FOR THE "ICNT"RD TEMPERATURE PERIOD"
7540  IF (ICNT > 3) THEN  PRINT "FOR THE "ICNT"TH TEMPERATURE PERIOD"
7550  PRINT : PRINT "ENTER THE HEATING RATE (DEG F/MIN)"
7560  IF (ICNT = 1) AND (NT = 3) THEN  INPUT "OR (RETURN) FOR DEFAULT OF
      3.6";RT$(1):RT(1) =  VAL (RT$(1)): IF RT(1) <  = 0 THEN RT$(1) = "
     3.6"
7570  IF (ICNT = 2) AND (NT = 3) THEN  INPUT "OR (RETURN) FOR DEFAULT OF
      0.0";RT$(2)
7580  IF (ICNT = 3) AND (NT = 3) THEN  INPUT "OR (RETURN) FOR DEFAULT OF
      1.98";RT$(3):RT(3) =  VAL (RT$(3)): IF RT(3) <  = 0 THEN RT$(3) =
     "1.98"
7590  IF (NT <  > 3) THEN  PRINT : PRINT : INPUT "HEATING RATE (DEG F/MI
     N): ";RT$(ICNT)
7600 RT(ICNT) =  VAL (RT$(ICNT))
7610  RETURN
8000  REM  SUBROUTINE TEMP
8001  IF FLAG = 1 THEN  VTAB 6
8005  IF ICNT = 1 THEN :TEMP$(1) =  STR$ (T7 * 1.8 + 32): GOTO 8090
8010  IF (ICNT = 2) THEN  PRINT "FOR THE "ICNT"ND TEMPERATURE PERIOD"
8020  IF (ICNT = 3) THEN  PRINT "FOR THE "ICNT"RD TEMPERATURE PERIOD"
8030  IF (ICNT > 3) THEN  PRINT "FOR THE "ICNT"TH TEMPERATURE PERIOD"
8035  IF FLAG = 1 THEN ICNT = ICNT + 1: VTAB 9: INPUT "ENTER TEMPERATURE
      AT END OF PERIOD       OR (RETURN) FOR DEFAULT VALUE OF         350
     DEG F ";TEMP$(ICNT): IF  VAL (TEMP$(ICNT)) <  = 0 THEN TEMP$(ICNT) =
     "350"
8037  IF FLAG = 1 THEN  GOTO 8090
8040  PRINT "ENTER THE TEMPERATURE (DEG. FAHRENHEIT)": PRINT "AT THE STA
     RT OF TEMPERATURE PERIOD
8050  IF (ICNT = 2) AND (NT = 3) THEN  INPUT "OR (RETURN) FOR DEFAULT OF
      275 ";TEMP$(2): IF  VAL (TEMP$(2)) <  = 0 THEN TEMP$(2) = "275"
8060  IF (ICNT = 3) AND (NT = 3) THEN  INPUT "OR (RETURN) FOR DEFAULT OF
      275 ";TEMP$(3): IF  VAL (TEMP$(3)) <  = 0 THEN TEMP$(3) = "275"
8070  IF (NT <  > 3) THEN  INPUT "TEMPERATURE (DEG F) ";TEMP$(ICNT)
8090 TEMP(ICNT) =  VAL (TEMP$(ICNT))
8100  RETURN
8500  REM
```

```
8520  FOR I = 1 TO LEN (C$) - 4):I$(I) =  MID$ (C$,I,1): NEXT I
8525  IF I$(2) = "" THEN I$(2) = "."
8530 F =  VAL ( RIGHT$ (A$,1)) - 1
8535 D$ = ""
8540  FOR I = 1 TO F:D$ = D$ + "0": NEXT I
8550 C$ = I$(2) + D$ + I$(1) + I$(3) + I$(4) + I$(5)
8560  RETURN
```

* U.S. GOVERNMENT PRINTING OFFICE: 1984 - 759-062/844